

# Physical and Flow Properties of Glass- Forming Chemicals ( $\text{V}_2\text{O}_5$ , $\text{SnO}$ , $\text{SnO}_2$ , $\text{Cr}_2\text{O}_3$ , $\text{FeCr}_2\text{O}_4$ , and $\text{ZrSiO}_4$ ) and Mixtures

June 2022

Seung Min Lee  
Carolyn A Burns  
Jaehun Chun  
Tongan Jin  
Dong-Sang Kim  
Renee L Russell  
William C Eaton  
John D Vienna

## DISCLAIMER

This report was prepared as an account of work sponsored by an agency of the United States Government. Neither the United States Government nor any agency thereof, nor Battelle Memorial Institute, nor any of their employees, makes **any warranty, express or implied, or assumes any legal liability or responsibility for the accuracy, completeness, or usefulness of any information, apparatus, product, or process disclosed, or represents that its use would not infringe privately owned rights.** Reference herein to any specific commercial product, process, or service by trade name, trademark, manufacturer, or otherwise does not necessarily constitute or imply its endorsement, recommendation, or favoring by the United States Government or any agency thereof, or Battelle Memorial Institute. The views and opinions of authors expressed herein do not necessarily state or reflect those of the United States Government or any agency thereof.

PACIFIC NORTHWEST NATIONAL LABORATORY  
*operated by*  
BATTELLE  
*for the*  
UNITED STATES DEPARTMENT OF ENERGY  
*under Contract DE-AC05-76RL01830*

Printed in the United States of America

Available to DOE and DOE contractors from the  
Office of Scientific and Technical Information,  
P.O. Box 62, Oak Ridge, TN 37831-0062;  
ph: (865) 576-8401  
fax: (865) 576-5728  
email: [reports@adonis.osti.gov](mailto:reports@adonis.osti.gov)

Available to the public from the National Technical Information Service  
5301 Shawnee Rd., Alexandria, VA 22312  
ph: (800) 553-NTIS (6847)  
email: [orders@ntis.gov](mailto:orders@ntis.gov) <<https://www.ntis.gov/about>>  
Online ordering: <http://www.ntis.gov>

# **Physical and Flow Properties of Glass-Forming Chemicals ( $V_2O_5$ , $SnO$ , $SnO_2$ , $Cr_2O_3$ , $FeCr_2O_4$ , and $ZrSiO_4$ ) and Mixtures**

June 2022

Seung Min Lee  
Carolyn A Burns  
Jaehun Chun  
Tongan Jin  
Dong-Sang Kim  
Renee L Russell  
William C Eaton  
John D Vienna

Prepared for  
the U.S. Department of Energy  
under Contract DE-AC05-76RL01830

Pacific Northwest National Laboratory  
Richland, Washington 99354

## Executive Summary

For an efficient nuclear waste vitrification process at Hanford's Waste Treatment and Immobilization Plant (WTP), proper selection and consistent supply of glass-forming chemicals (GFCs) are crucial. Thorough characterization of the GFCs is required to reduce risks in operation of the vitrification facility.

Low-activity waste (LAW) will be blended with GFCs to form slurry feeds and then fed to melter and vitrified. To enhance properties of waste glasses, new chemicals are being introduced to the current GFC mixture.<sup>1,2,3</sup> In this study, three new GFCs were evaluated for enhanced LAW glass formulations: chromium oxide ( $\text{Cr}_2\text{O}_3$ ), vanadium oxide ( $\text{V}_2\text{O}_5$ ), and stannic oxide ( $\text{SnO}_2$ ). These three oxide components are included in enhanced waste glass formulations, and GFCs with the appropriate physical and flow properties are needed. As a starting point, single metal oxide GFCs,  $\text{Cr}_2\text{O}_3$ ,  $\text{V}_2\text{O}_5$ , and  $\text{SnO}_2$ , were sourced and tested. Then, alternative sources of Sn and Cr ( $\text{SnO}$  and  $\text{FeCr}_2\text{O}_4$ ) were tested along with an alternative zircon source ( $\text{ZrSiO}_4$ ).

This report documents the work performed to collect physical and flow property data on these new GFCs and melter feed slurries generated using these GFCs and simulated low-activity wastes.

To characterize these new individual GFCs and mixtures of the GFCs, an industrial bulk characterization consultant, Jenike and Johanson, was employed to measure physical and flow properties of individual GFCs and their mixtures. Pacific Northwest National Laboratory (PNNL) also measured several selected physical properties including data evaluation as a quality assurance step. In addition, PNNL measured physical and rheological properties of slurry melter feeds containing these GFCs.

All new individual GFCs, except for  $\text{ZrSiO}_4$ , used for this study were not considered as the original baseline 13 GFCs currently planned or used at the WTP. Therefore, these new GFCs may need to replace other existing GFCs or require new silos. Based on the measured property data and fundamental information of storage design,  $\text{Cr}_2\text{O}_3$ ,  $\text{SnO}_2$ , and  $\text{FeCr}_2\text{O}_4$  are not suggested to be used because of issues with ratholing, arching, and caking.  $\text{V}_2\text{O}_5$  and  $\text{SnO}$  might be acceptable to be used but can also raise concerns for stagnant materials in the silo with insufficient wall angle. Bead-type  $\text{ZrSiO}_4$  does not raise any concerns for use in current silos and hoppers. GFC mixtures and slurry feeds tested in this study did not raise any issues for use at the WTP.

---

<sup>1</sup> Vienna JD, GF Piepel, DS Kim, JV Crum, CE Lonergan, BA Stanfill, BJ Riley, SK Cooley and T Jin. 2016. *2016 Update of Hanford Glass Property Models and Constraints for Use in Estimating the Glass Mass to be Produced at Hanford by Implementing Current Enhanced Glass Formulation Efforts*. PNNL-25835, Pacific Northwest National Laboratory, Richland, WA.

<sup>2</sup> Vienna, JD, A Heredia-Langner, SK Cooley, AE Holmes, DS Kim, and NA Lumetta. 2022. *Glass Property-Composition Models for Support of Hanford WTP LAW Facility Operation*, PNNL-30932, Rev. 2, Pacific Northwest National Laboratory, Richland, WA.

<sup>3</sup> Muller I, KS Matlack, H Gan, and IL Pegg. 2019. *Optimization of Enhanced LAW Correlation Glasses for Processing*. VSL-19R4460-1, Rev. 0, Vitreous State Laboratory, The Catholic University of America, Washington, D.C., and Atkins Energy Federal EPC, Inc., Calverton, MD.



## Acknowledgments

The authors thank Jenike and Johanson for the measurements and data reported of the physical and flow properties of GFCs and their mixtures. We also thank Maura Zimmerschied, Matt Wilburn, Derek Dixon, and David MacPherson for reviewing data, tables, and figures associated with this report. The authors gratefully acknowledge the financial support provided by the U.S. Department of Energy Office of River Protection and the project direction provided by Albert A. Kruger.

## Acronyms and Abbreviations

ADSP	air displacement slurry pump
ASTM	American Society for Testing and Materials
ASME	The American Society of Mechanical Engineers
CFR	Code of Federal Regulations
CRV	concentrate receipt vessel
CS	carbon steel
C/N	carbon to nitrogen mole ratio
DFLAW	Direct Feed Low-Activity Waste
DOE	U.S. Department of Energy
DS	dissolved solids
DST	double-shell tank
ECE	evaporator concentrate effluent
EDE	evaporator dilute effluent
EH	effective head
EMF	Effluent Management Facility
EWG	enhanced waste glass
GFC	glass-forming chemical
GFSF	Glass Former Storage Facility
HR	hot rolled
ILST	interim LAW storage tank
J&J	Jenike and Johanson
LAW	low-activity waste
MFPV	melter feed preparation vessel
MFV	melter feed vessel
NIST	National Institute of Standards and Technology
NQA	Nuclear Quality Assurance
NQAP	Nuclear Quality Assurance Program
PNNL	Pacific Northwest National Laboratory
SS	stainless steel
SOP	standard operating procedure
TS	total solids
TSCR	Tank Side Cesium Removal
UDS	undissolved solids
WTP	Waste Treatment and Immobilization Plant

## Contents

Executive Summary .....	ii
Acknowledgments .....	iii
Acronyms and Abbreviations .....	iv
1.0 Introduction .....	1
1.1 Quality assurance .....	2
2.0 Conduct of Testing .....	3
2.1 Preparation of individual GFCs and their mixtures .....	3
2.2 Powder property measurement at J&J .....	7
2.2.1 Cohesive strength test .....	8
2.2.2 Compressibility test .....	9
2.2.3 Wall friction test .....	10
2.2.4 Permeability test .....	11
2.2.5 Impact chute test .....	12
2.2.6 Angle of repose test .....	13
2.2.7 Particle size distribution .....	14
2.3 Powder property measurement at PNNL .....	14
2.3.1 Particle density .....	14
2.3.2 Moisture content .....	14
2.3.3 Particle size distribution .....	15
2.3.4 Angle of repose .....	15
2.4 Preparation of slurry melter feeds and property measurements at PNNL .....	16
2.4.1 Water content, total solid, dissolved solid, and undissolved solid test .....	21
2.4.2 Density test .....	21
2.4.3 pH test .....	21
2.4.4 Shear strength, viscosity, and yield stress test .....	21
2.4.5 Settling test .....	22
3.0 Results and Discussion .....	23
3.1 Summary of data for physical and flow properties of GFCs .....	23
3.1.1 Particle size analysis .....	23
3.1.2 Cohesive strength test .....	28
3.1.3 Compressibility test .....	29
3.1.4 Wall friction tests .....	29
3.1.5 Permeability test .....	33
3.1.6 Chute angle tests .....	33
3.1.7 Angle of repose test .....	34
3.1.8 Particle density .....	35

3.1.9	Moisture content.....	36
3.2	Summary of data for physical and rheological properties of slurry feeds .....	37
3.2.1	Water content, total solids, dissolved solids, and undissolved solids .....	37
3.2.2	Slurry melter feed density .....	38
3.2.3	pH .....	38
3.2.4	Shear strength, viscosity, and yield stress .....	39
3.2.5	Settling test.....	40
3.3	Dimension of silos at WTP and comparison with GFC properties.....	42
4.0	Conclusion .....	44
4.1	Results, concerns, and suggestions for bulk powder GFCs .....	44
4.2	Acceptable ranges of physical and flow properties of GFCs.....	45
4.3	Results, concerns, and suggestions for slurry feeds .....	45
4.4	Criteria of physical and rheological properties of slurry feeds.....	46
5.0	References .....	48
Appendix A – Chemical Data Sheets from Vendor .....		A.1
Appendix B – Testing Results Sheets .....		B.1
Appendix C – Original Measured Data from Jenike and Johanson.....		C.1
Appendix D – Original Shear Strength and Viscosity Data Measured at PNNL .....		D.1
Appendix E – Original Particle Size Distribution Data Measured at PNNL.....		E.1

## Figures

Figure 1. Simplified flowsheet of GFCs and DFLAW at the WTP. For simplicity, one of two LAW treatment trains are shown within the LAW Vitrification Facility.....	2
Figure 2. Images of the six individual GFCs and seven GFC mixtures .....	7
Figure 3. Schematic of the shear unit for twisting (top) and shear testing (bottom).....	9
Figure 4. Schematic of the compressibility test.....	10
Figure 5. Schematic of the wall friction test .....	11
Figure 6. Schematic of the permeability test (left) and gas flow control box (right) .....	12
Figure 7. Schematic of the impact chute test.....	13
Figure 8. Images of the shapes of powder piles during angle of repose test .....	14
Figure 9. Image of the angle of repose instrument .....	15
Figure 10. Images of “as batched” slurry melter feeds of each batch composition.....	20
Figure 11. Images of (a) the 16 x 16 mm shear vane tool and (b) Z41Ti viscosity spindle.....	22
Figure 12. Comparison of the particle size distribution data between PNNL and J&J.....	27
Figure 13. V <sub>2</sub> O <sub>5</sub> stains on the surfaces of used materials (top: TIVAR 88, middle: 304 SS, bottom: mild CS). Unstained materials shown on the right for comparison. ....	31
Figure 14. Comparison of the average data of angle of repose between PNNL and J&J.....	35

## Tables

Table 1. Properties measured at PNNL and J&J .....	3
Table 2. Basic information on the purchased GFCs .....	4
Table 3. Compositions of GFC mixtures with Cr <sub>2</sub> O <sub>3</sub> , SnO <sub>2</sub> , and V <sub>2</sub> O <sub>5</sub> .....	4
Table 4. Compositions of GFC mixtures with FeCr <sub>2</sub> O <sub>4</sub> , ZrSiO <sub>4</sub> , and SnO .....	5
Table 5. Final glass compositions in wt% .....	16
Table 6. Chemicals needed to make 1-liter waste simulant of 5.6 M sodium with added GFCs .....	17
Table 7. Particle size distributions of materials.....	25
Table 8. Sieving results in wt% for SnO <sub>2</sub> and GFC mixtures .....	25
Table 9. Compared data of particle size distribution measured by PNNL and J&J .....	26
Table 10. Critical rathole dimension and minimum diameter for cohesive arch.....	28
Table 11. Bulk density of individual GFCs and mixtures.....	29
Table 12. Wall friction angles (degrees from vertical).....	32
Table 13. Permeability test results .....	33
Table 14. Impact chute angle (maximum angle from the horizontal).....	34
Table 15. Compared data of angle of repose measured by PNNL and J&J .....	35
Table 16. Particle density results.....	36
Table 17. Moisture content results .....	37

Table 18. Water content, total solids, dissolved solids, and undissolved solids in slurry feeds.....	38
Table 19. Density of slurry melter feeds and estimated g glass per a liter of feed .....	38
Table 20. Average pH of slurry feeds .....	39
Table 21. Shear strength of slurry feeds.....	39
Table 22. Viscosity and yield stress of slurry melter feeds .....	40
Table 23. The volume of the settled undissolved solids in slurry feeds (mL) .....	41
Table 24. Dimension of each silo at WTP.....	42
Table 25. Primary properties of GFCs and assessment .....	43
Table 26. Acceptable range of physical and flow properties of individual GFCs and their mixtures for WTP .....	45
Table 27. Criteria of physical and rheological properties of slurry melter feeds for EWG.....	47

## 1.0 Introduction

The Waste Treatment and Immobilization Plant (WTP) Low-Activity Waste (LAW) Facility will vitrify the LAW fraction of Hanford Site tank wastes. The pretreated LAW will be mixed with glass-forming chemicals (GFCs) to prepare slurry feeds that will be charged into electric melters, where the slurry feeds undergo chemical reactions and are converted to waste glass. GFCs composed of minerals and oxides constitute large portions of the slurry feeds, typically about 50 wt% or more, and allow the LAW to be made into acceptable glass (Muller et al. 2001).

As Figure 1 illustrates, the individual GFCs will be stored separately in silos and blended in a hopper at the Glass Former Storage Facility (GFSF) at the WTP (LaBryer 2019). The mixture of GFCs will then be transferred to a melter feed preparation vessel (MFPV). For Direct Feed Low-Activity Waste (DFLAW), the pretreated waste in the interim LAW storage tank (ILST) is transferred to a concentrate receipt vessel (CRV), where it is blended with offgas condensate concentrate and then the required volume of waste is transferred into a MFPV. The required amount of GFCs and waste will be mixed in the MFPV to prepare the slurry feeds, which are sampled for analysis. The slurry feed will be transferred to a melter feed vessel (MFV) in batches and will be continuously fed from the MFV to a melter through six feed nozzles (in each melter). The slurry feed spreads to cover the molten glass, dries to form a cold-cap, and eventually reacts to form a glass melt (Schumacher et al. 2003; Kim et al. 2012).

The enhanced waste glasses (EWGs) were designed to expand the composition region over which the LAW Facility can operate. These EWGs contain new GFCs ( $\text{Cr}_2\text{O}_3$ ,  $\text{SnO}_2$ , and  $\text{V}_2\text{O}_5$ ) that are not currently represented in the WTP baseline glass formers. The  $\text{SnO}_2$  is added to improve chemical durability,  $\text{V}_2\text{O}_5$  is added to increase sulfate solubility, and  $\text{Cr}_2\text{O}_3$  is added to reduce refractory corrosion in the EWGs. Additionally, it is anticipated that the baseline GFCs may need to be changed during the life of the Hanford mission due to changes in manufacturers or GFC sources. For example,  $\text{FeCr}_2\text{O}_4$ ,  $\text{SnO}$ , and  $\text{ZrSiO}_4$  beads can be considered as alternative sources of Cr, Sn, and Zr. When new GFCs are needed, it is important to assess the physical and flow properties of the GFCs because they can affect storage, transfer, mixing, and/or melting processes (Rieck 2015).

The new proposed GFCs ( $\text{Cr}_2\text{O}_3$ ,  $\text{SnO}_2$ ,  $\text{V}_2\text{O}_5$ ,  $\text{FeCr}_2\text{O}_4$ ,  $\text{SnO}$ , and bead-type  $\text{ZrSiO}_4$ ) for this study have been assessed for physical and flow properties as well as slurry feed properties with them incorporated. Measured property data can provide better understanding of correlations between properties of GFCs as well as their effects on GFC mixtures (Schumacher 2003) and slurry feeds (Chun et al. 2011). Evaluating properties of GFCs and understanding their correlations will be helpful when GFCs are selected, stored, and processed in facilities. Therefore, the results of property measurements, their correlations, and evaluations are presented in this report.

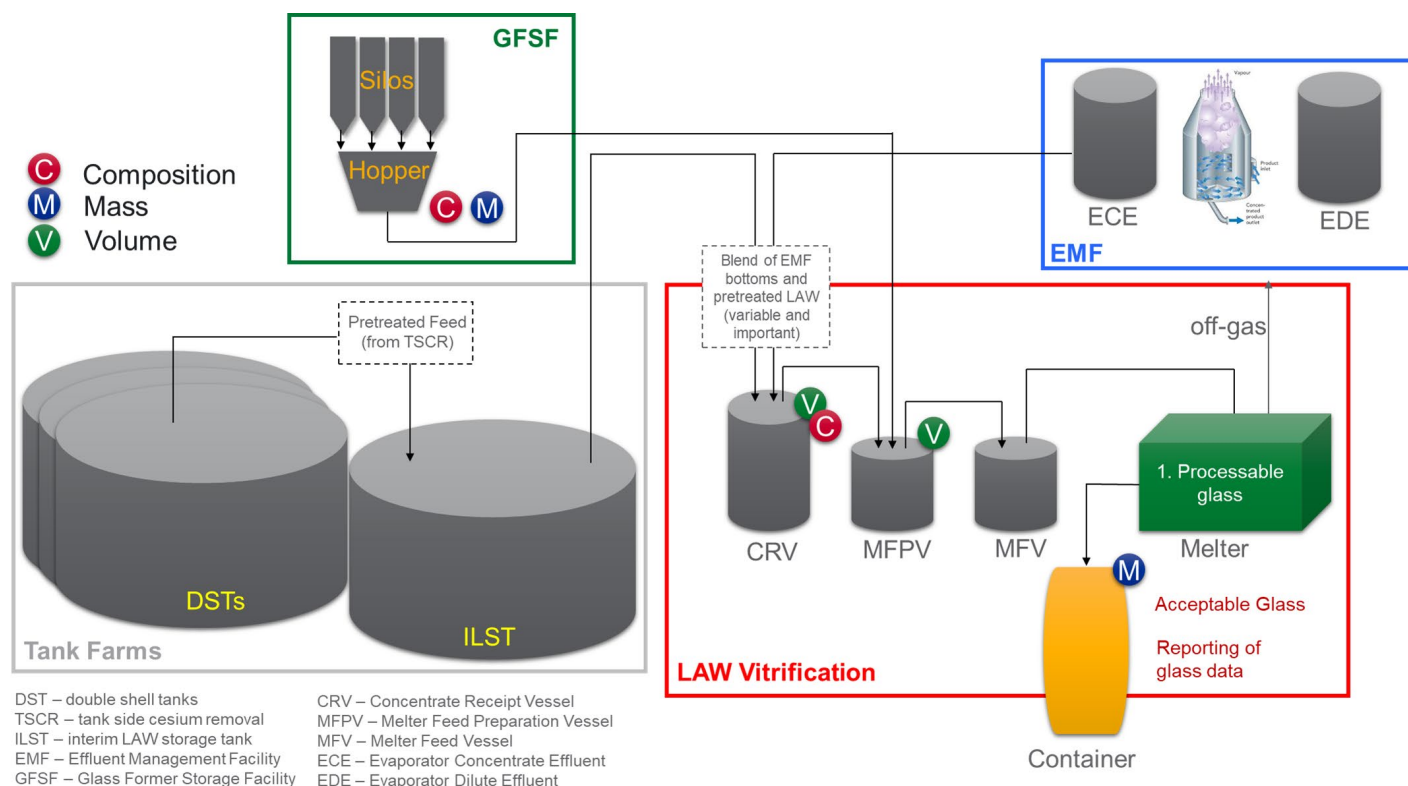


Figure 1. Simplified flowsheet of GFCs and DFLAW at the WTP. For simplicity, one of two LAW treatment trains are shown within the LAW Vitrification Facility.

## 1.1 Quality assurance

This work was performed in accordance with the Pacific Northwest National Laboratory (PNNL) Nuclear Quality Assurance Program (NQAP). The NQAP complies with DOE Order 414.1D, *Quality Assurance*, and 10 CFR 830 Subpart A, *Quality Assurance Requirements*. The NQAP uses ASME NQA-1-2000, *Quality Assurance Requirements for Nuclear Facility Application* (ASME 2000), as its consensus standard and ASME NQA-1-2000, Subpart 4.2.1, as the basis for its graded approach to quality.

The NQAP works in conjunction with PNNL's laboratory-level Quality Management Program, which is based on the requirements as defined in DOE Order 414.1D and 10 CFR 830, *Nuclear Safety Management*, Subpart A, *Quality Assurance Requirements*.

The work of this report was performed to the quality assurance level of applied research with a technology readiness level of 4.



## 2.0 Conduct of Testing

This section describes the physical and flow property measurements for individual GFCs ( $\text{SnO}_2$ ,  $\text{SnO}$ ,  $\text{V}_2\text{O}_5$ ,  $\text{Cr}_2\text{O}_3$ ,  $\text{FeCr}_2\text{O}_4$ , and  $\text{ZrSiO}_4$ ) and their mixtures (seven different batches) conducted at Jenike and Johanson (J&J) and PNNL. Physical and rheological properties of seven LAW slurry feeds that contain these GFC mixtures were also measured by PNNL.

Table 1 shows where each of the property measurements was performed. Tests for angle of repose and particle size distribution were performed by both J&J and PNNL and the results of these two properties were compared.

Tests at J&J were performed in accordance with ASTM procedures. J&J has had substantial involvement in developing and maintaining these procedures.

Table 1. Properties measured at PNNL and J&J

Test	Sample type	PNNL	J&J
Cohesive strength	Bulk powder		✓
Wall friction	Bulk powder		✓
Compressibility	Bulk powder		✓
Particle size distribution	Bulk powder	✓	✓
Permeability	Bulk powder		✓
Chute angle	Bulk powder		✓
Angle of repose	Bulk powder	✓	✓
Particle density	Bulk powder	✓	
Moisture content	Bulk powder	✓	
Water content	Slurry	✓	
Slurry density	Slurry	✓	
pH	Slurry	✓	
Viscosity and yield stress	Slurry	✓	
Shear strength	Slurry	✓	
Settling test	Slurry	✓	

### 2.1 Preparation of individual GFCs and their mixtures

Table 2 shows the GFCs along with vendors and grade used in this study. PNNL evaluated chemical products from several vendors by cost, purity, and availability of large quantity supply. Finally, chemical products that had high purity and availability at an industrial scale were purchased. See Appendix A for detailed information of purchased GFCs.

Table 2. Basic information on the purchased GFCs

New GFC	Vendor	Grade
V <sub>2</sub> O <sub>5</sub>	U.S. Vanadium	99% purity, <200 mesh
SnO <sub>2</sub>	Ferro	98% purity, <325 mesh
SnO	Atotech	99% purity, 50% 44 µm
Cr <sub>2</sub> O <sub>3</sub>	Venator	99% purity, <325 mesh
FeCr <sub>2</sub> O <sub>4</sub>	Prince	100% purity, <38 µm
ZrSiO <sub>4</sub>	Ceroglass	95% purity, 70-125 µm

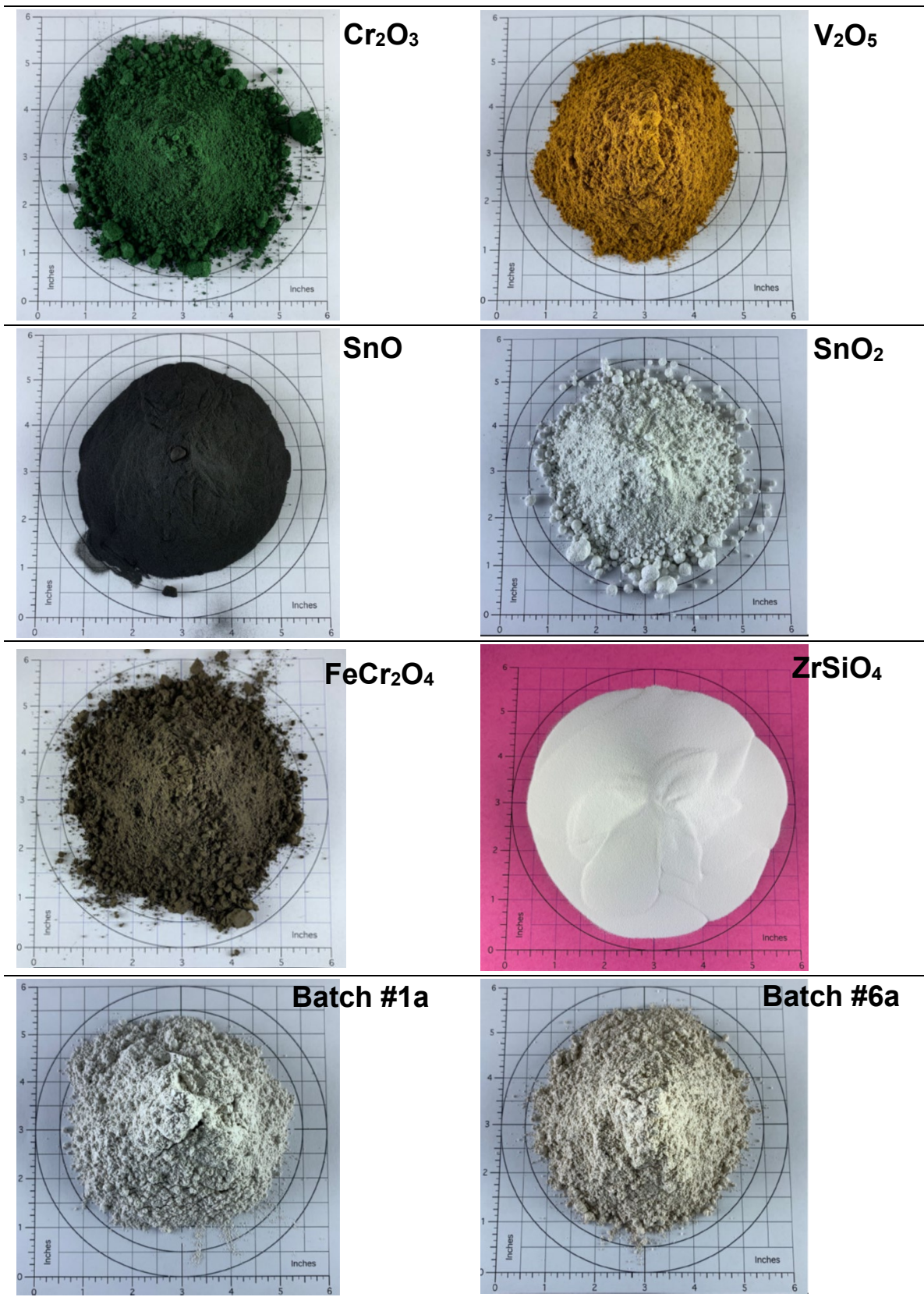
To obtain a range of representative GFC blends, a series of representative LAW compositions was selected. Waste estimates were based on individual CRV content estimates (snapshots) from the WTP Dynamic (G2) Flowsheet Model run MRQ07-0003 baseline case (Lee 2007). Ten waste compositions were selected from this run that span the range of potential waste loading limiting factors. These include wastes with the highest and lowest Na:S, Na:K, and Na:Cl ratios in this projected feed vector (Vienna et al. 2018; Lumetta et al. 2020). An enhanced glass was formulated for each of the 10 wastes according to the method described by Lumetta et al. (2020). Three of the ten glasses were selected with variable content of Cr<sub>2</sub>O<sub>3</sub>, SnO<sub>2</sub>, and V<sub>2</sub>O<sub>5</sub>: (1) maximum tin oxide and chromium oxide and minimum vanadium oxide (glass #1); (2) medium tin oxide, chromium oxide, and vanadium oxide (glass #6); and (3) minimum tin oxide, no chromium oxide, and maximum vanadium oxide (glass #9). Table 3 and 4 provide compositions of each GFC mixture. Note that SnO<sub>2</sub> in Batch #1b was replaced by SnO for Batch #1-1 to see how it changed properties in mixtures and slurry feeds. Figure 2 displays the six individual GFCs purchased and the seven GFC mixtures batched at PNNL. They were all then shipped to J&J for property measurements.

Table 3. Compositions of GFC mixtures with Cr<sub>2</sub>O<sub>3</sub>, SnO<sub>2</sub>, and V<sub>2</sub>O<sub>5</sub>

Component		GFC mass g/l waste					
		Batch #1a		Batch #6a		Batch #9a	
		grams	wt%	grams	wt%	grams	wt%
Kyanite	Al <sub>2</sub> SiO <sub>5</sub>	61.56	7.77	82.93	9.99	181.74	11.00
Boric acid	H <sub>3</sub> BO <sub>3</sub>	117.27	14.80	140.94	16.98	245.76	14.88
Wollastonite	CaSiO <sub>3</sub>	104.94	13.24	95.03	11.45	292.52	17.71
Lithium carbonate	Li <sub>2</sub> CO <sub>3</sub>	0.00	0.00	0.00	0.00	208.80	12.64
Olivine	Mg <sub>2</sub> SiO <sub>4</sub>	30.88	3.90	33.94	4.09	0.00	0.00
Chromium oxide	Cr <sub>2</sub> O <sub>3</sub>	5.36	0.68	0.22	0.03	0.00	0.00
Silica	SiO <sub>2</sub>	270.02	34.08	263.25	31.72	431.03	26.09
Zincite	ZnO	28.42	3.59	0.00	0.00	0.00	0.00
Zircon	ZrSiO <sub>4</sub>	81.44	10.28	99.92	12.04	168.71	10.21
Vanadium pentoxide	V <sub>2</sub> O <sub>5</sub>	0.00	0.00	35.16	4.24	67.58	4.09
Stannic oxide	SnO <sub>2</sub>	43.34	5.47	24.12	2.91	4.24	0.26
Sucrose	C <sub>12</sub> H <sub>22</sub> O <sub>11</sub>	49.09	6.20	54.47	6.56	51.64	3.13
Sum		792.32	100.00	829.98	100.00	1,652.00	100.00

Table 4. Compositions of GFC mixtures with  $\text{FeCr}_2\text{O}_4$ ,  $\text{ZrSiO}_4$ , and  $\text{SnO}$

Component		GFC mass g/l waste							
		Batch #1b		Batch #6b		Batch #9b		Batch #1-1	
		grams	wt%	grams	wt%	grams	wt%	grams	wt%
Kyanite	$\text{Al}_2\text{SiO}_5$	55.04	6.91	78.10	9.40	171.59	10.31	55.04	6.95
Boric Acid	$\text{H}_3\text{BO}_3$	116.45	14.63	141.15	16.98	254.69	15.31	116.45	14.70
Wollastonite	$\text{CaSiO}_3$	106.43	13.37	98.58	11.86	306.01	18.39	106.44	13.44
Hematite	$\text{Fe}_2\text{O}_3$	0.00	0.00	0.33	0.04	1.14	0.07	0.00	0.00
Lithium Carbonate	$\text{Li}_2\text{CO}_3$	0.00	0.00	0.00	0.00	205.65	12.36	0.00	0.00
Olivine	$\text{Mg}_2\text{SiO}_4$	26.69	3.35	32.81	3.95	0.00	0.00	26.69	3.37
Chromite	$\text{FeCr}_2\text{O}_4$	13.69	1.72	0.59	0.07	0.07	0.00	13.69	1.73
Silica	$\text{SiO}_2$	273.04	34.30	265.90	31.99	435.07	26.15	273.04	34.48
Zincite	$\text{ZnO}$	30.64	3.85	0.00	0.00	0.00	0.00	30.64	3.87
Zircon	$\text{ZrSiO}_4$	81.52	10.24	99.96	12.03	167.55	10.07	81.52	10.29
Vanadium pentoxide	$\text{V}_2\text{O}_5$	0.00	0.00	35.19	4.23	67.14	4.03	0.00	0.00
Stannic oxide	$\text{SnO}_2$	43.38	5.45	24.07	2.90	3.43	0.21	0.00	0.00
Stannous oxide	$\text{SnO}$	0.00	0.00	0.00	0.00	0.00	0.00	39.39	4.97
Sucrose	$\text{C}_{12}\text{H}_{22}\text{O}_{11}$	49.09	6.17	54.47	6.55	51.64	3.13	49.09	6.20
Sum		795.97	100.00	831.14	100.00	1,663.96	100.00	791.98	100.00





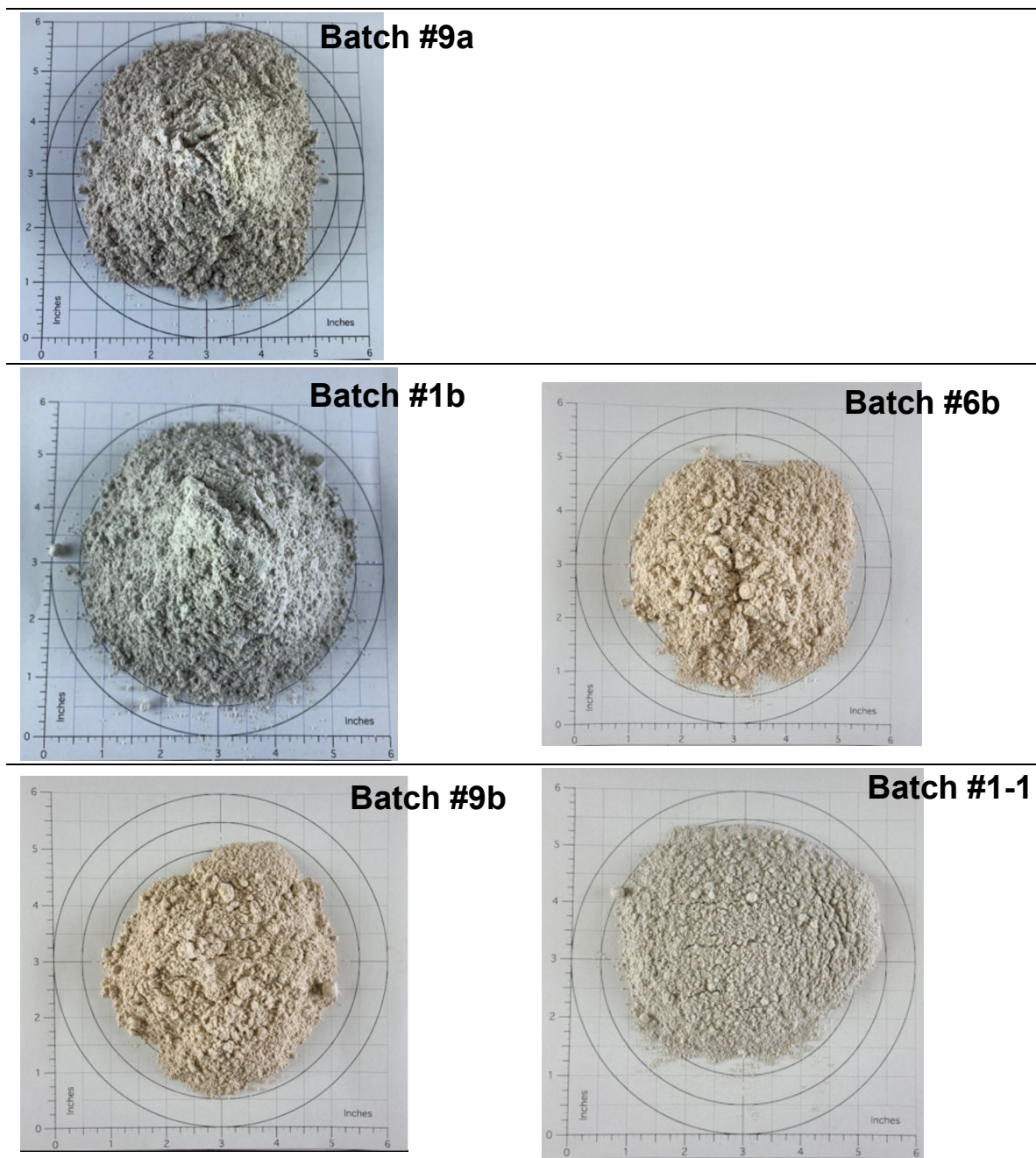


Figure 2. Images of the six individual GFCs and seven GFC mixtures

## 2.2 Powder property measurement at J&J

Six individual GFCs and seven GFC mixtures were tested in consistent experimental conditions at room temperature at J&J for the seven properties shown in Table 1. In this section, more detailed experimental methods will be explained for each of these properties.

### 2.2.1 Cohesive strength test

The cohesive strength tests were conducted using J&J standard operating procedure (SOP) *Determination of the Instantaneous and Time Yield Loci for Shear Testing*, 12/23/15. This procedure of the test is according to ASTM D6128-16 (ASTM 2016).

These tests were performed under continuous flow conditions upon receipt and after a 7-day (individual GFCs) or 1-day (blended GFCs) “at rest” period to obtain information on property changes that result from storing dry bulk materials under static conditions. These durations were based on the possible length of the wait at the WTP. If these bulk powder materials are expected to stay in the silos or hoppers for longer periods, then these materials need to be characterized again after resting for a longer period.

The flow function measured by a Jenike (direct) shear test apparatus is shown in Figure 3. This test is performed in three primary steps: pre-consolidation (or twisting), consolidation, and shear.

The typical test cell size is 95 mm in diameter and 40 mm tall including the mold ring, which results in a volume of 286 cm<sup>3</sup>. Alternate cell sizes may be used, ranging from 25 to 203 mm diameter. Generally, 12 to 15 cells are used during a continuous flow test.

For the measurement of cohesive shear strength, the base, ring, and mould are filled with bulk solid. Then, a predetermined weight is placed on the twisting top and 30 twists are applied. The weight, mould, and twisting top are removed, and a shear cover is placed on the bulk solid. A predetermined set of weights is placed directly on the cover. The stem motor switch applies a steady force to the ring. Some weights are removed and the force in the reverse direction is applied to the ring again. These steps are repeated, and the consolidating loads are recorded.

This test measures the tendency of material particles to stick to one another, on a bulk scale, and resist relative motion as a function of the pressures that are acting on them. This information is useful in determining minimum outlet dimensions and critical rathole diameters, depending on the flow pattern that develops within a container during gravity discharge.

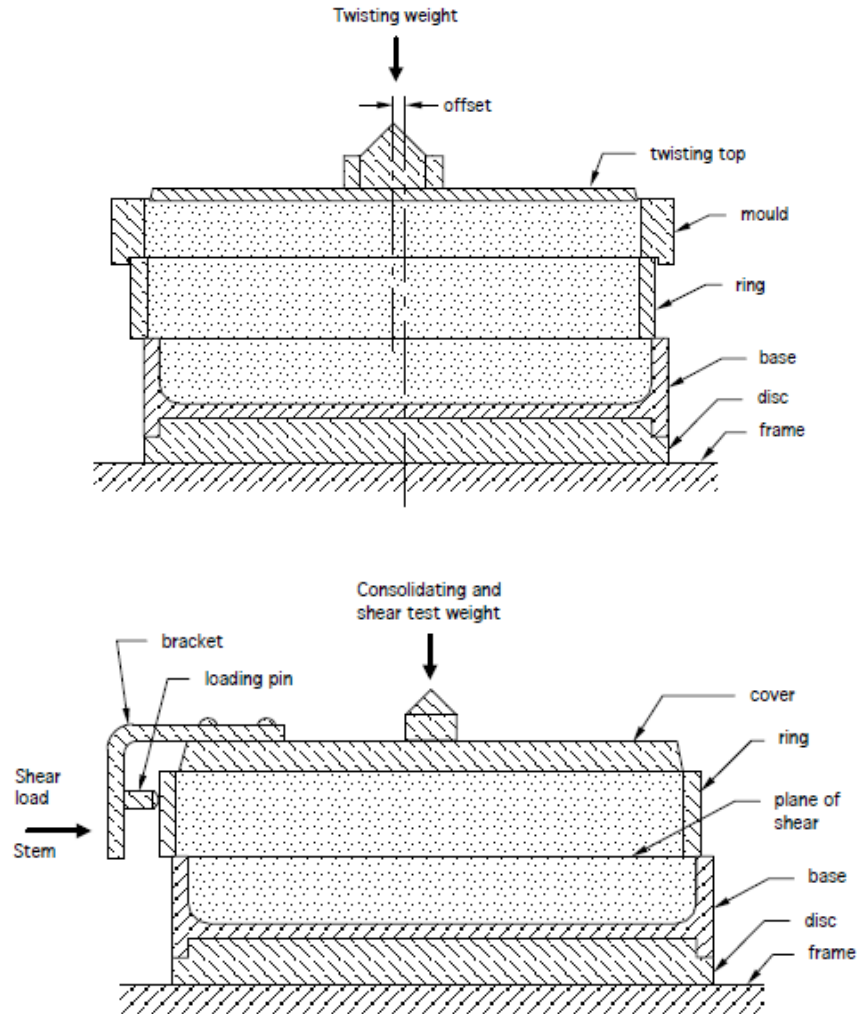


Figure 3. Schematic of the shear unit for twisting (top) and shear testing (bottom)

### 2.2.2 Compressibility test

This test measures the bulk density of a mass of particles as a function of consolidating pressure applied to it using ASTM D6683-19 (ASTM 2019). A test cell for this measurement is shown in Figure 4. The base is filled with the bulk solid to be measured and the cover is placed on it. The weight hanger is then placed on the cover and the indicator holder is placed on the base. After stabilizing the indicator, a load is recorded with an applied weight. A series of weights on the weight hanger is used. After the test is completed, the indicator holder, weights, weight hanger, and cover are all removed, and the net weight of the material is calculated.

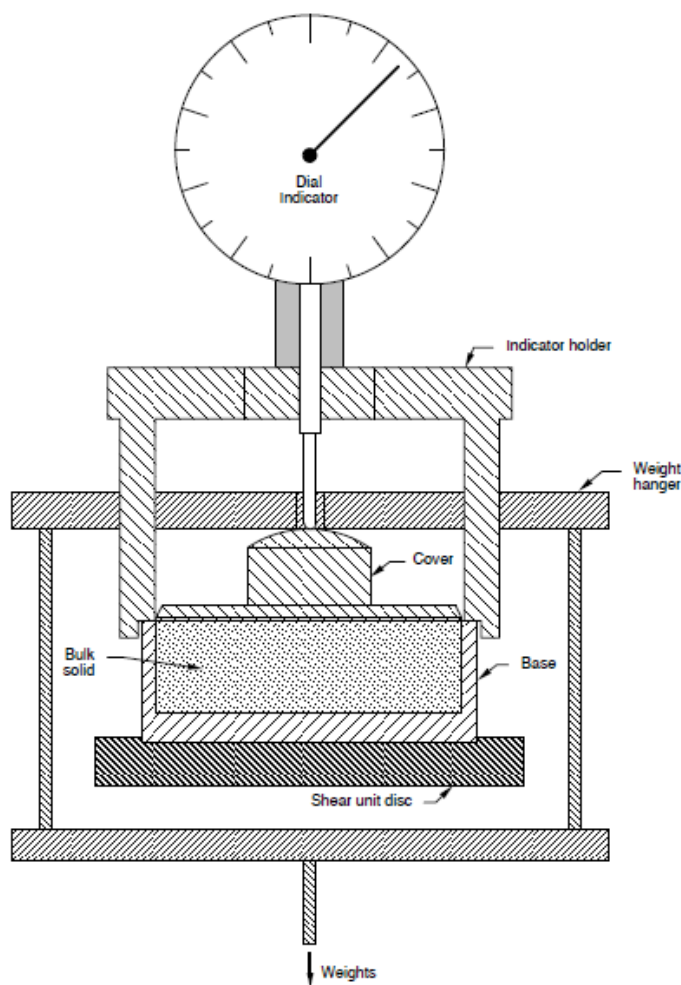


Figure 4. Schematic of the compressibility test

### 2.2.3 Wall friction test

This test measures the frictional drag of a mass of material particles sliding against a stationary wall surface that is representative of the inside of a converging hopper filled with material. This information is useful in determining the tendency of material to slide along a hopper surface that is tapered at a given angle.

The wall friction test was measured using the J&J SOP *Wall Friction Angles (Instantaneous and Time Wall Yield Loci) using the Jenike Shear Tester*, 3/21/18 method. This procedure is conducted according to ASTM Standard D6128-16 (ASTM 2016).

These wall friction tests were performed under continuous flow conditions upon receipt and after a 7-day (individual GFCs) or 1-day (blended GFCs) “at rest” period to obtain information on property changes that occur as a result of storing dry bulk materials under static conditions.

For the measurement of wall friction angle, three different materials of plates, where powder samples slide during testing, were used: 304 stainless steel (SS) sheet; mild carbon steel (CS) hot rolled (HR) plate; and TIVAR 88. For the additional test, TIVAR 88-2, which has a more



advanced surface than TIVAR 88, was used on GFC mixture batch #1a for comparison. These plates represent the inside of a hopper wall. The surface of each plate has different friction that affects the sliding tendency of powder materials against the plate. A ring and stem are placed on the wall sample and filled with the bulk solid. A predetermined weight is loaded on the top of the cover and 30 twists to the top are applied. The weight, mould, and twisting top are then removed. A shear cover is placed on the bulk solid and a predetermined set of weights is directly stacked on the cover. A steady force is applied, and the shear force is measured. The measurements are repeated. Figure 5 displays a schematic of the wall friction test.

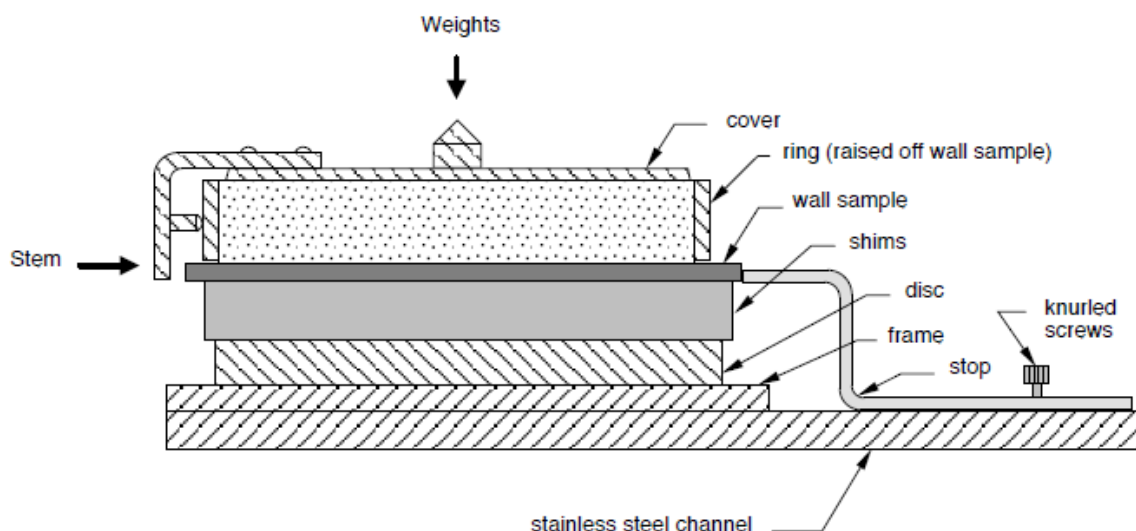


Figure 5. Schematic of the wall friction test

#### 2.2.4 Permeability test

This test measures the ability of air (or other suitable gas) to flow through a bed of particles when a pressure differential occurs across the bed. This value, along with compressibility test results, is used to determine limiting steady flow rates from vessels in gravity discharge, to prevent flooding or starving. It also allows for the determination of suitability of a material for dense phase pneumatic conveying.

The permeability test was measured using the J&J SOP *Gas Permeability of Bulk Solids using Gas Flow Controllers*, 8/22/14 method. The procedure of the test was developed by J&J. A 1-L sample of the bulk solid is placed in the test cylinder of the typical permeability test cell and gas flow control boxes (see Figure 6) with a spoon, layer after layer, distributing each layer lightly and uniformly with the spoon. The excess material is scraped off so that it is level with the top of the cylinder. The weight of the material is obtained and the air pressure to be applied to the cylinder is determined. The air pressure is added and when the flow rate has reached a constant value, the test is stopped, and the value is recorded. The cover is placed on the material in the cell and tapped lightly on the opposite sides of the cylinder with a plastic hammer. Then the height of the material in the cylinder is measured. The tapping is repeated with slightly more force each time and readings are taken until no further movement is made in the material.

When the gas velocity is low, flow through a packed bed is laminar. Darcy's law can be used to relate gas velocities to gas-pressure gradients within or across the bed and can be expressed as

$$u = -\frac{K}{\gamma} \left( \frac{dp}{dx} \right) \quad (1)$$

where  $u$  is the superficial relative gas velocity through the bed of solids,  $K$  is the permeability factor of the bulk solid,  $\gamma$  is bulk density of the solid in the bed, and  $dp/dx$  is the gas-pressure gradient acting at the point in the bed of solids where the velocity is being calculated. The permeability factor,  $K$ , has a unit of velocity and is inversely proportional to the viscosity of the gas. This permeability factor is usually a strong function of the bulk density of the material and has a linear relationship with the bulk density.

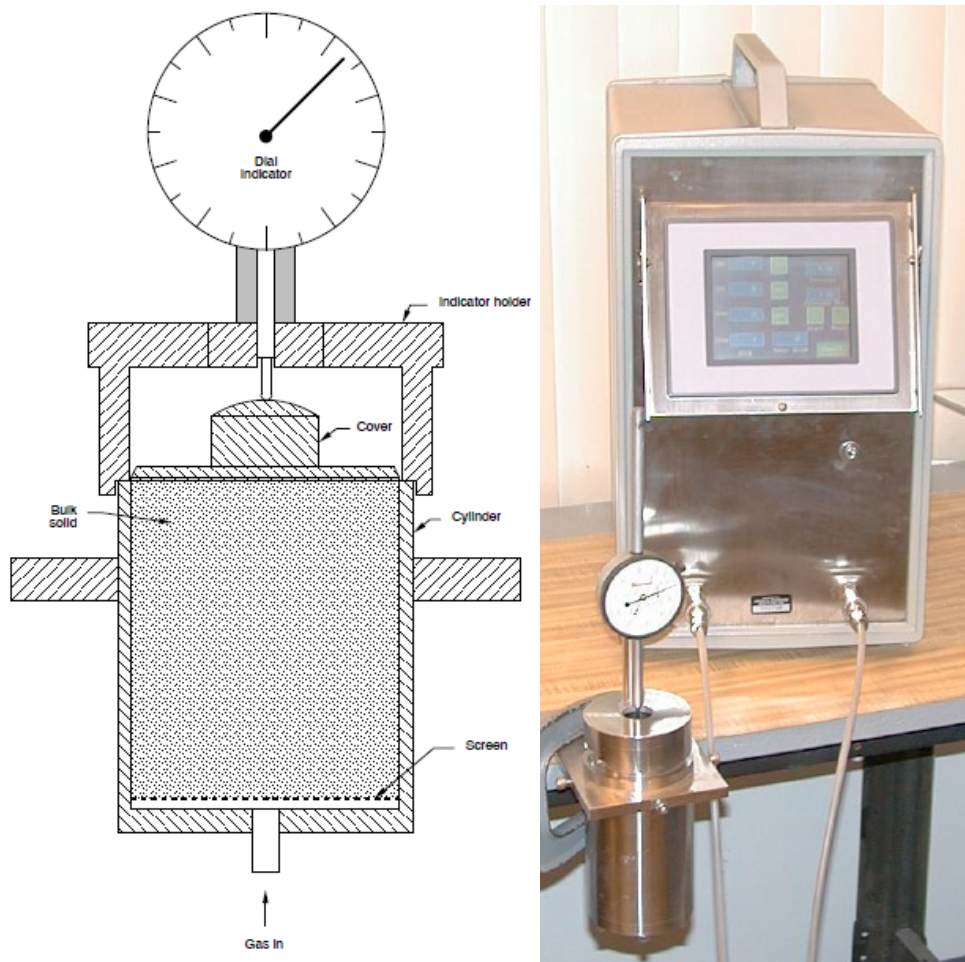


Figure 6. Schematic of the permeability test (left) and gas flow control box (right)

### 2.2.5 Impact chute test

This test measures the minimum chute angles required for non-converging flat chutes to maintain flow after impact. A minimum chute angle required to maintain flow is expressed as a function of the initial impact pressure and is measured from the horizontal chute. This property can be affected by impact pressure, moisture content, temperature, and chute surface.

The chute angle test was measured using the J&J SOP *Adherence to Wall Surfaces using a Manual Chute Tester*, 3/4/16 method. The procedure for this test was developed by J&J.

For the measurement of the impact chute angle, three different plate materials were used: 304 SS sheet; mild CS HR plate and TIVAR 88. The wall coupon and aluminum ring were placed on the plate (see Figure 7) and filled with a material. A 3.75-inch-diameter separator was placed on the sample and the weight to the sample was applied for approximately 15 seconds. Without disturbing, the weight was removed from the ring and sample. Then, the inclination cycle of the tester began. When the ring and material slid on the plate, the motion stopped automatically, and the angle was recorded. Tests were repeated (five trials are typically required at each pressure). When the angle reaches 90°, no additional runs at that pressure are required.

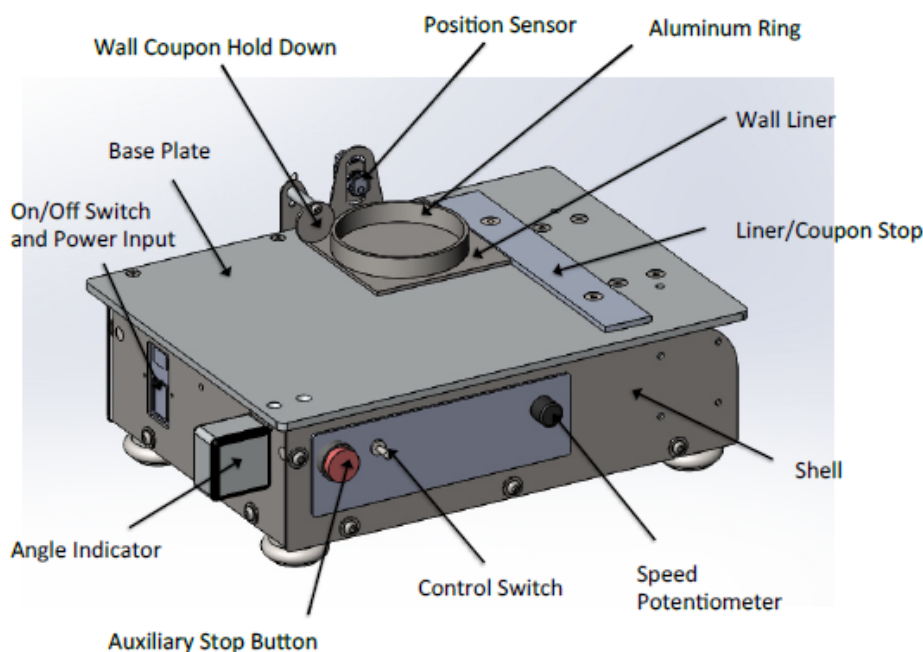


Figure 7. Schematic of the impact chute test

### 2.2.6 Angle of repose test

This test measures the angle that a pile of material will form when a material pours down on a horizontal surface. The angle is measured between the surface of the pile and the horizontal surface on which it rests. This angle can vary depending on how the pile is formed (e.g., drop height and flow rate) and where the angle is measured on the pile. Note that tests for the angle of repose were performed in triplicate and with minimal particle momentum; thus, actual surcharge angle values in the field may be lower because there are various methods of pile formation. There are three distinguishable shapes of piles (straight, concave up, and concave down), as shown in Figure 8. The customized procedure for the test is conducted according to ASTM D6393 (ASTM 2021). One liter of homogenous material was prepared, and a stainless-steel cone was filled with material. The cone was slowly raised, discharging the material to form a pile. After complete discharge of the material, the angle of the pile was measured in four quadrants. This test was repeated three times for each material.

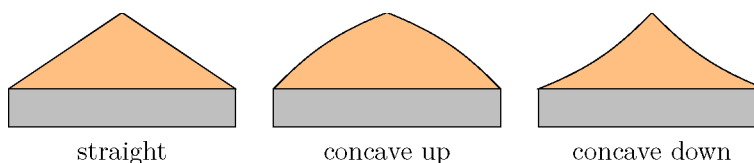


Figure 8. Images of the shapes of powder piles during angle of repose test

### 2.2.7 Particle size distribution

This test measures the particle size of materials using a laser diffraction particle size analyzer or sieving. It is helpful to understand the agglomeration tendency of the particles and the strength of materials. J&J SOP *Particle Size Distribution using Laser Diffraction (Malvern)*, 12/8/17 was used for the measurements of particle size distributions via the Malvern Mastersizer 2000 employing dry dispersion with the Scirocco unit. The method involves passing the dispersed sample through a laser beam and measuring the intensity of the light scattered by the particles at different angles.

J&J did not use the laser diffraction method for SnO<sub>2</sub> because of large agglomeration (see Figure 2). Instead, the sieving method, J&J SOP *Sieve Test Procedure Using Ro-Tap*, 3/2/09 was used for this chemical as well as GFC mixtures, Batch #1b, #6b, #9b, and #1-1. Shaking, tapping, and/or vibration was used to promote flow through the set of sieves. This can result in dispersing weak agglomerates and/or breaking weak particles. The sieve opening sizes used are nominal and are specified in ASTM Standard E-11.

## 2.3 Powder property measurement at PNNL

Samples of the same GFCs and GFC blends characterized by J&J were analyzed for particle size distribution, angle of repose, particle density, and moisture content at PNNL. The methods used by PNNL are discussed in the following sections.

### 2.3.1 Particle density

The room-temperature density of each powder was measured according to PNNL procedure *Density Using a Gas Pycnometer* (EWG-OP-045)<sup>1</sup> using the AccuPyc II 1340 gas pycnometer. The powder was dried in the oven before measuring density. The dried sample was loaded into a vial and placed within the instrument. The instrument then determined the density by the difference in amount of helium gas needed to fill the vial with powder versus without powder. The pycnometer was calibrated within 6 months of the testing and the calibration was checked before and after measurements for that day using a National Institute of Standards and Technology (NIST)-traceable standard tungsten carbide ball.

### 2.3.2 Moisture content

This test measures the quantity of water contained in a material using a moisture analyzer, Mettler Toledo HR83. Tests were performed in accordance with PNNL procedure *Operation of the Mettler Toledo HR83 Moisture Analyzer* (OP-LPTTS-010).<sup>2</sup> The powder, at least 5 g, was

<sup>1</sup> Russell RL. 2017. *Density Using a Gas Pycnometer*. EWG-OP-0045, Rev. 0.0, Pacific Northwest National Laboratory, Richland, Washington.

<sup>2</sup> Burns C. 2019. *Operation of the Mettler Toledo HR83 Moisture Analyzer*. OP-LPTTS-010, Rev. 0, Pacific Northwest National Laboratory, Richland, Washington.

loaded into a dish and placed into the instrument that runs at 95 °C and 105 °C to analyze moisture content. The results were reported in wt% moisture.

### 2.3.3 Particle size distribution

Particle size distribution of powder samples was performed in accordance with PNNL procedure *Size Analysis Using Malvern MS2000* (OP-WTPSP-003).<sup>1</sup> A dry dispersion unit and a wet dispersion unit were used to perform measurement. Using NIST Standard SRM 1003C, a performance check was carried out to verify acceptance criteria of measurement before and after actual samples were measured. PNNL was able to measure the particle size distribution for SnO<sub>2</sub> and did not use the sieving method.

### 2.3.4 Angle of repose

The method of angle of repose employed at PNNL is slightly different from the method used at J&J. Tests were performed in accordance with PNNL procedure *Measurement of Angle of Repose* (OP-WTPSP-166),<sup>2</sup> which is based on ASTM D6393 (ASTM 2021). About 200 mL of the powder sample was poured into the instrument by a scoop. Using vibration of the instrument, powder material flowed through a 710-μm sieve above a glass funnel, fell, and was stacked on a circular metal pan (see Figure 9). When a pile formed, no more powder was introduced. Then, the height of the pile was measured, and the angle of the pile was calculated.

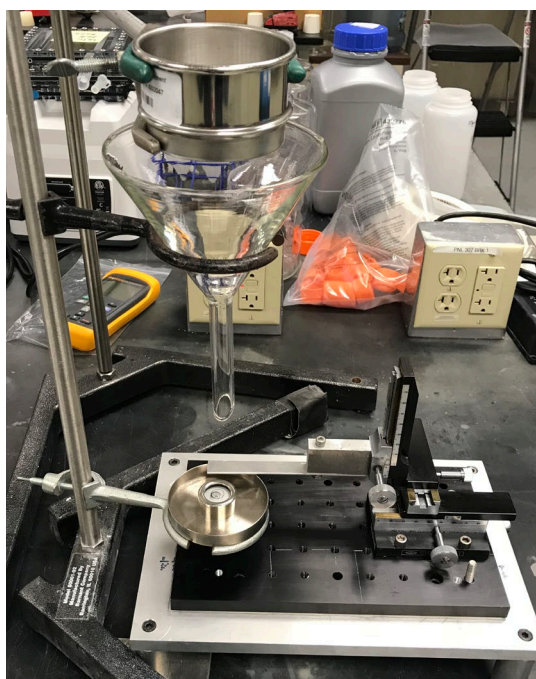


Figure 9. Image of the angle of repose instrument

<sup>1</sup> Burns C. 2019. *Size Analysis Using Malvern MS2000*. OP-WTPSP-003, Rev. 3, Pacific Northwest National Laboratory, Richland, Washington.

<sup>2</sup> Daniel R. 2021. *Measurement of Angle of Repose*. OP-WTPSP-166, Rev. 0, Pacific Northwest National Laboratory, Richland, Washington.



## 2.4 Preparation of slurry melter feeds and property measurements at PNNL

Slurry feeds, batches #1, #1-1, #6, and #9, containing the composition of the GFC mixtures in Table 5, were batched by PNNL to obtain the desired glass compositions in Table 6. Based on these glass compositions, slurry feeds were calculated. However, the calculation of these slurry feeds yielded sodium molarities in the waste simulant portion greater than 6.5 M, which is above the high sodium molarity criteria for the DFLAW process (Russell and Chamberlain 2019; Ard 2019). Therefore, the slurry feed compositions were recalculated to dilute the waste simulants to a sodium molarity of 5.6 M for all feeds. Sucrose was added to each slurry feed to target a carbon to nitrogen mole ratio (C/N ratio) of 0.75. Table 6 provides the final composition of all slurry feeds. Figure 10 displays images of the “as batched” slurry melter feeds. Slurry feed samples were aliquoted and physical and rheological properties were measured on each one.

Table 5. Final glass compositions in wt%

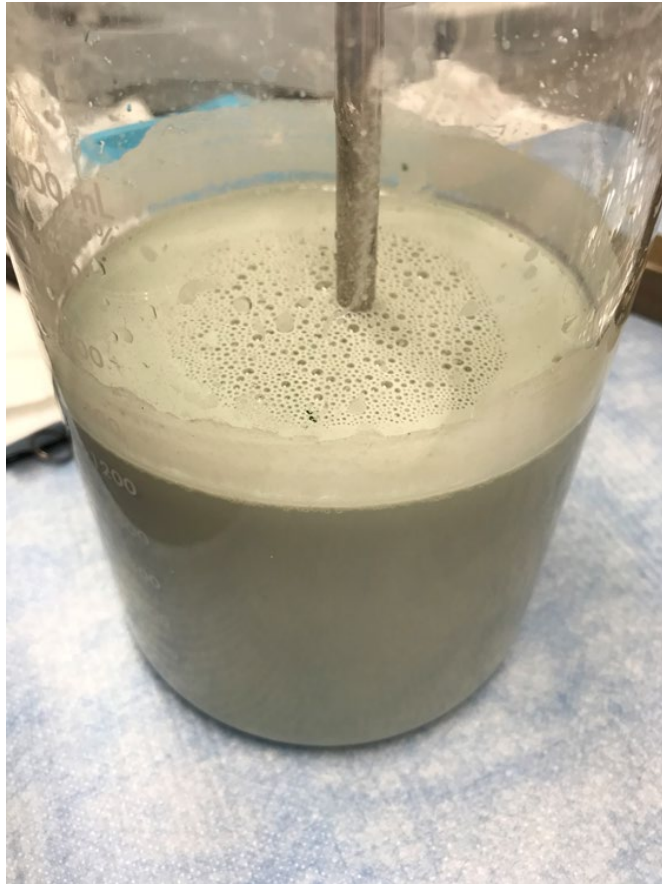
Component	Batch #								
	#1 and #1-1			#6			#9		
	Waste	GFC	Total	Waste	GFC	Total	Waste	GFC	Total
Al <sub>2</sub> O <sub>3</sub>	2.68	3.94	6.62	2.59	5.06	7.65	0.86	6.47	7.33
B <sub>2</sub> O <sub>3</sub>	0.01	6.87	6.88	0.13	7.98	8.12	0.04	8.21	8.26
CaO	-	5.05	5.05	-	4.42	4.42	-	8.03	8.03
Cl	0.21	-	0.21	0.44	-	0.44	0.11	-	0.11
Cr <sub>2</sub> O <sub>3</sub>	0.02	0.56	0.58	0.55	0.03	0.58	0.03	-	0.03
F	0.17	-	0.17	0.15	-	0.15	1.52	-	1.52
Fe <sub>2</sub> O <sub>3</sub>	-	0.33	0.33	0.02	0.35	0.37	0.00	0.12	0.13
K <sub>2</sub> O	3.61	0.02	3.63	0.07	0.02	0.09	0.33	0.04	0.36
Li <sub>2</sub> O	-	-	-	0.02	-	0.02	0.01	4.98	4.99
MgO	-	1.61	1.61	-	1.71	1.71	-	0.12	0.12
Na <sub>2</sub> O	20.99	0.01	21.00	23.38	0.01	23.38	13.91	0.01	13.92
P <sub>2</sub> O <sub>5</sub>	0.24	0.01	0.25	0.46	0.01	0.47	0.40	0.02	0.42
SiO <sub>2</sub>	0.04	40.25	40.28	0.15	39.29	39.44	0.06	41.97	42.03
SnO <sub>2</sub>	-	4.50	4.50	-	2.42	2.42	-	0.25	0.25
SO <sub>3</sub>	0.31	0.01	0.32	0.56	0.00	0.56	1.85	0.01	1.86
TiO <sub>2</sub>	-	0.12	0.12	-	0.15	0.15	-	0.18	0.18
V <sub>2</sub> O <sub>5</sub>	-	-	-	-	3.51	3.51	-	3.98	3.98
ZnO	-	2.95	2.95	-	-	-	-	-	-
ZrO <sub>2</sub>	-	5.50	5.50	-	6.52	6.52	-	6.50	6.50
SUM	28.27	71.73	100.00	28.51	71.49	100.00	19.12	80.88	100.00

Table 6. Chemicals needed to make 1-liter waste simulant of 5.6 M sodium with added GFCs

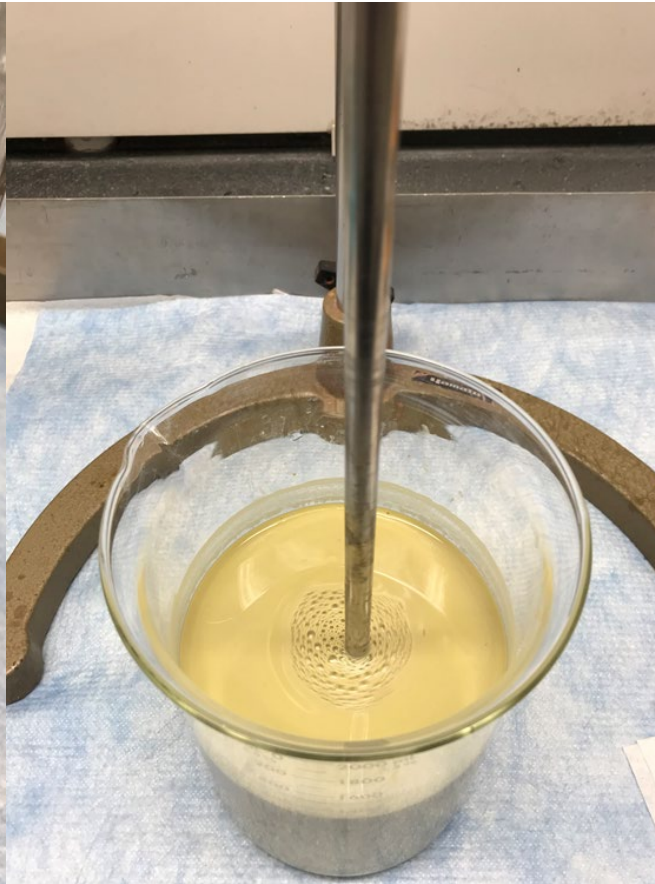
Batch #	#1a	#6a	#9a	#1b	#1-1	#6b	#9b
Na molarity	5.6 M	5.6 M	5.6 M	5.6 M	5.6 M	5.6 M	5.6 M
Waste component	Target weight (g/L)	Target weight (g/L)	Target weight (g/L)	Target weight (g/L)	Target weight (g/L)	Target weight (g/L)	Target weight (g/L)
Al(NO <sub>3</sub> ) <sub>3</sub> •9H <sub>2</sub> O	165.95	144.47	80.31	166.05	166.05	144.40	80.32
H <sub>3</sub> BO <sub>3</sub>	0.13	1.77	0.98	0.13	0.13	1.77	0.98
NaCl	2.85	5.33	2.29	2.85	2.85	5.33	2.29
Na <sub>2</sub> CrO <sub>4</sub>	0.43	8.92	0.69	0.43	0.43	8.92	0.69
NaF	3.17	2.51	42.12	3.17	3.17	2.51	42.13
Fe(NO <sub>3</sub> ) <sub>3</sub> •9H <sub>2</sub> O	NA	0.58	0.28	NA	NA	0.58	0.28
Li <sub>2</sub> CO <sub>3</sub>	NA	0.30	0.28	NA	NA	0.30	0.28
NaOH, 50% sol.	314.10	346.45	182.16	314.29	314.29	346.30	182.19
Na <sub>3</sub> PO <sub>4</sub> •12H <sub>2</sub> O	10.45	18.35	26.94	10.46	10.46	18.34	26.94
Na <sub>2</sub> SO <sub>4</sub>	4.60	7.44	41.21	4.60	4.60	7.44	41.22
SiO <sub>2</sub>	0.30	1.11	0.79	0.30	0.30	1.11	0.79
NaNO <sub>2</sub>	50.20	38.21	37.26	50.23	50.23	38.19	37.27
NaNO <sub>3</sub>	9.33	23.08	62.34	9.33	9.33	23.07	62.35
Na <sub>2</sub> C <sub>2</sub> O <sub>4</sub>	7.69	2.55	5.35	7.69	7.69	2.54	5.35
K <sub>2</sub> CO <sub>3</sub>	43.76	0.73	5.96	43.78	43.78	0.72	5.96
Na <sub>2</sub> CO <sub>3</sub>	28.56	NA	10.44	28.57	28.57	NA	10.44
Subtotal	641.50	601.78	499.39	641.88	641.88	601.53	499.47
GFC component	Target weight (g/L)	Target weight (g/L)	Target weight (g/L)	Target weight (g/L)	Target weight (g/L)	Target weight (g/L)	Target weight (g/L)
H <sub>3</sub> BO <sub>3</sub>	100.67	105.11	181.66	100.02	100.02	105.22	188.29
Li <sub>2</sub> CO <sub>3</sub>	NA	NA	155.88	NA	NA	NA	153.56
FeCr <sub>2</sub> O <sub>4</sub>	NA	NA	NA	11.78	11.78	0.44	0.05
Fe <sub>2</sub> O <sub>3</sub>	NA	NA	NA	NA	NA	0.25	0.86
Cr <sub>2</sub> O <sub>3</sub>	4.65	0.17	NA	NA	NA	NA	NA
ZnO	24.42	NA	NA	26.34	26.34	NA	NA
SnO <sub>2</sub>	37.22	18.00	3.14	37.28	NA	17.96	2.54
SnO	NA	NA	NA	NA	33.83	NA	NA

Batch #	#1a	#6a	#9a	#1b	#1-1	#6b	#9b
V <sub>2</sub> O <sub>5</sub>	NA	26.38	50.25	NA	NA	26.39	49.93
Mg <sub>2</sub> SiO <sub>4</sub>	29.28	27.96	NA	25.32	25.32	27.01	NA
Al <sub>2</sub> SiO <sub>5</sub>	54.03	63.23	137.34	48.33	48.33	59.53	129.70
ZrSiO <sub>4</sub>	70.54	75.18	125.83	70.02	70.02	75.19	124.98
CaSiO <sub>3</sub>	90.89	71.51	218.16	92.24	92.24	74.15	228.26
SiO <sub>2</sub>	232.94	197.30	320.17	235.69	235.69	199.20	323.22
C <sub>12</sub> H <sub>22</sub> O <sub>11</sub>	42.14	40.62	38.17	42.17	42.17	40.60	38.17
Subtotal	686.79	625.45	1230.59	689.20	685.75	625.93	1239.55
Total	1328.29	1227.23	1729.98	1331.08	1327.63	1227.46	1739.02

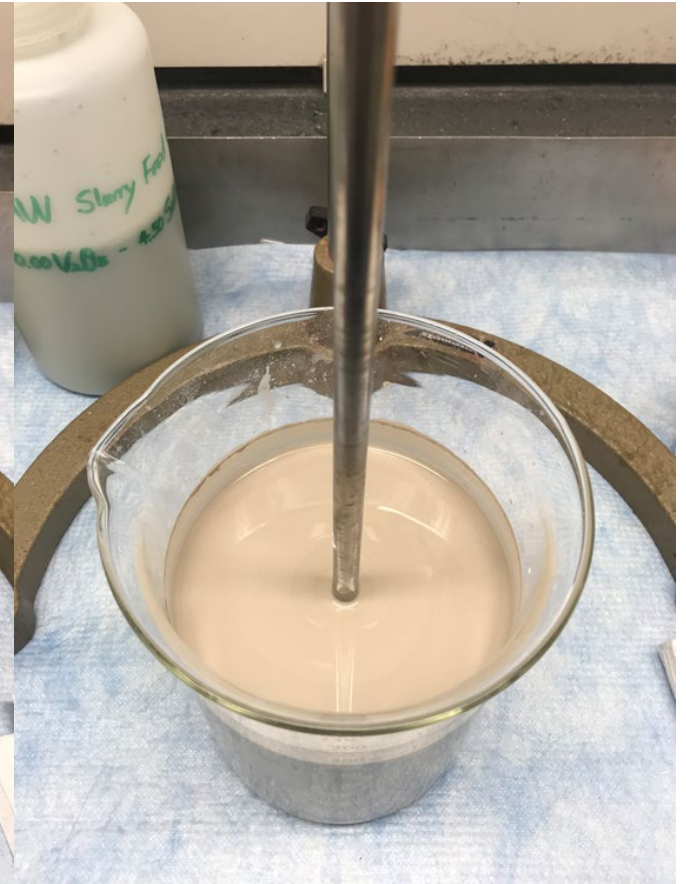




Batch #1a



Batch #6a



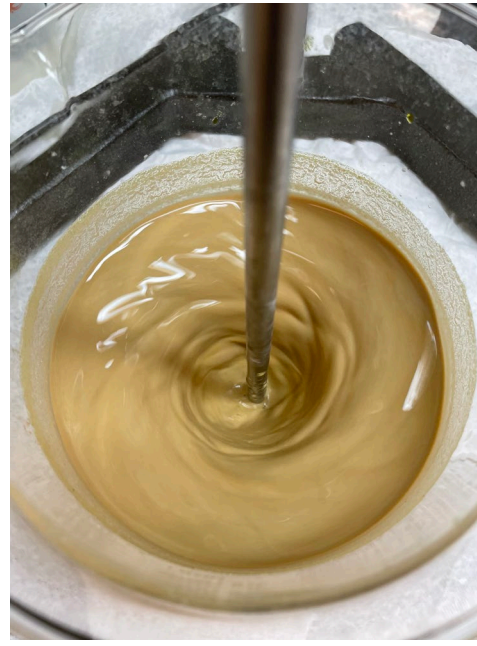
Batch #9a



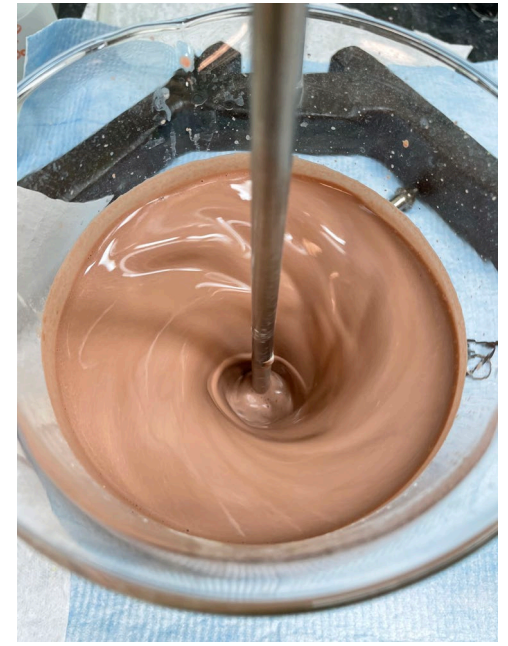
Batch #1b



Batch #1-1



Batch #6b



Batch #9b

Figure 10. Images of “as batched” slurry melter feeds of each batch composition

#### **2.4.1 Water content, total solid, dissolved solid, and undissolved solid test**

This test determined and verified water content in the slurry feeds by classifying total solids (TS) content, dissolved solids (DS) content, and undissolved solids (UDS) content. Properties were measured using the oven method. Slurry samples were centrifuged, and the supernatant was taken to determine the DS content. A supernatant and slurry feed were loaded on drying dishes, placed in an oven at 105 °C, and dried for 24 hours. The dried samples were cooled in a desiccator prior to weighing to avoid moisture uptake. The sample mass was weighed and recorded. The samples were put in the oven again for another 24 hours, cooled, and weighed for comparison. This was repeated until the weight became stable.

#### **2.4.2 Density test**

This test measured density of the slurry feeds using a certified glass pycnometer. The empty 25-mL pycnometer was weighed to obtain a tare weight. The slurry melter feed was added into the pycnometer to the 25-mL mark and its weight was recorded. The density was determined by dividing the net slurry feed weight by the 25-mL volume of the pycnometer.

#### **2.4.3 pH test**

The pH of the slurry was measured using a Thermo Scientific Orion Star model A215 pH meter and a ROSS Ultra pH/ATC (automatic temperature compensation) probe by placing it in the slurry feed and waiting for it to equilibrate. The instrument was calibrated using certified buffer solutions before actual samples were measured. The pH values were automatically adjusted from ambient temperature to 25 °C. Duplicate measurements were performed.

#### **2.4.4 Shear strength, viscosity, and yield stress test**

Shear strength tests were performed using a Haake VT550 rheometer with a 16 × 16 mm shear vane tool (see Figure 11a). The vane tool was inserted below the surface of the settled solids layer to a depth of 16 mm. Shear strength of the solid part in the slurry feed was measured at 0.3 rpm for 120 seconds as a function of settling/gelation time (24, 48, and 72 hours).

For the properties of yield stress and viscosity, flow curves were measured using a Haake RS600 rheometer coupled with a concentric cup measurement geometry using a Z41Ti spindle (see Figure 11b). Measurements were performed at 20 and 40 °C. A standard flow curve was used to measure the flow behavior of the slurry feeds with a 180-second pre-shear at 200 s<sup>-1</sup> before measurement. The standard protocol consists of a 300-second ramp-up from 0 to 1000 s<sup>-1</sup> followed by a 60-second hold at 1000 s<sup>-1</sup> and finally a 300-second down ramp from 1000 to 0 s<sup>-1</sup>. Viscosity was obtained by the ratio of yield stress and shear rate.





Figure 11. Images of (a) the 16 x 16 mm shear vane tool and (b) Z41Ti viscosity spindle

#### 2.4.5 Settling test

Undissolved materials in a slurry feed settle over time. This test measured the volume of settled undissolved materials in the slurry as a function of time using a 100-mL graduated cylinder (see pictures in Appendix B). Approximately 97 – 99 mL of slurry feed was placed in a graduated cylinder and settled for a month. The volume of the settled materials was monitored over time. The interval to monitor the volume changes was short in the beginning because large and heavy particles tend to settle quickly. The volume changes were monitored less frequently over time as the changes became slower.

## 3.0 Results and Discussion

In this section, the testing results are presented and discussed. Data sheets that summarize the properties measured for the dry GFC powders and slurry feeds as well as the associated information are presented in Appendix B.

### 3.1 Summary of data for physical and flow properties of GFCs

Each property for all the tested GFCs and their mixtures can be compared to give a better insight into the property relationships between individual GFCs and their mixtures. The flow and physical characteristics are also summarized and can be considered for information about the methods used and underlying concepts as well as application to the silos and hoppers for these chemicals. The original data from J&J are given in Appendix C.

#### 3.1.1 Particle size analysis

The calculated  $D_{10}$ ,  $D_{50}$ , and  $D_{90}$  for each GFC and mixture are given in Table 7. Note that in many cases, there was substantial variation among replicate samples, possibly a result of agglomeration and/or segregation of the material. The  $\text{SnO}_2$  was not tested via the Malvern laser diffraction system at J&J because it contained large agglomerates. At J&J, particle size for  $\text{SnO}_2$  was determined by sieving using the Ro-Tap. GFC mixtures, batch #1b, #6b, #9b, and #1-1, were also tested by the sieving method because J&J detected larger size than  $2000\text{ }\mu\text{m}$  (the limit of detection of the equipment) for those mixtures. The results of sieving are given in Table 8. However, the result from the sieving method for the  $\text{SnO}_2$  containing large agglomerates does not provide helpful information because of cohesiveness of the particles.

The results in this study show that  $\text{Cr}_2\text{O}_3$  and  $\text{SnO}_2$  primarily consist of very small particles ( $D_{50} < 5\text{ }\mu\text{m}$ ) and these fine particles in bulk powder most likely will be cohesive and sensitive to pressure as shown by the agglomeration and densified powder in a container.  $\text{FeCr}_2\text{O}_4$  consists of small particles as well ( $D_{50} < 15\text{ }\mu\text{m}$ ) and these particles in bulk powder will still be cohesive and sensitive to pressure. These fine particles may be related to a main cause of the ratholing or arching situation in silos and require a large outlet diameter in silos. GFCs that have larger particles (average particle sizes from  $50$  to  $100\text{ }\mu\text{m}$ ) appear to have better flow properties and would be recommended to avoid the ratholing or arching issue observed in testing with the smaller particle sizes.

Average particle size for  $\text{ZrSiO}_4$  is about  $100\text{ }\mu\text{m}$  and this bead-type powder will have better flow properties without any ratholing or arching issues in silos. The  $D_{90}$  values for all mixtures show large particle sizes due to agglomerates. These agglomerates in GFC mixtures would not be a problem in the blending hopper at WTP.

J&J and PNNL data on particle size distribution for the individual GFCs and their mixtures are given in Table 9 for comparison. PNNL used both a dry dispersion unit and a wet dispersion unit to measure data and both results are shown in Table 9. Data from the wet dispersion unit would be helpful to understand true particle sizes in bulk powders. A comparison of the particle size distribution by volume percent under 0 bar with a dry dispersion unit is plotted in Figure 12.

Based on the results, measured data normally show good agreement between J&J and PNNL. However, two data points in  $D_{90}$  values for  $\text{Cr}_2\text{O}_3$  and LAW batch #9a are somewhat different (see Figure 12). This could result from an agglomeration characteristic. For example, the

difference in the LAW batch #9a data could be primarily because of homogeneity of the mixtures, i.e., compositions of the chemicals in each collected sample may not be identical and the sample has different agglomeration behavior. The difference in the  $\text{Cr}_2\text{O}_3$  data could be because of sample selection and amount used for tests. Then, each selected sample has different agglomeration.

Table 7. Particle size distributions of materials

GFC	At 0 bar						At 3 bar					
	D <sub>10</sub> (μm)	D <sub>50</sub> (μm)	D <sub>90</sub> (μm)	Volume weighted mean (μm)	Surface weighted mean (μm)	Span = (D <sub>90</sub> – D <sub>10</sub> ) /D <sub>50</sub>	D <sub>10</sub> (μm)	D <sub>50</sub> (μm)	D <sub>90</sub> (μm)	Volume weighted mean (μm)	Surface weighted mean (μm)	Span = (D <sub>90</sub> – D <sub>10</sub> ) /D <sub>50</sub>
Cr <sub>2</sub> O <sub>3</sub>	1.4	4.2	10.6	5.2	3	2.17	1.2	2.8	7.6	3.7	2.3	2.31
V <sub>2</sub> O <sub>5</sub>	14	71.6	254.8	106.7	30.4	3.36	2.7	29.6	141.9	54	5.7	4.7
SnO	11.2	56.4	94.6	56.6	31.6	1.48	5.7	38.8	75.4	39.5	11.5	1.8
SnO <sub>2</sub>	NM	NM	NM	NM	NM	NM	NM	NM	NM	NM	NM	NM
FeCr <sub>2</sub> O <sub>4</sub>	2.7	13.9	38.3	17.7	6.3	2.57	1.5	10.2	37.3	15.3	3.6	3.51
ZrSiO <sub>4</sub>	70.4	100.1	141.6	103.6	96.4	0.71	70.3	98.3	137	101.5	95	0.68
LAW batch #1a	4.2	35.7	624.5	194.6	9.6	17.36	2.4	27.8	423.3	118.7	5.6	15.14
LAW batch #6a	5.1	51.2	618.5	213.4	12.5	11.97	3.4	47.6	564.7	186	9.7	11.79
LAW batch #9a	5	40.6	588.6	183.6	11.9	14.37	3.2	34.4	543.2	165.2	7.7	15.69
LAW batch #1b	8	103.3	779.4	293.8	18.7	7.47	4.1	96.8	593.7	223.4	12.3	6.09
LAW batch #1-1	8.1	145.8	721.6	287.7	19.2	4.89	5	85.6	565.3	204.2	13.5	6.55
LAW batch #6b	9.5	174.5	688.2	279.9	21.7	3.89	5.4	86.7	560.6	202	14	6.4
LAW batch #9b	9.1	72.8	629	219.3	20.1	8.51	5.7	66.4	553.5	186.7	14.3	8.25

NM means not measured.

Table 8. Sieving results in wt% for SnO<sub>2</sub> and GFC mixtures

Mesh size	μm	SnO <sub>2</sub>	LAW batch #1b	LAW batch #1-1	LAW batch #6b	LAW batch #9b
6 mesh	3350	0.0	0.03	0.16	0	0
12 mesh	1700	0.1	0.14	0.18	0	0
20 mesh	850	5.4	0.94	0.79	0.44	0.29
40 mesh	425	22.3	12.7	11.18	9.74	6.24
70 mesh	212	35.6	11.64	24.43	27.4	7.26
100 mesh	150	11.0	2.3	7.18	14	9.19
200 mesh	75	13.7	16.94	17.73	15.54	23.52
Pan	<75	11.7	55.31	38.85	32.88	53.49

Table 9. Compared data of particle size distribution measured by PNNL and J&J

Sample	Measured by J&J			Measured by PNNL					
	With a dry dispersion unit			With a dry dispersion unit			With a wet dispersion unit		
	D10, $\mu\text{m}$	D50, $\mu\text{m}$	D90, $\mu\text{m}$	D10, $\mu\text{m}$	D50, $\mu\text{m}$	D90, $\mu\text{m}$	D10, $\mu\text{m}$	D50, $\mu\text{m}$	D90, $\mu\text{m}$
Cr <sub>2</sub> O <sub>3</sub>	1.4	4.2	10.6	1.7	6.8	417.5	1.8	4.3	13.5
V <sub>2</sub> O <sub>5</sub>	14.0	71.6	254.8	15.4	83.7	283.7	13.4	66.6	228.0
SnO	11.2	56.4	94.6	12.5	58.4	97.5	12.1	55.5	94.1
SnO <sub>2</sub>	NM	NM	NM	16.9	53.2	397.3	0.6	2.3	17.8
FeCr <sub>2</sub> O <sub>4</sub>	2.7	13.9	38.3	2.7	13.6	39.2	1.7	11.5	37.9
ZrSiO <sub>4</sub>	70.4	100.1	141.6	73.8	101.5	139.5	71.8	99.2	137.4
LAW batch #1a	4.2	35.7	624.5	6.1	58.5	872.1	1.3	14.2	60.5
LAW batch #6a	5.1	51.2	618.5	6.5	53.2	725.2	1.6	17.5	75.1
LAW batch #9a	5.0	40.6	588.6	5.7	35.8	319.6	2.0	17.1	78.1
LAW batch #1b	8	103.3	779.4	10.5	178.7	827.5	1.3	18.0	87.1
LAW batch #1-1	8.1	145.8	721.6	10.4	192.5	819.3	1.8	21.4	87.3
LAW batch #6b	9.5	174.5	688.2	11.7	209.8	785.0	2.0	23.6	97.3
LAW batch #9b	9.1	72.8	629.0	11.6	82.3	747.3	2.3	21.3	98.6
NM means not measured.									



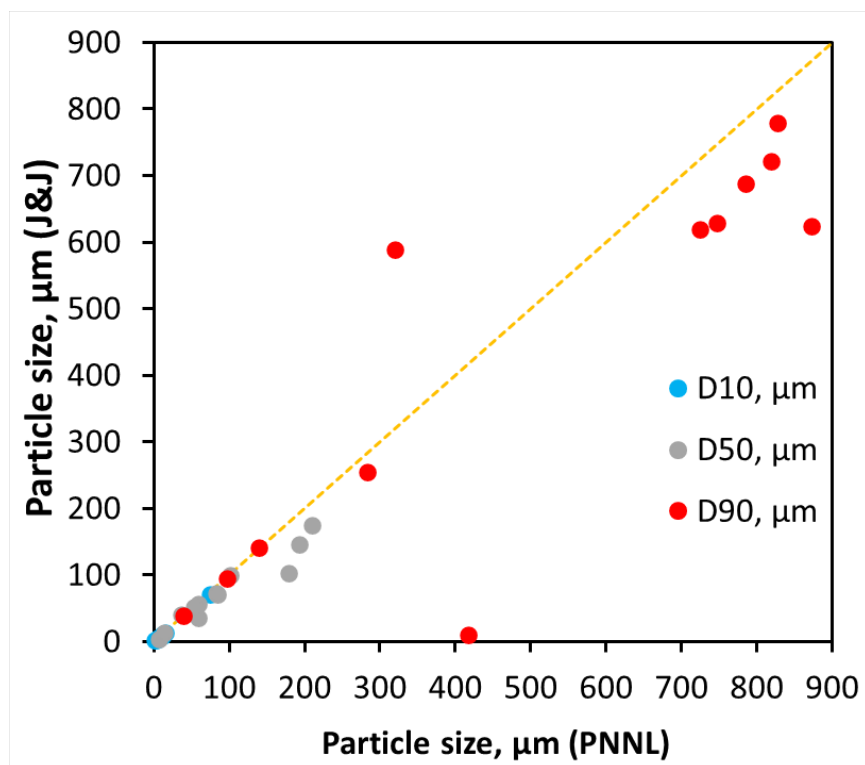


Figure 12. Comparison of the particle size distribution data between PNNL and J&J

### 3.1.2 Cohesive strength test

Several of the GFC materials ( $\text{Cr}_2\text{O}_3$ ,  $\text{SnO}_2$ ,  $\text{FeCr}_2\text{O}_4$ , and all mixtures) are pressure sensitive. Thus, if these materials are subjected to an overpressure due to vibration or impact loading, the minimum outlet diameter required to prevent a stable arch from forming in a mass flow silo can become quite large. Hence, these materials should be handled gently to avoid any overpressure.

Ratholing occurs at higher consolidation stresses, while arching is at lower consolidation stresses in silos. Critical ratholing dimensions were calculated using effective head (EH) under gravity discharge condition in a funnel flow silo. Table 10 shows the critical rathole dimension using a 10-foot EH in a funnel flow silo and the minimum diameter for a cohesive arch in a mass flow silo for these materials. Outlet size in a funnel flow bin must be greater than this value to prevent stable rathole formation. Arching conditions were determined by comparing the unconfined compressive strength and critical conditions in a mass flow silo.

WTP uses mass flow silos with different capacity depending on GFC materials; for example, silica has the biggest silo, while titanium dioxide, ferric oxide, zirconium silicate, and magnesium silicate have the smallest silos. The EH in these silos at WTP will be varied from ~8 to 14 feet but outlet diameters for all silos will be similar, ~0.83 ft (Suyderhoud 2017). Therefore, the data for minimum diameter for cohesive arch are more critical and will be used to be compared with silo dimensions at WTP to understand new GFC materials acceptance.

GFCs used in this study may be stored in small silos or they may be blended with other existing GFCs at WTP. However, because of the highly cohesive characteristic of  $\text{Cr}_2\text{O}_3$ ,  $\text{SnO}_2$ , and  $\text{FeCr}_2\text{O}_4$ , these materials stored in silos would bring a flowability concern. If they are blended with other GFCs and stored together, additional tests such as a segregation test need to be performed. In addition, transporting these materials to the facility should be considered.

GFC mixtures used in this study would not have any issues in a blending hopper at WTP while being processed.

Table 10. Critical rathole dimension and minimum diameter for cohesive arch

GFC	Minimum outlet diameter to avoid rathole in a funnel flow silo		Minimum diameter for cohesive arch in a mass flow silo	
	Continuous flow (ft)	After 7 days at rest (ft)	Continuous flow (ft)	After 7 days at rest (ft)
$\text{Cr}_2\text{O}_3$	14.2	14.5	3.3 (1.4)	4.0 (1.7)
$\text{V}_2\text{O}_5$	4.7	4.8	0.4 (0.2)	0.6 (0.3)
$\text{SnO}$	4.1	4.1	No minimum	No minimum
$\text{SnO}_2$	26.0	26.0	No minimum	No minimum
$\text{FeCr}_2\text{O}_4$	5.4	5.4	0.4 (0.2)	0.91 (0.4)
$\text{ZrSiO}_4$	0.8	0.8	no minimal	no minimal
	Continuous flow (ft)	After 1 day at rest (ft)	Continuous flow (ft)	After 1 day at rest (ft)
LAW batch #1a	7.9	8.1	0.8 (0.4)	1.7 (0.8)
LAW batch #6a	7.0	7.0	1.0 (0.5)	1.0 (0.5)
LAW batch #9a	7.4	8.1	0.6 (0.3)	1.7 (0.8)

LAW batch #1b	8.2	8.2	1.2 (0.6)	1.5 (0.7)
LAW batch #1-1	7.6	7.7	0.4 (0.2)	1.2 (0.6)
LAW batch #6b	7.5	7.5	0.4 (0.2)	0.4 (0.2)
LAW batch #9b	7.8	9.4	0.6 (0.3)	1.8 (0.9)

Note: Numbers in parentheses indicate minimum diameter in a transitional mass flow silo.

### 3.1.3 Compressibility test

The bulk density of most bulk solids varies with the consolidating pressure applied to them. As a result, it is not sufficient to describe a material simply as loose or compacted. Instead, this density/pressure relationship can often be expressed as a straight line on a log-log plot. Moisture, particle size and shape, and temperature can affect a material's bulk density also.

The ranges of bulk densities measured for all samples are shown in Table 11. The test results along with cohesive strength data were used to analyze outlet size requirements to prevent arching and ratholing. The results can also be used to determine storage vessel capacities based on varying pressures within a vessel and the suitability of dense phase conveying. If bulk densities of powders are too low or too high, they can be problematic in silos due to arching or ratholing when they flow. The relationship between bulk density and consolidating pressure for each sample is displayed in Appendix C.

Table 11. Bulk density of individual GFCs and mixtures

GFCs	Bulk density range (lb/ft <sup>3</sup> )
Cr <sub>2</sub> O <sub>3</sub>	65 – 144
V <sub>2</sub> O <sub>5</sub>	46 – 67
SnO	120 – 158
SnO <sub>2</sub>	61 – 102
FeCr <sub>2</sub> O <sub>4</sub>	82.2 – 136.5
ZrSiO <sub>4</sub>	136.5 – 141.1
LAW batch #1a	59 – 96
LAW batch #6a	63 – 100
LAW batch #9a	55 – 87
LAW batch #1b	57.9 – 89.2
LAW batch #1-1	60.3 – 89.1
LAW batch #6b	62.0 – 90.2
LAW batch #9b	50.4 – 75.5

### 3.1.4 Wall friction tests

In addition to a properly sized outlet, the design of a mass flow silo must consider the wall angles, materials of construction, and surface finish. The hopper walls must be steep enough and have sufficiently low friction to allow the material to flow along them.

GFCs used in this study were tested on three different wall materials, stainless steel, carbon steel, and TIVAR 88 (shown in Figure 13), and hopper angles (degree from vertical) with a 1-foot-diameter opening were calculated. The results are listed in Table 12. At WTP, wall

materials in silos are mild carbon steel and hopper angles vary between 28° and 36°. Based on measured data and silo actual dimensions, Cr<sub>2</sub>O<sub>3</sub>, SnO<sub>2</sub>, V<sub>2</sub>O<sub>5</sub>, and FeCr<sub>2</sub>O<sub>4</sub>, may raise a concern of stagnant materials in the silos because of insufficient wall slope angles. However, all silos at WTP will have an inside aeration system on the wall to let materials flow better. This subsidiary equipment may mitigate the stagnant issue in the silos. SnO, bead-type ZrSiO<sub>4</sub>, and all GFC mixtures would be acceptable in the current silos and blending hoppers.

With a wall friction test, a slip-stick (the cyclic adherence and release as the solids slide along the wall) was tested and reported. This behavior can lead to equipment vibration during gravity flow and should be considered as a potential problem. For the slip-stick data, the test cell was pushed at a constant low speed and the resulting shear force was measured. In general, most materials reach a steady value, but some materials experience slip-stick, where the value oscillates from a low value to a high value. The low and high values for a given cycle are selected and a slip-stick value is calculated in percentage ( $\frac{\text{low value}}{\text{high value}} \times 100$ ). Normally, slip-stick values above 85% are of minimal concern. When a slip-stick value is below 70%, slip-stick is considered high. The results of slip-stick for Cr<sub>2</sub>O<sub>3</sub>, SnO<sub>2</sub>, SnO, and ZrSiO<sub>4</sub> are shown in Table 12 and these new GFCs would not have any concerns of slip-stick in the silos at WTP.

V<sub>2</sub>O<sub>5</sub> was not tested for slip-stick but it stained the surfaces tested; see Figure 13. Note that this might pose a concern that the surface friction might change over time.

TIVAR 88-2 Lorien is a more advanced surface, allowing welding of joints. As a quick comparison, LAW batch #1a was tested using TIVAR 88-2 Lorien, and this showed an improvement in friction over the value for TIVAR 88, showing that the measured data of the wall friction angle from vertical with TIVAR 88-2 Lorien increased to 21° (33° for a transitional mass flow silo) under continuous flow status.



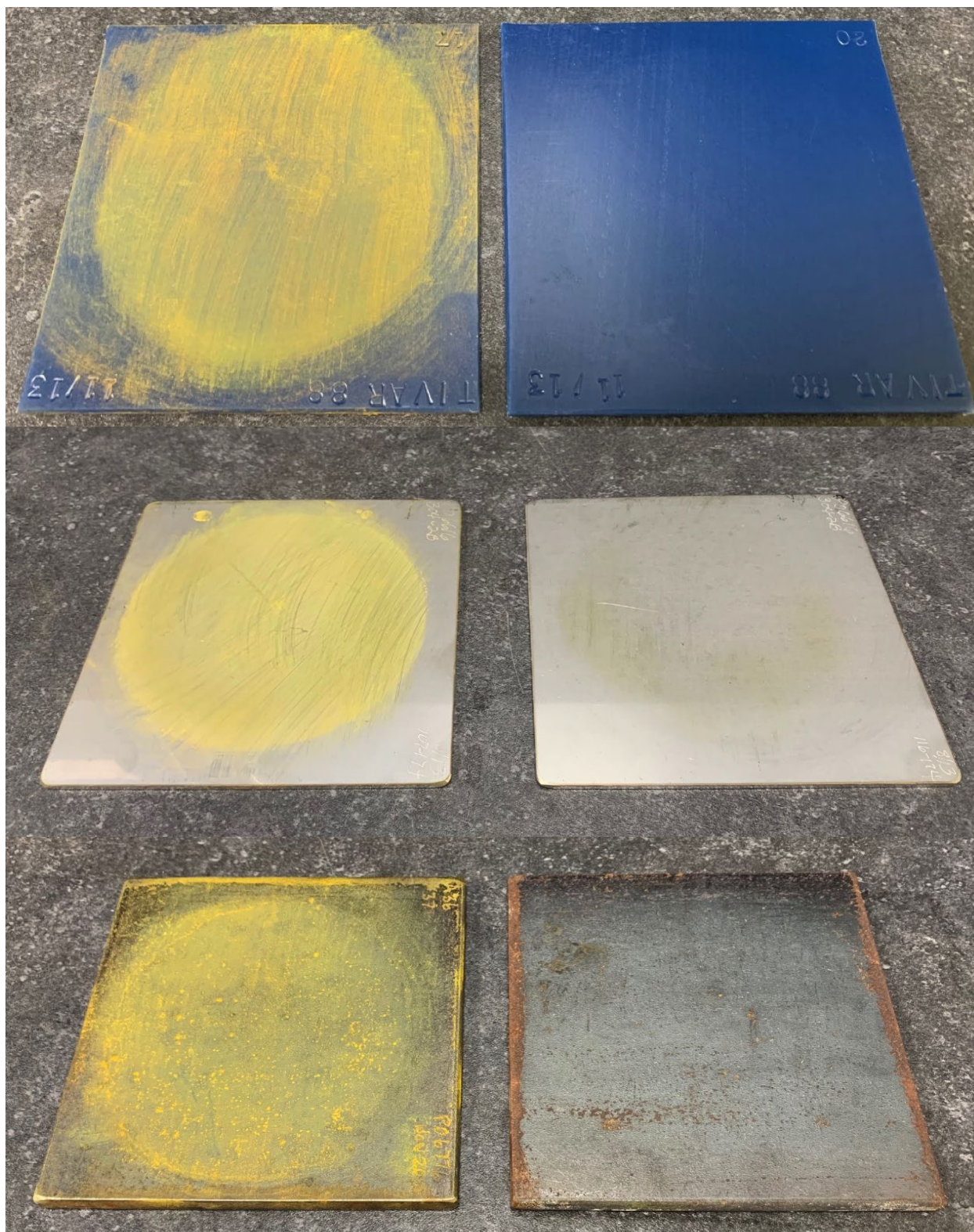


Figure 13. V<sub>2</sub>O<sub>5</sub> stains on the surfaces of used materials (top: TIVAR 88, middle: 304 SS, bottom: mild CS). Unstained materials shown on the right for comparison.

Table 12. Wall friction angles (degrees from vertical)

GFC	With 304 SS sheet, #2B finish, 12 ga			Mild CS HR plate, mill finish, 1/4-in.			TIVAR 88		
	Slip-stick %	Continuous flow	After 7 days at rest	Slip-stick %	Continuous flow	After 7 days at rest	Slip-stick %	Continuous flow	After 7 days at rest
Cr <sub>2</sub> O <sub>3</sub>	69	13° (24°)	13° (24°)	NM	0° (11°)	2° (11°)	82	21° (33°)	21° (33°)
V <sub>2</sub> O <sub>5</sub>	NM	5° (15°)	5° (15°)	NM	1° (11°)	1° (11°)	NM	12° (22°)	12° (22°)
SnO	NM	13° (24°)	13° (24°)	84	10° (22°)	6° (18°)	69	10° (23°)	10° (23°)
SnO <sub>2</sub>	NM	6° (17°)	6° (17°)	84	none (8°)	none (8°)	NM	14° (25°)	14° (25°)
FeCr <sub>2</sub> O <sub>4</sub>	NM	8° (18°)	8° (18°)	NM	1° (11°)	1° (11°)	NM	8° (18°)	8° (18°)
ZrSiO <sub>4</sub>	60	26° (36°)	26° (36°)	82	23° (34°)	23° (34°)	NM	32° (42°)	32° (42°)
GFC	With 304 SS sheet, #2B finish, 12 ga			Mild CS HR plate, mill finish, 1/4-in.			TIVAR 88		
	Slip-stick %	Continuous flow	After 1 day at rest	Slip-stick %	Continuous flow	After 1 day at rest	Slip-stick %	Continuous flow	After 1 day at rest
LAW batch #1a	NM	14° (24°)	14° (24°)	NM	8° (18°)	5° (14°)	NM	13° (23°)	13° (23°)
LAW batch #6a	NM	12° (22°)	12° (22°)	NM	0° (9°)	0° (9°)	NM	6° (16°)	6° (16°)
LAW batch #9a	NM	14° (25°)	14° (25°)	NM	8° (19°)	5° (16°)	NM	15° (25°)	15° (25°)
LAW batch #1b	NM	13° (23°)	13° (23°)	NM	7° (17°)	7° (17°)	NM	12° (22°)	12° (22°)
LAW batch #1-1	80	13° (23°)	13° (23°)	NM	8° (18°)	8° (18°)	NM	8° (18°)	8° (18°)
LAW batch #6b	NM	13° (23°)	13° (23°)	NM	9° (19°)	9° (19°)	NM	9° (19°)	9° (19°)
LAW batch #9b	NM	12° (22°)	12° (22°)	NM	6° (17°)	6° (17°)	NM	9° (19°)	9° (19°)

Note: Numbers in parentheses indicate wall friction angles in a transitional hopper; NM = not measured.



### 3.1.5 Permeability test

A permeability test was run to determine critical steady-state discharge rates. Bulk solids with low permeability will generally have low permeability constant ( $K_0$ ) values, where  $K_0$  is a value of steepness in the linear relationship between  $K$ , the permeability of the bulk solid in air, and  $\gamma$ , the bulk density of the solid in the bed, in the Eq. (1). Permeability test results can also be used to calculate the critical steady solids discharge rates of fully deaerated material for a mass flow silo with a given outlet size and EH. The permeability test results are summarized in Table 13. The  $\text{Cr}_2\text{O}_3$  has a comparatively high  $K_0$  due to arching issue. Unlike  $\text{Cr}_2\text{O}_3$ ,  $\text{FeCr}_2\text{O}_4$  does not have any arching issues showing low mass flow rate.  $\text{ZrSiO}_4$  has a relatively high  $K_0$  and shows high mass flow rate due to bead-type particles. This is attributed to the presence of voids caused by the cohesiveness of the material, which allows air to channel through these voids. An arching issue was also observed in Batch #1b but not in Batch #1a. This may be due to increase of moisture in the mixture (see Table 17).

Table 13. Permeability test results

GFC	$K_0$ (fps)	Mass flow in a hopper with 1-ft opening and 10-ft EH (lb/h)
$\text{Cr}_2\text{O}_3$	0.156	Not possible due to arching
$\text{V}_2\text{O}_5$	0.0042	2,400 (4000)
SnO	0.0157	32,600 (41,400)
$\text{SnO}_2$	0.0238	21,200 (27,000)
$\text{FeCr}_2\text{O}_4$	0.000751	400 (800)
$\text{ZrSiO}_4$	0.03869	772000 (982000)
LAW batch #1a	0.0013	200 (600)
LAW batch #6a	0.00099	200 (400)
LAW batch #9a	0.0017	600 (1000)
LAW batch #1b	0.001556	not possible due to arching (600)
LAW batch #1-1	0.002446	1400 (2000)
LAW batch #6b	0.00245	1200 (2000)
LAW batch #9b	0.003718	1400 (2400)

Note: Numbers in parentheses indicate flow rate in a transitional mass flow hopper.

### 3.1.6 Chute angle tests

Tests were run to determine angles required for non-converging flat chutes to clean off a 1/2-inch layer after an impact that reduces the velocity to zero. Chute angle increased as impact pressure increased.  $\text{Cr}_2\text{O}_3$ ,  $\text{SnO}_2$ , and  $\text{FeCr}_2\text{O}_4$  showed substantial increase of angles at higher pressure because they are fine powders and cohesive, whereas bead-type  $\text{ZrSiO}_4$  showed no effect of pressure on chute angles. It is important to control consistent discharge of the GFCs. The results of the chute angle tests are summarized in Table 14.

At WTP, individual GFCs or blended GFCs between silos and hoppers will be transferred in pipelines by the aeration system. Therefore, the chute angle data would not matter or would not need to be considered. Maintaining bulk powders with less fine powders, which are the causes of dust and clogging issues, will be more important in the facilities at WTP.

Table 14. Impact chute angle (maximum angle from the horizontal)

GFCs	With 304 SS sheet, #2B finish, 12 ga		Mild CS HR plate, mill finish, 1/4-in.		TIVAR 88	
	Impact pressure 4 psf	Impact pressure 80 psf	Impact pressure 4 psf	Impact pressure 80 psf	Impact pressure 4 psf	Impact pressure 80 psf
Cr <sub>2</sub> O <sub>3</sub>	24°	90°	35°	90°	29°	90°
V <sub>2</sub> O <sub>5</sub>	29°	34°	34°	39°	30°	38°
SnO	29°	30°	28°	30°	26°	28°
SnO <sub>2</sub>	30°	68°	34°	83°	33°	58°
FeCr <sub>2</sub> O <sub>4</sub>	30°	59°	34°	73°	34°	51°
ZrSiO <sub>4</sub>	21°	21°	23°	26°	24°	26°
LAW batch #1a	27°	39°	34°	52°	29°	36°
LAW batch #6a	30°	43°	36°	48°	34°	40°
LAW batch #9a	29°	50°	33°	50°	31°	50°
LAW batch #1b	28°	35°	33°	41°	32°	42°
LAW batch #1-1	26°	37°	28°	42°	27°	46°
LAW batch #6b	30°	40°	29°	42°	30°	36°
LAW batch #9b	26°	39°	28°	48°	28°	49°

### 3.1.7 Angle of repose test

Table 15 provides the results from angle-of-repose tests for each material by both J&J and PNNL. The angle is referenced from the horizontal. Note that a range has been provided; this reflects the change in angle from the base of the pile to its top, as well as around the pile's circumference. The shape of the pile for each sample tested is shown in Appendix B. The angle of repose can be used in determining silo and stockpile capacities but should not be used to specify hopper angles for mass flow.

As mentioned earlier, PNNL performed angle of repose and particle size distribution to compare measured data with J&J. As seen below, there was reasonable agreement for measured data between PNNL and J&J. Bead-type ZrSiO<sub>4</sub> has spherical shape particles, and they don't pile up well on the small stage in the equipment at PNNL resulting in smaller angles.

Data of angle of repose measured by J&J tend to have a wider range than PNNL's data, which show more consistency. Batches #1a and #6a show larger gaps between PNNL and J&J. This may be mainly because batched powders were not blended homogeneously or mixtures picked up moisture. Comparison of average angle is plotted in Figure 14.

Table 15. Compared data of angle of repose measured by PNNL and J&J

Sample	Measured by J&J		Measured by PNNL	
	average	range	average	range
Cr <sub>2</sub> O <sub>3</sub>	35°	32°– 40°	34°	33°– 35°
V <sub>2</sub> O <sub>5</sub>	42°	34°– 50°	45°	44°– 45°
SnO	26°	25°– 28°	26°	25°– 26°
SnO <sub>2</sub>	33°	31°– 34°	34°	32°– 36°
FeCr <sub>2</sub> O <sub>4</sub>	42°	38°– 46°	41°	41°– 42°
ZrSiO <sub>4</sub>	22°	20°– 23°	13°	13°– 14°
LAW batch #1a	34°	26°– 38°	39°	38°– 39°
LAW batch #6a	34°	26°– 40°	41°	41°– 42°
LAW batch #9a	33°	25°– 39°	34°	33°– 34°
LAW batch #1b	36°	25°– 42°	37°	36°– 39°
LAW batch #1-1	36°	31°– 44°	38°	37°– 38°
LAW batch #6b	37°	31°– 43°	39°	38°– 39°
LAW batch #9b	37°	34°– 40°	41°	40°– 42°

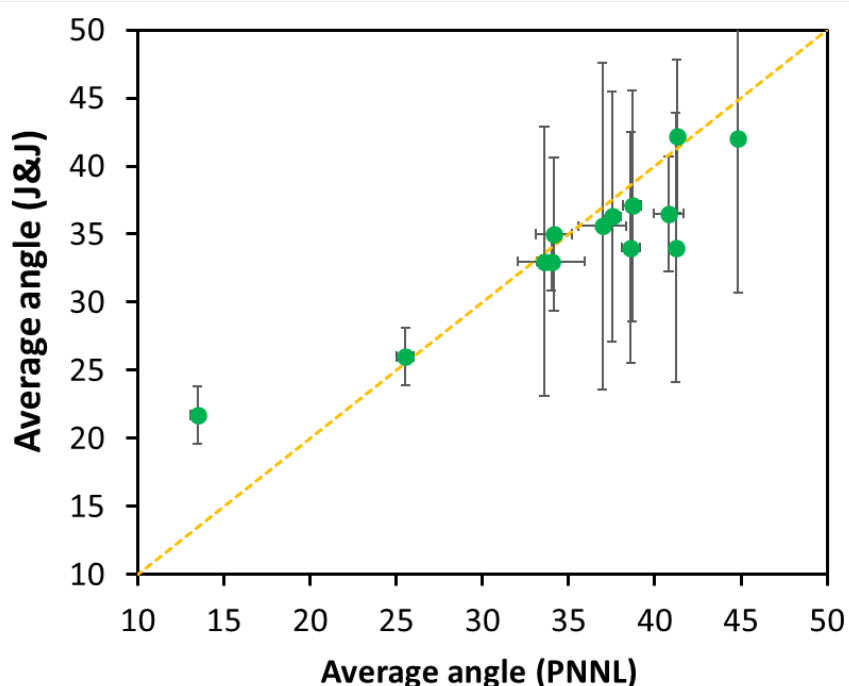


Figure 14. Comparison of the average data of angle of repose between PNNL and J&J

### 3.1.8 Particle density

Particle density was measured at PNNL. For each material, replicate measurements were performed, and the average of the measurements is shown in Table 16. As expected, stannous oxide and stannic oxide had high particle densities and GFC mixtures had low densities because of dominant components such as silica (2.65 g/cm<sup>3</sup>), boric acid (1.51 g/cm<sup>3</sup>), and wollastonite (2.90 g/cm<sup>3</sup>). Big differences in particle densities of GFCs might be a cause of GFC separation in mixing GFCs together and in slurry feeds.

Table 16. Particle density results

GFCs	Average (g/cm <sup>3</sup> )
Cr <sub>2</sub> O <sub>3</sub>	5.2319 (±0.0063)
V <sub>2</sub> O <sub>5</sub>	3.3880 (±0.0275)
SnO	6.2685 (±0.0106)
SnO <sub>2</sub>	7.2081 (±0.1627)
FeCr <sub>2</sub> O <sub>4</sub>	4.3236 (±0.0023)
ZrSiO <sub>4</sub>	3.8094 (±0.0021)
LAW batch #1a	2.7762 (±0.0249)
LAW batch #6a	2.6689 (±0.0316)
LAW batch #9a	2.5402 (±0.0512)
LAW batch #1b	2.7840 (±0.0027)
LAW batch #1-1	2.7742 (±0.0023)
LAW batch #6b	2.7169 (±0.0013)
LAW batch #9b	2.6565 (±0.0018)

Note: Numbers in parentheses indicate standard deviation.

### 3.1.9 Moisture content

Moisture content properties were calculated using equations as expressed below.

$$wt\% \text{ of water} = \frac{\text{wet weight} - \text{dry weight}}{\text{wet weight}} \times 100\% \quad (2)$$

$$wt\% \text{ of TS} = \frac{\text{dry weight}}{\text{wet weight}} \times 100\% \quad (3)$$

$$wt\% \text{ of DS} = \frac{\text{dry weight (supernatant)}}{\text{wet weight (supernatant)}} \times 100\% \quad (4)$$

$$wt\% \text{ of UDS} = \left(1 - \frac{100 - wt\% \text{ of TS}}{100 - wt\% \text{ of DS}}\right) \times 100\% \quad (5)$$

Moisture content was measured at PNNL in duplicate, and results were averaged. As shown in Table 17, individual GFCs have about 0.2% moisture in powders but moisture was higher in mixtures – about 4% in GFC mixture #1a and 5% in other GFC mixtures. This increase in GFC mixtures might arise from moisture being captured when GFCs were blended, or other individual GFCs, such as boric acid or sucrose, might have been exposed to a high moisture environment previously. Bulk powders exposed to high moisture in silos can cause increase of cohesion and decrease of bulk density that result in flowability change.

Table 17. Moisture content results

GFC	Average (%)
Cr <sub>2</sub> O <sub>3</sub>	0.093 (±0.018)
V <sub>2</sub> O <sub>5</sub>	0.267 (±0.049)
SnO	0.200 (±0.003)
SnO <sub>2</sub>	0.195 (±0.013)
FeCr <sub>2</sub> O <sub>4</sub>	0.1415 (±0.0064)
ZrSiO <sub>4</sub>	0.0315 (±0.0191)
LAW batch #1a	3.738 (±0.247)
LAW batch #6a	4.964 (±0.117)
LAW batch #9a	4.534 (±0.305)
LAW batch #1b	4.4900 (±0.1725)
LAW batch #1-1	4.8585 (±0.1280)
LAW batch #6b	5.3095 (±0.0983)
LAW batch #9b	4.8050 (±0.0297)

Note: Numbers in parentheses indicate standard deviation.

## 3.2 Summary of data for physical and rheological properties of slurry feeds

After batching several slurry feeds, tests of their physical and rheological properties were performed, and the results are discussed in this section. These results can help understand the effects of GFCs on slurry feeds and may help provide solutions for potential issues in the MFPV, MFV, sample loop, air displacement slurry pump (ADSP), or transfer line. All slurry feeds tested in this study did not show any issues and the results were within the acceptable ranges, but LAW slurry feed #1-1 might raise attention to potential issues because of oxidation of SnO. The original raw data from measurements are attached in Appendix D.

### 3.2.1 Water content, total solids, dissolved solids, and undissolved solids

Water and solid (dissolved and undissolved) contents were determined using the weight loss of the slurry and supernatant samples after 24 hours drying in the oven, and the results are shown in Table 18. It was assumed that all weight loss was water. These properties depend on waste

loading and water addition in slurry feeds. It will be important to maintain total solids in slurry feeds at the facility.

**Table 18. Water content, total solids, dissolved solids, and undissolved solids in slurry feeds**

Feed ID	Water content (wt%)	Total solids (wt%)	Dissolved solids (wt%)	Undissolved solids (wt%)
LAW slurry feed #1a	46.75	53.25	34.22	28.94
LAW slurry feed #6a	50.08	49.92	31.50	26.89
LAW slurry feed #9a	38.92	61.08	29.58	44.73
LAW slurry feed #1b	46.29	53.71	35.49	28.25
LAW slurry feed #1-1	45.51	54.49	36.02	28.88
LAW slurry feed #6b	50.07	49.93	33.11	25.14
LAW slurry feed #9b	38.36	61.64	30.96	44.44

### 3.2.2 Slurry melter feed density

Densities of the slurry feeds were measured at PNNL and results are shown in Table 19. Density of a slurry feed depends on waste loading, GFC composition, and water content. This property affects feed behavior in storage and pipelines, so it will be important to sustain density of the slurry feeds in the MFV. Based on the batch sheet and the measured slurry feed, the target glass per a liter of feed batched was estimated and they are shown in Table 19.

**Table 19. Density of slurry melter feeds and estimated g glass per a liter of feed**

Feed ID	Feed density (kg/L)	g glass per a liter feed
LAW slurry feed #1a	1.579	662
LAW slurry feed #6a	1.525	615
LAW slurry feed #9a	1.680	833
LAW slurry feed #1b	1.586	662
LAW slurry feed #1-1	1.574	657
LAW slurry feed #6b	1.524	595
LAW slurry feed #9b	1.685	834

### 3.2.3 pH

The average pH values measured at PNNL are reported in Table 20. The measured values of pH of slurry feeds depend on composition of waste slurry (especially sodium content), water content, and composition of GFCs such as boric acid. High waste loading leads to high pH and low waste loading leads to low pH.



Table 20. Average pH of slurry feeds

Feed ID	Average pH
LAW slurry feed #1a	12.76 ( $\pm 0.01$ )
LAW slurry feed #6a	12.58 ( $\pm 0.01$ )
LAW slurry feed #9a	9.21 ( $\pm 0.01$ )
LAW slurry feed #1b	13.19 ( $\pm 0.01$ )
LAW slurry feed #1-1	13.02 ( $\pm 0.01$ )
LAW slurry feed #6b	12.78 ( $\pm 0.01$ )
LAW slurry feed #9b	9.19 ( $\pm 0.00$ )
Note: Numbers in parentheses indicate standard deviation.	

### 3.2.4 Shear strength, viscosity, and yield stress

It was noted that the settled solids layer in these slurry feeds had two distinct solid layers: a dense layer composed of rapidly settling particles and a less dense layer of slower settling solids. Shear strength measurements are significantly influenced by the dense solids layer; the variation in shear strength reflected in Table 21 arises from slight variations in the penetration depth of the vane tool into the dense settled solids layer. LAW slurry feed #9 has a higher settled solid layer than #1 and #6 because of low waste loading, so the vane tool was rotated in the top part of the solid layer which is a less dense area yielding low shear strength values with less variation. The vane tool in LAW slurry feed #6a might touch the bottom of the sample bottle slightly because of a low settled solid layer showing high values of shear strength. To accurately measure the shear strength of the dense settled solids, the experimental setup would need to be modified to make sure that the vane tool was completely immersed in the dense layer, which was not the case for the measurements for the LAW slurry feeds #1a and #6a reported here.

Table 21. Shear strength of slurry feeds

Feed ID	Shear strength, Pa ( $16 \times 16$ mm vane, measurement depth 16 mm)		
	Gelling period		
	24 hours	48 hours	72 hours
LAW slurry feed #1a	130.6	181.3	25.1
LAW slurry feed #6a	1518.0	1478.0	399.8
LAW slurry feed #9a	22.2	38.5	19.8
LAW slurry feed #1b	16.32	32.65	NM
LAW slurry feed #1-1	43.53	108.8	NM
LAW slurry feed #6b	25.65	30.32	NM
LAW slurry feed #9b	25.54	31.48	NM
Note: NM means not measured.			

Flow curves were measured, and a Bingham fit was applied to the data from 200 to 800  $\text{s}^{-1}$  for all. However, this fit range was reduced to 150 to 600  $\text{s}^{-1}$  for the 40 °C measurement of LAW slurry feed #6a because Taylor vortices began to form at higher shear rates. The Bingham yield stress and viscosity values measured are given in Table 22. Measured yield stress and viscosity for the three slurry feeds used in this study meet the current design basis limits for LAW melter feeds at WTP. The limits of the recommended LAW melter feed rheology are described with the

following parameters:  $0 \text{ Pa} < \text{yield stress} < 15 \text{ Pa}$  and  $0.9 \text{ mPa}\cdot\text{s} < \text{viscosity} < 90 \text{ mPa}\cdot\text{s}$  (Deng et al. 2016). Viscosity appears to vary directly with slurry pH.

The original rheological data measured by PNNL are given in Appendix D.

Table 22. Viscosity and yield stress of slurry melter feeds

Feed ID	Temperature ( $^{\circ}\text{C}$ )	Down ramp ( $\text{s}^{-1}$ )	Yield stress (Pa)	Viscosity ( $\text{mPa}\cdot\text{s}$ )
LAW slurry feed #1a	20	200–800	0.1473	13.39
	40	200–800	0.0707	7.22
LAW slurry feed #6a	20	200–800	-0.0182	10.84
	40	150–600	0.0117	5.73
LAW slurry feed #9a	20	200–800	-0.0673	29.06
	40	200–800	0.8730	18.17
LAW slurry feed #1b	20	250–800	0.2201	12.17
	40	250–800	0.2369	7.429
LAW slurry feed #1-1	20	250–800	0	12.74
	40	250–750	0	6.606
LAW slurry feed #6b	20	250–800	0.546	12.18
	40	250–800	0.236	5.983
LAW slurry feed #9b	20	250–800	0.02837	33.23
	40	250–800	0	20.07

### 3.2.5 Settling test

The volume of the settled materials in the used slurry was monitored as a function of time, and the results are displayed in Table 23. The images of the final results are shown in Appendix B. Solids in the slurry melter feed settled quite quickly for the three melter feeds. Slurry feeds #9a and #9b, which contain less water and more GFCs, settled the fastest, while other feeds, which contain more water and less GFC content, showed slower settling rates. Interestingly, solids in slurry feed #1-1 settled quickly but the volume started to increase after 1 week. Bubbles were observed in the settled solid layer. The oxidation of metastable SnO could be a cause of this volume expansion. Slurry feeds settling too fast or volume expansion like slurry feed #1-1 may be an issue in the MFPV or MFV at the WTP if the facility were to lose power or operation was interrupted.

Table 23. The volume of the settled undissolved solids in slurry feeds (mL)

Duration	Feed ID						
	LAW slurry feed #1a	LAW slurry feed #6a	LAW slurry feed #9a	LAW slurry feed #1b	LAW slurry feed #1-1	LAW slurry feed #6b	LAW slurry feed #9b
Used slurry	97	96	98	99	99.5	98.5	99.5
5 minutes	97	96	97	99	98.5	98	99.5
10 minutes	96	94	97	98	97.8	97	99
15 minutes	96	94	97	97.8	97.5	96.5	98.8
20 minutes	96	93	96.5	97.5	97	96	98.5
30 minutes	95.5	92.5	96	97	96.5	95	98.1
40 minutes	95	92	95.5	96.5	96	94.5	98
50 minutes	94.5	91	94.5	96	95.3	93.5	97.5
1 hour	94	90	94	95.5	95	92.5	97
2 hours	92	85	87.5	92.7	91	87	94.5
4 hours	87	73.5	72	87.1	83	74.5	89.2
5 hours	NM	NM	NM	84.5	78.5	68.2	86.6
6 hours	83.5	64.5	71	81.5	73.9	62	84.1
24 hours	44	41.5	70	45	39	38	70
32 hours	NM	NM	NM	44	39	37	70
48 hours	41.5	41	70	43.5	39	37	70
72 hours	NM	NM	NM	43.5	39	37	70
76 hours	41	41	70	NM	NM	NM	NM
96 hours	NM	NM	NM	43.5	39	37	70
99 hours	41	41	70	NM	NM	NM	NM
124 hours	41	41	70	NM	NM	NM	NM
1 week	41	41	70	43.5	40	37	70
2 weeks	NM	NM	NM	43.5	42.5	37	70
3 weeks	41.5	41	70	43.5	44	37	70
1 month	41.5	41	70	43.5	45.5	37	70

Note: NM means not measured.

### 3.3 Dimension of silos at WTP and comparison with GFC properties

Another goal of this report is to compare measured properties of new GFCs with the dimension of silos at WTP to see whether new GFCs used in this study can be acceptable to the current silos or not. Table 24 displays the principal information of each silo dimension constructed at WTP such as capacity, inlet diameter, height, outlet diameter, wall angle, and interior materials. Measured property values of cohesive strength, wall friction angle, particle size distribution, bulk density, and angle of repose for new GFCs used in this study will be compared to the information displayed in Table 24. For example,  $\text{Cr}_2\text{O}_3$  which has high bulk density and angle of repose and contains very fine particles ( $D_{50} < 5 \mu\text{m}$ ) requires large outlet diameter ( $> 1.4 \text{ ft}$ ) and stiff hopper angles ( $< 11^\circ$  from vertical). If  $\text{Cr}_2\text{O}_3$  is stored in any silos at WTP, some issues of arching, rat-hole formation, and caking may be observed because of its high cohesive characteristics. Therefore,  $\text{Cr}_2\text{O}_3$  will not be acceptable. As we carry out this process, we can anticipate acceptance of new GFCs to the silos at WTP. Table 25 shows primary properties and assessment for six new GFCs used in this study. After assessment,  $\text{Cr}_2\text{O}_3$ ,  $\text{SnO}_2$ , and  $\text{FeCr}_2\text{O}_4$  seem unacceptable to be used in silos at WTP because of possible issues of ratholing, arching, and caking.

Table 24. Dimension of each silo at WTP

Facility	Capacity (ft <sup>3</sup> )	Height (ft)	Inlet (ft)	Outlet (ft)	Angle (°)	Internal materials
SiO <sub>2</sub> silo (1)	8,500	78.4	14	0.833	36	CS A36
ZnO silo (2)	2,500	45.9	12	0.833	28 – 30	CS A36
Li <sub>2</sub> CO <sub>3</sub> silo (2)	2,500	45.9	12	0.833	28 – 30	CS A36
TiO <sub>2</sub> silo (3)	1,000	45.9	8	0.833	32	CS A36, A569
Fe <sub>2</sub> O <sub>3</sub> silo (3)	1,000	45.9	8	0.833	32	CS A36, A569
ZrSiO <sub>4</sub> silo (3)	1,000	45.9	8	0.833	32	CS A36, A569
Mg <sub>2</sub> SiO <sub>4</sub> silo (3)	1,000	45.9	8	0.833	32	CS A36, A569
H <sub>3</sub> BO <sub>3</sub> silo (4)	3,000	50.25	12	0.833	30 – 34	CS A36
Al <sub>2</sub> SiO <sub>5</sub> silo (4)	2,175	50.25	10	0.833	32 – 35	CS A36
CaSiO <sub>3</sub> silo (4)	3,000	50.25	12	0.833	32 – 33	CS A36
C <sub>12</sub> H <sub>22</sub> O <sub>11</sub> silo (4)	1,800	45.9	9	0.833	32	CS A36
Na <sub>2</sub> CO <sub>3</sub> silo (5)	1,500	45.9	9	0.833	30	CS A36
Na <sub>2</sub> B <sub>4</sub> O <sub>7</sub> silo (5)	2,150	50.25	11	0.833	28 – 29	CS A36
Note: Numbers in parentheses indicate GFC groups. Silos in the same group use the same weigh hopper.						

Table 25. Primary properties of GFCs and assessment

GFC	Cohesive strength	Wall friction	Bulk density	Angle of repose	Particle size distribution	Assessment	Criteria
	Outlet size (ft)	Vertical angle (°)	Density (lb/ft <sup>3</sup> )	Slope angle (°)	D <sub>50</sub> (μm)		
FeCr <sub>2</sub> O <sub>4</sub>	> 0.2	< 11	82.2 – 136.5	42.2	13.9	Unacceptable	Fine particle, high density, stiff wall
ZrSiO <sub>4</sub>	No minimum	< 34	136.5 – 141.1	21.7	100.1	Acceptable	Highly flowable
Cr <sub>2</sub> O <sub>3</sub>	> 1.4	< 11	65 – 144	35	4.2	Unacceptable	Very fine particle, cohesive
V <sub>2</sub> O <sub>5</sub>	> 0.2	< 11	46 – 67	42	71.6	Acceptable	Low density, medium particle
SnO	No minimum	< 22	120 – 158	26	56.4	Acceptable	Not cohesive
SnO <sub>2</sub>	No minimum	< 8	61 – 102	33	53.2	Unacceptable	Stiff wall angle, cohesive

## 4.0 Conclusion

New GFCs have the potential to improve glass characteristics and/or expand the compositional matrix for the EWG program. As a part of consideration for use in the WTP, the physical and flow properties of the new GFCs as bulk powders or within slurry feeds must be evaluated. Tests for the physical and flow properties of individual GFCs and their mixtures were performed at both J&J and PNNL, and tests for the physical and rheological properties of slurry feeds containing these GFCs were performed at PNNL. Evaluating properties of GFCs and understanding their correlations were then carried out.

Measured data in this study indicate that GFCs containing very fine powders can result in problems such as ratholing, arching, and caking during storage or transport. The properties of mixtures and slurry feeds containing these fine powders might be degraded during operation. Our final opinion from the property results is presented in this section. We also mention several concerns observed during property tests and our suggestions to resolve concerns. Lastly, we include acceptable ranges and criteria for properties of GFCs and slurry feeds using property data for future reference.

### 4.1 Results, concerns, and suggestions for bulk powder GFCs

New GFCs ( $\text{Cr}_2\text{O}_3$ ,  $\text{V}_2\text{O}_5$ ,  $\text{SnO}$ ,  $\text{SnO}_2$ ,  $\text{FeCr}_2\text{O}_4$ , and  $\text{ZrSiO}_4$ ) for EWG and their blends (labelled batches #1, #6, #9, and #1-1) were introduced and characterized in this study. The results addressed in this report demonstrate that

- $\text{Cr}_2\text{O}_3$ ,  $\text{SnO}_2$ , and  $\text{FeCr}_2\text{O}_4$  can bring issues of arching, rat-hole formation, and caking because of very fine particles ( $< 20 \mu\text{m}$ ) and high cohesiveness when they are stored in the silos or transported,
- $\text{V}_2\text{O}_5$  and  $\text{SnO}$  are likely acceptable to be used in current silos but may have stagnant materials in the bottom of the silo because wall angles in silos are not stiff enough,
- Bead-type  $\text{ZrSiO}_4$  shows better flow properties, and no issues are identified,
- GFC mixtures should be fine in the blending hopper,
- These GFCs and their mixtures containing fine particles are sensitive to pressure and hence they should be handled carefully in storage and transport under dry conditions.

During sample preparation and property tests, several concerns that could cause processing challenges were observed. The concerns and suggestions demonstrate that

- $\text{SnO}_2$  powder had large agglomerates (the largest one observed was about 1.5 inches across). Many large agglomerates in bulk materials can affect flow properties,
- Moisture content increased in the GFC mixtures in this study. It is important to keep GFCs dry during handling and storage because high moisture content in bulk powders affects their flowability. GFC mixtures containing high moisture resulted in lower permeability and bigger outlet diameter requirements of hoppers to maintain flowability,
- Measuring permeability of  $\text{Cr}_2\text{O}_3$  was prevented by arching because of high cohesiveness. Discharge issues may be seen in silos during operation with  $\text{Cr}_2\text{O}_3$ ,
- $\text{V}_2\text{O}_5$  stained the surface of materials during testing (see Figure 13). This staining might be a concern if it would cause the surface friction of the silo to change over time,



- GFCs with bigger particle sizes (or coarse- or pellet-type GFCs) can help mitigate ratholing and arching in silos. However, using different particle sizes of GFCs requires additional tests to examine other properties,
- SnO showed better physical and flow properties than SnO<sub>2</sub>. An attempt to substitute SnO for SnO<sub>2</sub> could be possible but would require additional property data such as melter tests,
- For a high cohesive GFC, mixing it with other GFCs might help resolve the issues of rathole or arch formation. However, if this scenario is considered, additional property tests such as a material segregation tests are needed,
- Use of lower surface friction wall materials (stainless steel instead of carbon steel) may help GFCs flow better in silos,
- Evaluating other potential and promising substitutes for Cr<sub>2</sub>O<sub>3</sub>, V<sub>2</sub>O<sub>5</sub>, SnO<sub>2</sub>, and FeCr<sub>2</sub>O<sub>4</sub> is recommended.

## 4.2 Acceptable ranges of physical and flow properties of GFCs

We propose acceptable ranges of physical and flow properties of GFCs using the design of silos and hoppers at WTP and property data of GFCs that have been measured (Deng et al. 2016; LaBryer et al. 2019; Rieck et al. 2015; Schumacher et al. 2003; Suyderhoud et al. 2017; Lee et al. 2021). These criteria would be helpful to evaluate new GFCs for use in the facility at WTP in the future, and those are summarized in Table 26.

Table 26. Acceptable range of physical and flow properties of individual GFCs and their mixtures for WTP

Properties	Acceptable range
Cohesive strength, minimum outlet diameter (with transitional silos and hoppers)	< 0.8 ft
Compressibility	50 – 150 lb/ft <sup>3</sup>
Wall friction angle	< 30°
Permeability	> 200 lb/hr
Impact chute under 4 psf of pressure (from horizontal)	< 45°
Angle of repose (from horizontal)	< 45°
Particle size distribution (volume weight mean)	55 – 200 μm
Particle density	90 – 300 lb/ft <sup>3</sup>
Moisture content	< 0.3 wt%

## 4.3 Results, concerns, and suggestions for slurry feeds

PNNL performed tests of water content, slurry density, pH, viscosity, shear strength, and settling rate, which are major parameters to characterize slurry feeds. These parameters are affected primarily by the amount of GFCs per unit volume of slurry feed. The results demonstrate that

- LAW slurry feed #9, which possesses low waste loading and high GFC content, exhibits high slurry density, low water content, high viscosity, rapid settling rate, and low shear

strength in the settled particle layer. However, its properties are still within the acceptable range for the WTP and shouldn't be an issue in processing,

- LAW slurry feeds #1 and #6, which possess similar high waste loading and low GFC content, show opposite results to those from LAW slurry feed #9, as expected,
- From the experimental results and previous studies, the slurry feed that contains more  $\text{Cr}_2\text{O}_3$ ,  $\text{SnO}_2$ , and  $\text{ZnO}$ , which are fine particles ( $< 20 \mu\text{m}$ ), exhibits densification of the settled solids layer in the slurry feed because of the combination of bigger particles and smaller particles,

No issues or problems were observed with any of the slurry melter feeds containing six new GFCs proposed. However, only one caution was observed when  $\text{SnO}$  was used in the slurry feed.

- LAW slurry feed #1-1 containing  $\text{SnO}$  showed bubble creation and volume expansion in the settled solid layer because of oxidation of  $\text{SnO}$  in slurry feeds. Such a slurry feed may raise concern if it settles quickly and is not agitated for longer than 48 hours in the MFPV or MFV before entering a melter.
- There are no suggestions for the slurry feeds as no issues were observed.

#### 4.4 Criteria of physical and rheological properties of slurry feeds

All slurry feeds used in this study meet the current design basis limits. If new melter feeds do not meet the limits, feeding sequence during operation in the facility at WTP might have problems such as turbulent flow or blockage in pipelines. Success criteria of physical and rheological properties for slurry melter feeds would be helpful for operation (Ard et al. 2019; Lee et al. 2007; Muller et al. 2001, 2017, and 2019; Russell et al. 2019) and is shown in Table 27.

Table 27. Criteria of physical and rheological properties of slurry feeds for EWG

Properties	Criteria	Preferable range
wt% moisture, TS, DS, and UDS	Values are related to waste composition, glass composition, and water content. Less water content would be good for high melting rate but total solid level should be limited for feed transport or feed pump. Total solid level is limited to less than 60 wt% at WTP.	TS: 20 – 60 wt%
Slurry feed density	Density really depends on waste loading/GFC composition and water content. Density of a slurry melter feed affects feed behavior in storage and pipelines. Density should be no more than 1.85 kg/L at WTP.	1.5 – 1.8 kg/L
pH	Values vary significantly depending on waste composition and glass composition because of sodium content and boric acid. High waste loading leads to high pH and low waste loading leads to low pH. Sodium molarity is limited to 5 – 6 M at WTP, so water content can affect pH as well.	7.0 – 13.5
Viscosity	This value depends on water content, GFC composition, and temperature. It is important to keep consistent viscosity at consistent temperature because it affects flowability from MFV to a melter.	< 90 mPa s with 200 s <sup>-1</sup> at 40°C
Shear strength	This value depends on water content, particle sizes of GFCs, GFC composition, and sucrose ratio. Settled solids part in the slurry melter feed can be less dense if particle sizes of GFCs are all similar.	1 – 500 Pa
Settling rate	Settling rate is related to GFC composition, type of GFCs, and water content. Slurry melter feeds will be agitated in MFPV and MFV. However, if solids settle very quickly or settled solid parts are too dense in slurry melter feeds, that would be a problem.	> 12 hours

## 5.0 References

10 CFR 830, *Nuclear Safety Management*. Code of Federal Regulations.

Ard KE. 2019. *Document for Specification for the Tank-Side Cesium Removal Demonstration Project*. Report No. RPP-SPEC-61910, Rev. 2, Washington River Protection Solutions, Richland, WA.

ASME. 2000. *Quality Assurance Requirements for Nuclear Facility Application*. ASME NQA-1-2000, American Society of Mechanical Engineers, New York, NY.

ASTM. 2016. *Standard Test Method for Shear Testing of Bulk Solids Using the Jenike Shear Tester*. ASTM D6128-16, West Conshohocken, PA.

ASTM. 2019. *Standard Test Method for Measuring Bulk Density Values of Powders and Other Bulk Solids as Function of Compressive Stress*. ASTM D6683-19, West Conshohocken, PA.

ASTM. 2021. *Standard Test Method for Bulk Solids Characterization by Carr Indices*. ASTM D6393-21, West Conshohocken, PA.

Chun J, T Oh, M Luna, and M Schweiger. 2011. "Effect of particle size distribution on slurry rheology: Nuclear waste simulant slurries." *Colloids and Surfaces A: Physicochem. Eng. Aspects* 384:304–310. <https://doi.org/10.1016/j.colsurfa.2011.04.003>

Deng Y, RC Chen, R Gimpel, B Slettene, MR Gross, K Jun, and R Fundak. 2016. *Flowsheet Bases, Assumptions, and Requirements*. 24590-WTP-RPT-PT-02-005, Rev. 8, Bechtel National, Inc., Richland, WA.

DOE Order 414.1D, *Quality Assurance*. U.S. Department of Energy, Washington, D.C.

Kim DS, JD Vienna, and AA Kruger. 2012. *Preliminary ILAW Formulation Algorithm Description*. Report No. 24590-LAW-RPT-RT-04-0003, Rev. 1, Bechtel National, Inc., Richland, WA. <https://www.osti.gov/servlets/purl/1110191>

LaBryer J. 2019. *Document for Glass Former Chemicals*. 24590-BOF-3PS-MH00-W0001, Rev. 0, Bechtel National, Inc., Richland, WA.

Lee E. 2007. *Dynamic (G2) Flowsheet Assessment of the Effect of M-12 Modifications on Pretreatment Capacity*. 24590-WTP-RPT-PO-07-002, Rev. 0, River Protection Project, Hanford Tank Waste Treatment and Immobilization Plant, Richland, WA.

Lumetta NA, DS Kim, and JD Vienna. 2020. *Preliminary Enhanced LAW Glass Formulation Algorithm*. PNNL-29475, Pacific Northwest National Laboratory, Richland, WA.

Muller I, H Gan, and IL Pegg. 2001. *Physical and Rheological Properties of Waste Simulants and Melter Feeds for RPP-WTP LAW Vitrification*. VSL-01R3520-1, Rev. 0, Vitreous State Laboratory, The Catholic University of America, Washington, D.C.

Rieck BT. 2015. *Document for Alternate Glass Forming Chemical Qualification Matrix*. 24590-BOF-POSP-PENG-18-00022, Rev. 0, Bechtel National, Inc., Richland, WA.

Russell RM and Chamberlain BE. 2019. *Document for Waste Acceptance Criteria for the Low Activity Waste Pretreatment Systems*. RPP-RPT-60636, Rev. 1, Washington River Protection Solutions, Richland, WA.

Schumacher R. 2003. *Document for Characterization of HLW and LAW Glass Formers*. Report No. WSRC-TR-2002-00282, Rev. 1, Savannah River Site, Aiken, SC.

<https://sti.srs.gov/fulltext/tr2002282r1/tr2002282r1.pdf>

Suyderhoud P. 2017. *Document for System Description for the WTP Glass Formers Reagent System*. 24590-WTP-3YD-GFR-00001, Rev. 2, Bechtel National, Inc., Richland, WA.

Vienna JD, NA Lumetta, DS Kim, and AA Kruger. 2018. "Robust and High-Waste Loaded Glass Formulations for Hanford Low-Activity Waste - 19050," in Waste Management 2018, WM Symposia, Phoenix, AZ.

## Appendix A – Chemical Data Sheets from Vendor

This appendix displays the original chemical data sheets of four individual glass-forming chemicals that vendors provided for this testing.

**DAVIS COLORS®**  
**MAPICO®**  
**SILO®**

**VENATOR**

10001 Woodloch Forest Dr, The Woodlands, TX 77380  
Phone: (844) 341-4780

**CERTIFICATE OF ANALYSIS:**

**GB8500LCB50**

**GB8500 GREEN CHROMIUM OXIDE**

---

**CUSTOMER:** Azelis Americas (GMZ)

**City / State:** Vandalia / OH

**LOT NUMBER:** 190314-01

**MANF. DATE:** 14-Mar-2019

**Order Number:** O-19-19115

**CUSTOMER ITEM CODE:** 10016901

**QUANTITY REPRESENTED:** 3,500 LB

**SHIP DATE:** 1/8/2020

**CUSTOMER PO #:** 7201458

**CUSTOMER Fax #:**

---

QUALITY CRITERIA	S P E C I F I C A T I O N		TEST RESULTS
	Min	Max	Test
Masstone DE		1.00	0.40 CIELab Units
Masstone DL	-0.85	0.85	-0.14 CIELab Units
Masstone Da	-1.00	1.00	0.38 CIELab Units
Masstone Db	-1.00	1.00	-0.28 CIELab Units
Tint DE		1.00	0.05 CIELab Units
Tint DL	-0.85	0.85	0.05 CIELab Units
Tint Da	-1.00	1.00	0.00 CIELab Units
Tint Db	-1.00	1.00	-0.01 CIELab Units
pH of a 10 wt-% Slurry	4.0		5.7
Moisture%		1.00	0.16 %
Water Soluble Salts		0.50	0.37 %
325 Mesh Retention		0.300	0.170 %
Chromium Oxide (Cr2O3)	98.0000		99.1580 %

---

Customer Contact: Customer Service Representative 844-341-4780

Date: 1/8/2020

---

Information contained herein is, to the best of our knowledge, true and accurate, but all recommendations or suggestions are made without guarantee. Since the conditions of use are beyond our control, Venator disclaims any liability incurred in connection with the use of our products and information contained herein. No person is authorized to make any statement or recommendation not contained herein, and any such statement or recommendation so made shall not bind Venator. Furthermore, nothing contained herein shall be construed as a recommendation to use any product with existing patents covering any material or its use, and no license implied or in fact is granted herein under the claims of any patents.

Figure A.1. Cr<sub>2</sub>O<sub>3</sub> chemical data sheet





**Certificate of Analysis & Packing Slip**

Shipment Packet ID: 6975

Date Shipped: 5/6/2020

Page 1 of 1

Battelle for US DOE  
ATTENTION: Carolyn Burns AM:  
APEL/117  
790 6th Street  
Richland, WA 99354

Product : HP V2O5  
Customer Order # : 92023349  
USV Order # : C0-0163  
Scale Ticket # :

Carrier : FEDEX  
Seal # :  
Container # :  
Chemistry Units : Percent

Total Net Weight	Total V Weight	Total V2O5 Weight	Total Packages
50.00	27.96	49.92	1

Shipping Instructions:  
Ship FedEx 2nd day Collect  
Acct # 131704928-0

Bill of Lading Description:  
UN2862, Vanadium Pentoxide, 6.1, PG III  
Schedule B 2825.30.0010

Description of Articles:  
MATERIAL SAFETY DATA SHEET ATTACHED.  
CERTIFICATE OF ANALYSIS ATTACHED.  
Country of manufacture USA.

Final Q.A. Approval

					Fe	K	Mo	Na	Si	V	V2O4	V2O5
HP V2O5	1	H200167-98	1 pkgs	50 lbs	0.066	< 0.005	0.01	0.006	< 0.004	55.92	0.73	99.83
Overall Lot Chemistries (weighted avg)					0.066	< 0.005	0.01	0.006	< 0.004	55.92	0.73	99.83

Figure A.2. V<sub>2</sub>O<sub>5</sub> chemical data sheet



Ferro Corporation  
1789 Transelco Drive  
Penn Yan NY 14527  
USA  
Tel: 315-536-3357  
Fax: 315-536-8091

Battelle  
For The US Doe  
790 6th Street  
Richland WA 99354

### Certificate of analysis

Repeat printout

Date  
02/12/2021  
Purchase order item/date  
92023505 / 05/04/2020  
Delivery item/date  
83116403 900001 / 05/18/2020  
Order item/date  
1875934 000010 / 05/05/2020  
CUSTOMER NUMBER  
2501584

Ferro Material: 1014651 301 Tin Oxide 50 Lb Pail  
Customer Code:

Batch 909955 / Quantity 50.000 LB  
Inspection lot 30001710978 from 05/06/2020

Characteristic	Unit	Value	Lower Limit	Upper Limit
+325 Mesh Screen	%	< 0.00	-	1.00
Horiba LA-950 D50	µm	1.69	-	2.80
Loss on Ignition	%	0.41		0.50
Al <sub>2</sub> O <sub>3</sub>	%	0.001		0.010
CaO	%	0.0108	-	0.0500
Fe <sub>2</sub> O <sub>3</sub>	%	0.0035	-	0.0500
Na <sub>2</sub> O	%	0.0039	-	0.0100
SiO <sub>2</sub>	%	0.0034	-	0.0100
TiO <sub>2</sub>	%	0.0048	-	0.0100

The information contained in this certificate was established in our laboratories and is to the best of our knowledge and belief correct. The information is intended to show only the general nature of the products to which it relates and is not to be taken as a guarantee of the individual characteristics of any items supplied. Any liability on our part exceeding the liability stated in the Contract pursuant to which this certificate is issued is hereby expressly excluded.

Brandon Striker  
Quality Manager

Figure A.3. SnO<sub>2</sub> chemical data sheet



Atotech USA, LLC  
Quality Control  
1750 Overview drive  
Rock Hill, SC 29731-2000  
QC Lab Tel: (803) 817-3575 - Fax: (803) 817-3606  
Customer Service: (800) 752-8464 (US Customers Only)

Repeat printout

READE INT'L C/O BATELLE FOR US DOE  
790 8TH STREET  
RICHLAND WA 99354

#### Inspection Certificate

Date: 02/12/2021  
Article-No: 2201176-0055-5-000  
Material: STANNOUS OXIDE  
Charge: 0008  
Remain.Shelf Life: 05/2022  
Atotech Order No: 5002225819  
Delivery No: 5006385187  
Cust.Mat.No:  
Cust.Order No: 92023503

This is to certify that the product identified has been tested under controlled laboratory conditions and found to meet our specifications and quality assurance standards.

Manufacturing date: 05/06/2020

Qualitative characteristic(s)	Valid value(s)	Actual value	Method
Appearance	Fine homogeneous powder	Fine homogeneous powder	9727-PHY
Color	Blue Black	Black	9727-PHY

Quantitative characteristic(s)	Lower Limit	Upper Limit	Value	Unit	Method
Content: Sn(II)			86.7	%W/W	4649RCOA
By-product: Fe			0.005	%W/W	4649RCOA

Manager  
Laboratory Manager

Figure A.4. SnO chemical data sheet



## SAFETY DATA SHEET

### 1. Identification

Product identifier	CHROMOX; ChromeCAST	
Other means of identification		
Product code	100829, 103115	
Synonyms	Chromite (Cr <sub>2</sub> FeO <sub>4</sub> ) * Chrome ore * IRON CHROMITE	
Recommended use	Not available.	
Recommended restrictions	None known.	
Manufacturer/Importer/Supplier/Distributor information		
Manufacturer		
Company name	Prince Minerals, Inc.	
Address	21 West 46th Street Fourteenth Floor New York, NY 10036 United States	
Telephone	General Information	(713) 955-5398
Website	www.princecorp.com	
E-mail	Not available.	
Emergency phone number	CHEMTREC	(800) 424-9300

### 2. Hazard(s) identification

<b>Physical hazards</b>	Not classified.
<b>Health hazards</b>	Not classified.
<b>Environmental hazards</b>	Not classified.
<b>OSHA defined hazards</b>	Not classified.
<b>Label elements</b>	
Hazard symbol	None.
Signal word	None.
Hazard statement	The substance does not meet the criteria for classification.
<b>Precautionary statement</b>	
Prevention	Observe good industrial hygiene practices.
Response	Wash hands after handling.
Storage	Store away from incompatible materials.
Disposal	Dispose of waste and residues in accordance with local authority requirements.
<b>Hazard(s) not otherwise classified (HNOC)</b>	None known.
<b>Supplemental information</b>	None.

### 3. Composition/information on ingredients

#### Substances

The manufacturer lists no ingredients as hazardous according to OSHA 29 CFR 1910.1200.

Chemical name	Common name and synonyms	CAS number	%
Chromite (Cr <sub>2</sub> FeO <sub>4</sub> )	Chromite (Cr <sub>2</sub> FeO <sub>4</sub> ) Chrome ore IRON CHROMITE	1308-31-2	100

\*Designates that a specific chemical identity and/or percentage of composition has been withheld as a trade secret.

### 4. First-aid measures


<b>Inhalation</b>	Move to fresh air. Call a physician if symptoms develop or persist.
-------------------	---

Material name: CHROMOX; ChromeCAST  
100829, 103115 Version #: 02 Revision date: 10-28-2014 Issue date: 10-28-2014

SDS US  
1 / 6

Figure A.5. FeCr<sub>2</sub>O<sub>4</sub> chemical data sheet

<b>SiLibeads Ceramicbeads Type Z</b>				Version: V5/2011	
<i>EU Safety Data Sheet according to Attachment II EC Reg. 1907/2006 (REACH)</i>					
First created on:	25.03.2011	Updated on:	25.03.2011		
Next inspection on:	25.03.2012	Printed on:	25.03.2011		

  
SiLi  
SEGMENT LITHIUM



### 3. Composition / detailed information on the ingredients

#### 3.1 Chemical characteristics

Description: Beads made of Zirconium Silicate

#### 3.2 Ingredients

Name	Symbol, R-/S-phrases	Percentage % (w/w)	CAS No.	EC No. (EINECS)	REACH Reg.No.
main components		reference value			
Zirconium dioxide $ZrO_2$	Xi, R36/37, S26-39 no hazardous substances	67,50 %	1314-23-4	215-227-2	----
Hafnium dioxide $HfO_2$			12055-23-1	235-013-2	----
Silicon dioxide $SiO_2$ <sup>(1)</sup>	amorphous, no hazardous substance	27,50 %	7631-86-9	231-545-4	----
further <sup>(2)</sup>		5,00 %			

<sup>(1)</sup> Silica glass, free from crystalline forms of silica

<sup>(2)</sup> Further: Traces of radioactive components with natural origin (U + Th < 0,05 %)

The heavy metal content of SiLibeads Type Z remain within the permitted limits of European Directive 2002/95/EC - RoHS

### 4. First-aid measures

General Advice:	Remove soiled Clothes. In case of persisting discomfort please contact a physician. To helpers: Please protect yourself.
After Inhalation:	Provide fresh air.
After Skin Contact:	Clean Skin with water and soap.
After Eye Contact:	Remove particle carefully from the affected eye. If needed, remove contact lense. Rinse eye thoroughly with plenty of water. Consult a physician if needed.
After Swallowing:	Consult a physician after swallowing large quantities.
Advise to the physician:	Irritation of skin, mucosa, eyes and to the respiratory system through dust are possible. Decontamination and symptomatic treatments are in most cases sufficient.

### 5. Fire fighting actions

Suitable extinguishing agents:	The product itself is neither combustible nor explosive. extinguishing agents have to be coordinated with the surrounding fire.
For safety reason unsuitable extinguishing agents:	Largely unknown

Figure A.6.  $ZrSiO_4$  chemical data sheet

## Appendix B – Testing Results Sheets

Table B.1 through Table B.13 display data sheets that summarize the physical and flow properties of the dry powders, both individual GFCs and their mixtures, as measured by the vendor, J&J, and/or PNNL. Data from J&J are highlighted in red and data from PNNL are highlighted in blue in the data sheets.


In the data sheets, the property of cohesive strength is expressed in feet. These results are driven by the flow function, unconfined compressive strength (lbf/ft<sup>2</sup>) vs. major consolidating pressure (lbf/ft<sup>2</sup>), and the bulk density (lbf/ft<sup>3</sup>).

Table B.14 through Table B.20 display data sheets that summarize the results of physical and rheological property measurements of the slurry feeds performed at PNNL. In the data sheets, for the measurement of shear strength, the vane was mistakenly lowered a little bit closer to the container bottom at 48 hours. Hence, the value tends to be higher than the value for 24 hours.

The settling test was set to monitor solids settling in the slurry feed as a function of time at room temperature. The test was performed for 30 days without any disturbance and the volume of the settled solid portion was recorded (see images in Table B.14 through Table B.20).

Table B.1. Data sheet for chromium oxide ( $\text{Cr}_2\text{O}_3$ )

Oxide	Cr <sub>2</sub> O <sub>3</sub>
Grade	Technical, 99% purity, 325 mesh
Vendor	Venator, TX USA Lot: 190314-01
Cost for bulk	\$16.98/lb




<b>Data from vendor</b>					
Chemical purity					
Cr <sub>2</sub> O <sub>3</sub>					
99.158%					
<b>Measured data</b>					
Cohesive strength					
To avoid rathole (effective head = 10 ft)		Minimum diameter for cohesive arch			
Continuous flow	7 days at rest	Continuous flow	7 days at rest		
14.2 ft	14.5 ft	3.3 ft	4.0 ft		
Compressibility (bulk density as a function of consolidating pressure)					
Bulk density	65–144 lb/ft <sup>3</sup>	Particle density	327 lb/ft <sup>3</sup>		
Wall friction angle (degrees from vertical), Conical hopper (outlet diameter 1 ft)					
Wall material	Slip-stick	Continuous flow	After 7 days at rest		
304 SS sheet, #2B finish	69%	13°	13°		
Mild CS HR plate	n/a	0°	0°		
TIVAR 88	82%	21°	21°		
Permeability (limiting flow rate), 1-ft-diameter opening, effective head = 10 ft					
K0	0.156 fps	Critical flow rate	Not possible due to arch		
Impact chute (maximum angle from horizontal)					
Material	Impact pressure 4 psf		Impact pressure 8 psf		
304 SS sheet, #2B finish	24°		90°		
Mild CS HR plate	35°		90°		
TIVAR 88	29°		90°		
Angle of repose (degrees from horizontal)					
Average	35°	Range	32° - 40°		
Particle size distribution by volume percent					
At 0 bar		At 3 bar			
D <sub>10</sub>	D <sub>50</sub>	D <sub>90</sub>	D <sub>10</sub>	D <sub>50</sub>	D <sub>90</sub>
1.4 μm	4.2 μm	10.6 μm	1.2 μm	2.8 μm	7.6 μm
Moisture content		0.093 wt%			



Table B.2. Data sheet for vanadium pentoxide (V<sub>2</sub>O<sub>5</sub>)


Oxide	V <sub>2</sub> O <sub>5</sub>
Grade	Technical, 99% purity 140 mesh
Vendor	U.S. Vanadium, AR USA Lot: H200167-98
Cost for bulk	\$27.98/lb



<b>Data from vendor</b>					
Chemical purity					
V <sub>2</sub> O <sub>5</sub>	Fe	K	Mo	Na	Si
99.83%	0.066%	<0.005%	0.01%	0.006%	<0.004%
<b>Measured data</b>					
<b>Cohesive strength</b>					
To avoid rathole (effective head = 10 ft)			Minimum diameter for cohesive arch		
Continuous flow	7 days at rest		Continuous flow	7 days at rest	
4.7 ft	4.8 ft		0.4 ft	0.6 ft	
<b>Compressibility (bulk density as a function of consolidating pressure)</b>					
<b>Bulk density</b>		46 – 67 lb/ft <sup>3</sup>		<b>Particle density</b>	212 lb/ft <sup>3</sup>
<b>Wall friction angle (degrees from vertical), Conical hopper (outlet diameter 1 ft)</b>					
Material	Slip-stick		Continuous flow	7 days at rest	
304 SS sheet, #2B finish	n/a		5°	5°	
Mild CS HR plate	n/a		1°	1°	
TIVAR 88	n/a		12°	12°	
<b>Permeability (limiting flow rate), 1-ft-diameter opening, effective head = 10 ft</b>					
K0	0.0042 fps		Critical flow rate	2400 lb/h	
<b>Impact chute (maximum angle from horizontal)</b>					
Material	Impact pressure 4 psf		Impact pressure 8 psf		
304 SS sheet, #2B finish	29°		34°		
Mild CS HR plate	34°		39°		
TIVAR 88	30°		38°		
<b>Angle of repose (degrees from horizontal)</b>					
Average	42°		Range	34° - 50°	
<b>Particle size distribution by volume percent</b>					
At 0 bar			At 3 bar		
D <sub>10</sub>	D <sub>50</sub>	D <sub>90</sub>	D <sub>10</sub>	D <sub>50</sub>	D <sub>90</sub>
14 µm	71.6 µm	254.8 µm	2.7 µm	29.6 µm	141.9 µm
<b>Moisture content</b>			0.2665 wt%		

Table B.3. Data sheet for stannous oxide (SnO)


Oxide	SnO				
Grade	Technical, 99% purity, 200 mesh				
Vendor	Atotech, SC USA Lot: 5002225819				
Cost for bulk	\$32.15/lb				



<b>Data from vendor</b>					
Chemical purity					
SnO	Fe				
99.99%	0.005%				
<b>Measured data</b>					
Cohesive strength					
To avoid rathole (effective head = 10 ft)			Minimum diameter for cohesive arch		
Continuous flow	7 days at rest		Continuous flow	7 days at rest	
4.1 ft	4.1 ft		No minimum	No minimum	
Compressibility (bulk density as a function of consolidating pressure)					
Bulk density	120 – 158 lb/ft³		Particle density	391 lb/ft³	
Wall friction angle (degrees from vertical), Conical hopper (outlet diameter 1 ft)					
Material	Slip-stick		Continuous flow	7 days at rest	
304 SS sheet, #2B finish	n/a		13°	13°	
Mild CS HR plate	84%		10°	6°	
TIVAR 88	69%		10°	10°	
Permeability (limiting flow rate), 1-ft-diameter opening, effective head = 10 ft					
K0	0.0157 fps		Critical flow rate	32,600 lb/h	
Impact chute (maximum angle from horizontal)					
Material	Impact pressure 4 psf		Impact pressure 8 psf		
304 SS sheet, #2B finish	29°		30°		
Mild CS HR plate	28°		30°		
TIVAR 88	26°		28°		
Angle of repose (degrees from horizontal)					
Average	26°		Range	25° - 28°	
Particle size distribution by volume percent					
At 0 bar			At 3 bar		
D <sub>10</sub>	D <sub>50</sub>	D <sub>90</sub>	D <sub>10</sub>	D <sub>50</sub>	D <sub>90</sub>
11.2 µm	56.4 µm	94.6 µm	5.7 µm	38.8 µm	75.4 µm
Moisture content			0.2 wt%		

Table B.4. Data sheet for stannic oxide (SnO<sub>2</sub>)


Oxide	SnO <sub>2</sub>
Grade	Technical, 99.0% purity, 325 mesh
Vendor	Ferro, NY USA LOT: 909955
Cost for bulk	\$63.76/lb



Data from vendor							
Chemical purity							
SnO <sub>2</sub>	Al <sub>2</sub> O <sub>3</sub>	CaO	Fe <sub>2</sub> O <sub>3</sub>	Na <sub>2</sub> O	SiO <sub>2</sub>	TiO <sub>2</sub>	
99.98%	0.001%	0.01%	0.004%	0.004%	0.003%	0.005%	
Measured data							
Cohesive strength							
To avoid rathole (effective head = 10 ft)				Minimum diameter for cohesive arch			
Continuous flow		7 days at rest		Continuous flow		7 days at rest	
26 ft		26 ft		No minimum		No minimum	
Compressibility (bulk density as a function of consolidating pressure)							
Bulk density		61–102 lb/ft <sup>3</sup>		Particle density		450 lb/ft <sup>3</sup>	
Wall friction angle (degrees from vertical), Conical hopper (outlet diameter 1 ft)							
Material		Slip-stick		Continuous flow		7 days at rest	
304 SS sheet, #2B finish		n/a		6°		6°	
Mild CS HR plate		84%		No data		No data	
TIVAR 88		n/a		14°		14°	
Permeability (limiting flow rate), 1-ft-diameter opening, effective head = 10 ft							
K0		0.0238 fps		Critical flow rate		21,200 lb/h	
Impact chute (maximum angle from horizontal)							
Material		Impact pressure 4 psf			Impact pressure 8 psf		
304 SS sheet, #2B finish		30°			68°		
Mild CS HR plate		34°			83°		
TIVAR 88		33°			58°		
Angle of repose (degrees from horizontal)							
Average		33°		Range		31°–34°	
Particle size distribution by volume percent at 0 bar							
D <sub>10</sub>		D <sub>50</sub>			D <sub>90</sub>		
0.5 μm		2.2 μm			11.3 μm		
Particle size distribution by sieving (weight percent)							
6 mesh	12 mesh	20 mesh	40 mesh	70 mesh	100 mesh	200 mesh	Pan
3350 μm	1700 μm	850 μm	425 μm	212 μm	150 μm	75 μm	<75 μm
0%	0.1%	5.4%	22.3%	35.6%	11%	13.7%	11.7%
Moisture content				0.1945 wt%			

Table B.5. Data sheet for GFC Batch #1a (0.00V<sub>2</sub>O<sub>5</sub>–4.50SnO<sub>2</sub>)


Component	wt%
Al <sub>2</sub> SiO <sub>5</sub>	7.77
H <sub>3</sub> BO <sub>3</sub>	14.80
CaSiO <sub>3</sub>	13.24
Li <sub>2</sub> CO <sub>3</sub>	-
Mg <sub>2</sub> SiO <sub>4</sub>	3.90
Cr <sub>2</sub> O <sub>3</sub>	0.68
SiO <sub>2</sub>	34.08
ZnO	3.59
ZrSiO <sub>4</sub>	10.28
V <sub>2</sub> O <sub>5</sub>	-
SnO <sub>2</sub>	5.47
C <sub>12</sub> H <sub>22</sub> O <sub>11</sub>	6.20
Sum	100.00



Measured data					
Cohesive strength					
To avoid rathole (effective head = 10 ft)		Minimum diameter for cohesive arch			
Continuous flow	7 days at rest	Continuous flow	7 days at rest		
7.9 ft	8.1 ft	0.8 ft	1.7 ft		
Compressibility (bulk density as a function of consolidating pressure)					
Bulk density	59 – 96 lb/ft <sup>3</sup>	Particle density	173 lb/ft <sup>3</sup>		
Wall friction angle (degrees from vertical), Conical hopper (outlet diameter 1 ft)					
Material	Slip-stick	Continuous flow	7 days at rest		
304 SS sheet, #2B finish	n/a	14°	14°		
Mild CS HR plate	n/a	8°	5°		
TIVAR 88	n/a	13°	13°		
TIVAR 88-2 Lorien	n/a	21°	Not tested		
Permeability (limiting flow rate), 1-ft-diameter opening, effective head = 10 ft					
K0	0.0013 fps	Critical flow rate	200 lb/h		
Impact chute (maximum angle from horizontal)					
Material	Impact pressure 4 psf		Impact pressure 8 psf		
304 SS sheet, #2B finish	27°		39°		
Mild CS HR plate	34°		52°		
TIVAR 88	29°		36°		
Angle of repose (degrees from horizontal)					
Average	34°	Range	26°–38°		
Particle size distribution by volume percent					
At 0 bar		At 3 bar			
D <sub>10</sub>	D <sub>50</sub>	D <sub>90</sub>	D <sub>10</sub>	D <sub>50</sub>	D <sub>90</sub>
4.2 μm	35.7 μm	624.5 μm	2.4 μm	27.8 μm	423.3 μm
Moisture content		3.7375 wt%			

Table B.6. Data sheet for GFC Batch #6a (3.51V<sub>2</sub>O<sub>5</sub>–2.42SnO<sub>2</sub>)


Component	wt%
Al <sub>2</sub> SiO <sub>5</sub>	9.99
H <sub>3</sub> BO <sub>3</sub>	16.98
CaSiO <sub>3</sub>	11.45
Li <sub>2</sub> CO <sub>3</sub>	-
Mg <sub>2</sub> SiO <sub>4</sub>	4.09
Cr <sub>2</sub> O <sub>3</sub>	0.03
SiO <sub>2</sub>	31.72
ZnO	-
ZrSiO <sub>4</sub>	12.04
V <sub>2</sub> O <sub>5</sub>	4.24
SnO <sub>2</sub>	2.91
C <sub>12</sub> H <sub>22</sub> O <sub>11</sub>	6.56
Sum	100.00



Measured data					
Cohesive strength					
To avoid rathole (effective head = 10 ft)		Minimum diameter for cohesive arch			
Continuous flow	7 days at rest	Continuous flow	7 days at rest		
7.0 ft	7.0 ft	1.0 ft	1.0 ft		
Compressibility (bulk density as a function of consolidating pressure)					
Bulk density	63 – 100 lb/ft <sup>3</sup>	Particle density	167 lb/ft <sup>3</sup>		
Wall friction angle (degrees from vertical), Conical hopper (outlet diameter 1 ft)					
Material	Slip-stick	Continuous flow	7 days at rest		
304 SS sheet, #2B finish	n/a	12°	12°		
Mild CS HR plate	n/a	0°	0°		
TIVAR 88	n/a	6°	6°		
Permeability (limiting flow rate), 1-ft-diameter opening, effective head = 10 ft					
K0	0.00099 fps	Critical flow rate	200 lb/h		
Impact chute (maximum angle from horizontal)					
Material	Impact pressure 4 psf		Impact pressure 8 psf		
304 SS sheet, #2B finish	30°		43°		
Mild CS HR plate	36°		48°		
TIVAR 88	34°		40°		
Angle of repose (degrees from horizontal)					
Average	34°	Range	26°–40°		
Particle size distribution by volume percent					
At 0 bar		At 3 bar			
D <sub>10</sub>	D <sub>50</sub>	D <sub>90</sub>	D <sub>10</sub>	D <sub>50</sub>	D <sub>90</sub>
5.1 μm	51.2 μm	618.5 μm	3.4 μm	47.6 μm	564.7 μm
Moisture content		4.9635 wt%			

Table B.7. Data sheet for GFC Batch #9a (3.98V<sub>2</sub>O<sub>5</sub>–0.25SnO<sub>2</sub>)

Component	wt%
Al <sub>2</sub> SiO <sub>5</sub>	11.00
H <sub>3</sub> BO <sub>3</sub>	14.88
CaSiO <sub>3</sub>	17.71
Li <sub>2</sub> CO <sub>3</sub>	12.64
Mg <sub>2</sub> SiO <sub>4</sub>	-
Cr <sub>2</sub> O <sub>3</sub>	-
SiO <sub>2</sub>	26.09
ZnO	-
ZrSiO <sub>4</sub>	10.21
V <sub>2</sub> O <sub>5</sub>	4.09
SnO <sub>2</sub>	0.26
C <sub>12</sub> H <sub>22</sub> O <sub>11</sub>	3.13
Sum	100.00



Measured data					
Cohesive strength					
To avoid rathole (effective head = 10 ft)		Minimum diameter for cohesive arch			
Continuous flow	7 days at rest	Continuous flow	7 days at rest		
7.4 ft	8.1 ft	0.6 ft	1.7 ft		
Compressibility (bulk density as a function of consolidating pressure)					
Bulk density	55 – 87 lb/ft <sup>3</sup>	Particle density	159 lb/ft <sup>3</sup>		
Wall friction angle (degrees from vertical), Conical hopper (outlet diameter 1 ft)					
Material	Slip-stick	Continuous flow	7 days at rest		
304 SS sheet, #2B finish	n/a	14°	14°		
Mild CS HR plate	n/a	8°	5°		
TIVAR 88	n/a	15°	15°		
Permeability (limiting flow rate), 1-ft-diameter opening, effective head = 10 ft					
K0	0.0017 fps	Critical flow rate	600 lb/h		
Impact chute (maximum angle from horizontal)					
Material	Impact pressure 4 psf		Impact pressure 8 psf		
304 SS sheet, #2B finish	29°		50°		
Mild CS HR plate	33°		50°		
TIVAR 88	31°		50°		
Angle of repose (degrees from horizontal)					
Average	33°	Range	25°–39°		
Particle size distribution by volume percent					
At 0 bar		At 3 bar			
D <sub>10</sub>	D <sub>50</sub>	D <sub>90</sub>	D <sub>10</sub>	D <sub>50</sub>	D <sub>90</sub>
5.0 μm	40.6 μm	588.6 μm	3.2 μm	34.4 μm	543.2 μm
Moisture content		4.534 wt%			

Table B.8. Data sheet for chromium oxide ( $\text{FeCr}_2\text{O}_4$ )


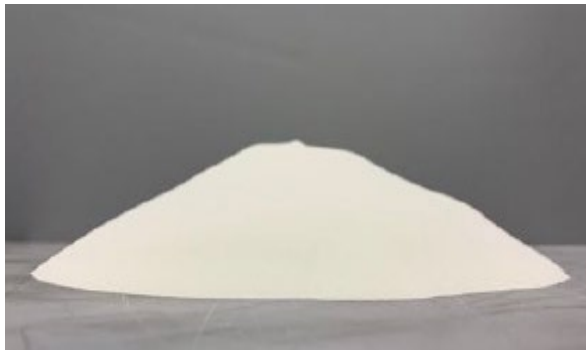
Oxide	FeCr <sub>2</sub> O <sub>4</sub>				
Grade	Technical, 100% purity, 38 μm				
Vendor	PRINCE Lot: 100829, 103115				
					
Cost for bulk	\$16.43/lb				
<b>Data from vendor</b>					
Chemical purity					
FeCr <sub>2</sub> O <sub>4</sub>					
100%					
<b>Measured data</b>					
Cohesive strength					
To avoid rathole (effective head = 10 ft)			Minimum diameter for cohesive arch		
Continuous flow	7 days at rest		Continuous flow	7 days at rest	
5.4 ft	5.4 ft		0.4 ft	0.9 ft	
Compressibility (bulk density as a function of consolidating pressure)					
Bulk density	82.2–136.5 lb/ft <sup>3</sup>		Particle density	270 lb/ft <sup>3</sup>	
Wall friction angle (degrees from vertical), Conical hopper (outlet diameter 1 ft)					
Wall material	Slip-stick		Continuous flow	After 7 days at rest	
304 SS sheet, #2B finish	N/A		8°	8°	
Mild CS HR plate	N/A		1°	1°	
TIVAR 88	N/A		8°	8°	
Permeability (limiting flow rate), 1-ft-diameter opening, effective head = 10 ft					
K <sub>0</sub>	0.00075 fps		Critical flow rate	400 lb/h	
Impact chute (maximum angle from horizontal)					
Material	Impact pressure 4 psf		Impact pressure 8 psf		
304 SS sheet, #2B finish	30°		59°		
Mild CS HR plate	34°		73°		
TIVAR 88	34°		51°		
Angle of repose (degrees from horizontal)					
Average	42.2°		Range	38° - 46°	
Particle size distribution by volume percent					
At 0 bar			At 3 bar		
D <sub>10</sub>	D <sub>50</sub>	D <sub>90</sub>	D <sub>10</sub>	D <sub>50</sub>	D <sub>90</sub>
2.7 μm	13.9 μm	38.3 μm	1.5 μm	10.2 μm	37.3 μm
Moisture content			0.1415 wt%		



Table B.9. Data sheet for vanadium pentoxide (ZrSiO<sub>4</sub>)


Oxide	ZrSiO <sub>4</sub>				
Grade	Bead type Z, 95% purity 70-125 μm				
Vendor	Ceroglass Lot: 1805020				
Cost for bulk	\$22/lb				



<b>Data from vendor</b>					
Chemical purity					
ZrO <sub>2</sub>	SiO <sub>2</sub>	Others	U+Th		
67.50%	27.50%	5.00%	<0.05%		
<b>Measured data</b>					
Cohesive strength					
To avoid rathole (effective head = 10 ft)			Minimum diameter for cohesive arch		
Continuous flow	7 days at rest		Continuous flow	7 days at rest	
0.8 ft	0.8 ft		No minimal	No minimal	
Compressibility (bulk density as a function of consolidating pressure)					
Bulk density	136.5 – 141.1 lb/ft <sup>3</sup>		Particle density	238 lb/ft <sup>3</sup>	
Wall friction angle (degrees from vertical), Conical hopper (outlet diameter 1 ft)					
Material	Slip-stick		Continuous flow	7 days at rest	
304 SS sheet, #2B finish	60 %		26°	26°	
Mild CS HR plate	82 %		23°	23°	
TIVAR 88	N/A		32°	32°	
Permeability (limiting flow rate), 1-ft-diameter opening, effective head = 10 ft					
K <sub>0</sub>	0.03869 fps		Critical flow rate	772000 lb/h	
Impact chute (maximum angle from horizontal)					
Material	Impact pressure 4 psf		Impact pressure 8 psf		
304 SS sheet, #2B finish	21°		21°		
Mild CS HR plate	23°		26°		
TIVAR 88	24°		26°		
Angle of repose (degrees from horizontal)					
Average	21.7°		Range	20° – 23°	
Particle size distribution by volume percent					
At 0 bar			At 3 bar		
D <sub>10</sub>	D <sub>50</sub>	D <sub>90</sub>	D <sub>10</sub>	D <sub>50</sub>	D <sub>90</sub>
70.4 μm	100.1 μm	141.6 μm	70.3 μm	98.3 μm	137.0 μm
Moisture content			0.0315 wt%		

Table B.10. Data sheet for GFC Batch #1b (0.00V<sub>2</sub>O<sub>5</sub>–4.50SnO<sub>2</sub>)

Component	wt%
Al <sub>2</sub> SiO <sub>5</sub>	6.91
H <sub>3</sub> BO <sub>3</sub>	14.63
CaSiO <sub>3</sub>	13.37
Fe <sub>2</sub> O <sub>3</sub>	0.00
Li <sub>2</sub> CO <sub>3</sub>	0.00
Mg <sub>2</sub> SiO <sub>4</sub>	3.35
FeCr <sub>2</sub> O <sub>4</sub>	1.72
SiO <sub>2</sub>	34.30
ZnO	3.85
ZrSiO <sub>4</sub>	10.24
V <sub>2</sub> O <sub>5</sub>	0.00
SnO <sub>2</sub>	5.45
C <sub>12</sub> H <sub>22</sub> O <sub>11</sub>	6.17
Sum	100.00




Measured data					
Cohesive strength					
To avoid rathole (effective head = 10 ft)		Minimum diameter for cohesive arch			
Continuous flow	7 days at rest	Continuous flow	7 days at rest		
8.2 ft	8.2 ft	1.2 ft	1.5 ft		
Compressibility (bulk density as a function of consolidating pressure)					
Bulk density	57.9 – 89.2 lb/ft <sup>3</sup>	Particle density	174 lb/ft <sup>3</sup>		
Wall friction angle (degrees from vertical), Conical hopper (outlet diameter 1 ft)					
Material	Slip-stick	Continuous flow	7 days at rest		
304 SS sheet, #2B finish	n/a	13°	13°		
Mild CS HR plate	n/a	7°	7°		
TIVAR 88	n/a	12°	12°		
Permeability (limiting flow rate), 1-ft-diameter opening, effective head = 10 ft					
K <sub>0</sub>	0.001556 fps	Critical flow rate	not possible due to arching		
Impact chute (maximum angle from horizontal)					
Material	Impact pressure 4 psf		Impact pressure 8 psf		
304 SS sheet, #2B finish	28°		35°		
Mild CS HR plate	33°		41°		
TIVAR 88	32°		42°		
Angle of repose (degrees from horizontal)					
Average	35.6°	Range	25° – 42°		
Particle size distribution by volume percent					
At 0 bar		At 3 bar			
D <sub>10</sub>	D <sub>50</sub>	D <sub>90</sub>	D <sub>10</sub>	D <sub>50</sub>	D <sub>90</sub>
8.0 μm	103.3 μm	779.4 μm	4.1 μm	96.8 μm	593.7 μm
Moisture content		4.4900 wt%			



Table B.11. Data sheet for GFC Batch #1-1 (0.00V<sub>2</sub>O<sub>5</sub>–4.50SnO<sub>2</sub>)


Component	wt%
Al <sub>2</sub> SiO <sub>5</sub>	6.95
H <sub>3</sub> BO <sub>3</sub>	14.70
CaSiO <sub>3</sub>	13.44
Fe <sub>2</sub> O <sub>3</sub>	0.00
Li <sub>2</sub> CO <sub>3</sub>	0.00
Mg <sub>2</sub> SiO <sub>4</sub>	3.37
FeCr <sub>2</sub> O <sub>4</sub>	1.73
SiO <sub>2</sub>	34.48
ZnO	3.87
ZrSiO <sub>4</sub>	10.29
V <sub>2</sub> O <sub>5</sub>	0.00
SnO	4.97
C <sub>12</sub> H <sub>22</sub> O <sub>11</sub>	6.20
Sum	100.00



Measured data					
Cohesive strength					
To avoid rathole (effective head = 10 ft)		Minimum diameter for cohesive arch			
Continuous flow	7 days at rest	Continuous flow	7 days at rest		
7.6 ft	7.7 ft	0.4 ft	1.2 ft		
Compressibility (bulk density as a function of consolidating pressure)					
Bulk density	60.3 – 89.1 lb/ft <sup>3</sup>	Particle density	173 lb/ft <sup>3</sup>		
Wall friction angle (degrees from vertical), Conical hopper (outlet diameter 1 ft)					
Material	Slip-stick	Continuous flow	7 days at rest		
304 SS sheet, #2B finish	80 %	13°	13°		
Mild CS HR plate	N/A	8°	8°		
TIVAR 88	N/A	8°	8°		
Permeability (limiting flow rate), 1-ft-diameter opening, effective head = 10 ft					
K <sub>0</sub>	0.002446 fps	Critical flow rate	1400 lb/h		
Impact chute (maximum angle from horizontal)					
Material	Impact pressure 4 psf		Impact pressure 8 psf		
304 SS sheet, #2B finish	26°		37°		
Mild CS HR plate	28°		42°		
TIVAR 88	27°		46°		
Angle of repose (degrees from horizontal)					
Average	36.2°	Range	31° – 44°		
Particle size distribution by volume percent					
At 0 bar		At 3 bar			
D <sub>10</sub>	D <sub>50</sub>	D <sub>90</sub>	D <sub>10</sub>	D <sub>50</sub>	D <sub>90</sub>
8.1 μm	145.8 μm	721.6 μm	5.0 μm	85.6 μm	565.3 μm
Moisture content		4.8585 wt%			

Table B.12. Data sheet for GFC Batch #6b (3.51V<sub>2</sub>O<sub>5</sub>–2.42SnO<sub>2</sub>)


Component	wt%
Al <sub>2</sub> SiO <sub>5</sub>	9.40
H <sub>3</sub> BO <sub>3</sub>	16.98
CaSiO <sub>3</sub>	11.86
Fe <sub>2</sub> O <sub>3</sub>	0.04
Li <sub>2</sub> CO <sub>3</sub>	0.00
Mg <sub>2</sub> SiO <sub>4</sub>	3.95
FeCr <sub>2</sub> O <sub>4</sub>	0.07
SiO <sub>2</sub>	31.99
ZnO	0.00
ZrSiO <sub>4</sub>	12.03
V <sub>2</sub> O <sub>5</sub>	4.23
SnO <sub>2</sub>	2.90
C <sub>12</sub> H <sub>22</sub> O <sub>11</sub>	6.55
Sum	100.00



Measured data					
Cohesive strength					
To avoid rathole (effective head = 10 ft)		Minimum diameter for cohesive arch			
Continuous flow	7 days at rest	Continuous flow	7 days at rest		
7.5 ft	7.5 ft	0.4 ft	0.4 ft		
Compressibility (bulk density as a function of consolidating pressure)					
Bulk density	62.0 – 90.2 lb/ft <sup>3</sup>	Particle density	170 lb/ft <sup>3</sup>		
Wall friction angle (degrees from vertical), Conical hopper (outlet diameter 1 ft)					
Material	Slip-stick	Continuous flow	7 days at rest		
304 SS sheet, #2B finish	N/A	13°	13°		
Mild CS HR plate	N/A	9°	9°		
TIVAR 88	N/A	9°	9°		
Permeability (limiting flow rate), 1-ft-diameter opening, effective head = 10 ft					
K <sub>0</sub>	0.00245 fps	Critical flow rate	1200 lb/h		
Impact chute (maximum angle from horizontal)					
Material	Impact pressure 4 psf		Impact pressure 8 psf		
304 SS sheet, #2B finish	30°		40°		
Mild CS HR plate	29°		42°		
TIVAR 88	30°		36°		
Angle of repose (degrees from horizontal)					
Average	37.1°	Range	31°– 43°		
Particle size distribution by volume percent					
At 0 bar		At 3 bar			
D <sub>10</sub>	D <sub>50</sub>	D <sub>90</sub>	D <sub>10</sub>	D <sub>50</sub>	D <sub>90</sub>
9.5 μm	174.5 μm	688.2 μm	5.4 μm	86.7 μm	560.6 μm
Moisture content		5.3095 wt%			

Table B.13. Data sheet for GFC Batch #9b (3.98V<sub>2</sub>O<sub>5</sub>–0.25SnO<sub>2</sub>)

Component	wt%
Al <sub>2</sub> SiO <sub>5</sub>	10.31
H <sub>3</sub> BO <sub>3</sub>	15.31
CaSiO <sub>3</sub>	18.39
Fe <sub>2</sub> O <sub>3</sub>	0.07
Li <sub>2</sub> CO <sub>3</sub>	12.36
Mg <sub>2</sub> SiO <sub>4</sub>	0.00
FeCr <sub>2</sub> O <sub>4</sub>	0.00
SiO <sub>2</sub>	26.15
ZnO	0.00
ZrSiO <sub>4</sub>	10.07
V <sub>2</sub> O <sub>5</sub>	4.03
SnO <sub>2</sub>	0.21
C <sub>12</sub> H <sub>22</sub> O <sub>11</sub>	3.10
Sum	100.00



Measured data					
Cohesive strength					
To avoid rathole (effective head = 10 ft)		Minimum diameter for cohesive arch			
Continuous flow	7 days at rest	Continuous flow	7 days at rest		
7.8 ft	9.4 ft	0.6 ft	1.8 ft		
Compressibility (bulk density as a function of consolidating pressure)					
Bulk density	50.4 – 75.5 lb/ft <sup>3</sup>	Particle density	166 lb/ft <sup>3</sup>		
Wall friction angle (degrees from vertical), Conical hopper (outlet diameter 1 ft)					
Material	Slip-stick	Continuous flow	7 days at rest		
304 SS sheet, #2B finish	N/A	12°	12°		
Mild CS HR plate	N/A	6°	6°		
TIVAR 88	N/A	9°	9°		
Permeability (limiting flow rate), 1-ft-diameter opening, effective head = 10 ft					
K <sub>0</sub>	0.003718 fps	Critical flow rate	1400 lb/h		
Impact chute (maximum angle from horizontal)					
Material	Impact pressure 4 psf		Impact pressure 8 psf		
304 SS sheet, #2B finish	26°		39°		
Mild CS HR plate	28°		48°		
TIVAR 88	28°		49°		
Angle of repose (degrees from horizontal)					
Average	36.5°	Range	34°– 40°		
Particle size distribution by volume percent					
At 0 bar		At 3 bar			
D <sub>10</sub>	D <sub>50</sub>	D <sub>90</sub>	D <sub>10</sub>	D <sub>50</sub>	D <sub>90</sub>
9.1 μm	72.8 μm	629.0 μm	5.7 μm	66.4 μm	553.5 μm
Moisture content		4.8050 wt%			

Table B.14. Data sheet for slurry melter feed #1a (0.00V<sub>2</sub>O<sub>5</sub>–4.50SnO<sub>2</sub>)

Feed ID	LAW feed #1 0.00V <sub>2</sub> O <sub>5</sub> – 4.50SnO <sub>2</sub>	
Na molarity	5.6 M	
Waste loading	28.27 wt%	
C/N ratio	0.75	
Water content	46.75 wt%	
Total solids	53.25 wt%	
Dissolved solids	34.22 wt%	
Undissolved solids	28.94 wt%	
Density	1579.06 g/L	
pH	12.76	
Shear strength	24 hours	130.6 Pa
	48 hours	181.3 Pa
	72 hours	25.06 Pa
Viscosity	20 °C	13.39 mPa·s
	40 °C	7.219 mPa·s
Settling test	5 minutes	100.00 vol%
	15 minutes	98.97 vol%
	30 minutes	98.45 vol%
	1 hour	96.91 vol%
	2 hours	94.85 vol%
	6 hours	86.08 vol%
	24 hours	45.36 vol%
	48 hours	42.78 vol%
	76 hours	42.27 vol%
	124 hours	42.27 vol%
	1 week	42.27 vol%
	3 weeks	42.28 vol%
	1 month	42.28 vol%

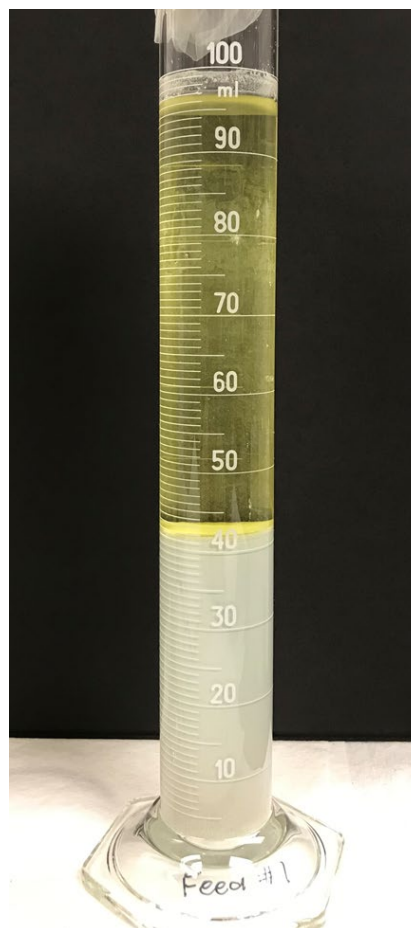


Table B.15. Data sheet for slurry melter feed #6a ( $3.51\text{V}_2\text{O}_5-2.42\text{SnO}_2$ )

Feed ID	LAW feed #6 $3.51\text{V}_2\text{O}_5 - 2.42\text{SnO}_2$	
Na molarity	5.6 M	
Waste loading	28.51 wt%	
C/N ratio	0.75	
Water content	50.08 wt%	
Total solids	49.92 wt%	
Dissolved solids	31.50 wt%	
Undissolved solids	26.89 wt%	
Density	1525.40 g/L	
pH	12.58	
Shear strength	24 hours	1518 Pa
	48 hours	1478 Pa
	72 hours	399.8 Pa
Viscosity	20 °C	10.84 mPa·s
	40 °C	5.73 mPa·s
Settling test	5 minutes	100.00 vol%
	15 minutes	97.92 vol%
	30 minutes	96.35 vol%
	1 hour	93.75 vol%
	2 hours	88.54 vol%
	6 hours	67.19 vol%
	24 hours	43.27 vol%
	48 hours	42.71 vol%
	76 hours	42.71 vol%
	124 hours	42.71 vol%
	1 week	42.71 vol%
	3 weeks	42.71 vol%
	1 month	42.71 vol%

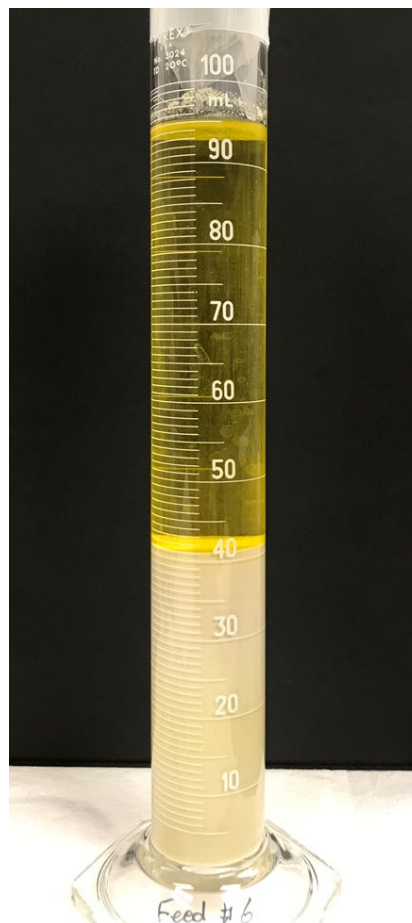




Table B.16. Data sheet for slurry melter feed #9a ( $3.98\text{V}_2\text{O}_5-0.25\text{SnO}_2$ )

Feed ID	LAW feed #9 $3.98\text{V}_2\text{O}_5 - 0.25\text{SnO}_2$	
Na molarity	5.6 M	
Waste loading	19.12 wt%	
C/N ratio	0.75	
Water content	38.92 wt%	
Total solids	61.08 wt%	
Dissolved solids	29.58 wt%	
Undissolved solids	44.73 wt%	
Density	1680.02 g/L	
pH	9.21	
Shear strength	24 hours	22.15 Pa
	48 hours	38.47 Pa
	72 hours	19.82 Pa
Viscosity	20 °C	29.06 mPa·s
	40 °C	18.17 mPa·s
Settling test	5 minutes	98.98 vol%
	15 minutes	98.98 vol%
	30 minutes	97.96 vol%
	1 hour	95.92 vol%
	2 hours	89.29 vol%
	6 hours	72.45 vol%
	24 hours	71.43 vol%
	48 hours	71.43 vol%
	76 hours	71.43 vol%
	124 hours	71.43 vol%
	1 week	71.43 vol%
	3 weeks	71.43 vol%
	1 month	71.43 vol%

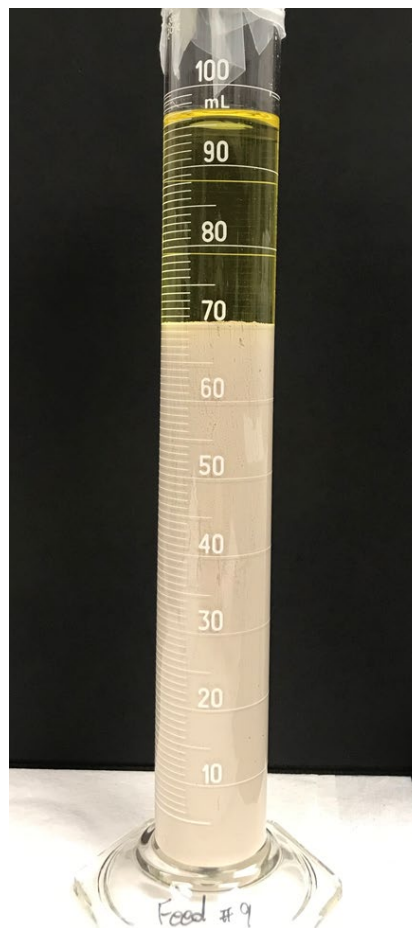


Table B.17. Data sheet for slurry feed #1b (0.00V<sub>2</sub>O<sub>5</sub>–4.50SnO<sub>2</sub>)

Feed ID			LAW slurry feed #1
Na molarity			5.6 M
Waste loading			28.24 wt%
C/N ratio			0.75
Water content			46.29 wt%
Total solids			53.71 wt%
Dissolved solids			35.49 wt%
Undissolved solids			28.25 wt%
Density			1585.65 g/L
pH			13.19
Shear strength	24 hours		16.32 Pa
	48 hours		32.65 Pa
	72 hours		N/A
Viscosity	20 °C		12.17 mPa·s
	40 °C		7.429 mPa·s
Settling test	5 minutes		100.00 vol%
	15 minutes		98.79 vol%
	30 minutes		97.98 vol%
	1 hour		96.46 vol%
	2 hours		93.64 vol%
	6 hours		82.32 vol%
	24 hours		45.45 vol%
	48 hours		43.94 vol%
	72 hours		43.94 vol%
	96 hours		43.94 vol%
	1 week		43.94 vol%
	3 weeks		43.94 vol%
	1 month		43.94 vol%

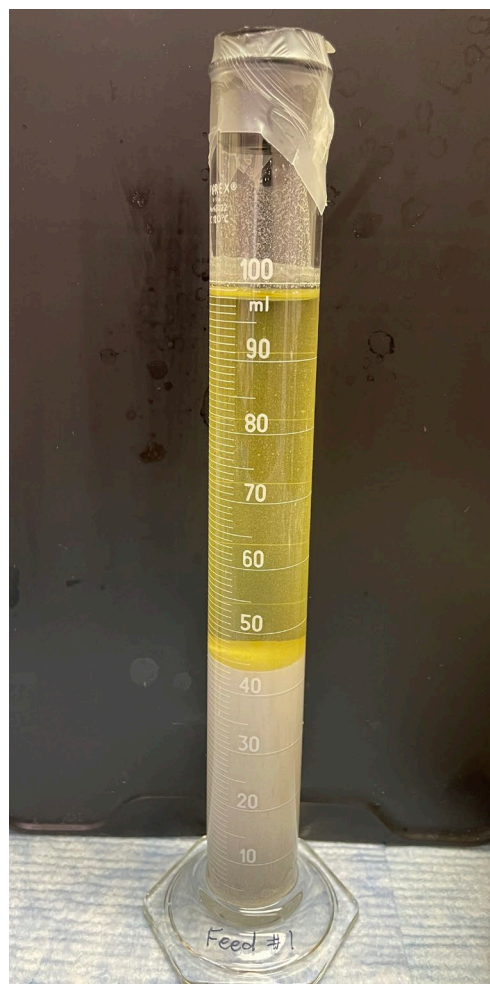


Table B.18. Data sheet for slurry feed #1-1 (0.00V<sub>2</sub>O<sub>5</sub>–4.50SnO<sub>2</sub>)

Feed ID		LAW slurry feed #1-1
Na molarity		5.6 M
Waste loading		28.24 wt%
C/N ratio		0.75
Water content		45.51 wt%
Total solids		54.49 wt%
Dissolved solids		36.02 wt%
Undissolved solids		28.88 wt%
Density		1574.24 g/L
pH		13.02
Shear strength	24 hours	45.53 Pa
	48 hours	108.8 Pa
	72 hours	N/A
Viscosity	20 °C	12.74 mPa·s
	40 °C	6.606 mPa·s
Settling test	5 minutes	98.99 vol%
	15 minutes	97.99 vol%
	30 minutes	96.98 vol%
	1 hour	95.48 vol%
	2 hours	91.46 vol%
	6 hours	74.27 vol%
	24 hours	39.20 vol%
	48 hours	39.20 vol%
	72 hours	39.20 vol%
	96 hours	39.20 vol%
	1 week	39.22 vol%
	3 weeks	41.51 vol%
	1 month	42.52 vol%

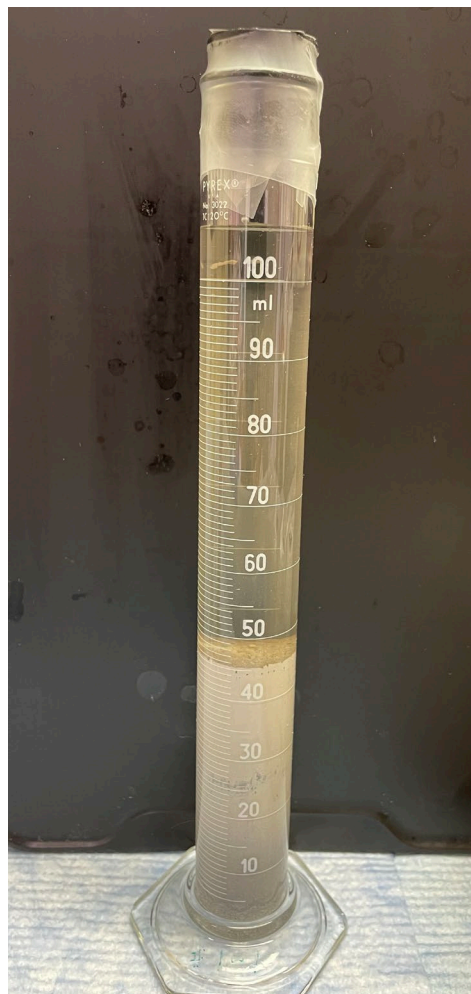


Table B.19. Data sheet for slurry feed #6b ( $3.51\text{V}_2\text{O}_5-2.42\text{SnO}_2$ )

Feed ID	LAW slurry feed #6	
Na molarity	5.6 M	
Waste loading	28.47 wt%	
C/N ratio	0.75	
Water content	50.07 wt%	
Total solids	49.93 wt%	
Dissolved solids	33.11 wt%	
Undissolved solids	25.14 wt%	
Density	1524.07 g/L	
pH	12.78	
Shear strength	24 hours	25.65 Pa
	48 hours	30.32 Pa
	72 hours	N/A
Viscosity	20 °C	12.18 mPa·s
	40 °C	5.983 mPa·s
Settling test	5 minutes	99.49 vol%
	15 minutes	97.97 vol%
	30 minutes	96.45 vol%
	1 hour	93.91 vol%
	2 hours	88.32 vol%
	6 hours	62.94 vol%
	24 hours	38.58 vol%
	48 hours	37.56 vol%
	72 hours	37.56 vol%
	96 hours	37.56 vol%
	1 week	37.56 vol%
	3 weeks	37.56 vol%
	1 month	37.56 vol%

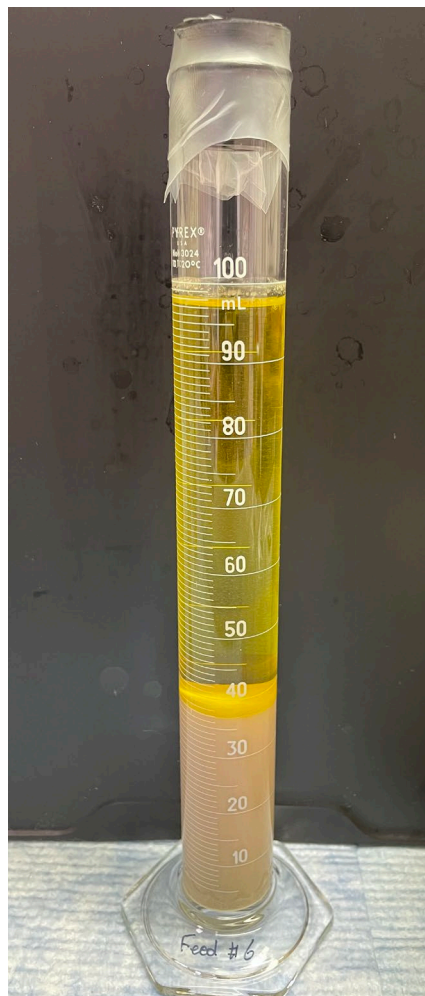
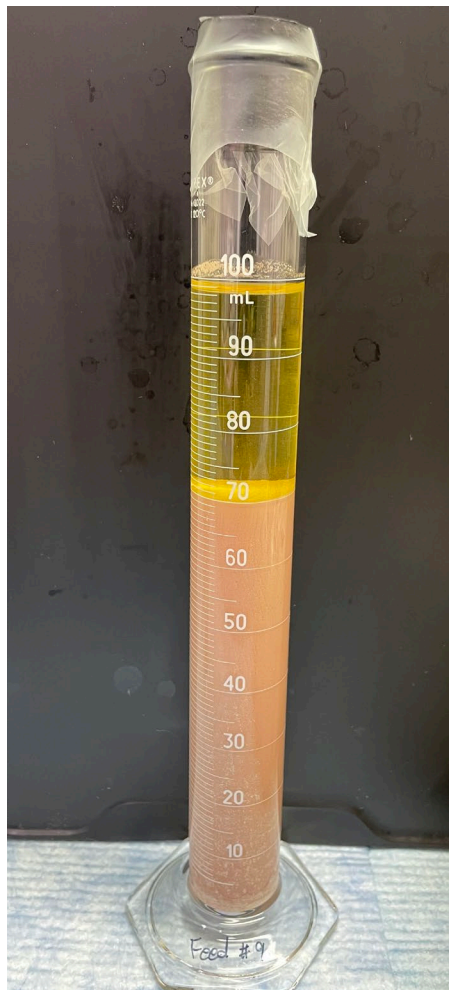


Table B.20. Data sheet for slurry feed #9b ( $3.98\text{V}_2\text{O}_5-0.25\text{SnO}_2$ )

Feed ID	LAW slurry feed #9	
Na molarity	5.6 M	
Waste loading	19.07 wt%	
C/N ratio	0.75	
Water content	38.36 wt%	
Total solids	61.64 wt%	
Dissolved solids	30.96 wt%	
Undissolved solids	44.44 wt%	
Density	1685.33 g/L	
pH	9.19	
Shear strength	24 hours	22.54 Pa
	48 hours	31.48 Pa
	72 hours	N/A
Viscosity	20 °C	33.23 mPa·s
	40 °C	20.07 mPa·s
Settling test	5 minutes	100.00 vol%
	15 minutes	99.30 vol%
	30 minutes	98.59 vol%
	1 hour	97.49 vol%
	2 hours	94.97 vol%
	6 hours	84.52 vol%
	24 hours	70.35 vol%
	48 hours	70.35 vol%
	72 hours	70.35 vol%
	96 hours	70.35 vol%
	1 week	70.35 vol%
	3 weeks	70.35 vol%
	1 month	70.35 vol%



## Appendix C – Original Measured Data from Jenike and Johanson

The figures in this section display experimental results of flow properties for individual glass-forming chemicals and their mixtures measured by Jenike and Johanson.

### Appendix C Table of Contents

• C.1	Cr <sub>2</sub> O <sub>3</sub> Properties.....	C.2
• C.2	V <sub>2</sub> O <sub>5</sub> Properties .....	C.13
• C.3	SnO Properties .....	C.24
• C.4	SnO <sub>2</sub> Properties .....	C.35
• C.5	LAW Batch #1a Properties.....	C.46
• C.6	LAW Batch #6a Properties.....	C.58
• C.7	LAW Batch #9a Properties.....	C.69
• C.8	FeCr <sub>2</sub> O <sub>4</sub> Properties.....	C.80
• C.9	ZrSiO <sub>4</sub> Properties .....	C.91
• C.5	LAW Batch #1b Properties.....	C.102
• C.5	LAW Batch #1-1 Properties.....	C.114
• C.6	LAW Batch #6b Properties.....	C.126
• C.7	LAW Batch #9b Properties.....	C.138

## C.1 Cr<sub>2</sub>O<sub>3</sub> properties

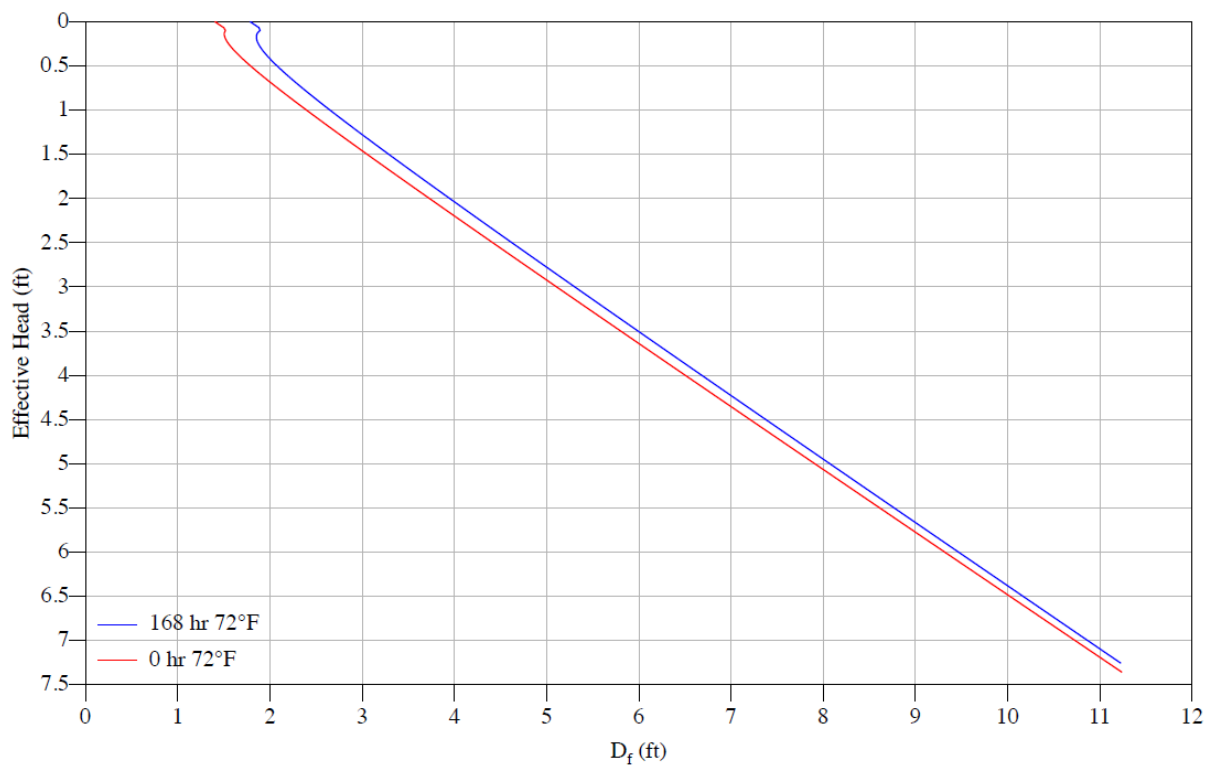


Figure C.1. Cr<sub>2</sub>O<sub>3</sub>: Critical rathole dimensions



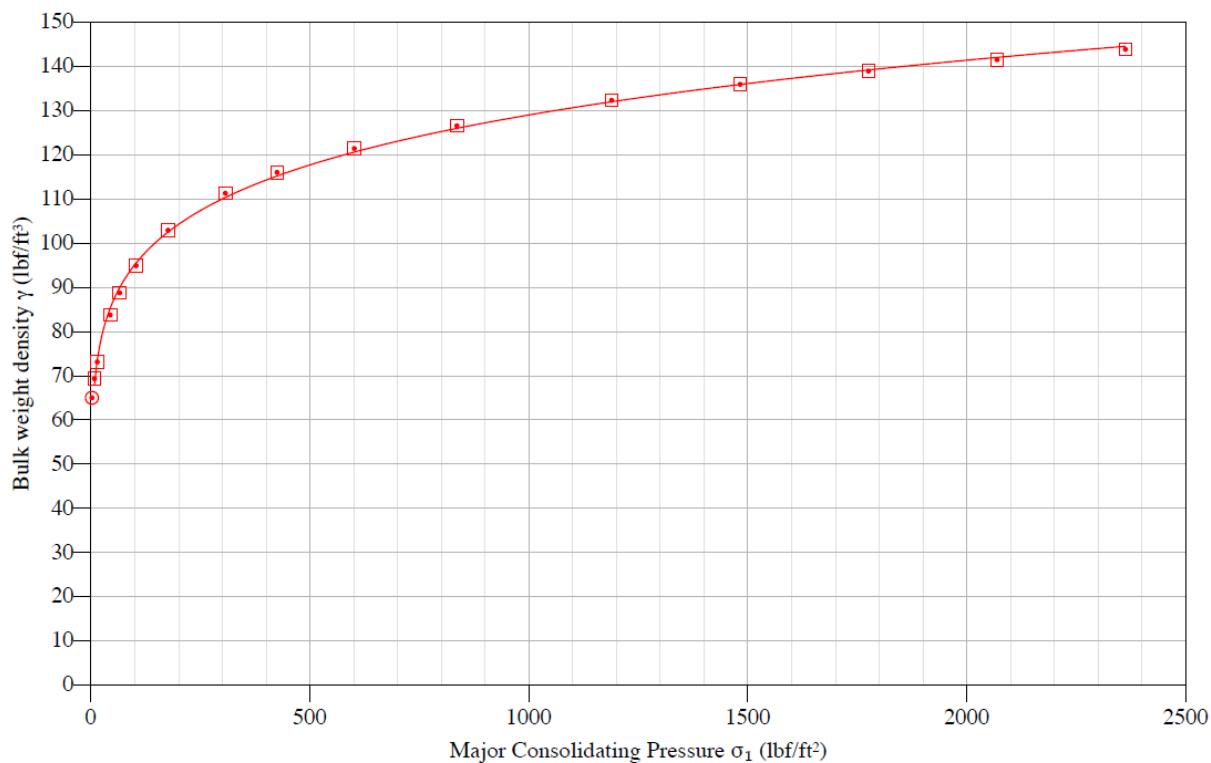


Figure C.2. Cr<sub>2</sub>O<sub>3</sub>: Compressibility curve

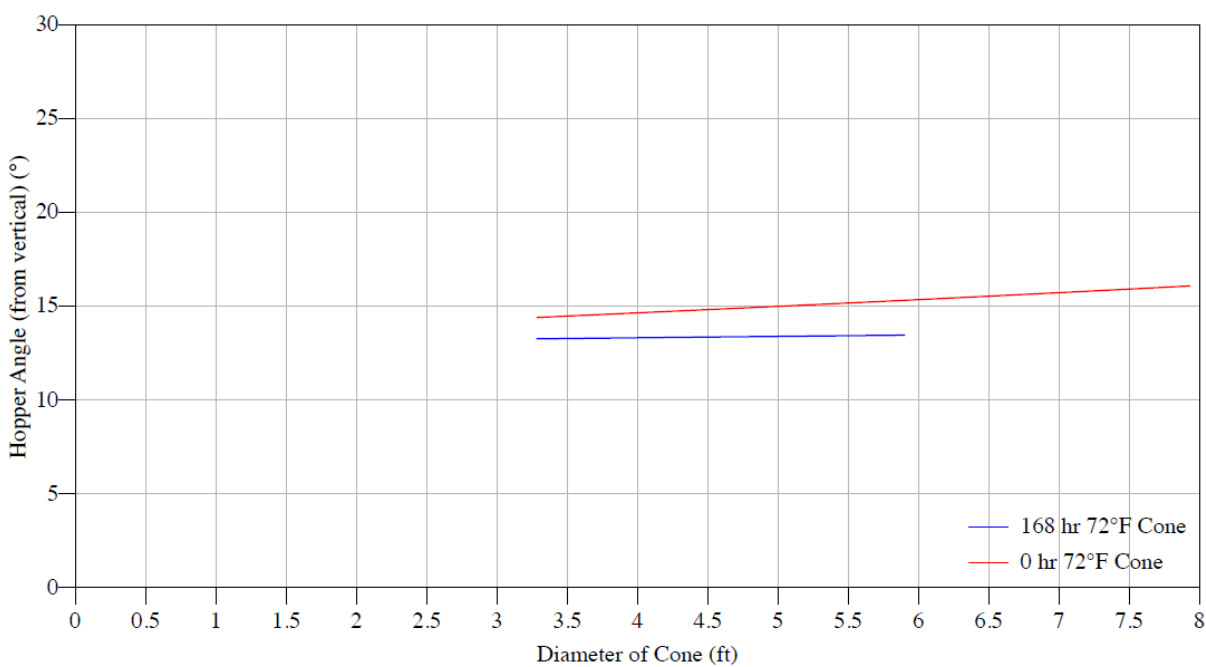


Figure C.3. Cr<sub>2</sub>O<sub>3</sub>: Conical hopper angles with 304 SS sheet

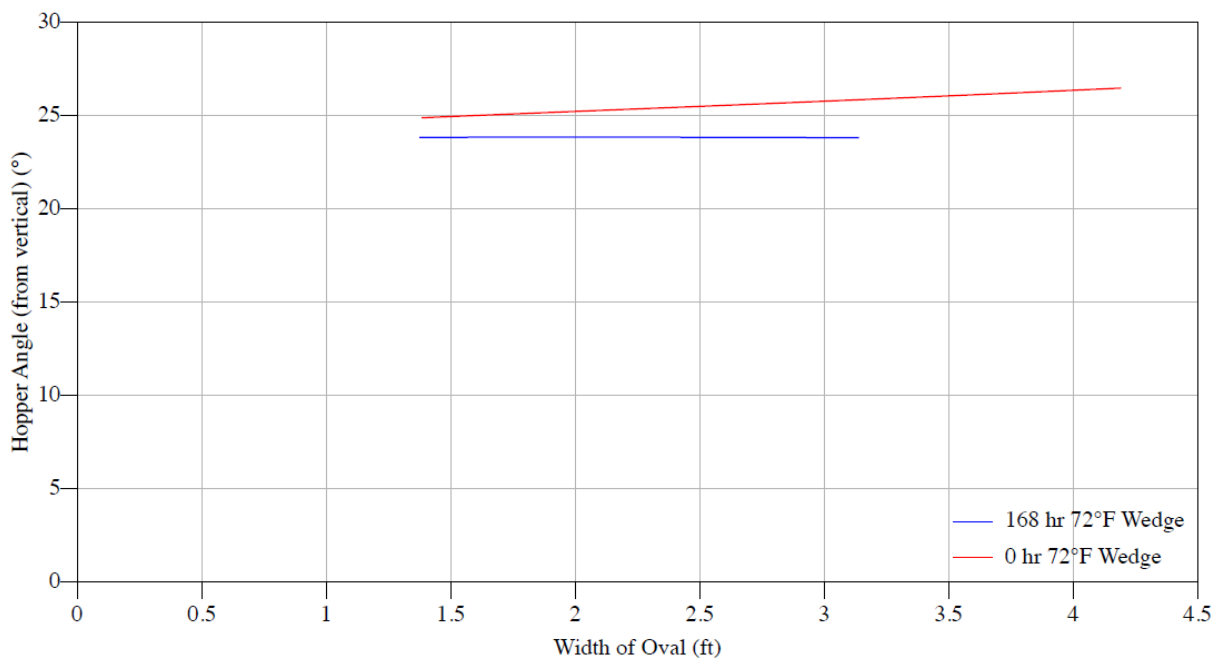


Figure C.4.  $\text{Cr}_2\text{O}_3$ : Wedge hopper angles with 304 SS sheet

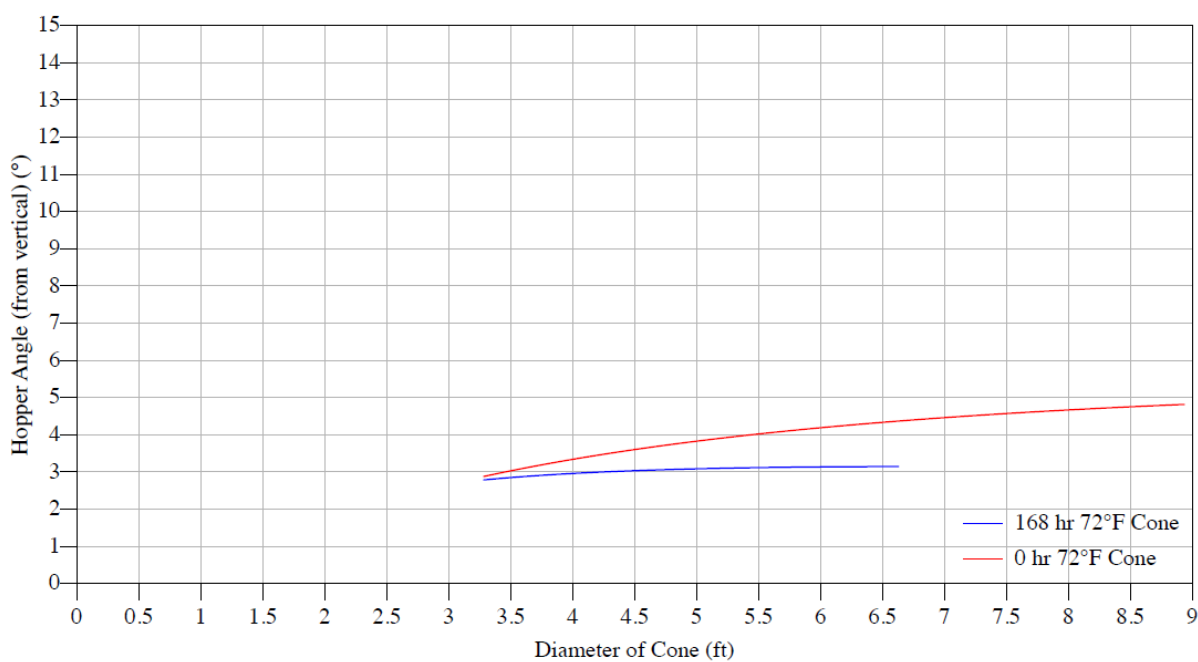


Figure C.5.  $\text{Cr}_2\text{O}_3$ : Conical hopper angles with mild CS HR plate

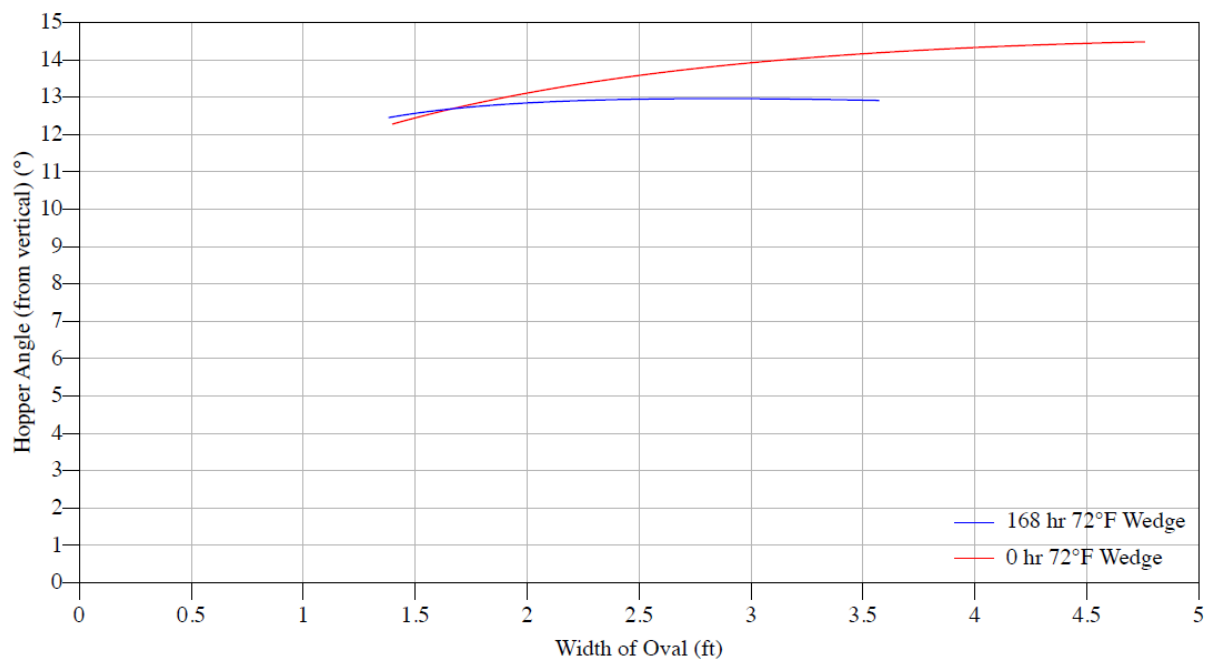


Figure C.6.  $\text{Cr}_2\text{O}_3$  Wedge hopper angles with mild CS HR plate

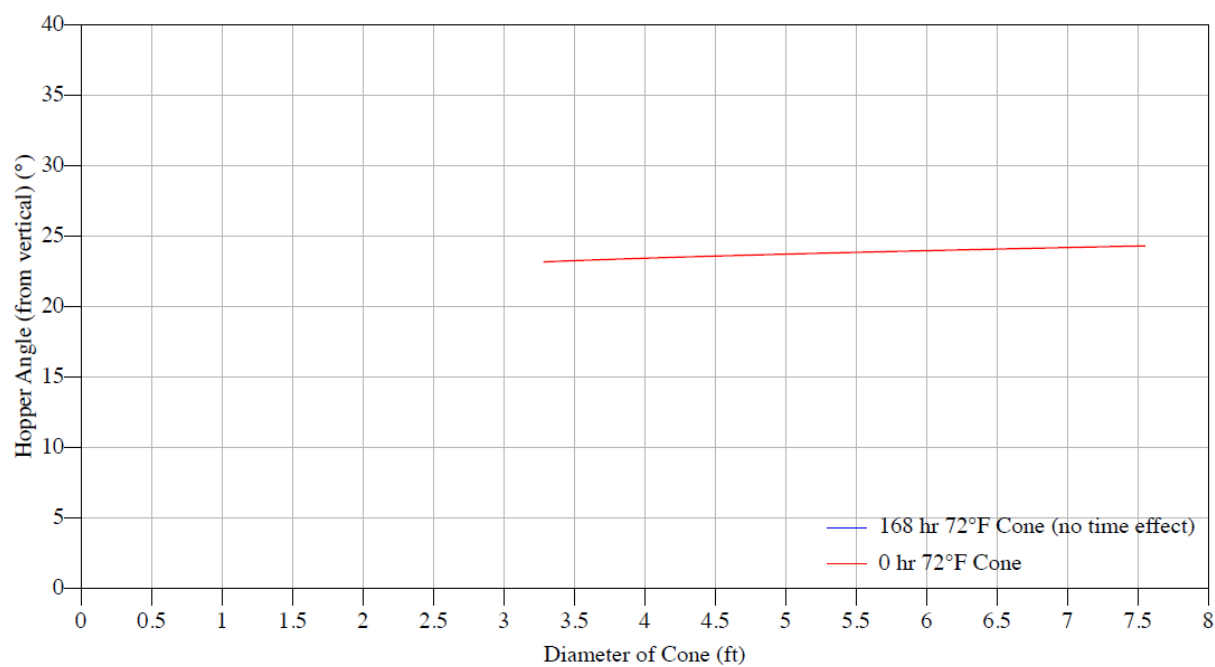


Figure C.7.  $\text{Cr}_2\text{O}_3$ : Conical hopper angles with TIVAR 88

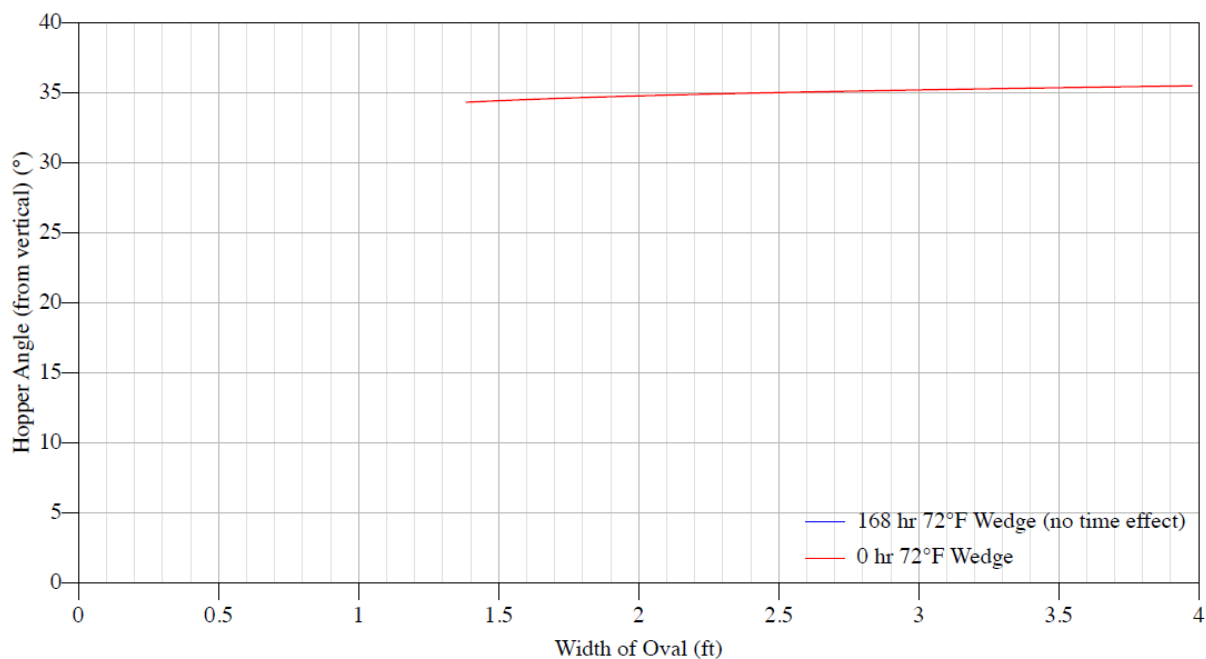


Figure C.8.  $\text{Cr}_2\text{O}_3$ : Wedge hopper angles with TIVAR 88

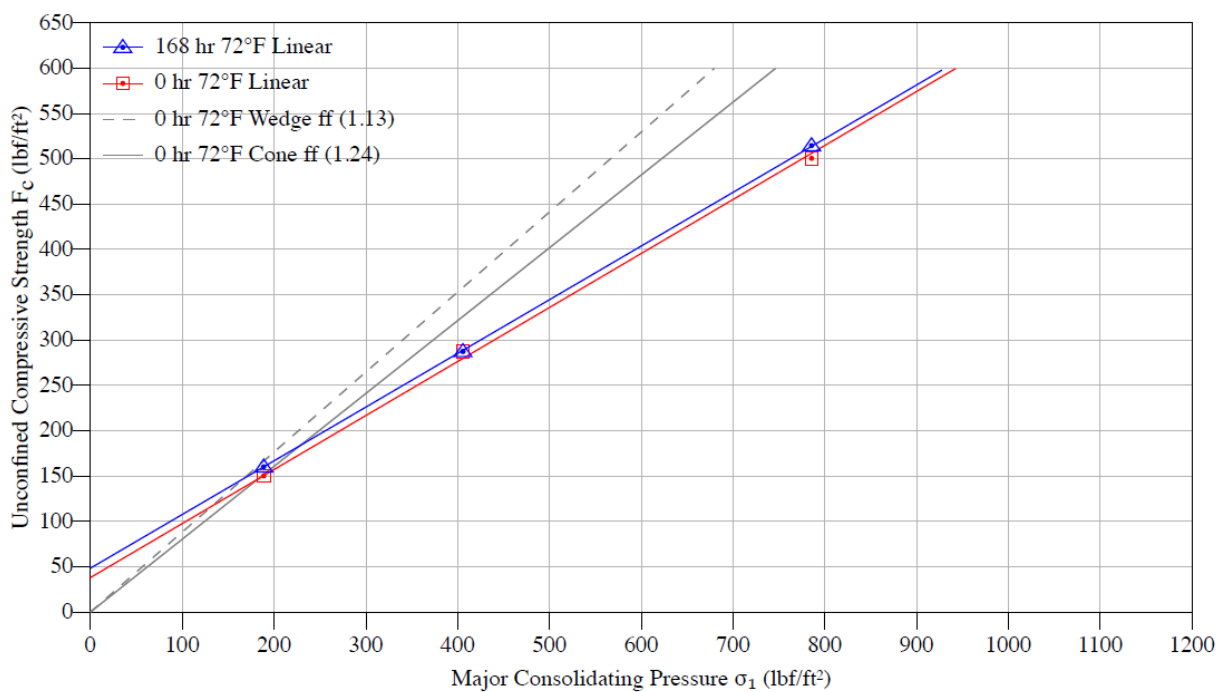


Figure C.9.  $\text{Cr}_2\text{O}_3$ : Flow function

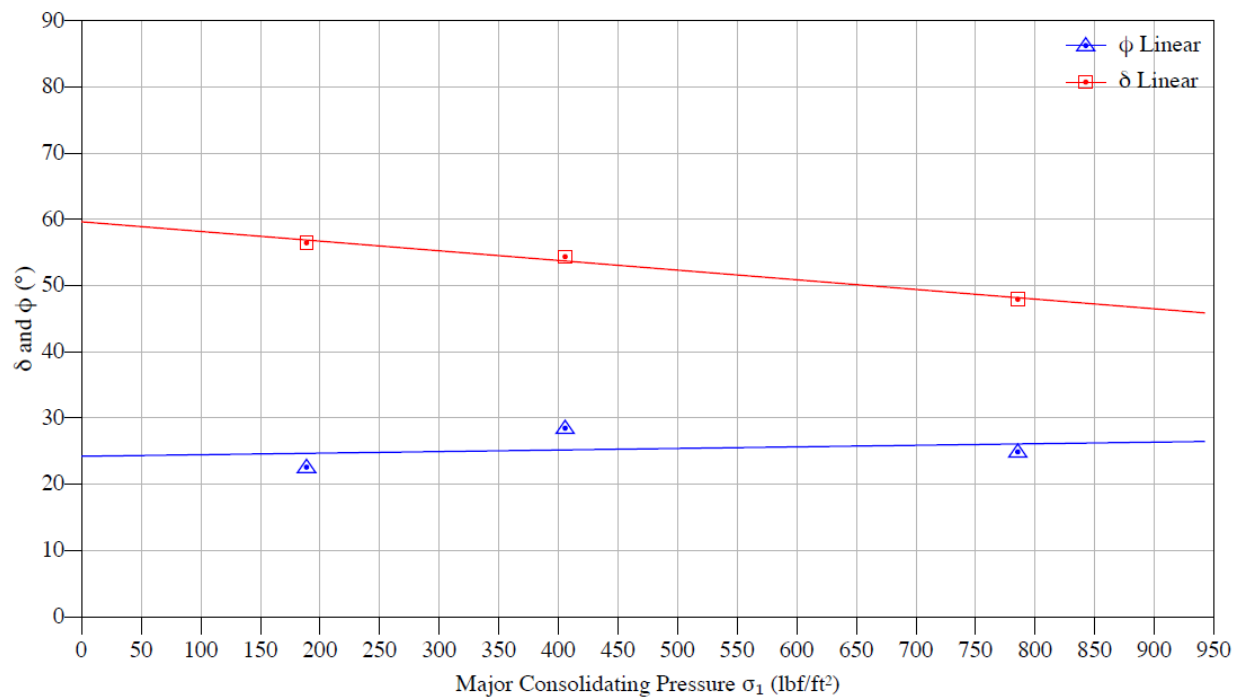


Figure C.10.  $\text{Cr}_2\text{O}_3$ : Effective angle of friction ( $\delta$ ) and kinematic angle of internal friction ( $\phi$ )

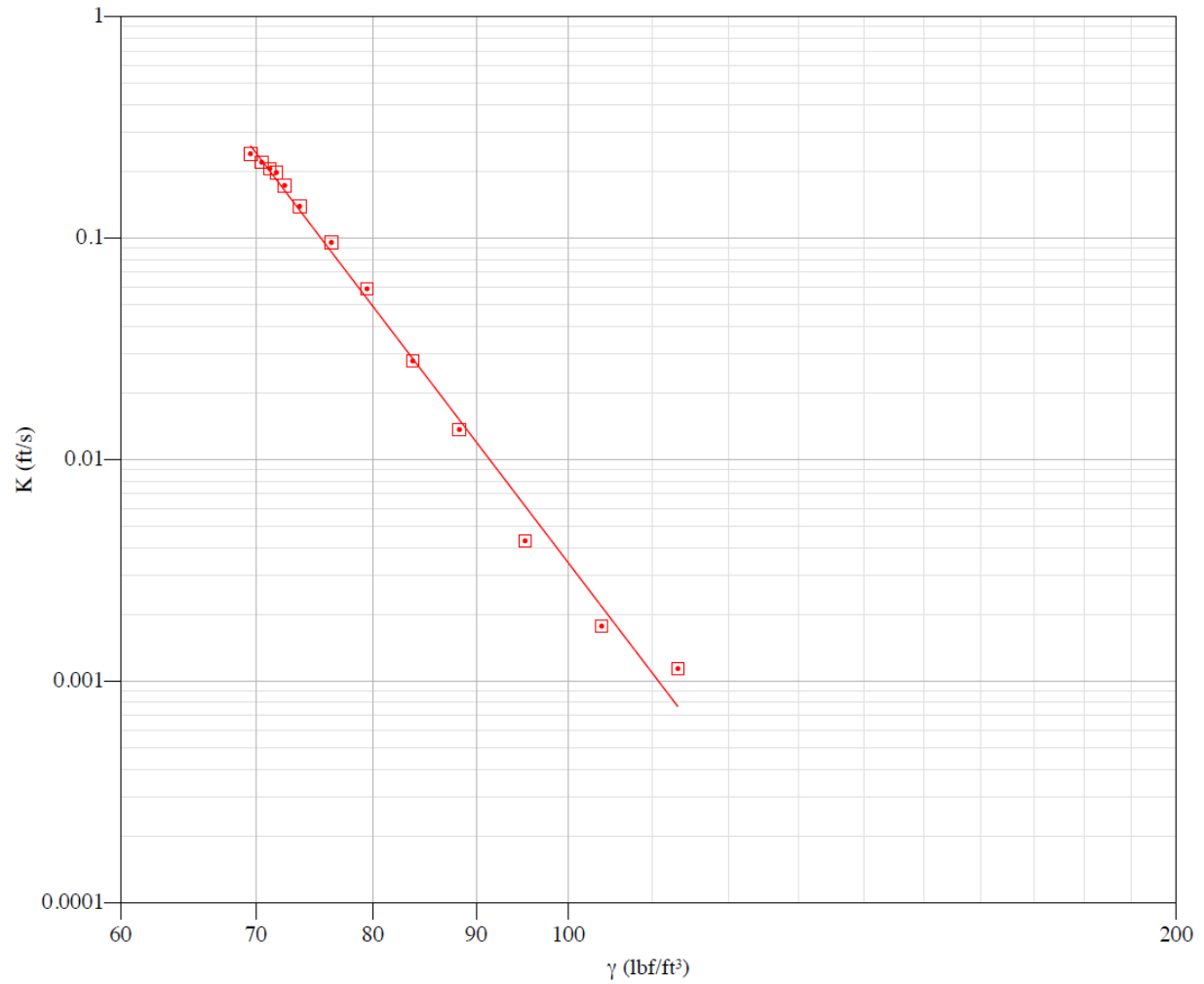


Figure C.11.  $\text{Cr}_2\text{O}_3$ : Permeability curve

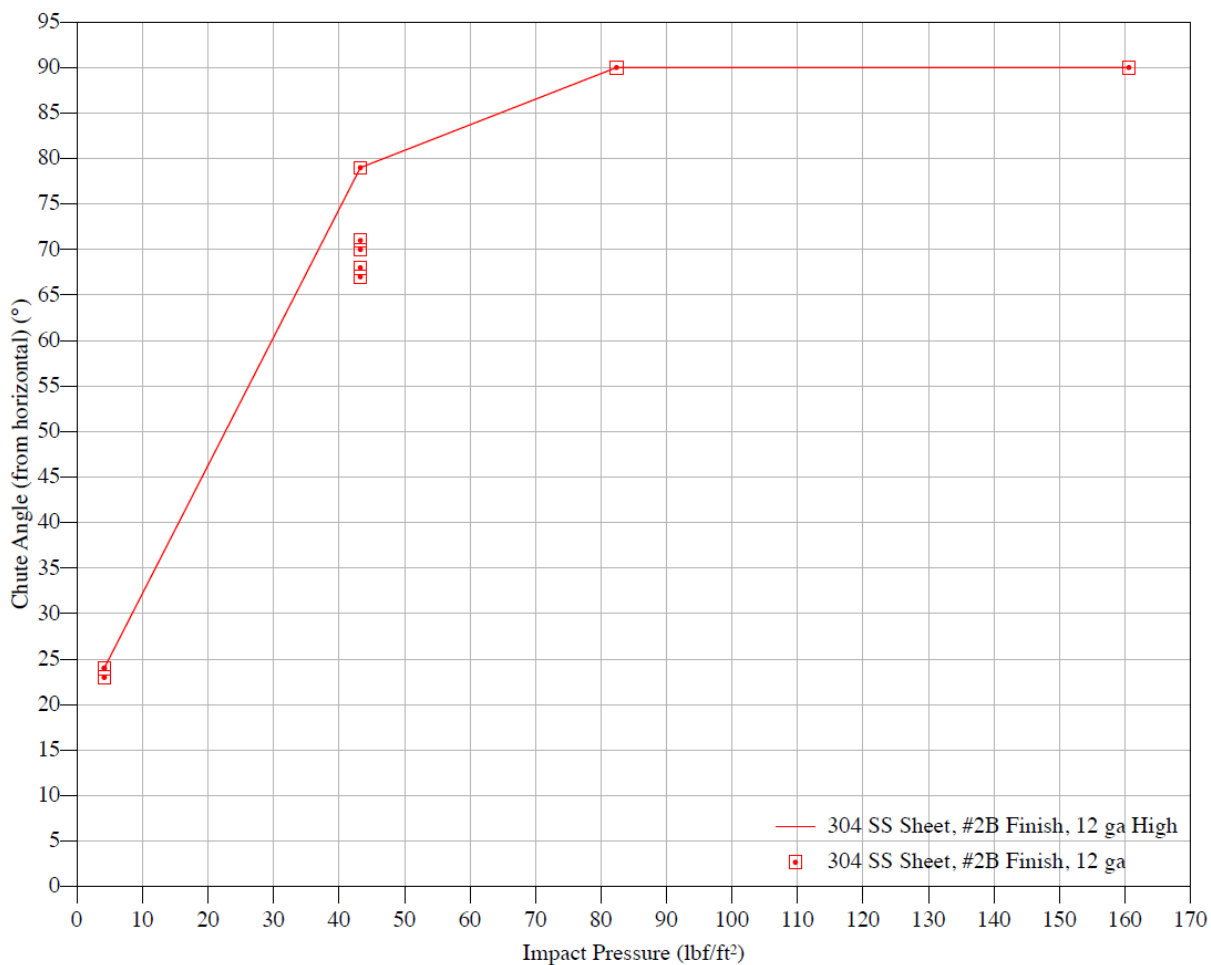


Figure C.12.  $\text{Cr}_2\text{O}_3$ : Chute curve with 304 SS sheet



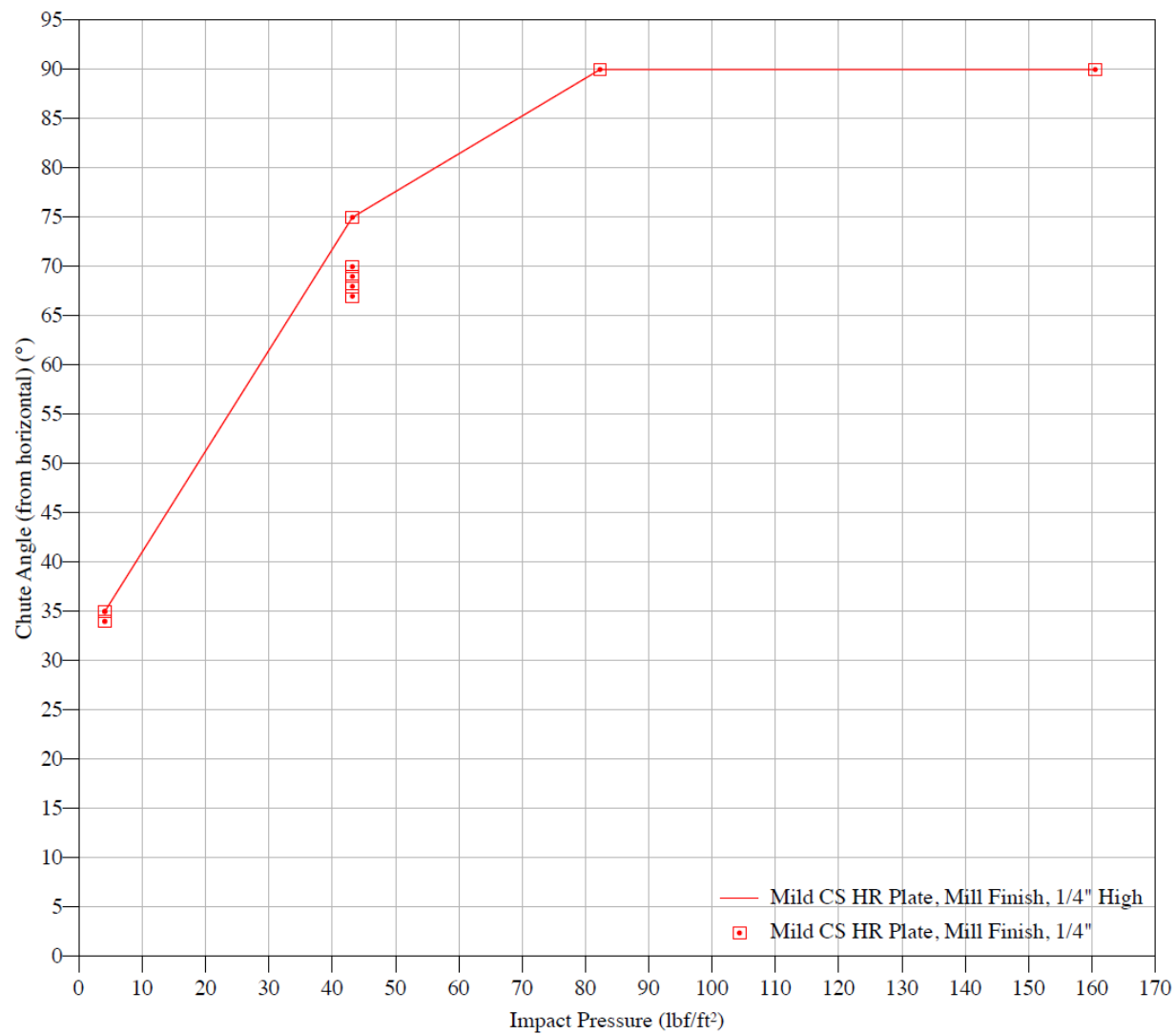


Figure C.13.  $\text{Cr}_2\text{O}_3$ : Chute curve with mild CS HR plate

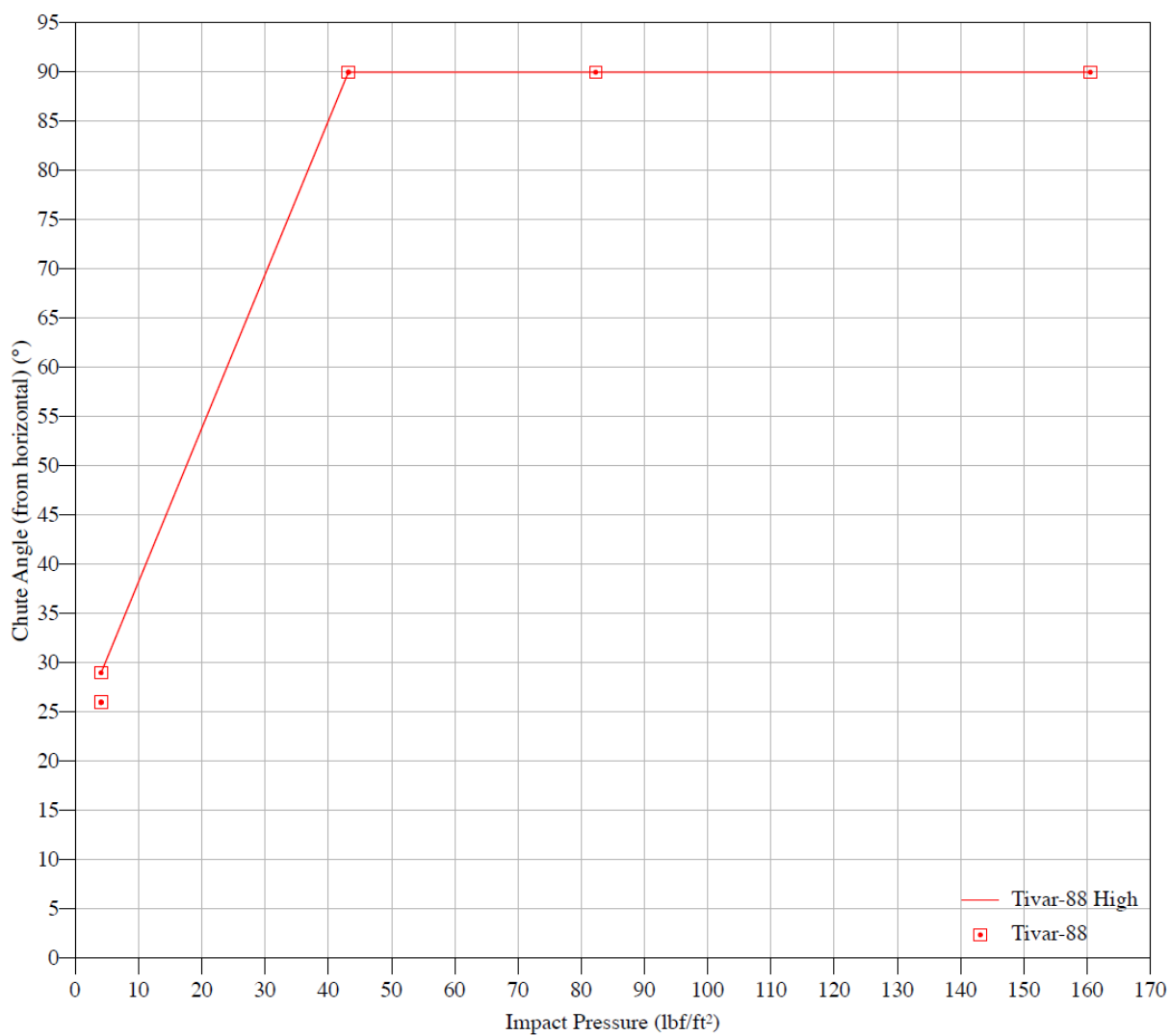


Figure C.14.  $\text{Cr}_2\text{O}_3$ : Chute curve with TIVAR 88

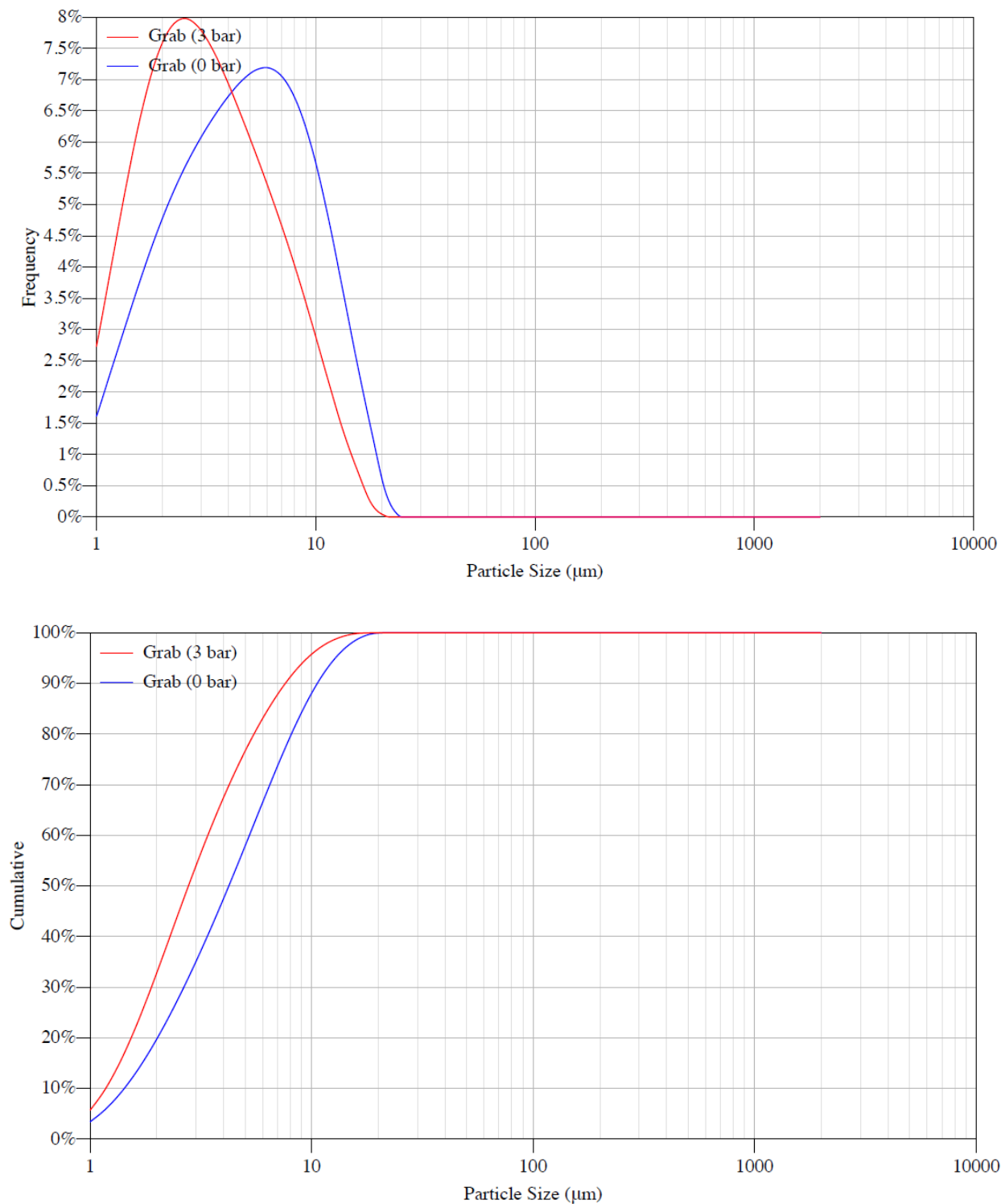


Figure C.15.  $\text{Cr}_2\text{O}_3$ : Particle size distribution by volume and pressure

## C.2 V<sub>2</sub>O<sub>5</sub> properties

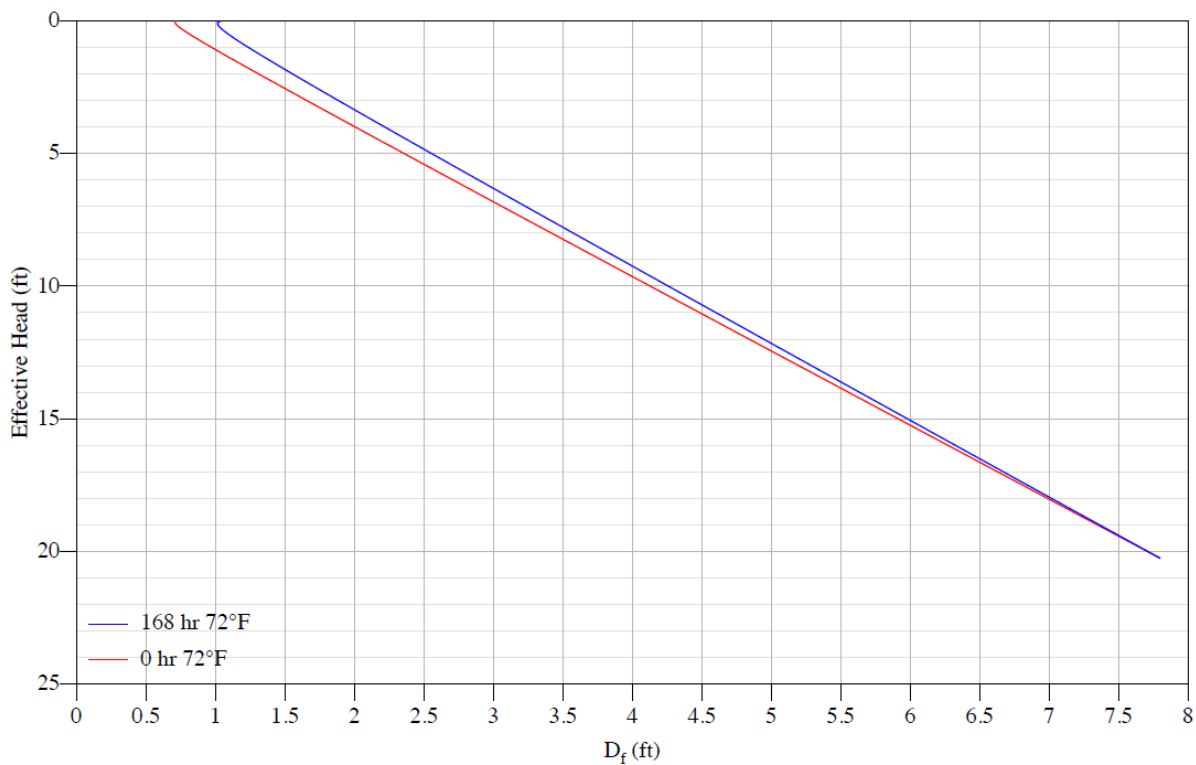


Figure C.16. V<sub>2</sub>O<sub>5</sub>: Critical rathole dimensions

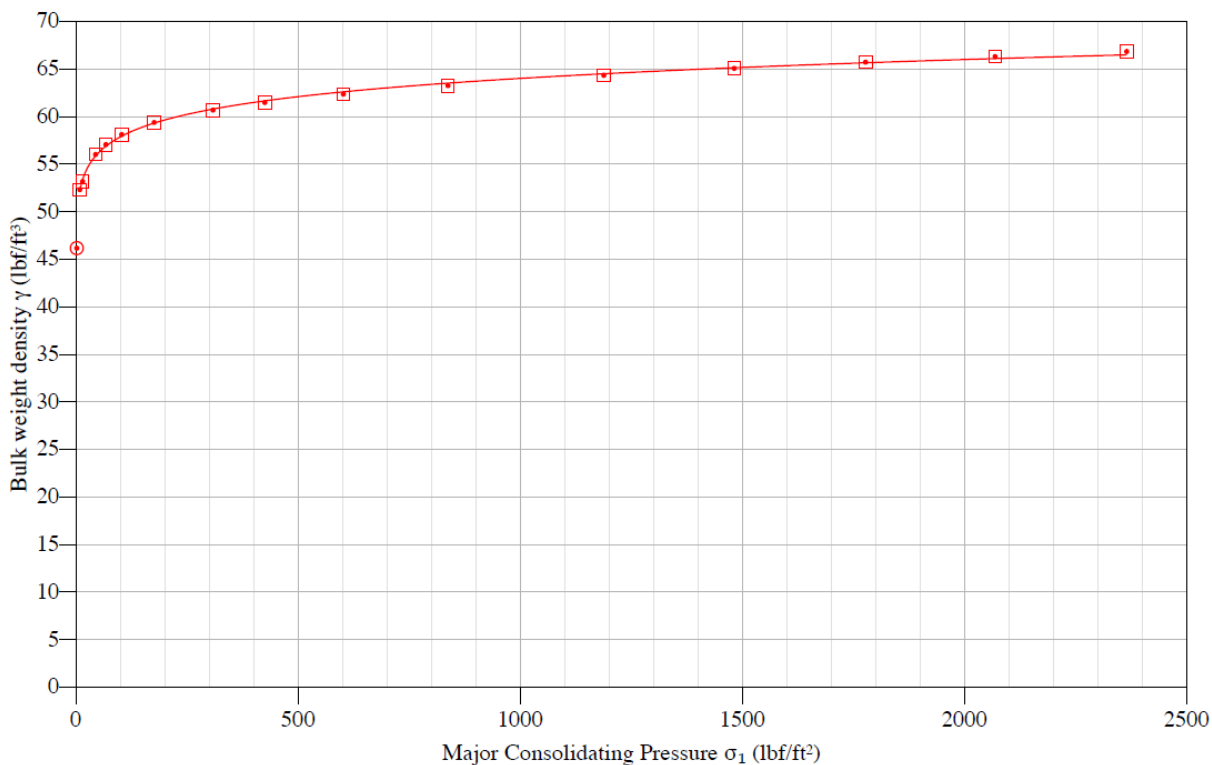


Figure C.17. V<sub>2</sub>O<sub>5</sub>: Compressibility curve

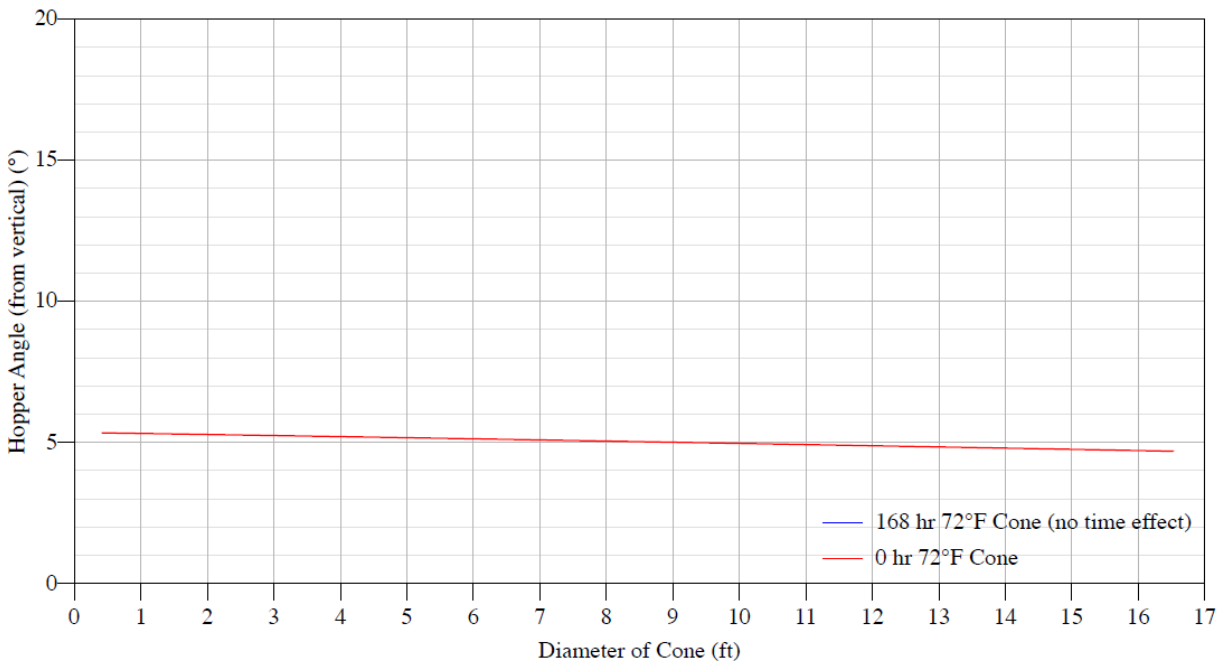


Figure C.18. V<sub>2</sub>O<sub>5</sub>: Conical hopper angles with 304 SS sheet

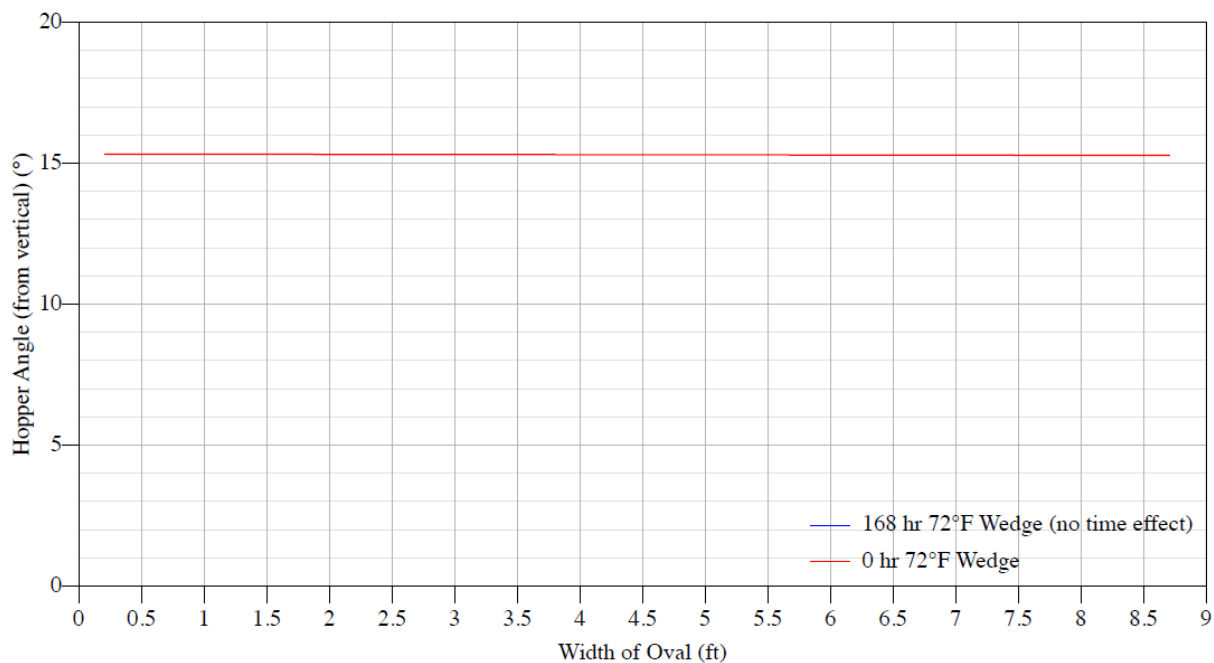


Figure C.19. V<sub>2</sub>O<sub>5</sub>: Wedge hopper angles with 304 SS sheet

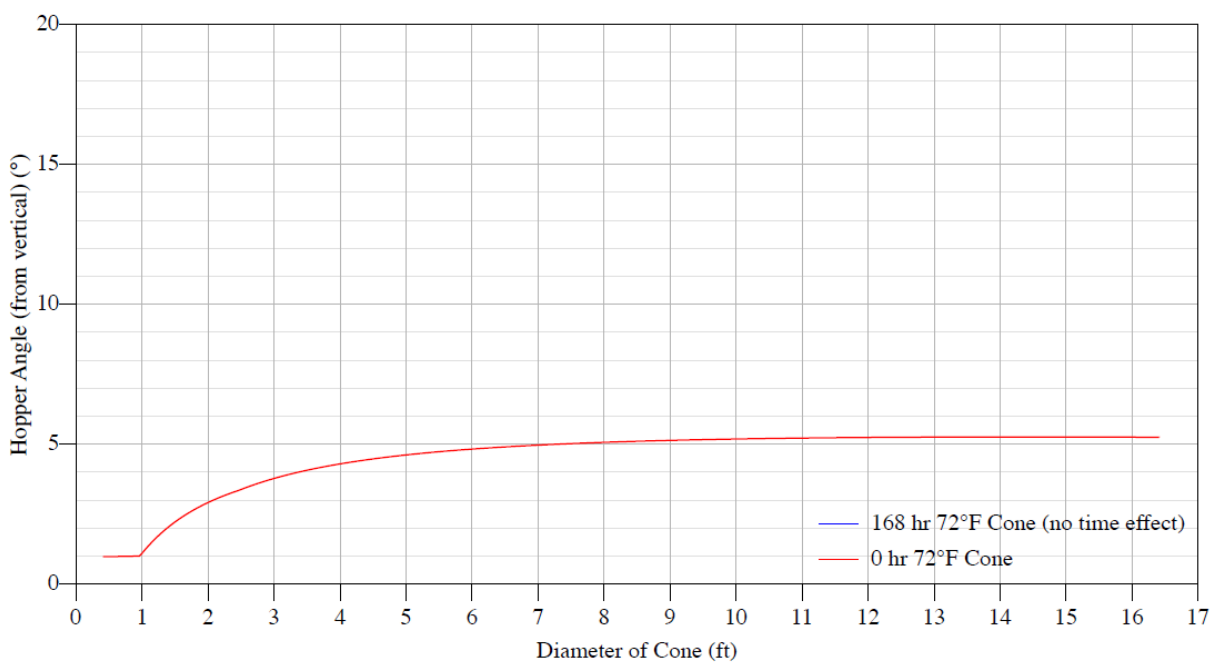


Figure C.20. V<sub>2</sub>O<sub>5</sub>: Conical hopper angles with mild CS HR plate

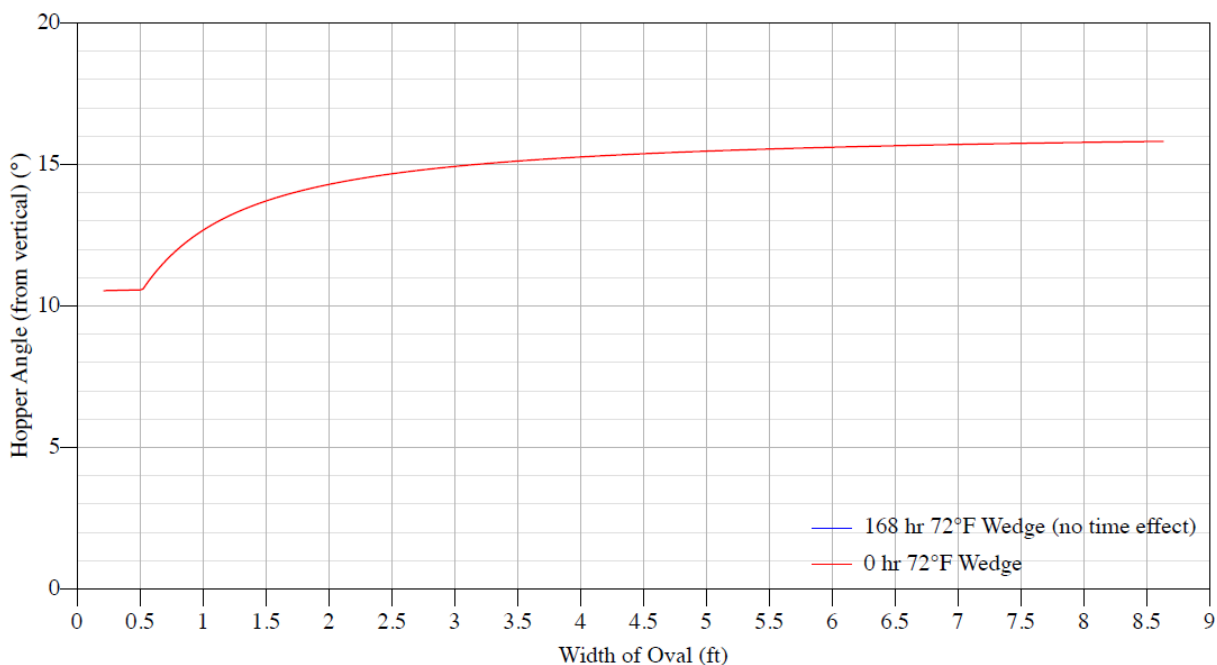


Figure C.21. V<sub>2</sub>O<sub>5</sub>: Wedge hopper angles with mild SC HR plate

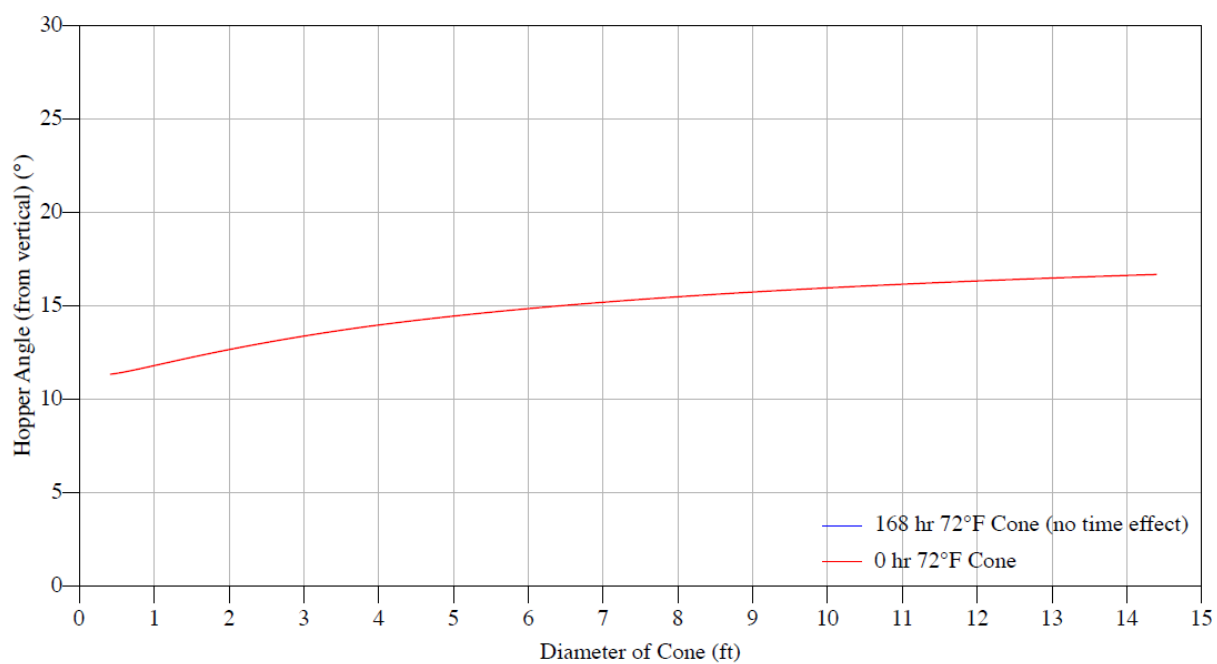


Figure C.22. V<sub>2</sub>O<sub>5</sub>: Conical hopper angles with TIVAR 88



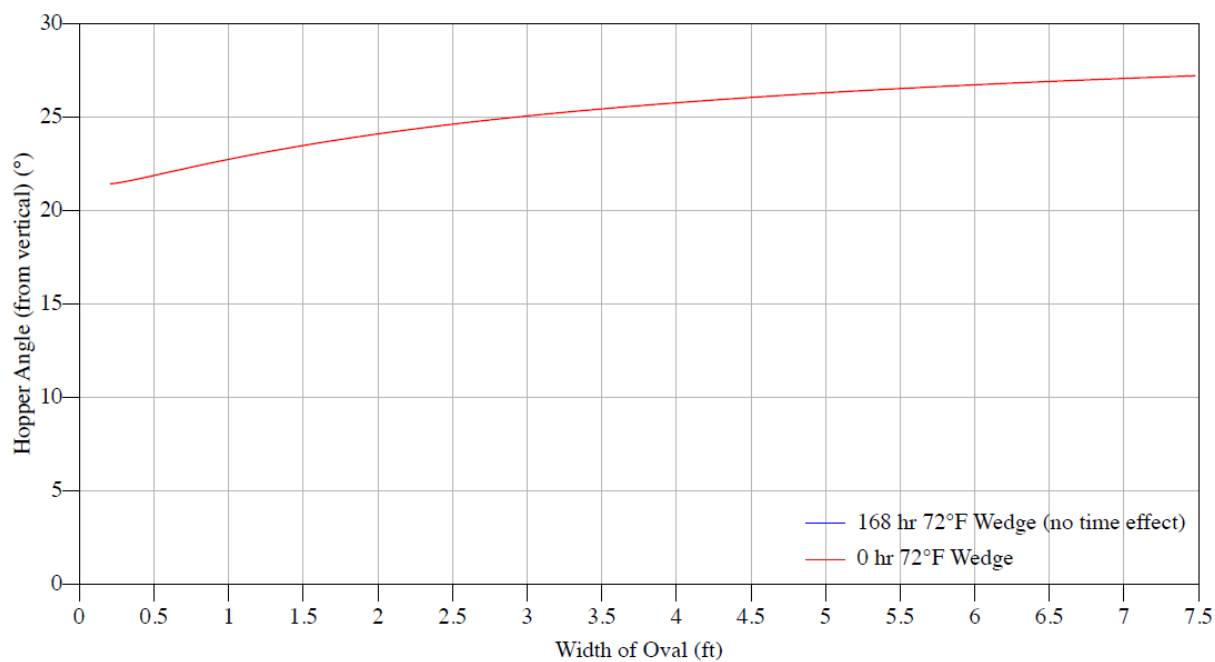


Figure C.23. V<sub>2</sub>O<sub>5</sub>: Wedge hopper angles with TIVAR 88

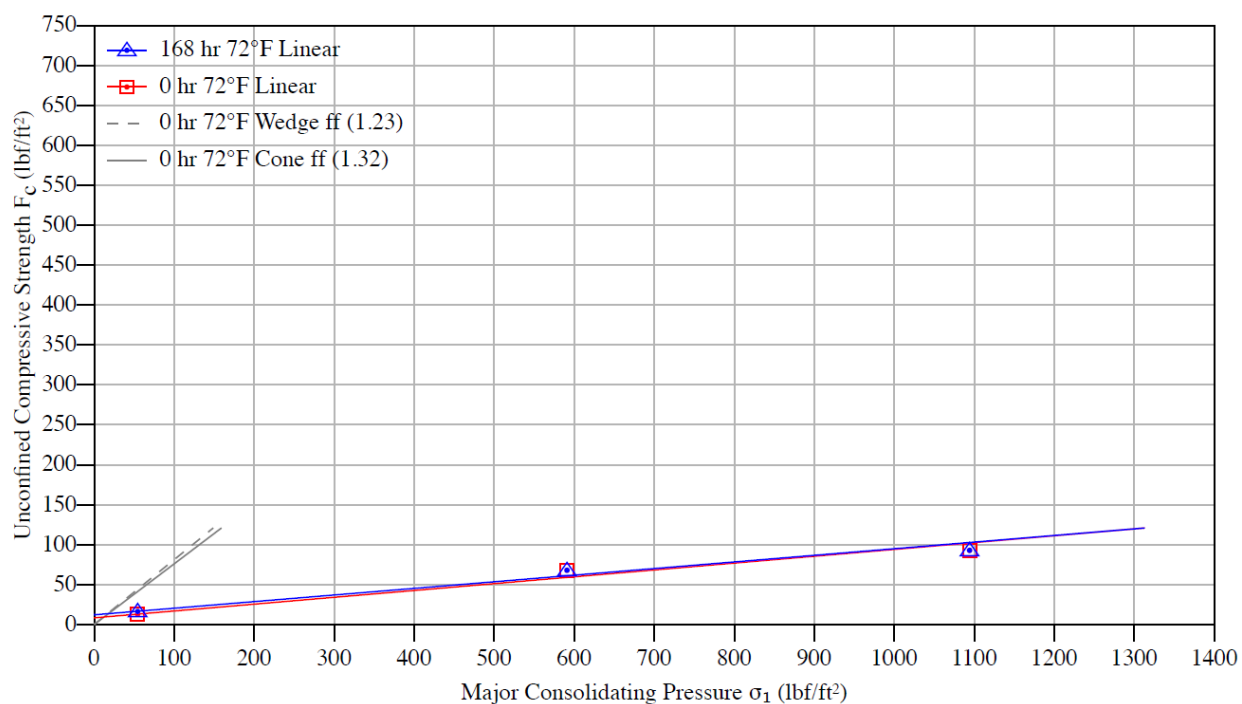


Figure C.24. V<sub>2</sub>O<sub>5</sub>: Flow function

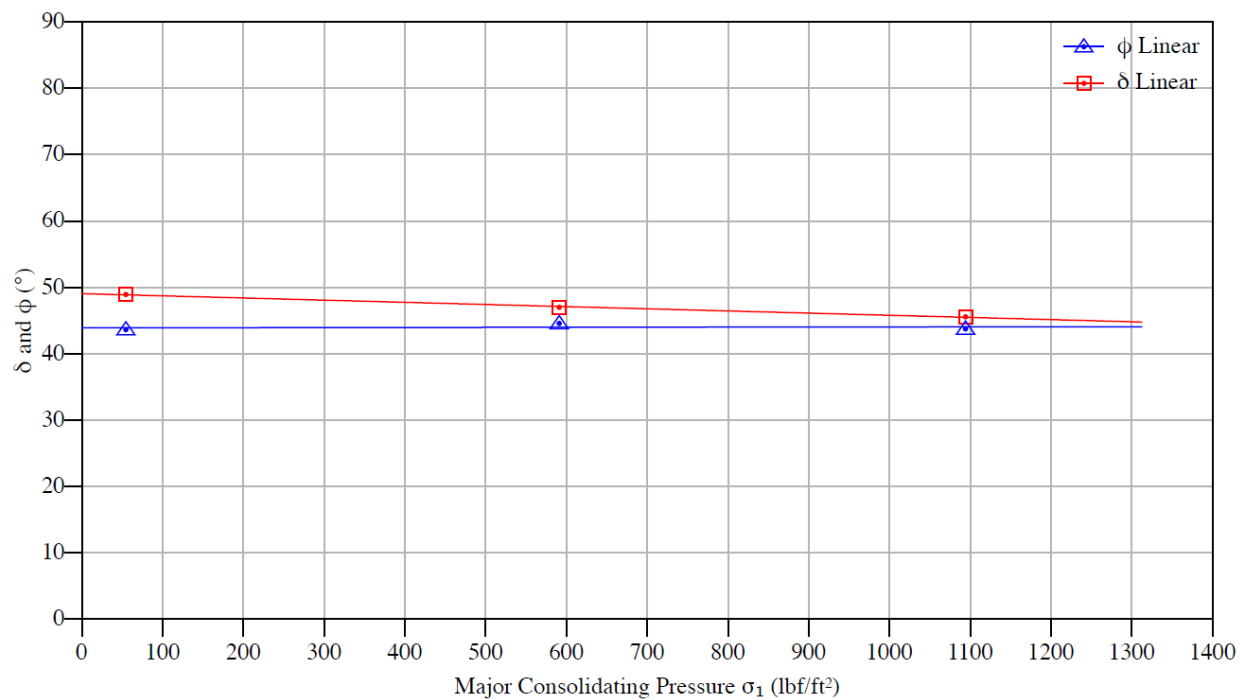


Figure C.25. V<sub>2</sub>O<sub>5</sub>: Effective angle of friction ( $\delta$ ) and kinematic angle of internal friction ( $\phi$ )

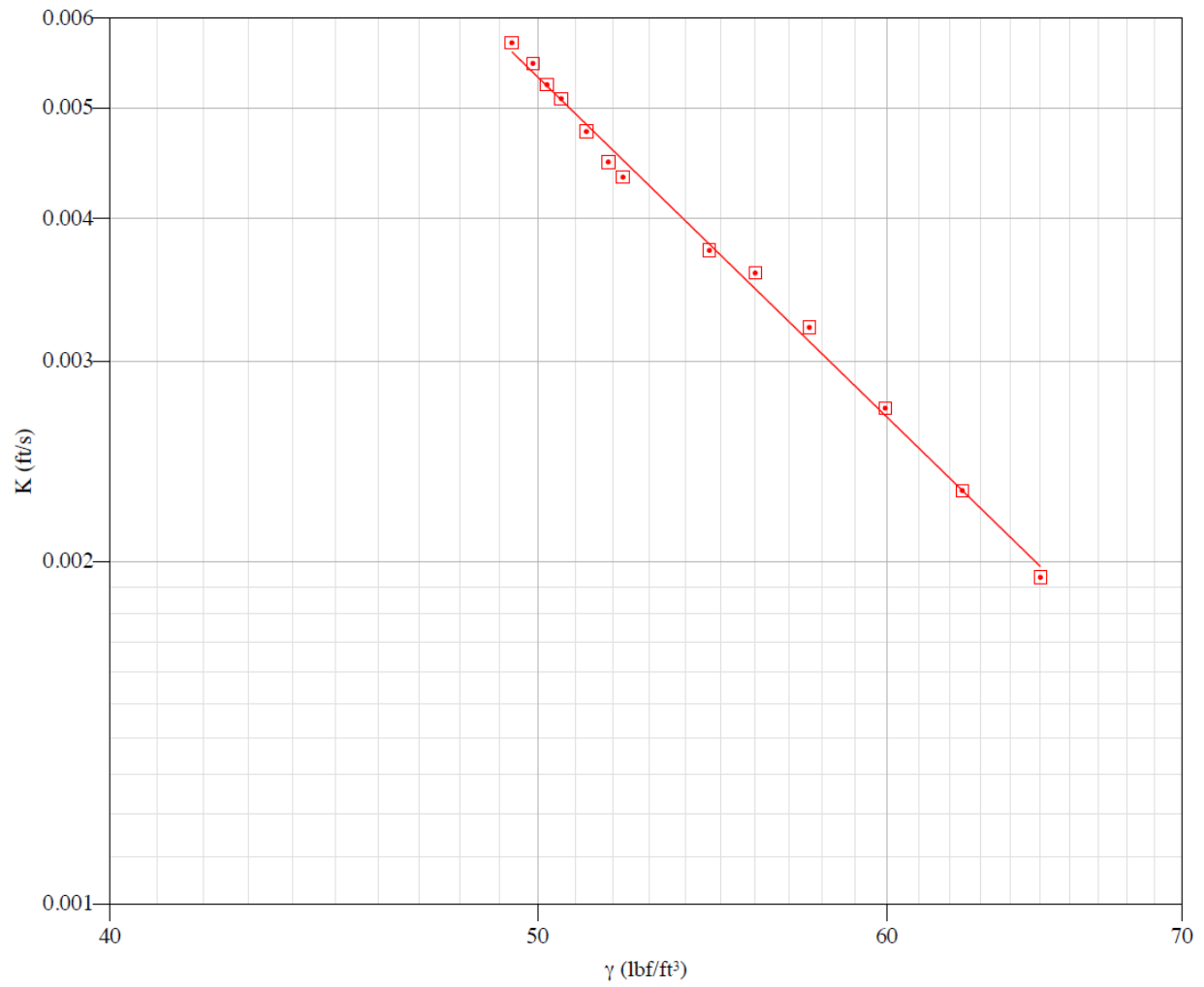


Figure C.26. V<sub>2</sub>O<sub>5</sub>: Permeability curve

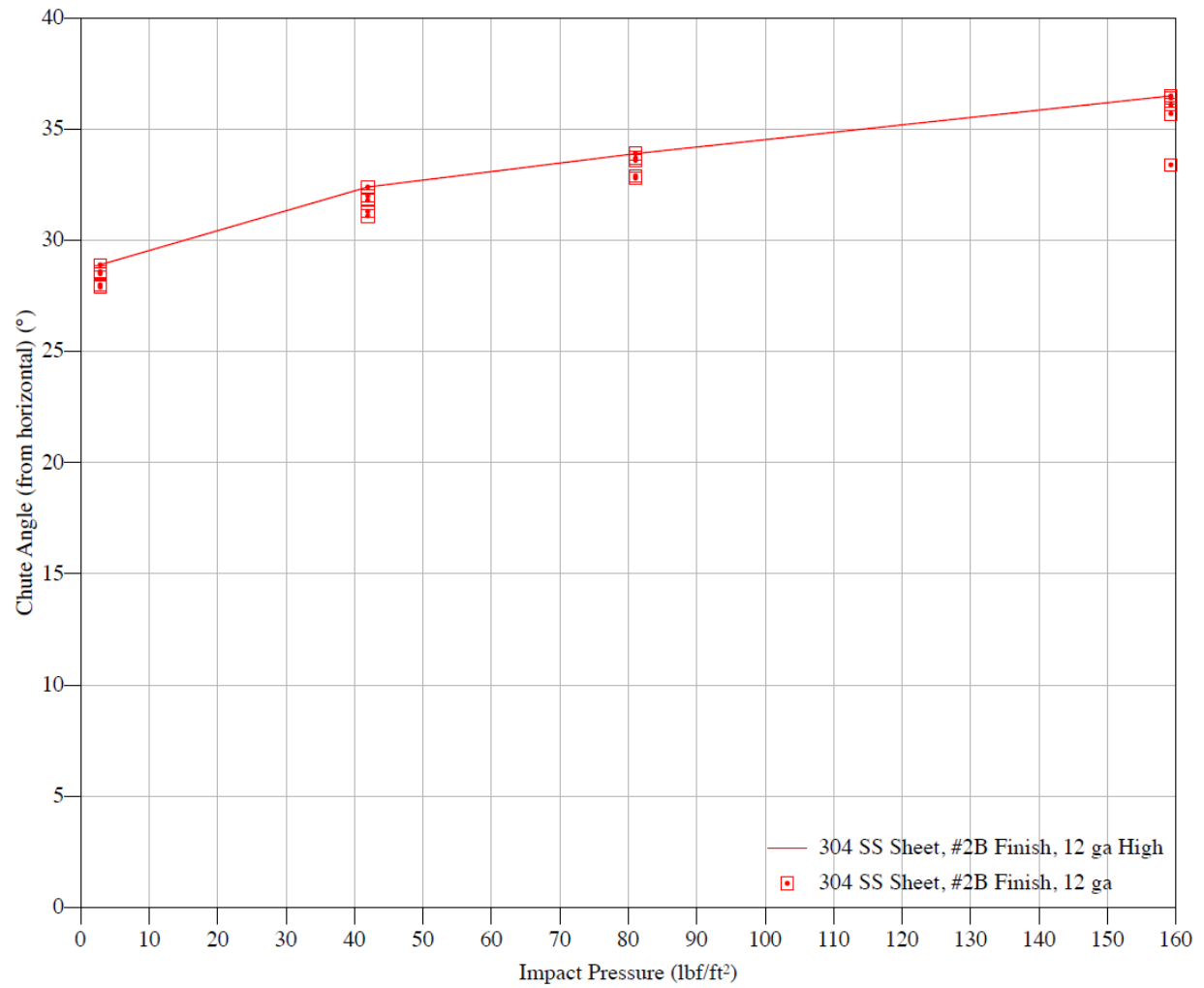


Figure C.27.  $V_2O_5$ : Chute curve with 304 SS sheet

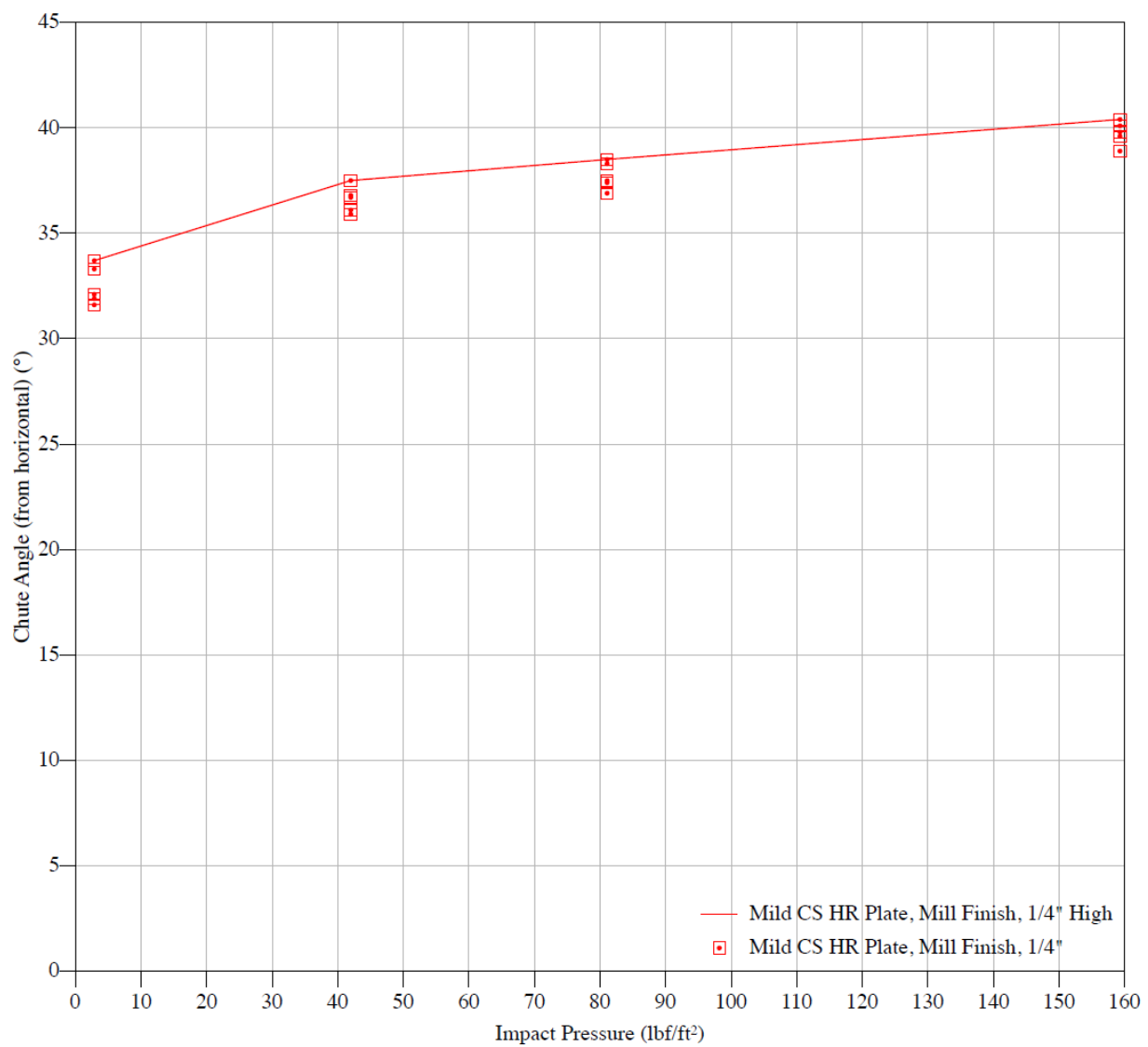


Figure C.28.  $V_2O_5$ : Chute curve with mild CS HR plate

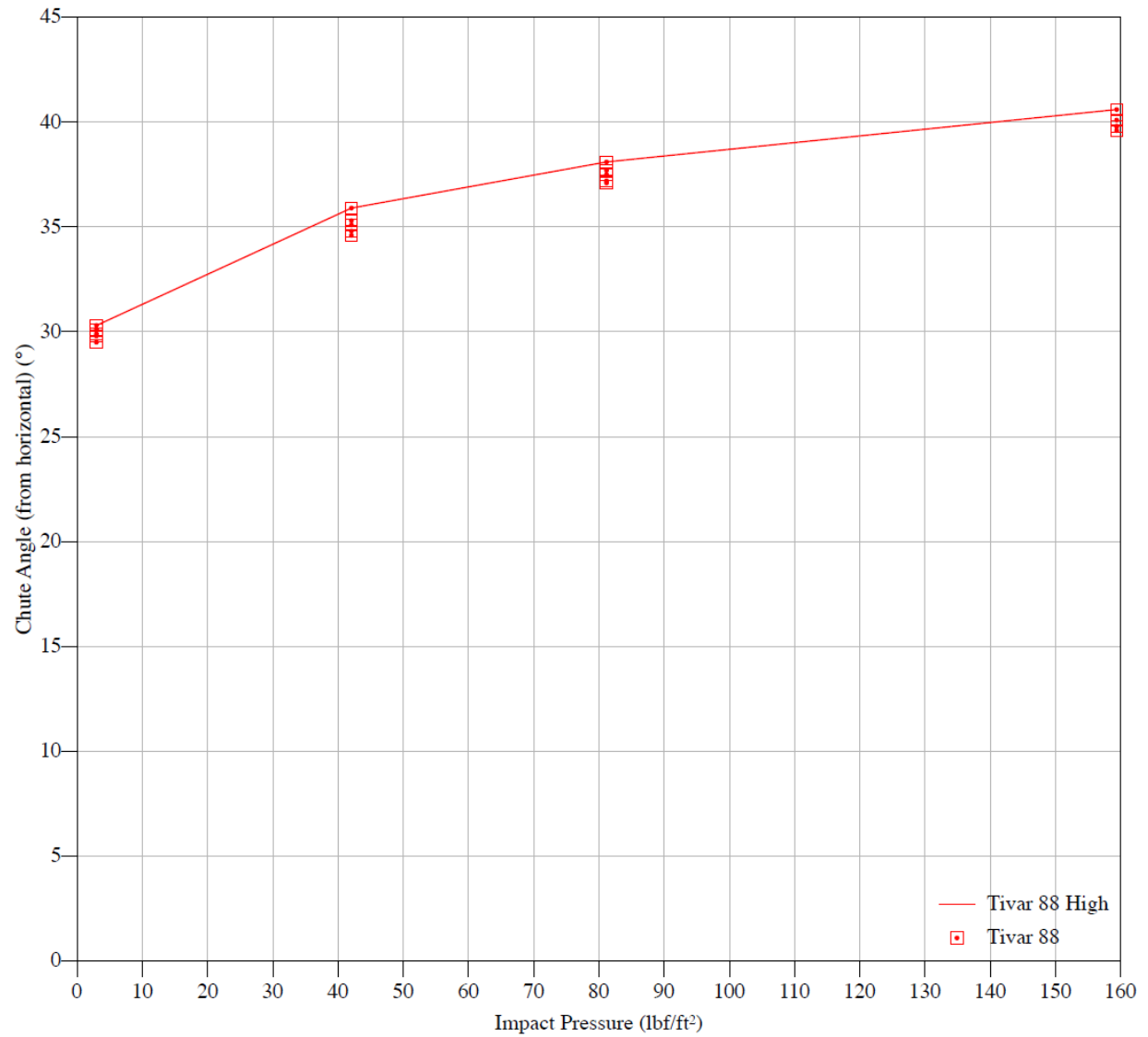


Figure C.29. V<sub>2</sub>O<sub>5</sub>: Chute curve with TIVAR 88

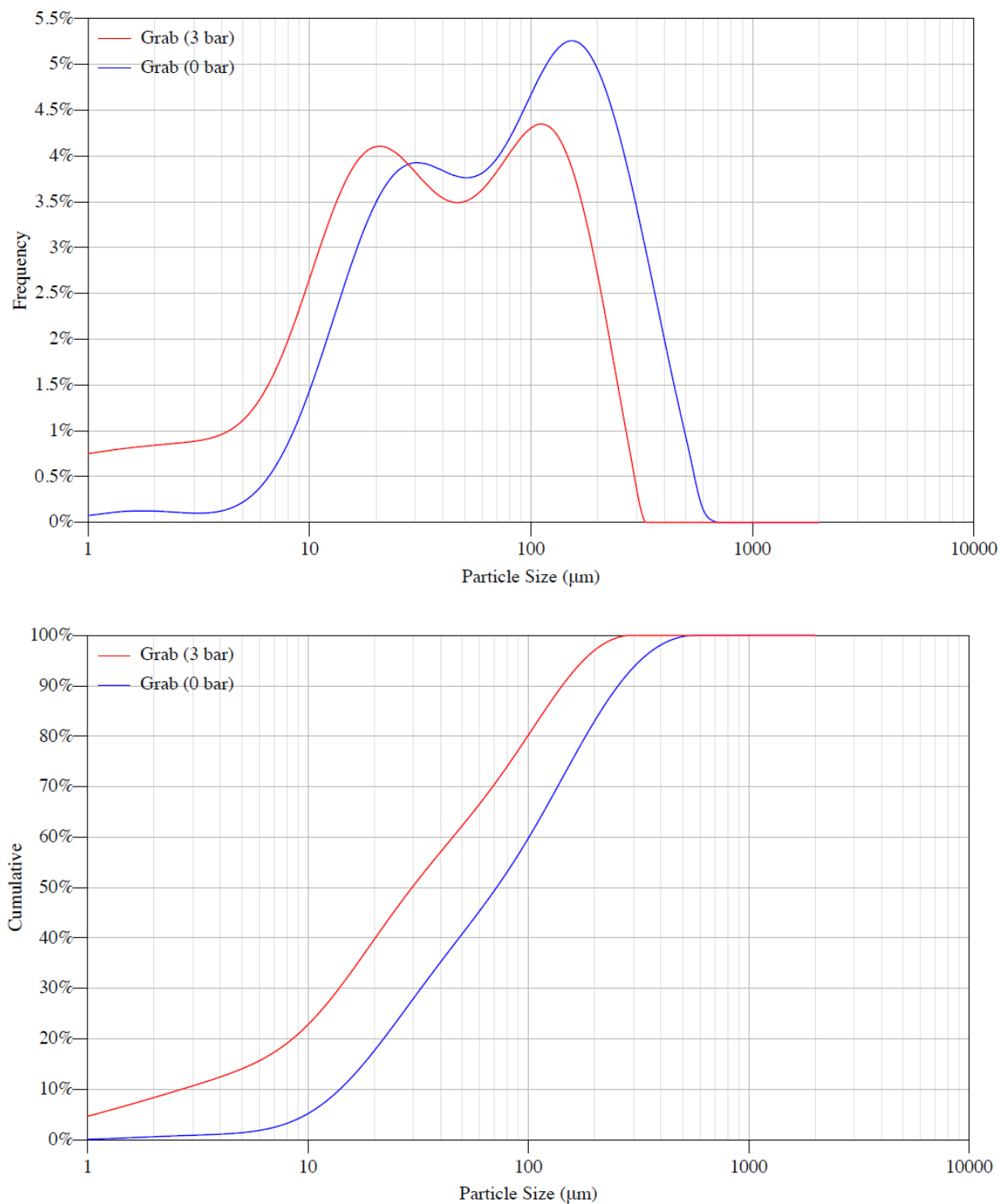


Figure C.30. V<sub>2</sub>O<sub>5</sub>: Particle size distribution by volume and pressure



### C.3 SnO properties

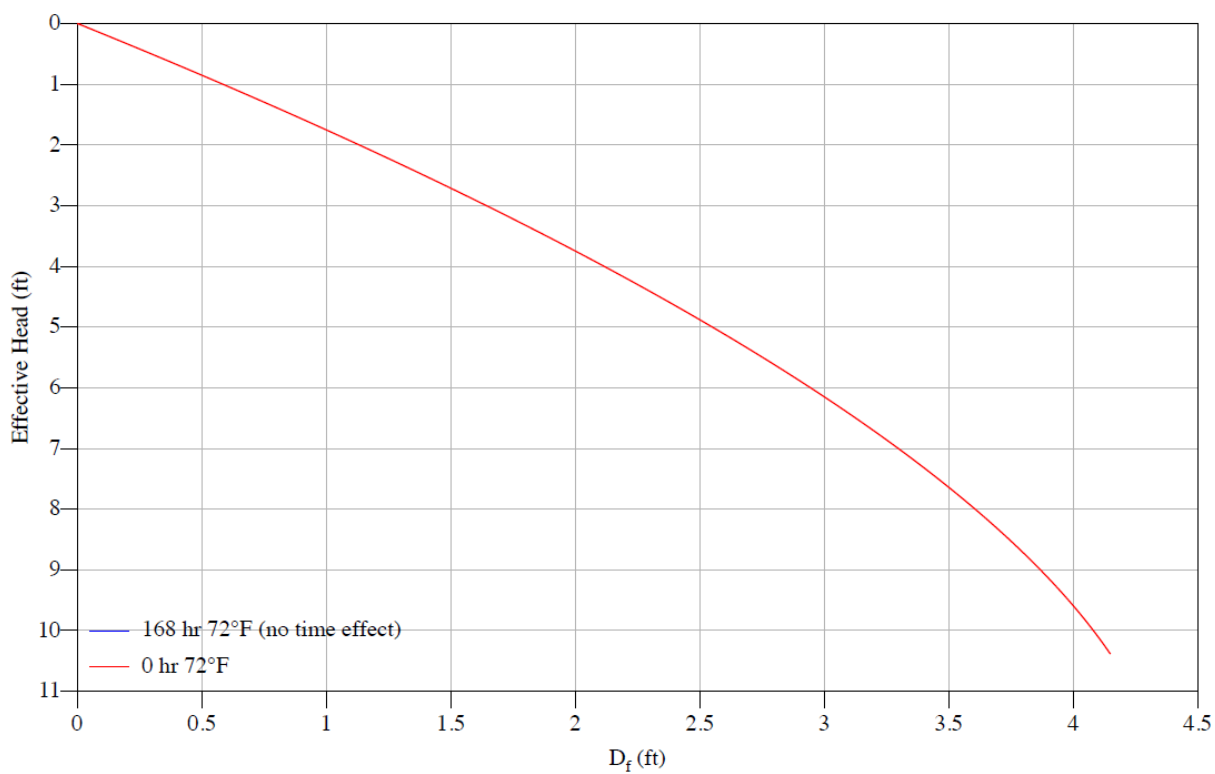


Figure C.31. SnO: Critical rathole dimensions

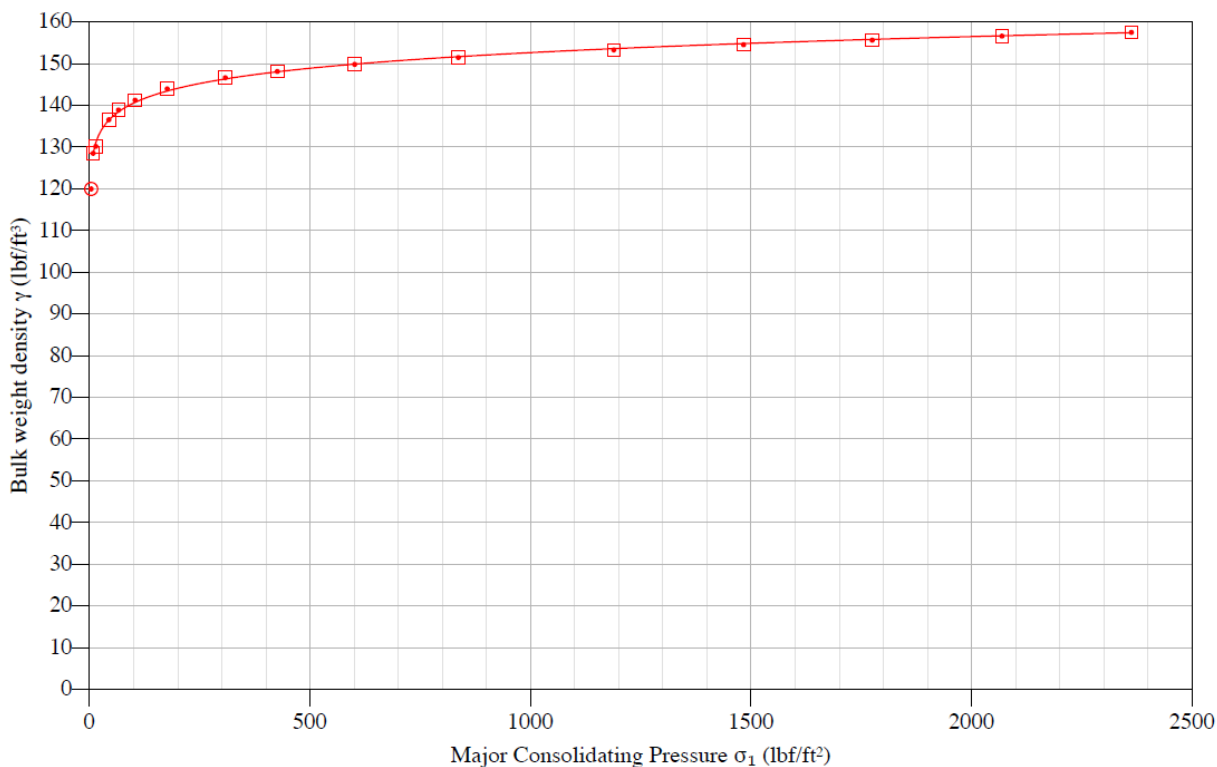


Figure C.32. SnO: Compressibility curve

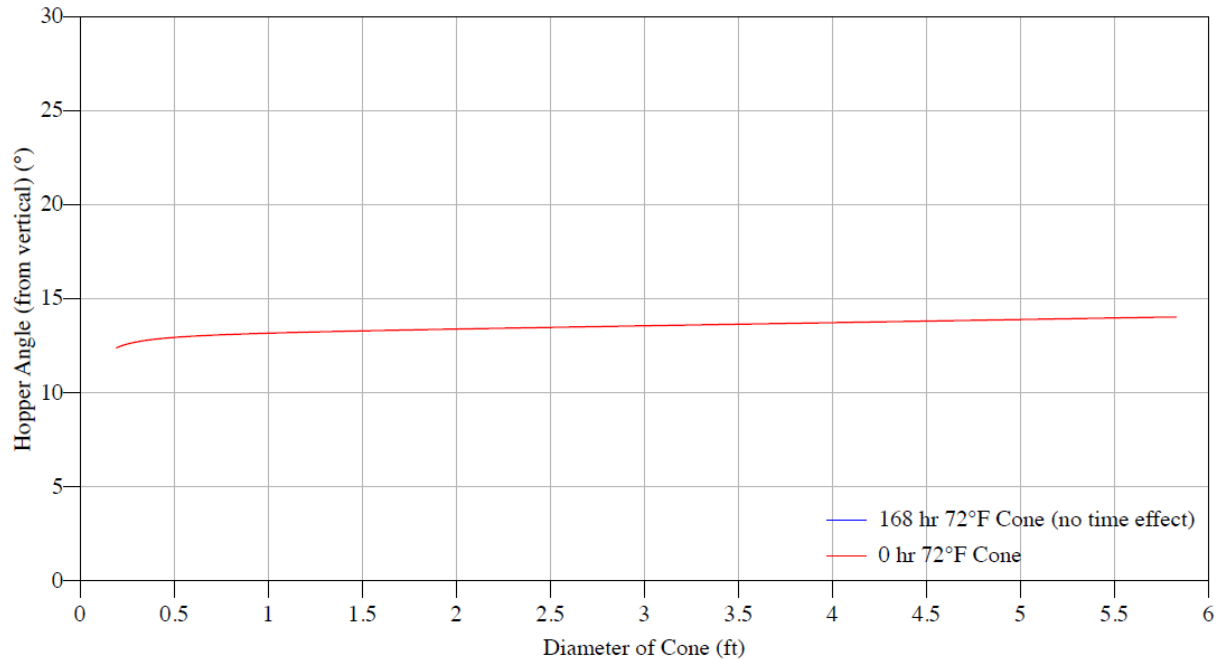


Figure C.33. SnO: Conical hopper angles with 304 SS sheet

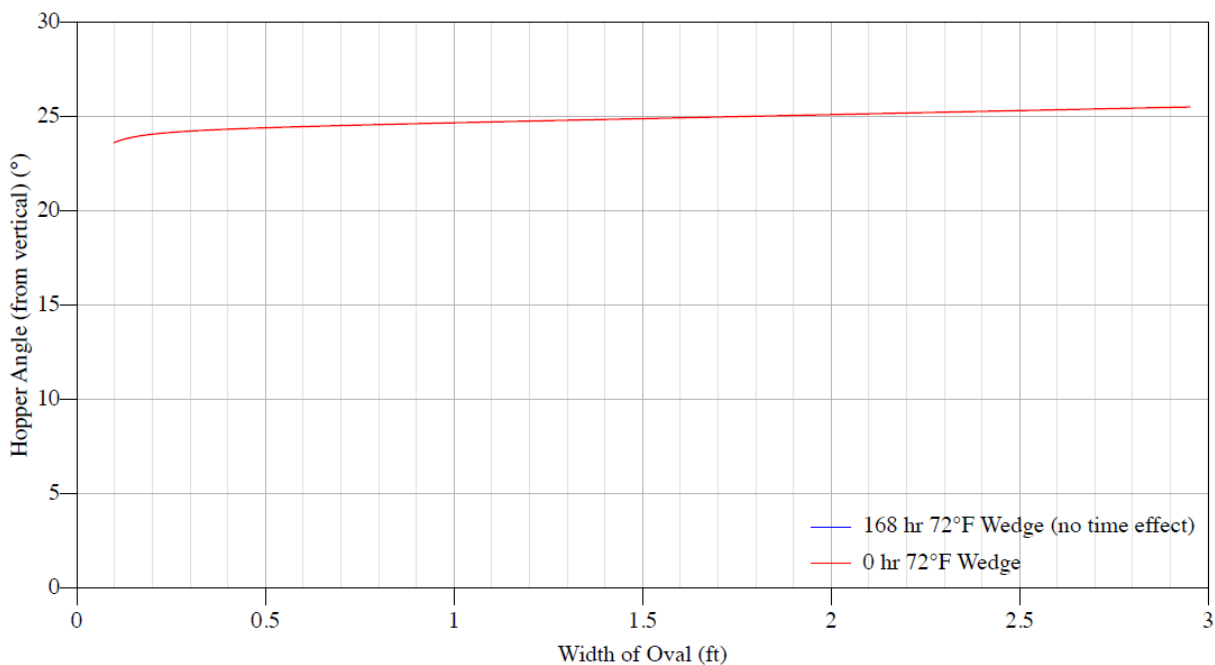


Figure C.34. SnO: Wedge hopper angles with 304 SS sheet

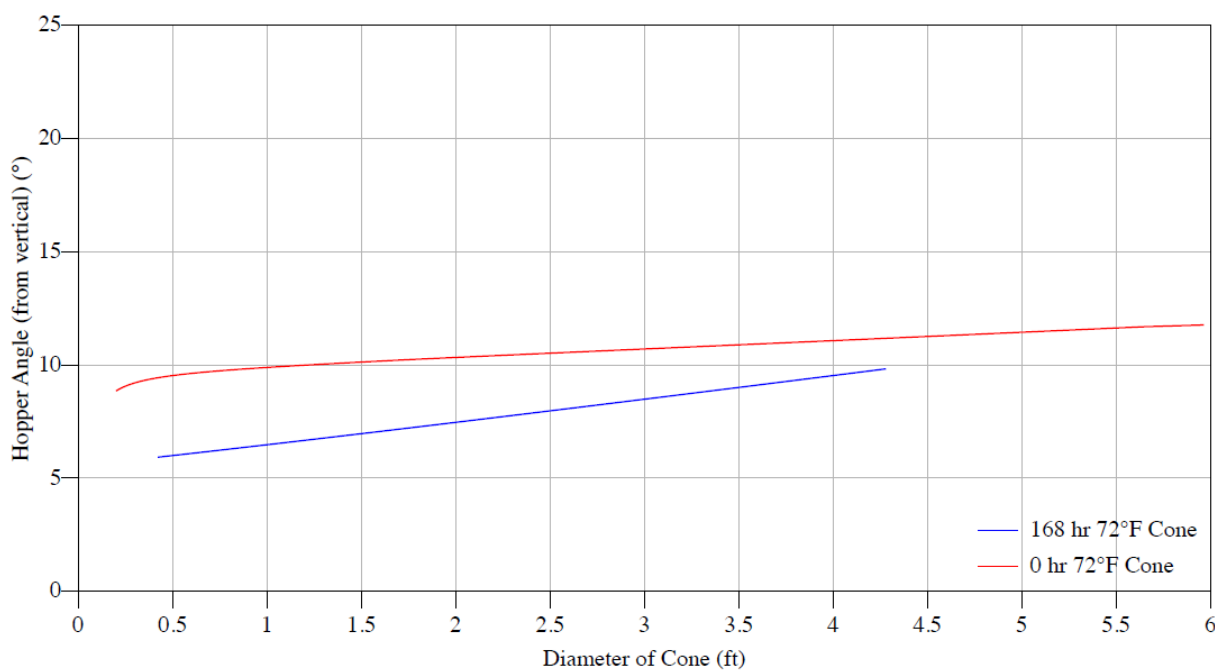


Figure C.35. SnO: Conical hopper angles with mild CS HR plate

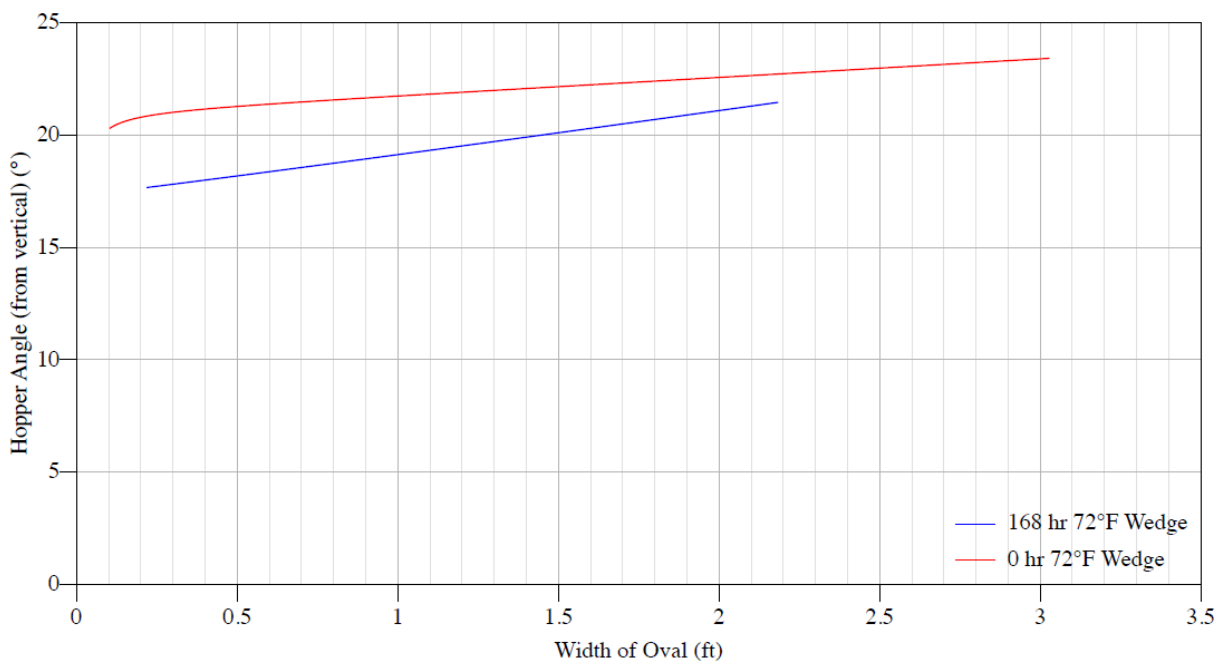


Figure C.36. SnO: Wedge hopper angles with mild CS HR plate

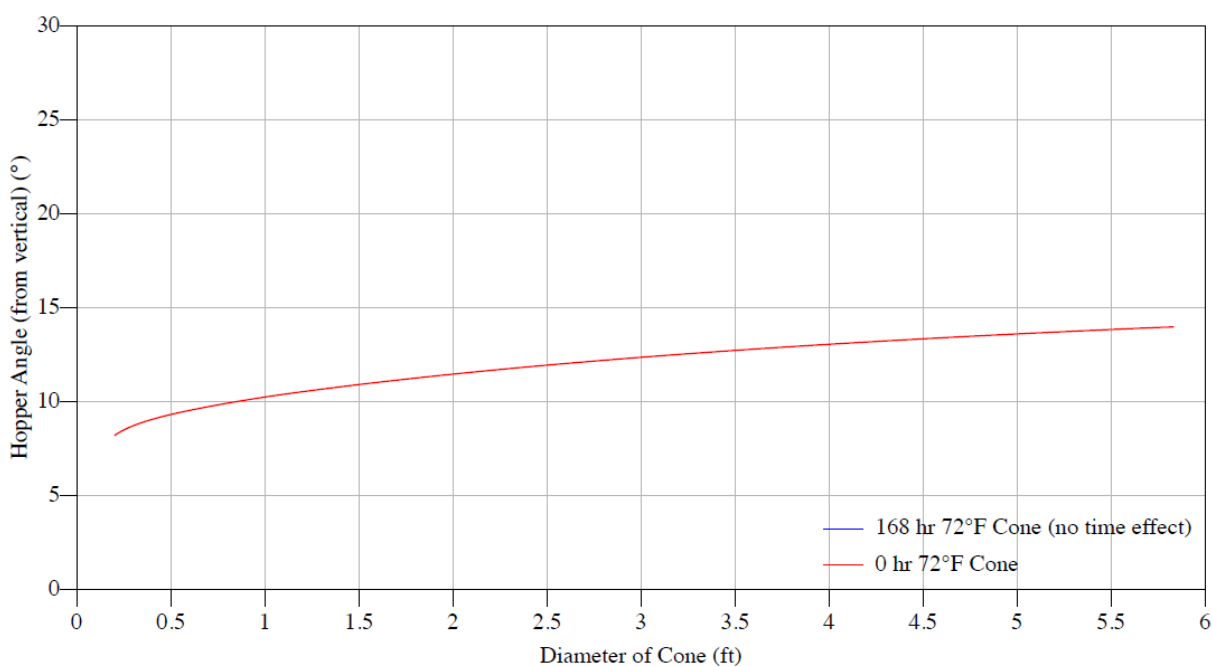


Figure C.37. SnO: Conical hopper angles with TIVAR 88

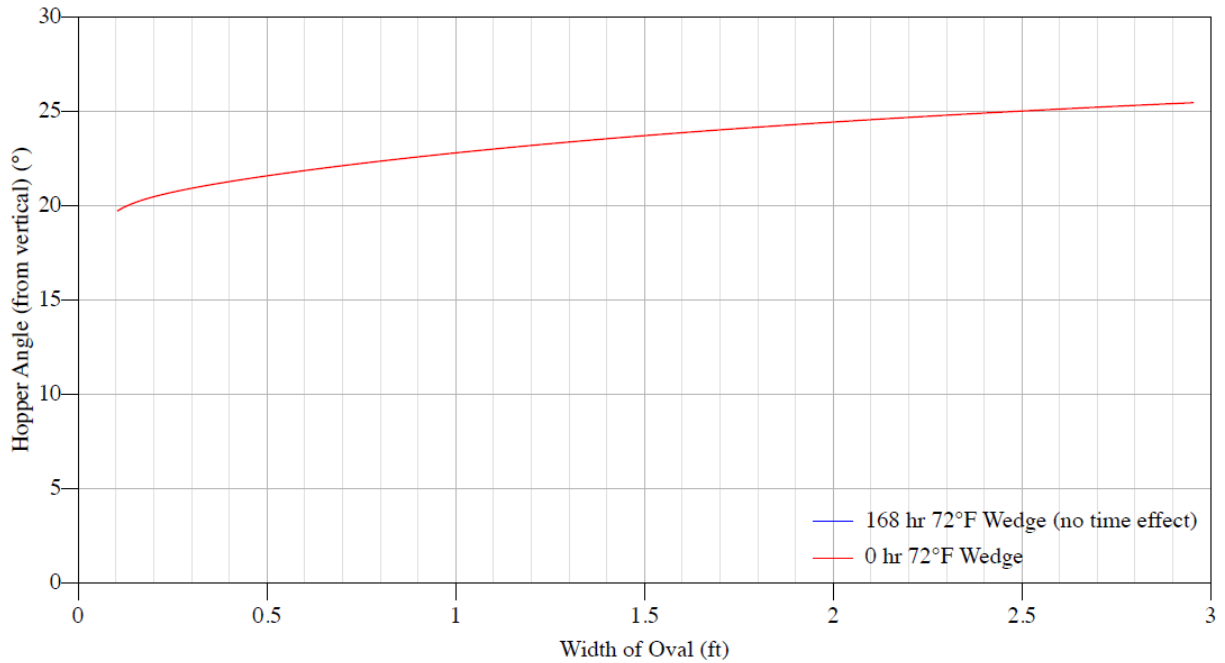


Figure C.38. SnO: Wedge hopper angles with TIVAR 88

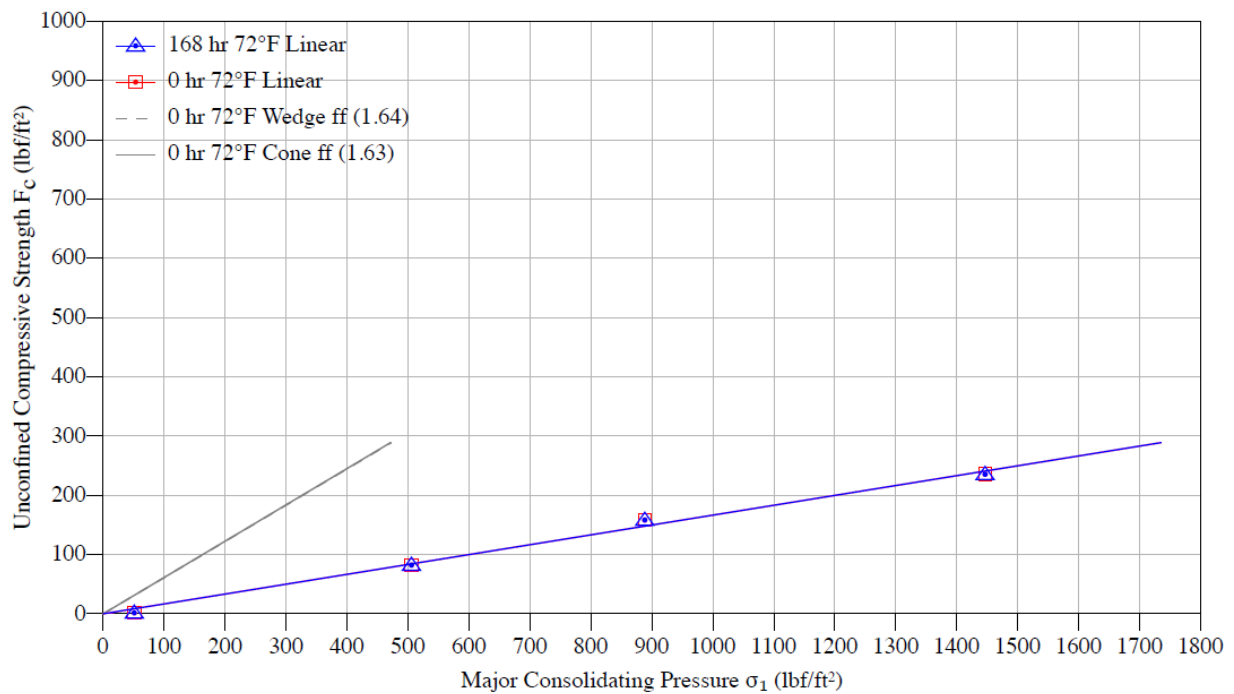


Figure C.39. SnO: Flow function

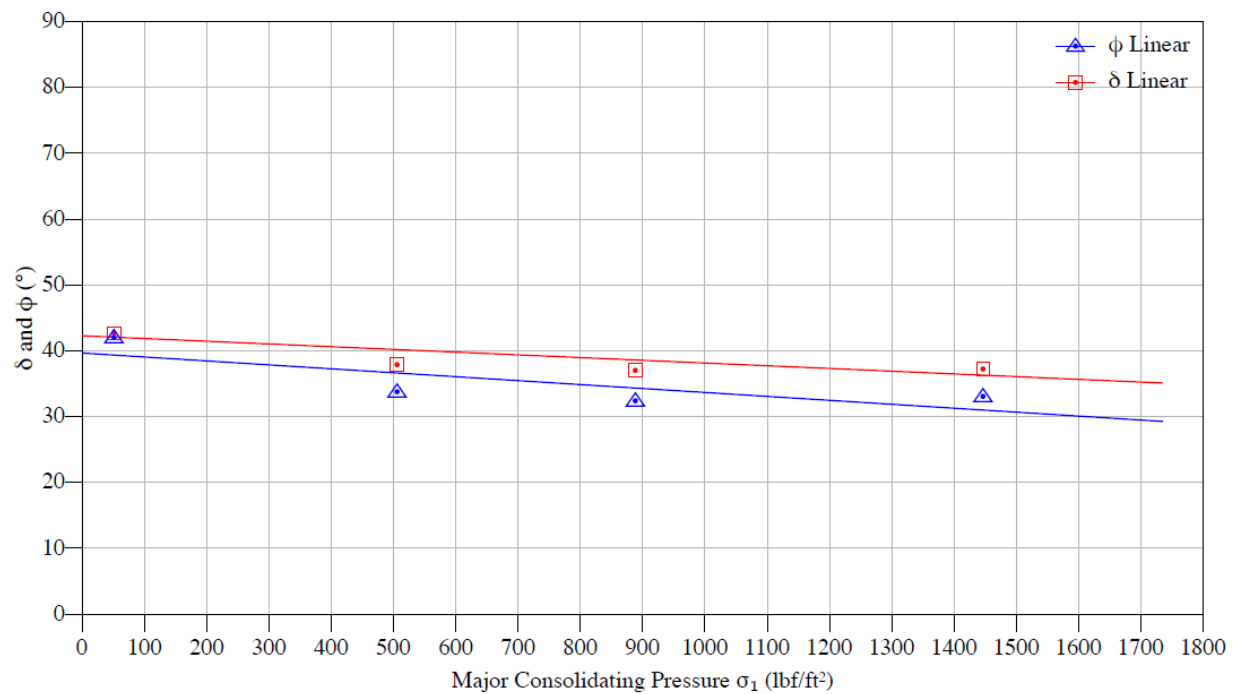


Figure C.40. SnO: Effective angle of friction ( $\delta$ ) and kinematic angle of internal friction ( $\phi$ )

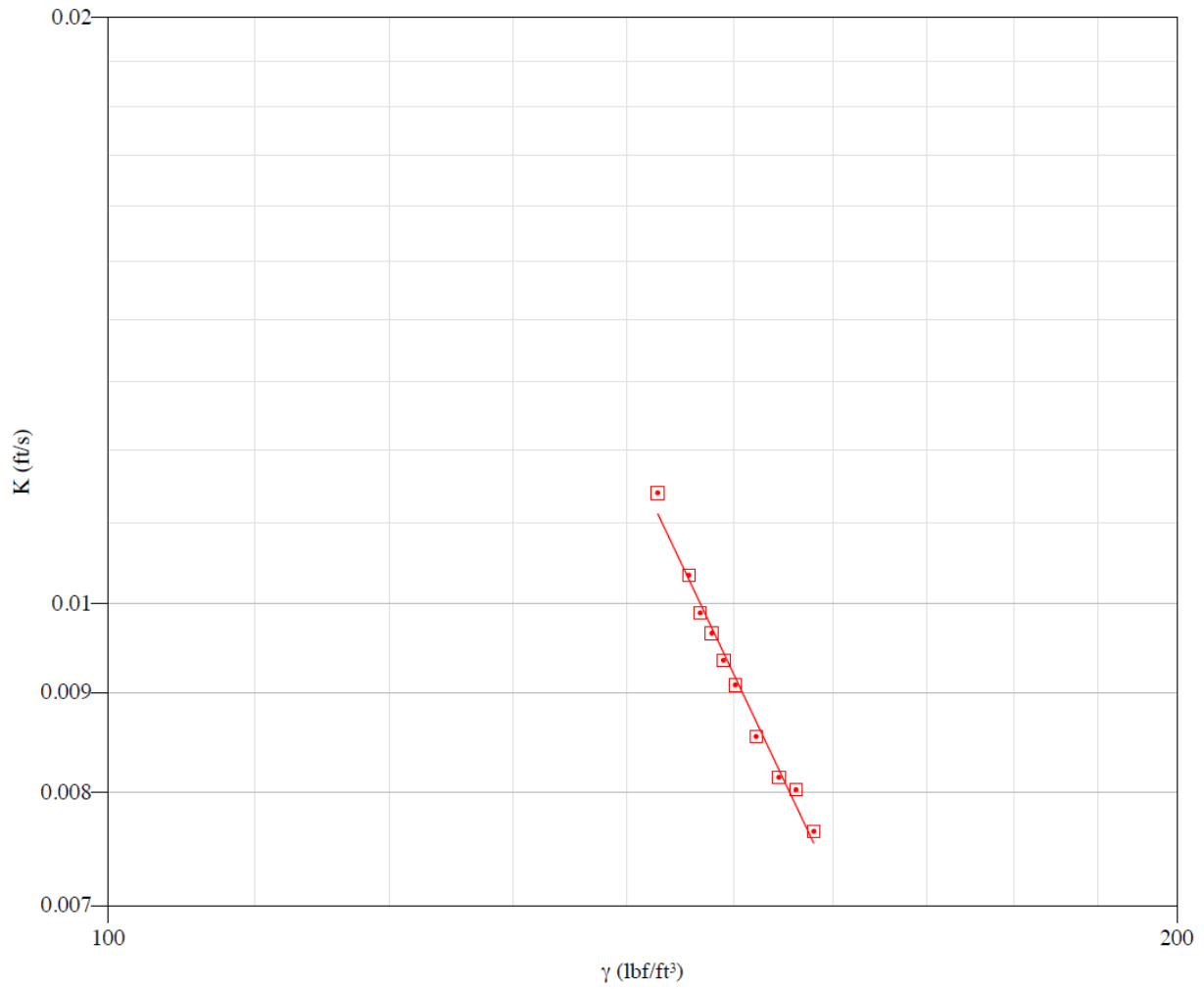


Figure C.41. SnO: Permeability curve



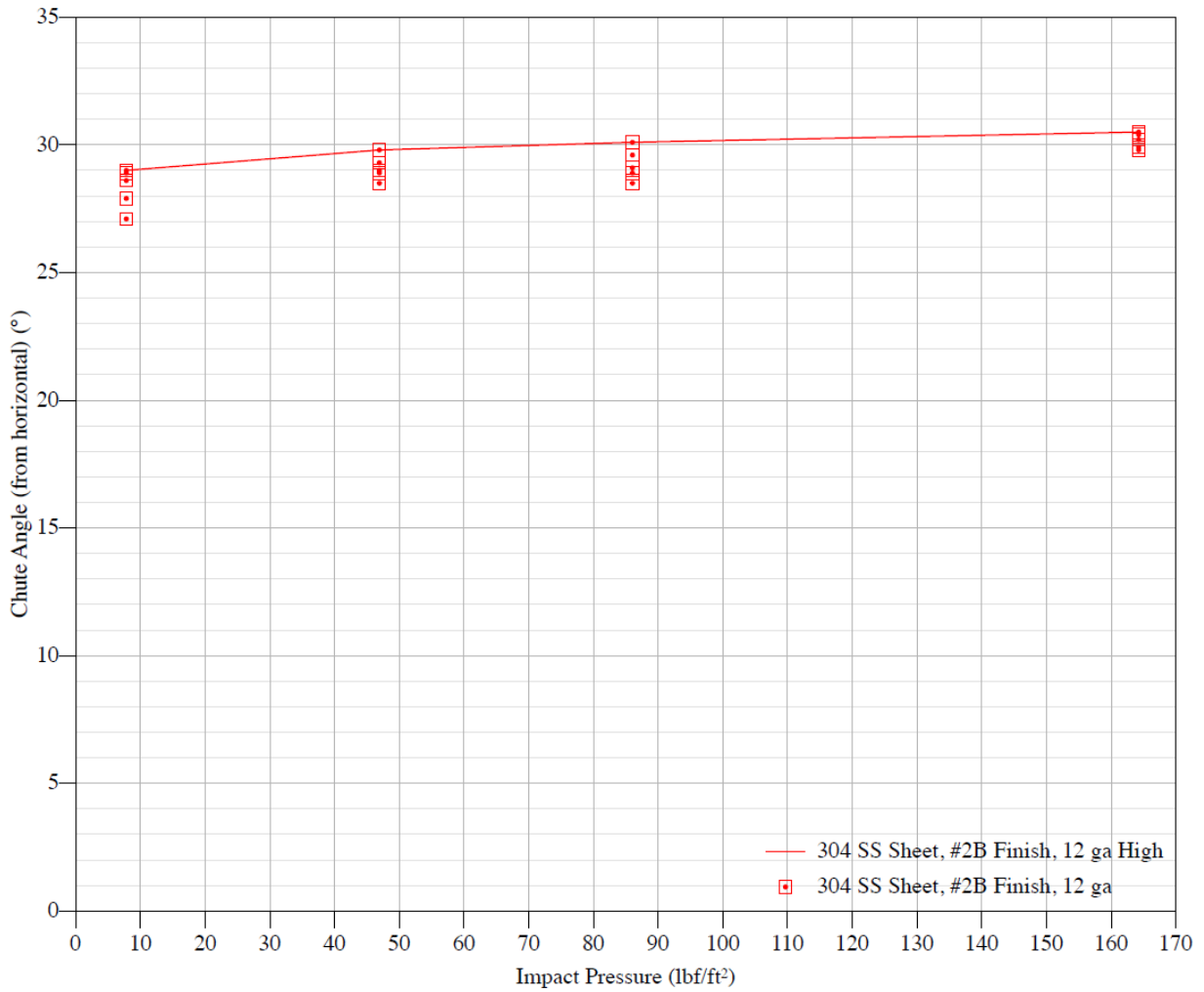


Figure C.42. SnO: Chute curve with 304 SS sheet

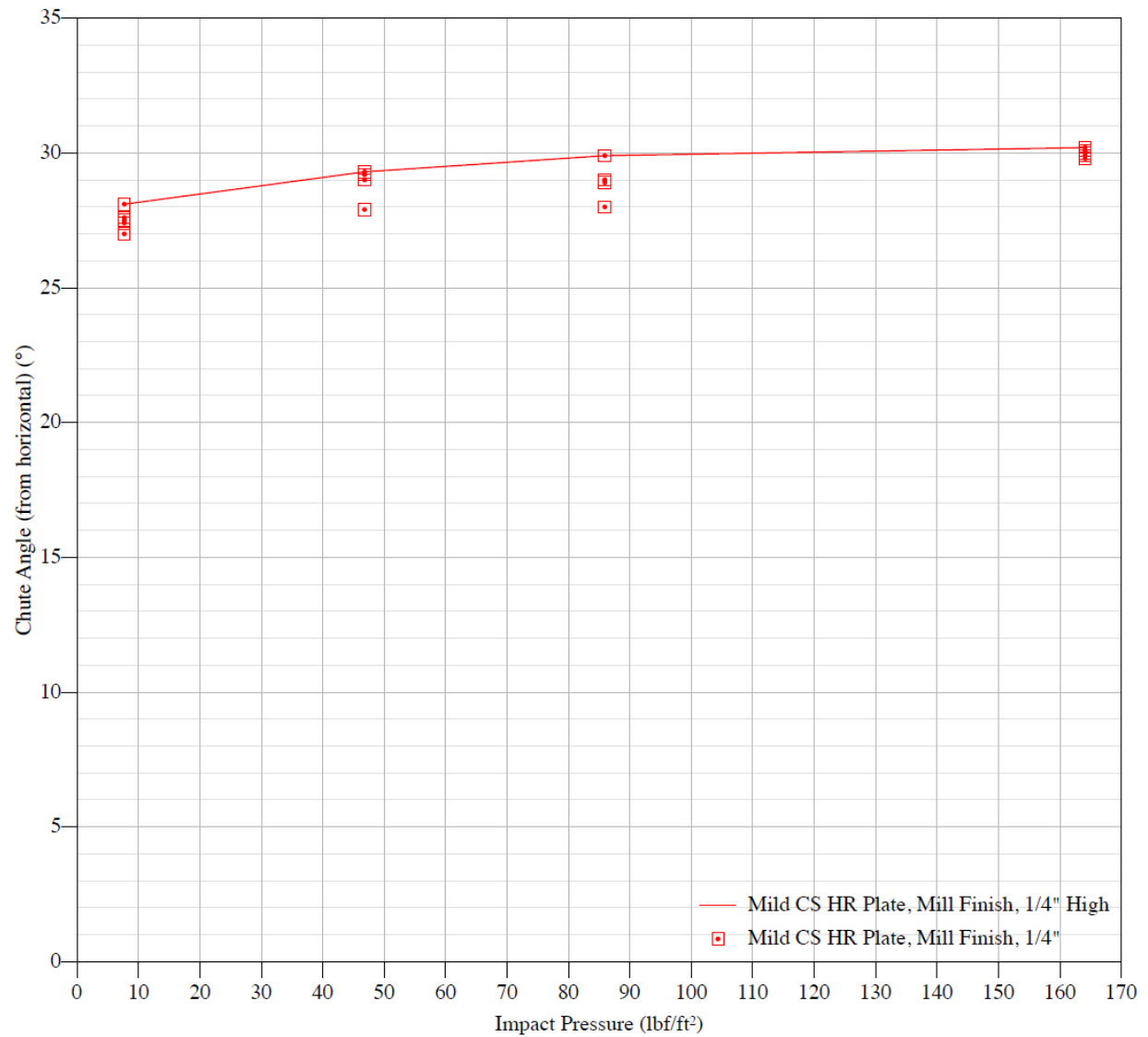


Figure C.43. SnO: Chute curve with mild CS HR plate

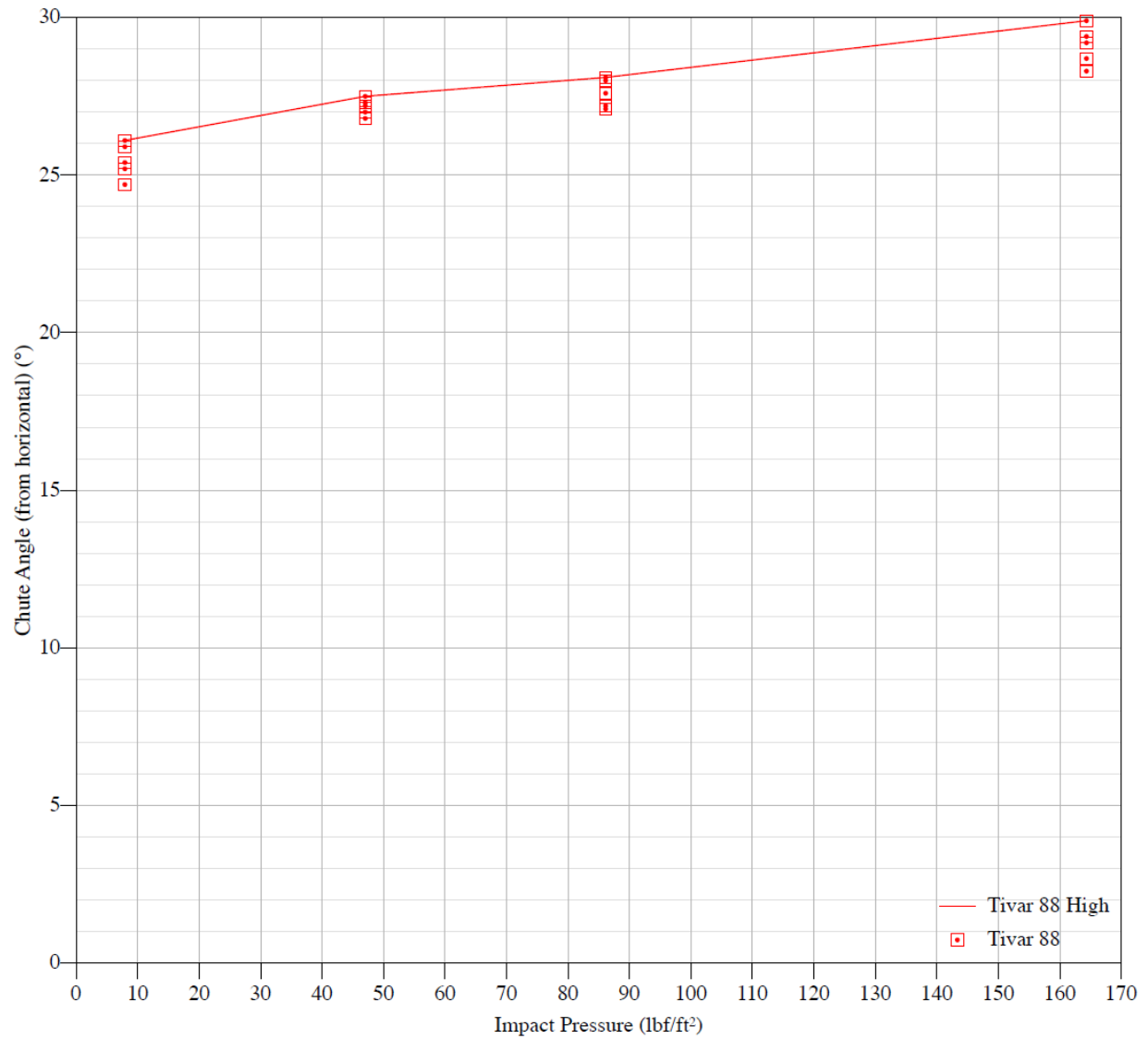


Figure C.44. SnO: Chute curve with TIVAR 88

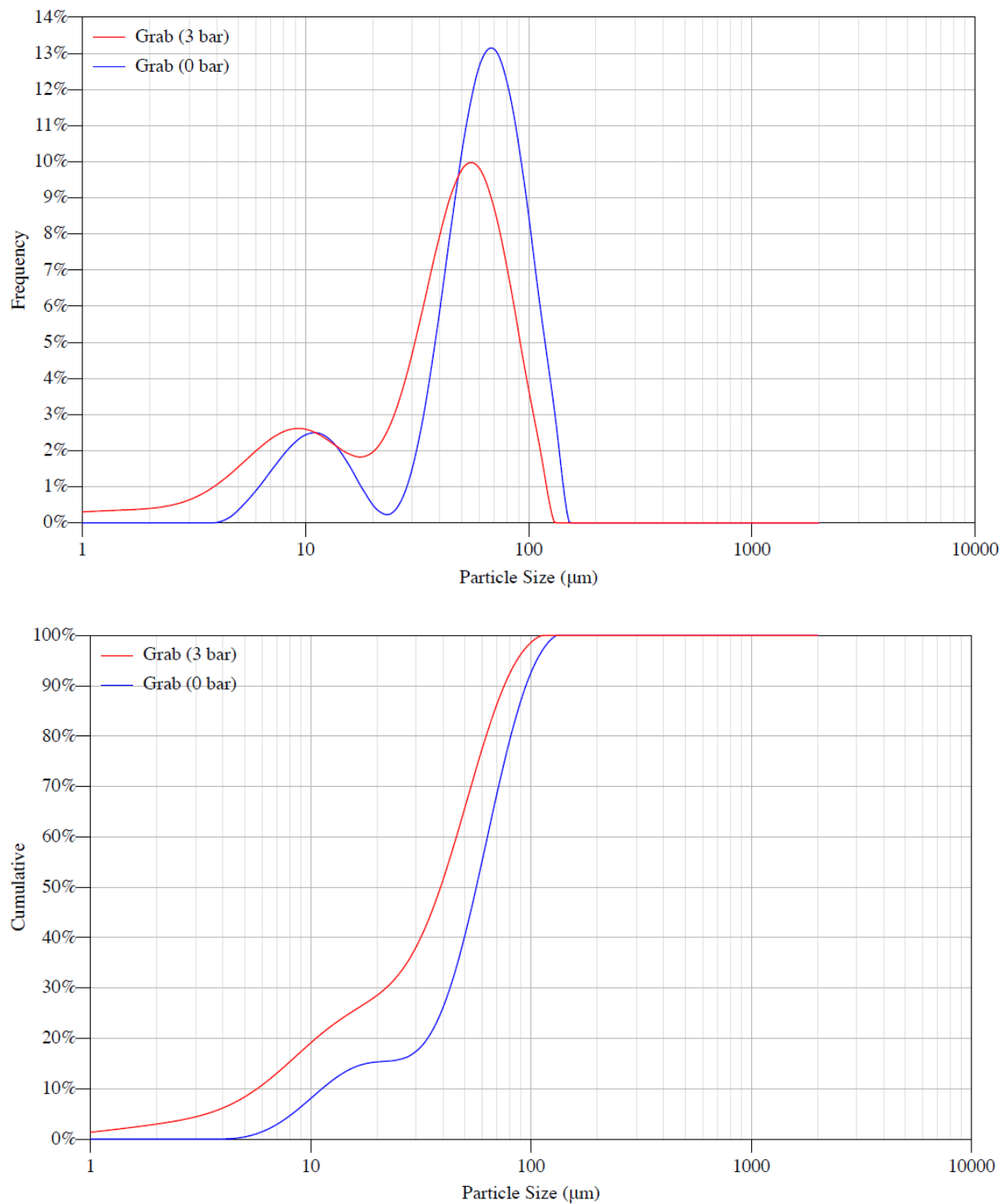


Figure C.45. SnO: Particle size distribution by volume and pressure

## C.4 SnO<sub>2</sub> properties

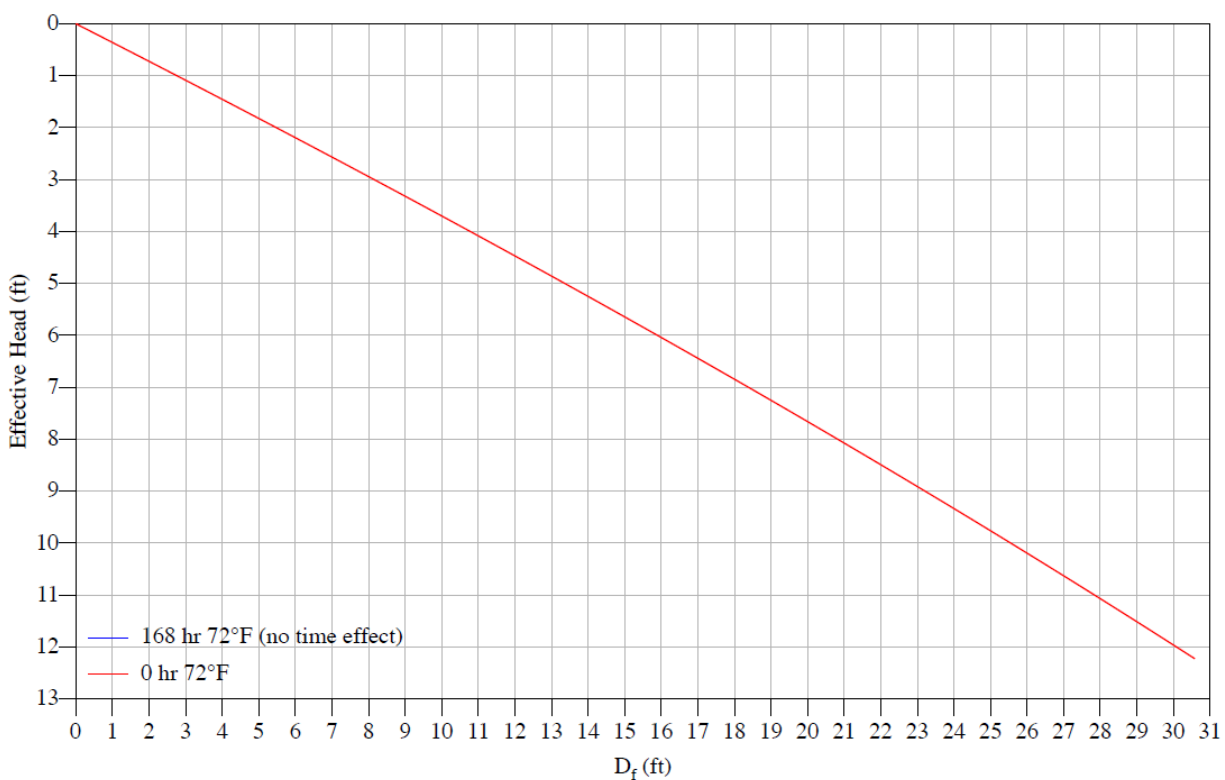


Figure C.46. SnO<sub>2</sub>: Critical rathole dimensions

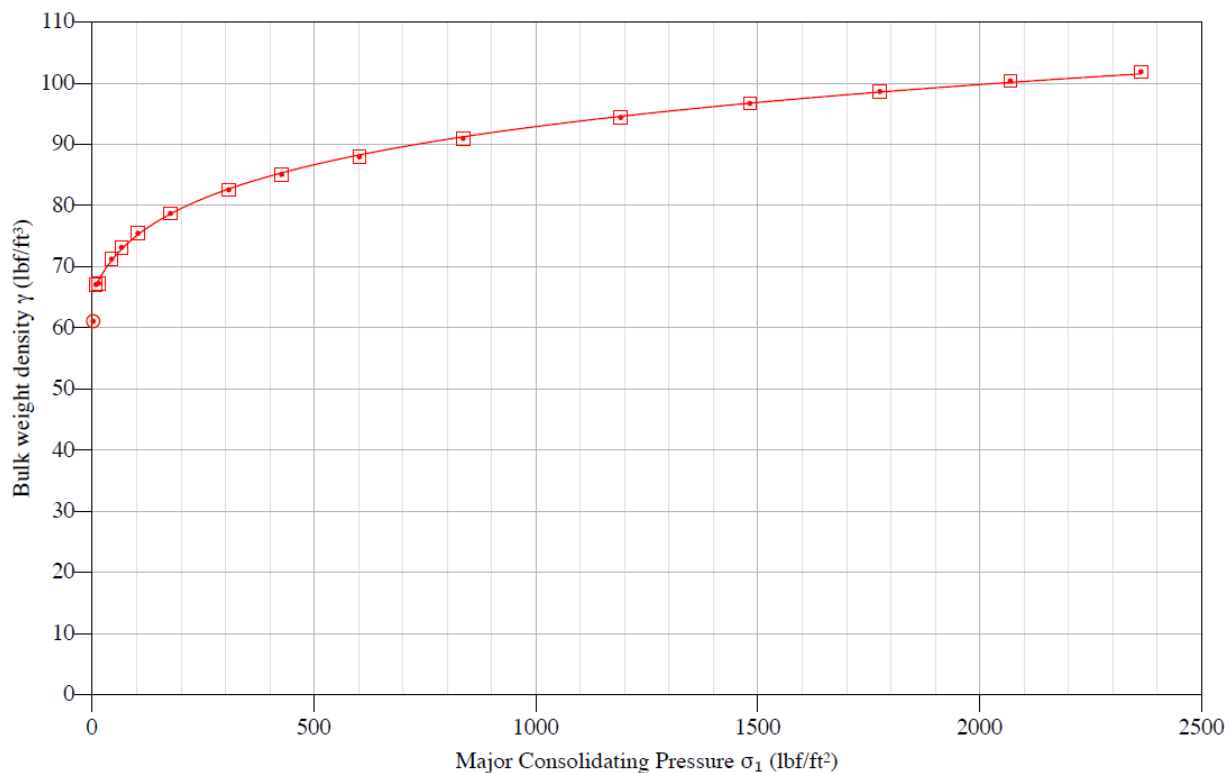


Figure C.47. SnO<sub>2</sub>: Compressibility curve

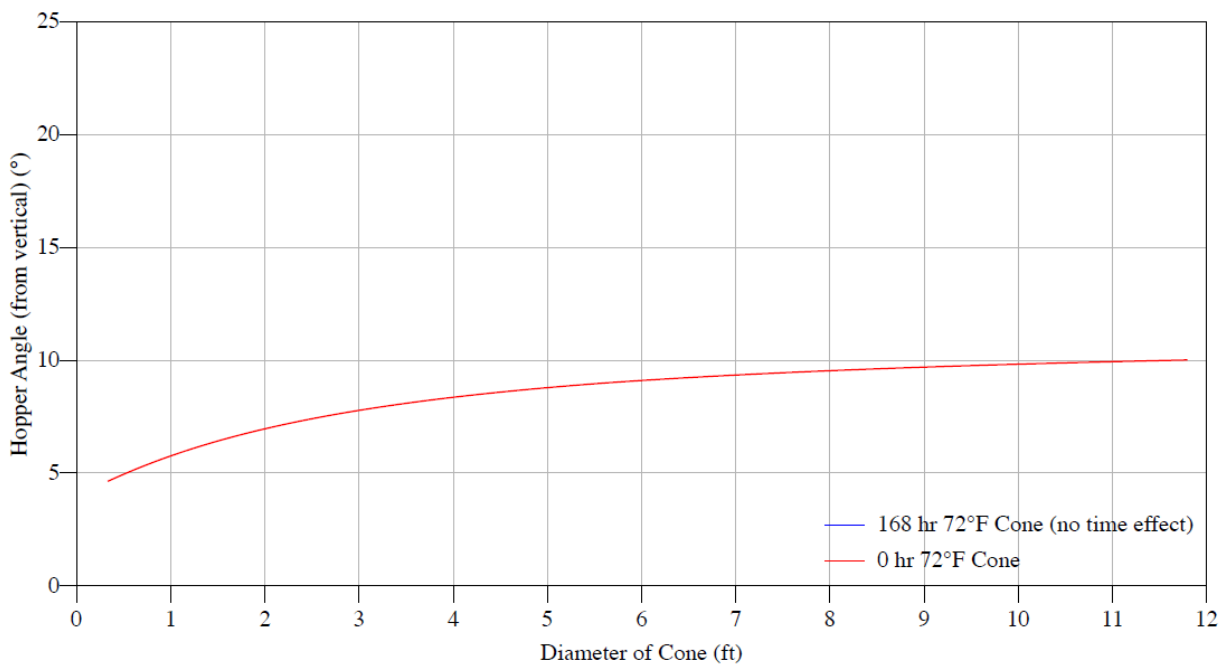


Figure C.48. SnO<sub>2</sub>: Conical hopper angles with 304 SS sheet

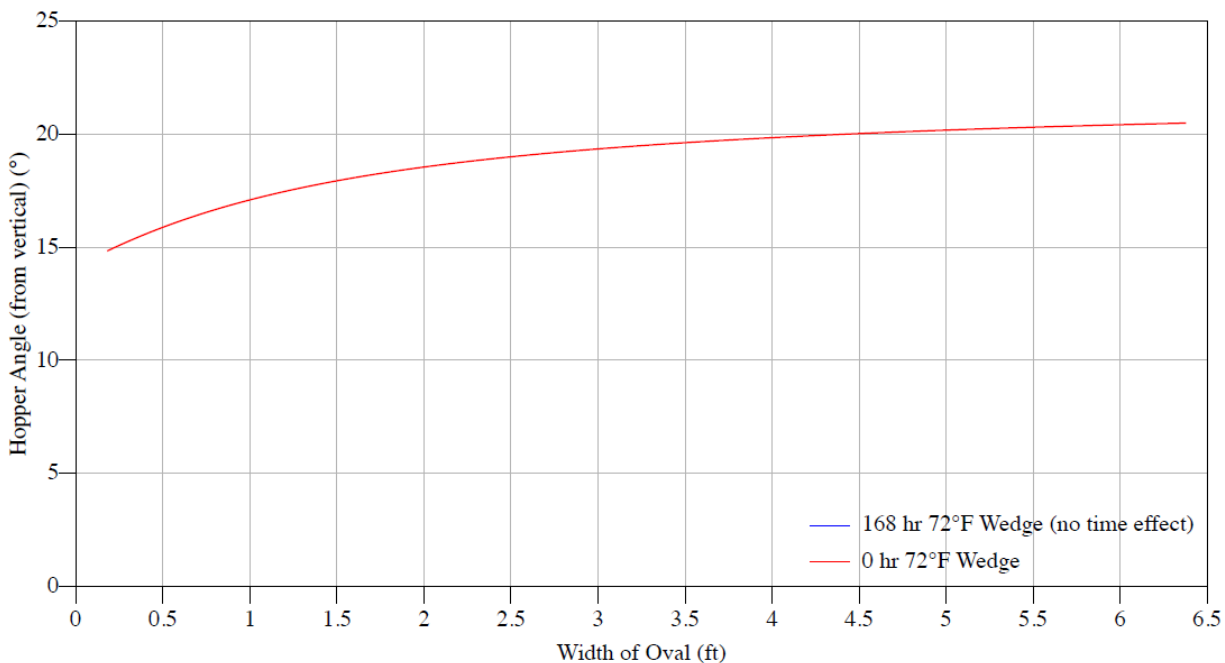


Figure C.49.  $\text{SnO}_2$ : Wedge hopper angles with 304 SS sheet

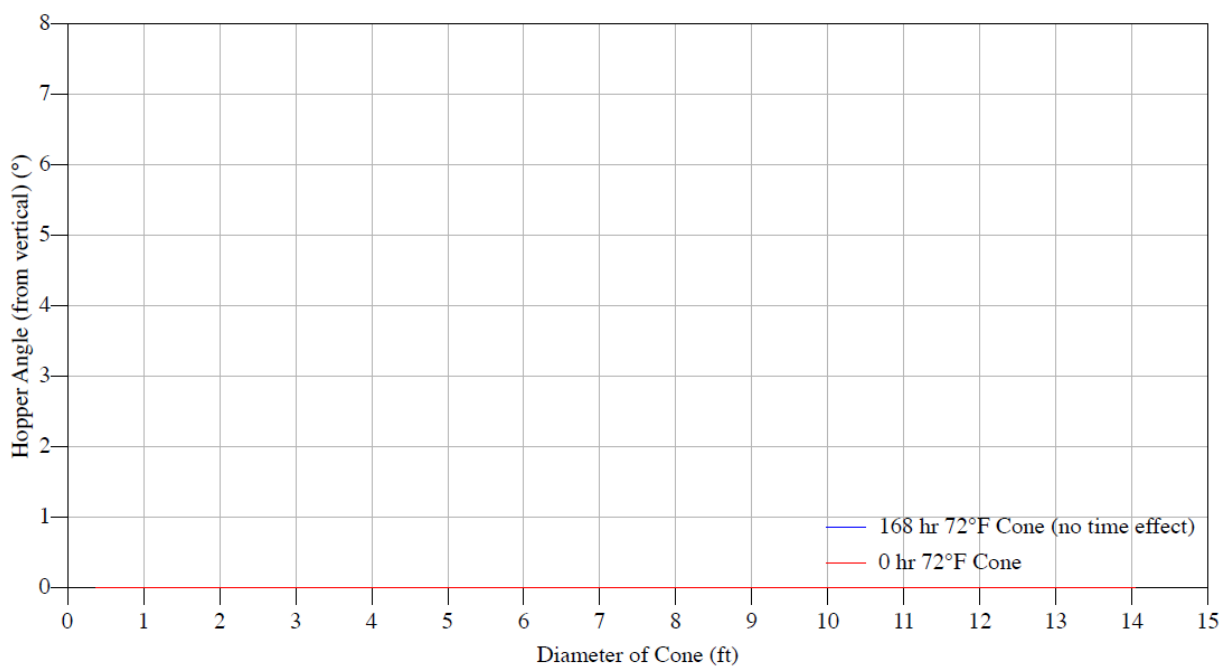


Figure C.50.  $\text{SnO}_2$ : Conical hopper angles with mild CS HR plate

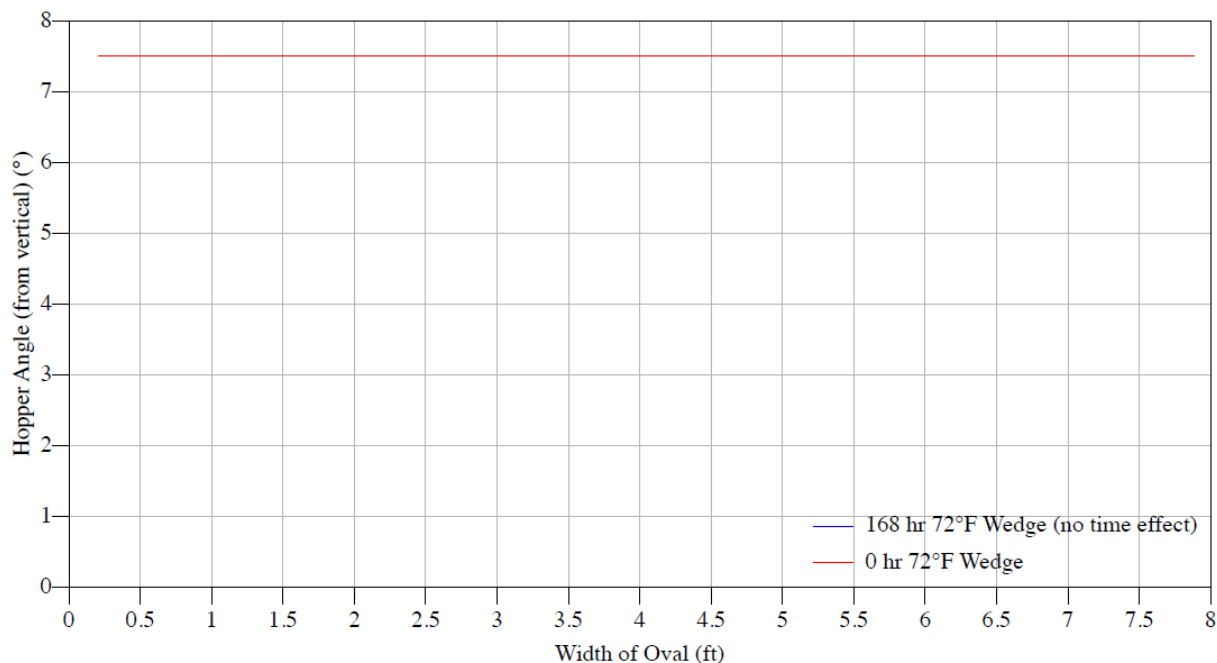


Figure C.51. SnO<sub>2</sub>: Wedge hopper angles with mild CS HR plate

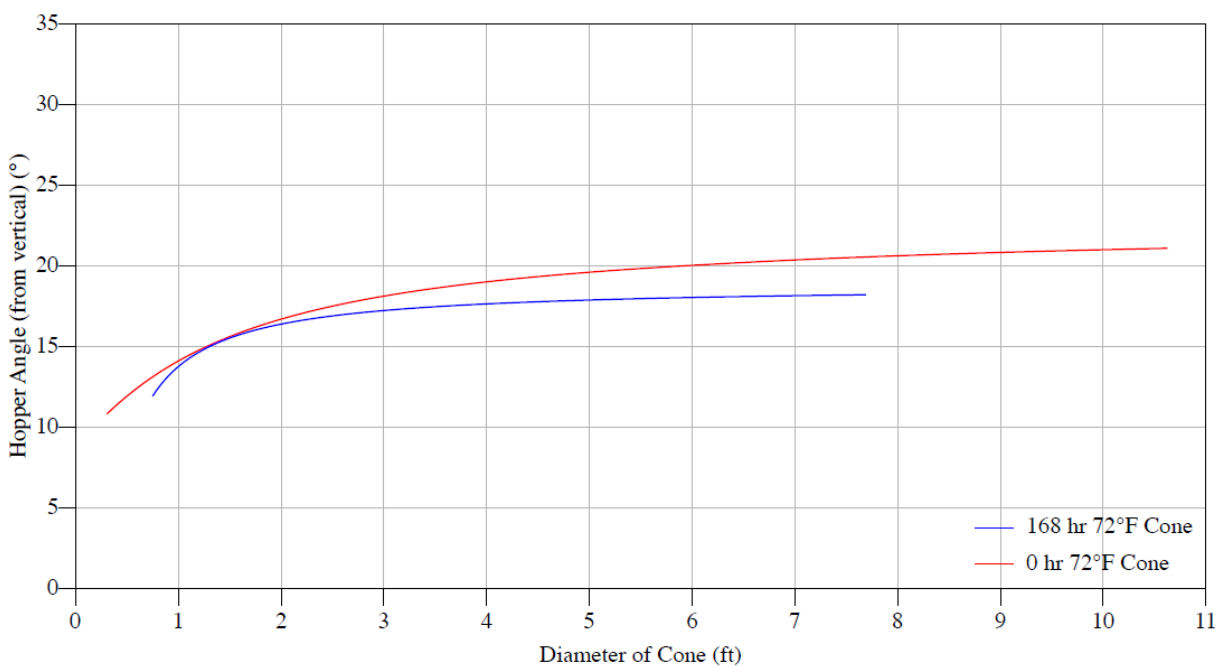


Figure C.52. SnO<sub>2</sub>: Conical hopper angles with TIVAR 88



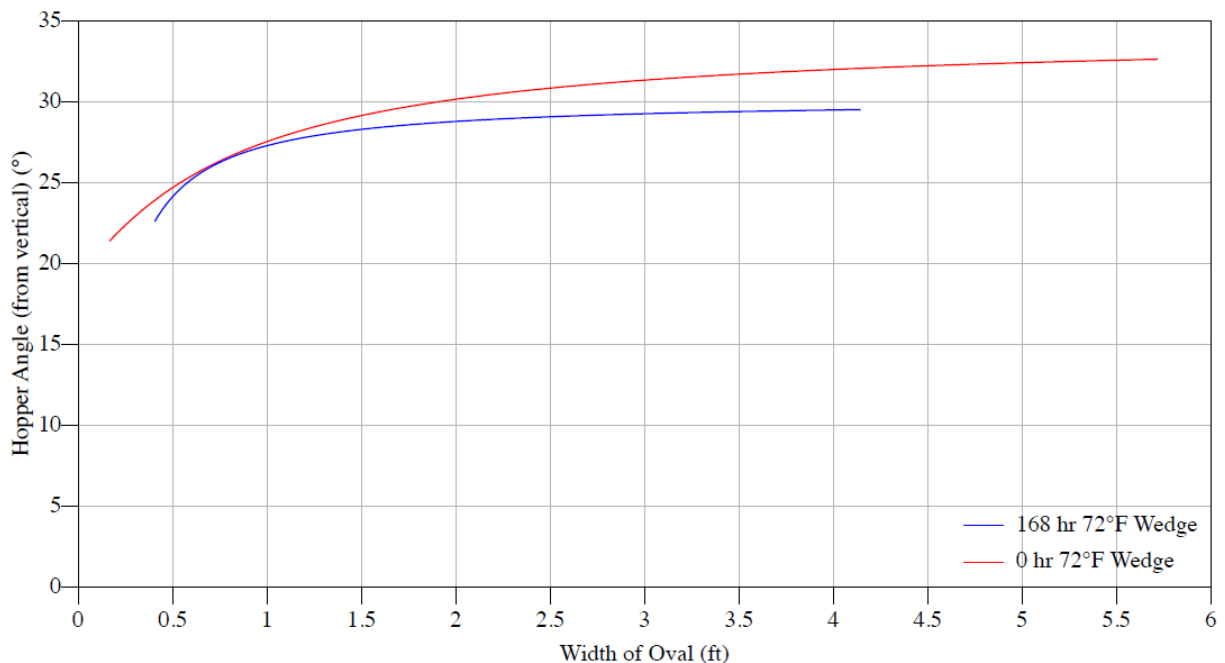


Figure C.53. SnO<sub>2</sub>: Wedge hopper angles with TIVAR 88

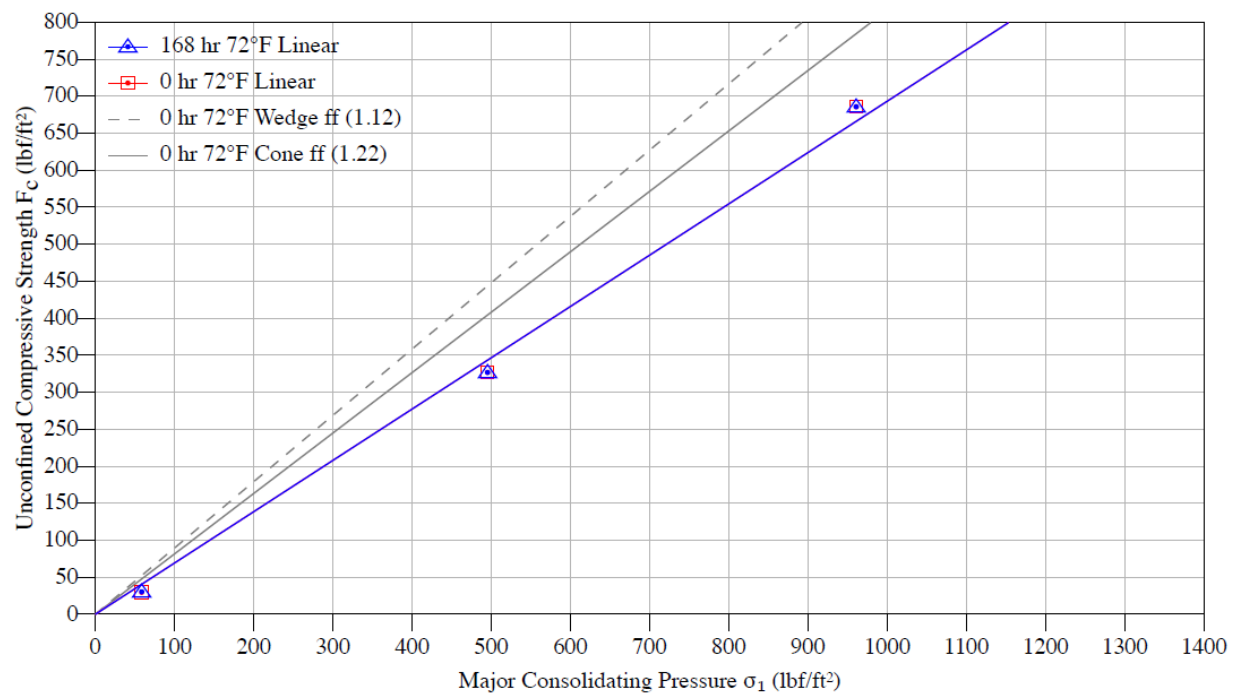


Figure C.54. SnO<sub>2</sub>: Flow function

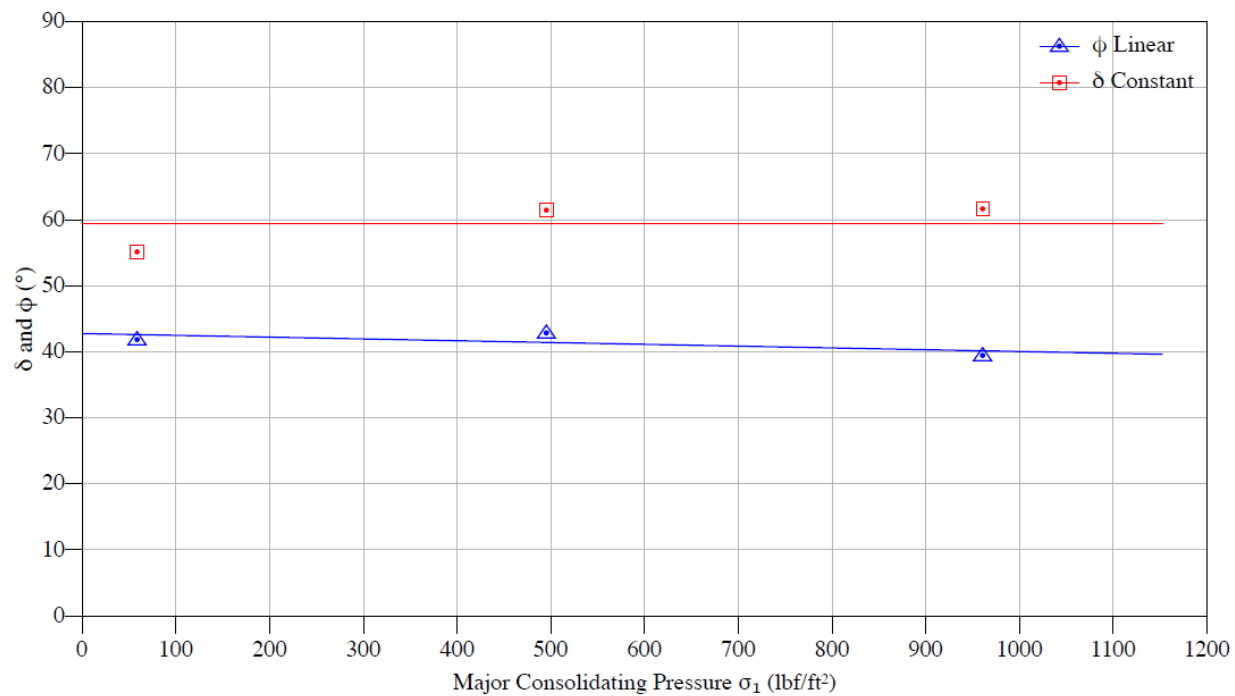


Figure C.55. SnO<sub>2</sub>: Effective angle of friction ( $\delta$ ) and kinematic angle of internal friction ( $\phi$ )

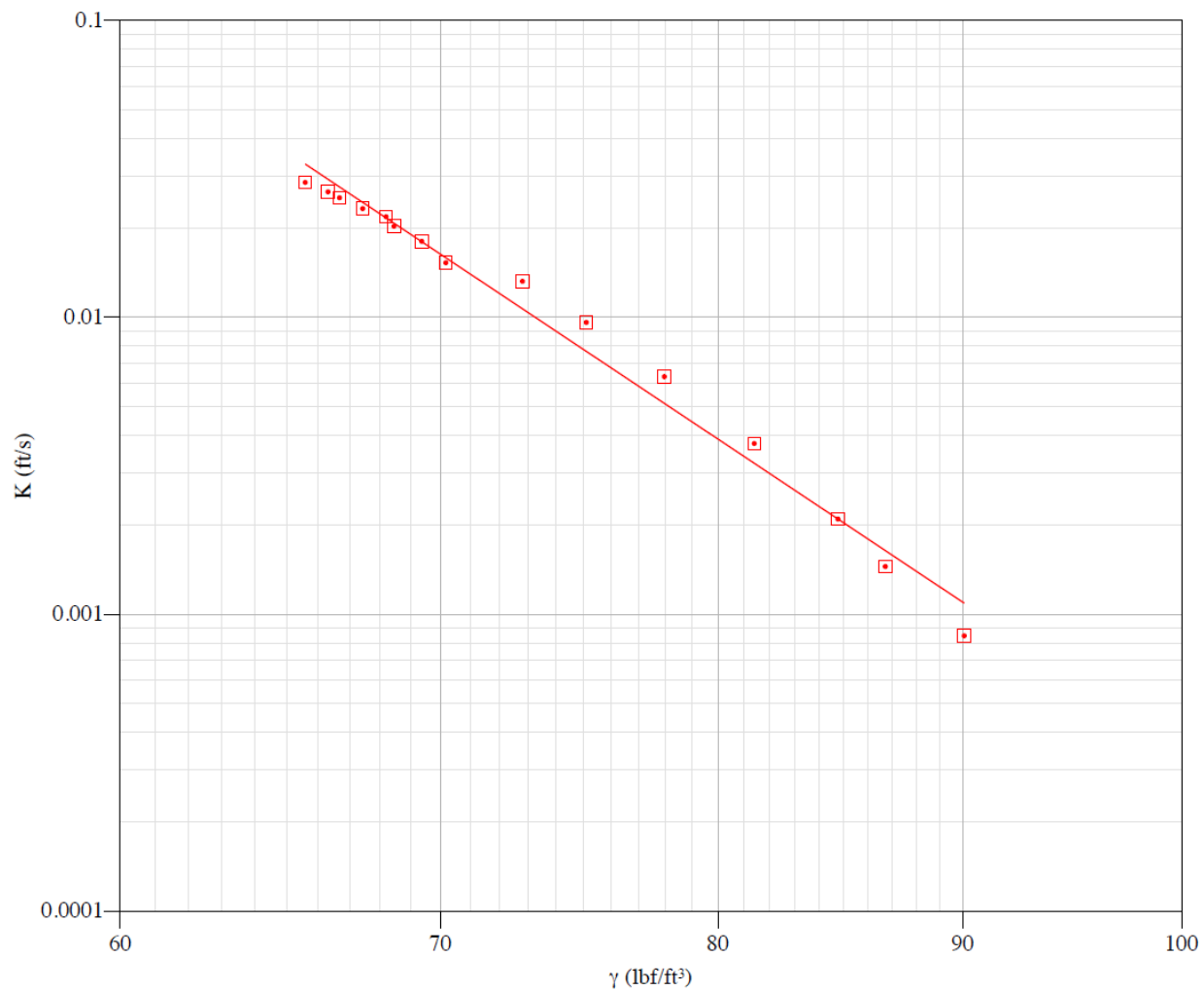


Figure C.56.  $\text{SnO}_2$ : Permeability curve

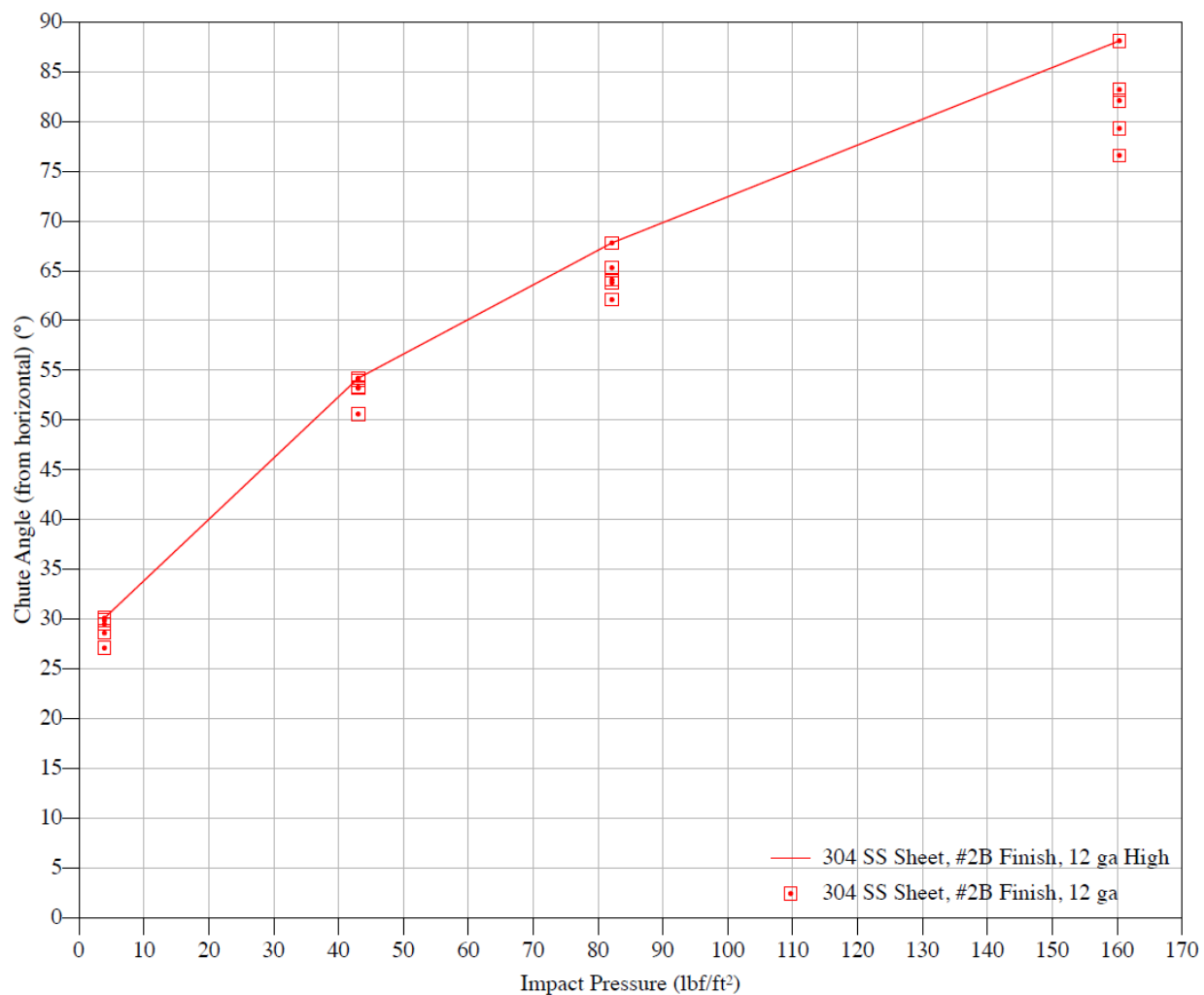


Figure C.57. SnO<sub>2</sub>: Chute curve with 304 SS sheet

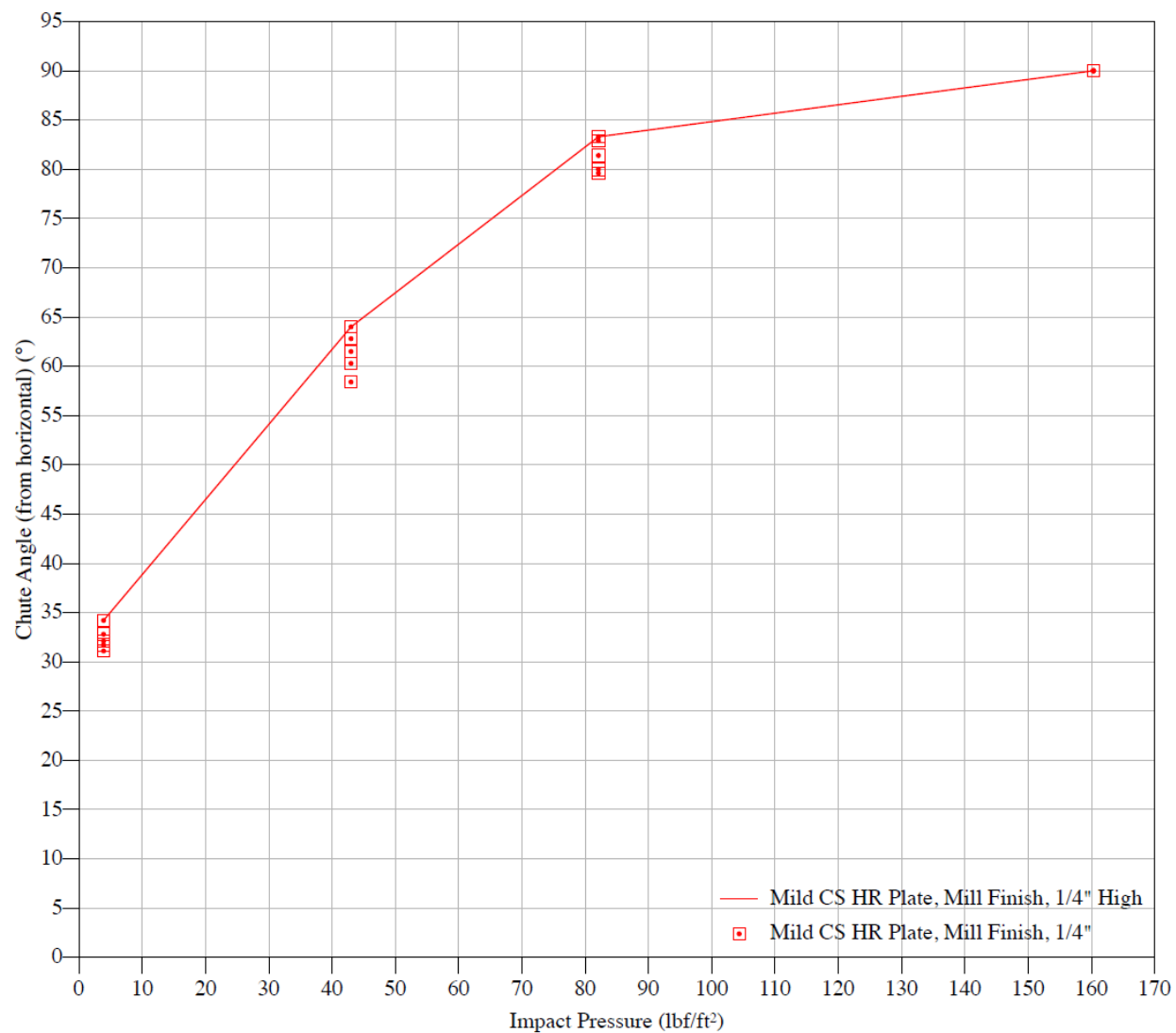


Figure C.58. SnO<sub>2</sub>: Chute curve with mild CS HR plate

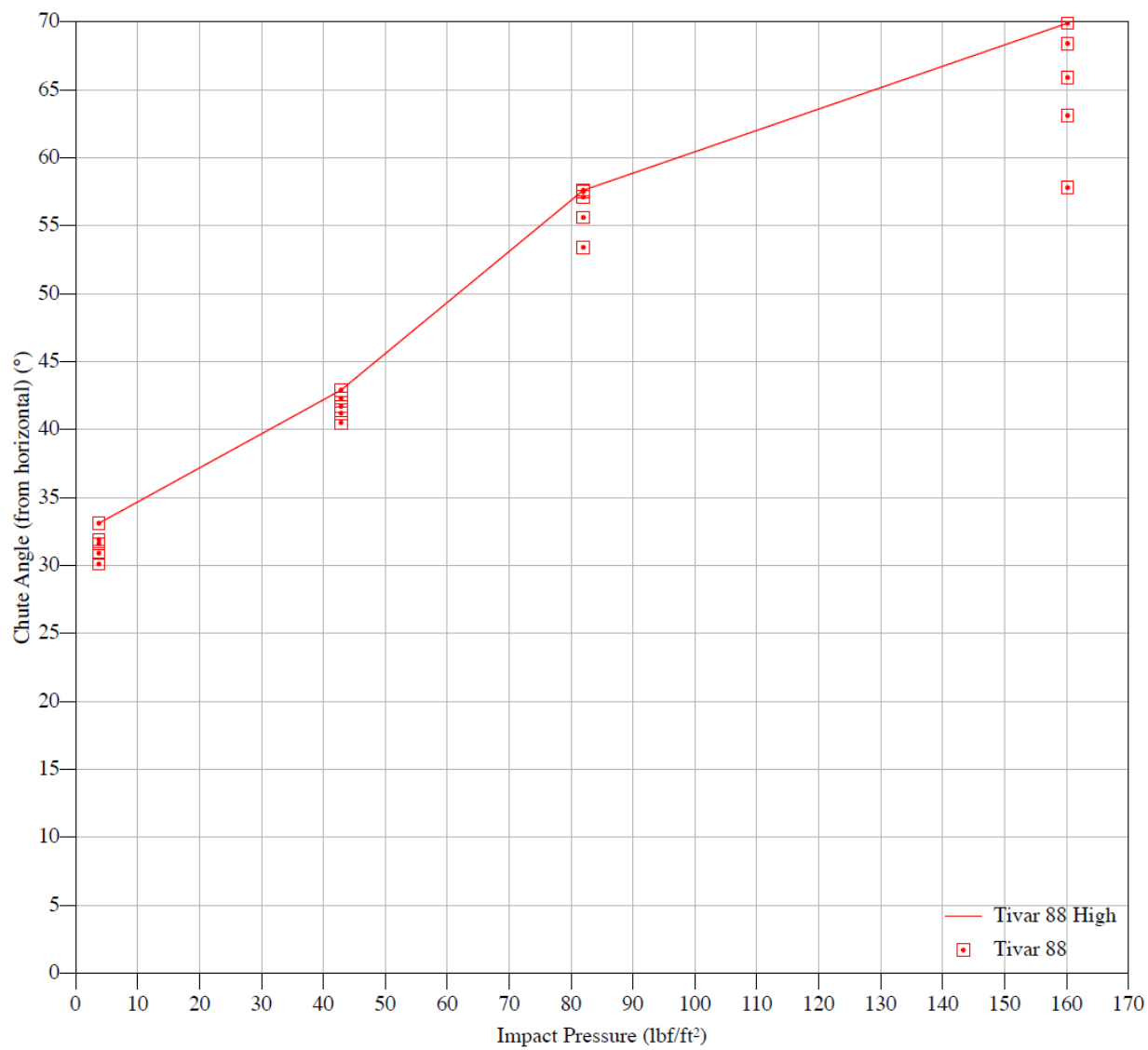


Figure C.59. SnO<sub>2</sub>: Chute curve with TIVAR 88

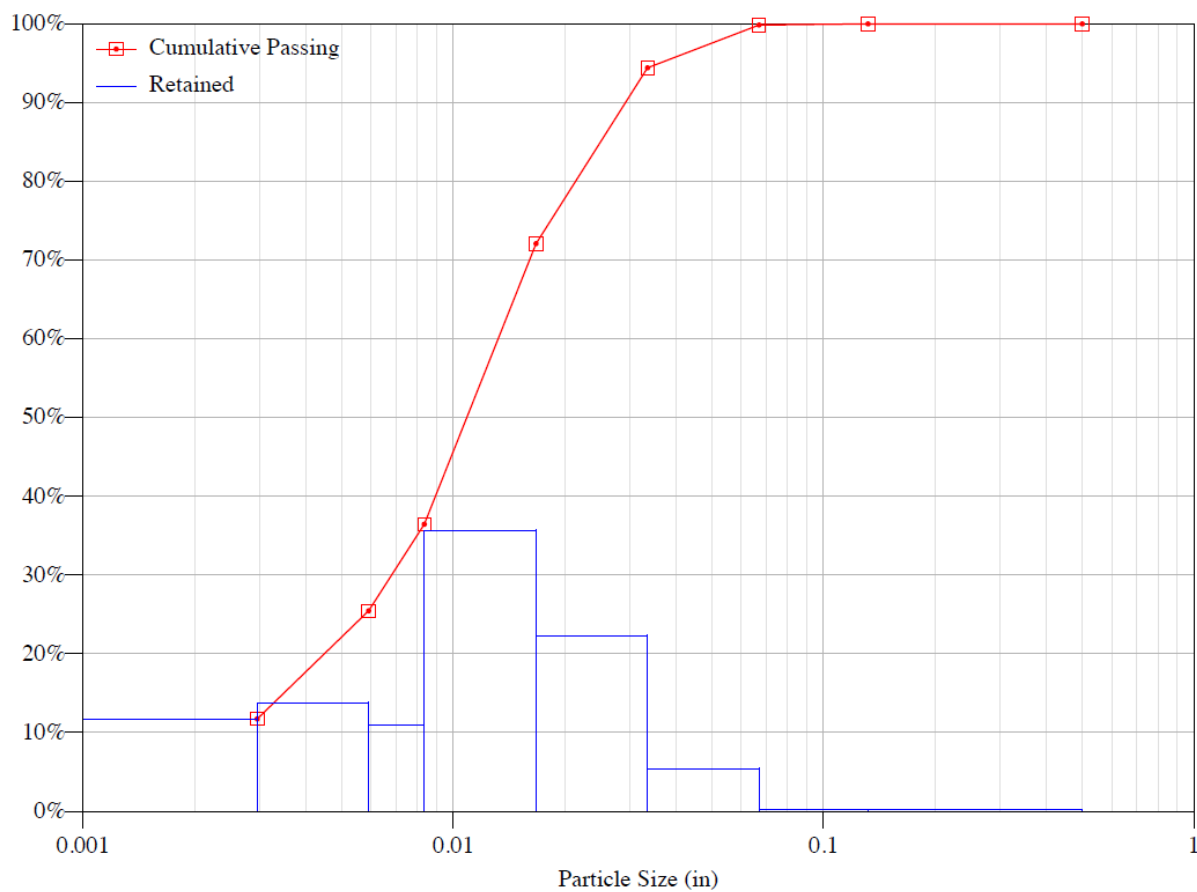


Figure C.60. SnO<sub>2</sub>: Particle size distribution by mass (after sieving)

## C.5 LAW batch #1a properties

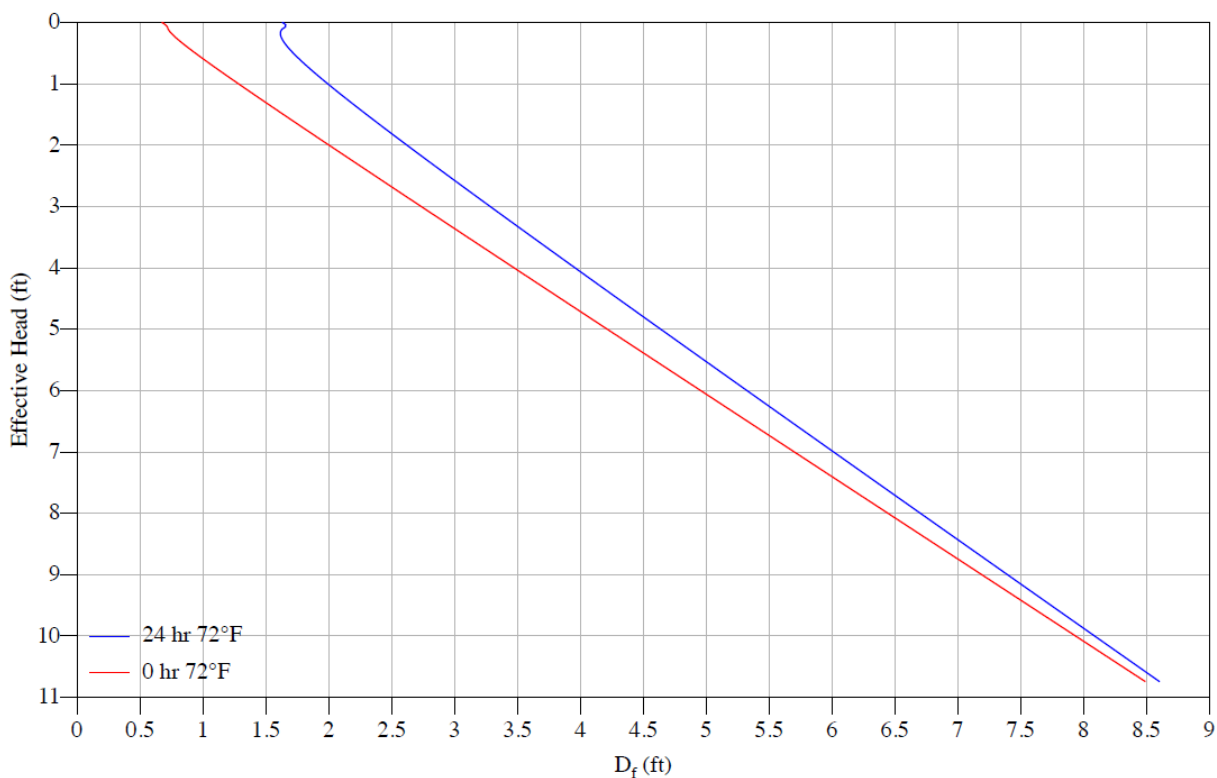


Figure C.61. Batch #1a: Critical rathole dimensions



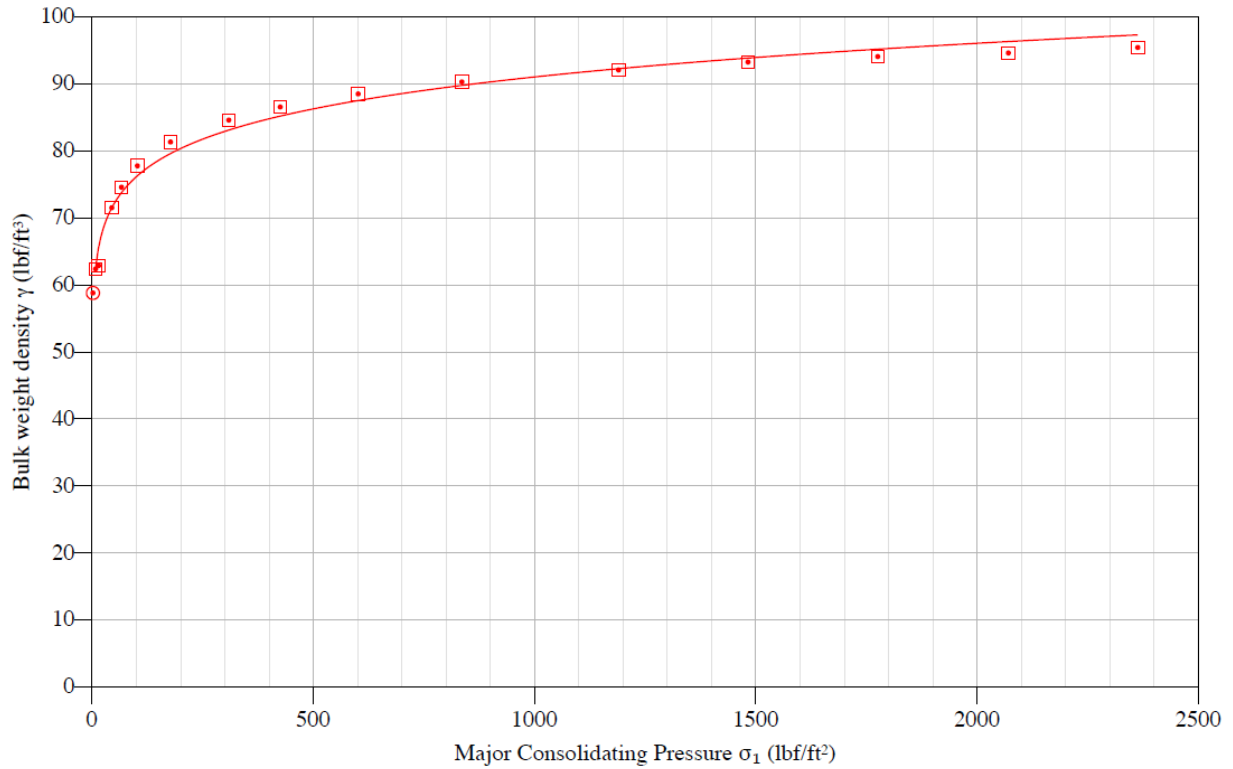


Figure C.62. Batch #1a: Compressibility curve

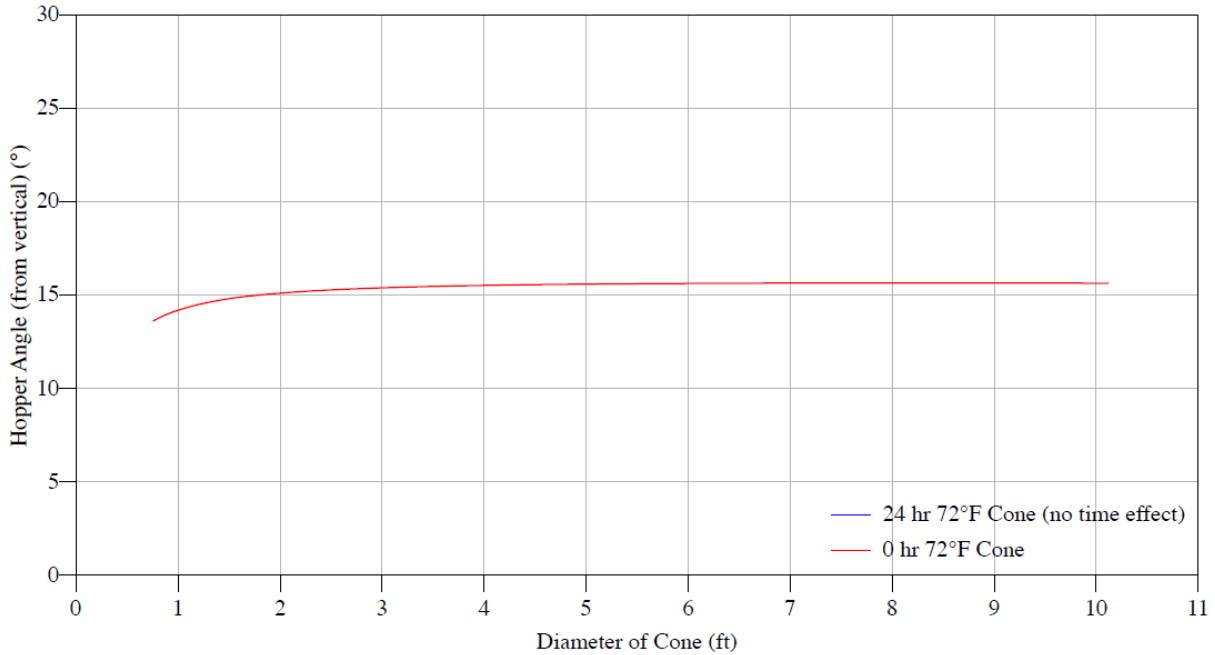


Figure C.63. Batch #1a: Conical hopper angles with 304 SS sheet

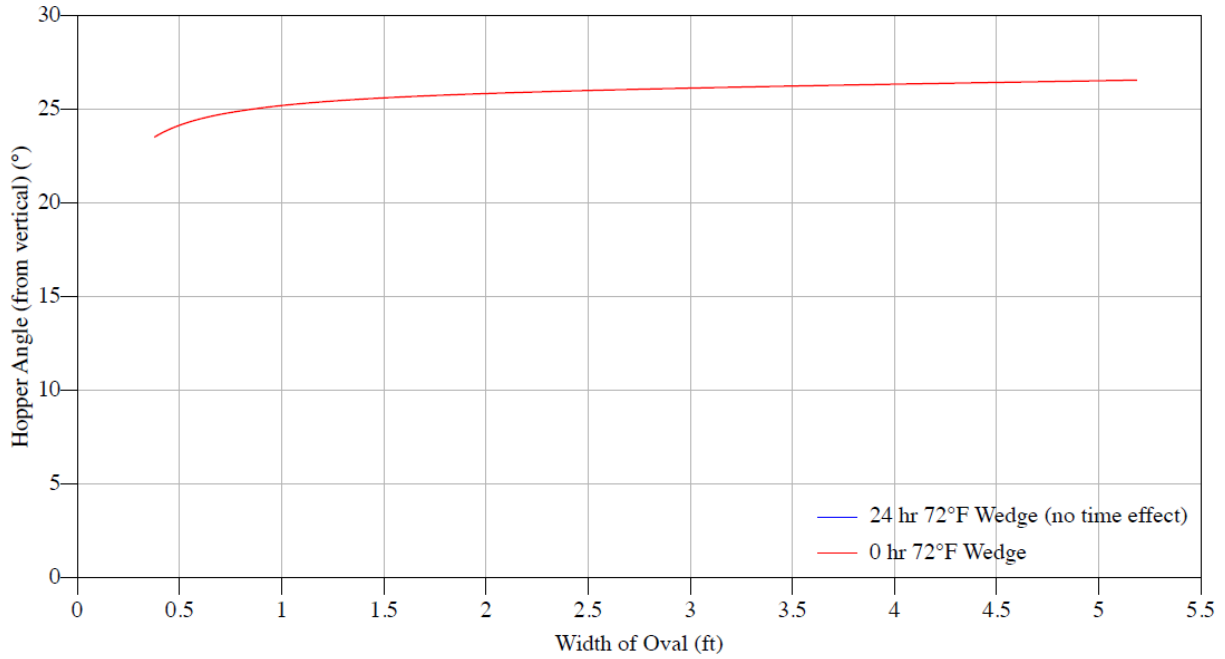


Figure C.64. Batch #1a: Wedge hopper angles with 304 SS sheet

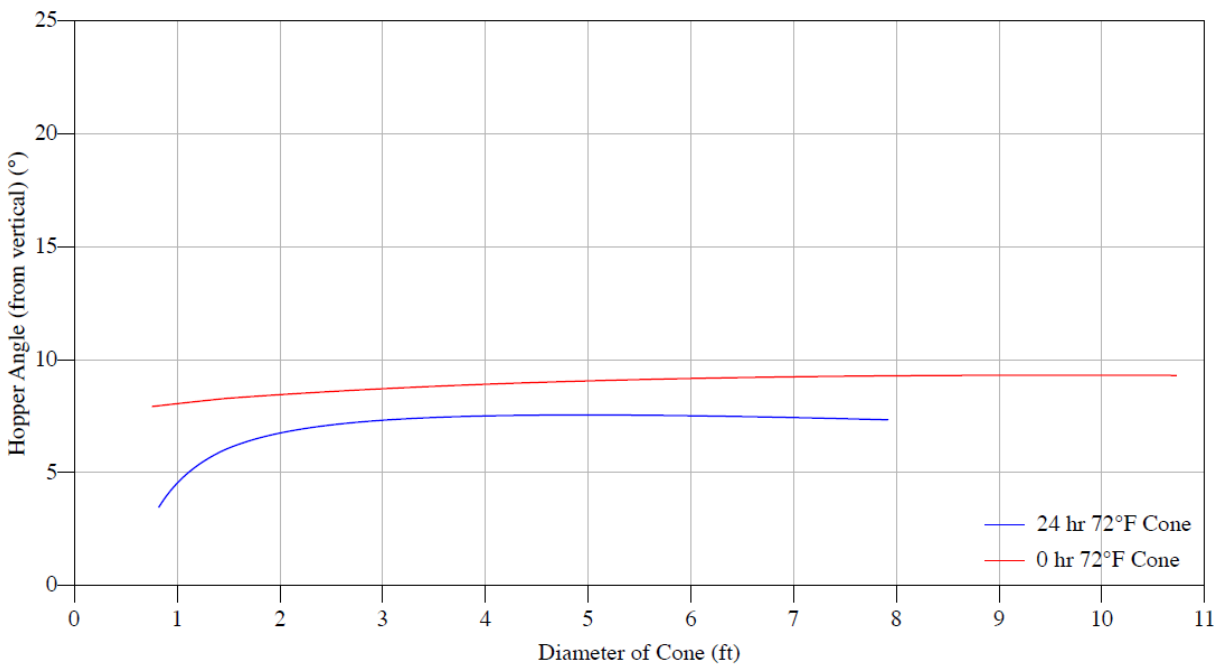


Figure C.65. Batch #1a: Conical hopper angles with mild CS HR plate

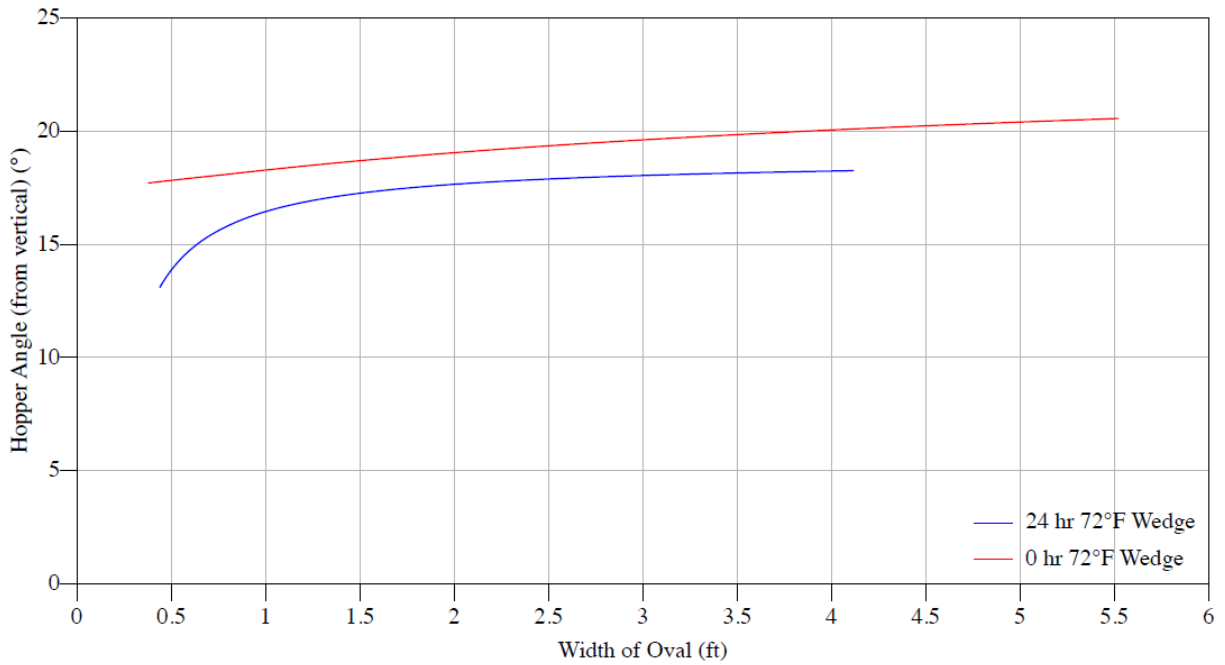


Figure C.66. Batch #1a: Wedge hopper angles with mild CS HR plate

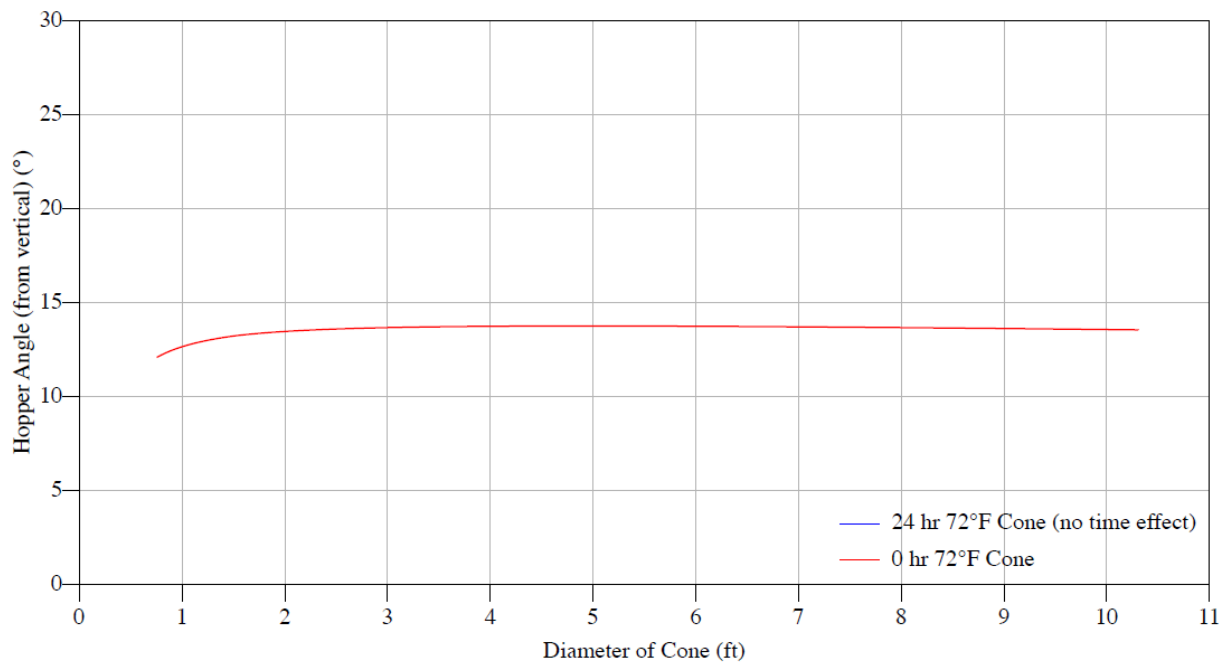


Figure C.67. Batch #1a: Conical hopper angles with TIVAR 88

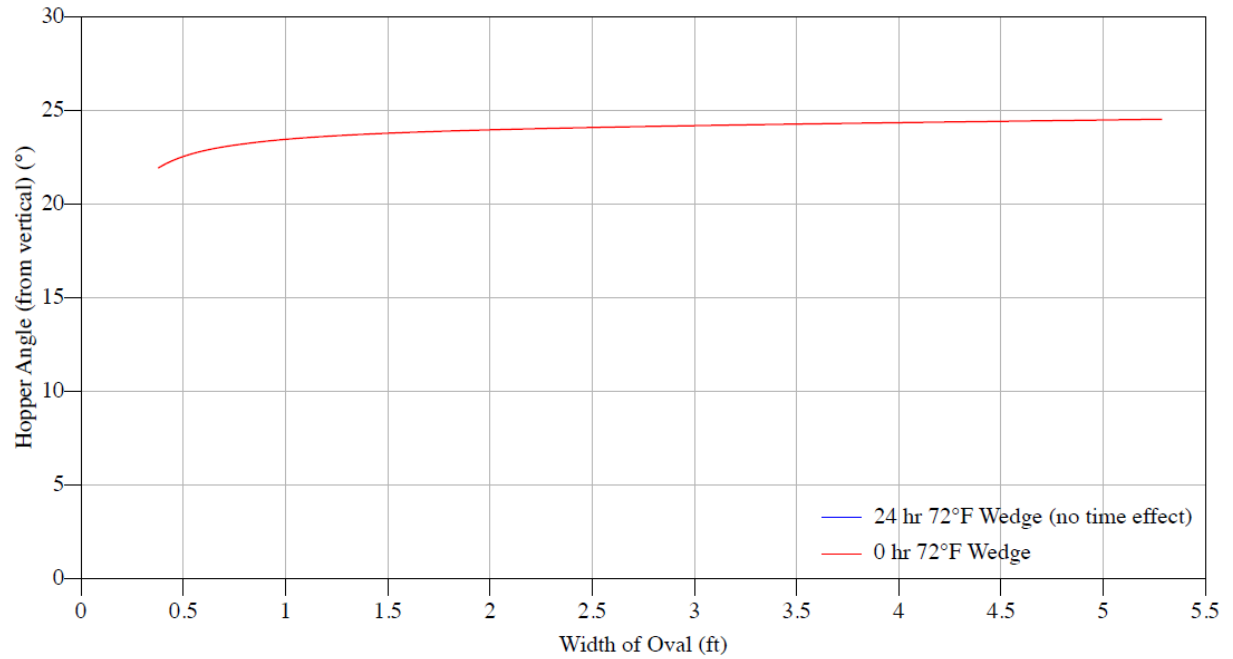


Figure C.68. Batch #1a: Wedge hopper angles with TIVAR 88

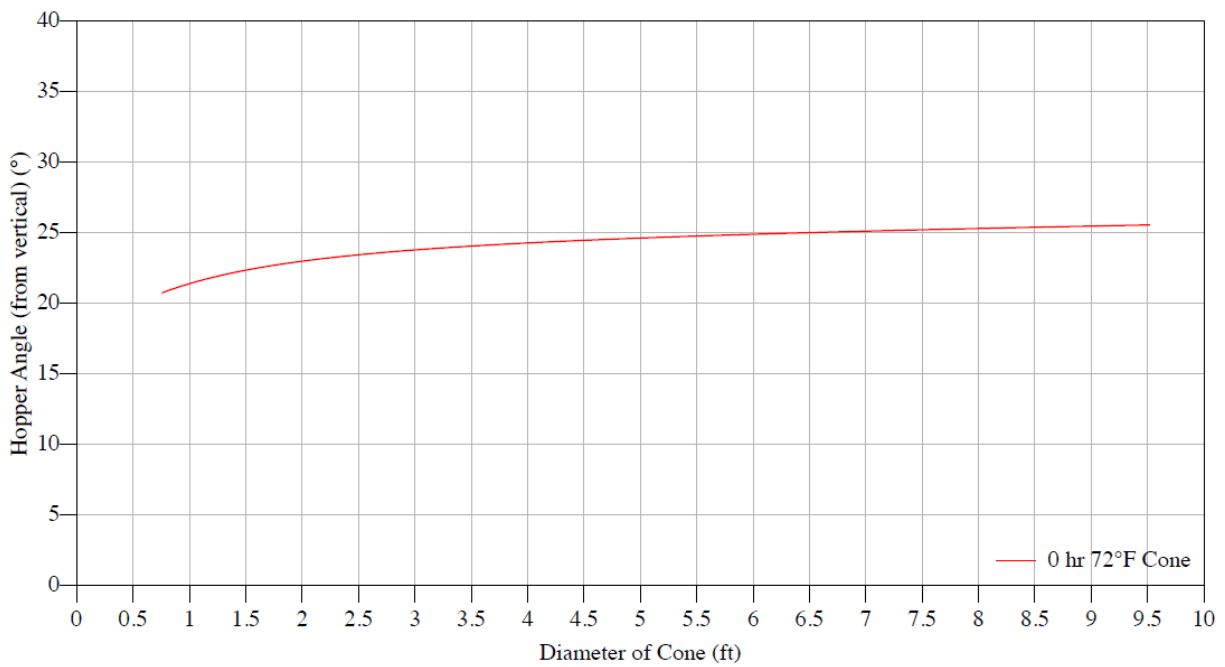


Figure C.69. Batch #1a: Conical hopper angles with TIVAR 88-2 Lorien

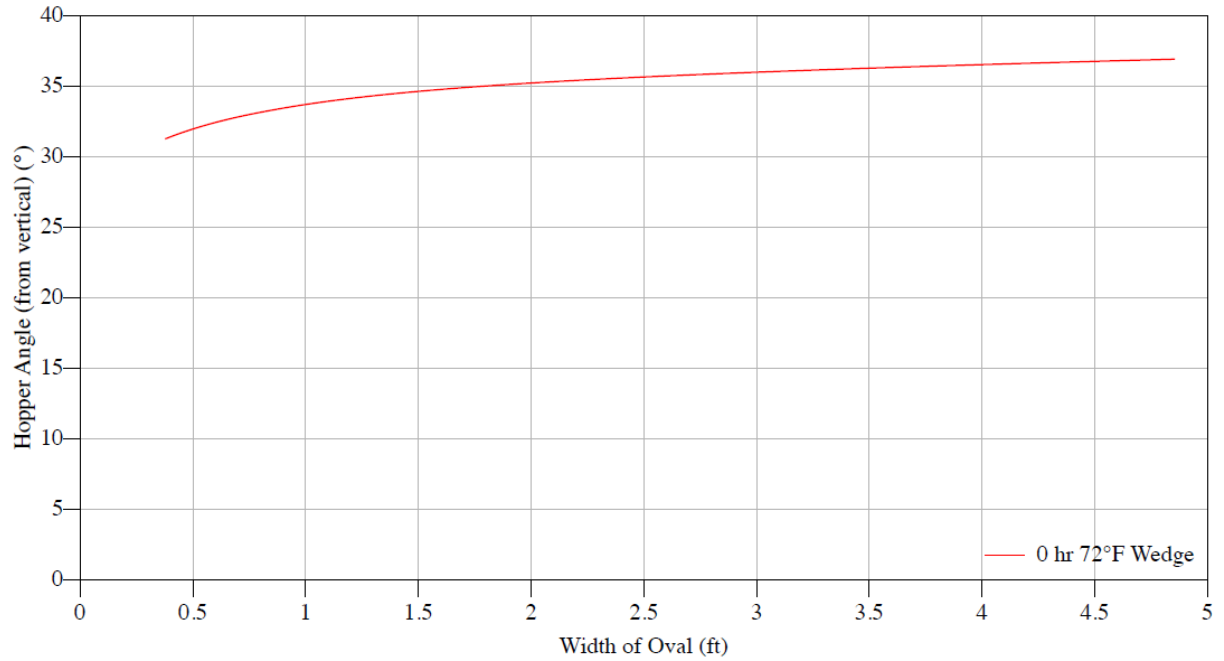


Figure C.70. Batch #1a: Wedge hopper angles with TIVAR 88-2 Lorien

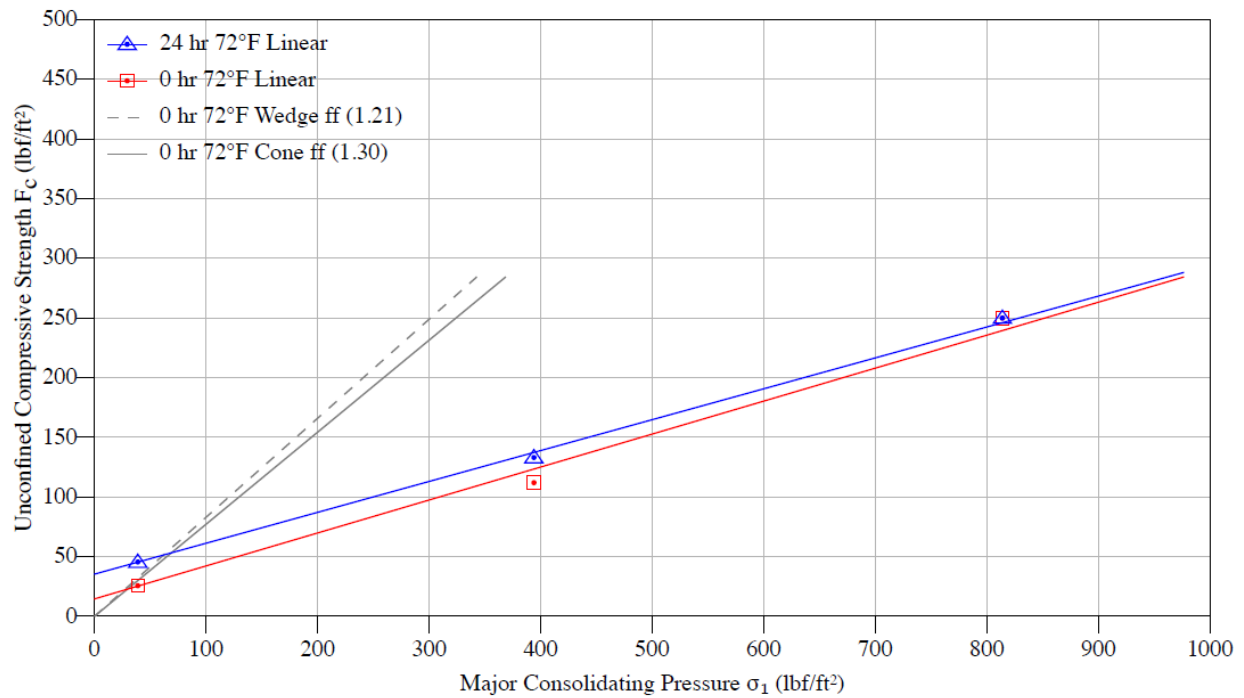


Figure C.71. Batch #1a: Flow function

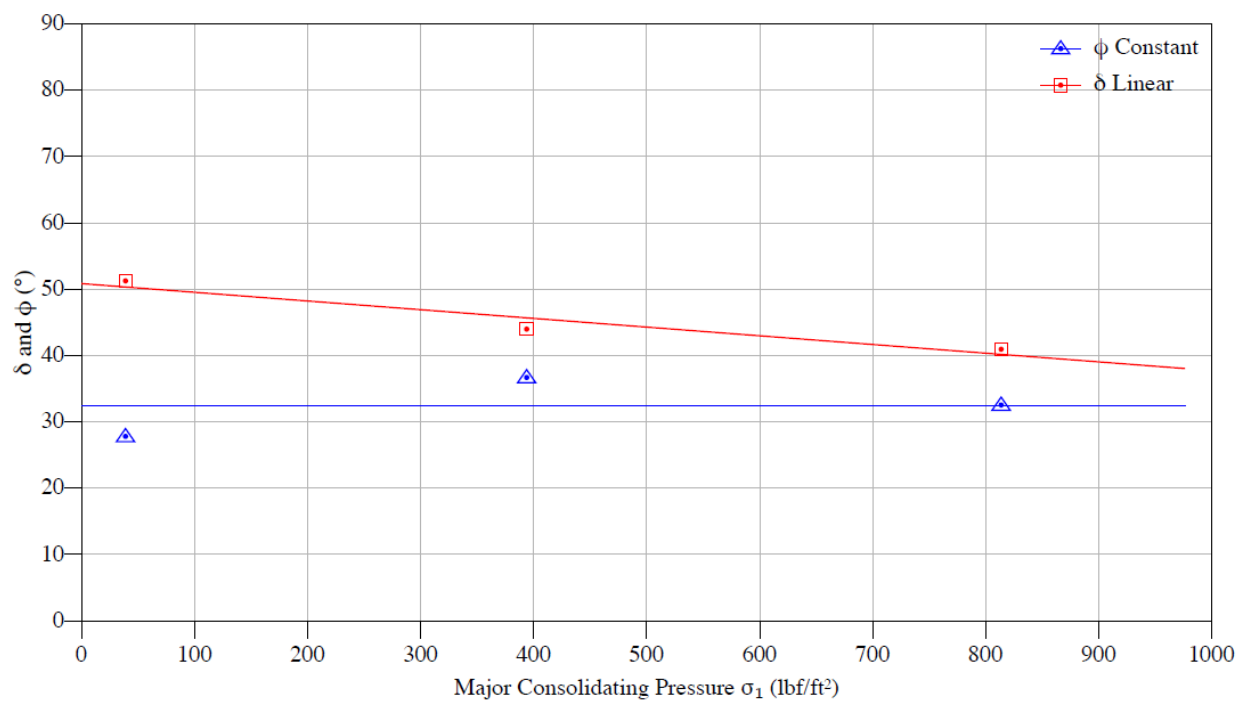


Figure C.72. Batch #1a: Effective angle of friction ( $\delta$ ) and kinematic angle of internal friction ( $\phi$ )

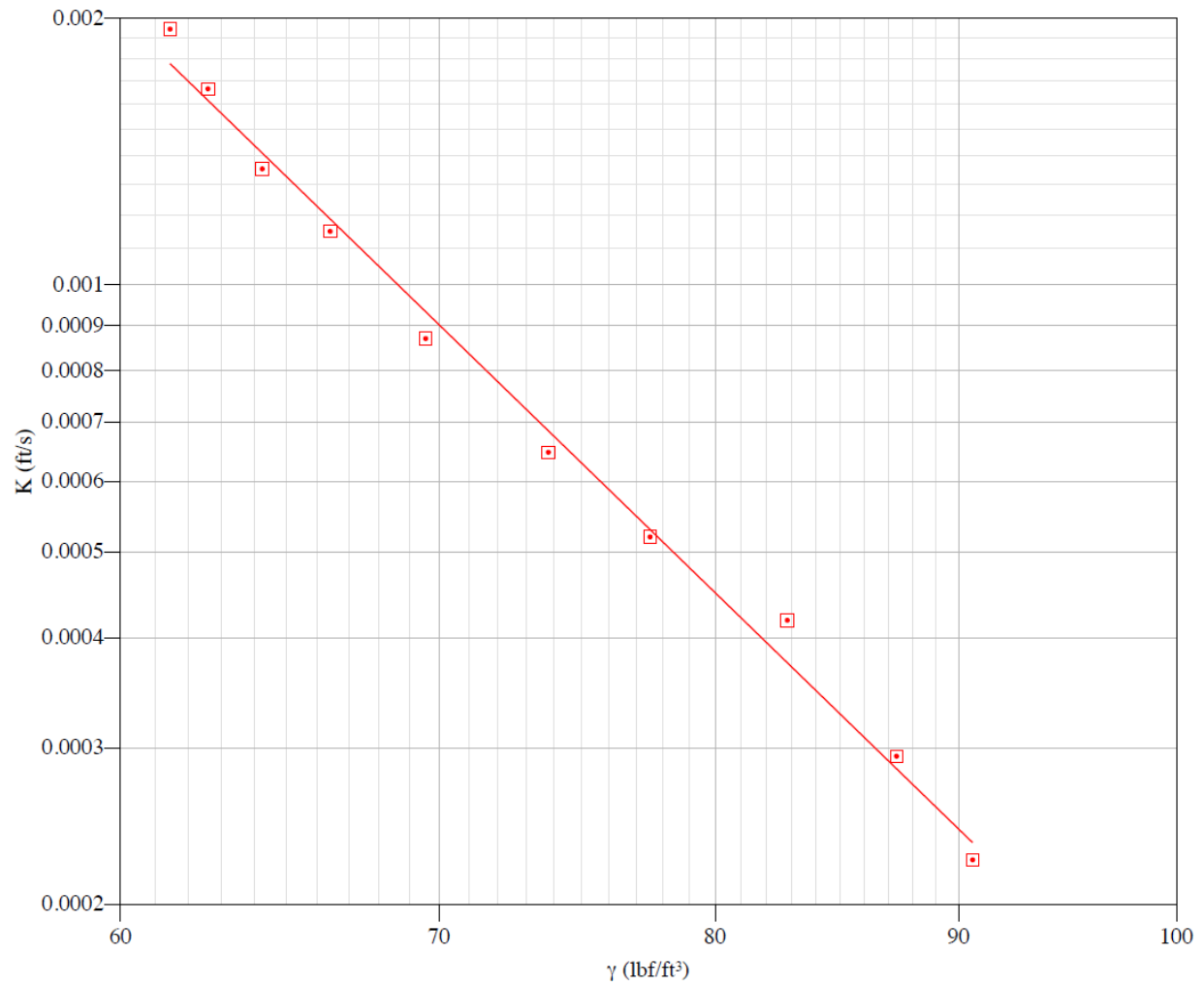


Figure C.73. Batch #1a: Permeability curve

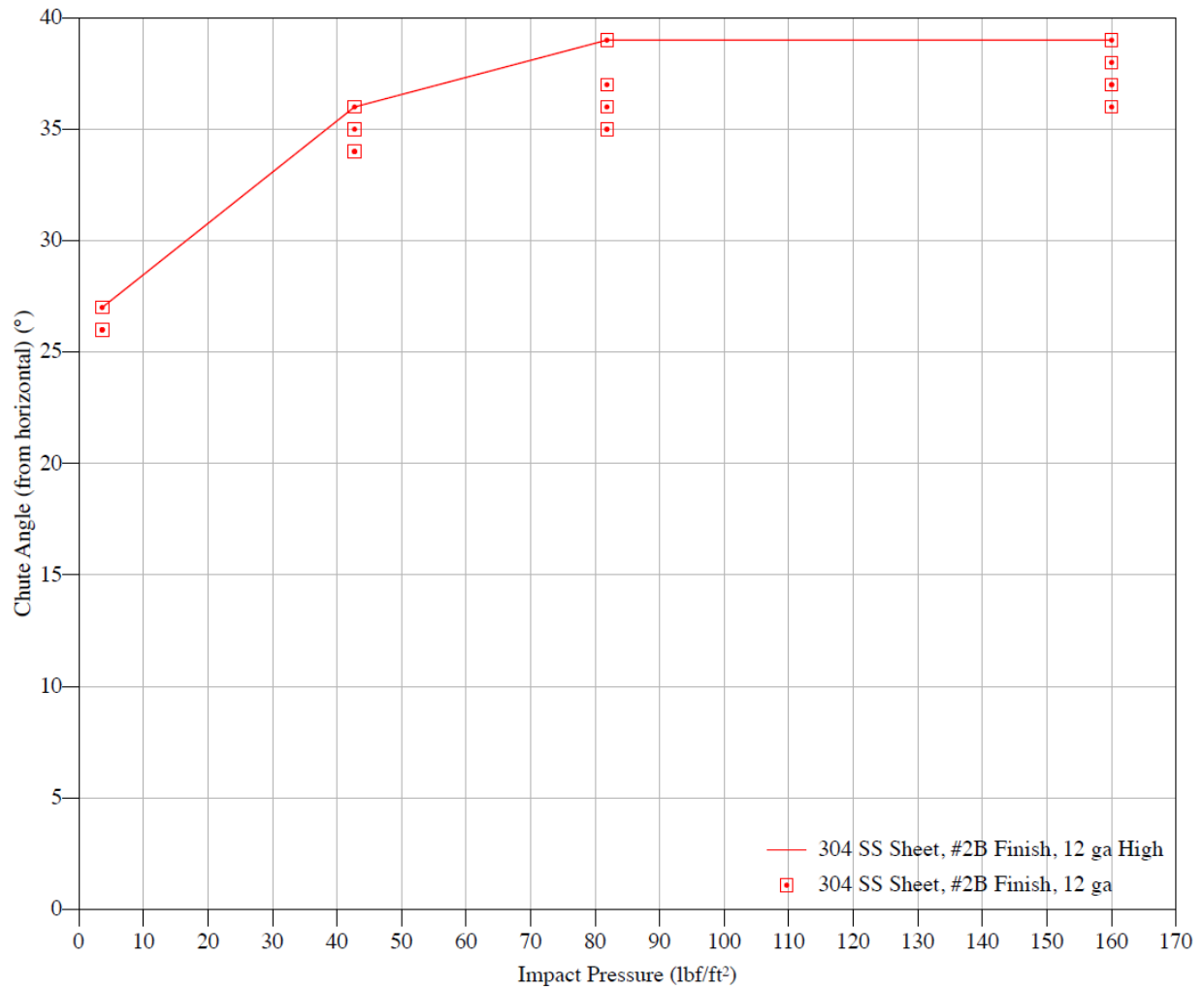


Figure C.74. Batch #1a: Chute curve with 304 SS sheet



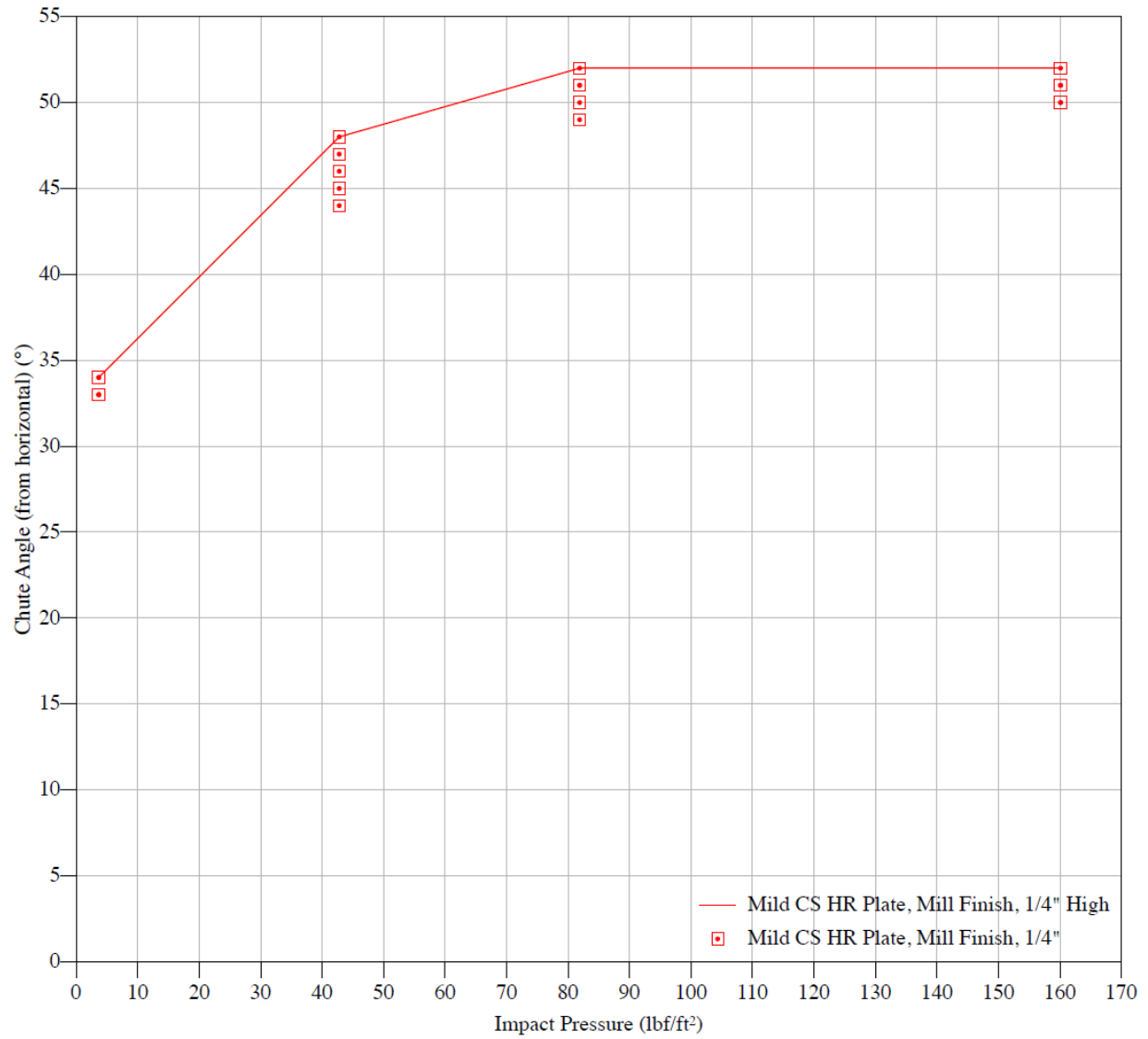


Figure C.75. Batch #1a: Chute curve with mild CS HR plate

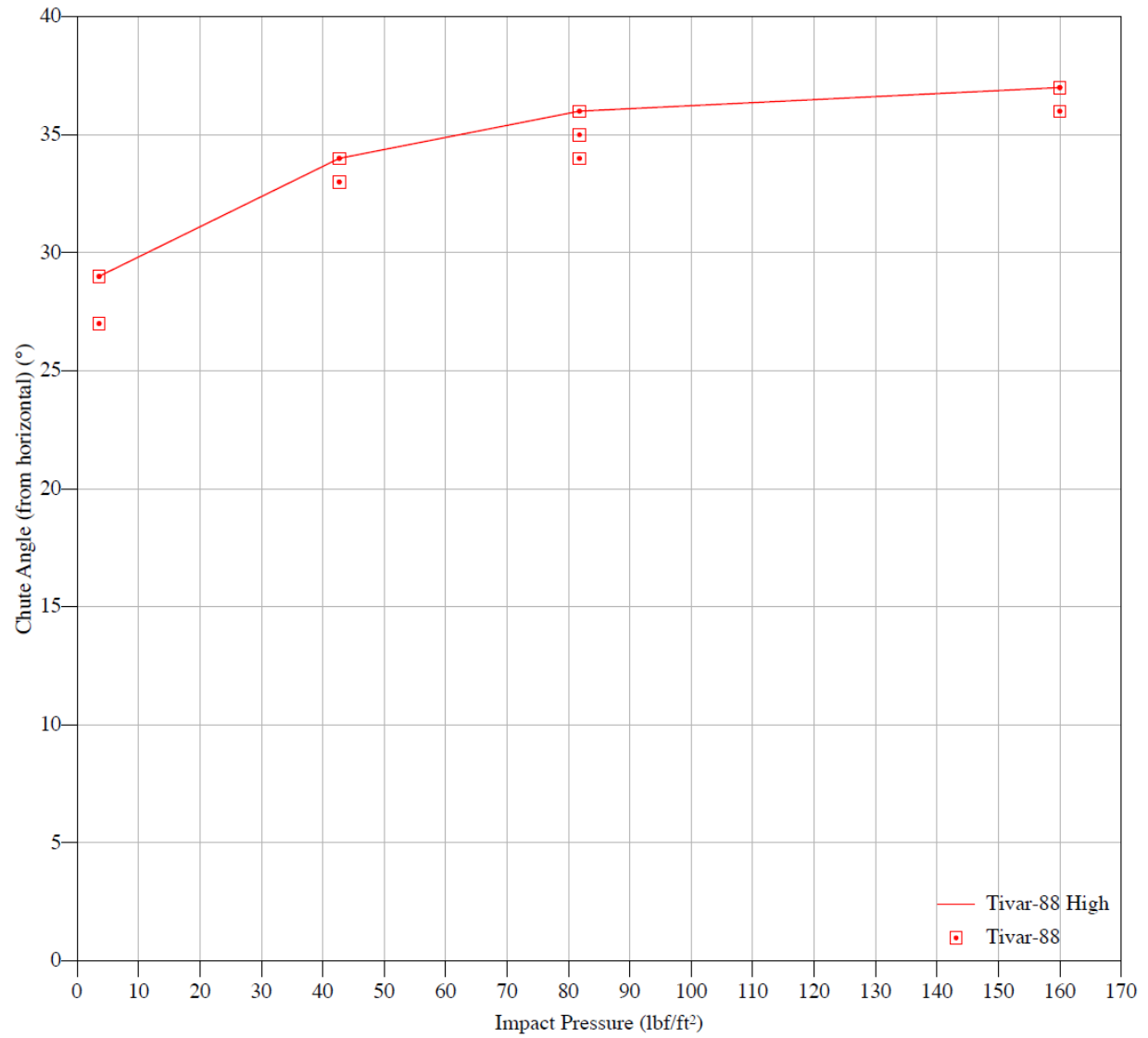


Figure C.76. Batch #1a: Chute curve with TIVAR 88

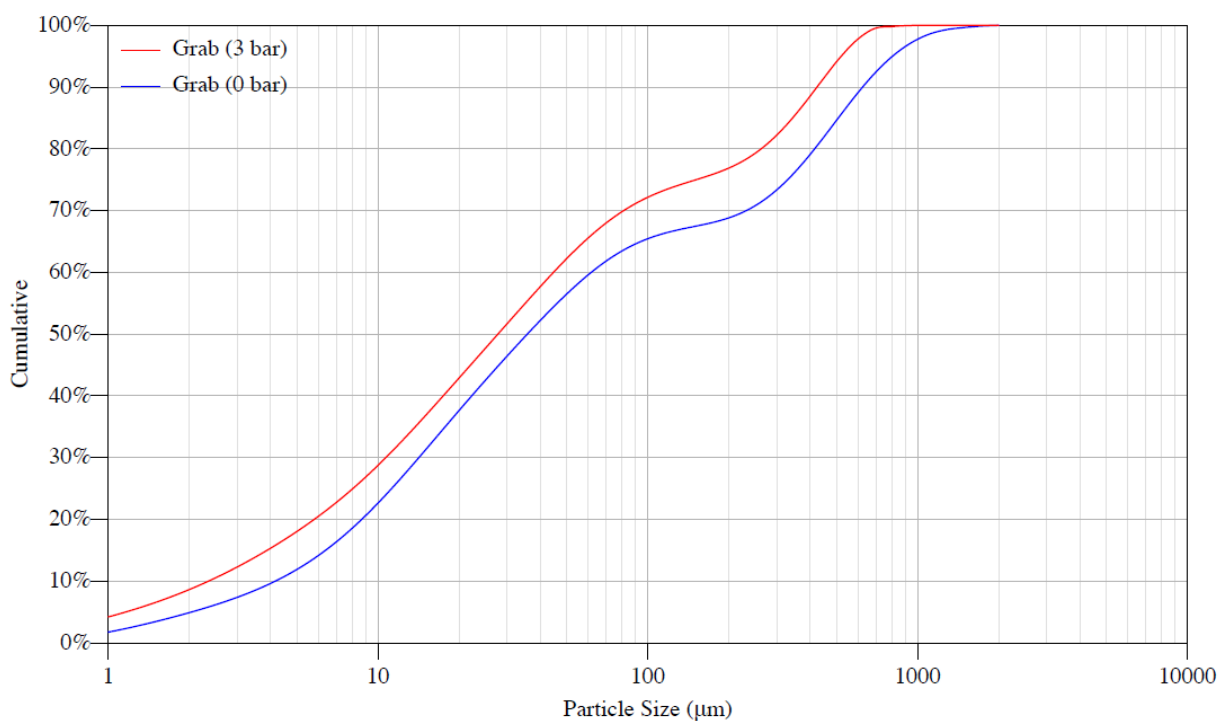
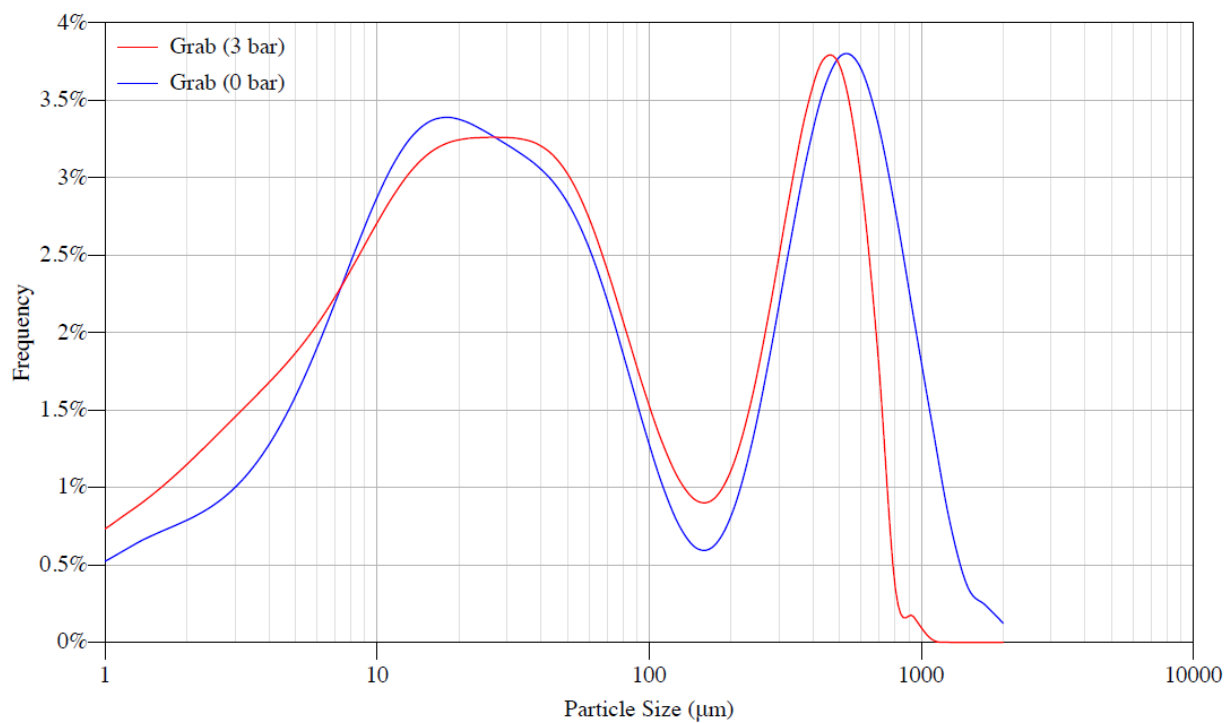


Figure C.77. Batch #1a: Particle size distribution by volume and pressure

## C.6 LAW batch #6a properties

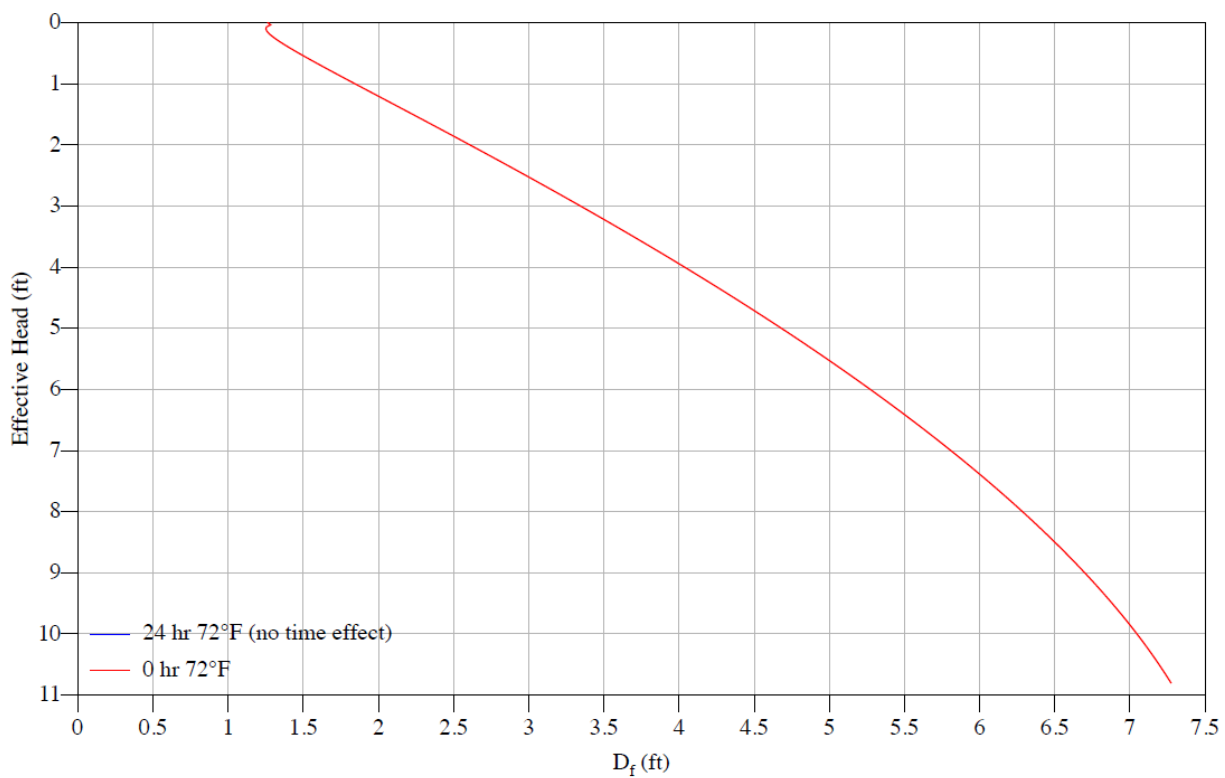


Figure C.78. Batch #6a: Critical rathole dimensions

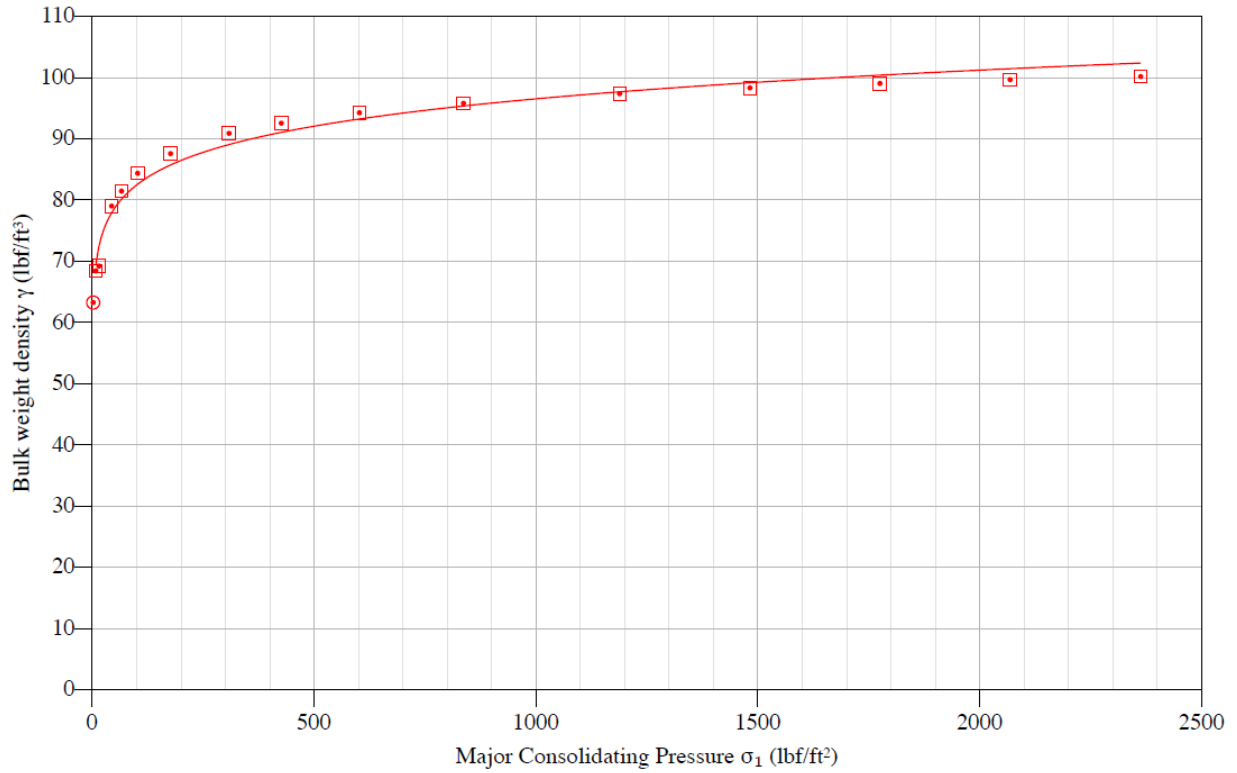


Figure C.79. Batch #6a: Compressibility curve

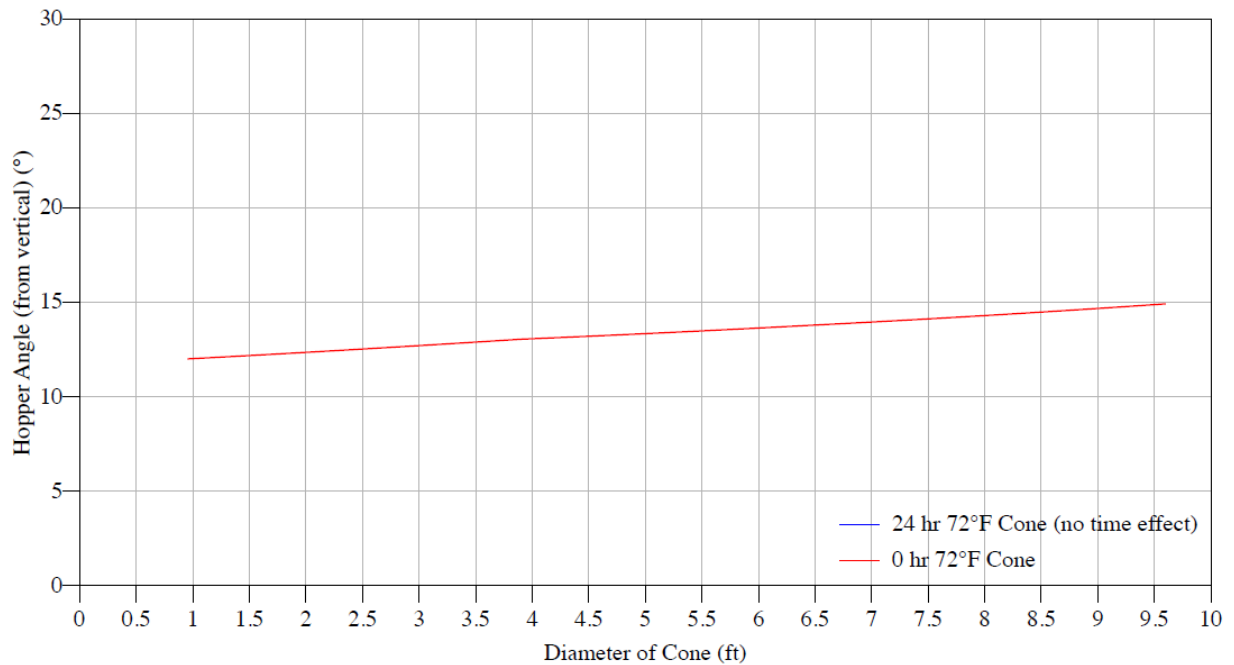


Figure C.80. Batch #6a: Conical hopper angles with 304 SS sheet

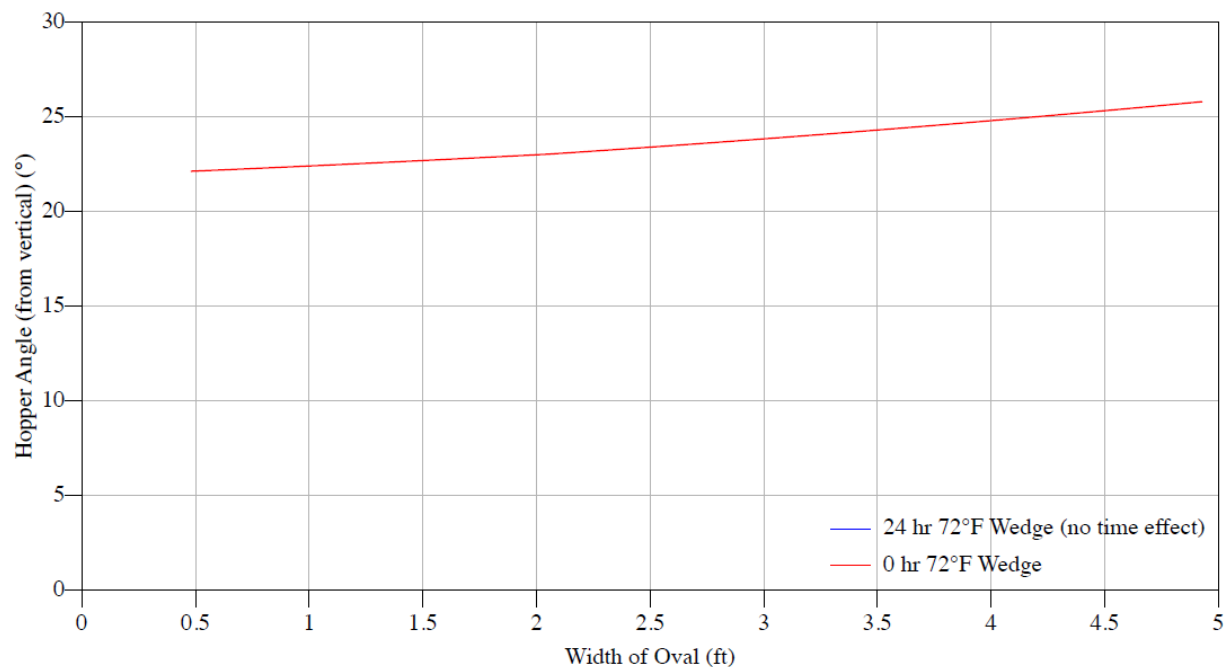


Figure C.81. Batch #6a: Wedge hopper angles with 304 SS sheet

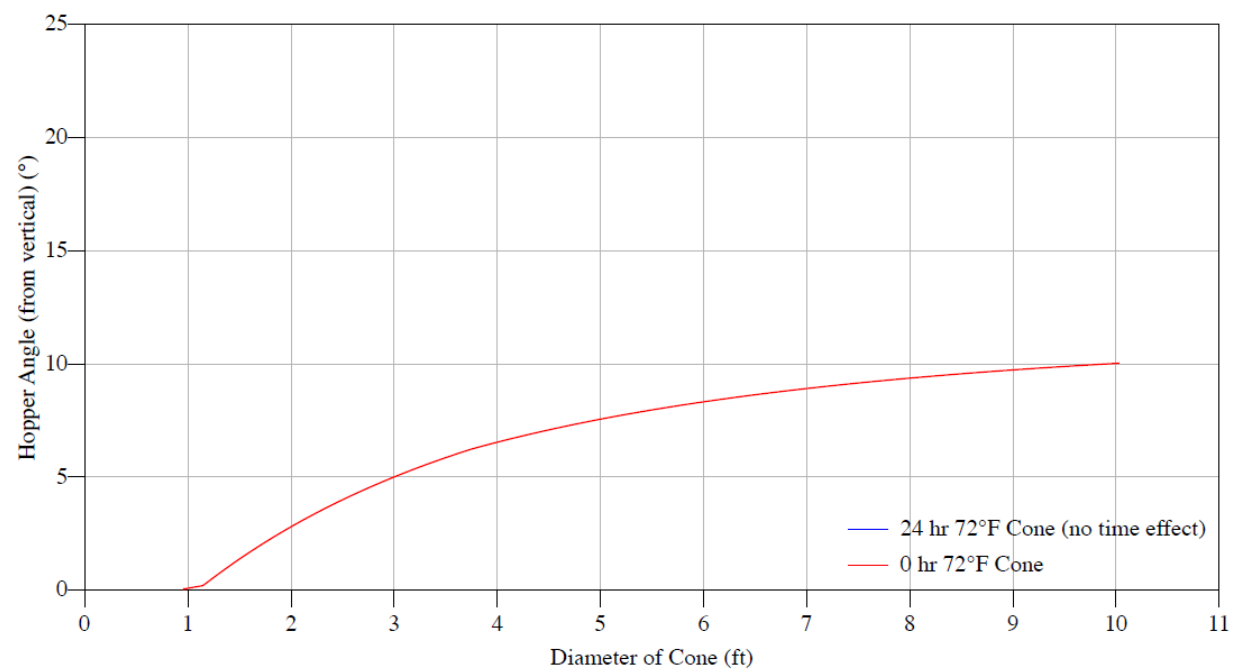


Figure C.82. Batch #6a: Conical hopper angles with mild CS HR plate

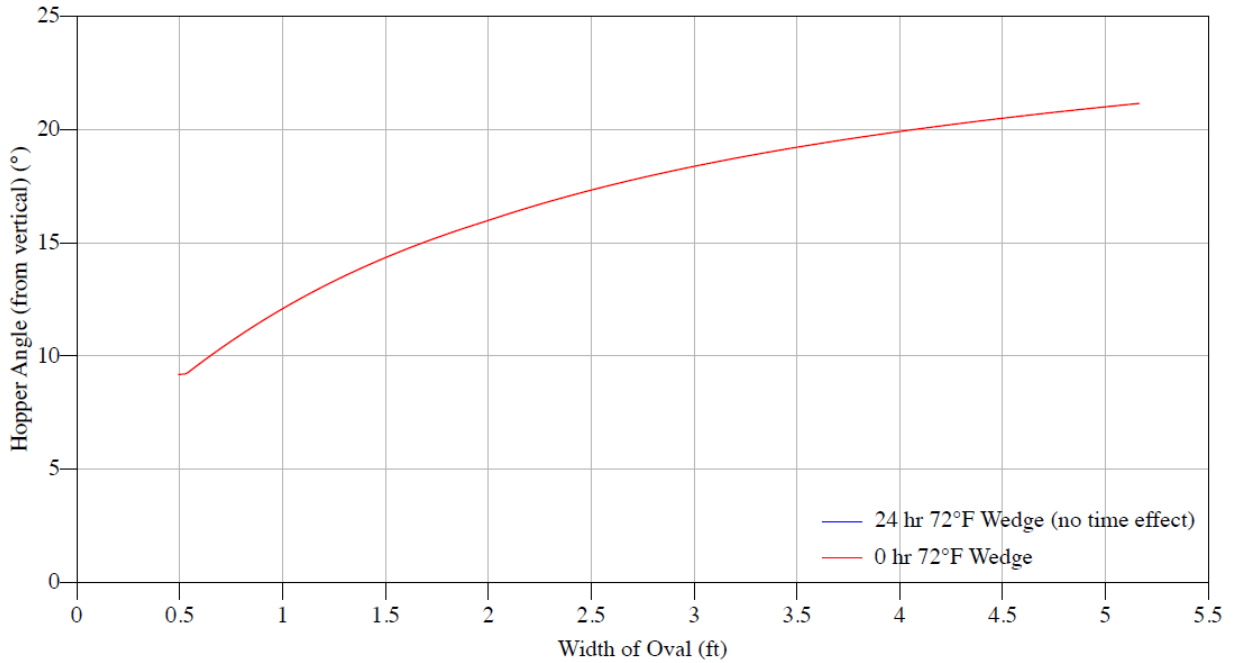


Figure C.83. Batch #6a: Wedge hopper angles with mild CS HR plate

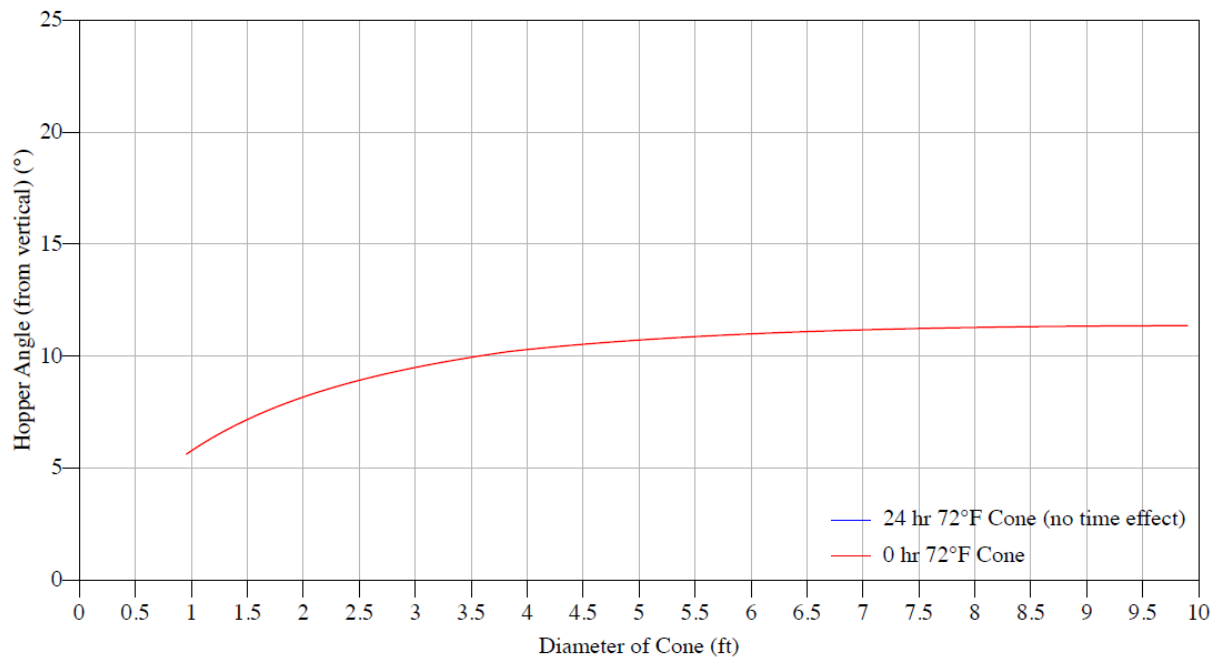


Figure C.84. Batch #6a: Conical hopper angles with TIVAR 88

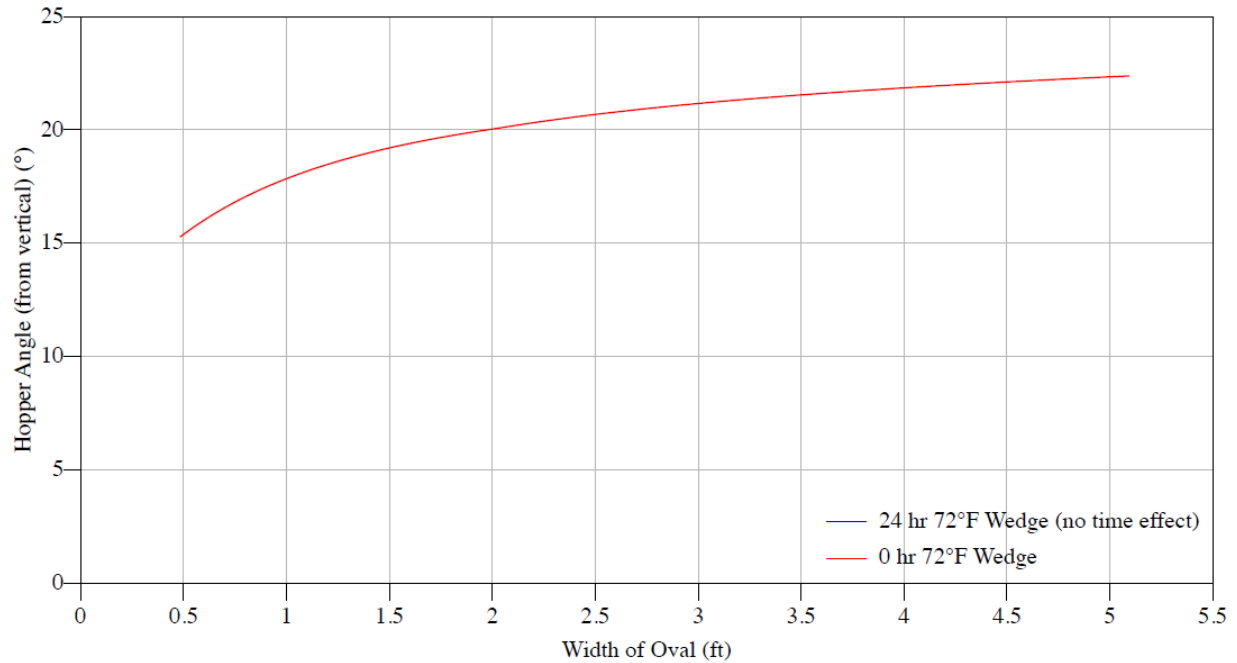


Figure C.85. Batch #6a: Wedge hopper angles with TIVAR 88

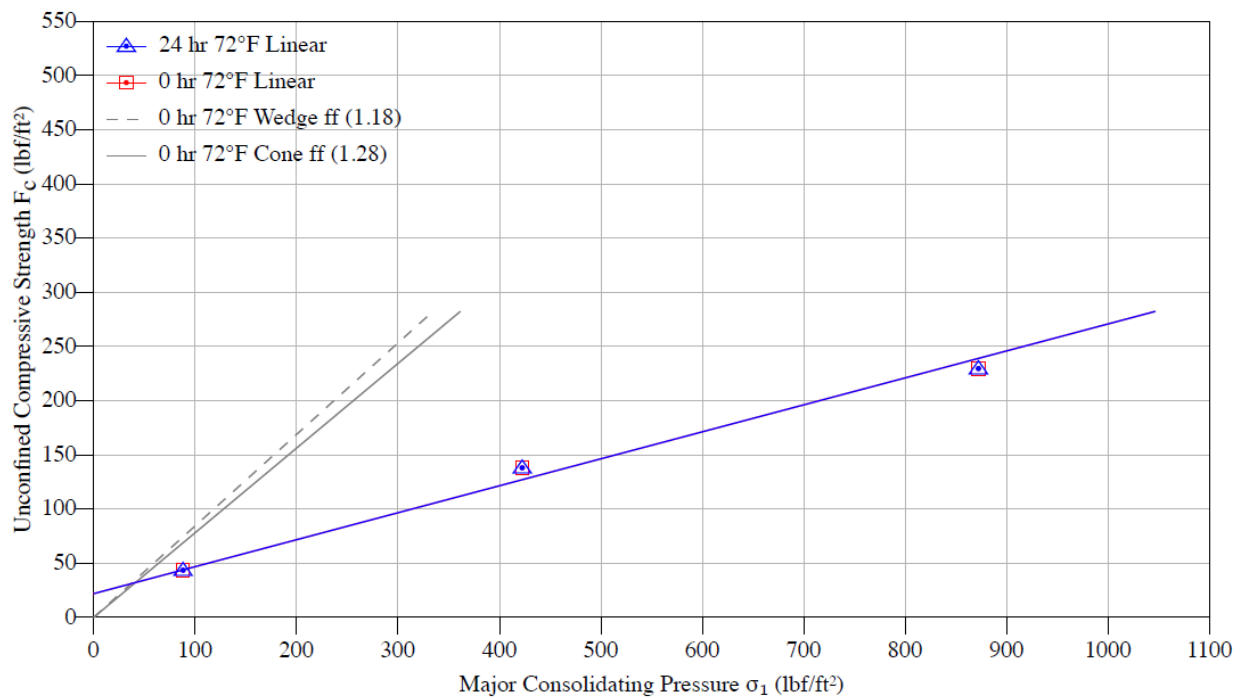


Figure C.86. Batch #6a: Flow function



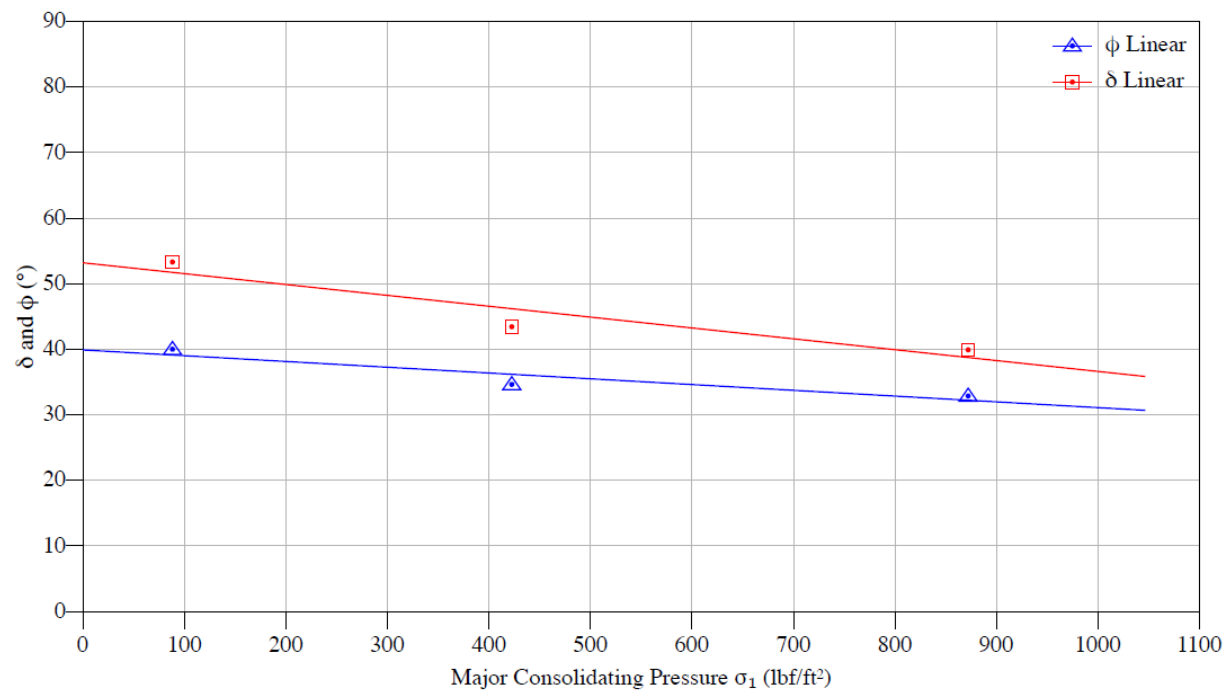


Figure C.87. Batch #6a: Effective angle of friction ( $\delta$ ) and kinematic angle of internal friction ( $\phi$ )

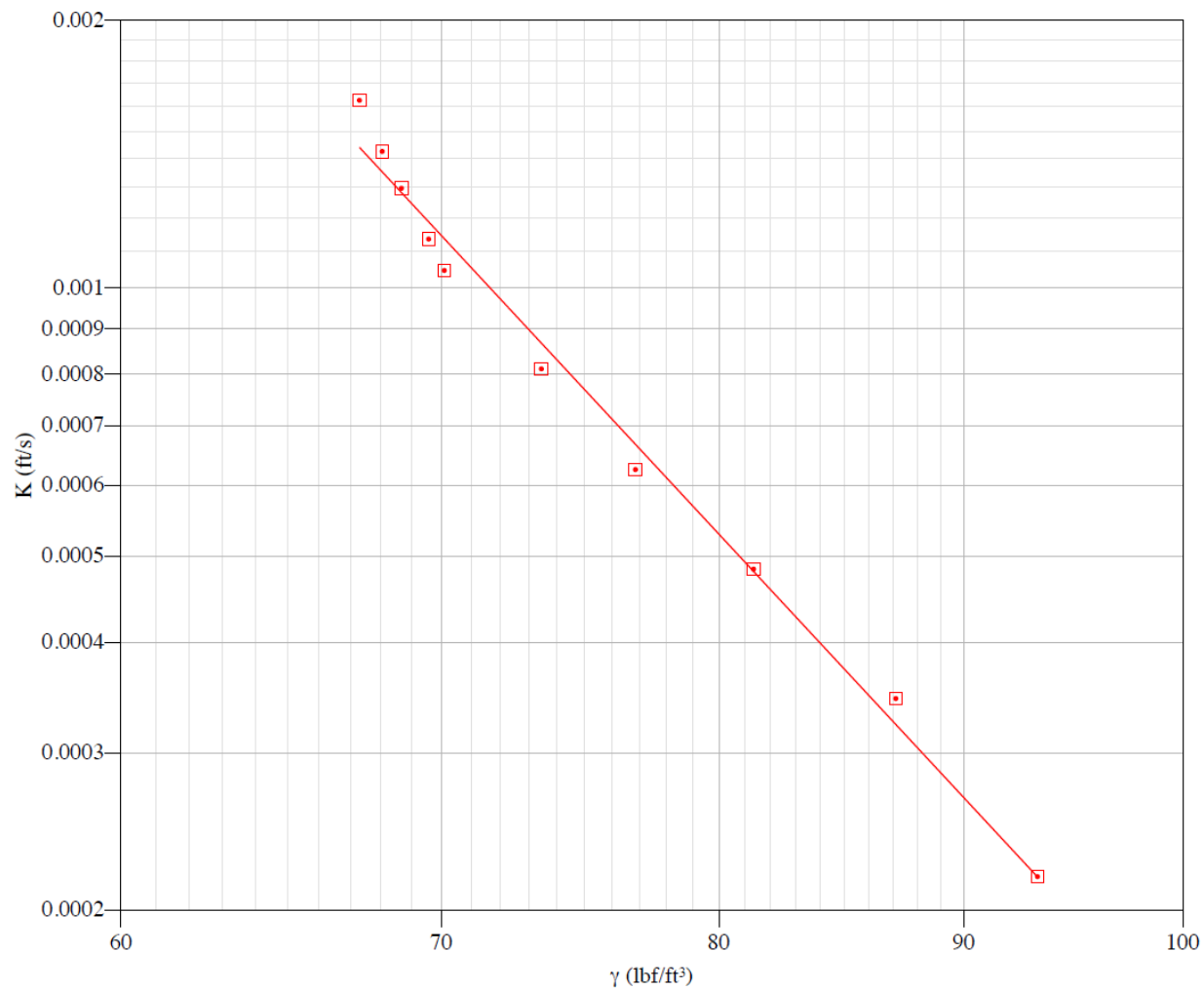


Figure C.88. Batch #6a: Permeability curve

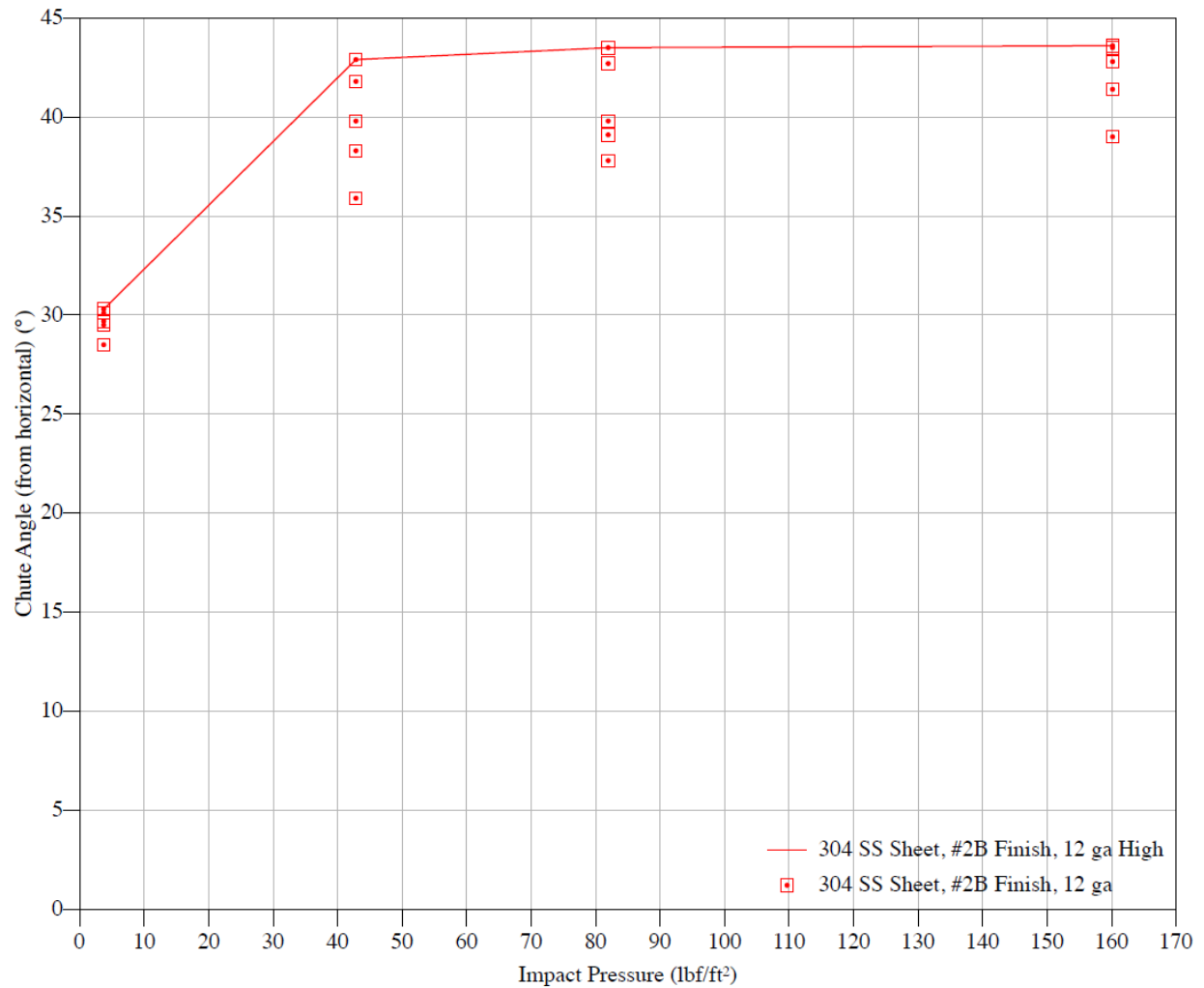


Figure C.89. Batch #6a: Chute curve with 304 SS sheet

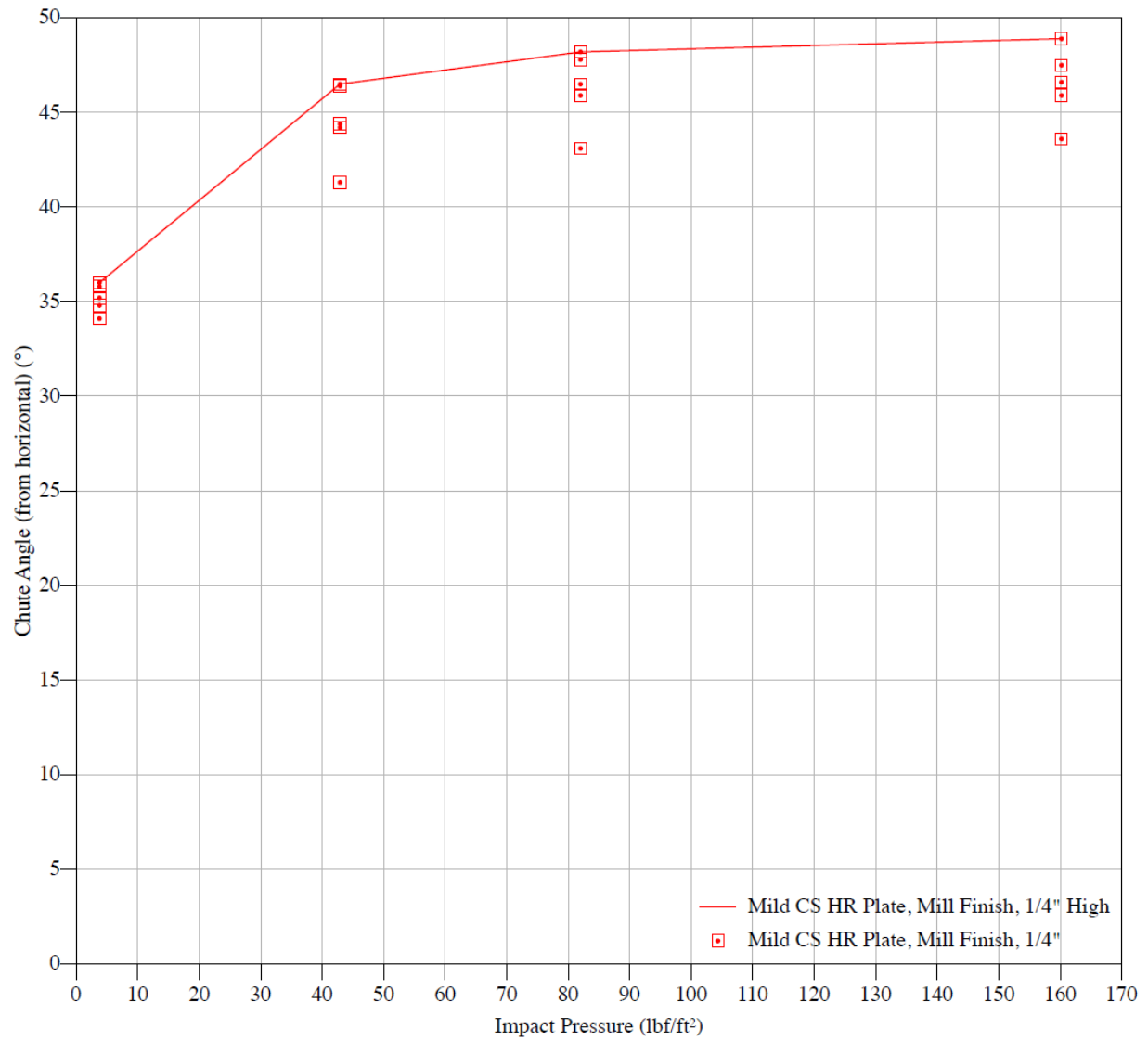


Figure C.90. Batch #6a: Chute curve with mild CS HR plate

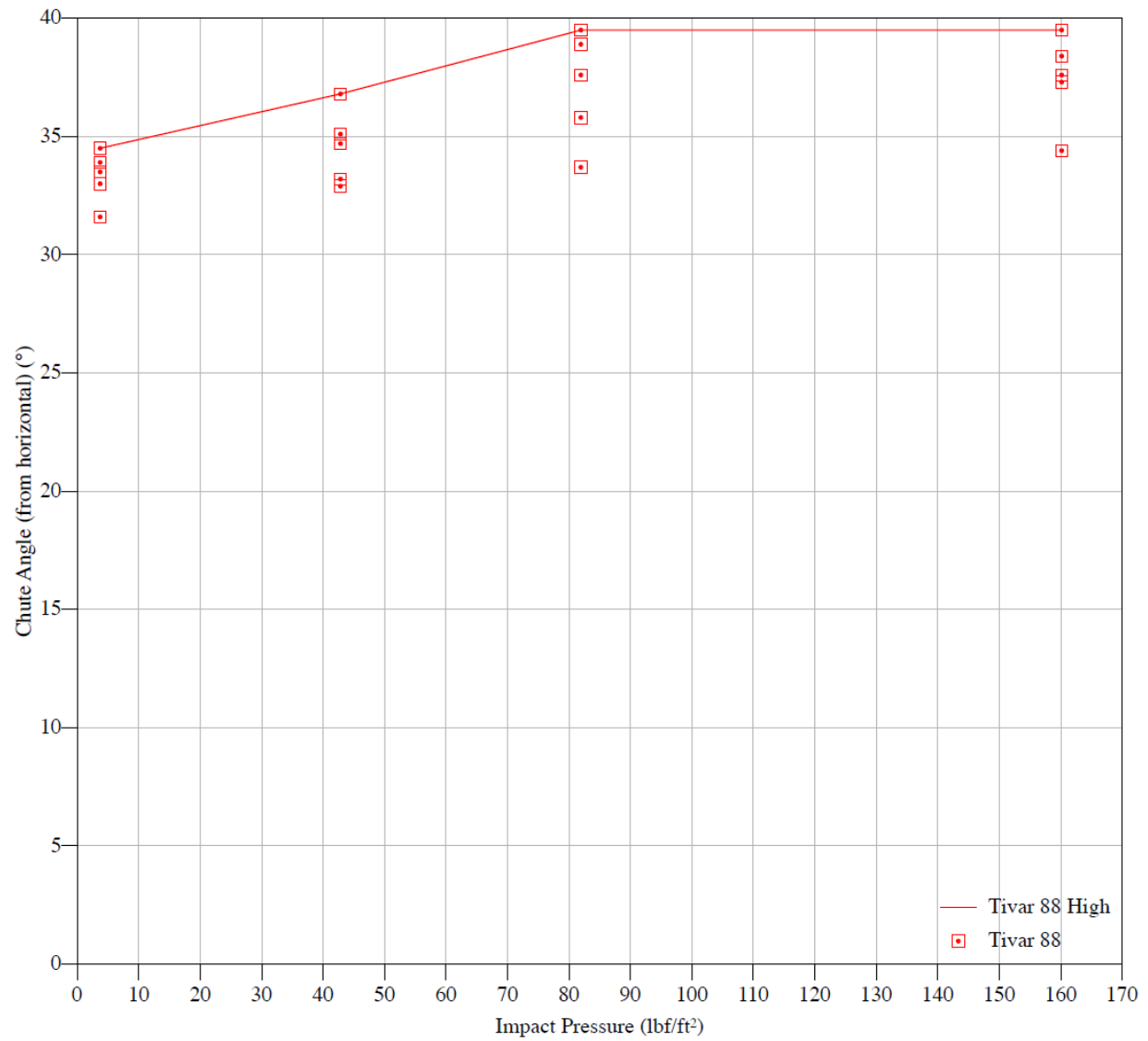


Figure C.91. Batch #6a: Chute curve with TIVAR 88

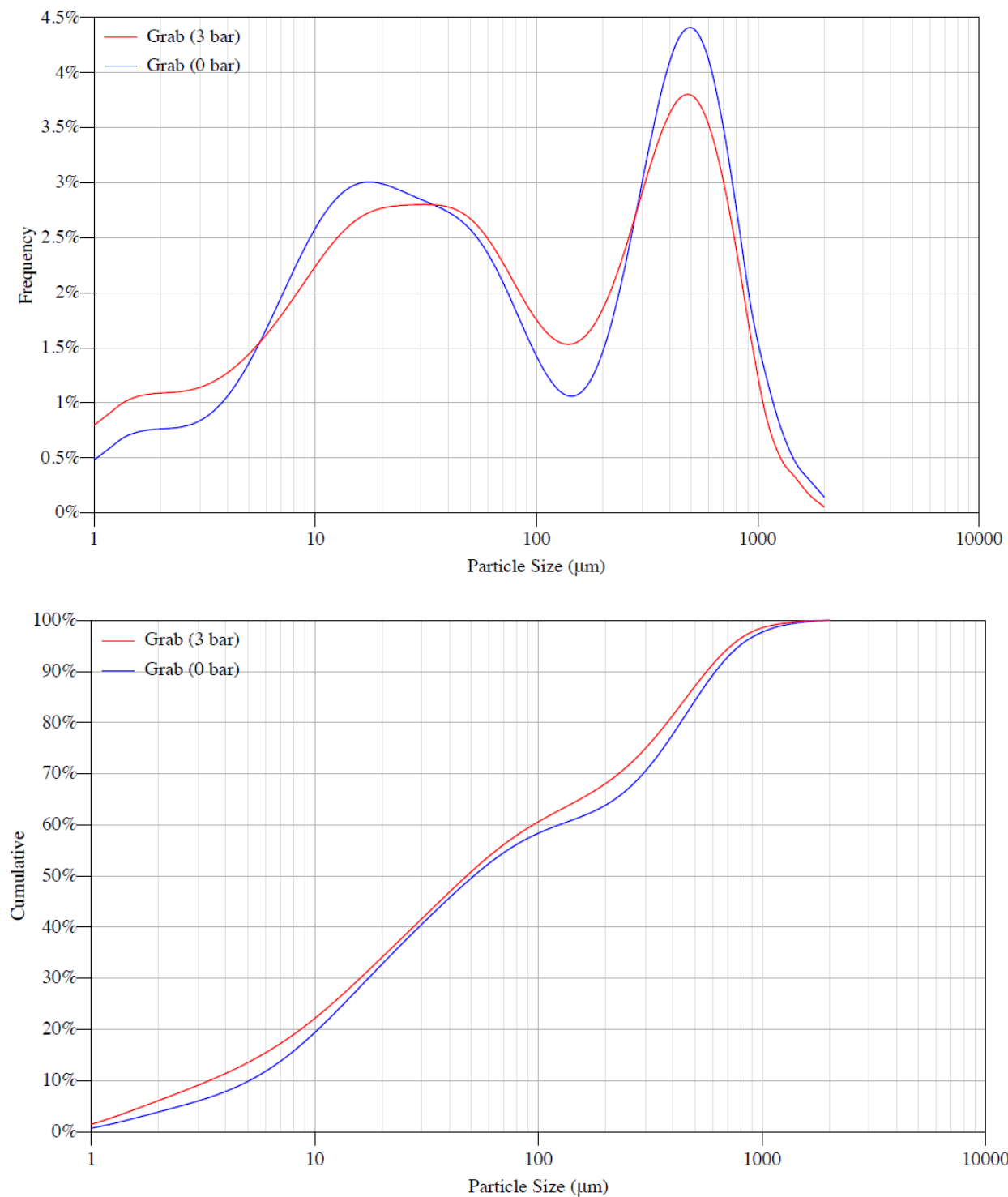


Figure C.92. Batch #6a: Particle size distribution by volume and pressure

## C.7 LAW batch #9a properties

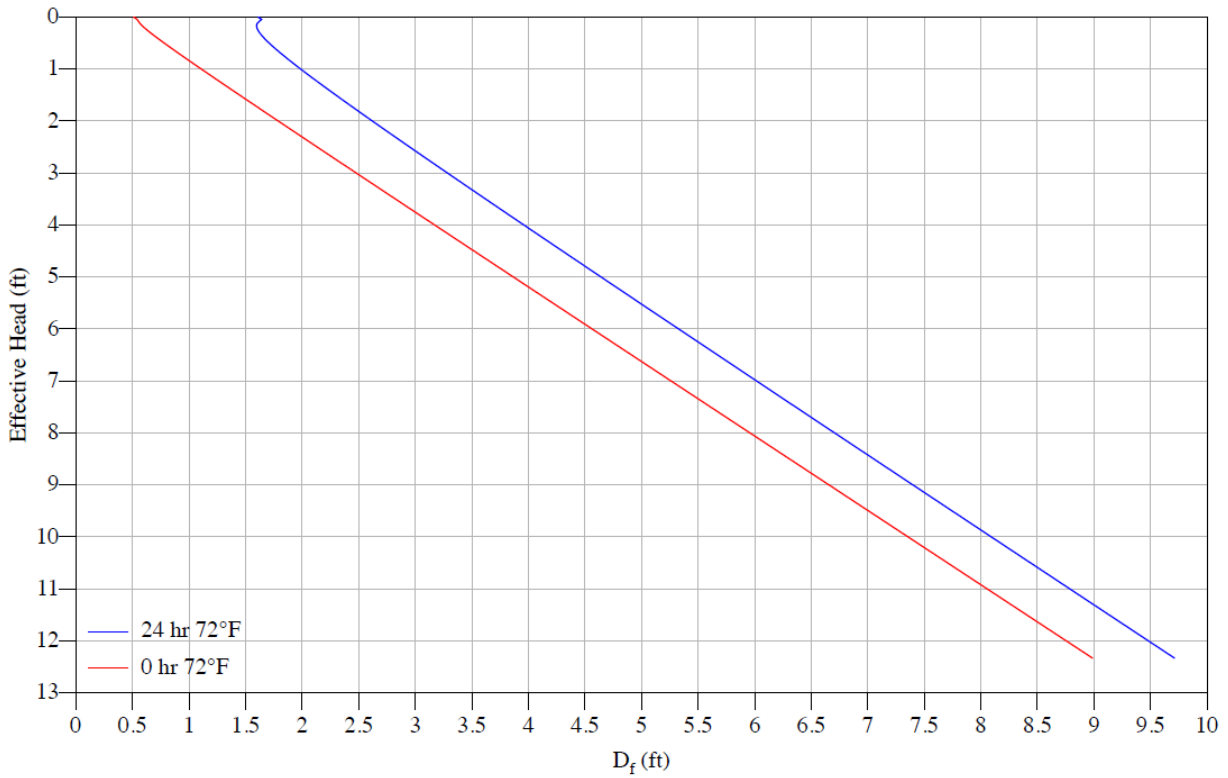


Figure C.93. Batch #9a: Critical rathole dimensions

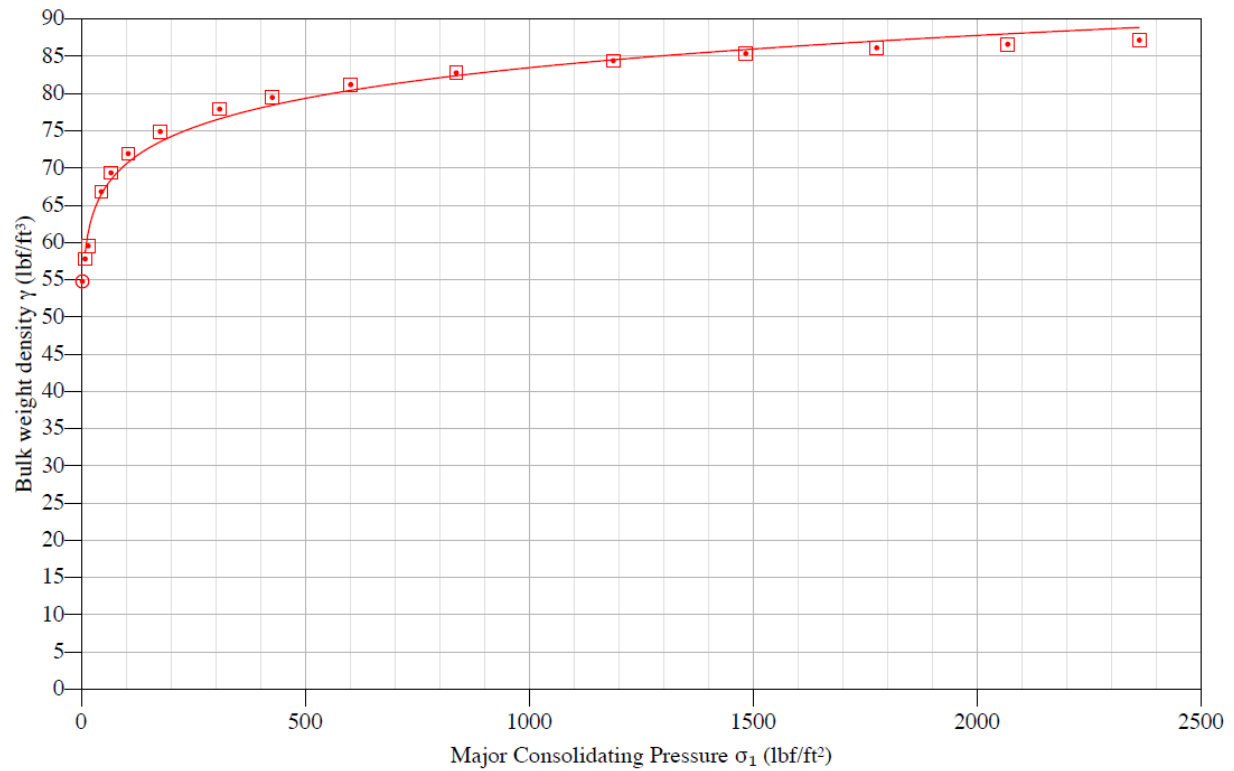


Figure C.94. Batch #9a: Compressibility curve

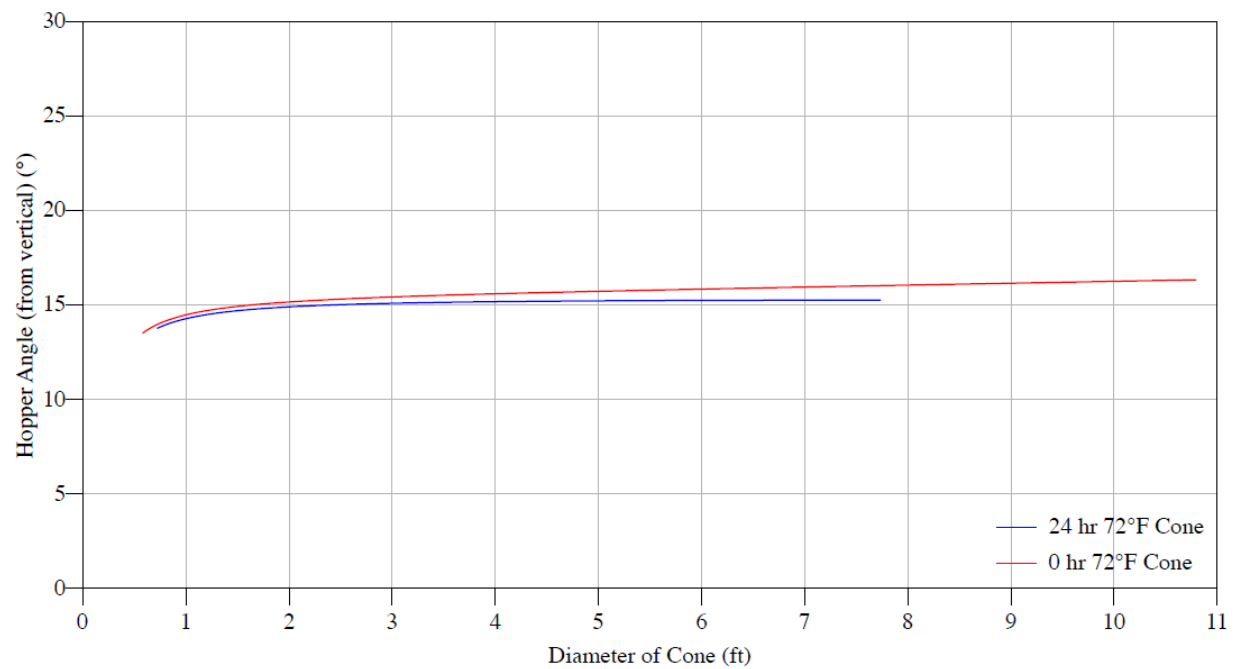


Figure C.95. Batch #9a: Conical hopper angles with 304 SS sheet



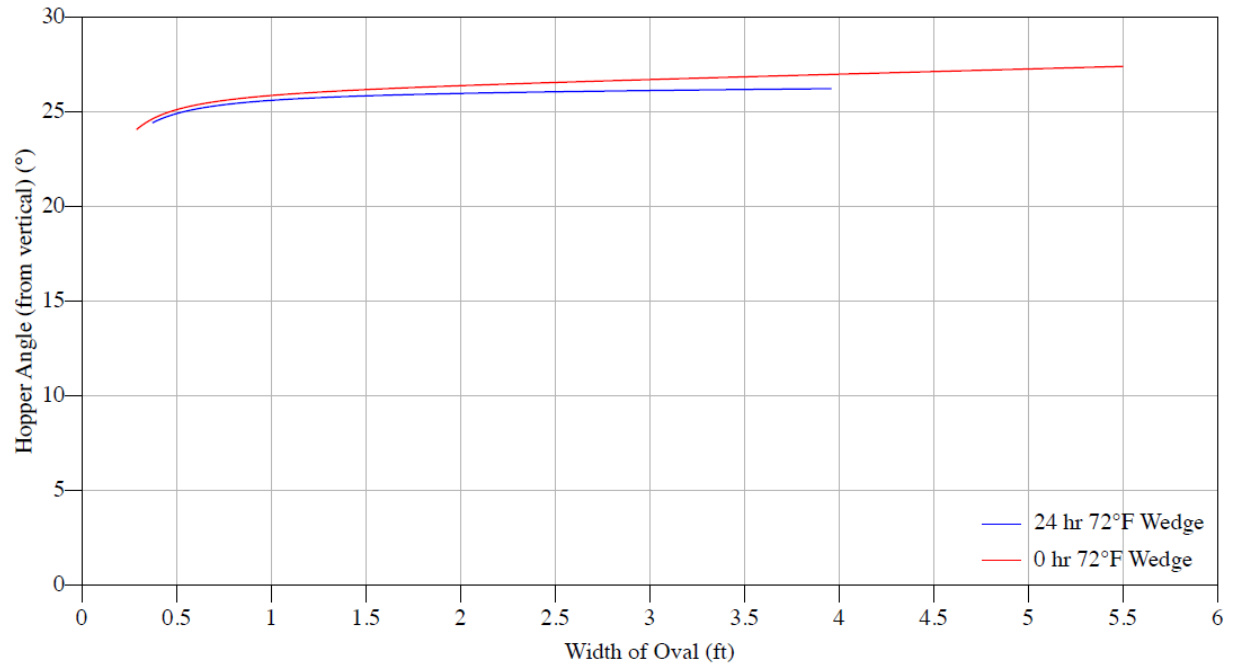


Figure C.96. Batch #9a: Wedge hopper angles with 304 SS sheet

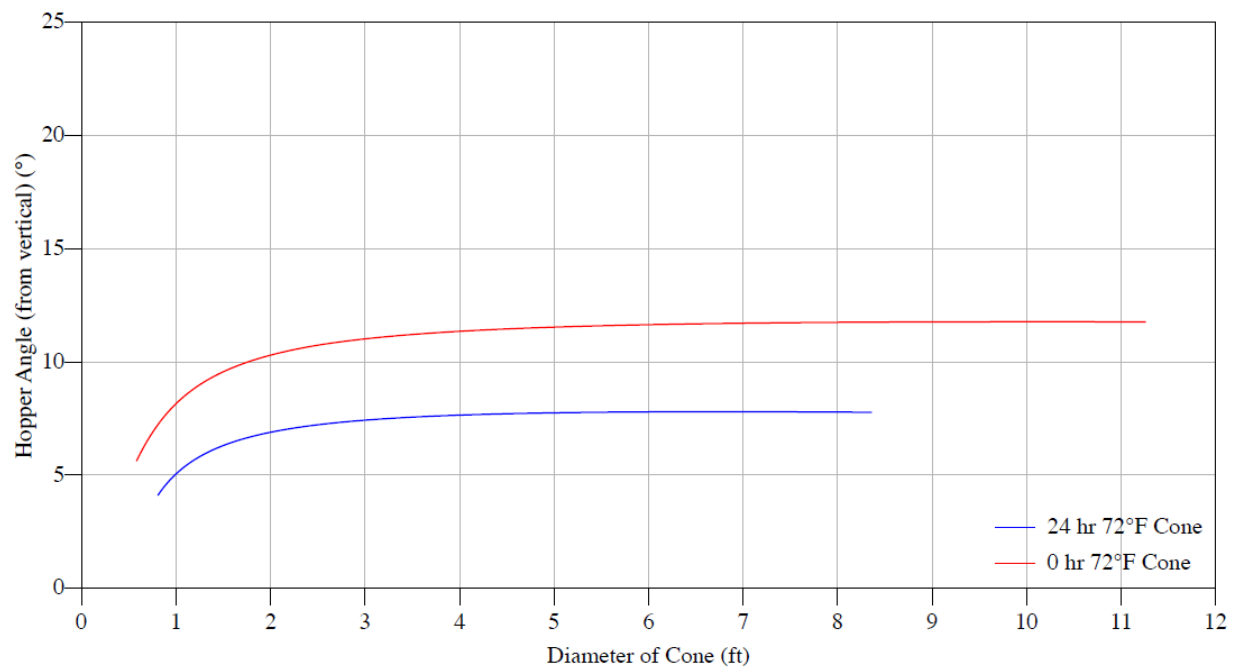


Figure C.97. Batch #9a: Conical hopper angles with mild CS HR plate

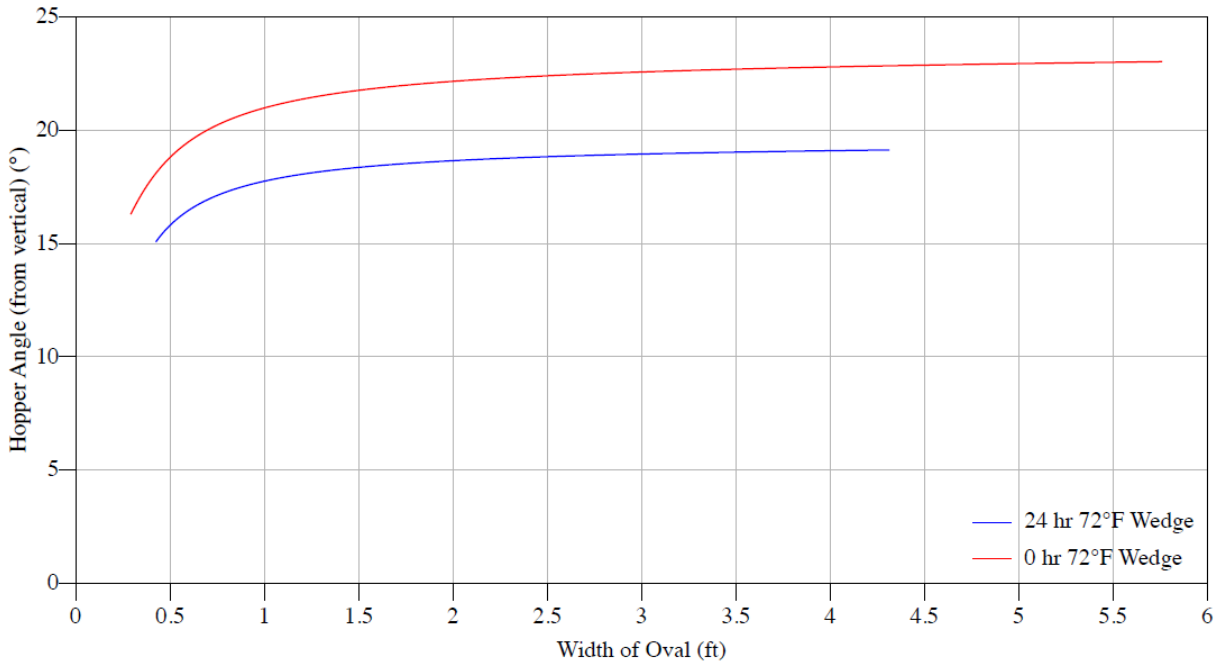


Figure C.98. Batch #9a: Wedge hopper angles with mild CS HR plate

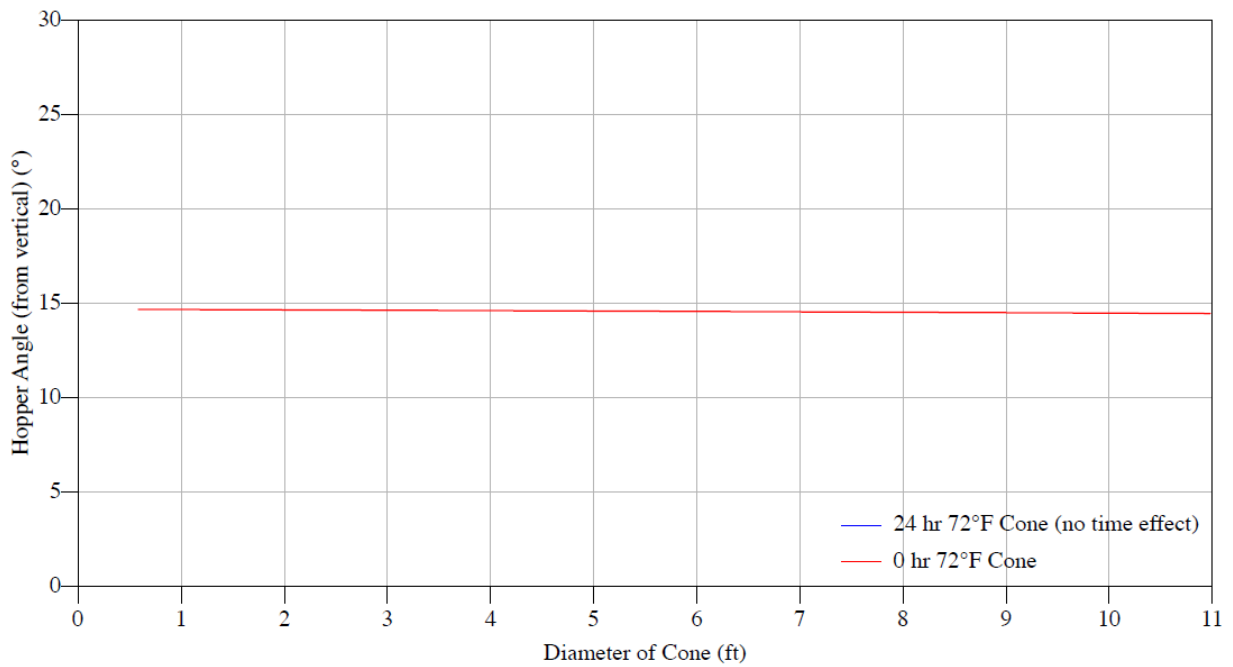


Figure C.99. Batch #9a: Conical hopper angles with TIVAR 88

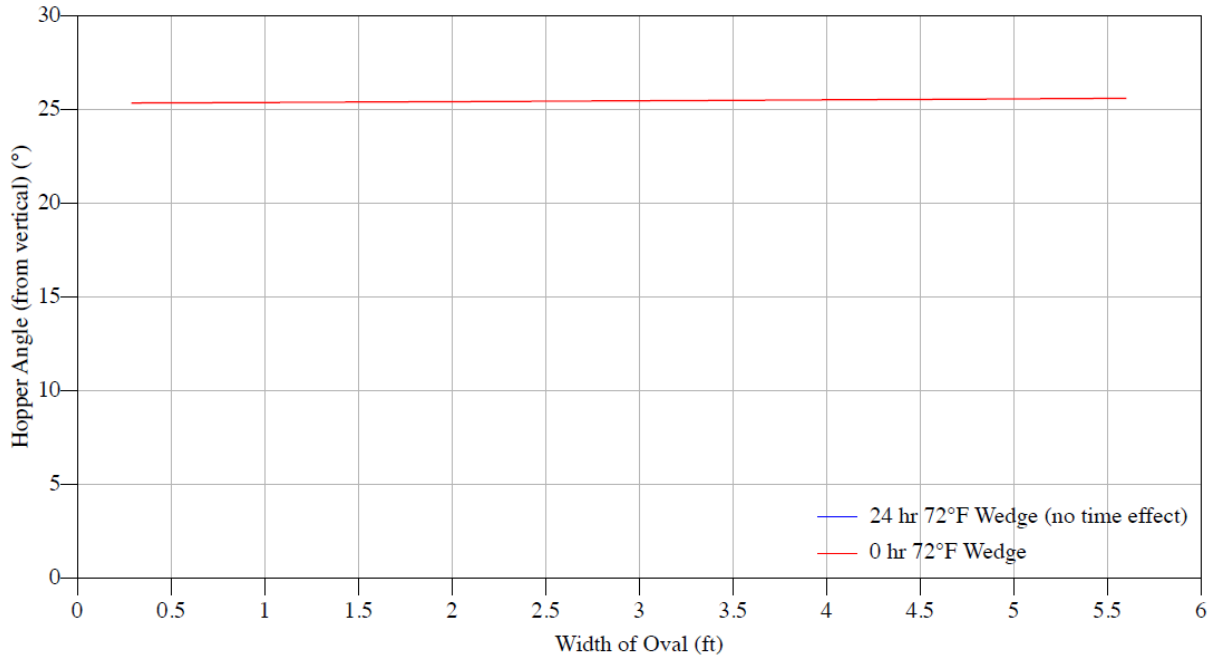


Figure C.100. Batch #9a: Wedge hopper angles with TIVAR 88

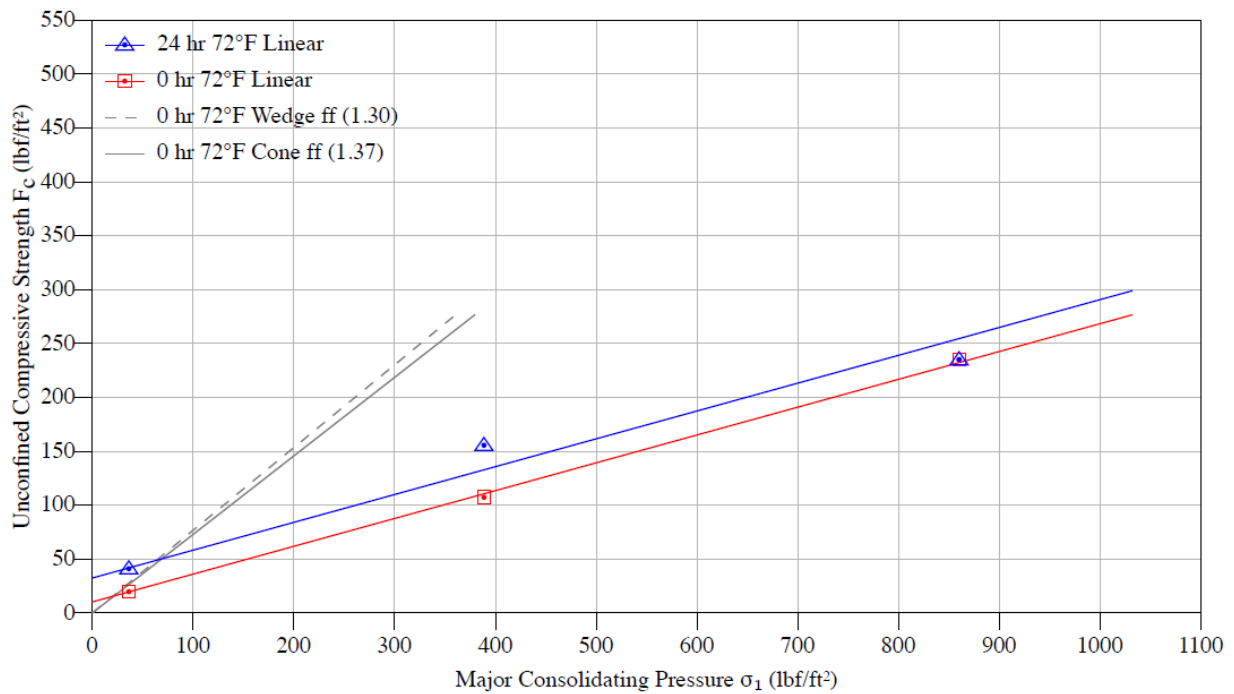


Figure C.101. Batch #9a: Flow function

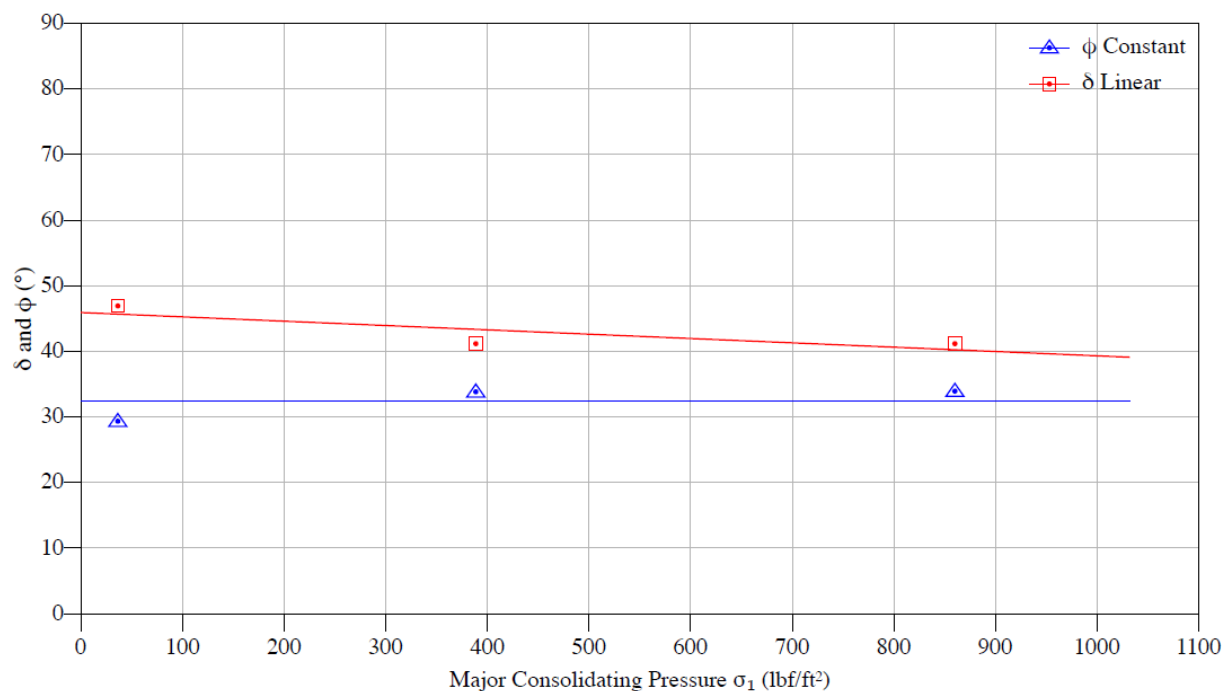


Figure C.102. Batch #9a: Effective angle of friction ( $\delta$ ) and kinematic angle of internal friction ( $\phi$ )

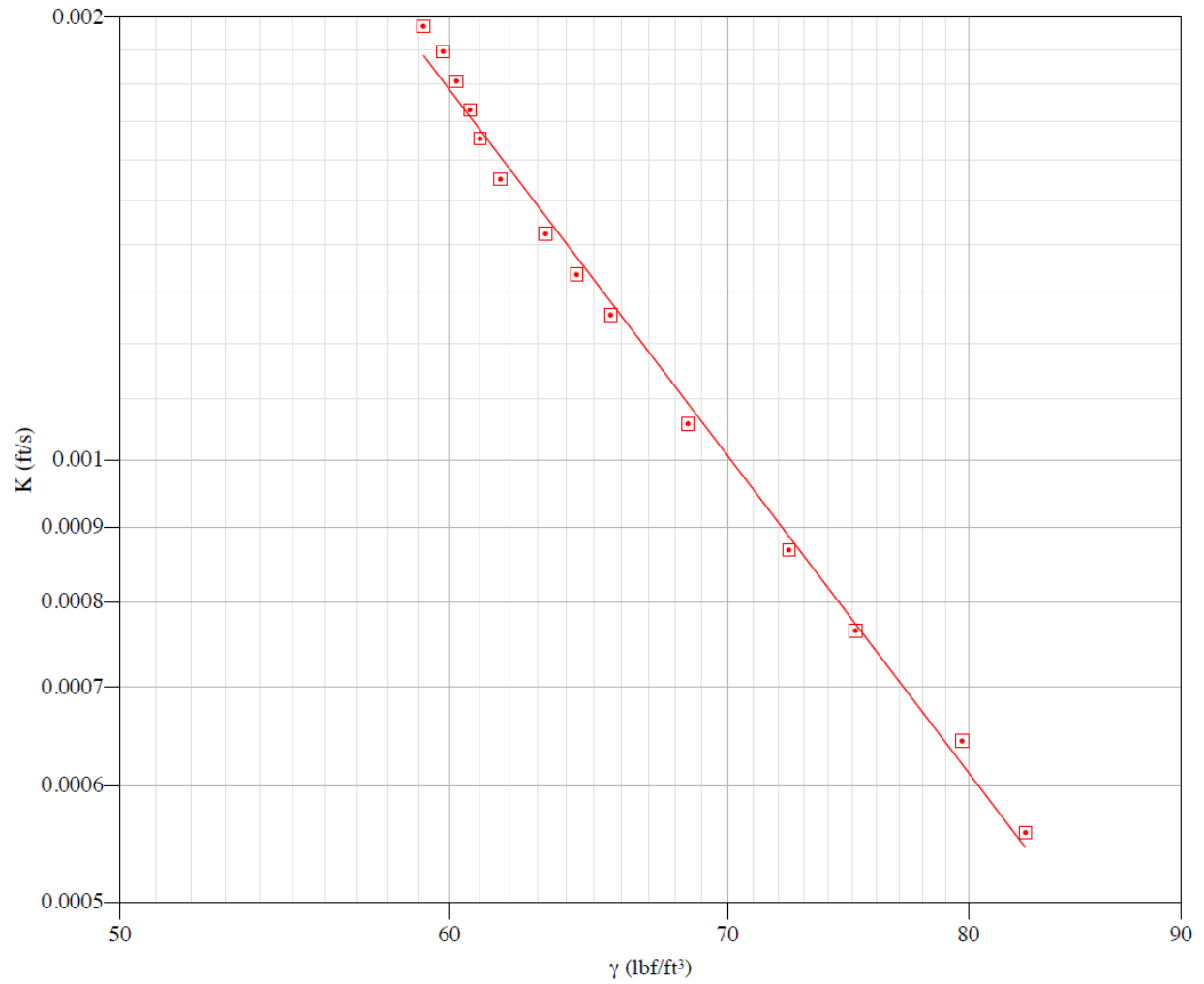


Figure C.103. Batch #9a: Permeability curve

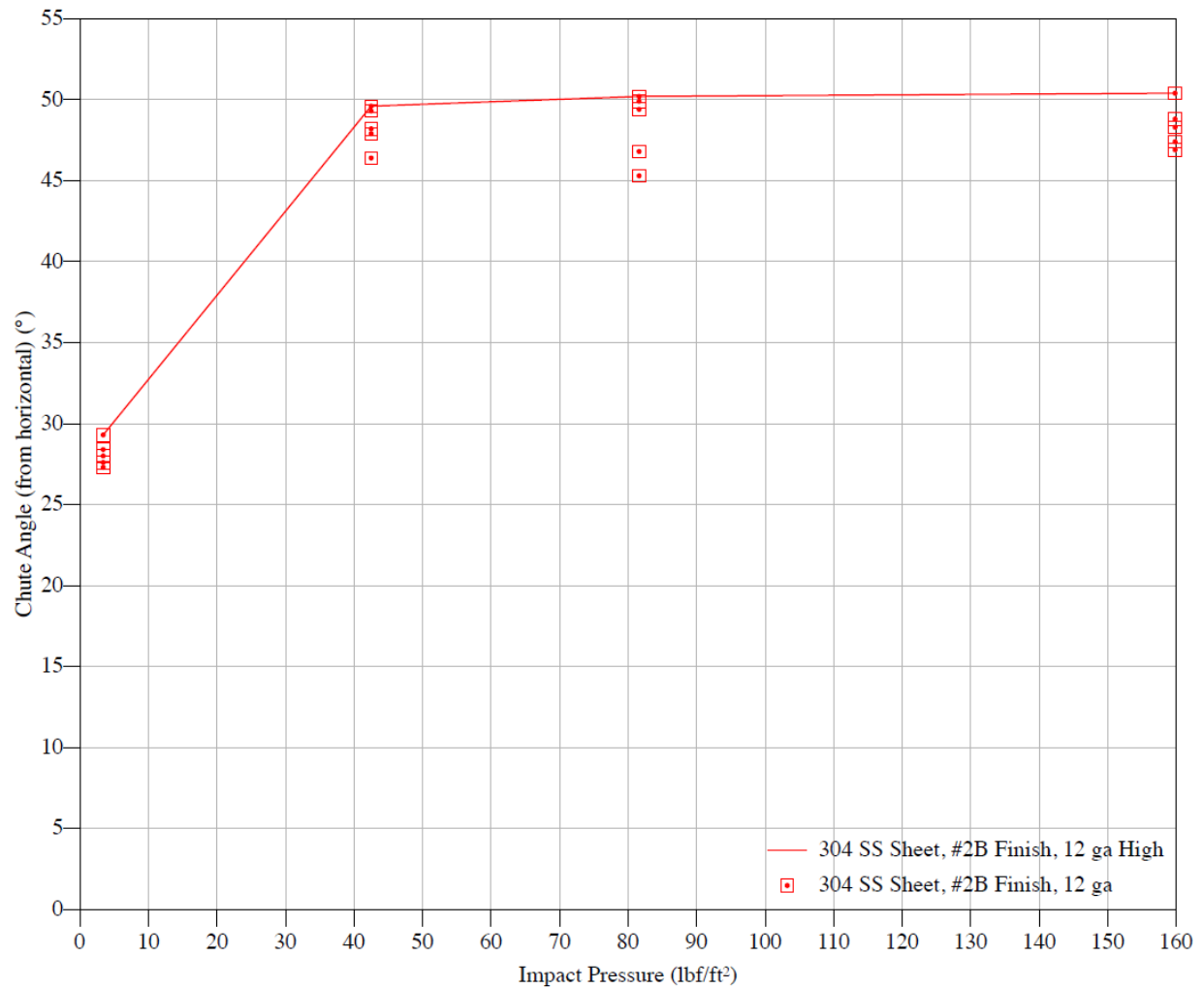


Figure C.104. Batch #9a: Chute curve with 304 SS sheet

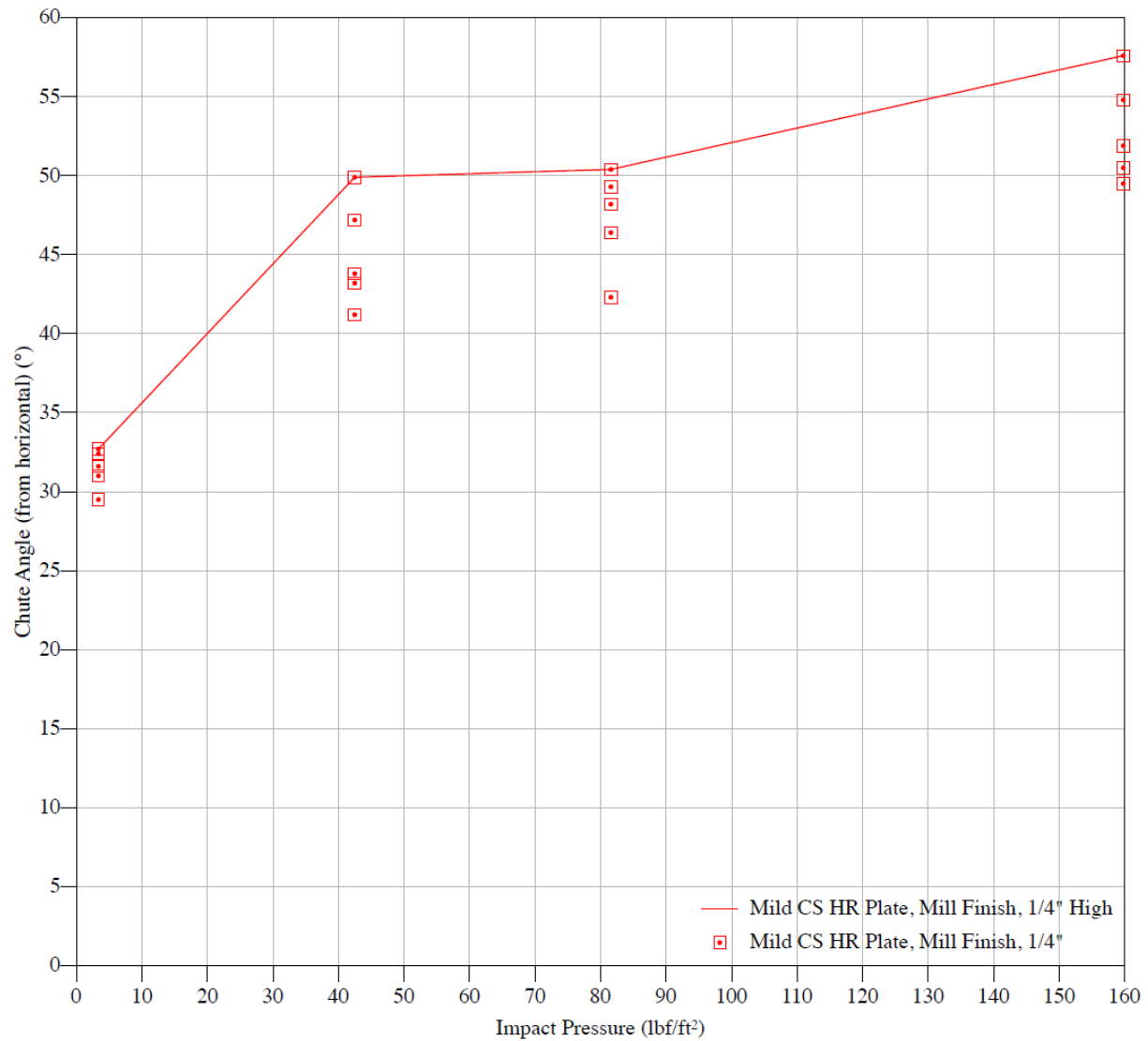


Figure C.105. Batch #9a: Chute curve with mild CS HR plate

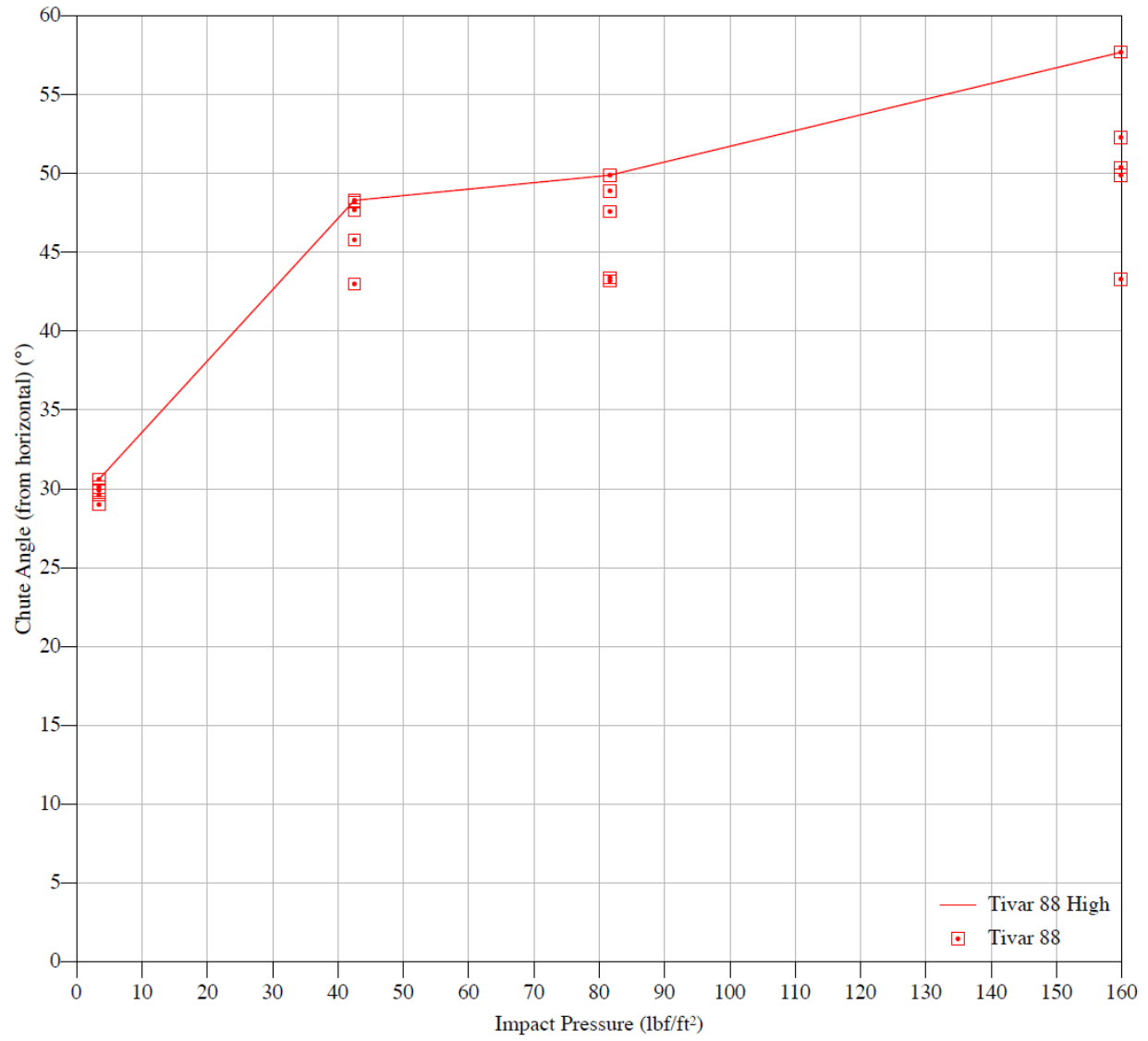


Figure C.106. Batch #9a: Chute curve with TIVAR 88



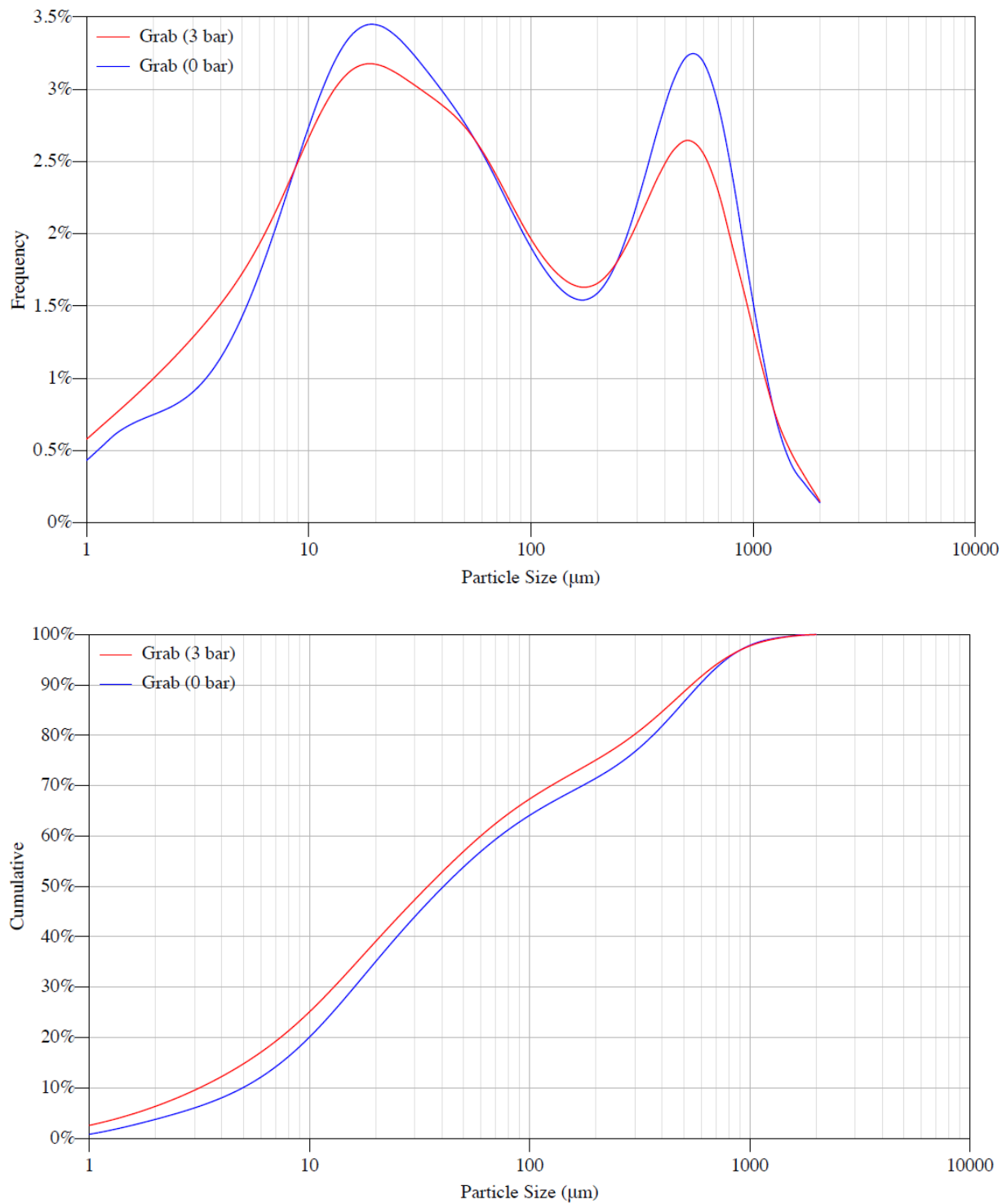


Figure C.107. Batch #9a: Particle size distribution by volume and pressure

## C.8 $\text{FeCr}_2\text{O}_4$

### Bin dimensions for dependable flow

Storage time at rest 0 hr

Temperature 72°F

Table 1.1: Critical outlet dimensions to prevent arching

P – Factor	$B_c$ ft	$B_p$ ft	$B_t$ ft
1.00	0.4	0.2	0.2
1.25	0.4	0.2	0.3
1.50	0.5	0.2	0.4
2.00	0.82	0.4	0.82

For detailed explanations of terms see pg. 166.

Figure 1.1: Critical rathole dimensions (P – Factor = 1)

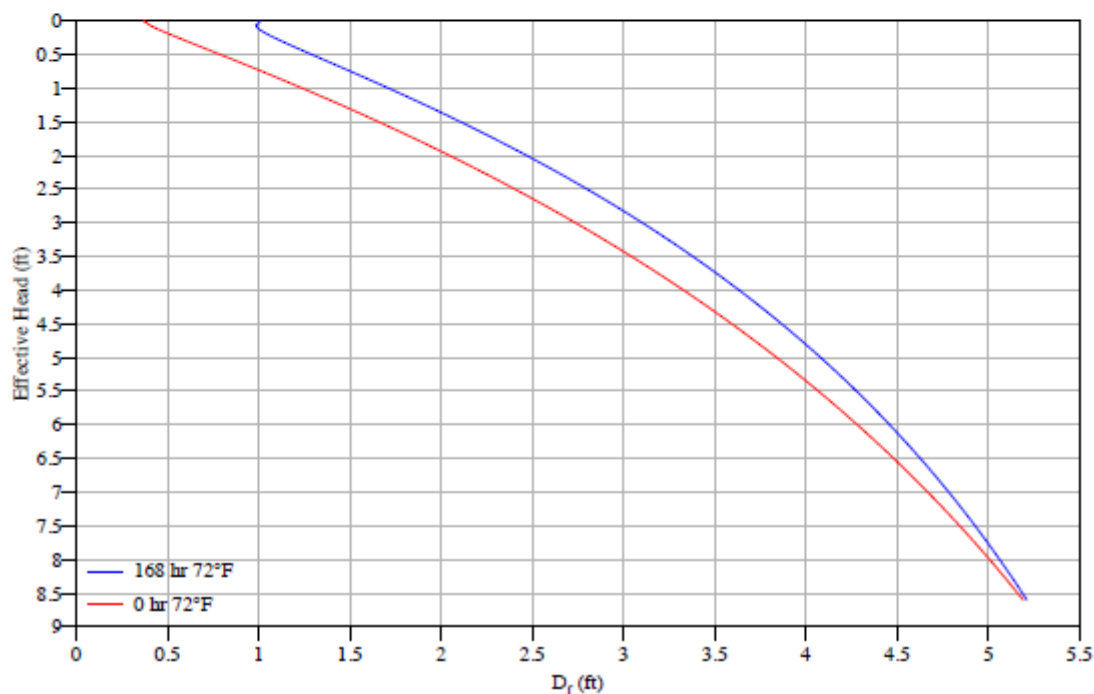


Figure C.108  $\text{FeCr}_2\text{O}_4$ : Critical rathole dimensions

## Bulk density

### Temperature 70°F

The bulk weight density,  $\gamma$ , is a function of the major consolidating pressure,  $\sigma_1$ , expressed in terms of Effective Head.

Table 1.3: Bulk weight density

Effective Head	ft	0.5	1	2.5	5	10	20
$\sigma_1$	lb/ft <sup>2</sup>	52.7	111	298.7	630.6	1331	2811
$\gamma$	lb/ft <sup>3</sup>	105.4	111.2	119.5	126.1	133.1	140.5

### Compressibility parameters

Bulk weight density,  $\gamma$ , is a function of the major consolidating pressure  $\sigma_1$ , as follows:

$$\gamma = \gamma_0 (\sigma_1 / \sigma_0)^\beta \quad \text{for } 91 < \gamma < 136.5 \text{ lb/ft}^3$$

Table 1.4: Compressibility parameters

$\gamma_0$	lb/ft <sup>3</sup>	95.2
$\sigma_0$	lb/ft <sup>2</sup>	13
$\beta$		0.0724
$\gamma_{\text{loose fill}}$	lb/ft <sup>3</sup>	82.2

Figure 1.2: Compressibility curve

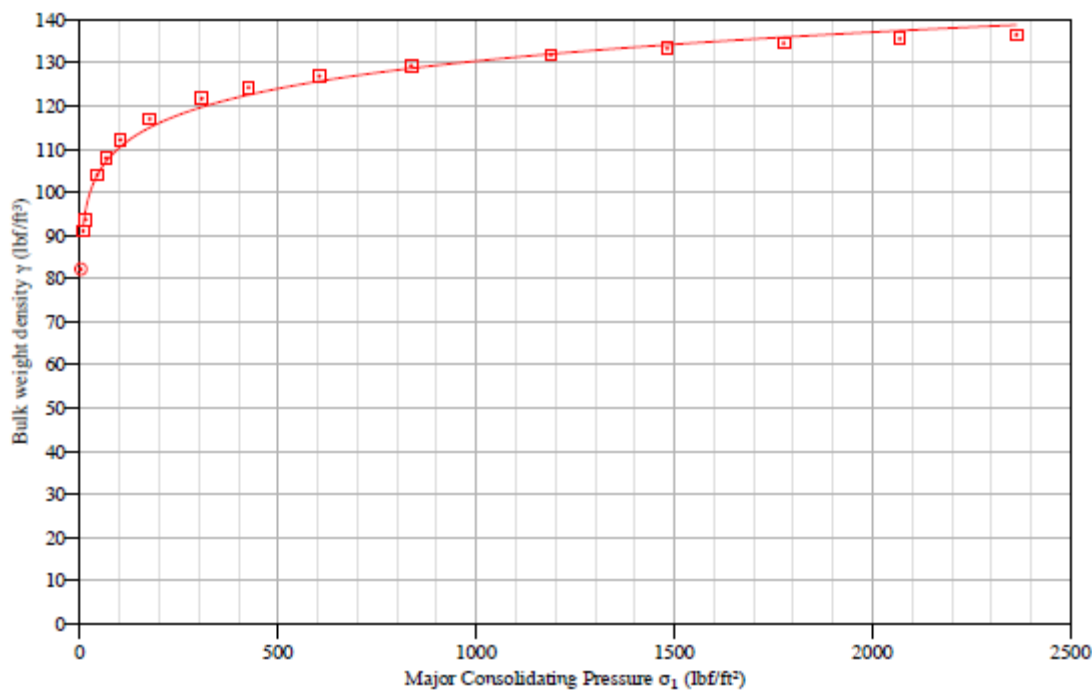


Figure C.109 FeCr<sub>2</sub>O<sub>4</sub>: Compressibility curve

## Maximum hopper angles for Mass Flow

Wall material 304 SS Sheet, #2B Finish, 12 ga

Figure 1.3: Conical hopper angles

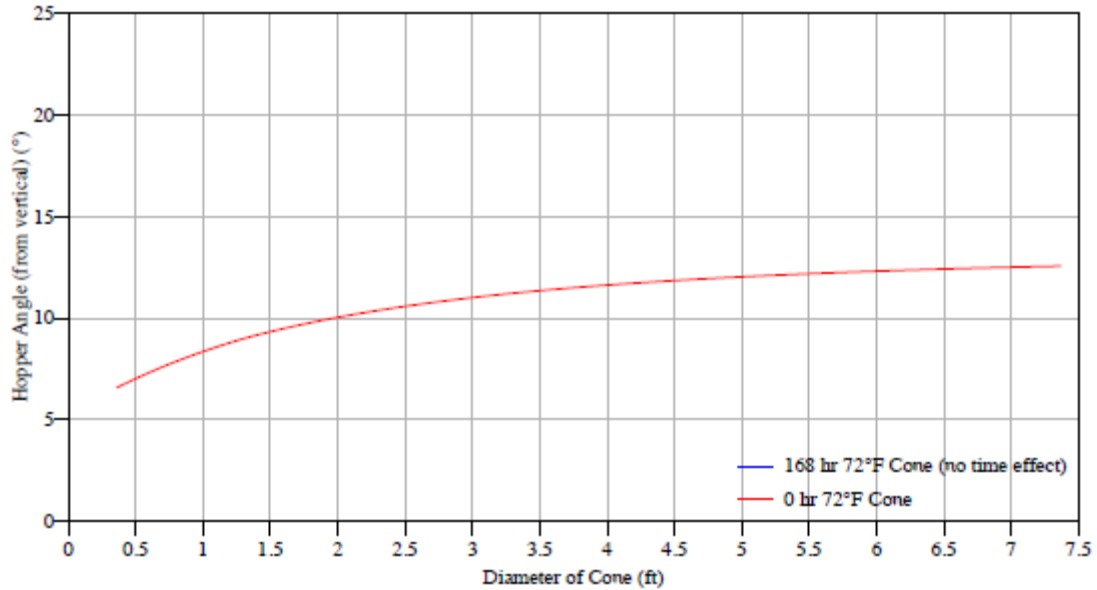


Figure 1.4: Wedge hopper angles

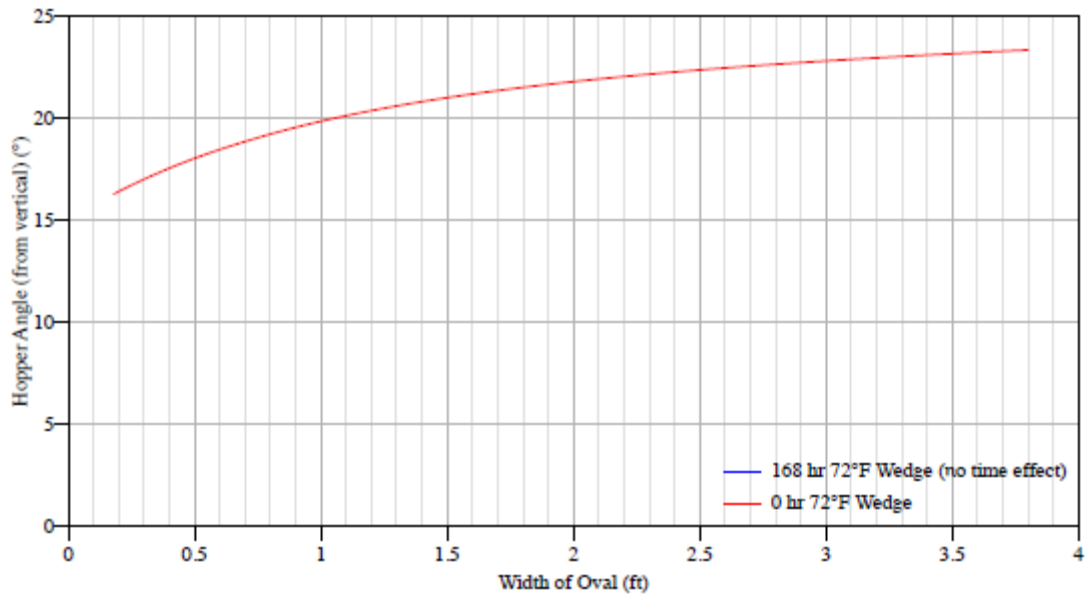


Figure C.110  $\text{FeCr}_2\text{O}_4$ : Conical hopper angles (Top) and Wedge hopper angles (Bottom) with 304 SS sheet

Wall material Mild CS HR Plate, Mill Finish, 1/4"

Figure 1.5: Conical hopper angles

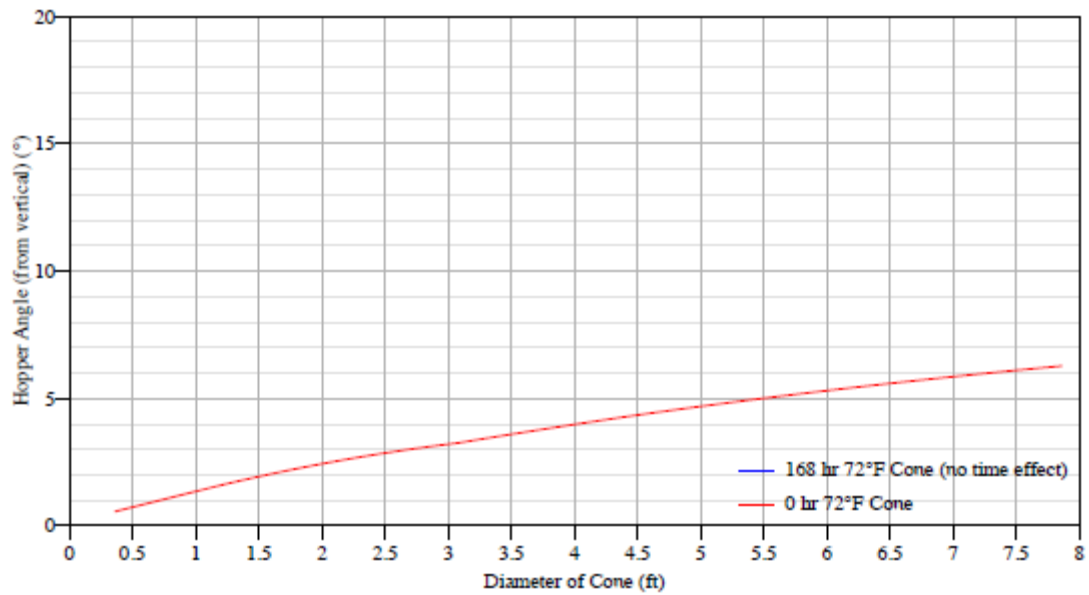


Figure 1.6: Wedge hopper angles

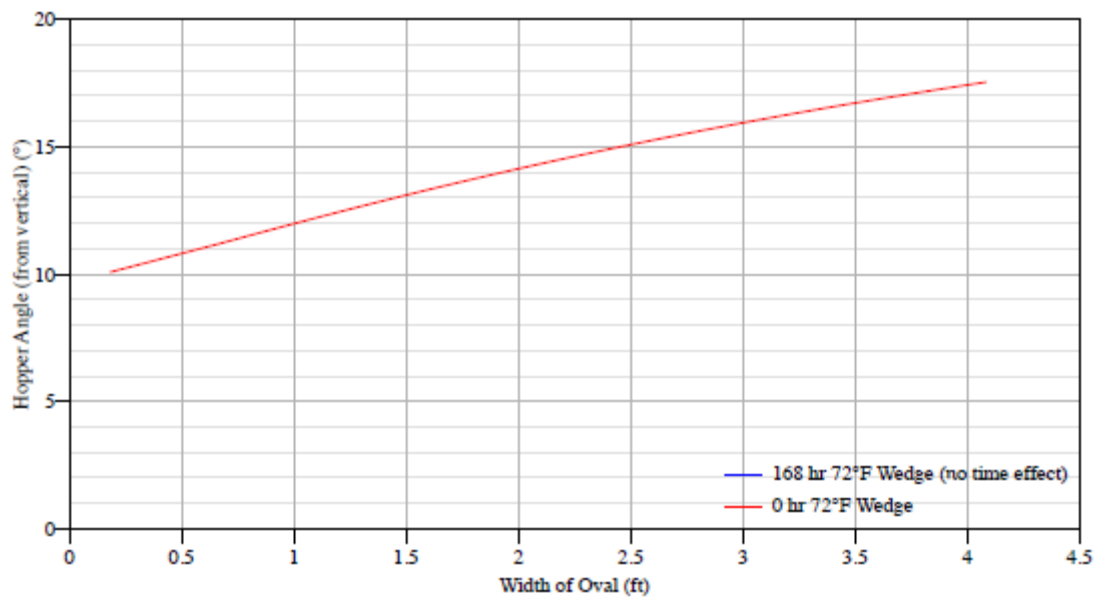


Figure C.111 FeCr<sub>2</sub>O<sub>4</sub>: Conical hopper angles (Top) and Wedge hopper angles (Bottom) with mild CS HR plate

Wall material Tivar-88

Figure 1.7: Conical hopper angles

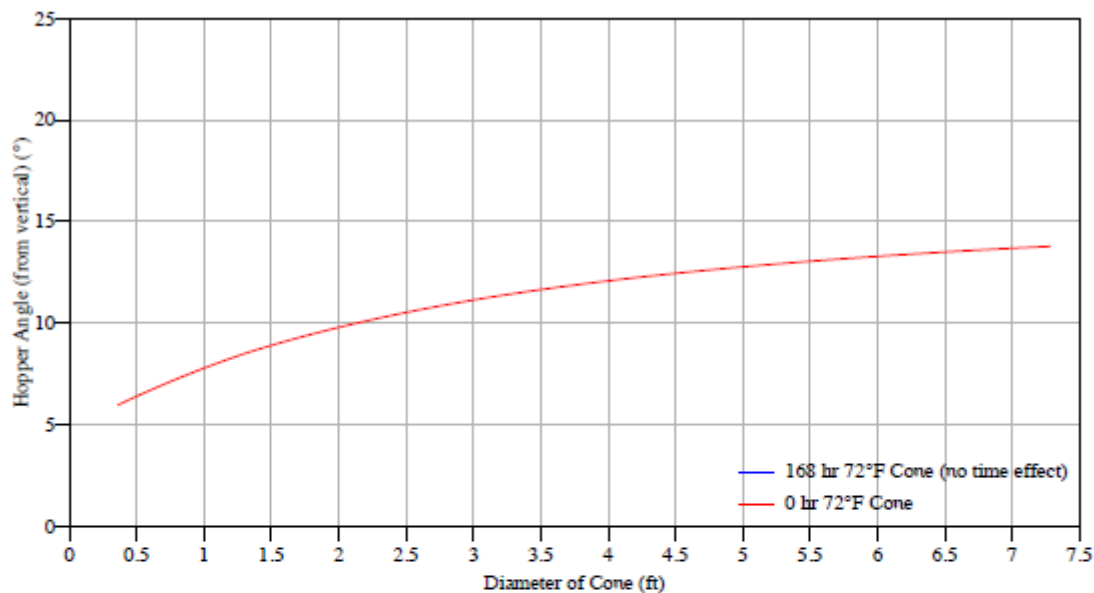


Figure 1.8: Wedge hopper angles

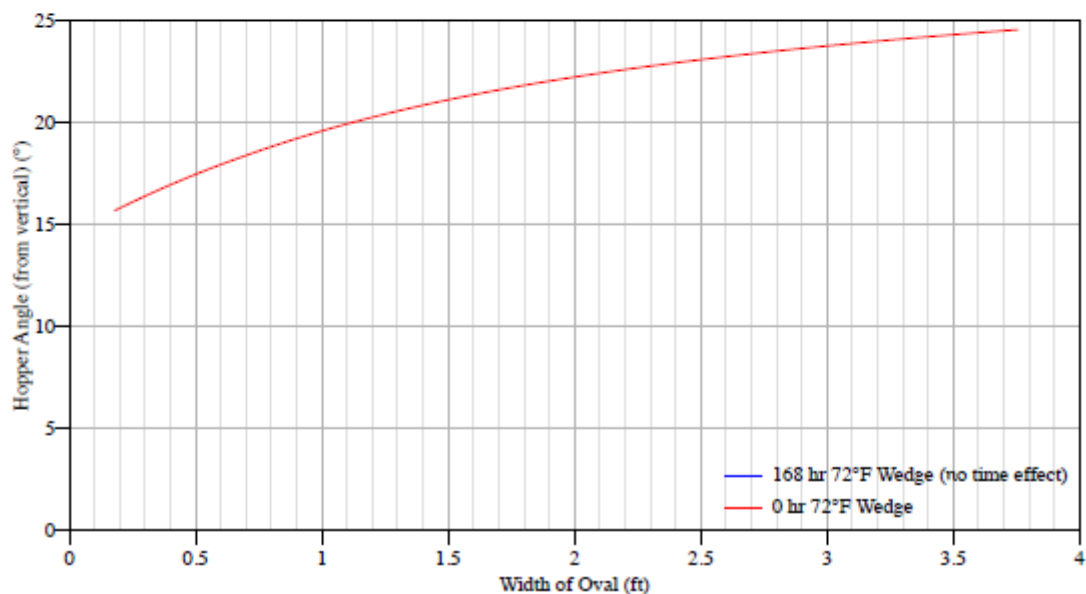


Figure C.112 FeCr<sub>2</sub>O<sub>4</sub>: Conical hopper angles (Top) and Wedge hopper angles (Bottom) with Tivar 88

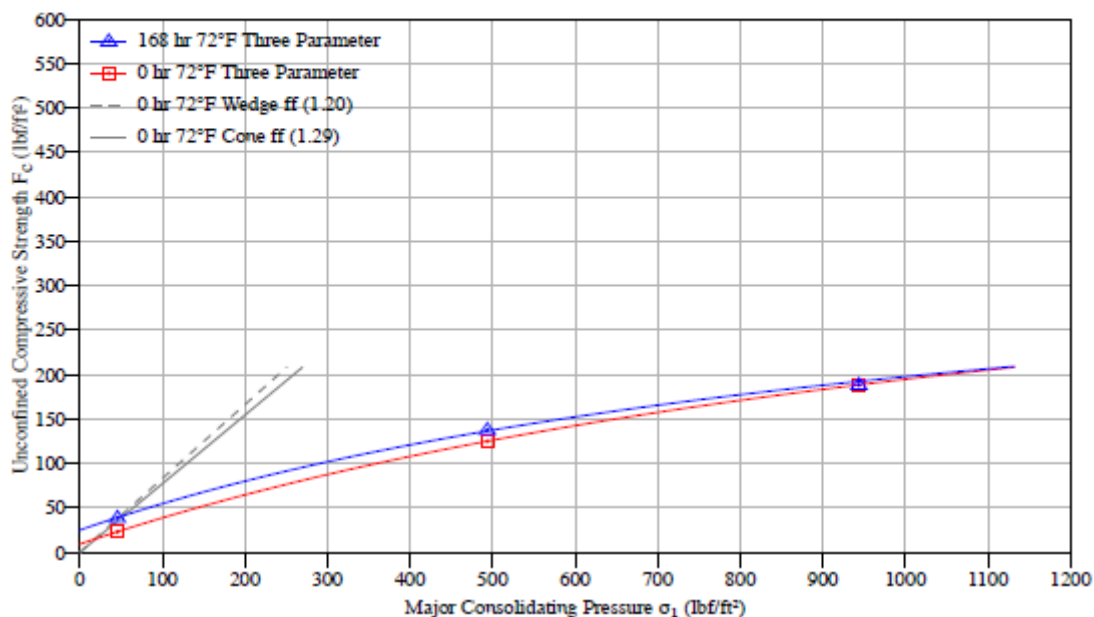


Figure C.113 FeCr<sub>2</sub>O<sub>4</sub>: Flow function

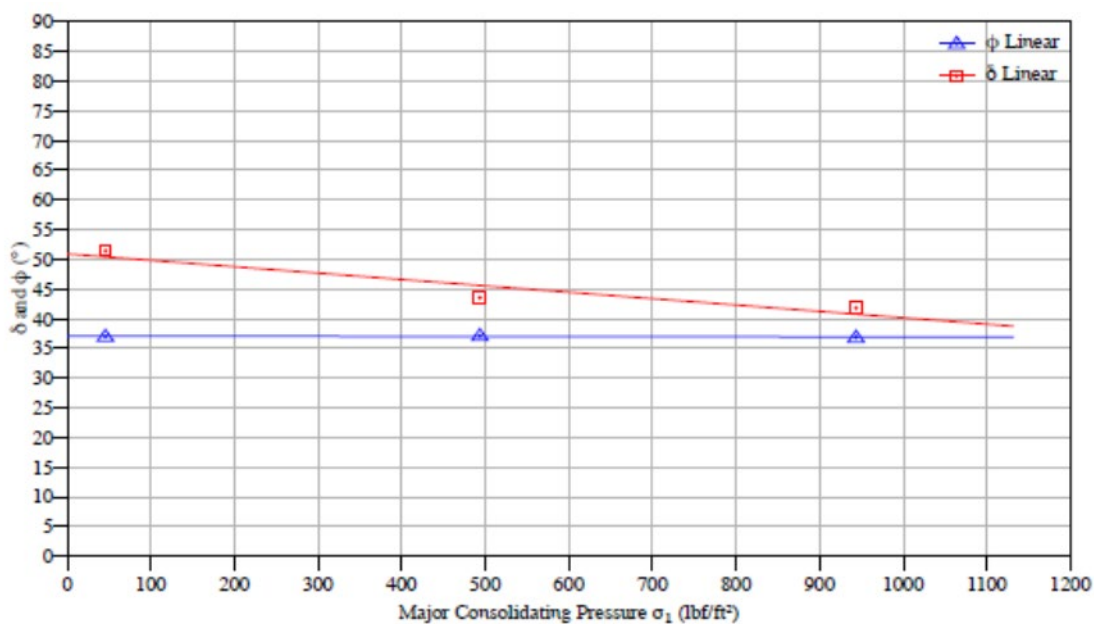


Figure C.114 FeCr<sub>2</sub>O<sub>4</sub>: Effective angle of friction ( $\delta$ ) and kinematic angle of internal friction ( $\phi$ )

## Air permeability test results

### Temperature 70°F

$K$  is a function of the bulk weight density of the solid

$$K = K_0 \left( \frac{\gamma}{\gamma_0} \right)^{-\alpha}$$

At 70°F, for  $\gamma$  between 85 and 137  $lb_f/ft^3$ :

Table 1.4: Permeability parameters

$K_0$	$ft/s$	0.0007511
$\gamma_0$	$lb_f/ft^3$	95.2
$\alpha$		4.909

Figure 1.15: Permeability curve

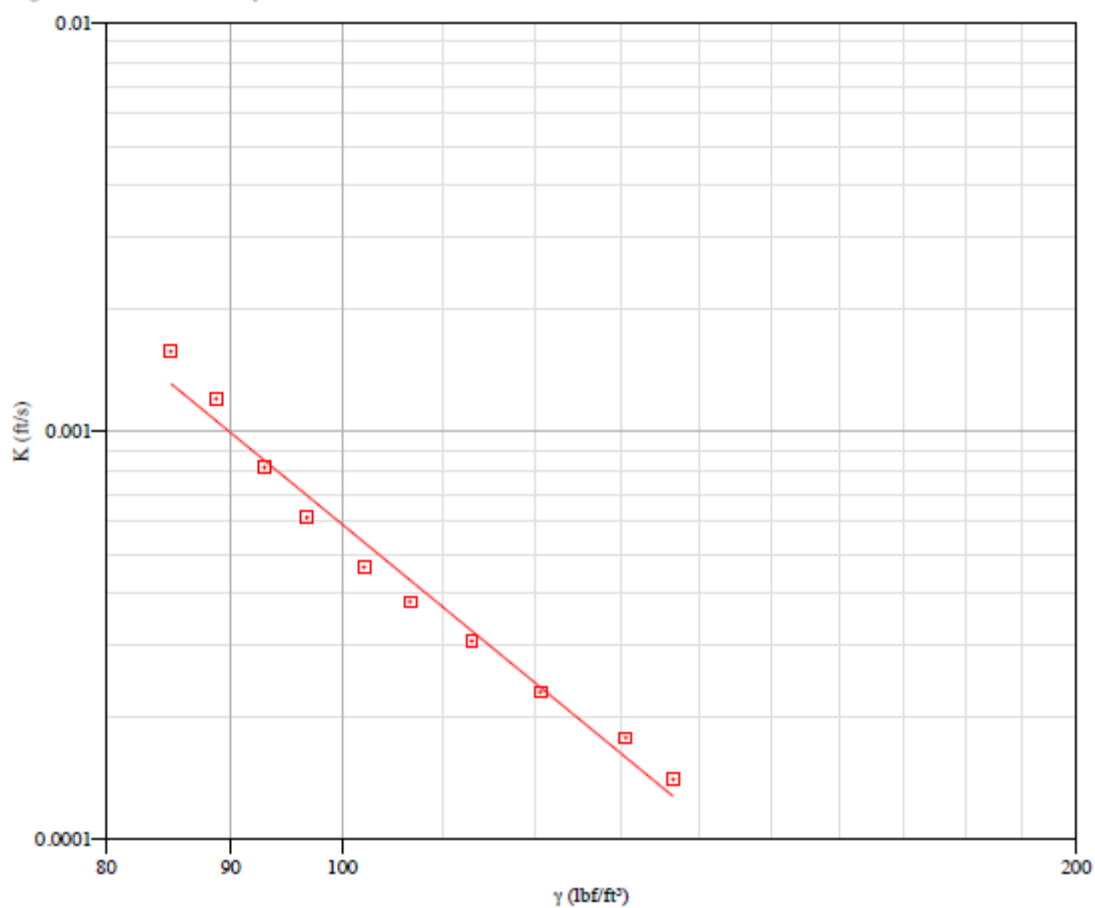


Figure C.115 FeCr<sub>2</sub>O<sub>4</sub>: Permeability curve



## Chute angles

Chute material 304 SS Sheet, #2B Finish, 12ga

Storage time at rest 0 hr

Chute temperature 72°F

Material temperature 71°F

Table 1.5: Measured chute clean-off angles (from horizontal)

Impact Pressure $lb_f/ft^2$	Angle $^\circ$
4.6	28 to 30
43.7	53 to 57
82.8	55 to 59
161.1	60 to 66

Figure 1.16: Chute curve

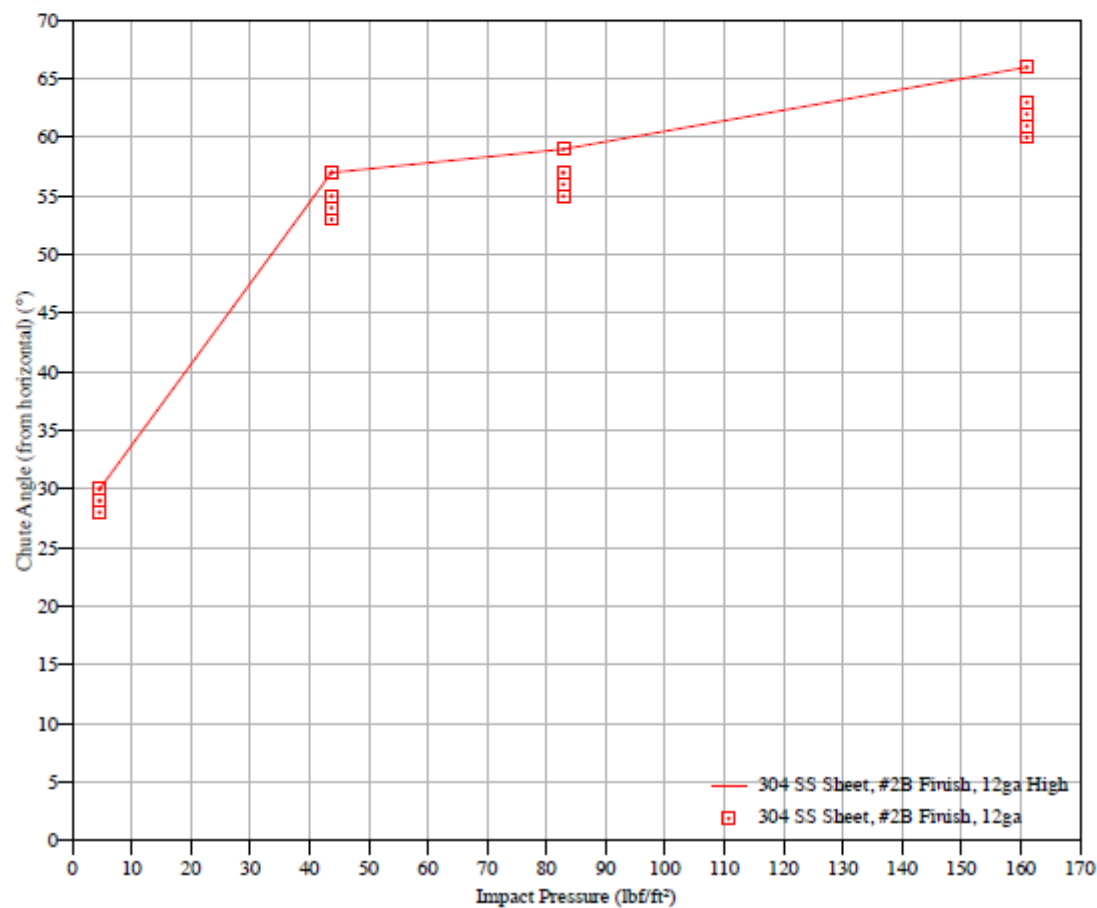


Figure C.116  $FeCr_2O_4$ : Chute curve with 304 SS sheet

Chute material Mild CS HR Plate, Mill Finish, 1/4"  
Storage time at rest 0 hr  
Chute temperature 72°F  
Material temperature 71°F

Table 1.6: Measured chute clean-off angles (from horizontal)

Impact Pressure $lb_f/ft^2$	Angle $^\circ$
4.7	33 to 34
43.8	60 to 67
82.9	59 to 73
161.1	69 to 78

Figure 1.17: Chute curve

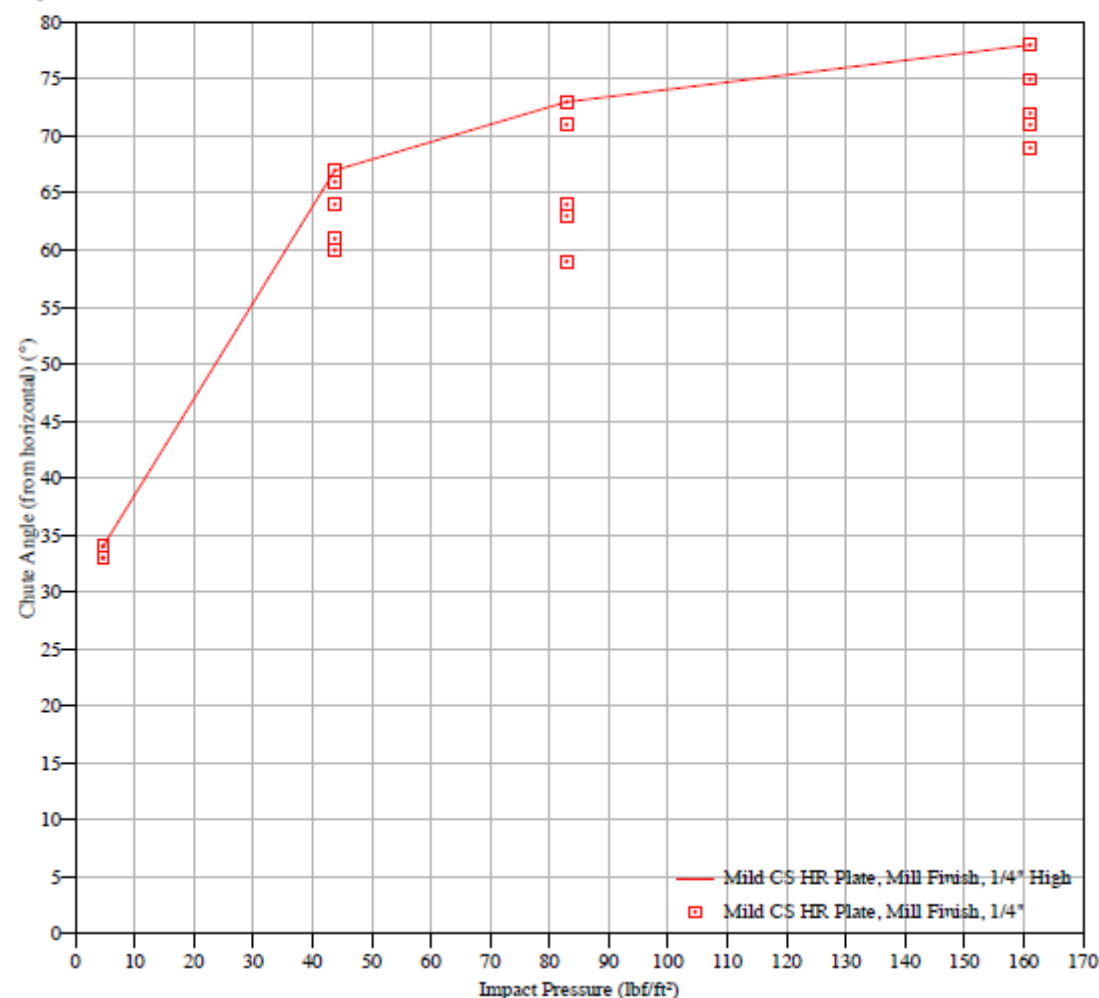


Figure C.117 FeCr<sub>2</sub>O<sub>4</sub>: Chute curve with mild CS HR plate

Chute material Tivar-88  
Storage time at rest 0 hr  
Chute temperature 72°F  
Material temperature 71°F

Table 1.7: Measured chute clean-off angles (from horizontal)

Impact Pressure $lb_f/ft^2$	Angle $^\circ$
4.5	32 to 34
43.7	48 to 51
82.8	42 to 51
161	38 to 50

Figure 1.18: Chute curve

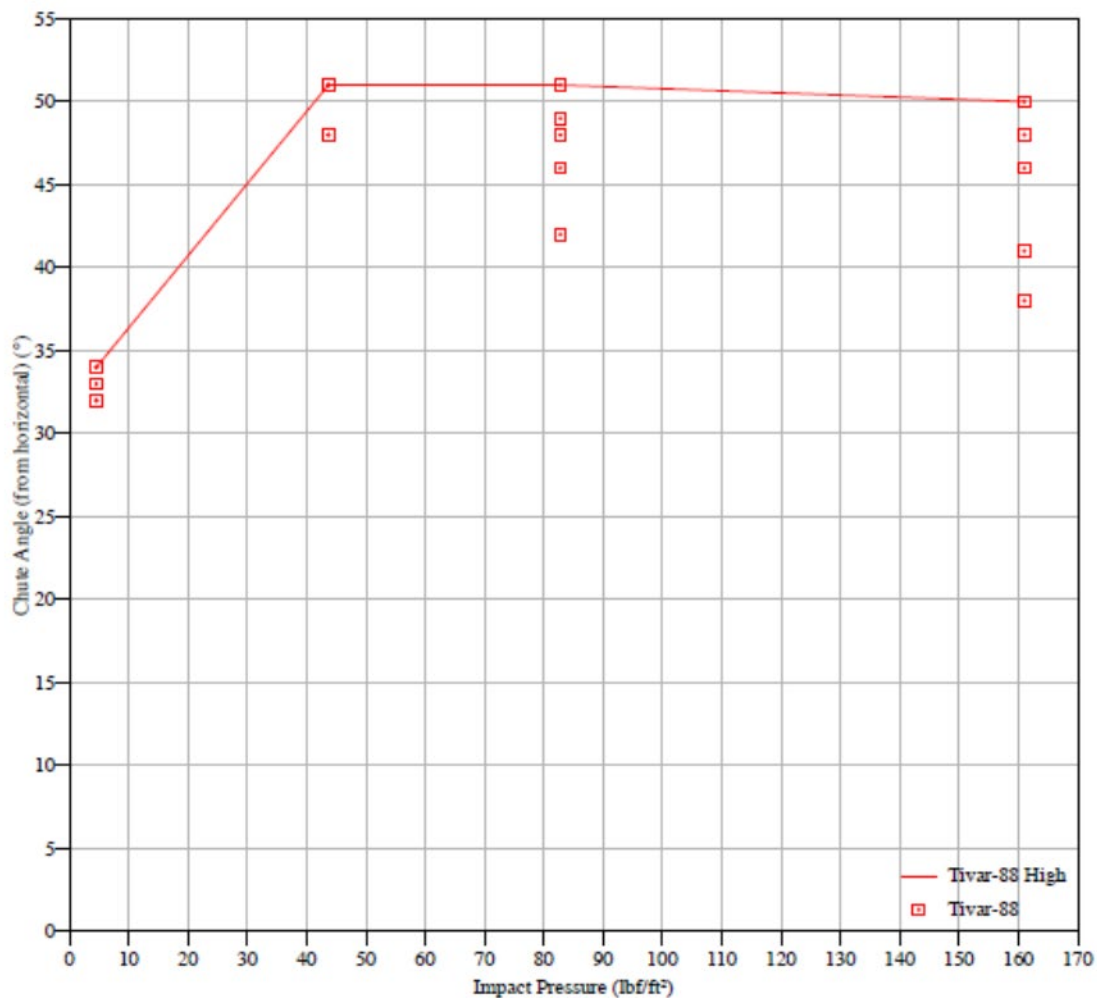


Figure C.118 FeCr<sub>2</sub>O<sub>4</sub>: Chute curve with Tivar 88

## Particle Size Distribution Analysis Comparison

Figure 1.21: Particle size distribution, by volume

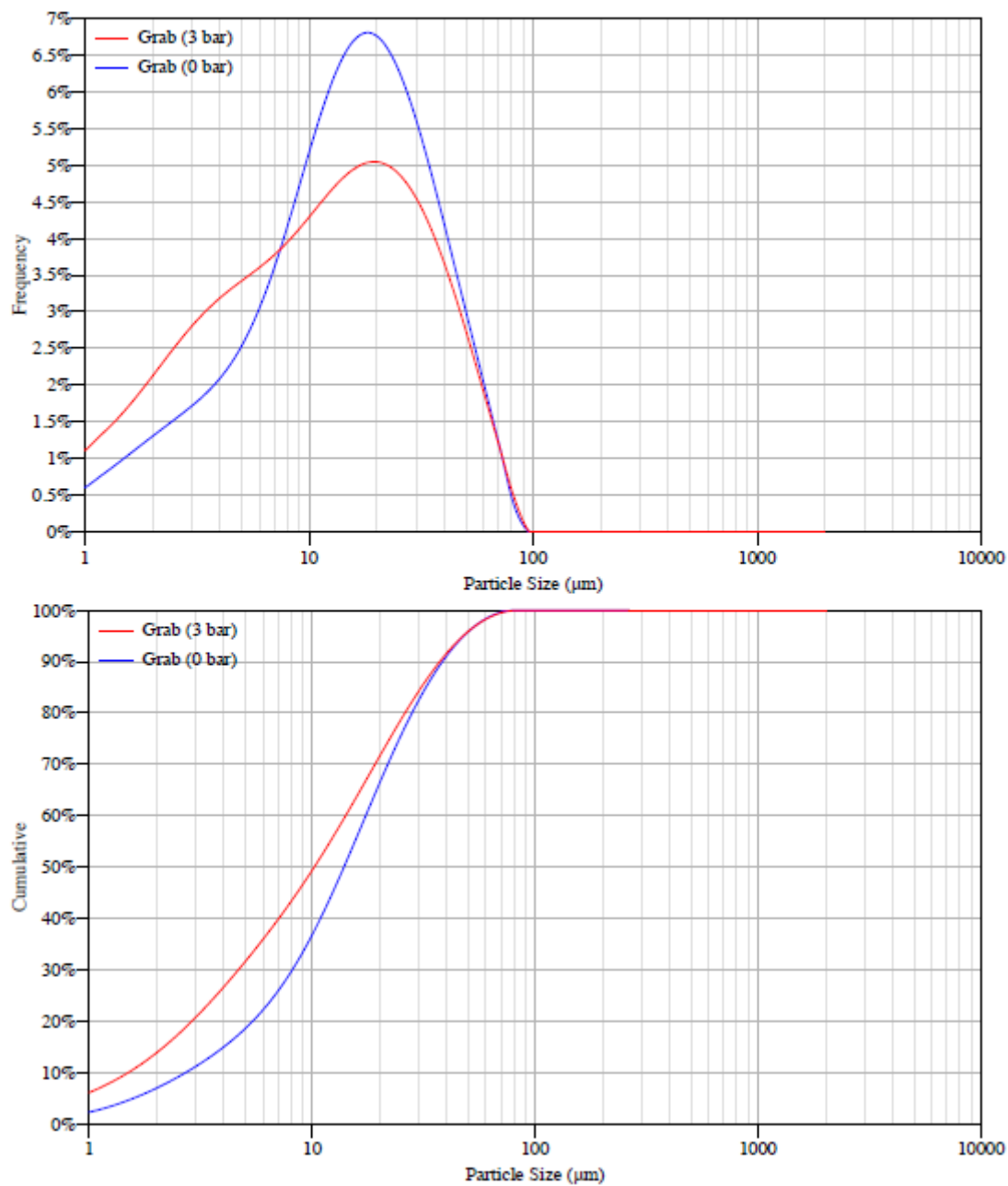


Figure C.119  $\text{FeCr}_2\text{O}_4$ : Particle size distribution by volume and pressure

## C.9 ZrSiO<sub>4</sub>

### Bin dimensions for dependable flow

Storage time at rest 0 hr

Temperature 72°F

Table 2.1: Critical outlet dimensions to prevent arching

P – Factor	B <sub>c</sub> ft	B <sub>p</sub> ft	B <sub>t</sub> ft
1.00	0.*	0.*	0.*
1.25	0.*	0.*	0.*
1.50	0.*	0.*	0.*
2.00	0.*	0.*	0.*

0.\* Denotes no minimum dimensions are given by the tests. Instead, the outlet size should be selected by consideration of particle interlocking, flow rate, etc.

For detailed explanations of terms see pg. 166.

Figure 2.1: Critical rathole dimensions (P – Factor = 1)

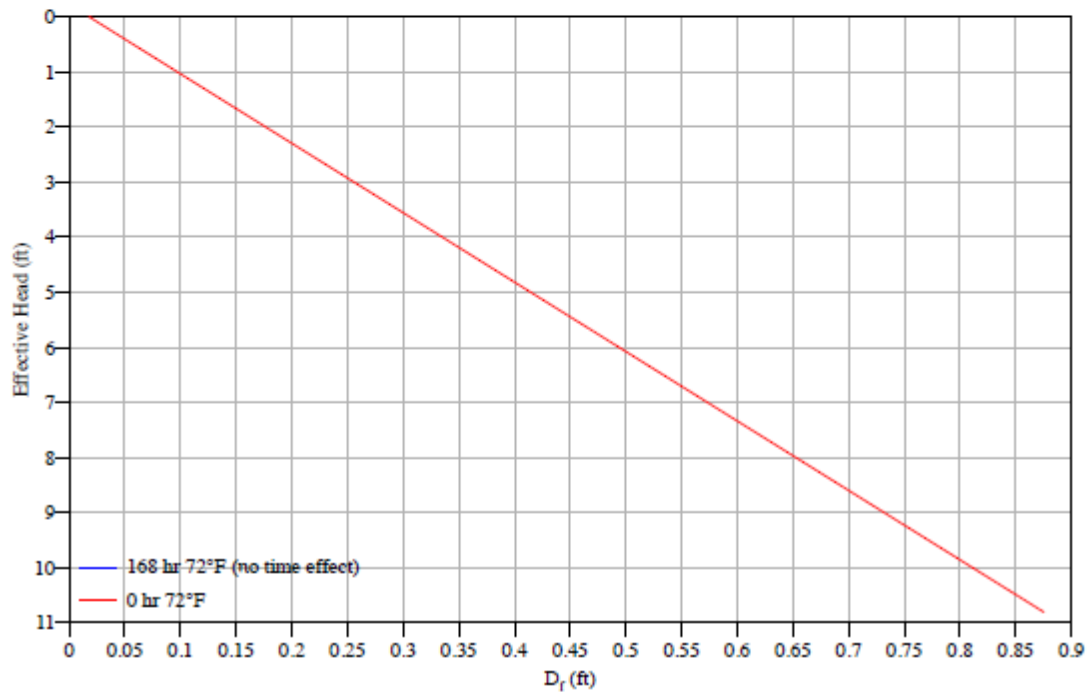


Figure C.120 ZrSiO<sub>4</sub>: Critical rathole dimensions

## Bulk density

### Temperature 70°F

The bulk weight density,  $\gamma$ , is a function of the major consolidating pressure,  $\sigma_1$ , expressed in terms of Effective Head.

Table 2.3: Bulk weight density

Effective Head	ft	0.5	1	2.5	5	10	20
$\sigma_1$	lb/ft <sup>2</sup>	69.5	139	349.8	701.7	1408	2826
$\gamma$	lb/ft <sup>3</sup>	139.1	139.4	139.9	140.3	140.8	141.3

### Compressibility parameters

Bulk weight density,  $\gamma$ , is a function of the major consolidating pressure  $\sigma_1$ , as follows:

$$\gamma = \gamma_m (1 + \sigma_1 / \sigma_m)^{\beta_m} \quad \text{for} \quad 138.6 < \gamma < 141.1 \text{ lb/ft}^3$$

Table 2.4: Compressibility parameters

$\gamma_m$	lb/ft <sup>3</sup>	138.4
$\sigma_m$	lb/ft <sup>2</sup>	46.01
$\beta_m$		0.00494
$\gamma_{\text{loose fill}}$	lb/ft <sup>3</sup>	136.5

Figure 2.2: Compressibility curve

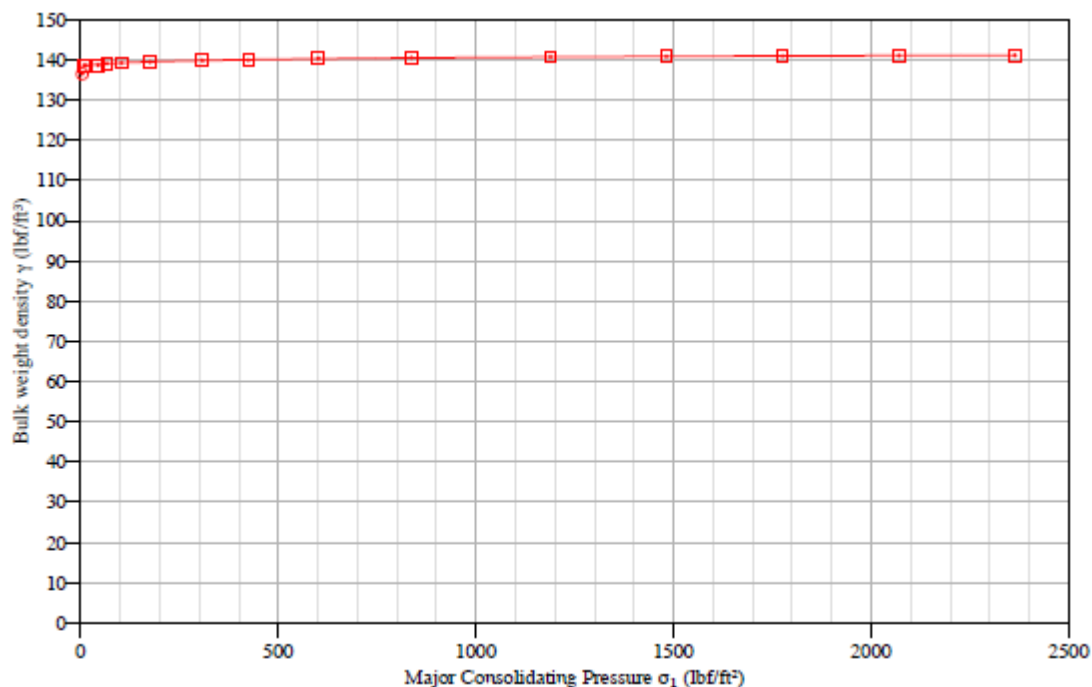


Figure C.121 ZrSiO<sub>4</sub>: Compressibility curve

## Maximum hopper angles for Mass Flow

Wall material 304 SS Sheet, #2B Finish, 12 ga

Figure 2.3: Conical hopper angles

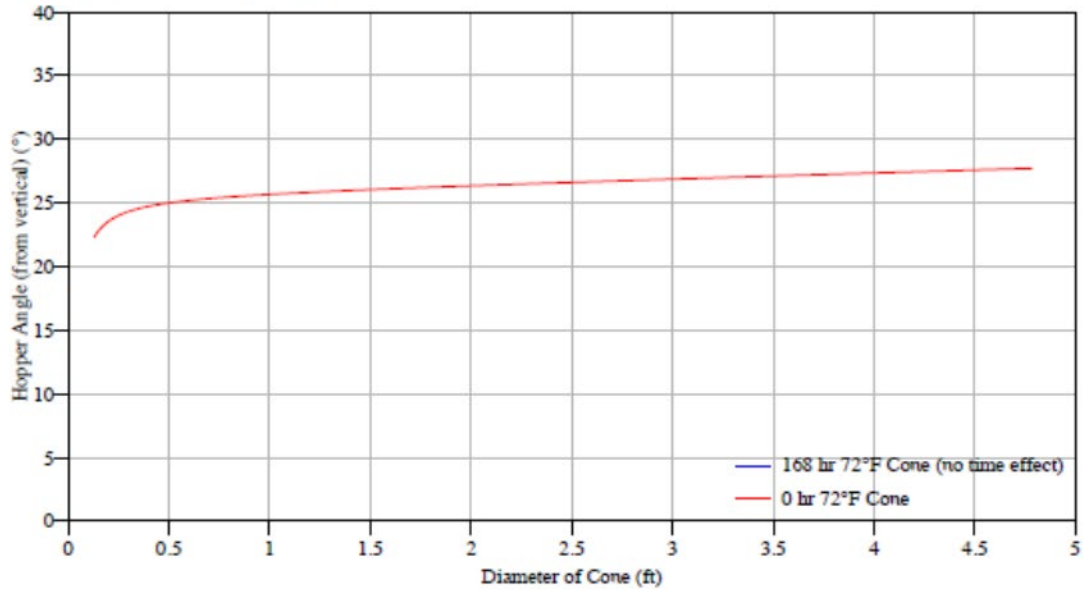


Figure 2.4: Wedge hopper angles

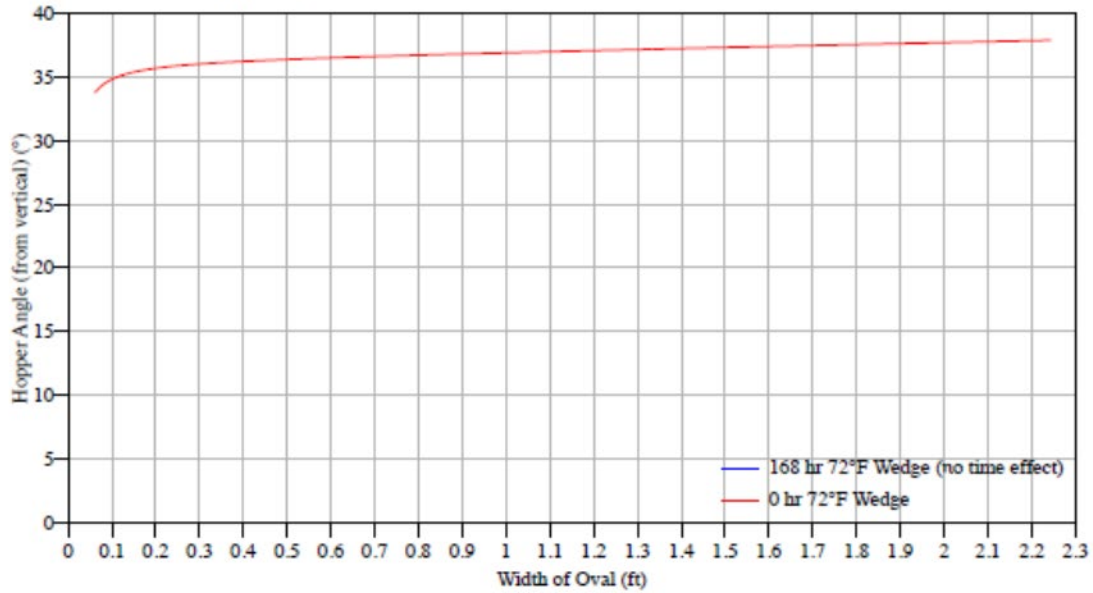


Figure C.122 ZrSiO<sub>4</sub>: Conical hopper angles (Top) and Wedge hopper angles (Bottom) with 304 SS sheet

Wall material Mild CS HR Plate, Mill Finish, 1/4"

Figure 2.5: Conical hopper angles

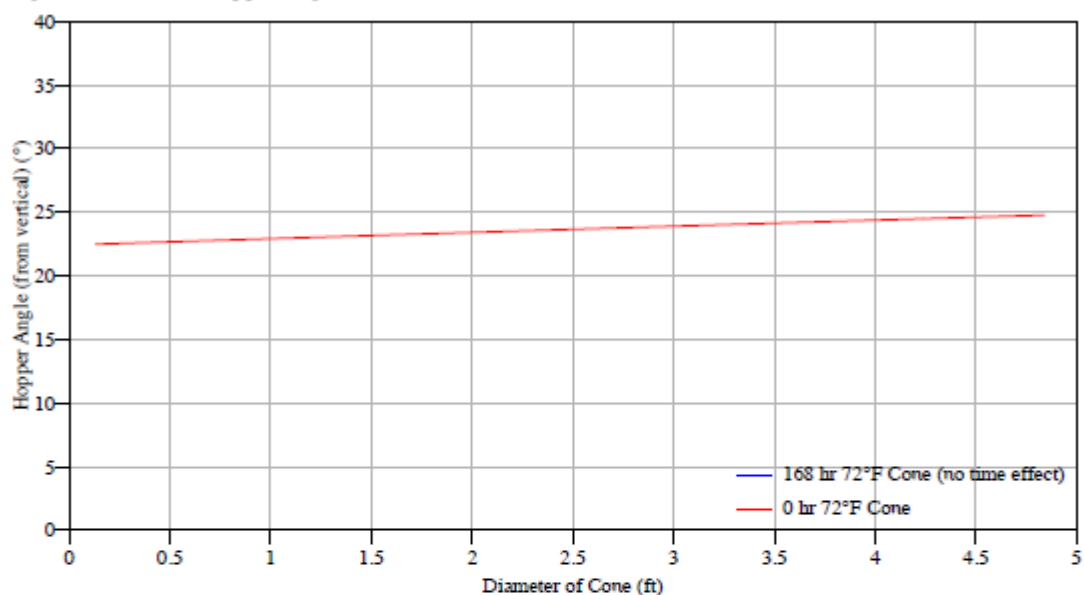


Figure 2.6: Wedge hopper angles

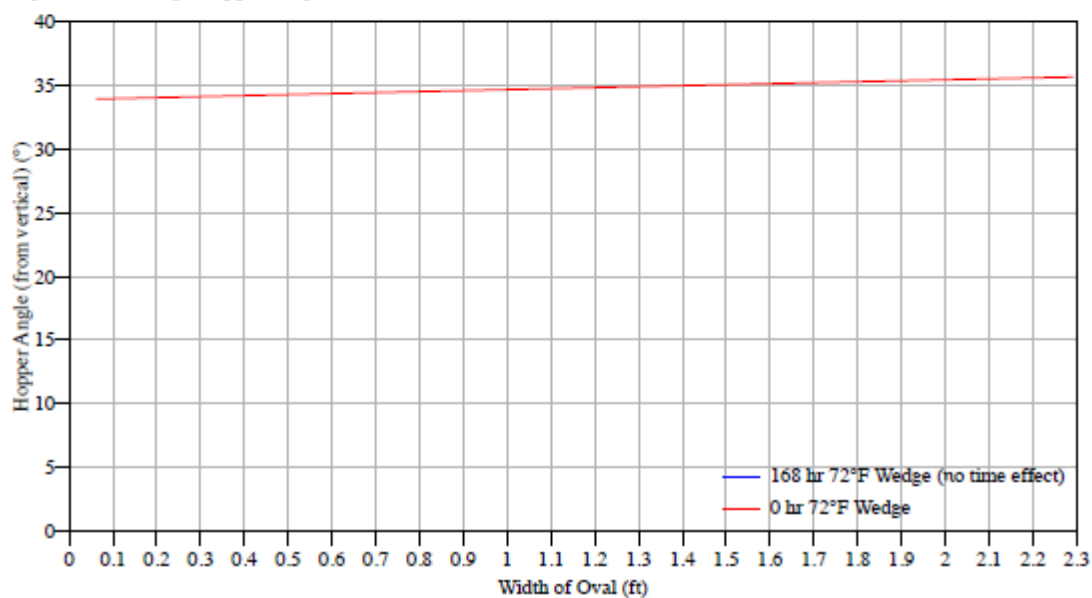


Figure C.123 ZrSiO<sub>4</sub>: Conical hopper angles (Top) and Wedge hopper angles (Bottom) with mild CS HR plate



Wall material Tivar-88

Figure 2.7: Conical hopper angles

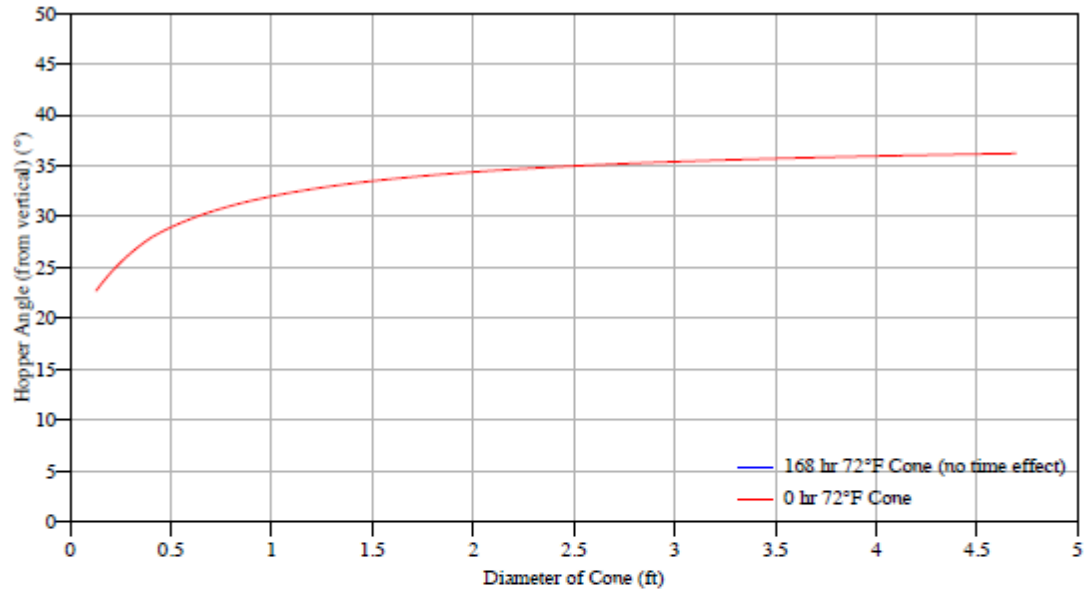


Figure 2.8: Wedge hopper angles

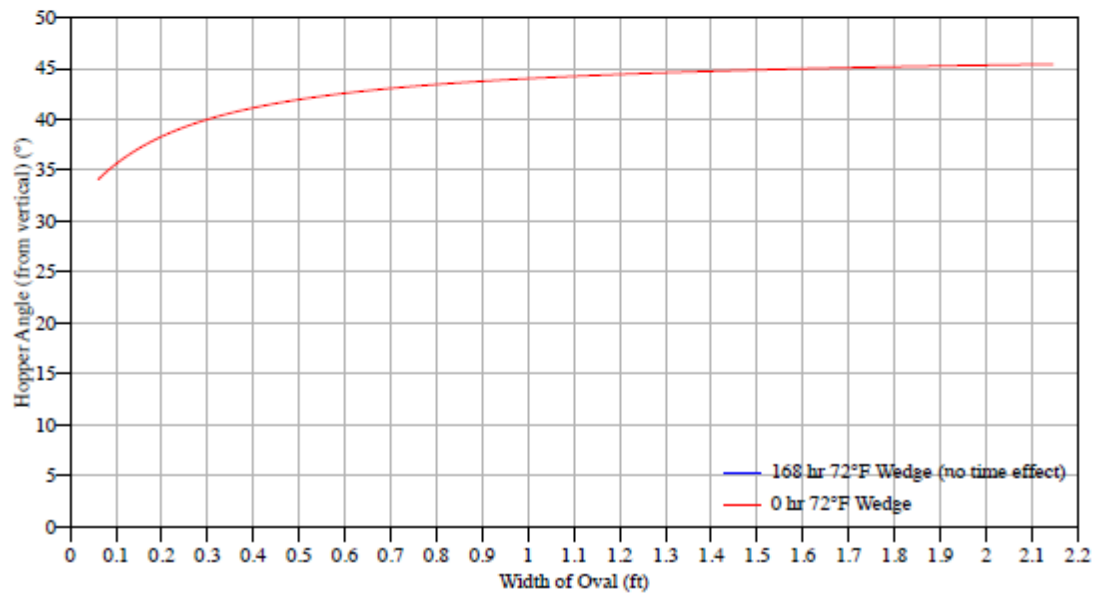


Figure C.124 ZrSiO<sub>4</sub>: Conical hopper angles (Top) and Wedge hopper angles (Bottom) with Tivar 88

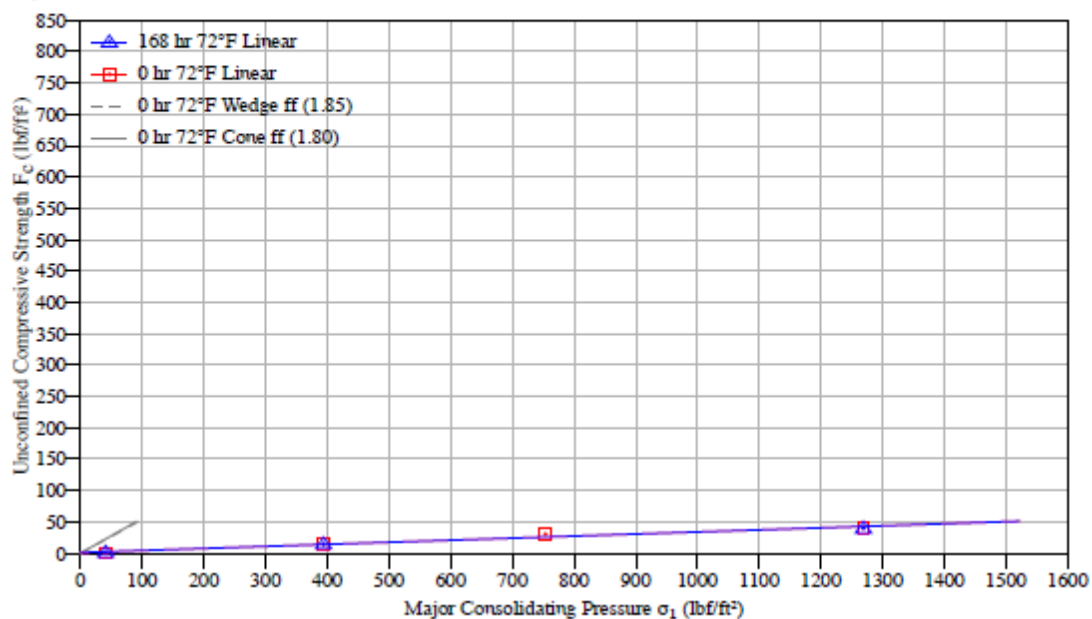


Figure C.125 ZrSiO<sub>4</sub>: Flow function

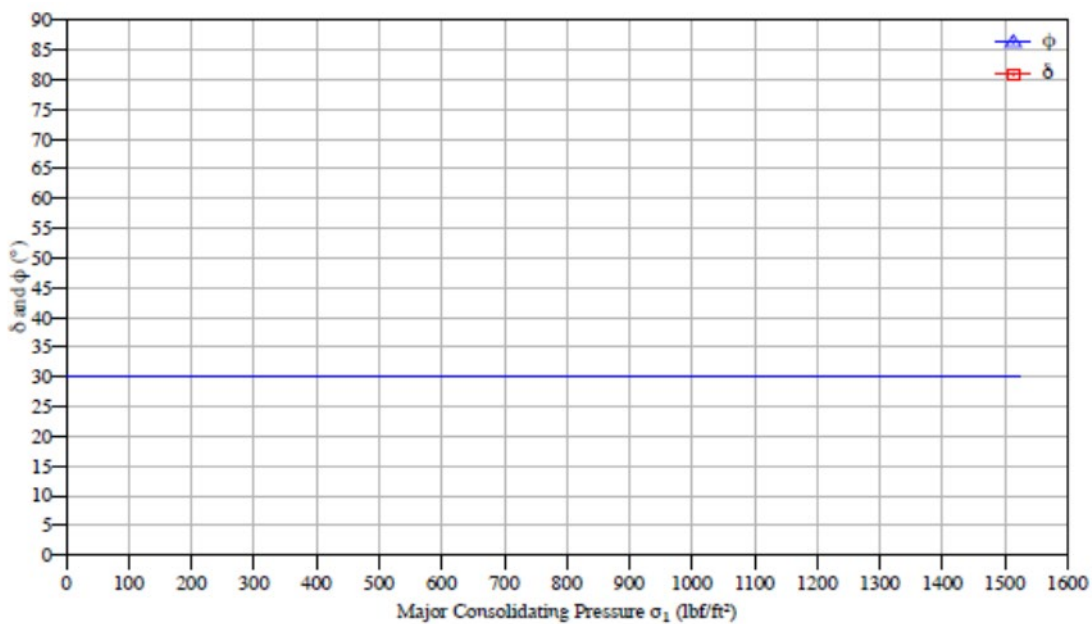


Figure C.126 ZrSiO<sub>4</sub>: Effective angle of friction ( $\delta$ ) and kinematic angle of internal friction ( $\phi$ )

## Air permeability test results

### Temperature 70°F

$K$  is a function of the bulk weight density of the solid

$$K = K_0 \left( \frac{\gamma}{\gamma_0} \right)^{-\alpha}$$

At 70°F, for  $\gamma$  between 134 and 145  $lb_f/ft^3$ :

Table 2.4: Permeability parameters

$K_0$	$ft/s$	0.03869
$\gamma_0$	$lb_f/ft^3$	139
$\alpha$		4.809

Figure 2.16: Permeability curve

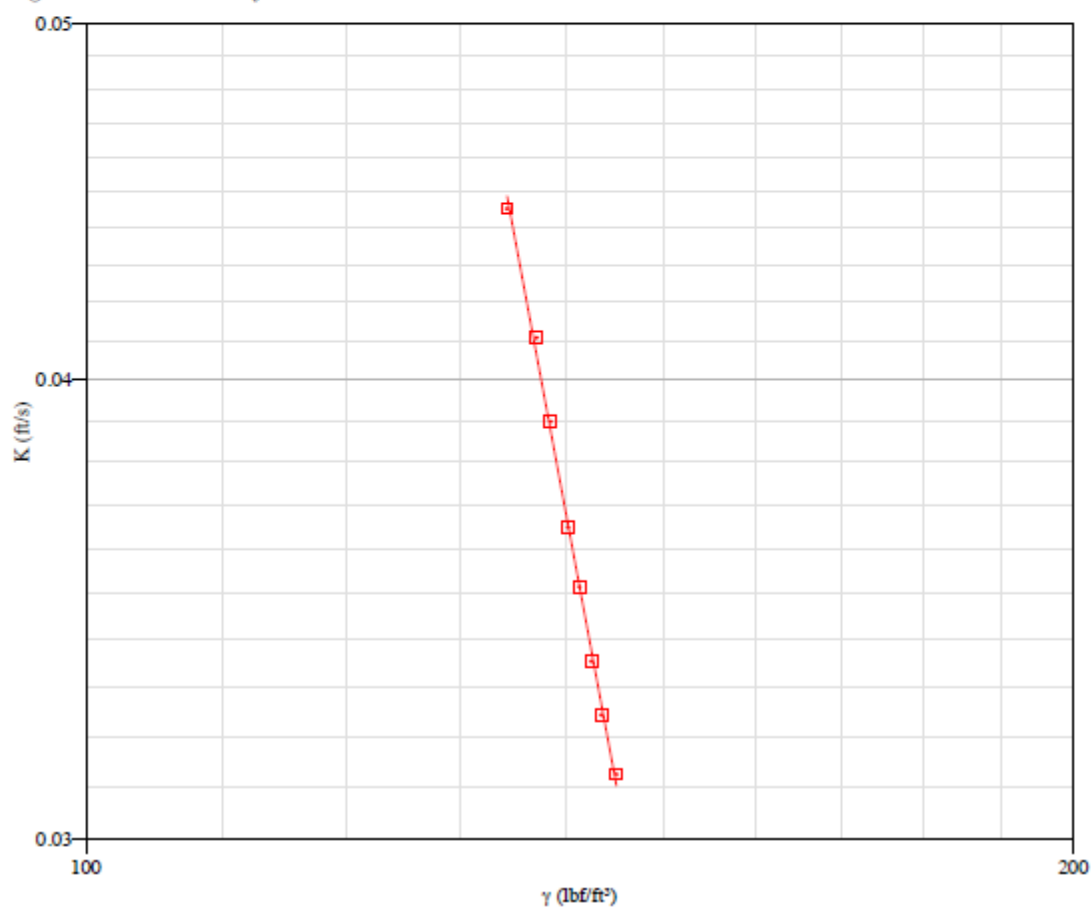


Figure C.127 ZrSiO<sub>4</sub>: Permeability curve

## Chute angles

Chute material 304 SS Sheet, #2B Finish, 12 ga

Storage time at rest 7 min

Chute temperature 72°F

Material temperature 71°F

Table 2.5: Measured chute clean-off angles (from horizontal)

Impact Pressure $lb_f/ft^2$	Angle $^\circ$
7.9	19 to 21
47	20 to 21
86.1	19 to 21
164.4	20 to 21

Figure 2.17: Chute curve

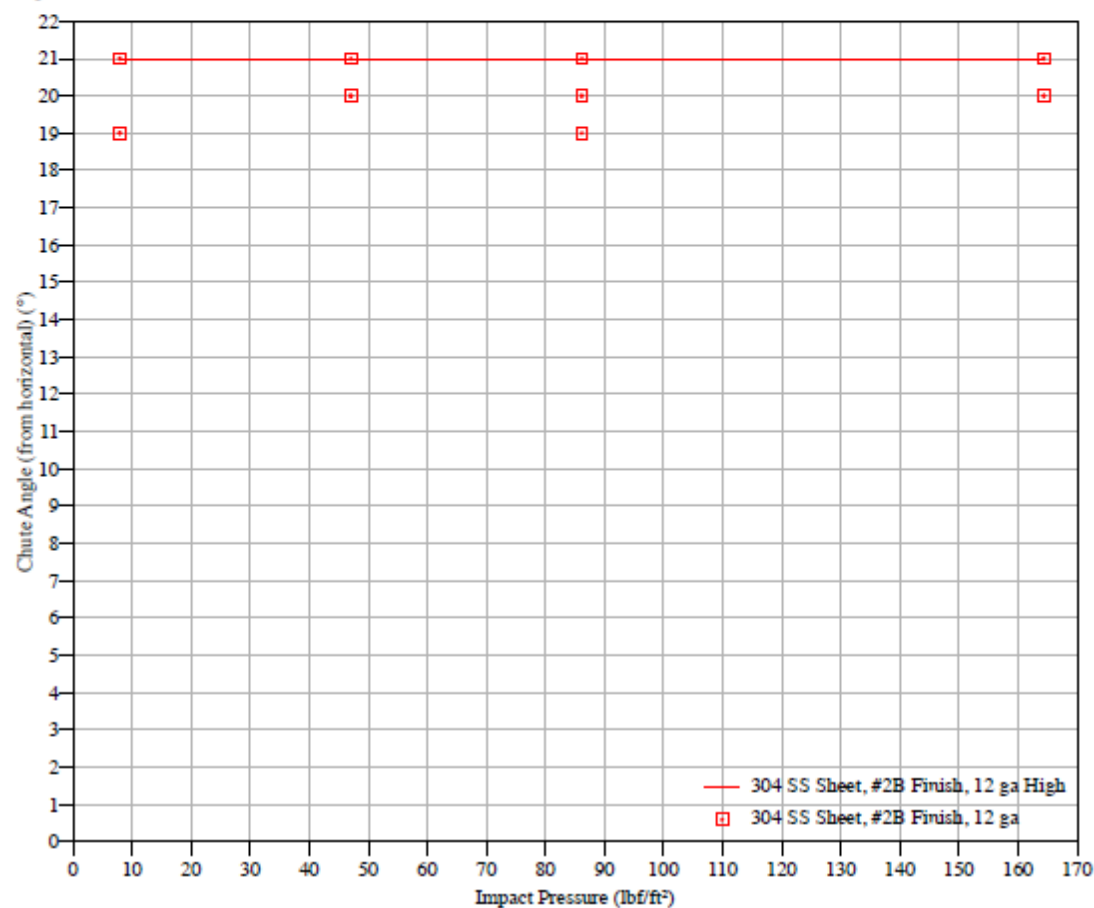


Figure C.128 ZrSiO<sub>4</sub>: Chute curve with 304 SS sheet

Chute material Mild CS HR Plate, Mill Finish, 1/4"  
Storage time at rest 0 hr  
Chute temperature 72°F  
Material temperature 71°F

Table 2.6: Measured chute clean-off angles (from horizontal)

Impact Pressure $lb_f/ft^2$	Angle $^\circ$
7.8	21 to 23
46.9	23 to 25
86	24 to 26
164.2	24 to 26

Figure 2.18: Chute curve

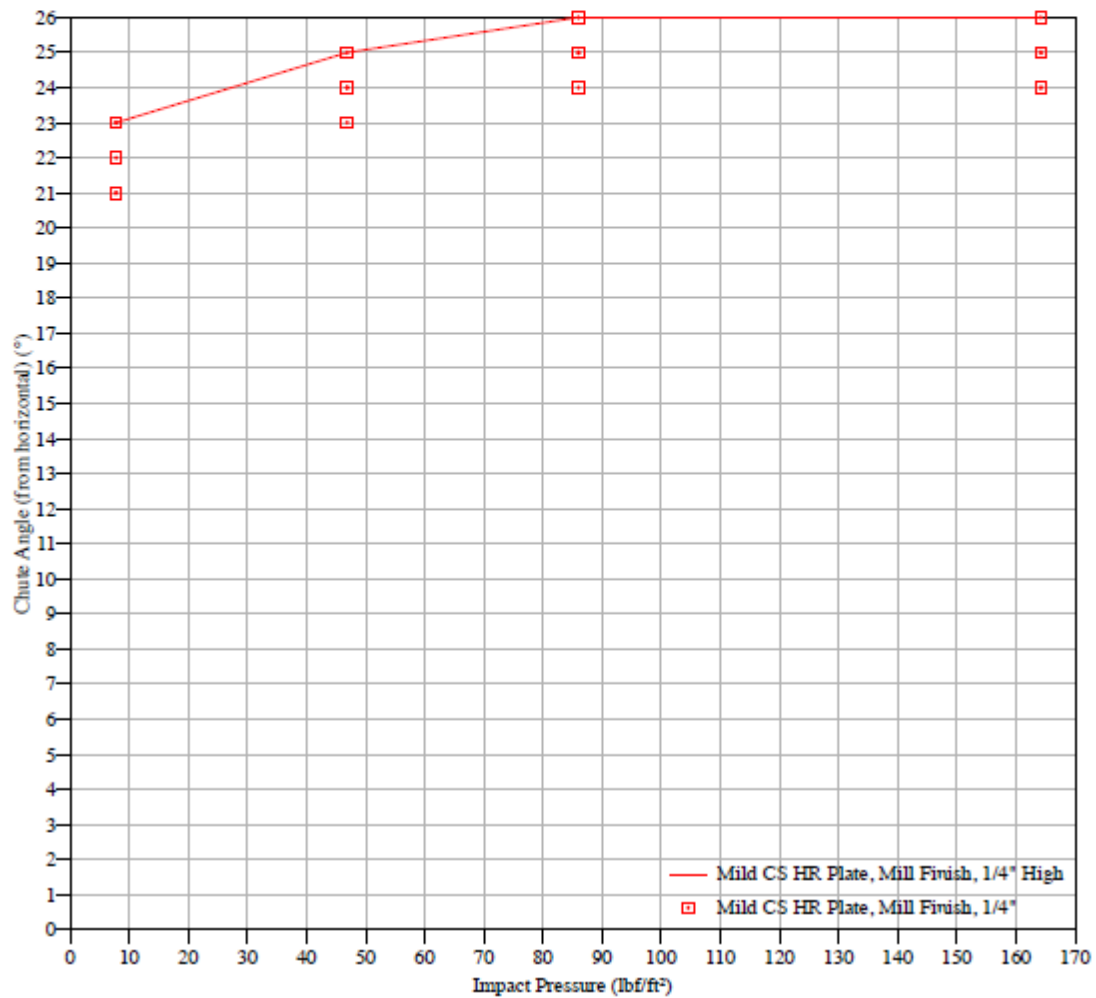


Figure C.129 ZrSiO<sub>4</sub>: Chute curve with mild CS HR plate

Chute material Tivar-88  
Storage time at rest 0 hr  
Chute temperature 72°F  
Material temperature 71°F

Table 2.7: Measured chute clean-off angles (from horizontal)

Impact Pressure $lb_f/ft^2$	Angle $^\circ$
7.8	23 to 24
46.9	24 to 25
86.1	25 to 26
164.3	24 to 26

Figure 2.19: Chute curve

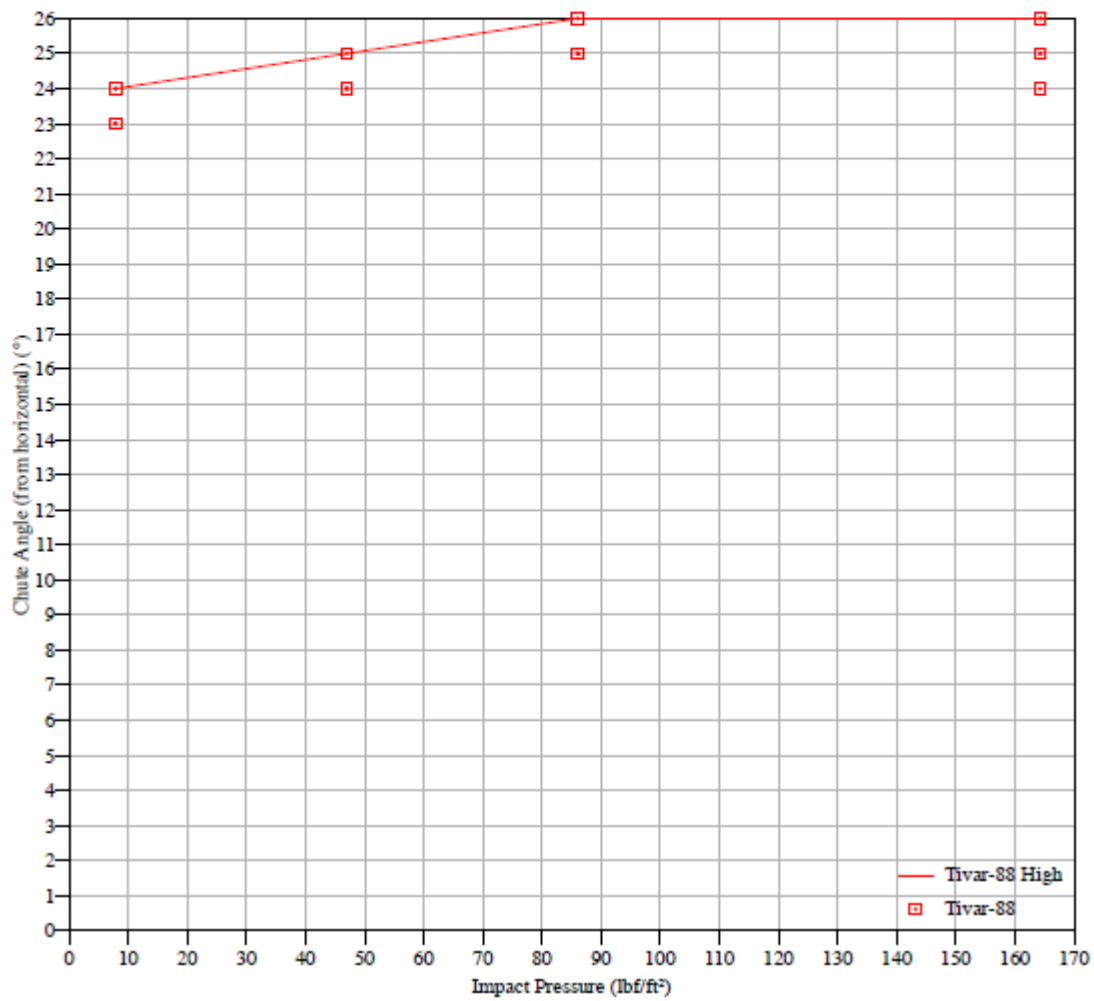


Figure C.130 ZrSiO<sub>4</sub>: Chute curve with Tivar 88

## Particle Size Distribution Analysis Comparison

Figure 2.22: Particle size distribution, by volume

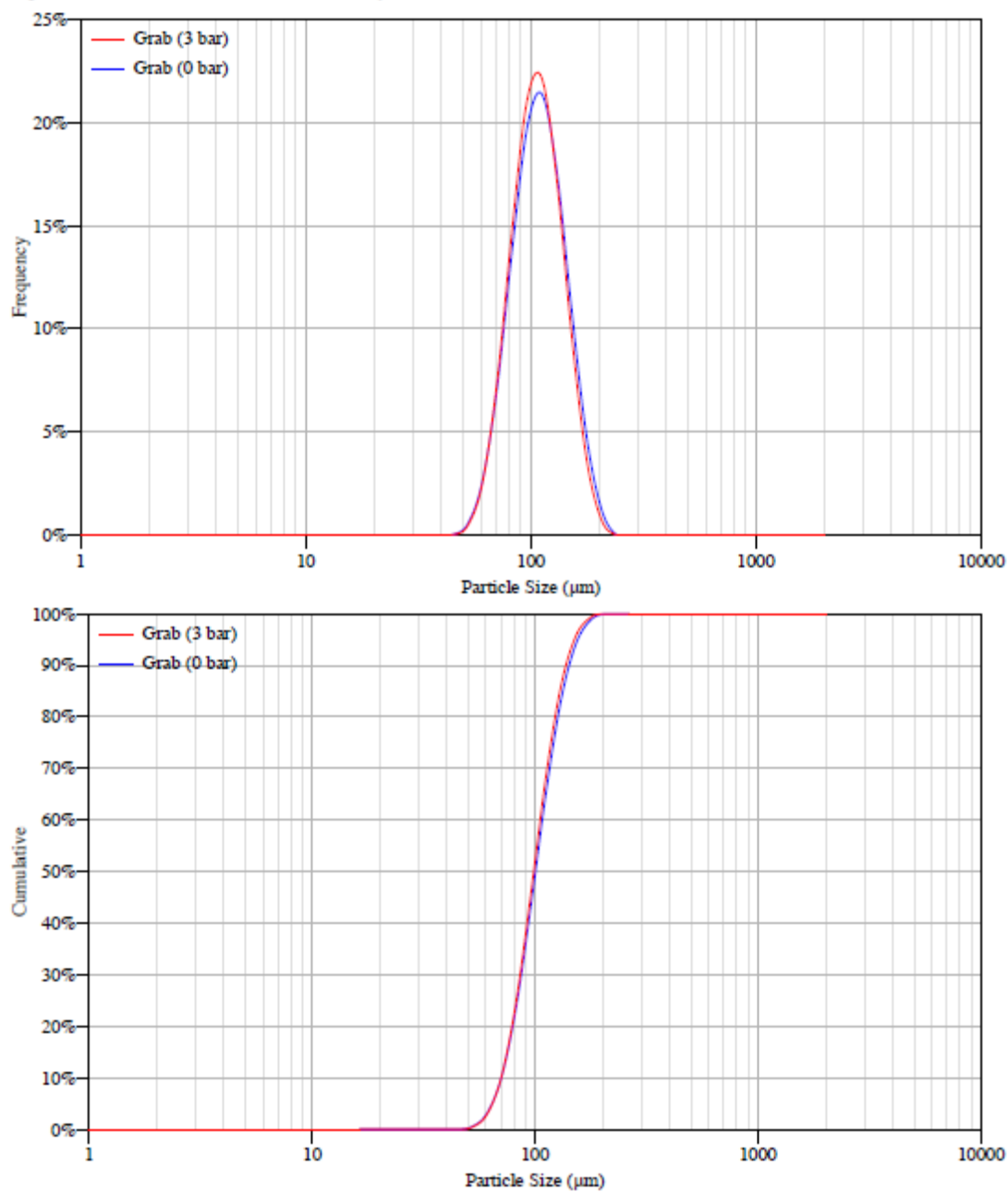


Figure C.131 ZrSiO<sub>4</sub>: Particle size distribution by volume and pressure

## C.10 LAW batch #1b

### Bin dimensions for dependable flow

Storage time at rest 0 hr

Temperature 72°F

Table 3.1: Critical outlet dimensions to prevent arching

P – Factor	B <sub>c</sub> ft	B <sub>p</sub> ft	B <sub>f</sub> ft
1.00	1.2	0.6	0.7
1.25	1.4	0.7	0.95
1.50	1.7	0.8	1.5
2.00	+++	***	***

+++ Denotes unassisted gravity flow is impossible. However, diameters of only up to 9.65 ft were simulated by our tests. If larger diameters are practical for your application, further testing at higher pressures might reveal conditions under which unassisted gravity flow is possible.

\*\*\* Denotes unassisted gravity flow is impossible. However, widths of only up to 4.8 ft were simulated by our tests. If larger widths are practical for your application, further testing at higher pressures might reveal conditions under which unassisted gravity flow is possible.

For detailed explanations of terms see pg. 166.

Figure 3.1: Critical rathole dimensions (P – Factor = 1)

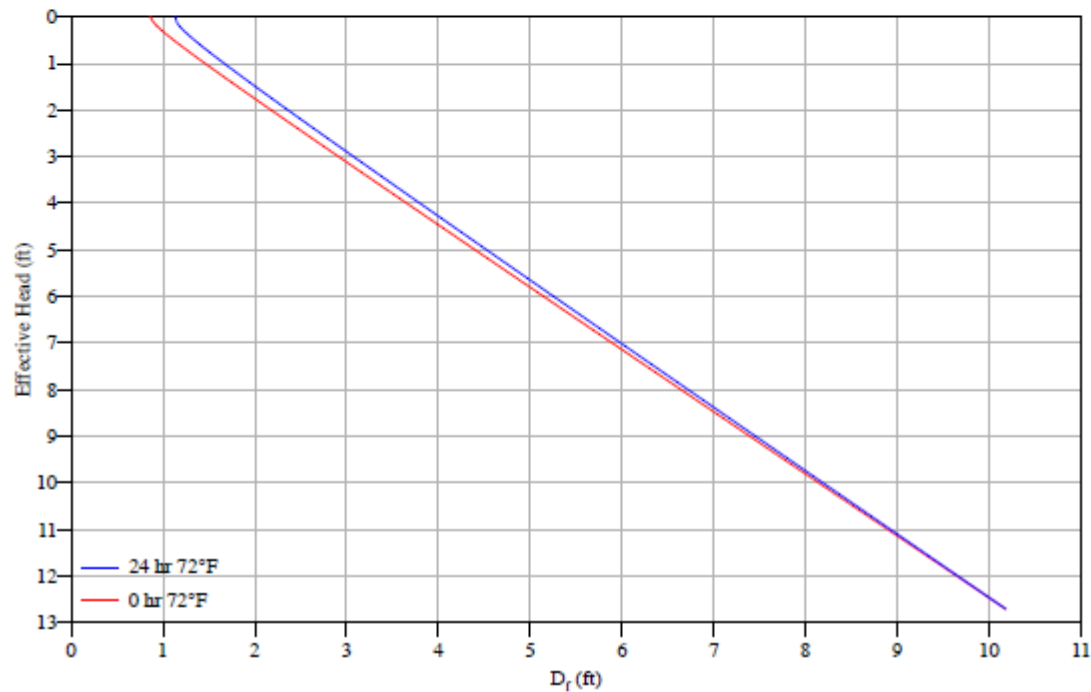


Figure C.132 LAW batch #1b: Critical rathole dimensions



## Bulk density

### Temperature 71°F

The bulk weight density,  $\gamma$ , is a function of the major consolidating pressure,  $\sigma_1$ , expressed in terms of Effective Head.

Table 3.3: Bulk weight density

Effective Head	ft	0.5	1	2.5	5	10	20
$\sigma_1$	lb/ft <sup>2</sup>	33.7	70.7	189	399	841.3	1774
$\gamma$	lb/ft <sup>3</sup>	67.3	70.7	75.7	79.8	84.1	88.7

### Compressibility parameters

Bulk weight density,  $\gamma$ , is a function of the major consolidating pressure  $\sigma_1$ , as follows:

$$\gamma = \gamma_m (1 + \sigma_1 / \sigma_m)^{\beta_m} \quad \text{for } 62.7 < \gamma < 89.2 \text{ lb/ft}^3$$

Table 3.4: Compressibility parameters

$\gamma_m$	lb/ft <sup>3</sup>	56.8
$\sigma_m$	lb/ft <sup>2</sup>	3.35
$\beta_m$		0.0712
$\gamma_{\text{loose fill}}$	lb/ft <sup>3</sup>	57.9

Figure 3.2: Compressibility curve

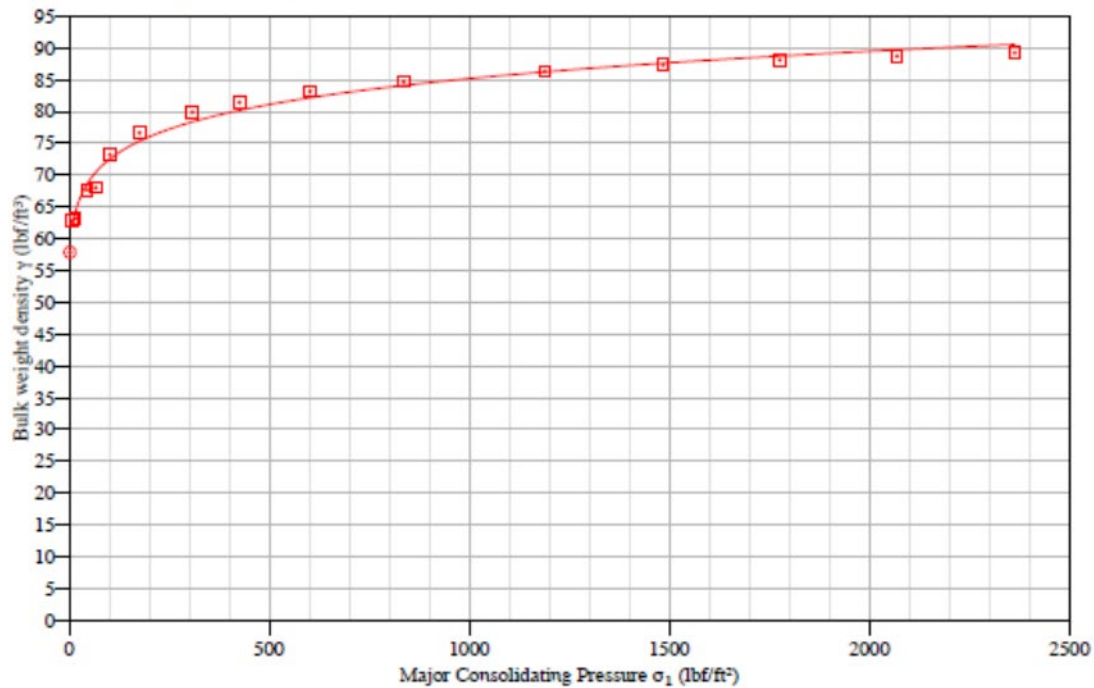


Figure C.133 LAW batch #1b: Compressibility curve

## Maximum hopper angles for Mass Flow

Wall material 304 SS Sheet, #2B Finish, 12 ga

Figure 3.3: Conical hopper angles

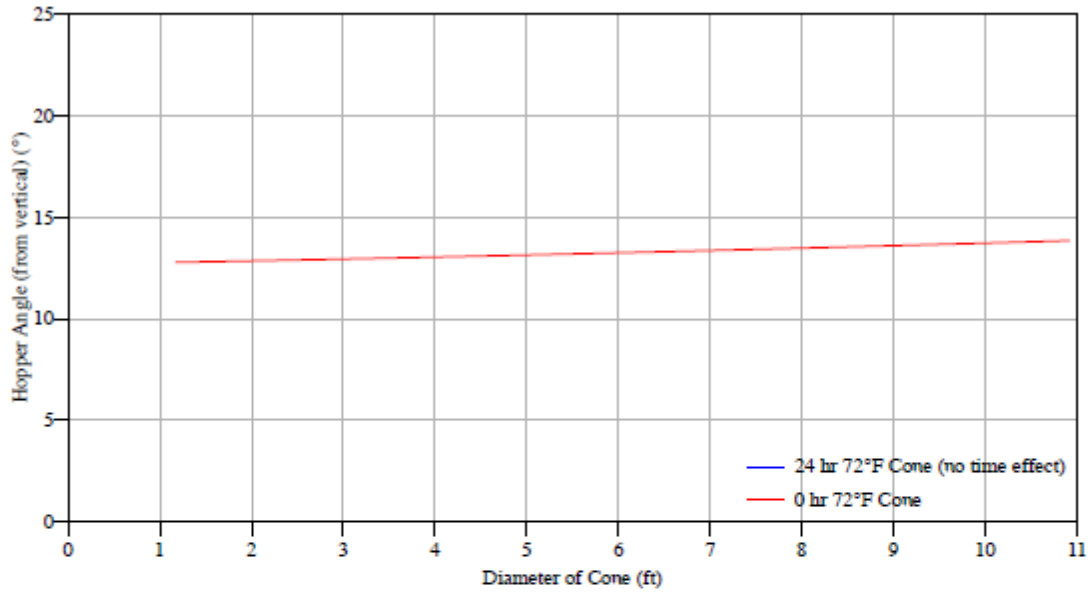


Figure 3.4: Wedge hopper angles

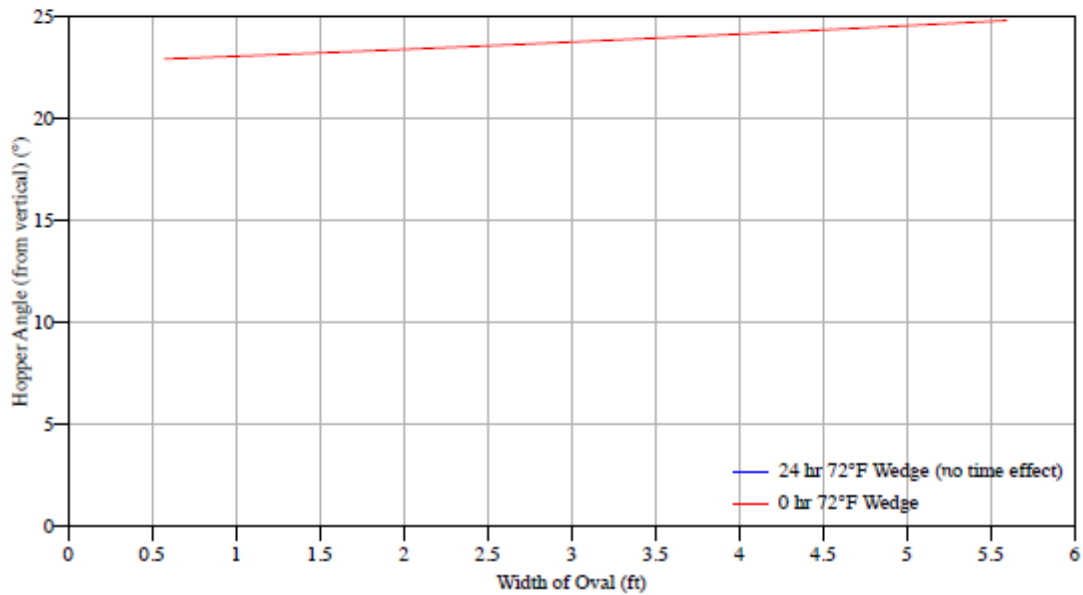


Figure C.134 LAW batch #1b: Conical hopper angles (Top) and Wedge hopper angles (Bottom) with 304 SS sheet

Wall material Mild CS HR Plate, Mill Finish, 1/4"

Figure 3.5: Conical hopper angles

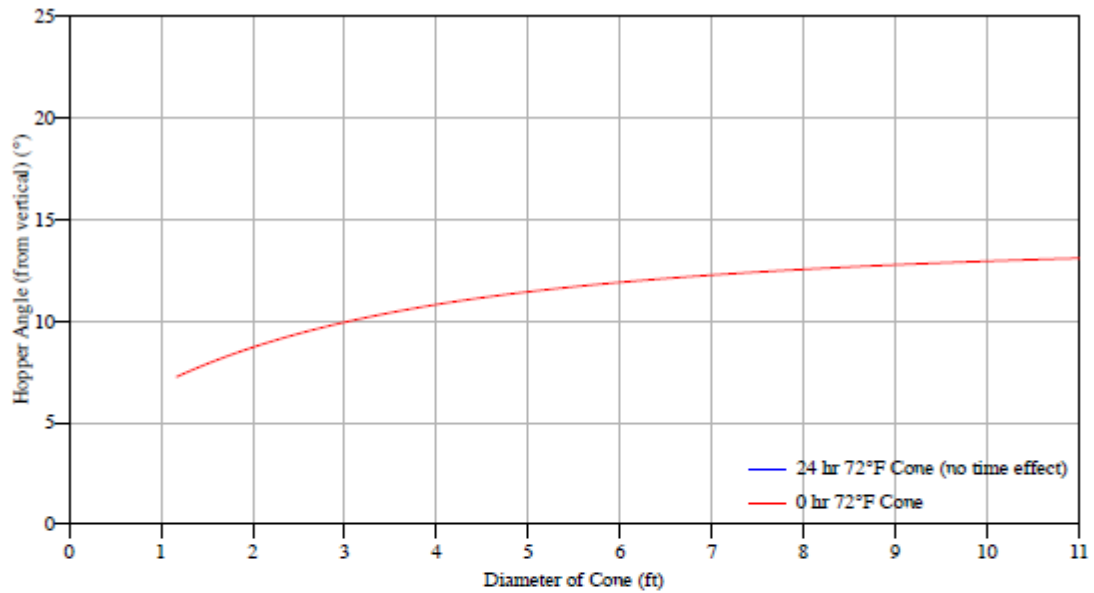


Figure 3.6: Wedge hopper angles

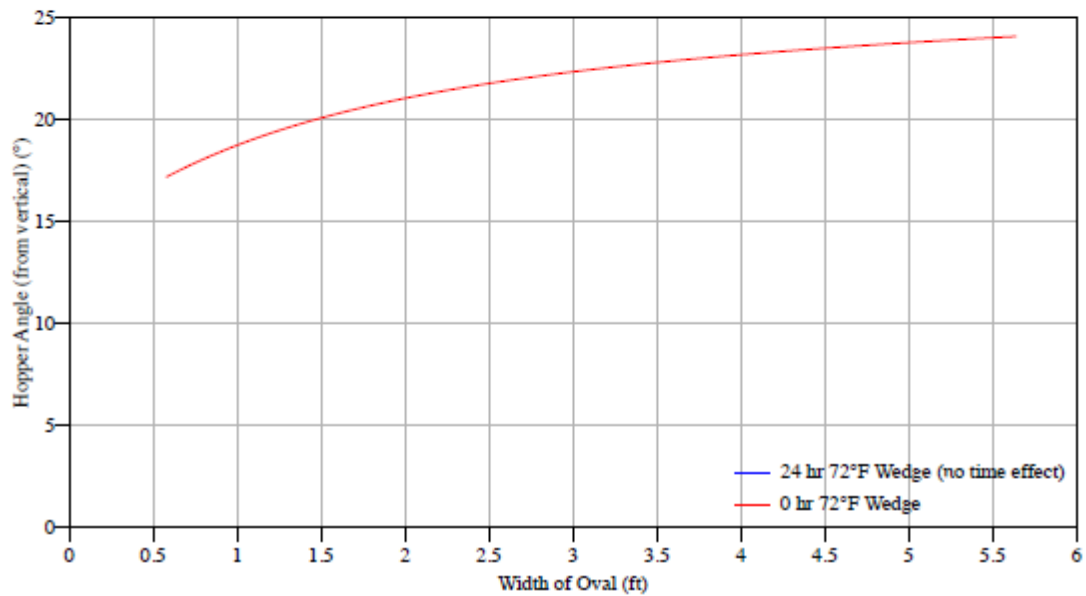


Figure C.135 LAW batch #1b: Conical hopper angles (Top) and Wedge hopper angles (Bottom) with mild CS HR plate

Wall material Tivar-88

Figure 3.7: Conical hopper angles

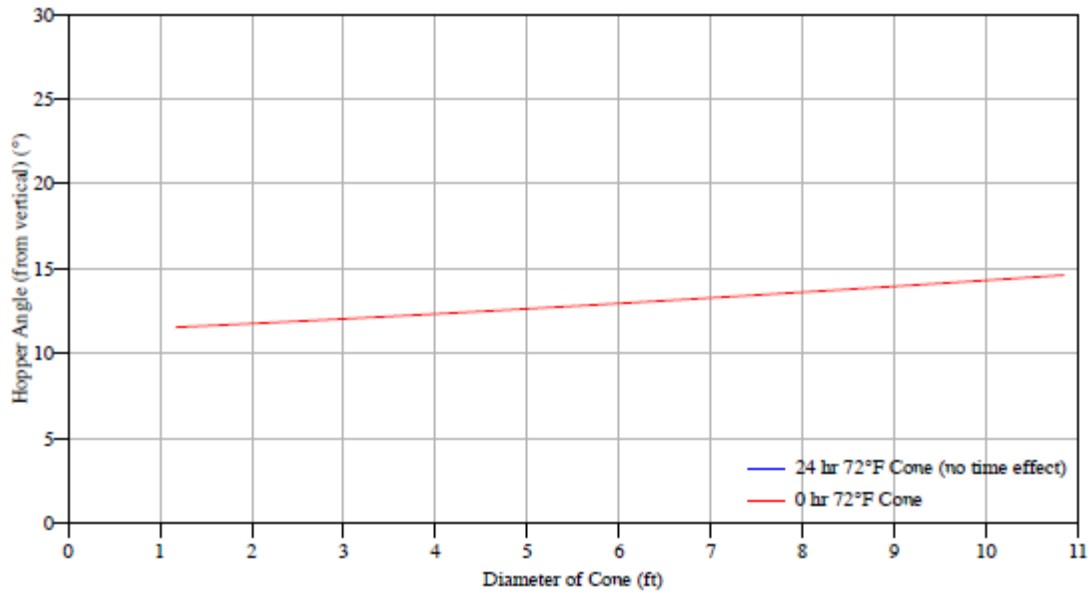


Figure 3.8: Wedge hopper angles

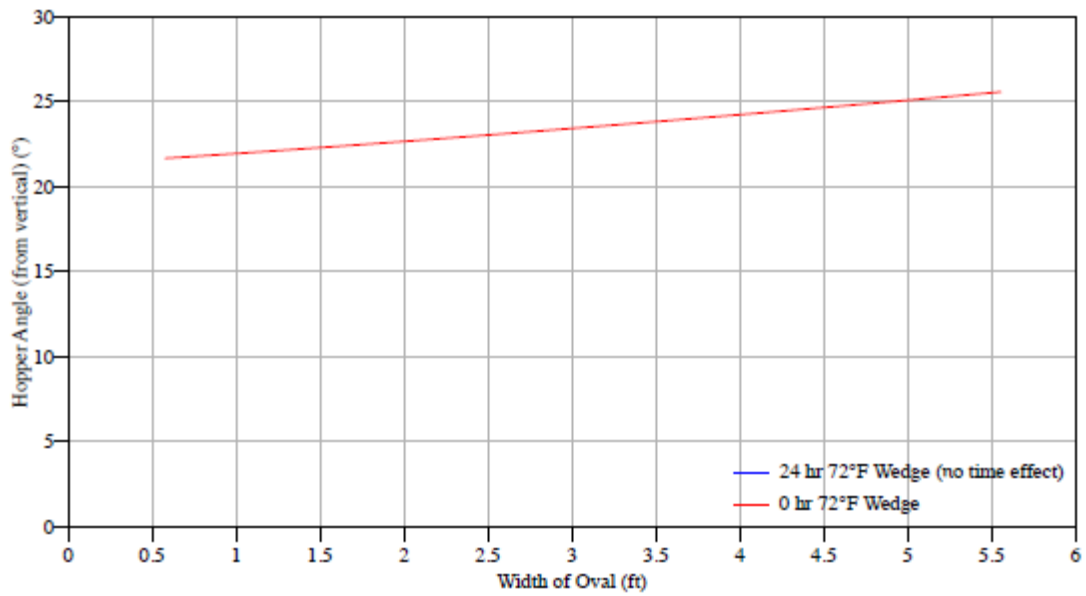


Figure C.136 LAW batch #1b: Conical hopper angles (Top) and Wedge hopper angles (Bottom) with Tivar 88

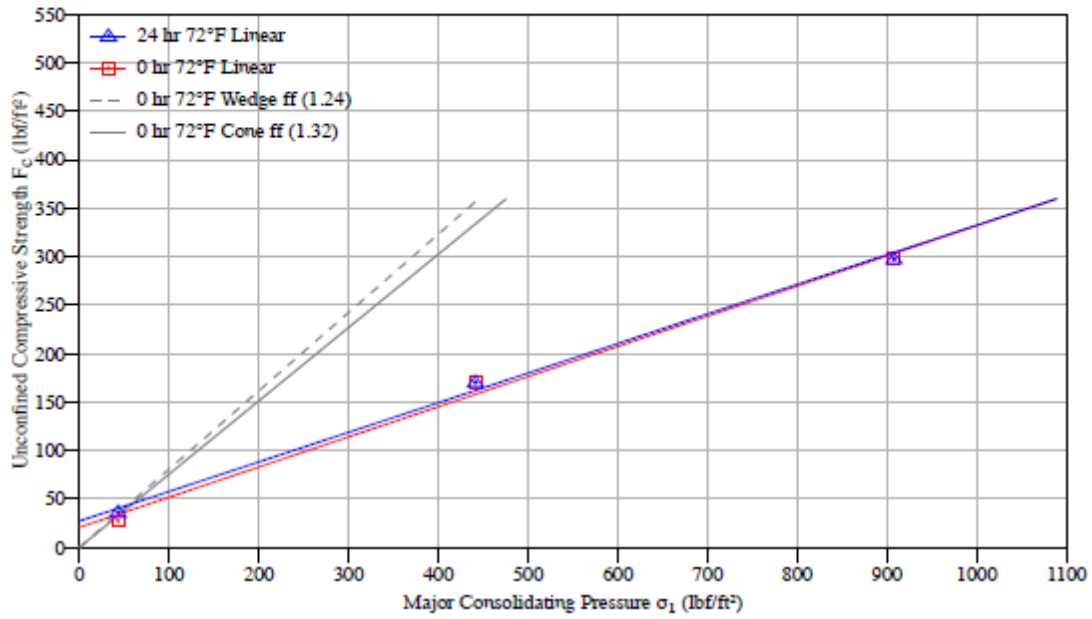


Figure C.137 LAW batch #1b: Flow function

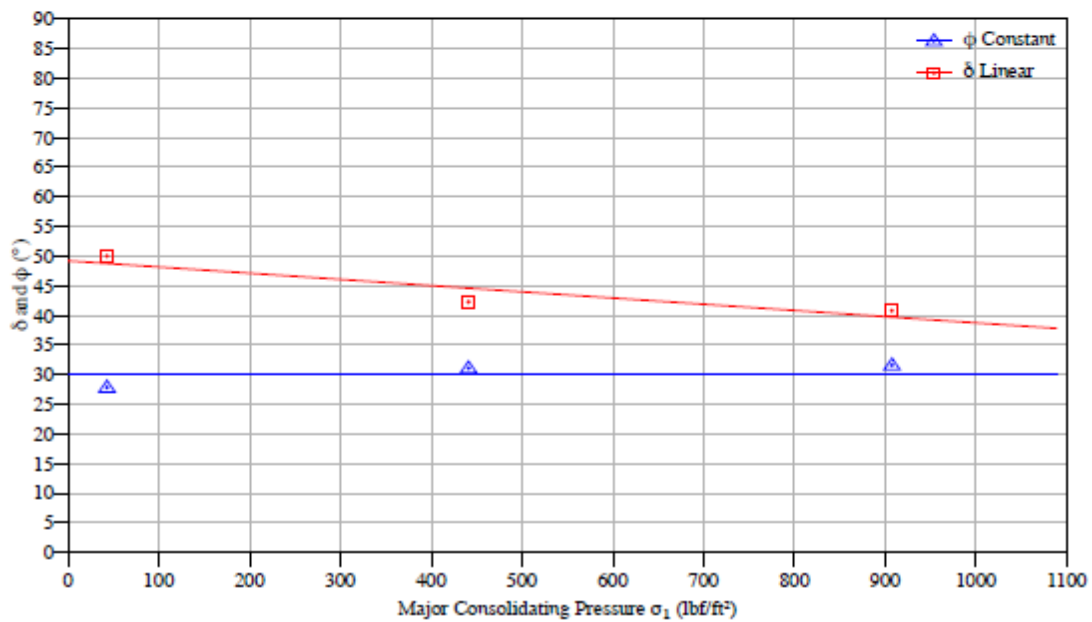


Figure C.138 LAW batch #1b: Effective angle of friction ( $\delta$ ) and kinematic angle of internal friction ( $\phi$ )

## Air permeability test results

### Temperature 71°F

K is a function of the bulk weight density of the solid

$$K = K_0 \left( \frac{\gamma}{\gamma_0} \right)^{-\alpha}$$

At 71°F, for  $\gamma$  between 61 and 90  $lb_f/ft^3$ :

Table 3.4: Permeability parameters

$K_0$ $ft/s$	0.001556
$\gamma_0$ $lb_f/ft^3$	63.5
$\alpha$	5.442

Figure 3.15: Permeability curve

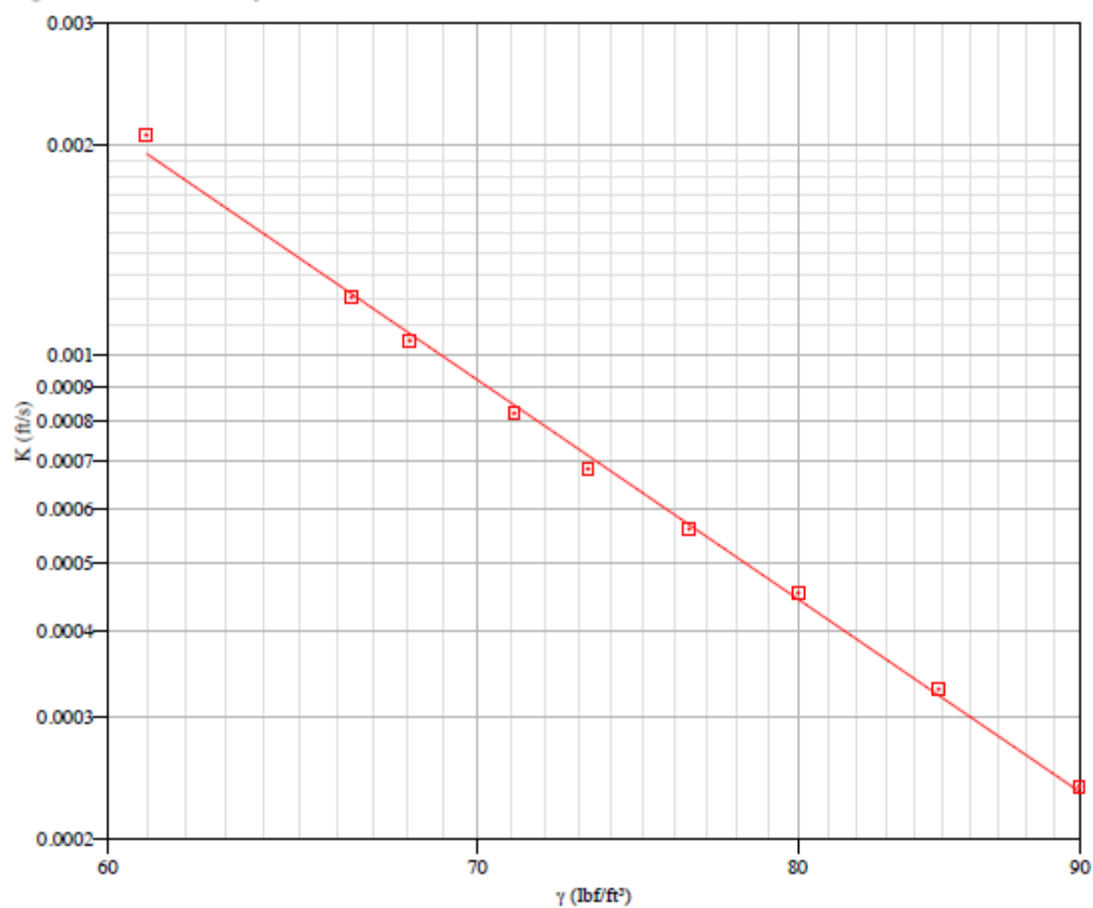


Figure C.139 LAW batch #1b: Permeability curve

## Chute angles

Chute material 304 SS Sheet, #2B Finish, 12 ga

Storage time at rest 0 hr

Chute temperature 72°F

Material temperature 70°F

Table 3.5: Measured chute clean-off angles (from horizontal)

Impact Pressure $lb_f/ft^2$	Angle $^\circ$
3.5	25 to 28
42.7	29 to 34
81.8	31 to 35
160	29 to 35

Figure 3.16: Chute curve

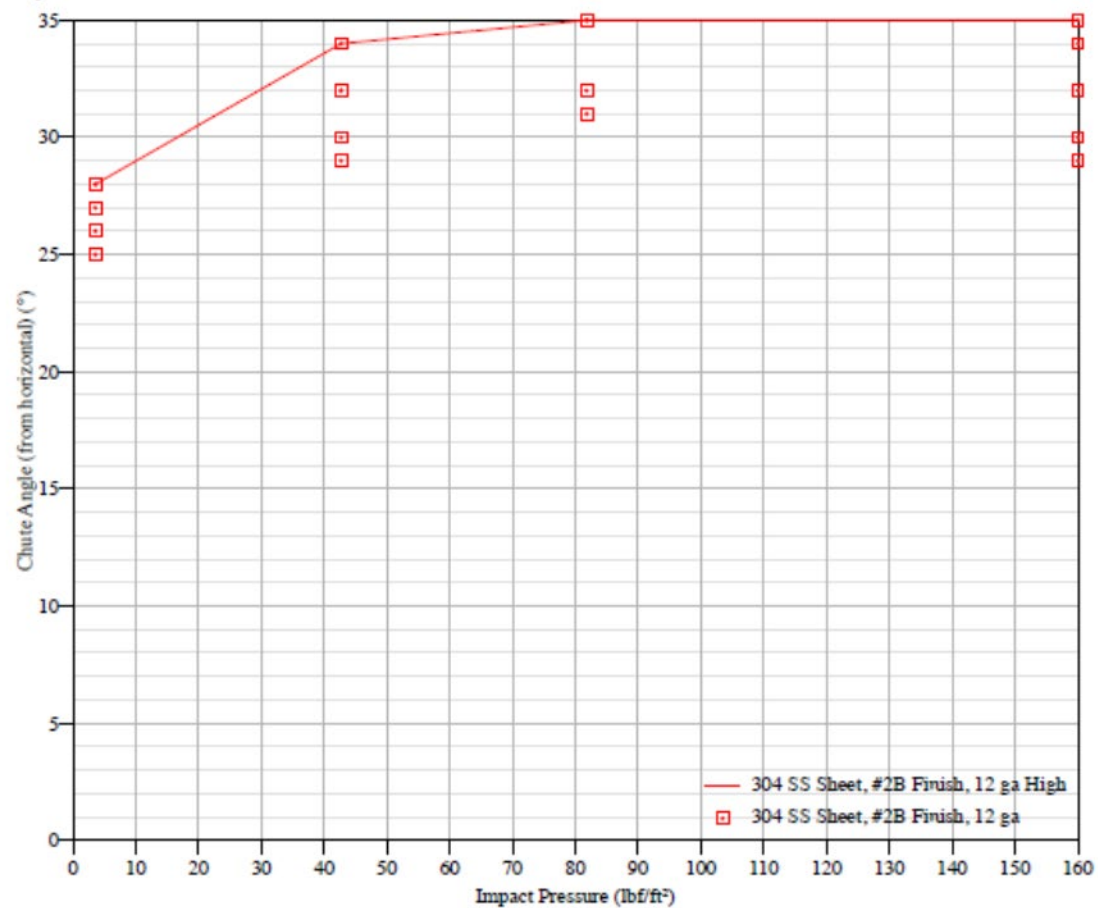


Figure C.140 LAW batch #1b: Chute curve with 304 SS sheet

Chute material Mild CS HR Plate, Mill Finish, 1/4"  
Storage time at rest 0 hr  
Chute temperature 72°F  
Material temperature 70°F

Table 3.6: Measured chute clean-off angles (from horizontal)

Impact Pressure $lb_f/ft^2$	Angle $^\circ$
3.7	30 to 33
42.8	37 to 39
81.9	39 to 41
160.1	38 to 43

Figure 3.17: Chute curve

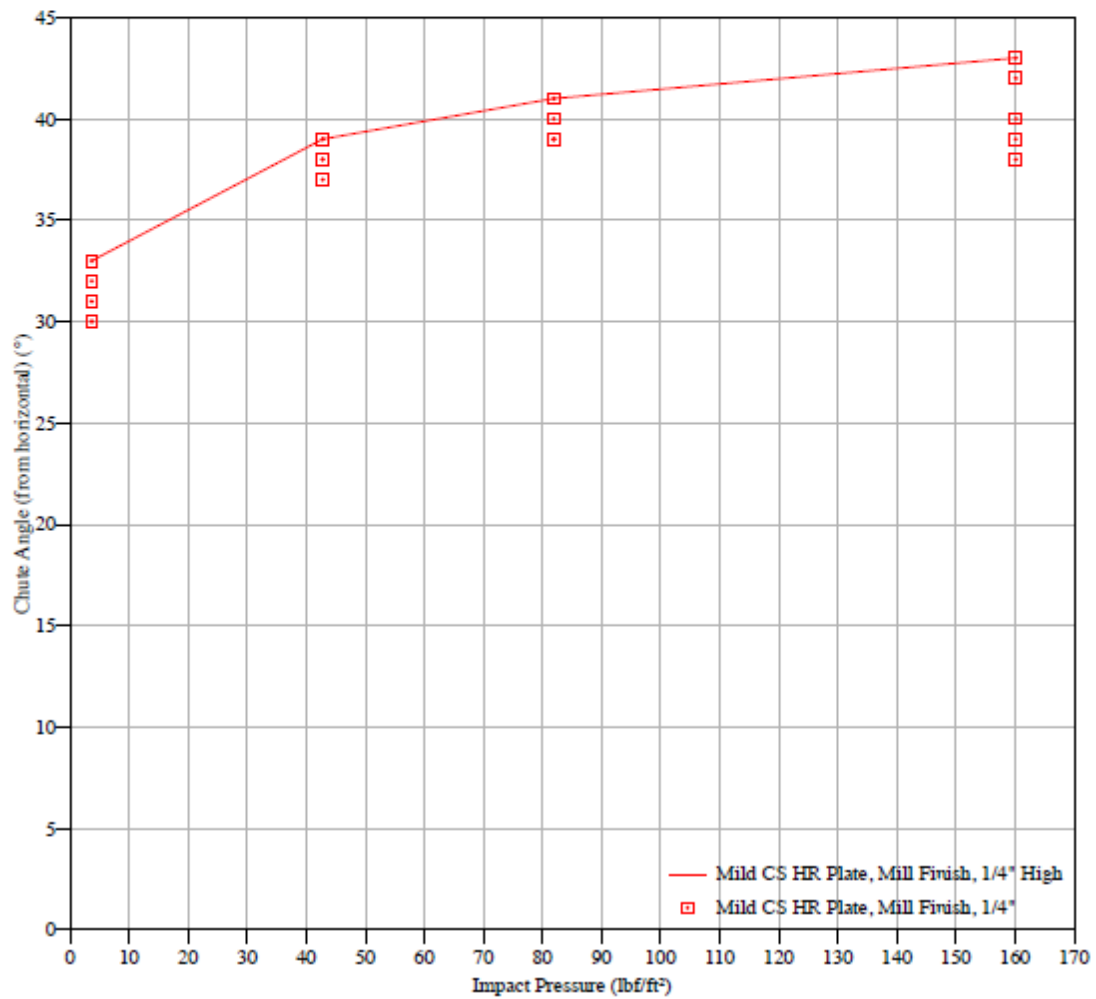


Figure C.141 LAW batch #1b: Chute curve with mild CS HR plate



Chute material Tivar-88  
Storage time at rest 0 hr  
Chute temperature 72°F  
Material temperature 70°F

Table 3.7: Measured chute clean-off angles (from horizontal)

Impact Pressure $lb_f/ft^2$	Angle $^\circ$
3.6	29 to 32
42.7	37 to 42
81.8	37 to 42
160.1	39 to 44

Figure 3.18: Chute curve

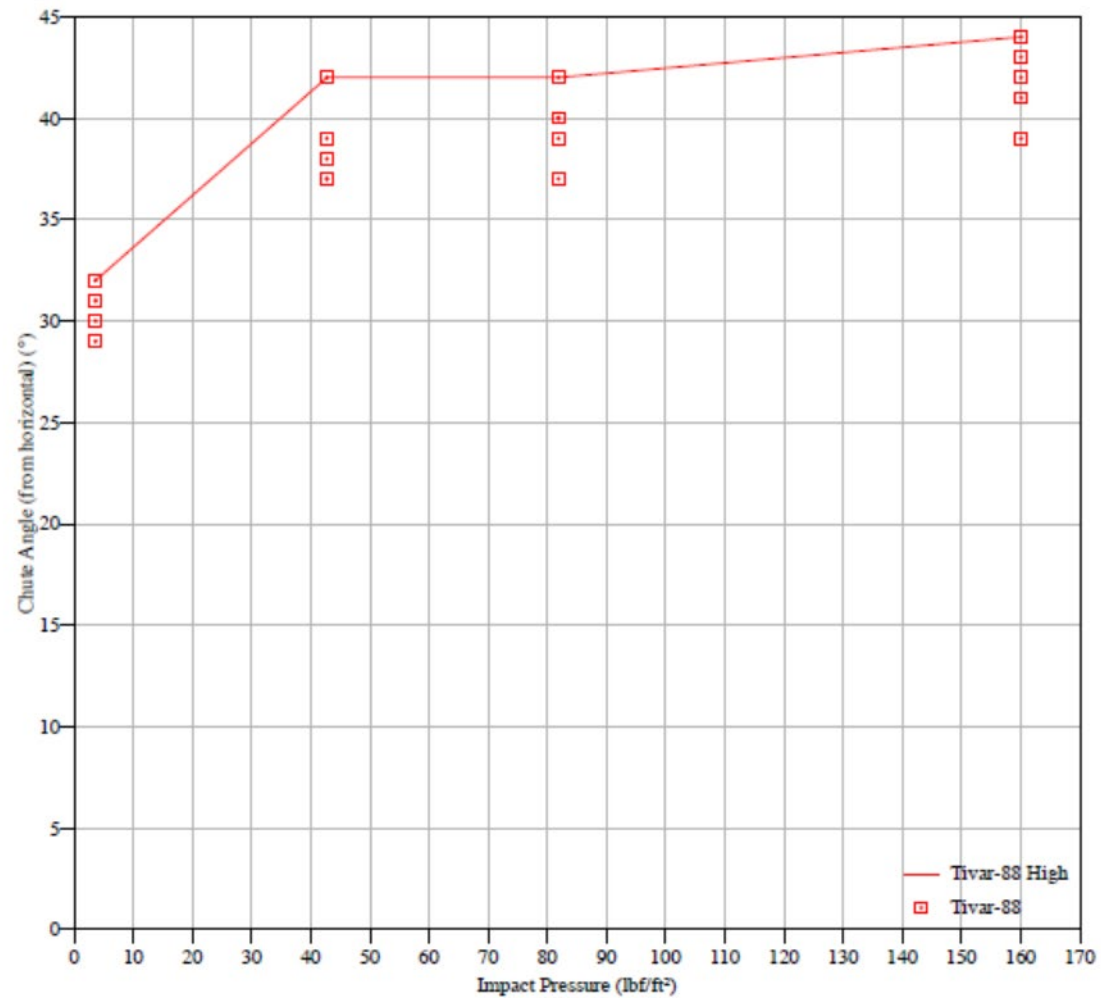


Figure C.142 LAW batch #1b: Chute curve with Tivar 88

## Particle Size Distribution Analysis Comparison

Figure 3.22: Particle size distribution, by volume

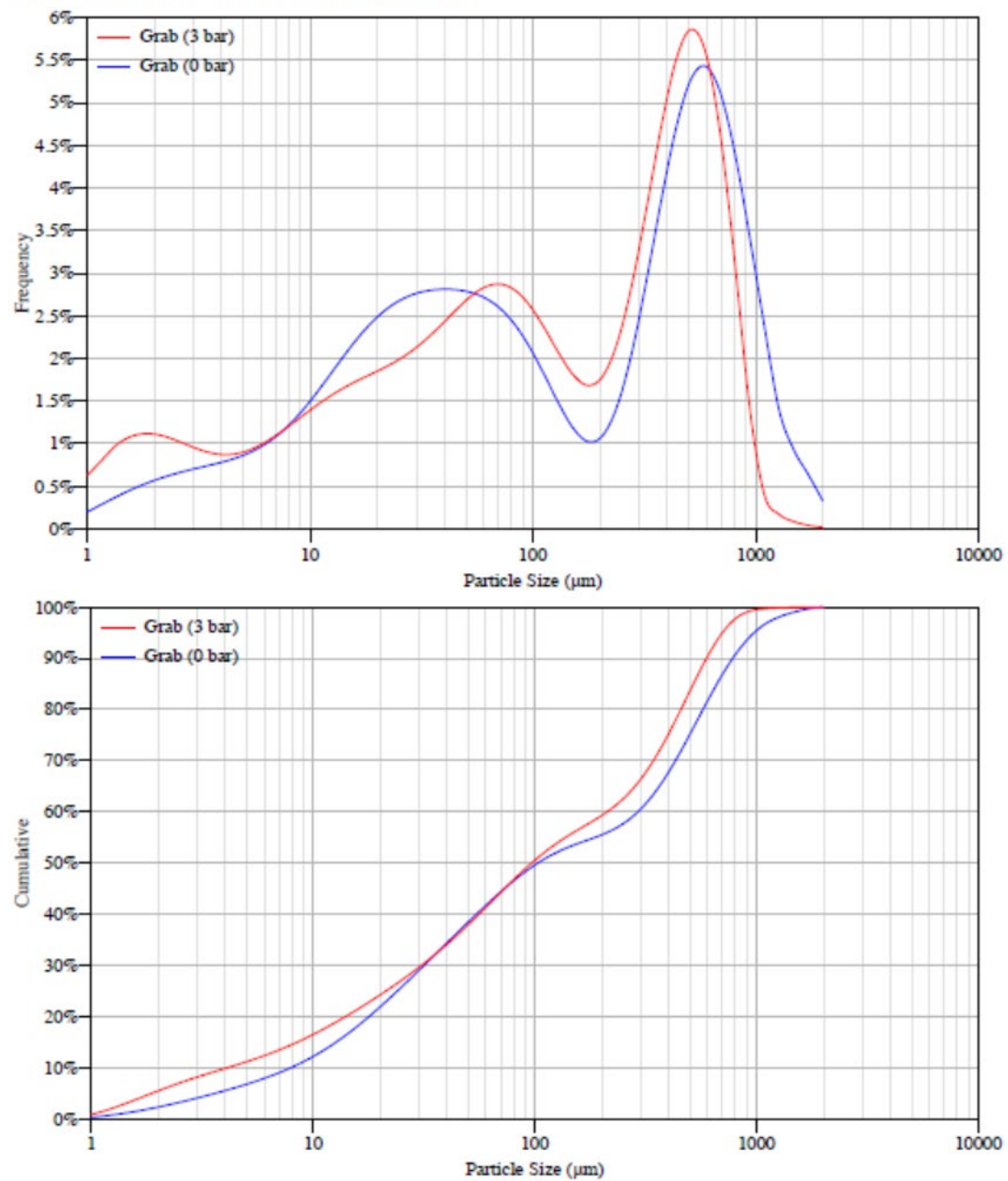


Figure C.143 LAW batch #1b: Particle size distribution by volume and pressure

## Particle Size Distribution

### Particle Size Distribution By Sieving

Table 3.8: Reference via Ro-Tap w/ tapper

Sieve name	Size	Retained %	Particle	Size
ASTM #6	3.35 mm	0.03	p <sub>80</sub>	0.0116 in
ASTM #12	1.7 mm	0.14	p <sub>90</sub>	0.0206 in
ASTM #20	850 μm	0.94		
ASTM #40	425 μm	12.70		
ASTM #70	212 μm	11.64		
ASTM #100	150 μm	2.30		
ASTM #200	75 μm	16.94		
PAN	0 μm	55.31		
	Total	100.00		
	Sieving Yield	99.65		
	Initial Total Mass	139.12 gm		

Figure 3.19: Particle size distribution, by mass

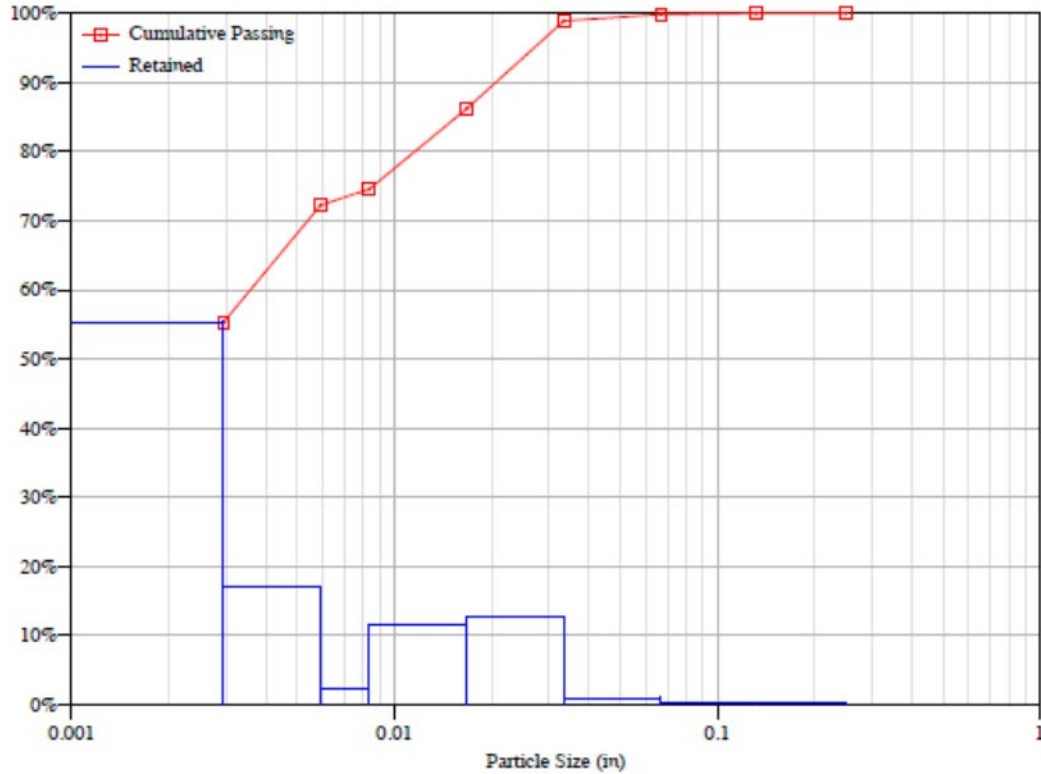


Figure C.144 LAW batch #1b: Particle size distribution by sieving (mass %)

## C.11 LAW batch #1-1

### Bin dimensions for dependable flow

Storage time at rest 0 hr

Temperature 72°F

Table 4.1: Critical outlet dimensions to prevent arching

P – Factor	B <sub>c</sub> ft	B <sub>p</sub> ft	B <sub>f</sub> ft
1.00	0.4	0.2	0.2
1.25	0.5	0.2	0.3
1.50	0.5	0.2	0.4
2.00	0.81	0.3	2

For detailed explanations of terms see pg. 166.

Figure 4.1: Critical rathole dimensions (P – Factor = 1)

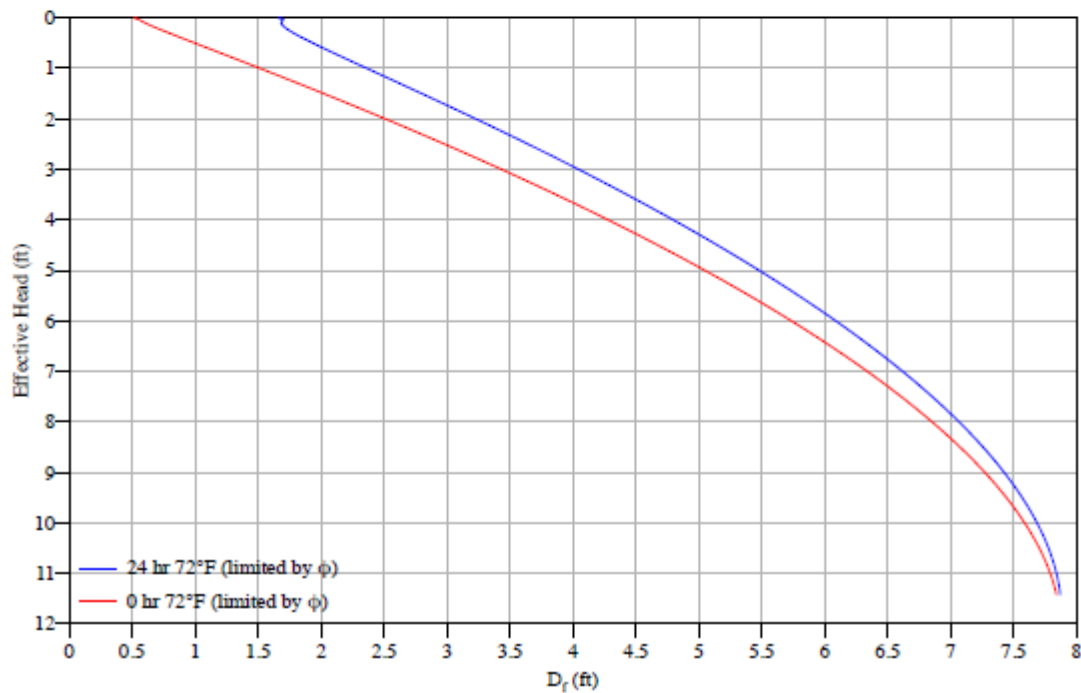


Figure C.145 LAW batch #1-1: Critical rathole dimensions

## Bulk density

### Temperature 72°F

The bulk weight density,  $\gamma$ , is a function of the major consolidating pressure,  $\sigma_1$ , expressed in terms of Effective Head.

Table 4.3: Bulk weight density

Effective Head	ft	0.5	1	2.5	5	10	20
$\sigma_1$	lb/ft <sup>2</sup>	35.1	73.4	194	405.9	848.1	1772
$\gamma$	lb/ft <sup>3</sup>	70.2	73.4	77.7	81.2	84.8	88.6

### Compressibility parameters

Bulk weight density,  $\gamma$ , is a function of the major consolidating pressure  $\sigma_1$ , as follows:

$$\gamma = \gamma_0(\sigma_1/\sigma_0)^\beta \quad \text{for} \quad 64.3 < \gamma < 89.1 \text{ lb/ft}^3$$

Table 4.4: Compressibility parameters

$\gamma_0$	lb/ft <sup>3</sup>	66.2
$\sigma_0$	lb/ft <sup>2</sup>	13
$\beta$		0.0593
$\gamma_{\text{loose fill}}$	lb/ft <sup>3</sup>	60.3

Figure 4.2: Compressibility curve

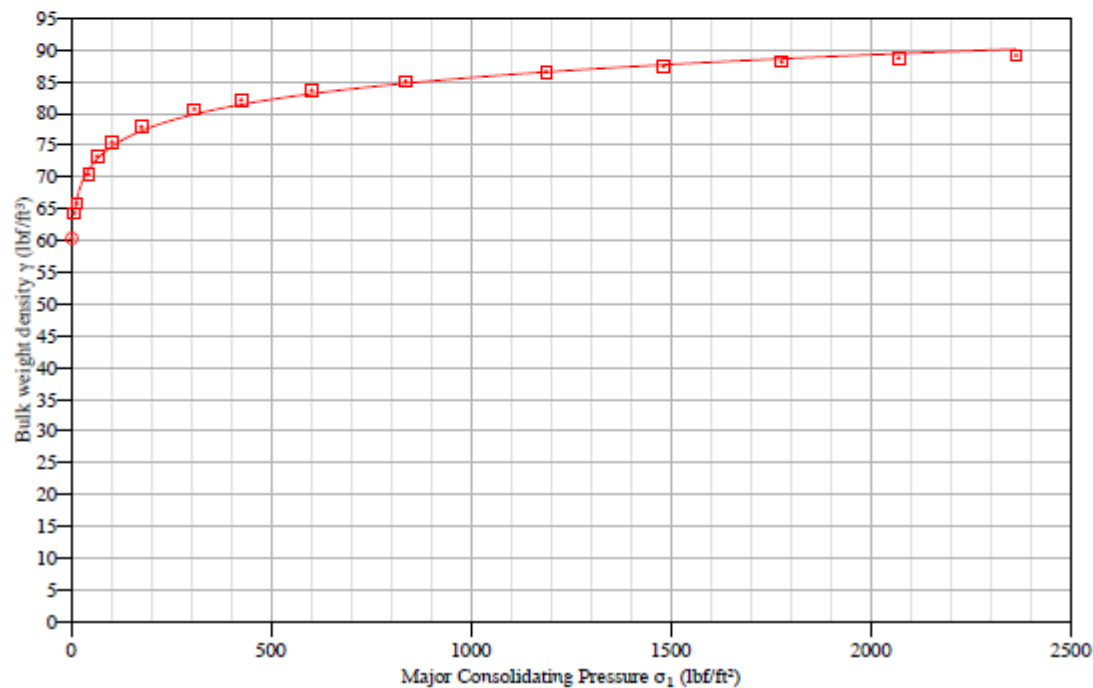


Figure C.146 LAW batch #1-1: Compressibility curve

## Maximum hopper angles for Mass Flow

Wall material 304 SS Sheet, #2B Finish, 12 ga

Figure 4.3: Conical hopper angles

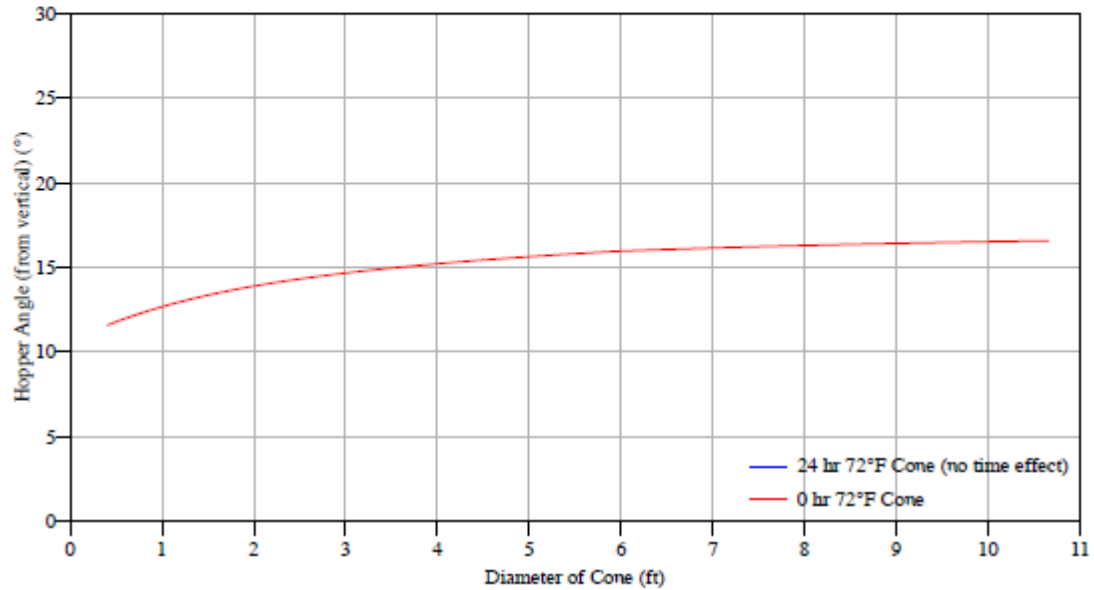


Figure 4.4: Wedge hopper angles

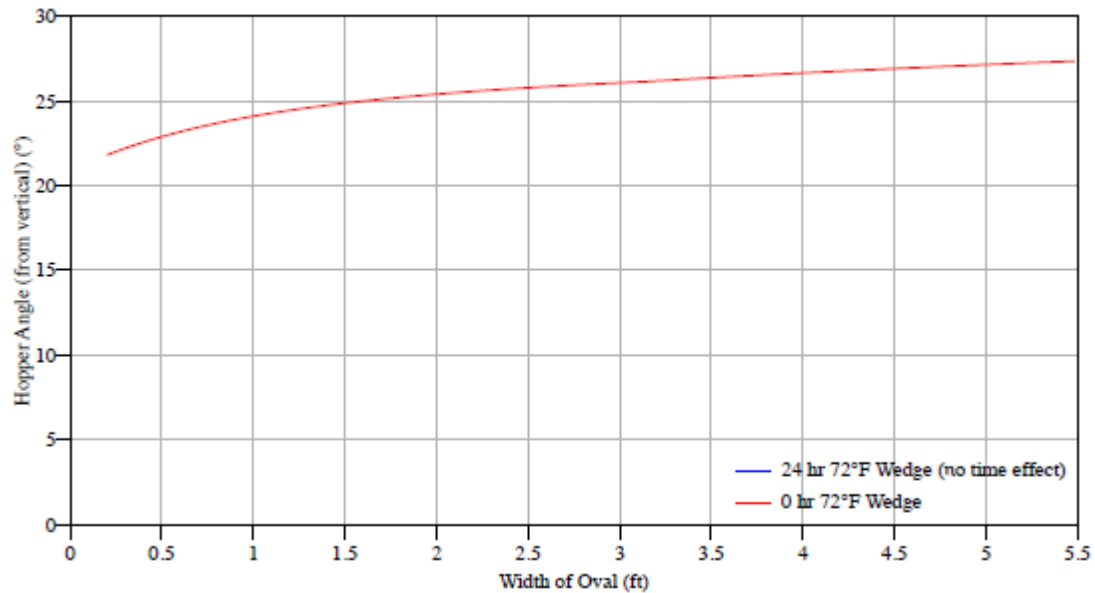


Figure C.147 LAW batch #1-1: Conical hopper angles (Top) and Wedge hopper angles (Bottom) with 304 SS sheet

Wall material Mild CS HR Plate, Mill Finish, 1/4"

Figure 4.5: Conical hopper angles

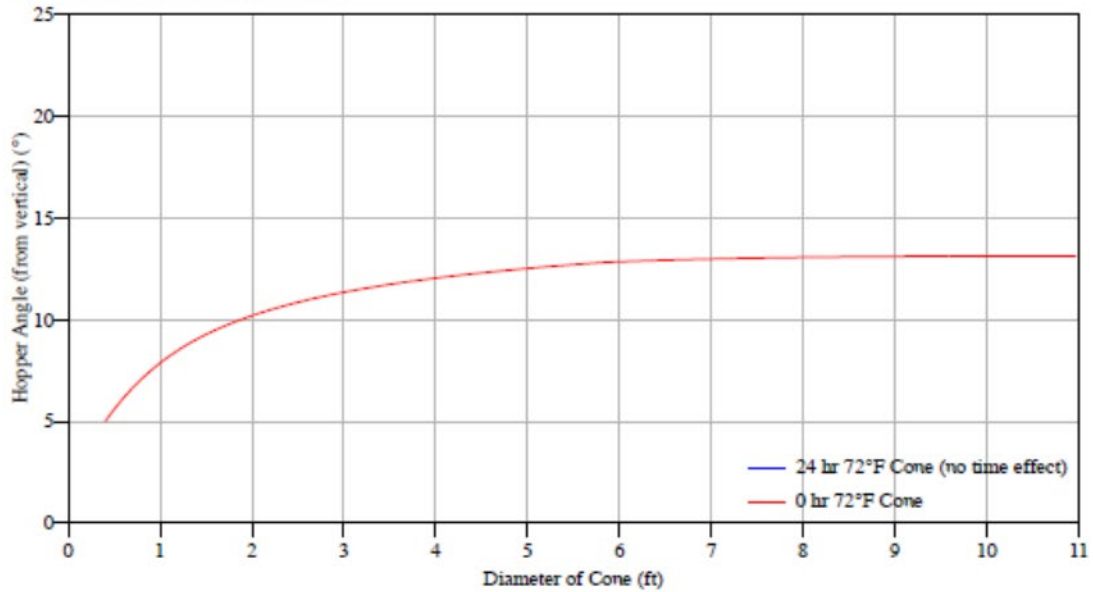


Figure 4.6: Wedge hopper angles

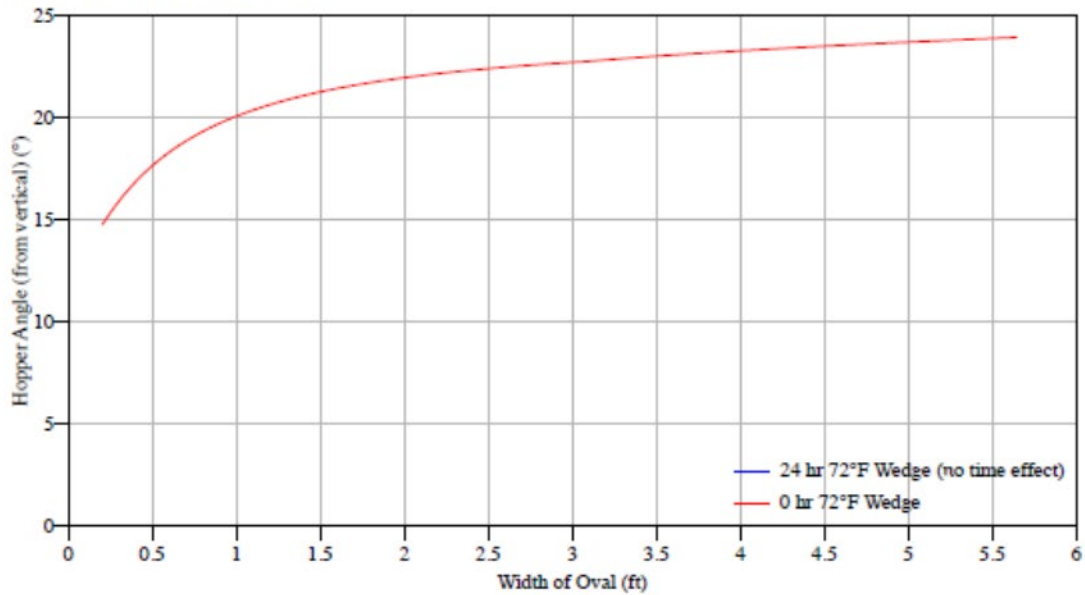


Figure C.148 LAW batch #1-1: Conical hopper angles (Top) and Wedge hopper angles (Bottom) with mild CS HR plate

Wall material Tivar-88

Figure 4.7: Conical hopper angles

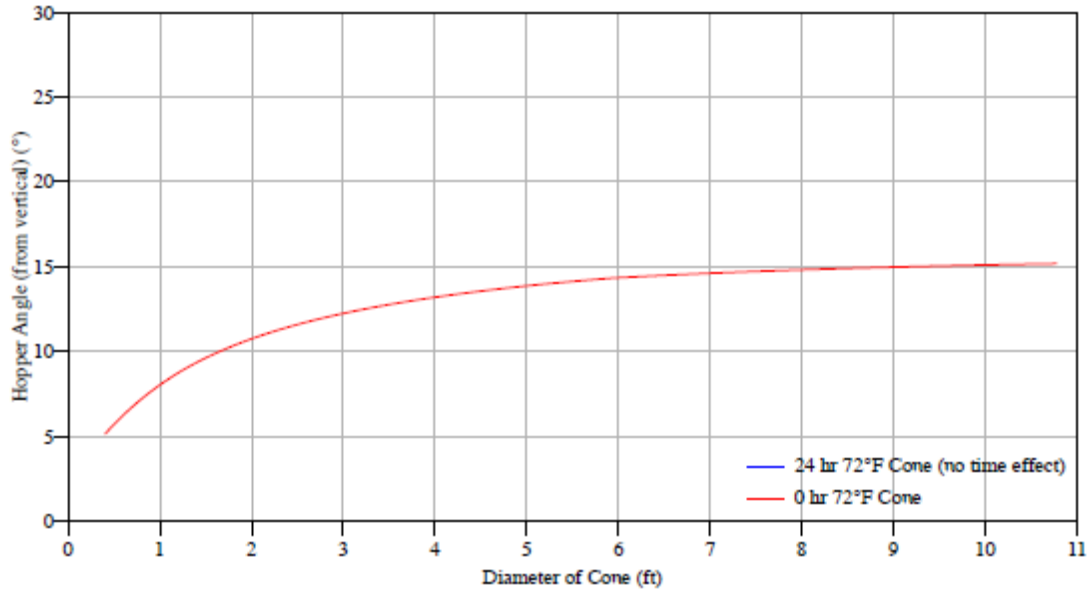


Figure 4.8: Wedge hopper angles

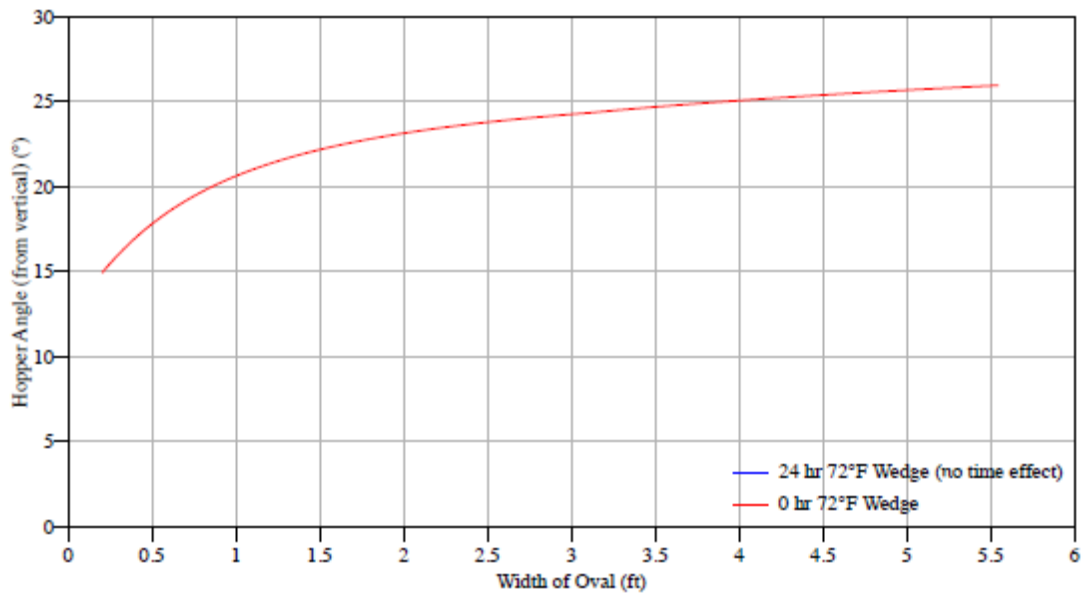


Figure C.149 LAW batch #1-1: Conical hopper angles (Top) and Wedge hopper angles (Bottom) with Tivar 88



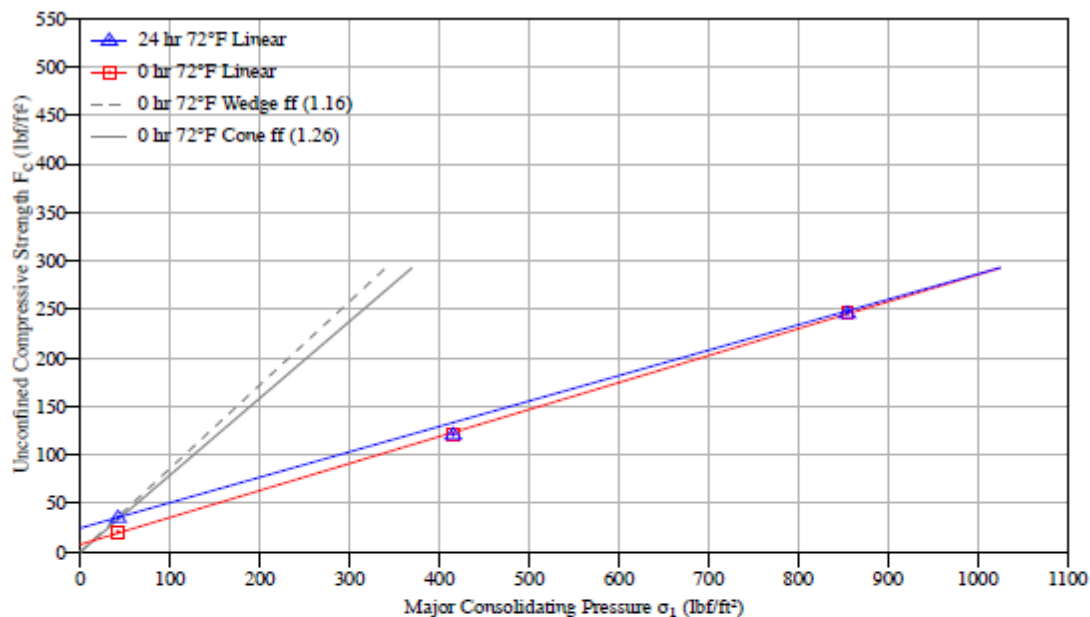


Figure C.150 LAW batch #1-1: Flow function

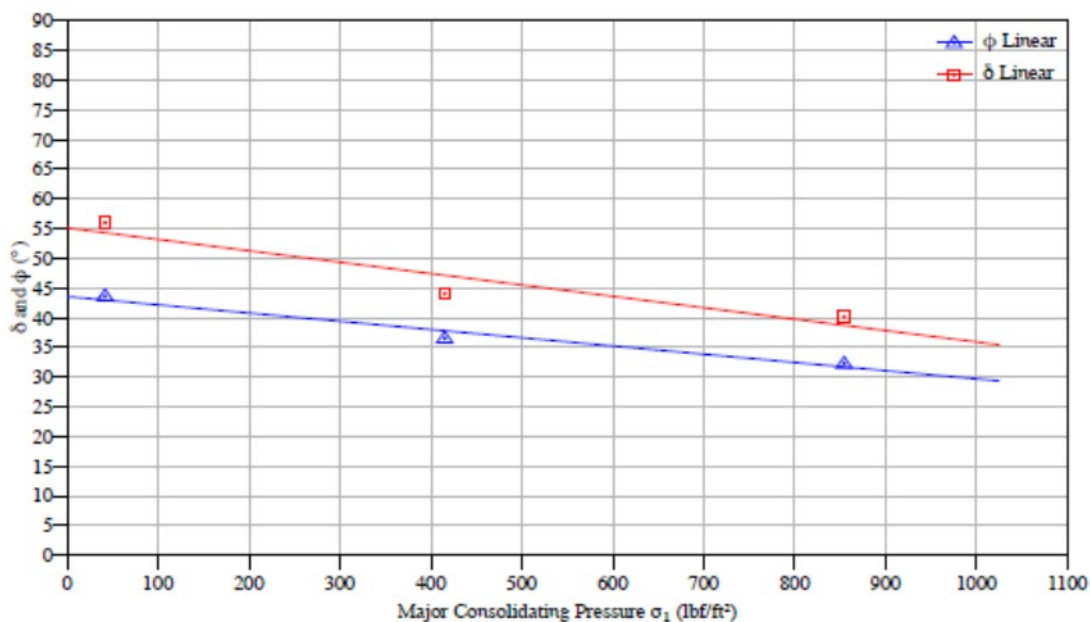


Figure C.151 LAW batch #1-1: Effective angle of friction ( $\delta$ ) and kinematic angle of internal friction ( $\phi$ )

## Air permeability test results

### Temperature 72°F

$K$  is a function of the bulk weight density of the solid

$$K = K_0 \left( \frac{\gamma}{\gamma_0} \right)^{-\alpha}$$

At room temperature, for  $\gamma$  between 62.6 and 82.8  $lb_f/ft^3$ :

Table 4.4: Permeability parameters

$K_0$ $ft/s$	0.002446
$\gamma_0$ $lb_f/ft^3$	66.2
$\alpha$	2.706

Figure 4.15: Permeability curve

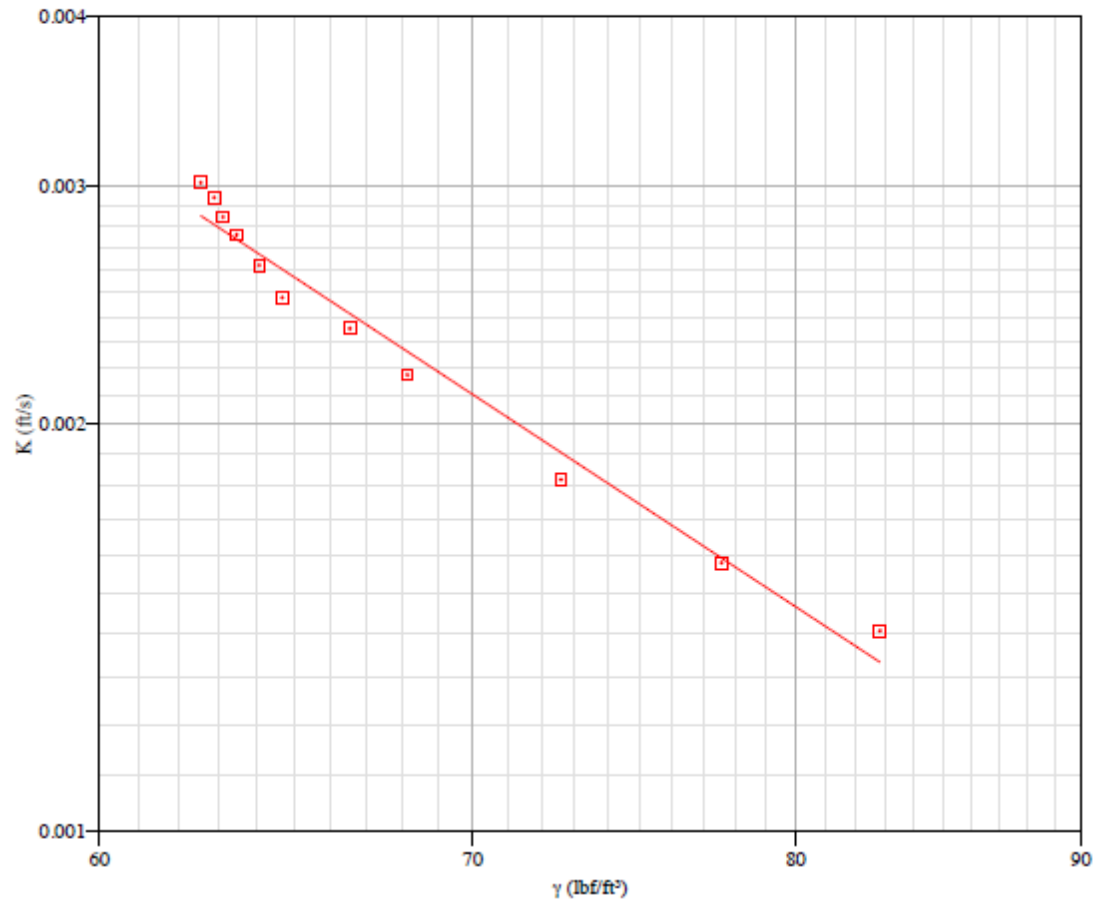


Figure C.152 LAW batch #1-1: Permeability curve

## Chute angles

Chute material 304 SS Sheet, #2B Finish, 12 ga

Storage time at rest 0 hr

Chute temperature 72°F

Material temperature 72°F

Table 4.5: Measured chute clean-off angles (from horizontal)

Impact Pressure $lb_f/ft^2$	Angle $^\circ$
4.2	24 to 26
43.3	29 to 32
82.4	35 to 37
160.6	37 to 40

Figure 4.16: Chute curve

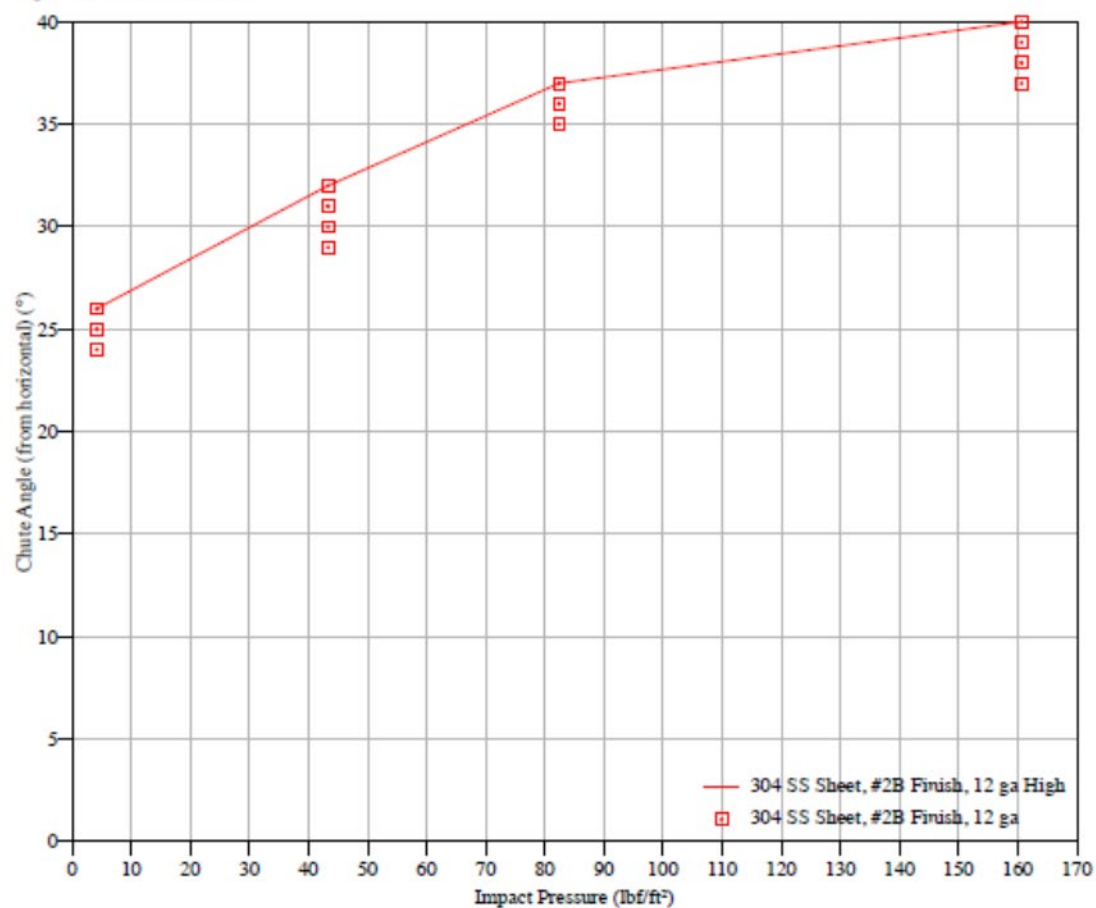


Figure C.153 LAW batch #1-1: Chute curve with 304 SS sheet

Chute material Mild CS HR Plate, Mill Finish, 1/4"  
Storage time at rest 0 hr  
Chute temperature 72°F  
Material temperature 72°F

Table 4.6: Measured chute clean-off angles (from horizontal)

Impact Pressure $lb_f/ft^2$	Angle $^\circ$
4.2	26 to 28
43.3	35 to 37
82.4	41 to 42
160.6	44 to 46

Figure 4.17: Chute curve

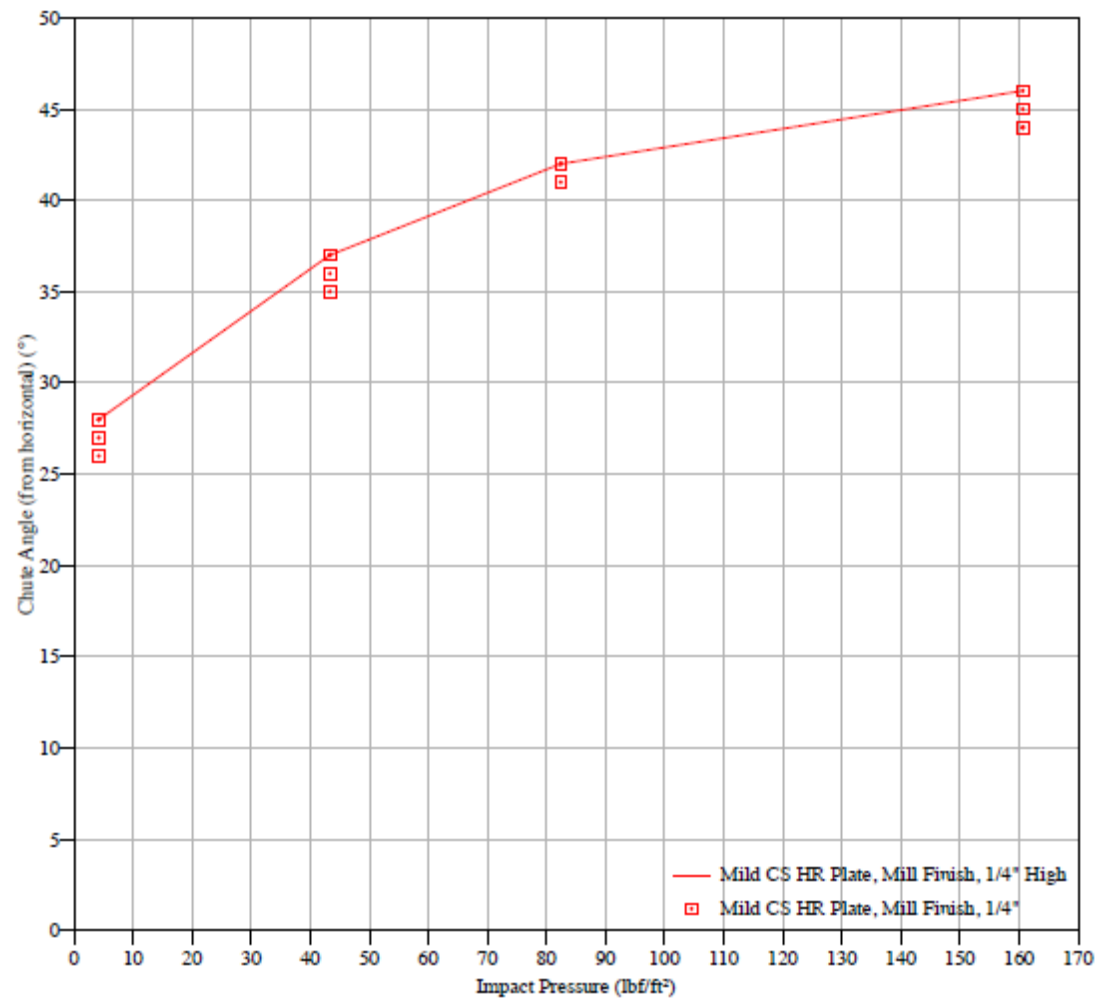


Figure C.154 LAW batch #1-1: Chute curve with mild CS HR plate

Chute material Tivar-88  
Storage time at rest 0 hr  
Chute temperature 72°F  
Material temperature 72°F

Table 4.7: Measured chute clean-off angles (from horizontal)

Impact Pressure $lb_f/ft^2$	Angle $^\circ$
4.2	24 to 27
43.3	36 to 39
82.4	44 to 46
160.6	45 to 49

Figure 4.18: Chute curve

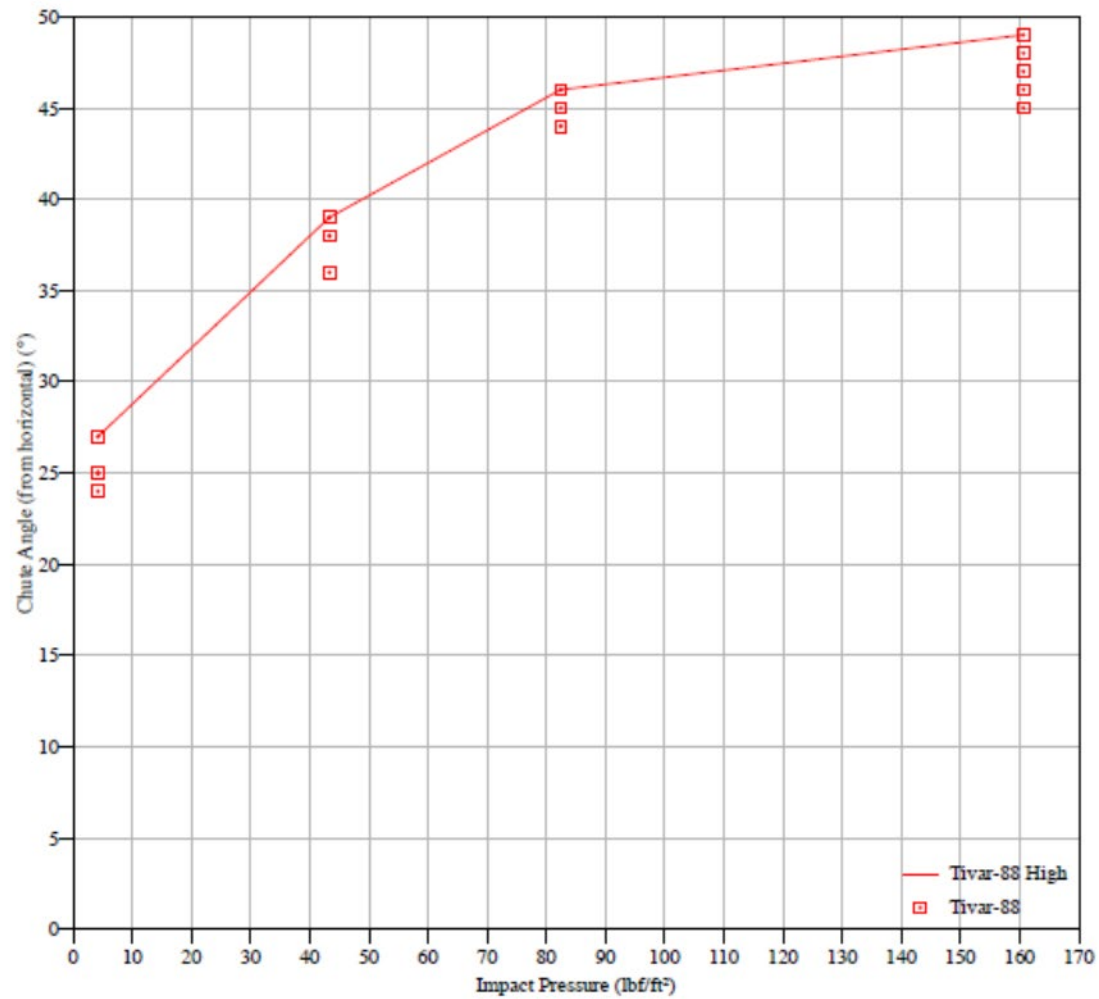


Figure C.155 LAW batch #1-1: Chute curve with Tivar 88

## Particle Size Distribution Analysis Comparison

Figure 4.22: Particle size distribution, by volume

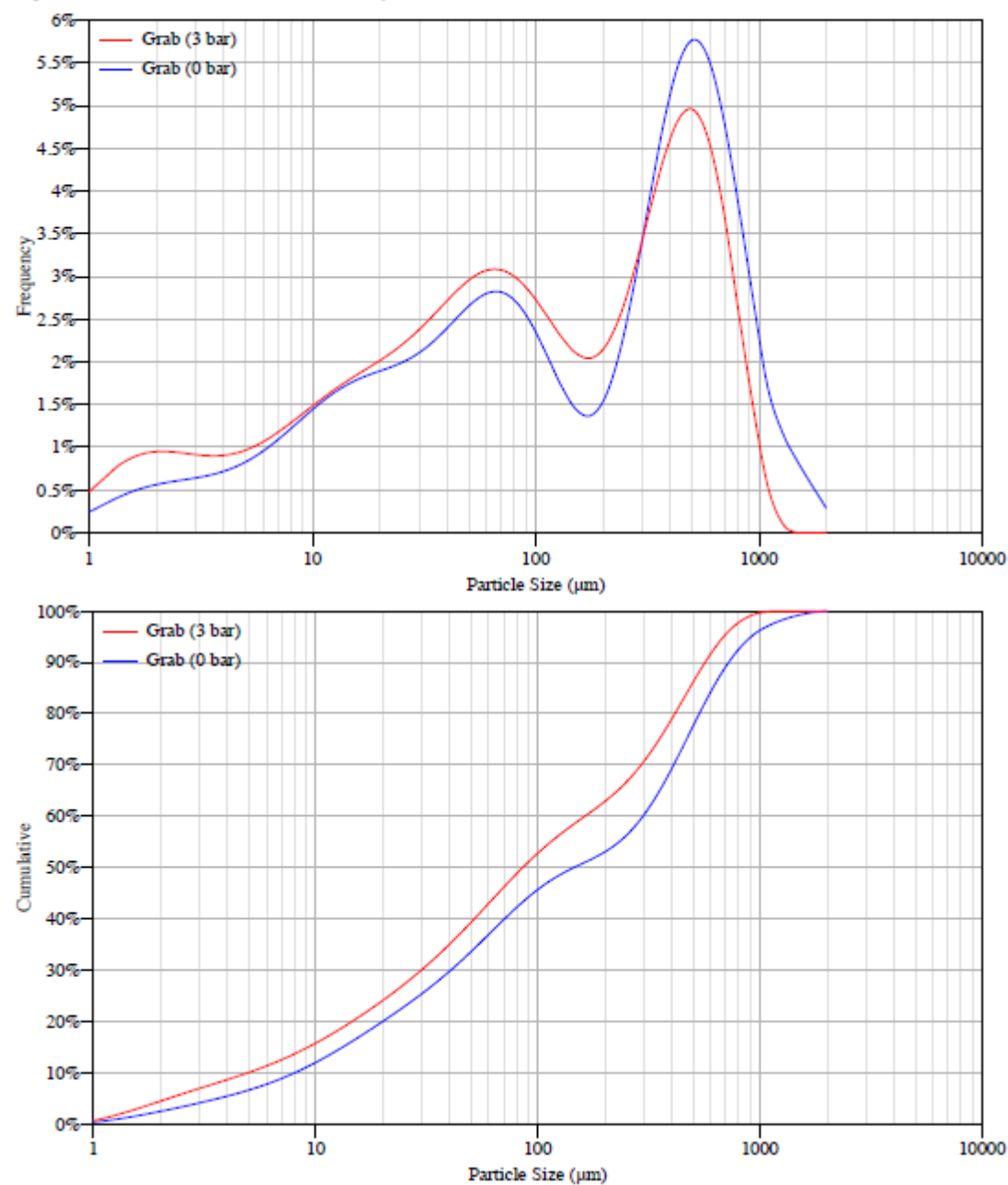


Figure C.156 LAW batch #1-1: Particle size distribution by volume and pressure

## Particle Size Distribution

### Particle Size Distribution By Sieving

Table 4.8: Reference via Ro-Tap w/ tapper

Sieve name	Size	Retained %
ASTM #6	3.35 mm	0.16
ASTM #12	1.7 mm	0.18
ASTM #20	850 $\mu$ m	0.79
ASTM #40	425 $\mu$ m	11.18
ASTM #70	212 $\mu$ m	24.43
ASTM #100	150 $\mu$ m	7.18
ASTM #200	75 $\mu$ m	17.73
PAN	0 $\mu$ m	38.35
	Total	100.00
	Sieving Yield	99.38
	Initial Total Mass	121.81 gm

Particle	Size
p50	0.0047 in
p80	0.0134 in
p90	0.0193 in

Figure 4.19: Particle size distribution, by mass

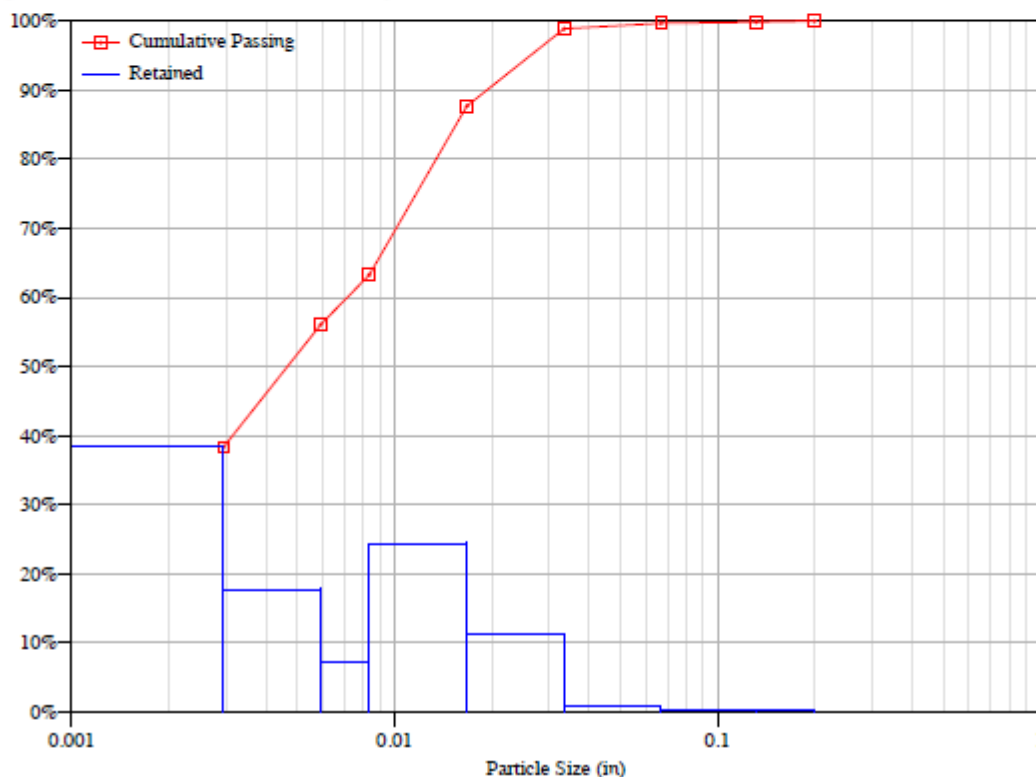


Figure C.157 Law batch #1-1: Particle size distribution by sieving (mass %)

## C.12 LAW batch #6b

### Bin dimensions for dependable flow

Storage time at rest 0 hr

Temperature 72°F

Table 5.1: Critical outlet dimensions to prevent arching

P – Factor	B <sub>c</sub> ft	B <sub>p</sub> ft	B <sub>t</sub> ft
1.00	0.4	0.2	0.2
1.25	0.5	0.2	0.3
1.50	0.5	0.3	0.3
2.00	0.7	0.3	0.6

For detailed explanations of terms see pg. 166.

Figure 5.1: Critical rathole dimensions (P – Factor = 1)

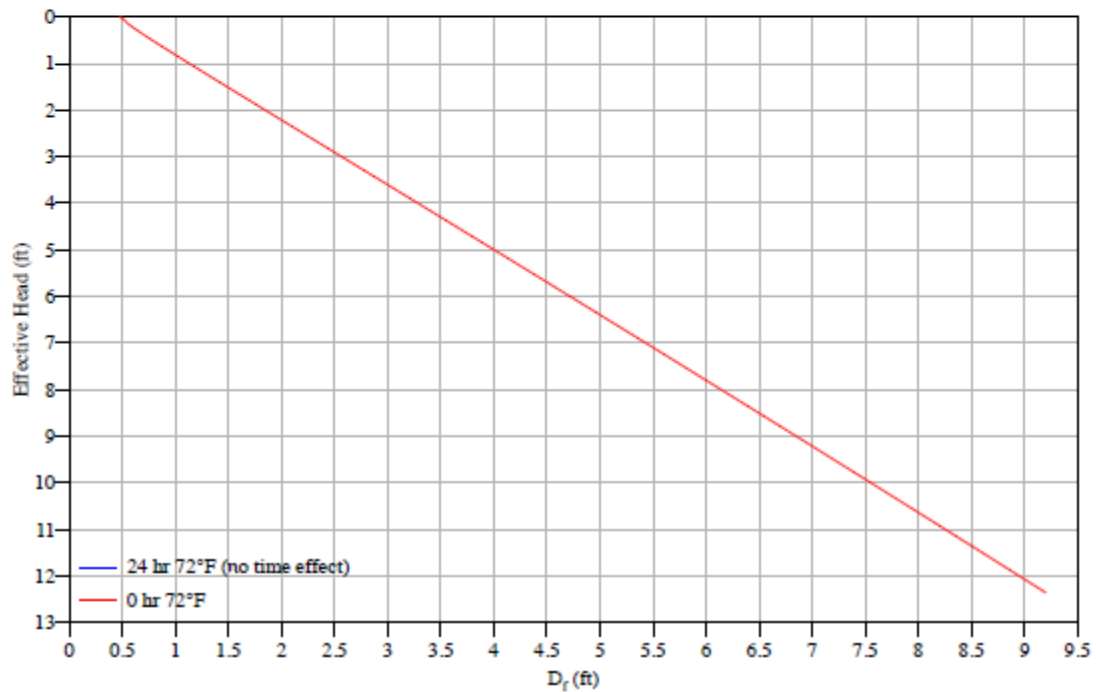


Figure C.158 LAW batch #6b: Critical rathole dimensions



## Bulk density

### Temperature 72°F

The bulk weight density,  $\gamma$ , is a function of the major consolidating pressure,  $\sigma_1$ , expressed in terms of Effective Head.

Table 5.3: Bulk weight density

Effective Head	ft	0.5	1	2.5	5	10	20
$\sigma_1$	lb $f$ /ft <sup>2</sup>	35.8	74.8	198	414.1	865.2	1808
$\gamma$	lb $f$ /ft <sup>3</sup>	71.6	74.8	79.3	82.8	86.5	90.4

### Compressibility parameters

Bulk weight density,  $\gamma$ , is a function of the major consolidating pressure  $\sigma_1$ , as follows:

$$\gamma = \gamma_0(\sigma_1/\sigma_0)^\beta \quad \text{for } 64.8 < \gamma < 90.2 \text{ lb}/\text{ft}^3$$

Table 5.4: Compressibility parameters

$\gamma_0$	lb $f$ /ft <sup>3</sup>	67.4
$\sigma_0$	lb $f$ /ft <sup>2</sup>	13
$\beta$		0.0594
$\gamma_{\text{loose fill}}$	lb $f$ /ft <sup>3</sup>	62

Figure 5.2: Compressibility curve

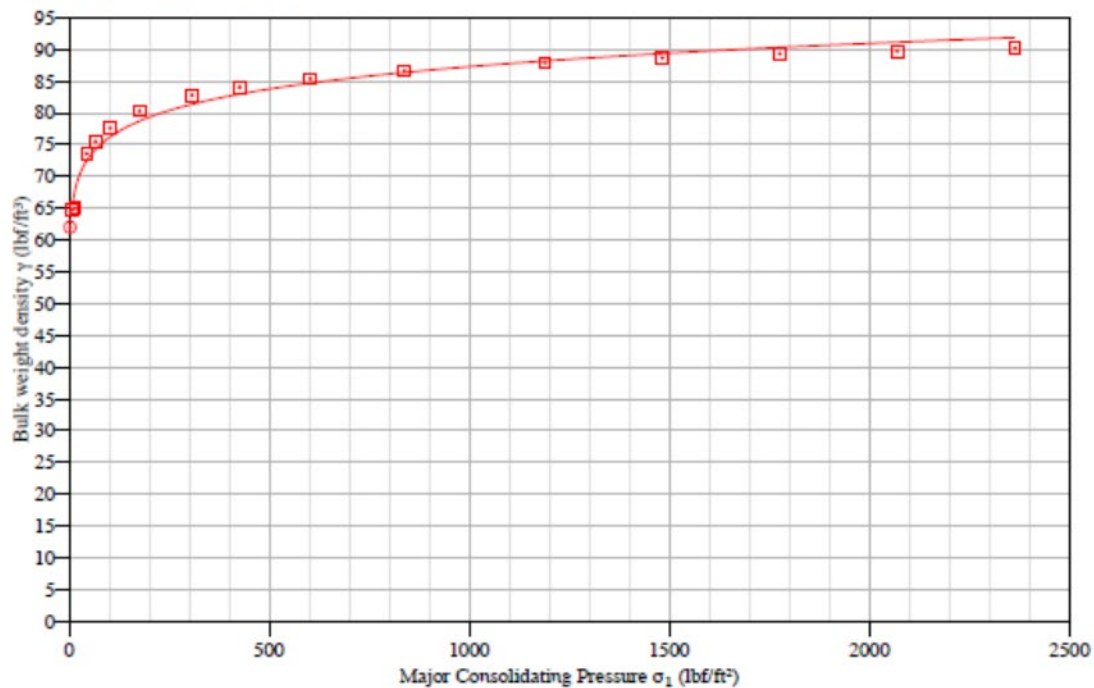


Figure C.159 LAW batch #6b: Compressibility curve

## Maximum hopper angles for Mass Flow

Wall material 304 SS Sheet, #2B Finish, 12 ga

Figure 5.3: Conical hopper angles

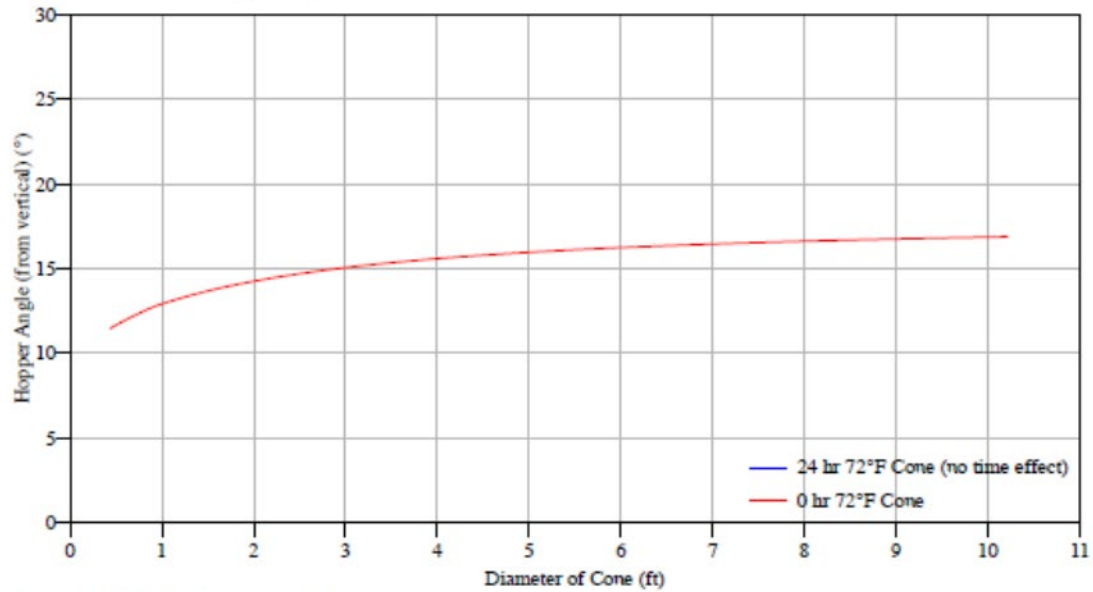


Figure 5.4: Wedge hopper angles

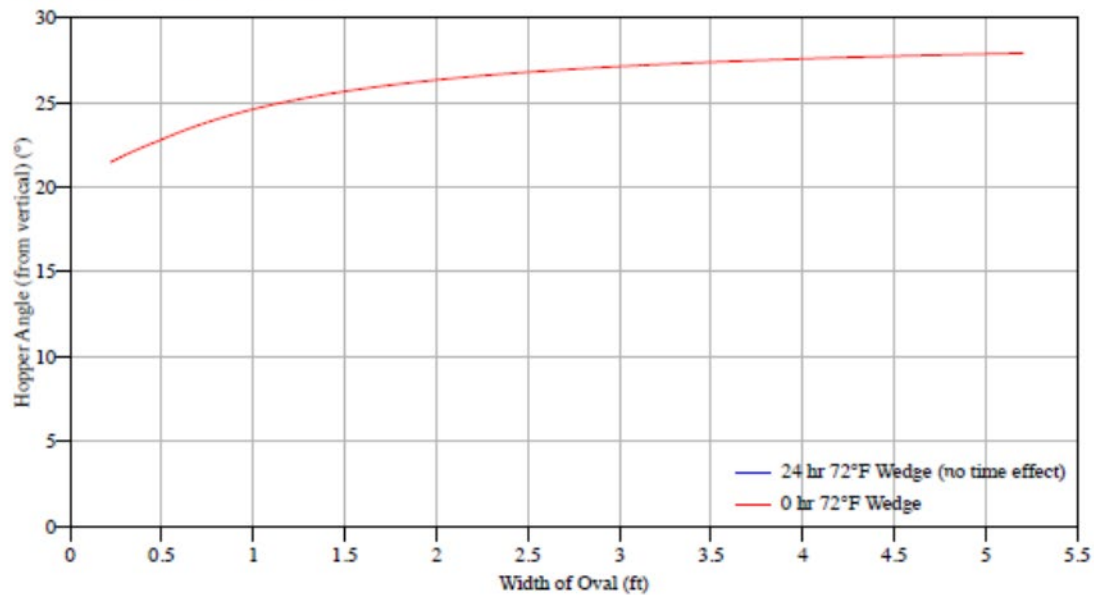


Figure C.160 LAW batch #6b: Conical hopper angles (Top) and Wedge hopper angles (Bottom) with 304 SS sheet

Wall material Mild CS HR Plate, Mill Finish, 1/4"

Figure 5.5: Conical hopper angles

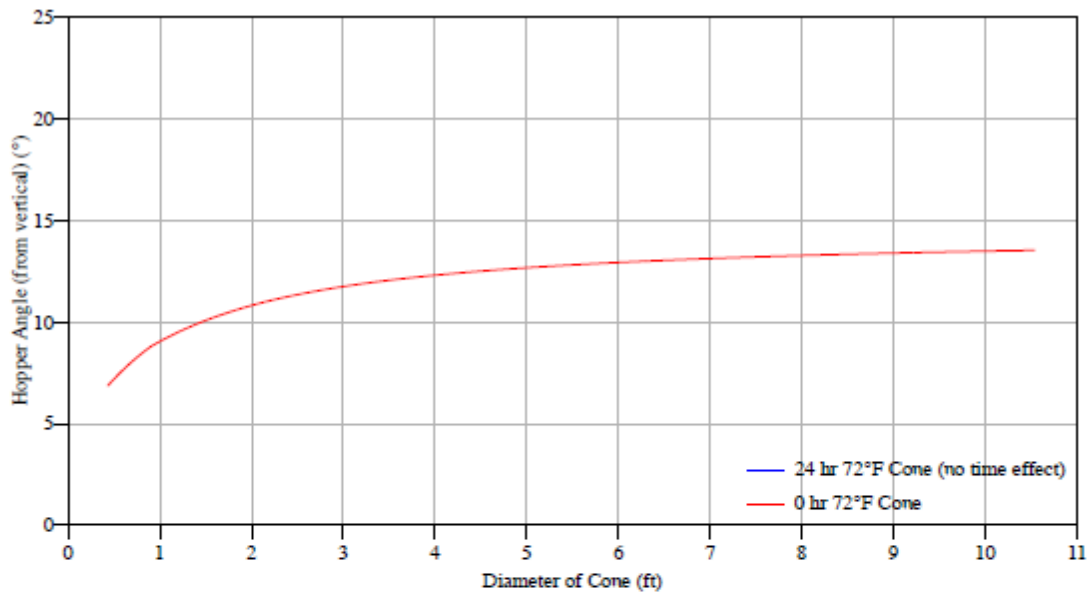


Figure 5.6: Wedge hopper angles

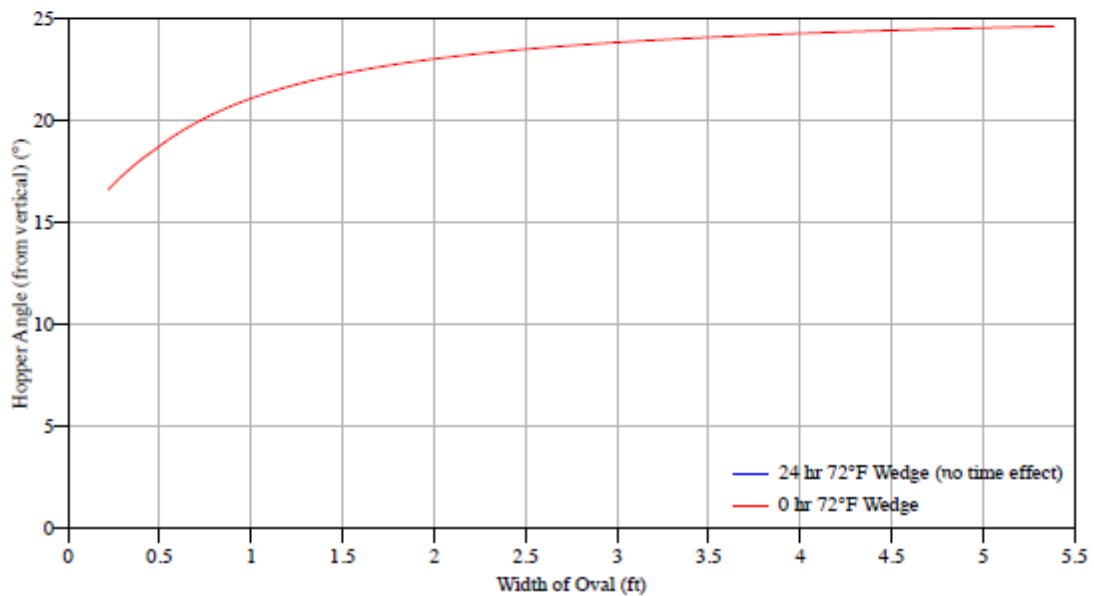


Figure C.161 LAW batch #6b: Conical hopper angles (Top) and Wedge hopper angles (Bottom) with mild CS HR plate

Wall material Tivar-88

Figure 5.7: Conical hopper angles

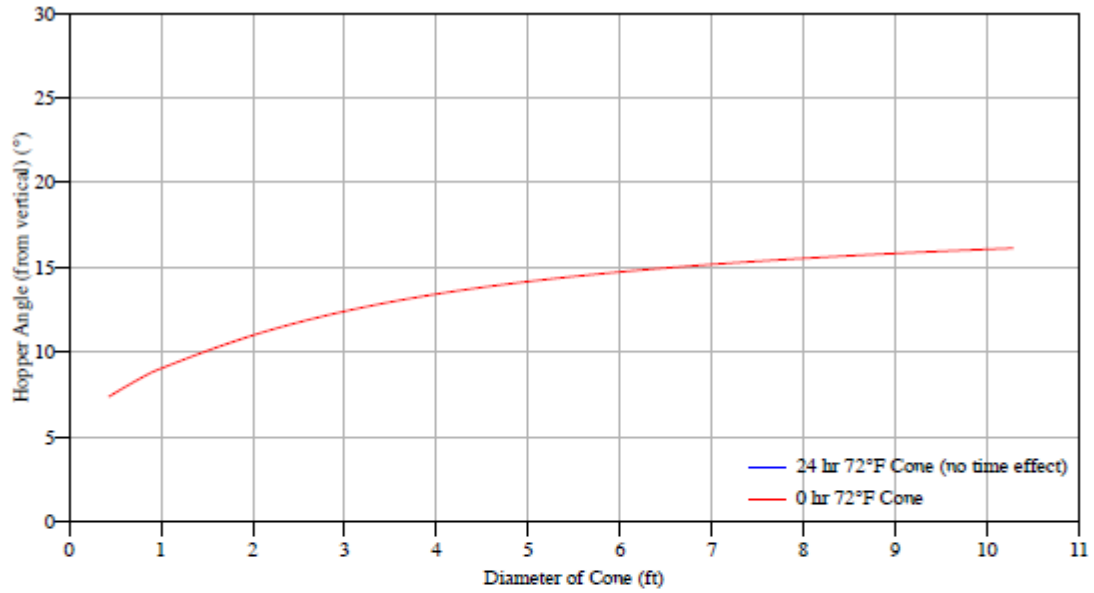


Figure 5.8: Wedge hopper angles

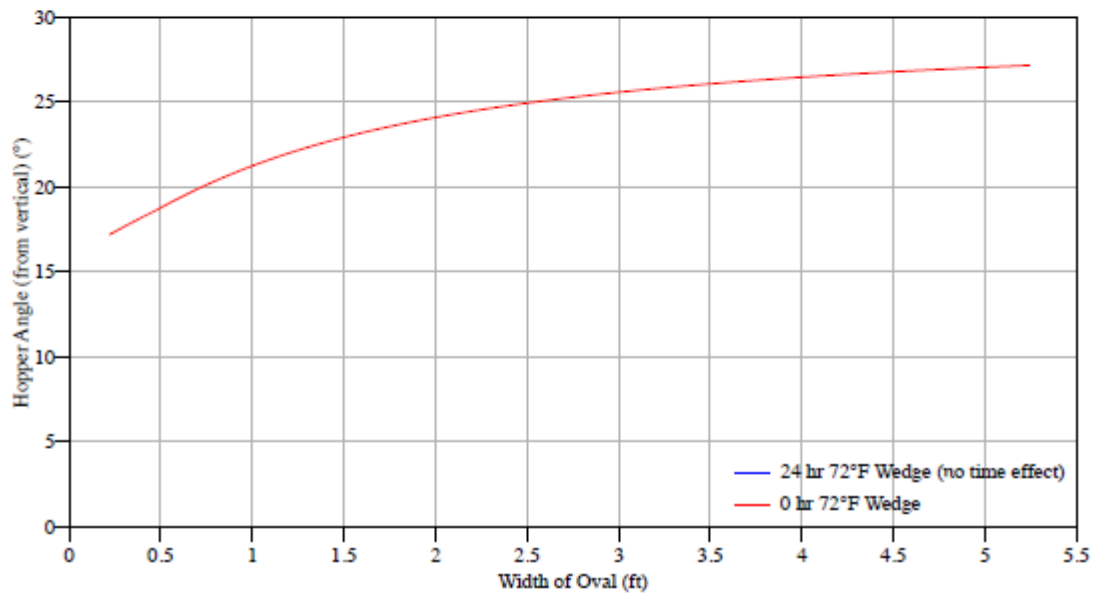


Figure C.162 LAW batch #6b: Conical hopper angles (Top) and Wedge hopper angles (Bottom) with Tivar 88

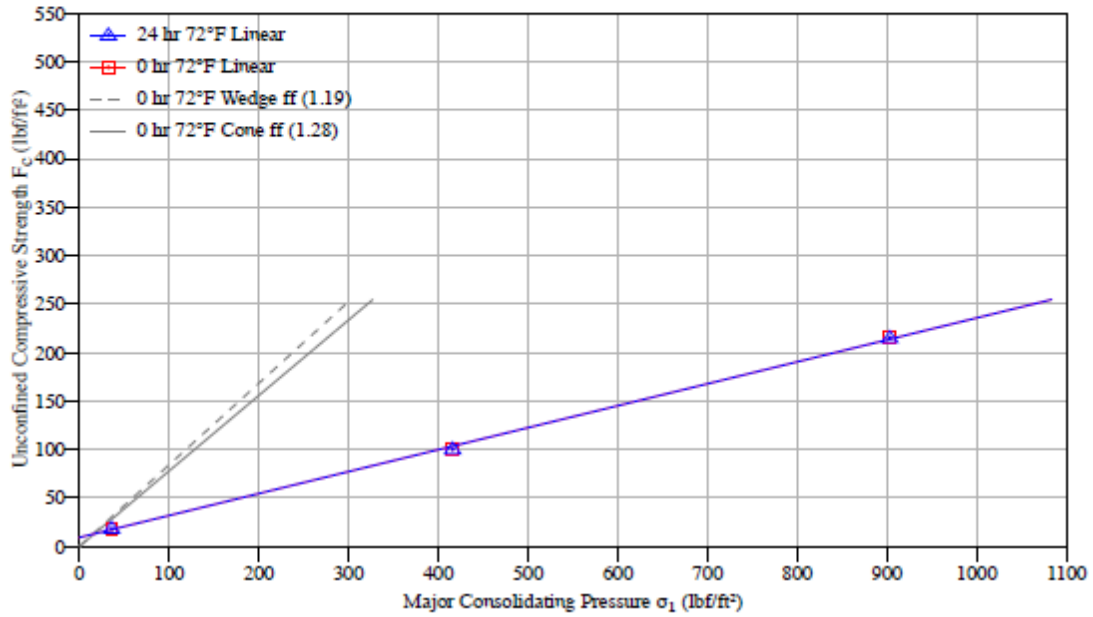


Figure C.163 LAW batch #6b: Flow function

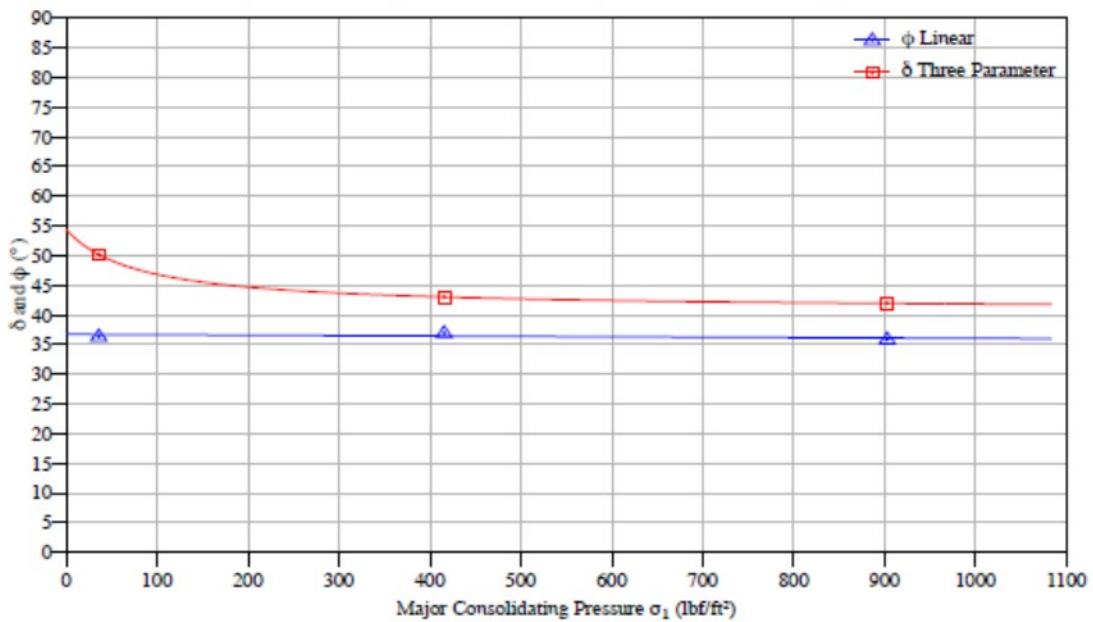


Figure C.164 LAW batch #6b: Effective angle of friction ( $\delta$ ) and kinematic angle of internal friction ( $\phi$ )

## Air permeability test results

### Temperature 72°F

$K$  is a function of the bulk weight density of the solid

$$K = K_0 \left( \frac{\gamma}{\gamma_0} \right)^{-\alpha}$$

At room temperature, for  $\gamma$  between 63.7 and 88.3  $lb/ft^3$ :

Table 5.4: Permeability parameters

$K_0$	$ft/s$	0.00245
$\gamma_0$	$lb/ft^3$	67.4
$\alpha$		2.248

Figure 5.15: Permeability curve

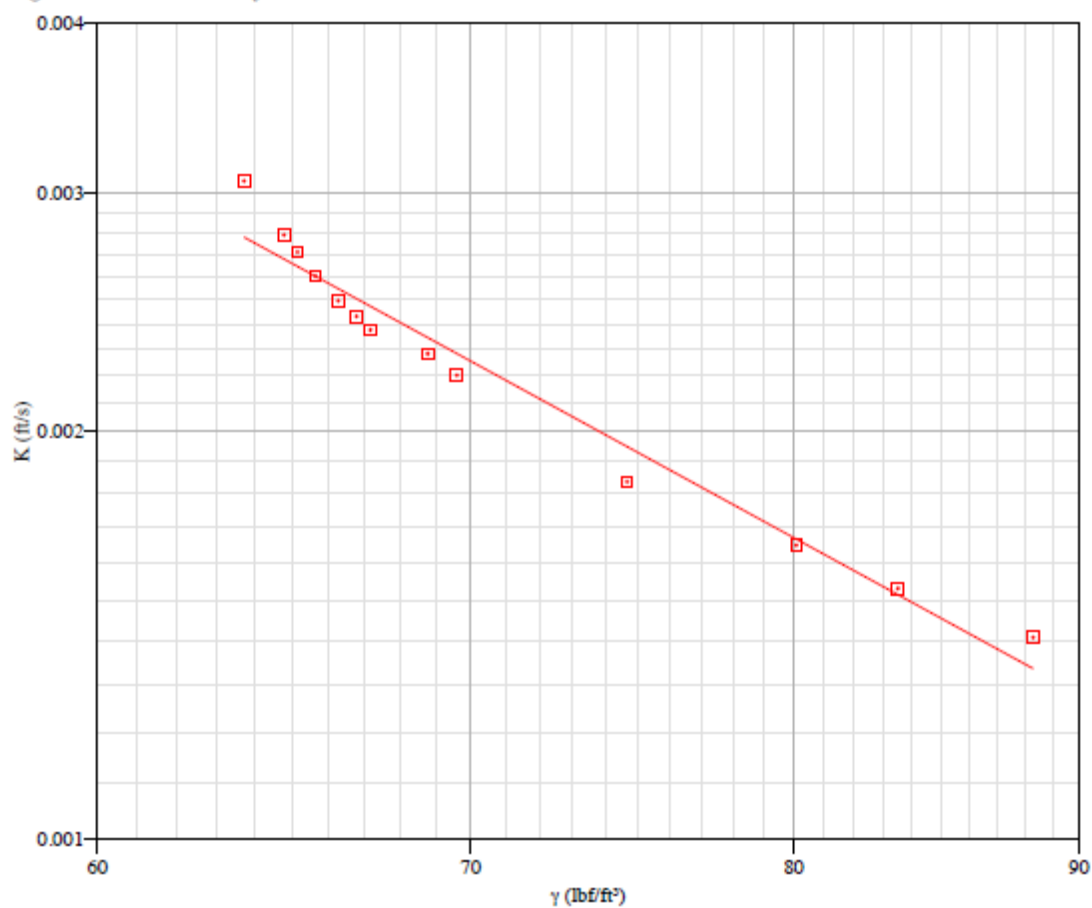


Figure C.165 LAW batch #6b: Permeability curve

## Chute angles

Chute material 304 SS Sheet, #2B Finish, 12 ga

Storage time at rest 0 hr

Chute temperature 72°F

Material temperature 71°F

Table 5.5: Measured chute clean-off angles (from horizontal)

Impact Pressure $lb_f/ft^2$	Angle $^\circ$
4.2	27 to 30
43.3	36 to 39
82.4	38 to 40
160.6	38 to 40

Figure 5.16: Chute curve

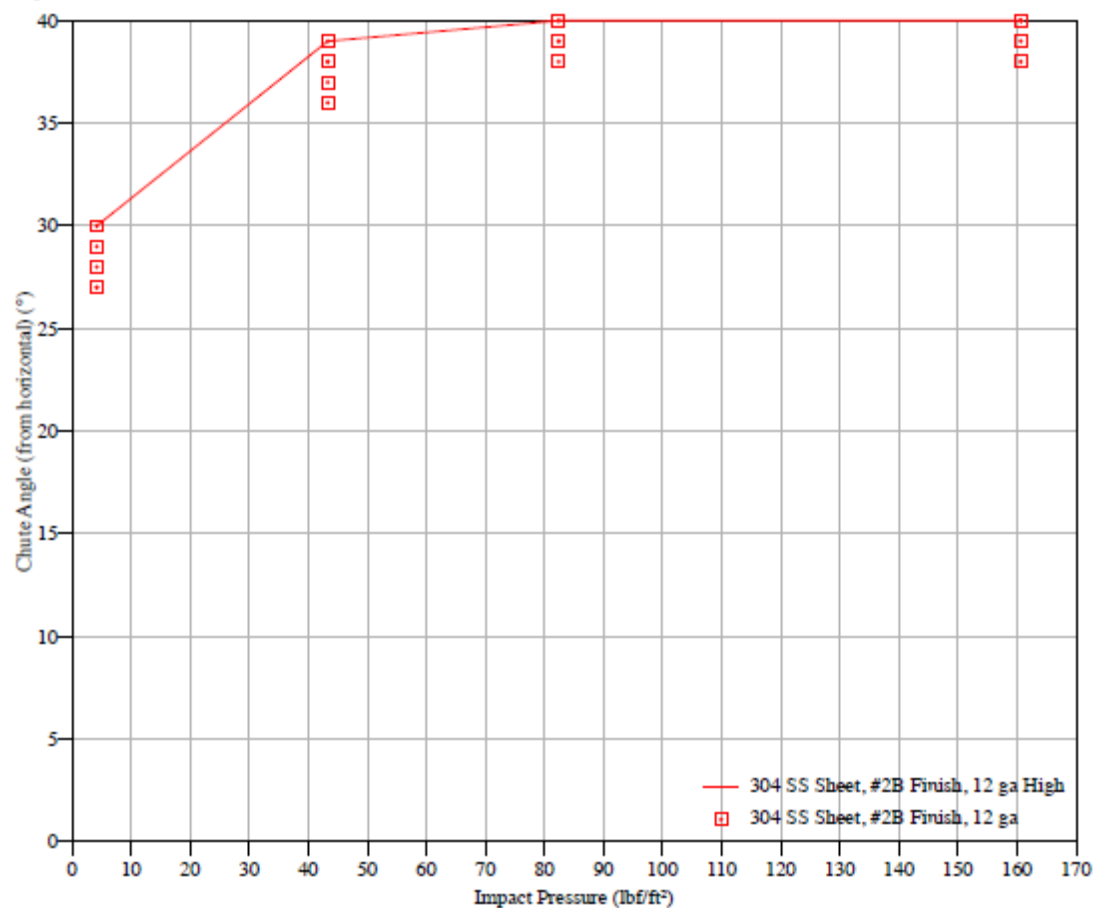


Figure C.166 LAW batch #6b: Chute curve with 304 SS sheet

Chute material Mild CS HR Plate, Mill Finish, 1/4"  
Storage time at rest 0 hr  
Chute temperature 72°F  
Material temperature 71°F

Table 5.6: Measured chute clean-off angles (from horizontal)

Impact Pressure $lb_f/ft^2$	Angle $^\circ$
4.2	27 to 29
43.3	38 to 40
82.4	40 to 42
160.6	45 to 47

Figure 5.17: Chute curve

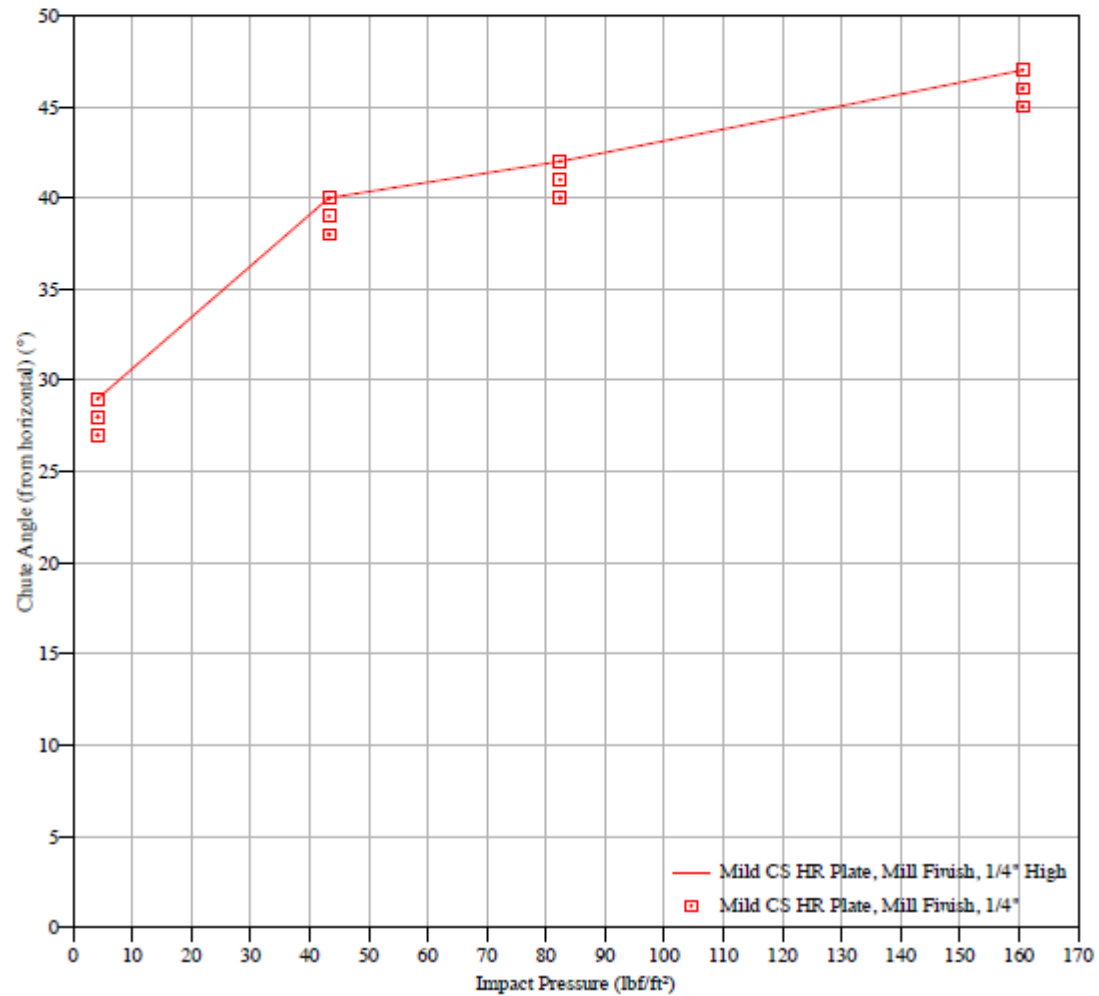


Figure C.167 LAW batch #6b: Chute curve with mild CS HR plate



Chute material Tivar-88  
Storage time at rest 0 hr  
Chute temperature 72°F  
Material temperature 71°F

Table 5.7: Measured chute clean-off angles (from horizontal)

Impact Pressure $lb_f/ft^2$	Angle $^\circ$
4.2	25 to 30
43.3	34 to 36
82.4	35 to 36
160.6	35 to 37

Figure 5.18: Chute curve

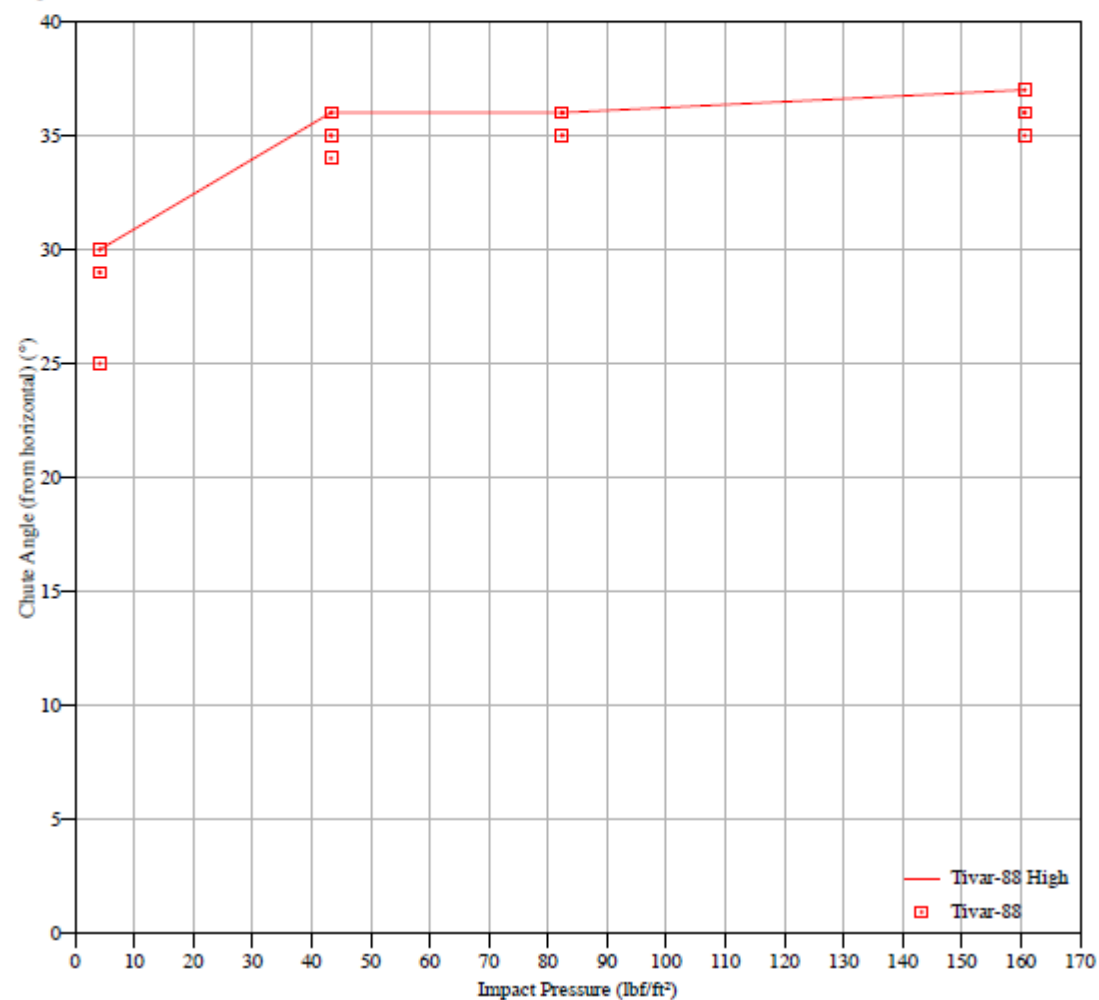


Figure C.168 LAW batch #6b: Chute curve with Tivar 88

## Particle Size Distribution Analysis Comparison

Figure 5.22: Particle size distribution, by volume

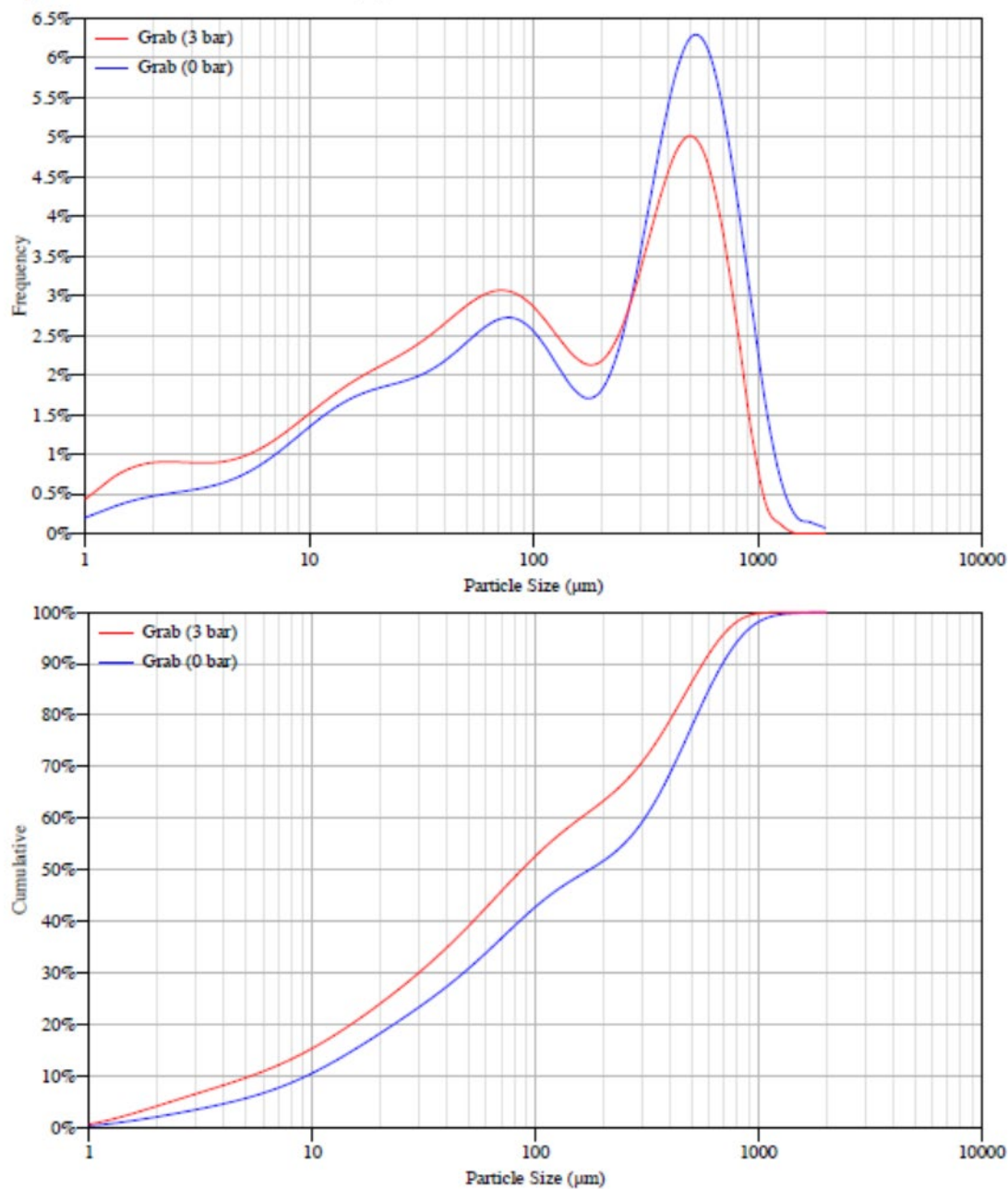


Figure C.169 LAW batch #6b: Particle size distribution by volume and pressure

## Particle Size Distribution

### Particle Size Distribution By Sieving

Table 5.8: Reference via Ro-Tap w/ tapper

Sieve name	Size	Retained %
ASTM #6	3.35 mm	0.00
ASTM #12	1.7 mm	0.00
ASTM #20	850 $\mu m$	0.44
ASTM #40	425 $\mu m$	9.74
ASTM #70	212 $\mu m$	27.40
ASTM #100	150 $\mu m$	14.00
ASTM #200	75 $\mu m$	15.54
PAN	0 $\mu m$	32.88
	Total	100.00
	Sieving Yield	99.15
	Initial Total Mass	89.951 gm

Particle	Size
$p_{50}$	0.0061 in
$p_{80}$	0.013 in
$p_{90}$	0.017 in

Figure 5.19: Particle size distribution, by mass

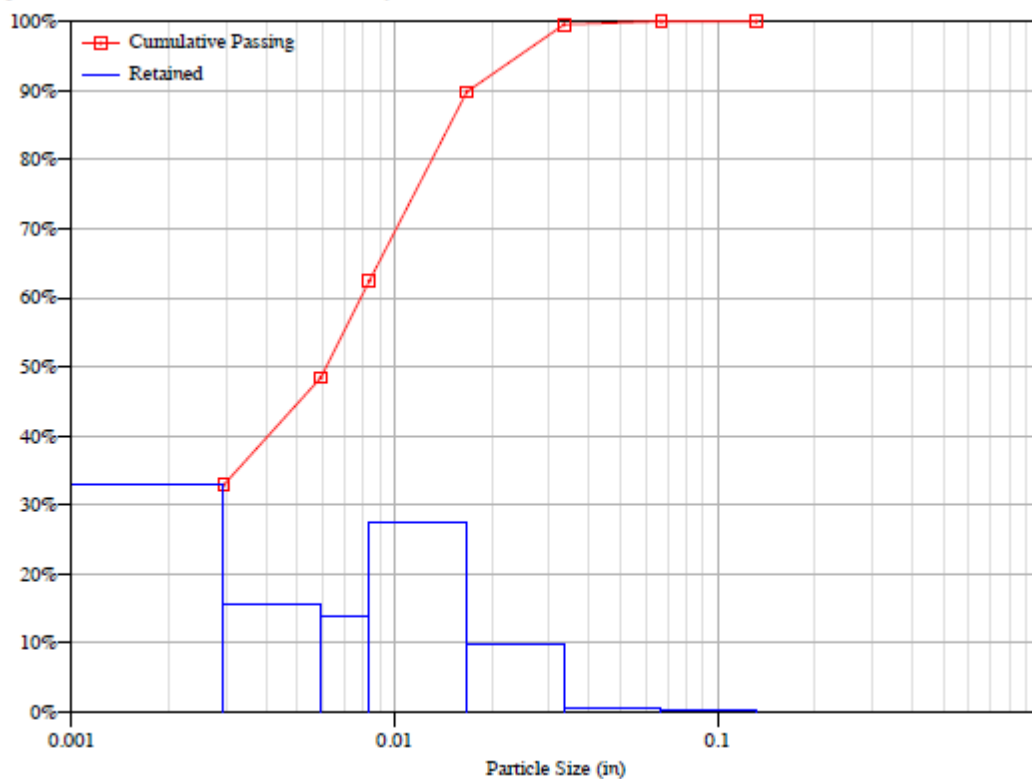


Figure C.170 Law batch #6b: Particle size distribution by sieving (mass %)

## C.13 LAW batch #9b

### Bin dimensions for dependable flow

Storage time at rest 0 hr

Temperature 72°F

Table 6.1: Critical outlet dimensions to prevent arching

P – Factor	B <sub>c</sub> ft	B <sub>p</sub> ft	B <sub>f</sub> ft
1.00	0.6	0.3	0.3
1.25	0.6	0.3	0.4
1.50	0.7	0.3	0.5
2.00	1	0.5	1

For detailed explanations of terms see pg. 166.

Figure 6.1: Critical rathole dimensions (P – Factor = 1)

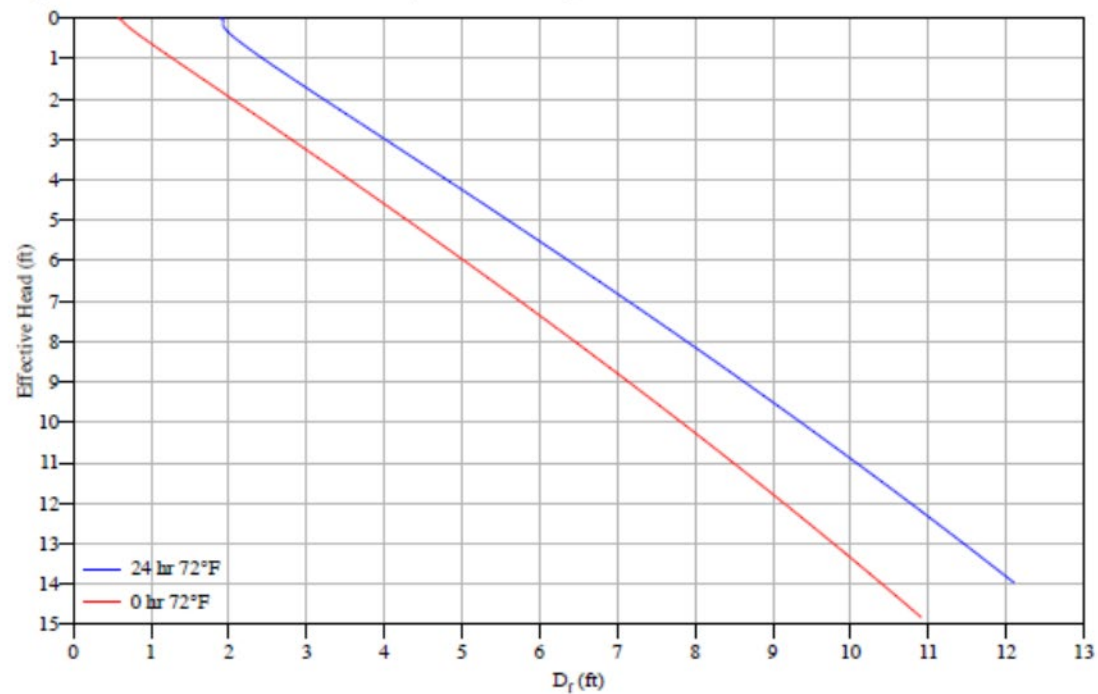


Figure C.171 LAW batch #9b: Critical rathole dimensions

## Bulk density

### Temperature 72°F

The bulk weight density,  $\gamma$ , is a function of the major consolidating pressure,  $\sigma_1$ , expressed in terms of Effective Head.

Table 6.3: Bulk weight density

Effective Head	ft	0.5	1	2.5	5	10	20
$\sigma_1$	lb/ft <sup>2</sup>	29	60.4	161	336.3	704.3	1475
$\gamma$	lb/ft <sup>3</sup>	57.7	60.4	64.2	67.3	70.4	73.7

### Compressibility parameters

Bulk weight density,  $\gamma$ , is a function of the major consolidating pressure  $\sigma_1$ , as follows:

$$\gamma = \gamma_0(\sigma_1/\sigma_0)^\beta \quad \text{for } 53.4 < \gamma < 75.5 \text{ lb/ft}^3$$

Table 6.4: Compressibility parameters

$\gamma_0$	lb/ft <sup>3</sup>	54.9
$\sigma_0$	lb/ft <sup>2</sup>	13
$\beta$		0.0623
$\gamma_{\text{loose fill}}$	lb/ft <sup>3</sup>	50.4

Figure 6.2: Compressibility curve

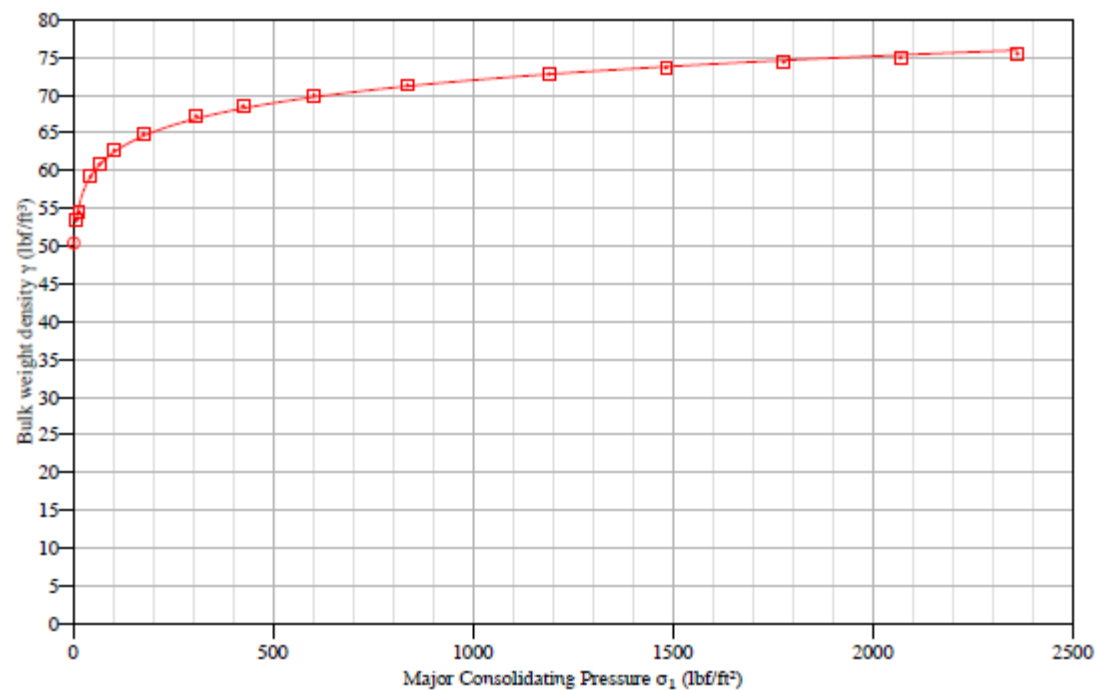


Figure C.172 LAW batch #9b: Compressibility curve

## Maximum hopper angles for Mass Flow

Wall material 304 SS Sheet, #2B Finish, 12 ga

Figure 6.3: Conical hopper angles

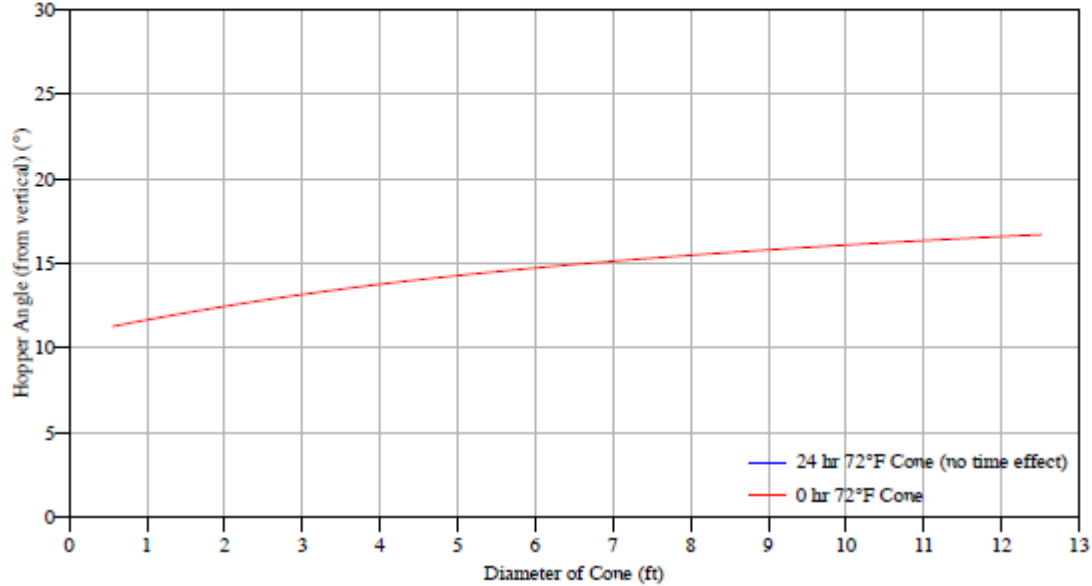


Figure 6.4: Wedge hopper angles

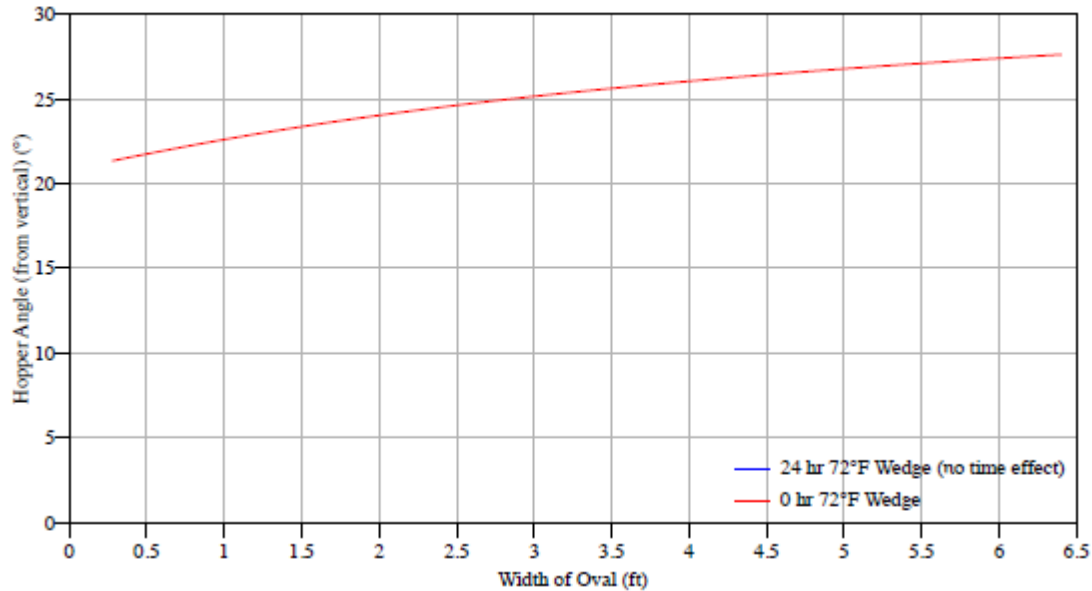


Figure C.173 LAW batch #9b: Conical hopper angles (Top) and Wedge hopper angles (Bottom) with 304 SS sheet

Wall material Mild CS HR Plate, Mill Finish, 1/4"

Figure 6.5: Conical hopper angles

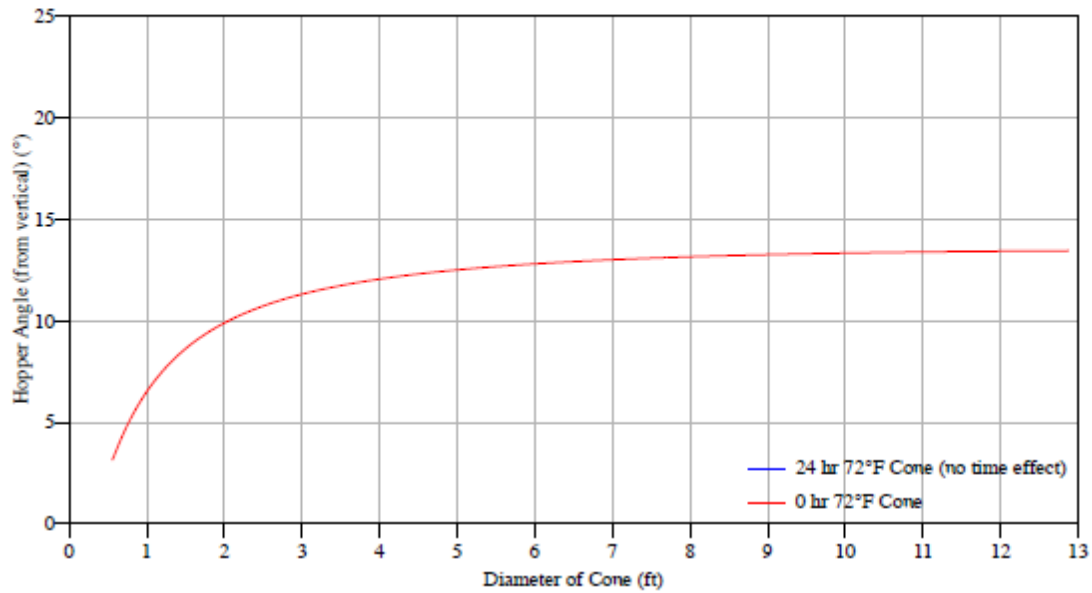


Figure 6.6: Wedge hopper angles

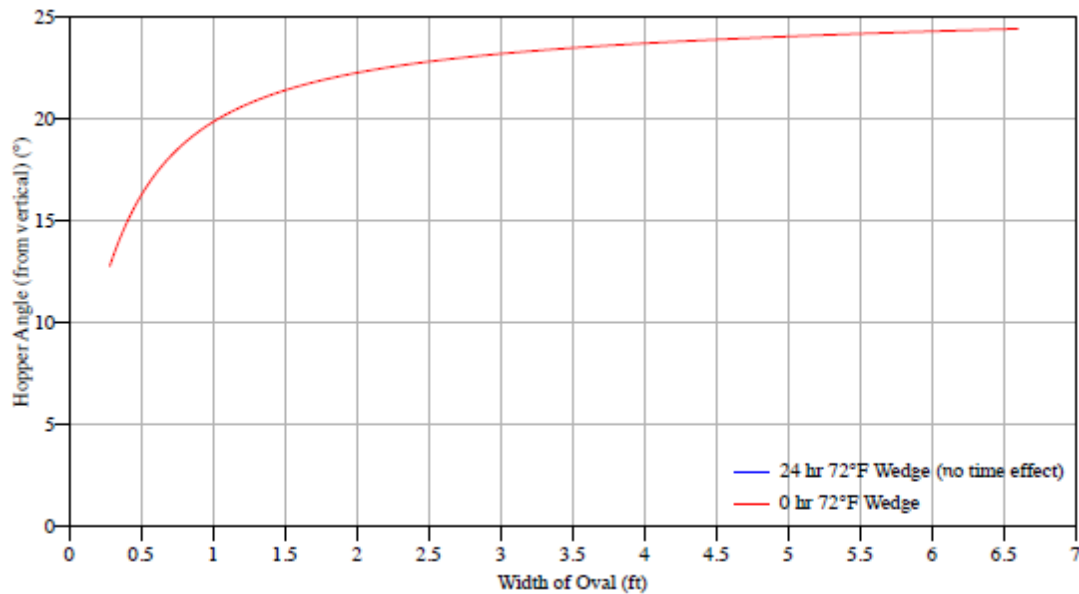


Figure C.174 LAW batch #9b: Conical hopper angles (Top) and Wedge hopper angles (Bottom) with mild CS HR plate

Wall material Tivar-88

Figure 6.7: Conical hopper angles

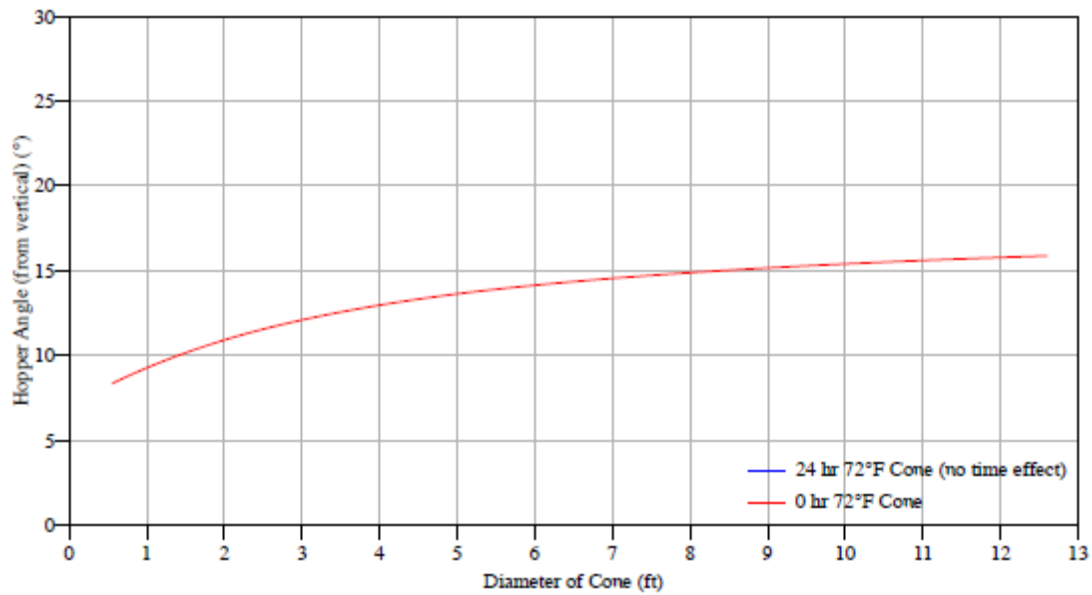


Figure 6.8: Wedge hopper angles

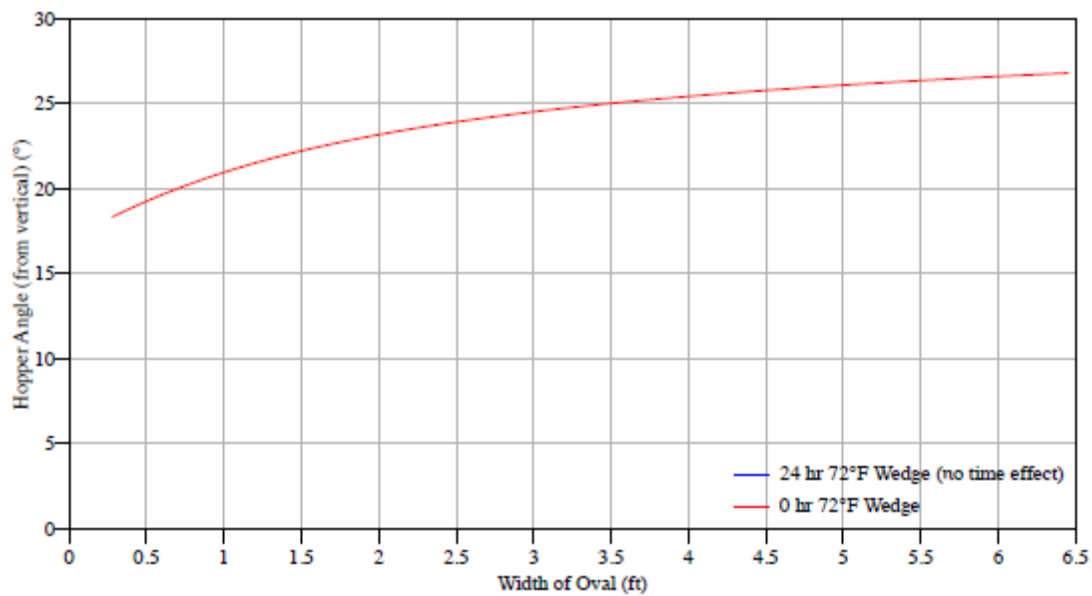


Figure C.175 LAW batch #9b: Conical hopper angles (Top) and Wedge hopper angles (Bottom) with Tivar 88



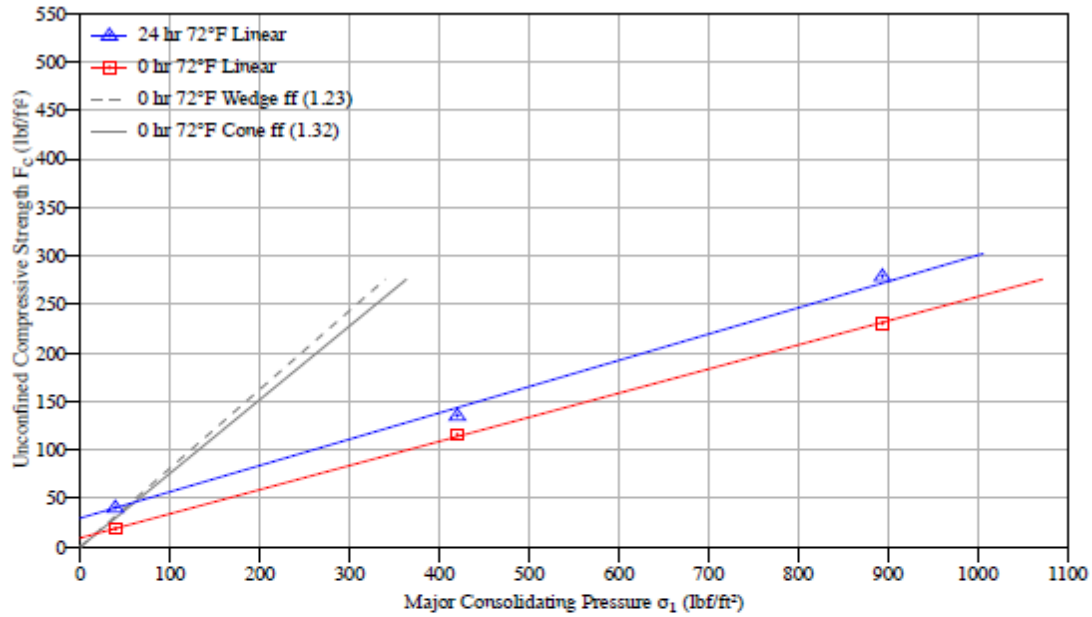


Figure C.176 LAW batch #9b: Flow function

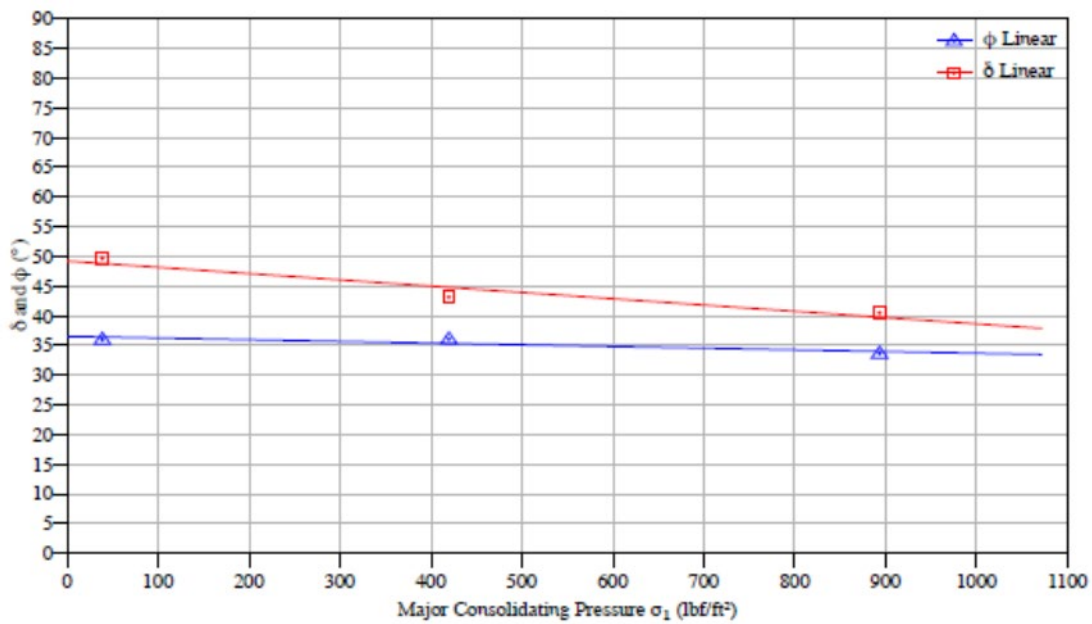


Figure C.177 LAW batch #9b: Effective angle of friction ( $\delta$ ) and kinematic angle of internal friction ( $\phi$ )

## Air permeability test results

### Temperature 72°F

$K$  is a function of the bulk weight density of the solid

$$K = K_0 \left( \frac{\gamma}{\gamma_0} \right)^{-\alpha}$$

At room temperature, for  $\gamma$  between 50.2 and 70  $lb_f/ft^3$ :

Table 6.4: Permeability parameters

$K_0$	$ft/s$	0.003718
$\gamma_0$	$lb_f/ft^3$	54.9
$\alpha$		3.076

Figure 6.15: Permeability curve

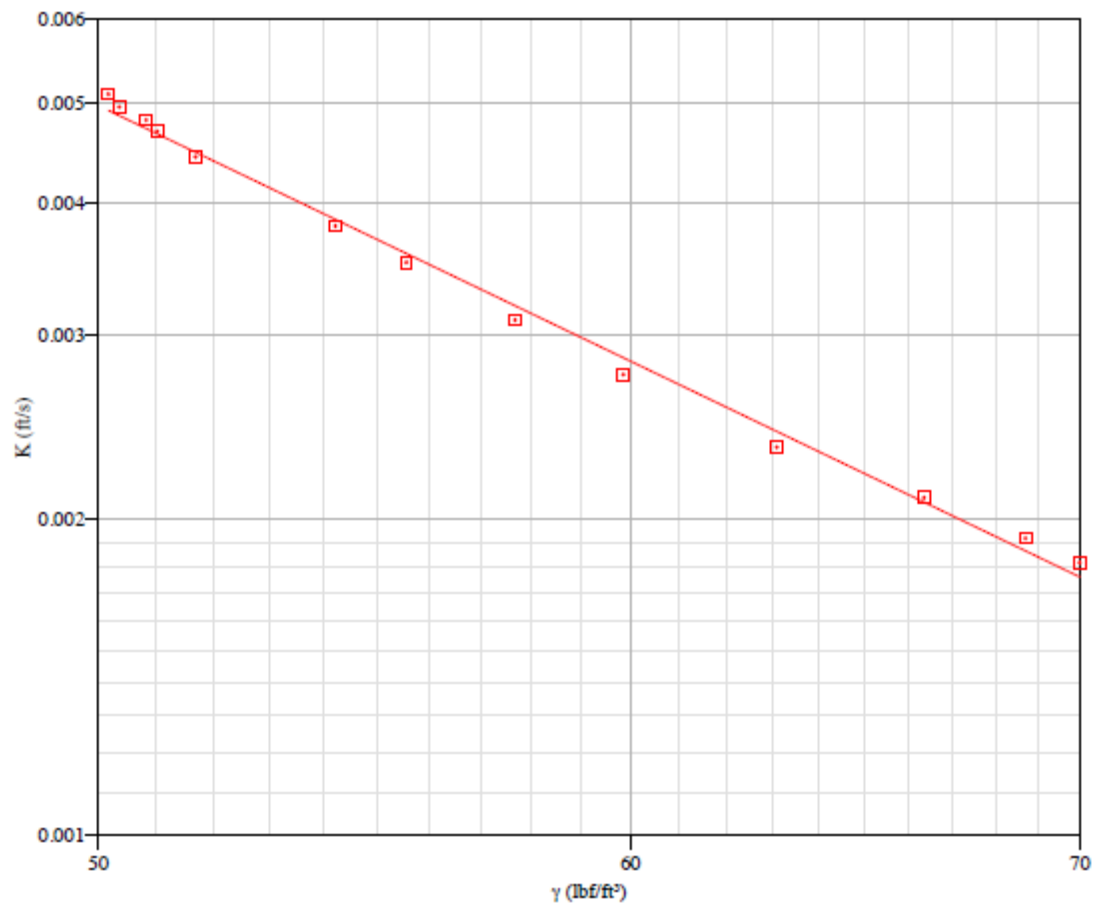


Figure C.178 LAW batch #9b: Permeability curve

## Chute angles

Chute material 304 SS Sheet, #2B Finish, 12 ga

Storage time at rest 0 hr

Chute temperature 72°F

Material temperature 72°F

Table 6.5: Measured chute clean-off angles (from horizontal)

Impact Pressure $lb_f/ft^2$	Angle $^\circ$
3.3	24 to 26
42.5	34 to 37
81.6	36 to 39
159.8	49 to 56

Figure 6.16: Chute curve

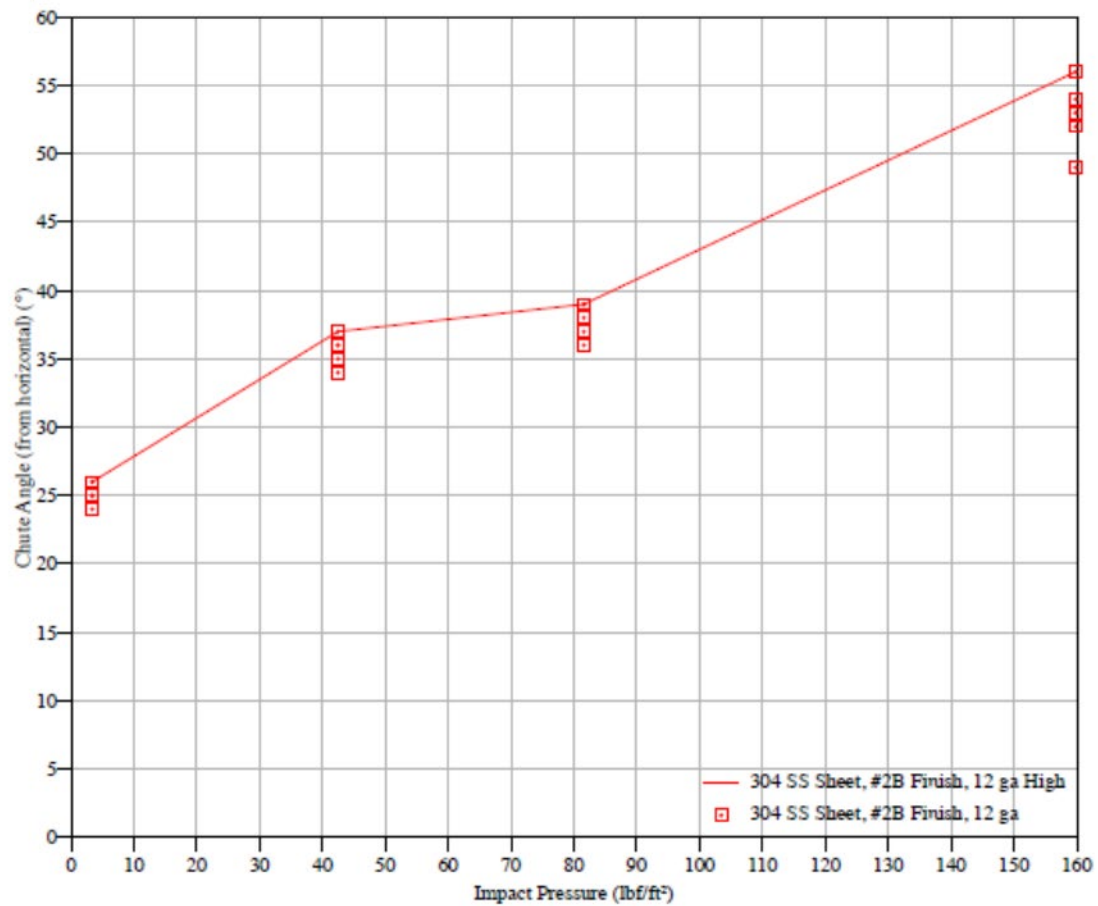


Figure C.179 LAW batch #9b: Chute curve with 304 SS sheet

Chute material Mild CS HR Plate, Mill Finish, 1/4"  
Storage time at rest 0 hr  
Chute temperature 72°F  
Material temperature 72°F

Table 6.6: Measured chute clean-off angles (from horizontal)

Impact Pressure $lb_f/ft^2$	Angle $^\circ$
3.3	26 to 28
42.5	36 to 38
81.6	40 to 48
159.8	53 to 56

Figure 6.17: Chute curve

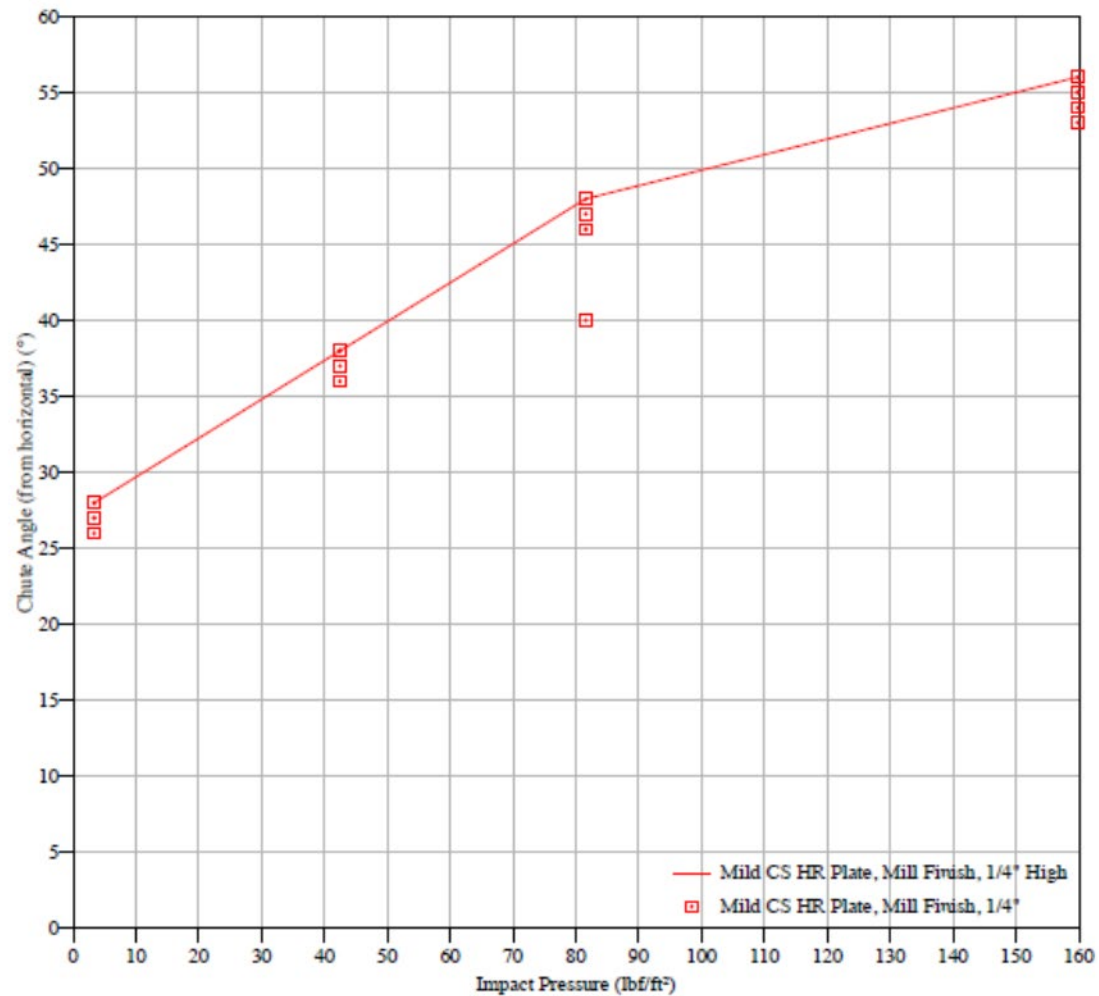


Figure C.180 LAW batch #9b: Chute curve with mild CS HR plate

Chute material Tivar-88  
Storage time at rest 0 hr  
Chute temperature 72°F  
Material temperature 72°F

Table 6.7: Measured chute clean-off angles (from horizontal)

Impact Pressure $lb_f/ft^2$	Angle $^\circ$
3.3	26 to 28
42.5	40 to 42
81.6	46 to 49
159.8	49 to 52

Figure 6.18: Chute curve

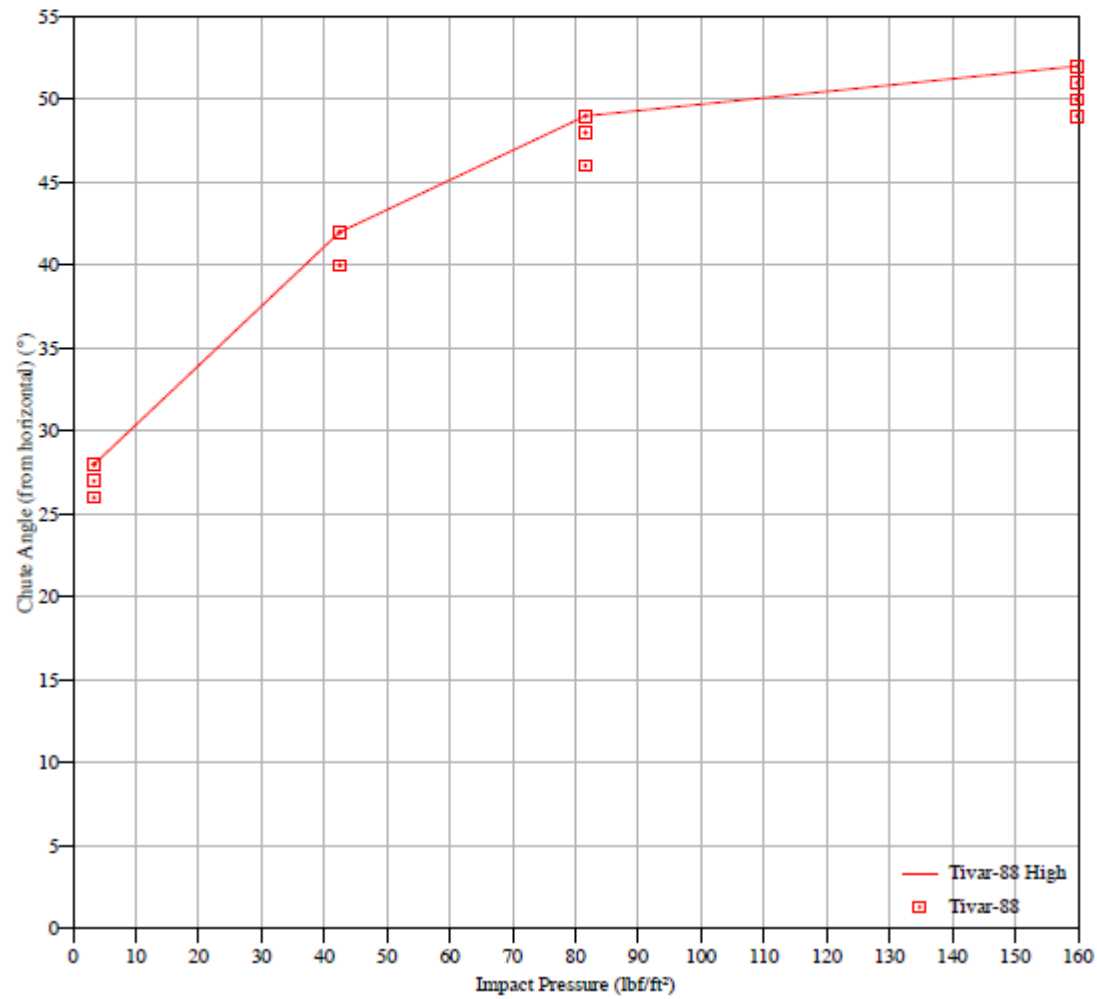


Figure C.181 LAW batch #9b: Chute curve with Tivar 88

## Particle Size Distribution Analysis Comparison

Figure 6.22: Particle size distribution, by volume

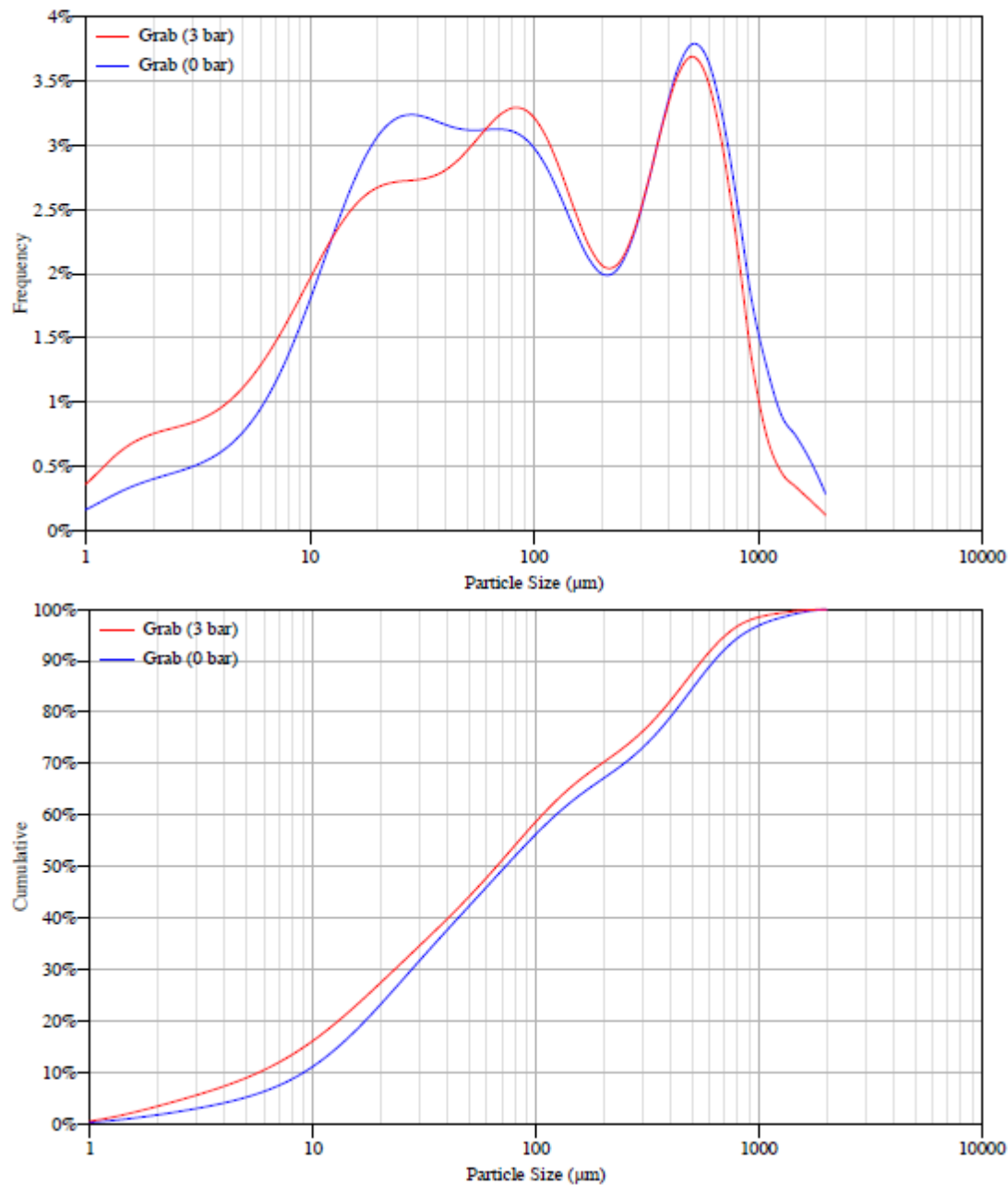


Figure C.182 LAW batch #9b: Particle size distribution by volume and pressure

## Particle Size Distribution

### Particle Size Distribution By Sieving

Table 6.8: Reference via Ro-Tap w/ taper

Sieve name	Size	Retained %	Particle	Size
ASTM #6	3.35 mm	0.00	p80	0.0066 in
ASTM #12	1.7 mm	0.00	p90	0.012 in
ASTM #20	850 $\mu$ m	0.29		
ASTM #40	425 $\mu$ m	6.24		
ASTM #70	212 $\mu$ m	7.26		
ASTM #100	150 $\mu$ m	9.19		
ASTM #200	75 $\mu$ m	23.52		
PAN	0 $\mu$ m	53.49		
	Total	100.00		
	Sieving Yield	98.81		
	Initial Total Mass	62.091 gm		

Figure 6.19: Particle size distribution, by mass

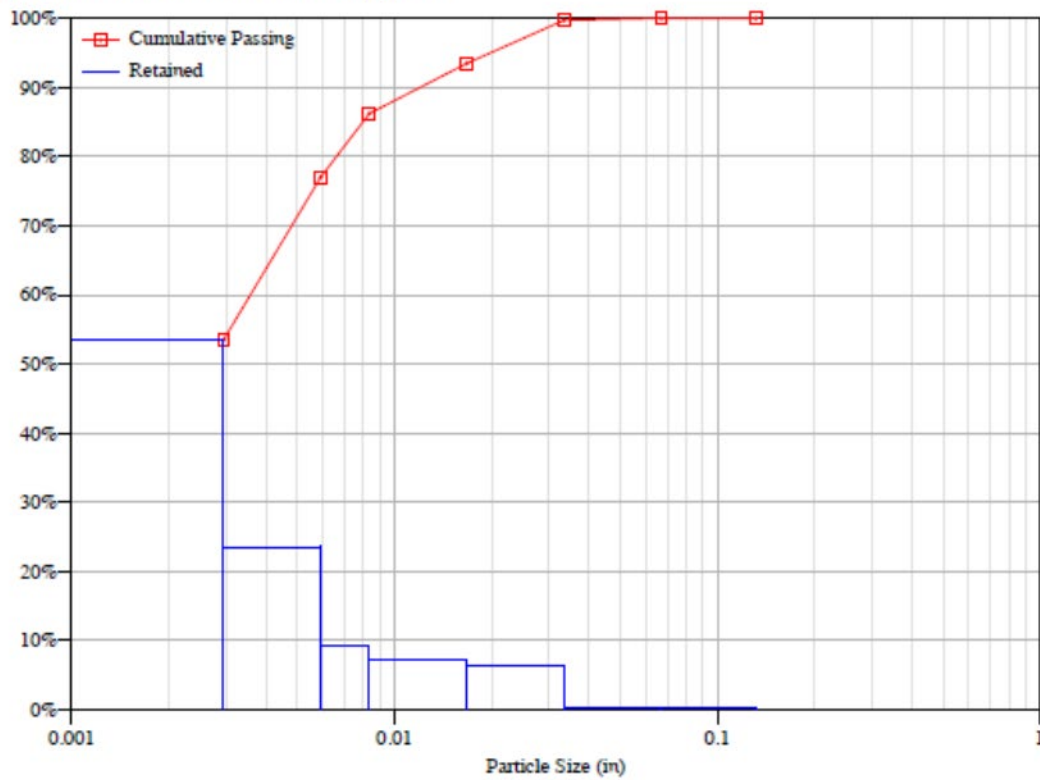


Figure C.183 LAW batch #9b: Particle size distribution by sieving (mass %)

## Appendix D – Original Shear Strength and Viscosity Data Measured at PNNL

The figures in this section display experimental results of rheological properties for slurry feeds generated by Pacific Northwest National Laboratory.

### Appendix D Table of Contents

- D.1 Shear Strength as a Function of Time..... D.1
- D.2 Yield Stress Versus Shear Rate..... D.14

### D.1 Shear strength as a function of time

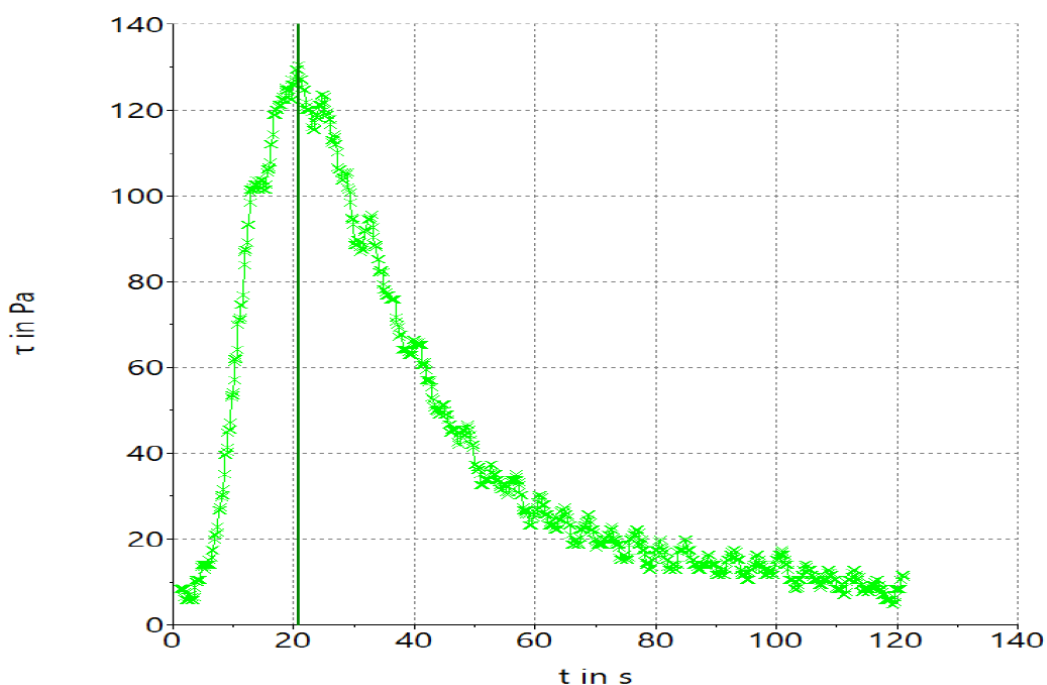


Figure D.1. Slurry feed #1a: Shear strength as a function of time after settling for 24 hours



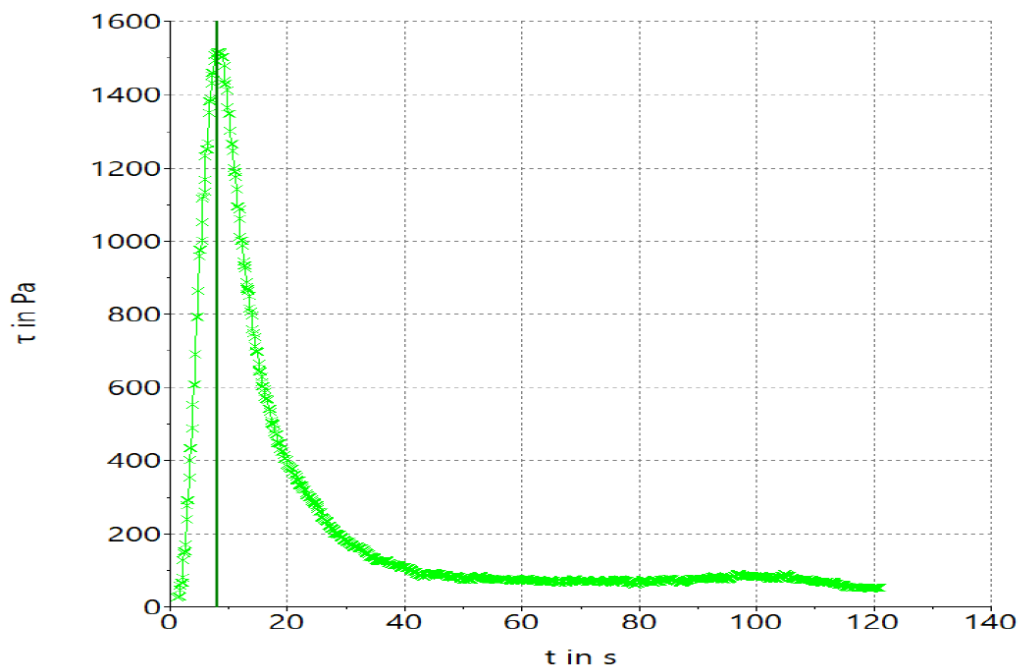


Figure D.2. Slurry feed #6a: Shear strength as a function of time after settling for 24 hours

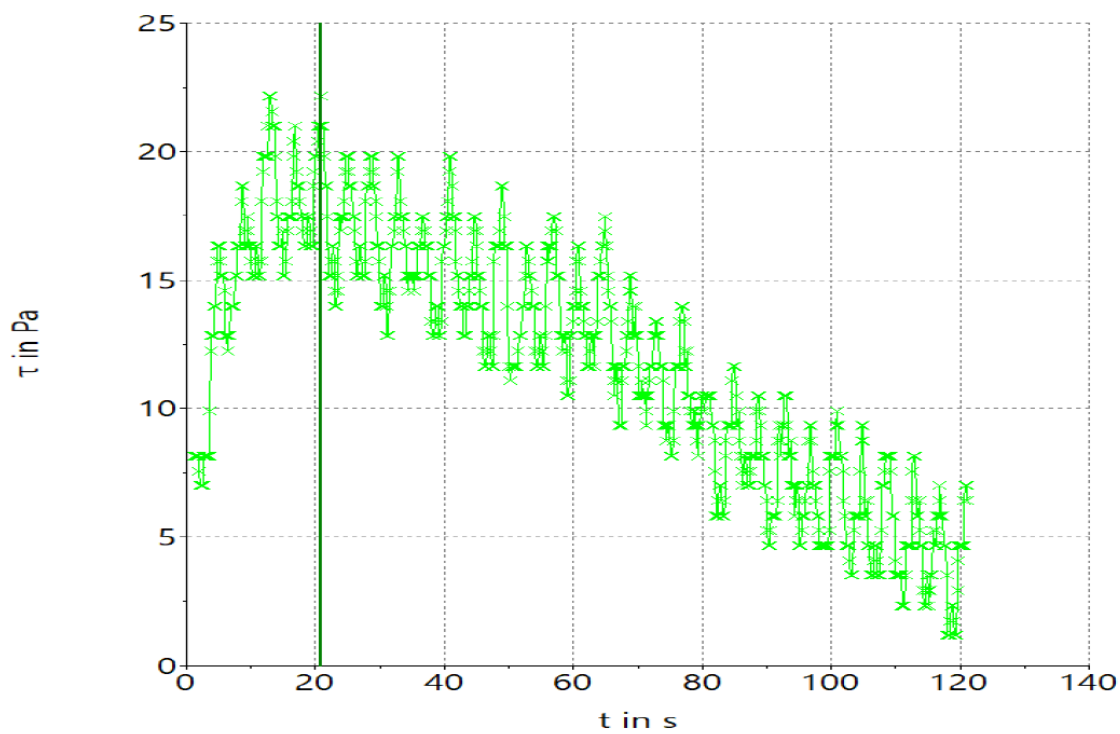


Figure D.3. Slurry feed #9a: Shear strength as a function of time after settling for 24 hours

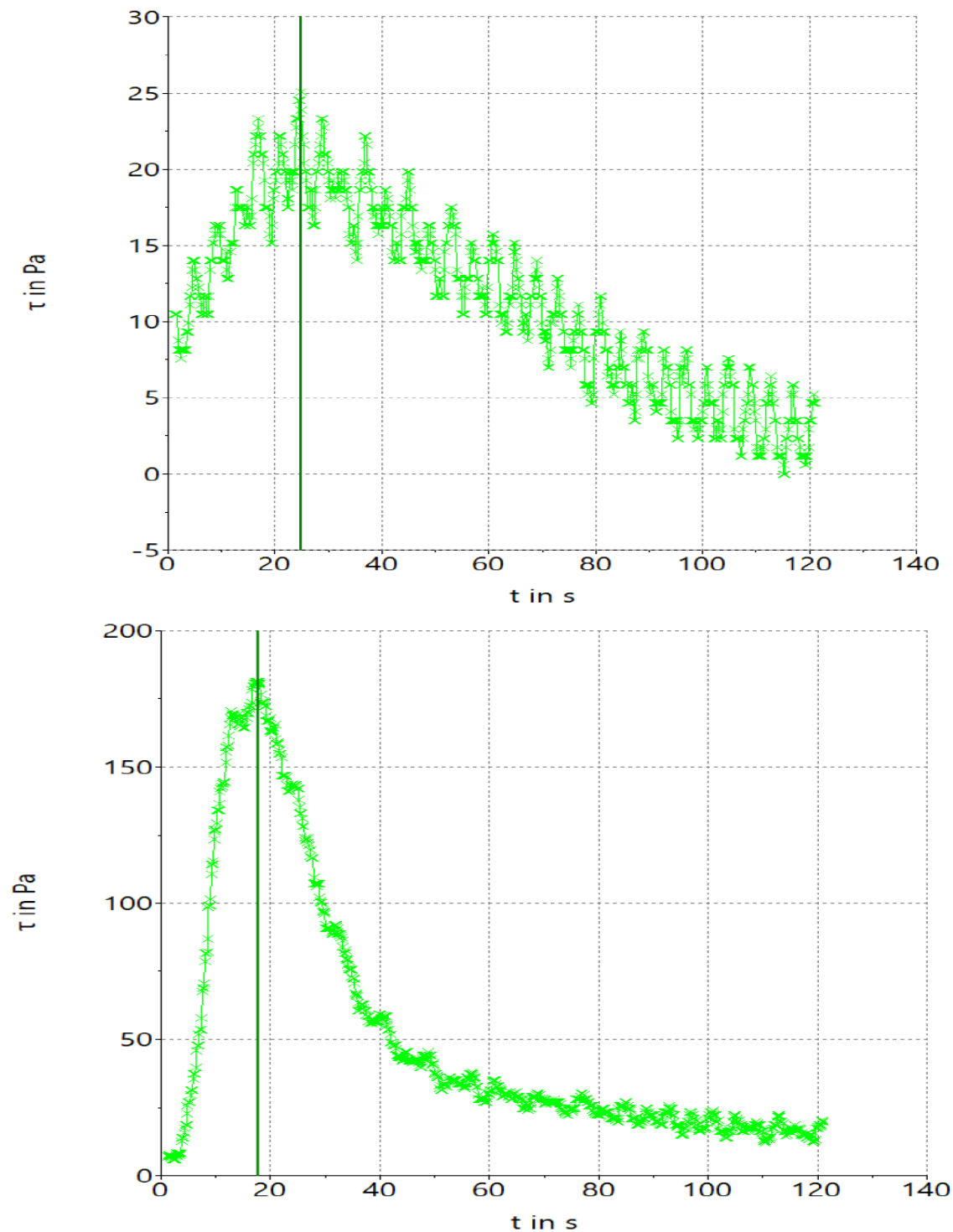


Figure D.4. Slurry feed #1a: Shear strength as a function of time after settling for 72 hours (top) and 48 hours (bottom, vane was inserted deeper)

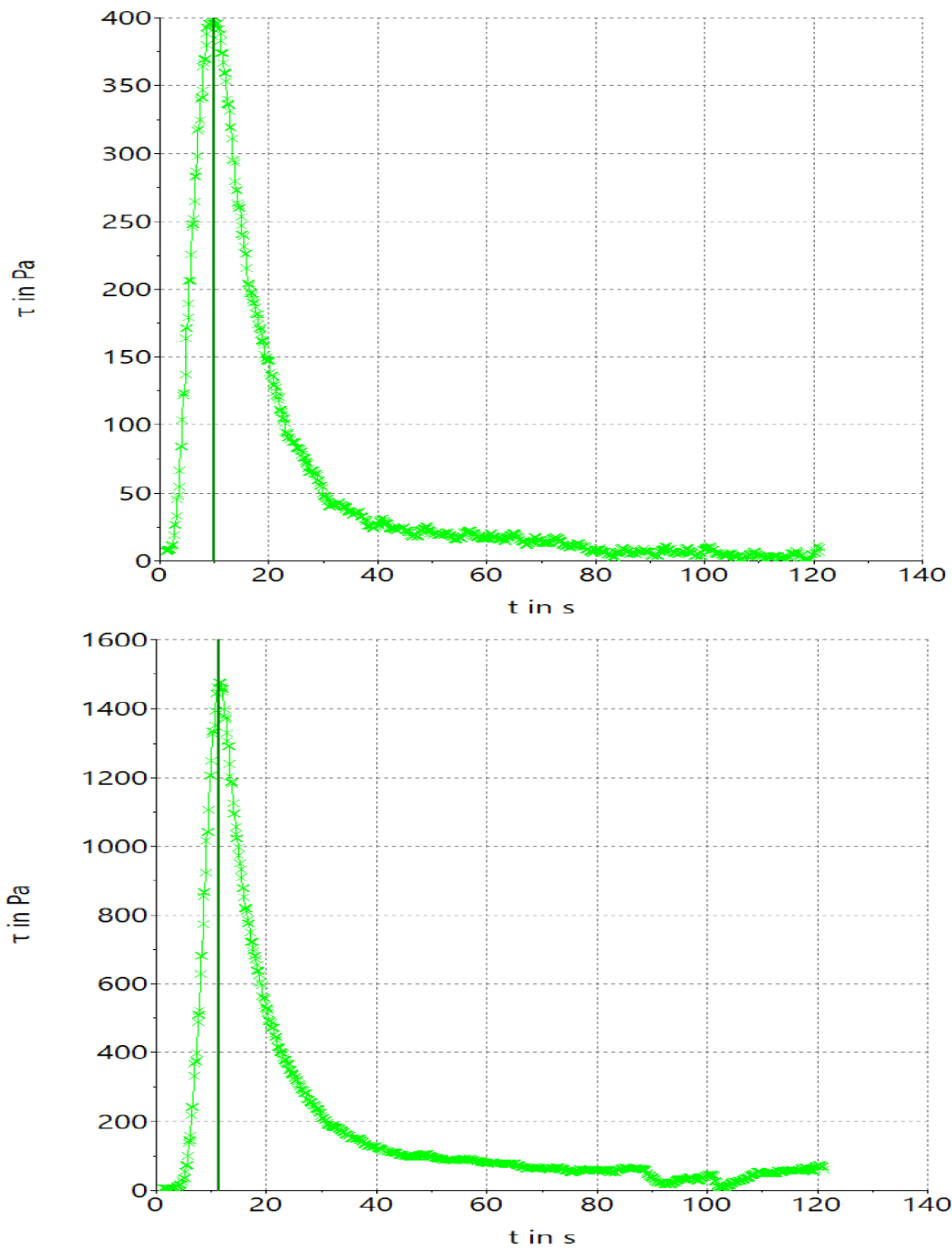


Figure D.5. Slurry feed #6a: Shear strength as a function of time after settling for 72 hours (top) and 48 hours (bottom, vane was inserted deeper)

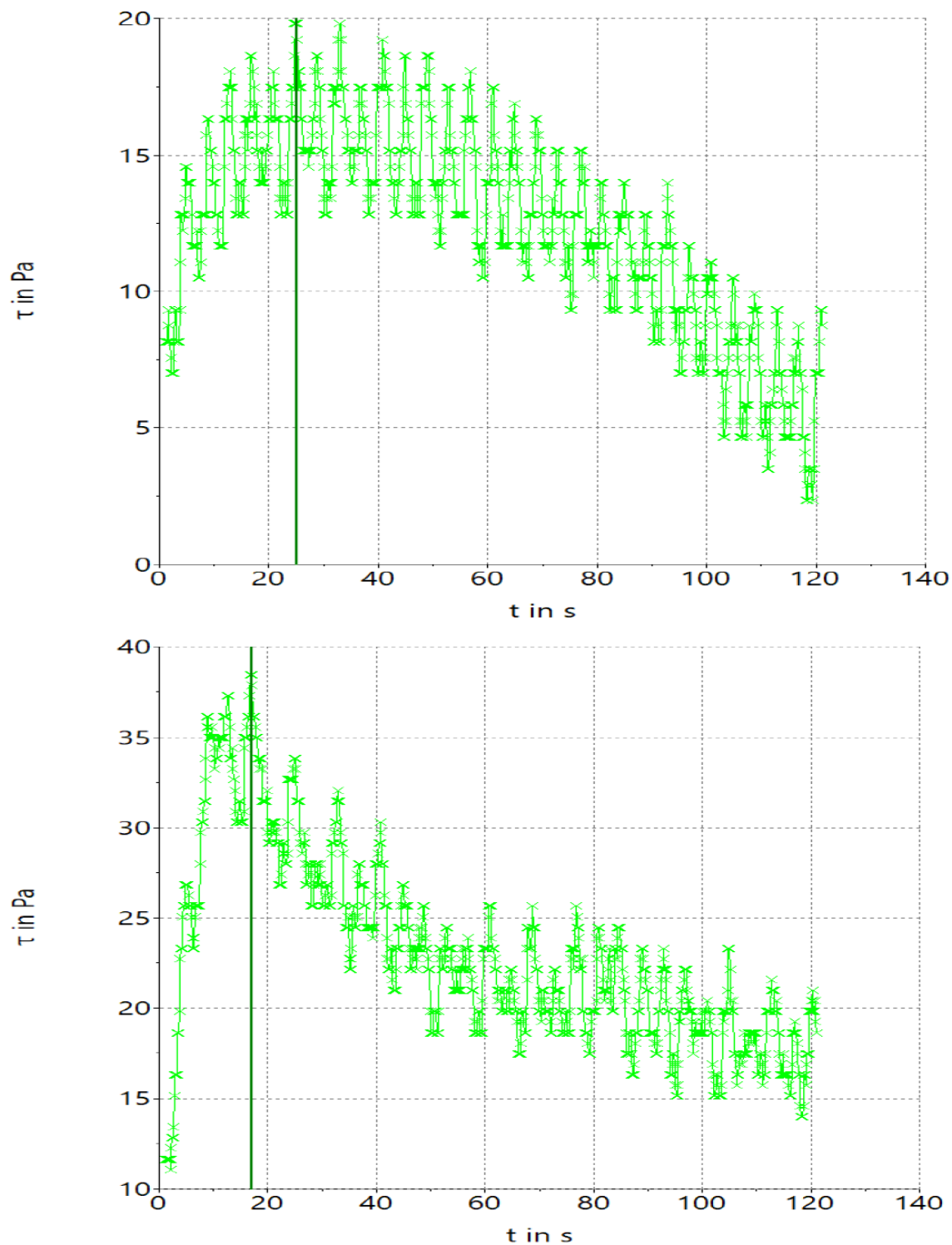
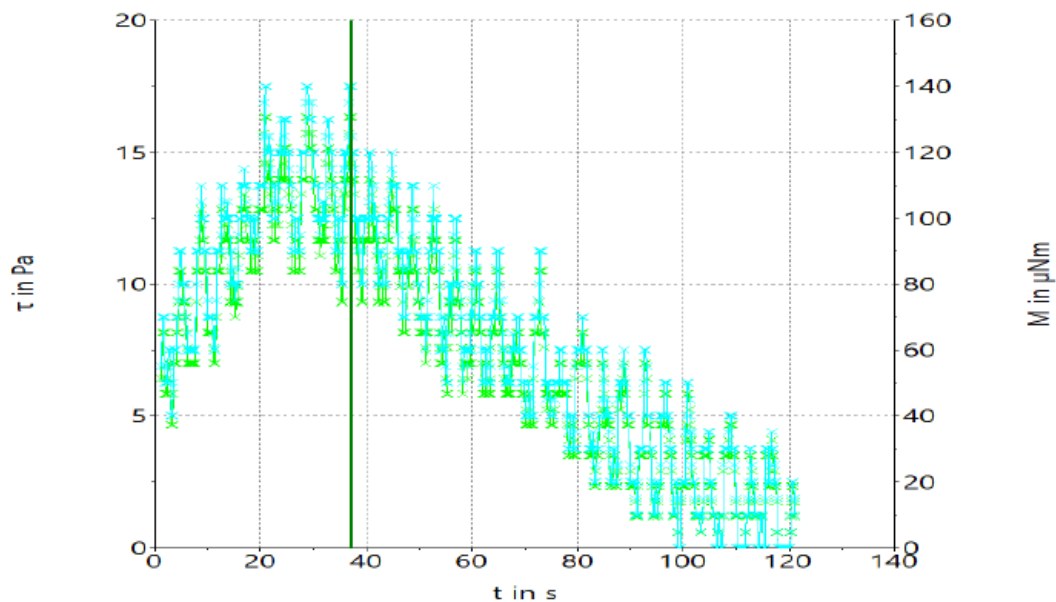


Figure D.6. Slurry feed #9a: Shear strength as a function of time after settling for 72 hours (top) and 48 hours (bottom, vane was inserted deeper)

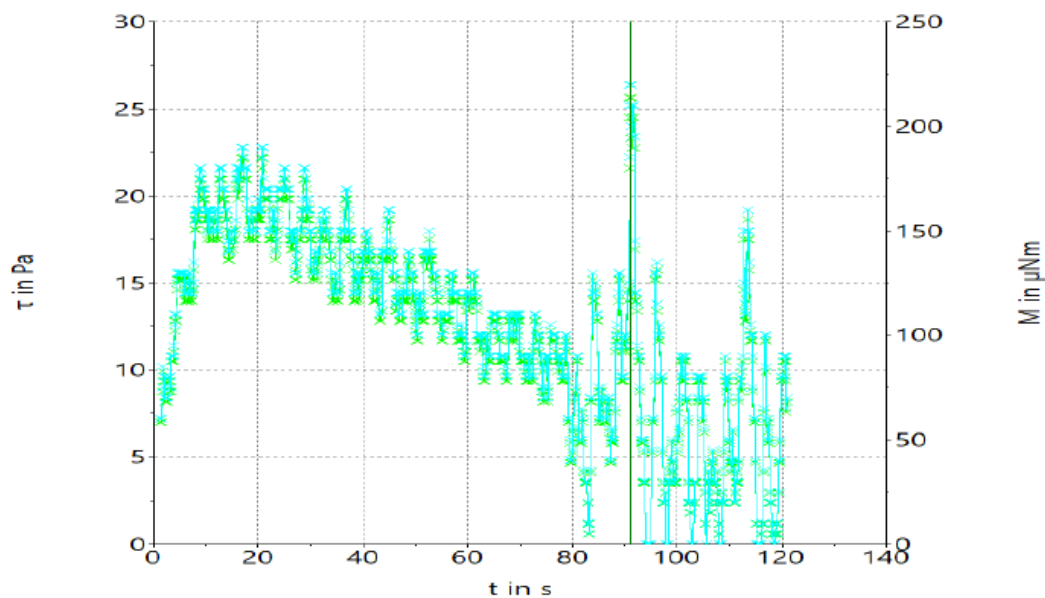


HAAKE RheoWin 4.86.0002

Filename: C:\Users\D3M966\Desktop\lala\GFCs-Seung Min FY 2020\GFC 10\_2021\Rheology 2021-EWG-TI-164\2021-10-22 LAW Slurry Feed #1-RT-1.1.r  
Job: C:\Users\Public\Documents\Thermo\RheoWin\Jobs\VT550 - 1.6x1.6 cm vane shear strength.rwj

C:\Users\D3M966\Desktop\lala\GFCs-Seung Min FY 2020\GFC  
10\_2021\Rheology 2021-EWG-TI-164\2021-10-22 LAW Slurry Feed  
#1-RT-1.1.rwd  
ID 7-4: Curve discussion :  
Method t in s τ in Pa  
-----  
Greatest value 37.12 16.32

Figure D.7 Melter feed #1b: Shear strength as a function of time after settling for 24 hours.



HAAKE RheoWin 4.86.0002

Filename: C:\Users\D3M966\Desktop\Jala\GFCs-Seung Min FY 2020\GFC 10\_2021\Rheology 2021-EWG-TI-164\2021-10-22 LAW Slurry Feed #6-RT-1.1.r

Job: C:\Users\Public\Documents\Thermo\RheoWin\Jobs\VT550 - 1.6×1.6 cm vane shear strength.rwj

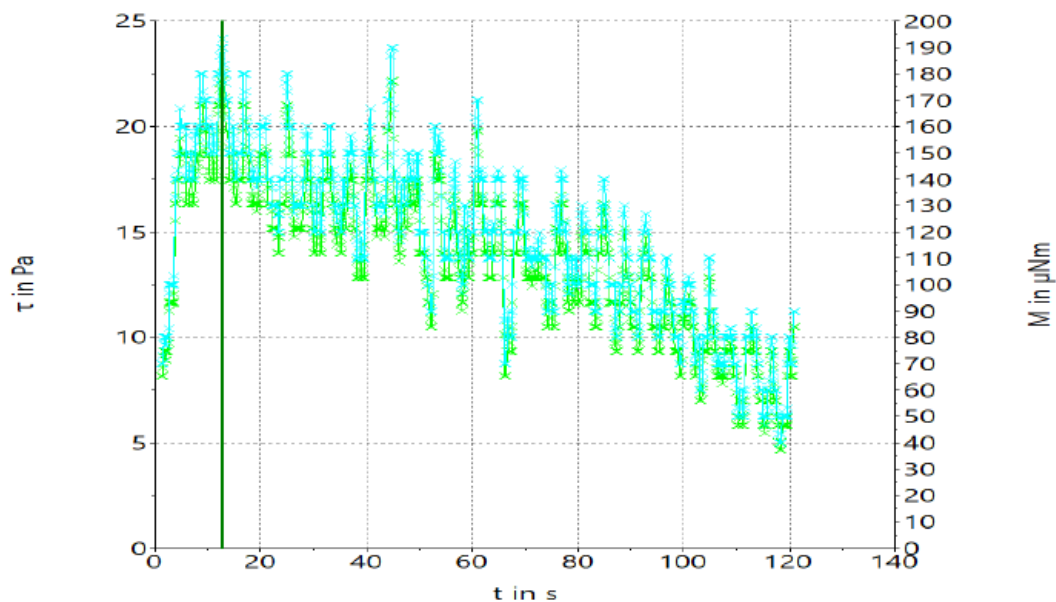
C:\Users\D3M966\Desktop\Jala\GFCs-Seung Min FY 2020\GFC  
10\_2021\Rheology 2021-EWG-TI-164\2021-10-22 LAW Slurry Feed  
#6-RT-1.1.rwd

ID 7-4: Curve discussion :

Method	t in s	τ in Pa
--------	--------	---------

Greatest value	91.20	25.65
----------------	-------	-------

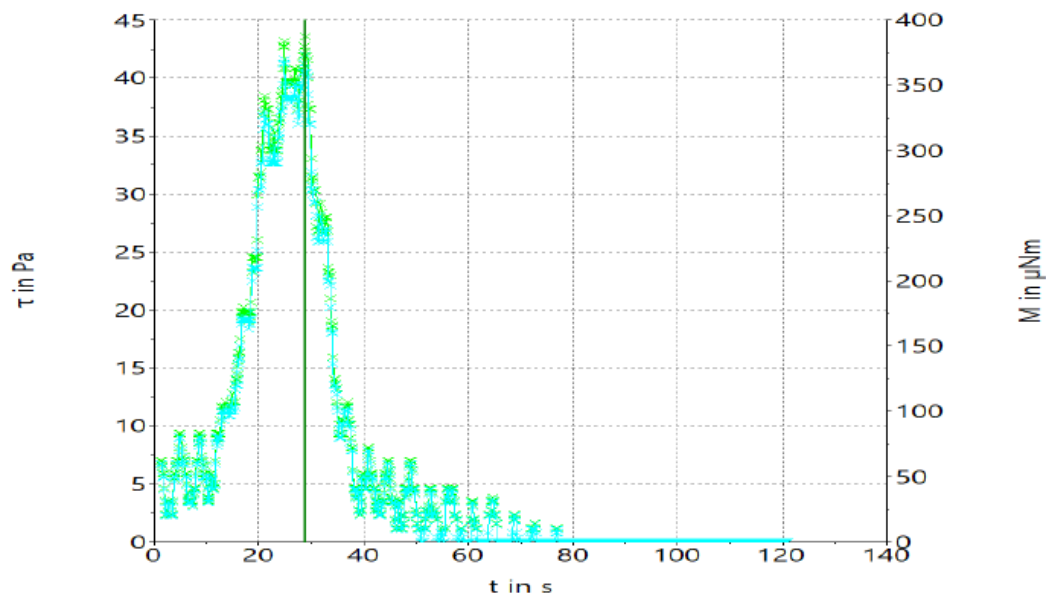
Figure D.8 Melter feed #6b: Shear strength as a function of time after settling for 24 hours.



HAAKE RheoWin 4.86.0002  
 Filename: C:\Users\D3M966\Desktop\lala\GFCs-Seung Min FY 2020\GFC 10\_2021\Rheology 2021-EWG-TI-164\2021-10-22 LAW Slurry Feed #9-RT-1.1.r  
 Job: C:\Users\Public\Documents\Thermo\RheoWin\Jobs\VT550 - 1.6×1.6 cm vane shear strength.rwj

C:\Users\D3M966\Desktop\lala\GFCs-Seung Min FY 2020\GFC  
 10\_2021\Rheology 2021-EWG-TI-164\2021-10-22 LAW Slurry Feed  
 #9-RT-1.1.rwd  
 ID 7-4: Curve discussion :  
 Method t in s τ in Pa  
 -----  
 Greatest value 12.83 22.54

Figure D.9 Melter feed #9b: Shear strength as a function of time after settling for 24 hours.



HAAKE RheoWin 4.86.0002

Filename: C:\Users\D3M966\Desktop\lala\GFCs-Seung Min FY 2020\GFC 10\_2021\Rheology 2021-EWG-TI-164\2021-10-22 LAW Slurry Feed #1-1 -RT-1.

Job: C:\Users\Public\Documents\Thermo\RheoWin\Jobs\VT550 - 1.6×1.6 cm vane shear strength.rwj

C:\Users\D3M966\Desktop\lala\GFCs-Seung Min FY 2020\GFC  
10\_2021\Rheology 2021-EWG-TI-164\2021-10-22 LAW Slurry Feed  
#1-1 -RT-1.1.rwd

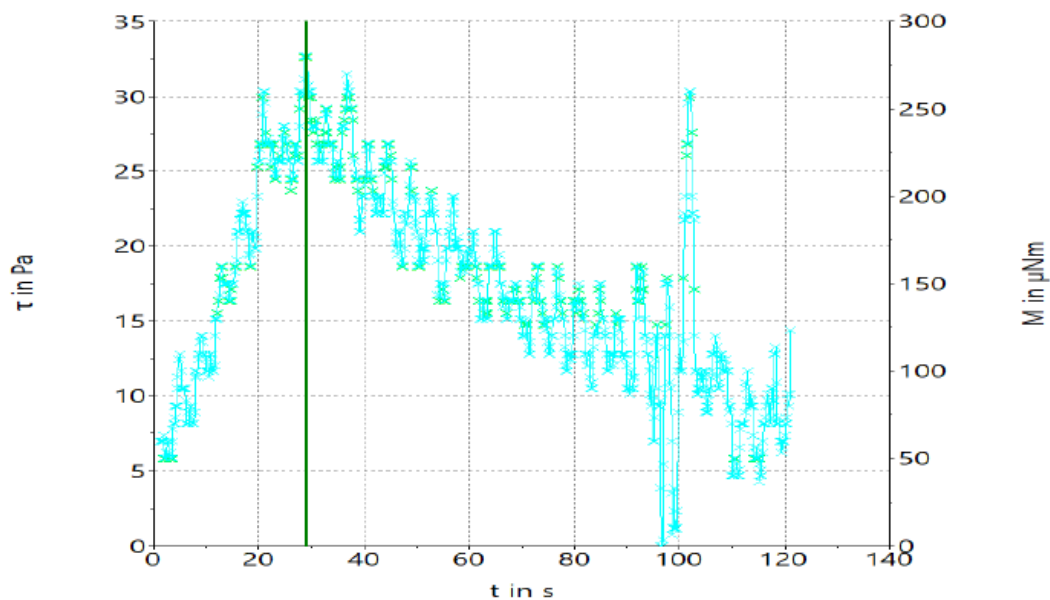
ID 7-4: Curve discussion :

Method	t in s	τ in Pa
--------	--------	---------

Greatest value	28.86	43.53
----------------	-------	-------

Figure D.10 Melter feed #1-1: Shear strength as a function of time after settling for 24 hours.





HAAKE RheoWin 4.86.0002

Filename: C:\Users\D3M966\Desktop\lala\GFCs-Seung Min FY 2020\GFC 10\_2021\Rheology 2021-EWG-TI-164\2021-10-21 LAW Slurry Feed -RT-1-1.1.n

Job: C:\Users\Public\Documents\Thermo\RheoWin\Jobs\VT550 - 1.6×1.6 cm vane shear strength.rwj

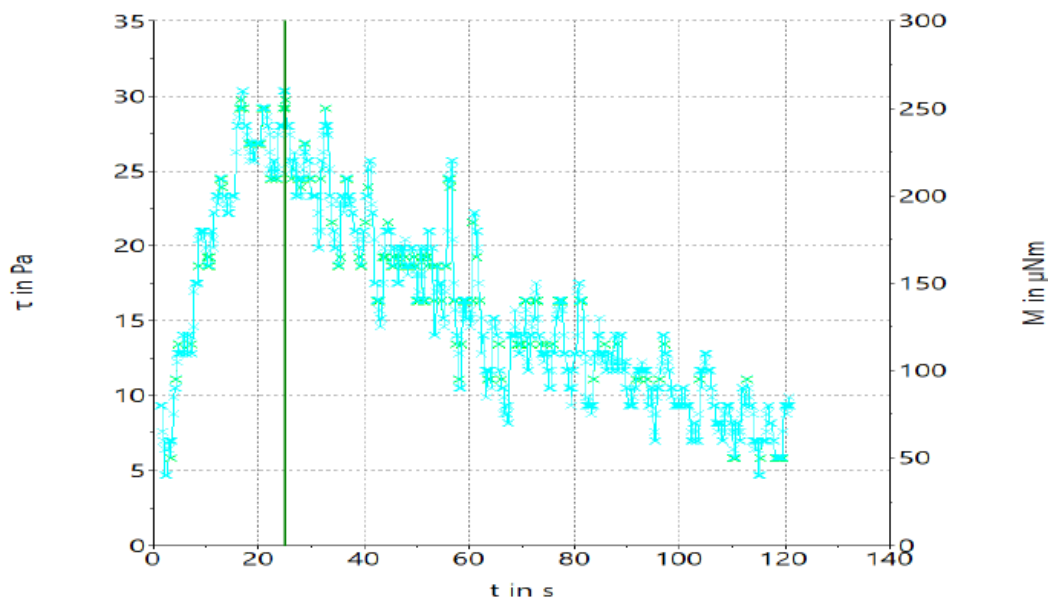
C:\Users\D3M966\Desktop\lala\GFCs-Seung Min FY 2020\GFC  
10\_2021\Rheology 2021-EWG-TI-164\2021-10-21 LAW Slurry Feed  
-RT-1-1.1.rwd

ID 7-4: Curve discussion :

Method	t in s	τ in Pa
--------	--------	---------

Greatest value	29.14	32.65
----------------	-------	-------

Figure D.11 Melter feed #1b: Shear strength as a function of time after settling for 48 hours.



HAAKE RheoWin 4.86.0002

Filename: C:\Users\D3M966\Desktop\lala\GFCs-Seung Min FY 2020\GFC 10\_2021\Rheology 2021-EWG-TI-164\2021-10-21 LAW Slurry Feed -RT-6-1.1.n

Job: C:\Users\Public\Documents\Thermo\RheoWin\Jobs\VT550 - 1.6×1.6 cm vane shear strength.rwj

C:\Users\D3M966\Desktop\lala\GFCs-Seung Min FY 2020\GFC  
10\_2021\Rheology 2021-EWG-TI-164\2021-10-21 LAW Slurry Feed  
-RT-6-1.1.rwd

ID 7-4: Curve discussion :

Method	t in s	τ in Pa
--------	--------	---------

Greatest value	25.01	30.32
----------------	-------	-------

Figure D.12 Melter feed #6b: Shear strength as a function of time after settling for 48 hours.

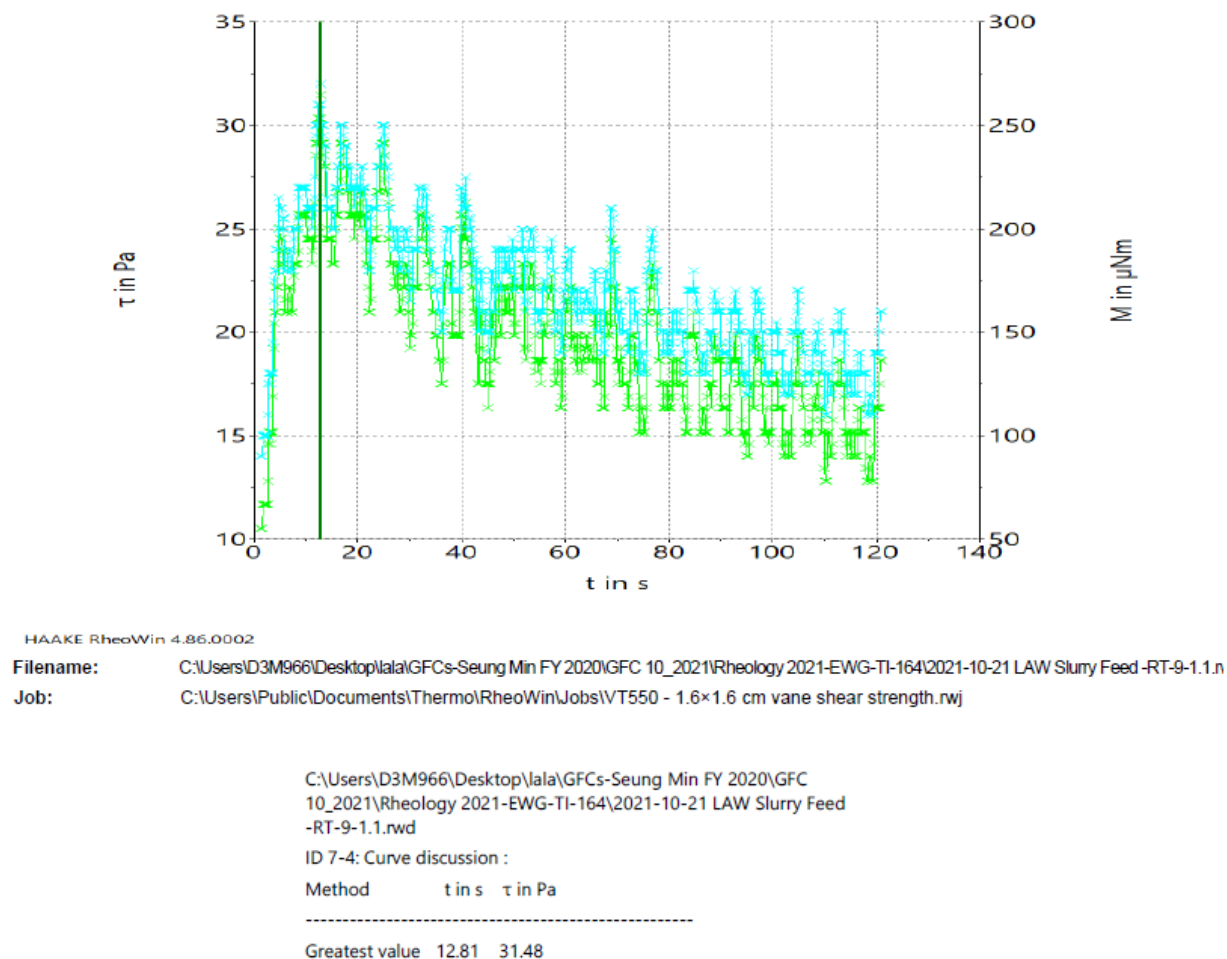
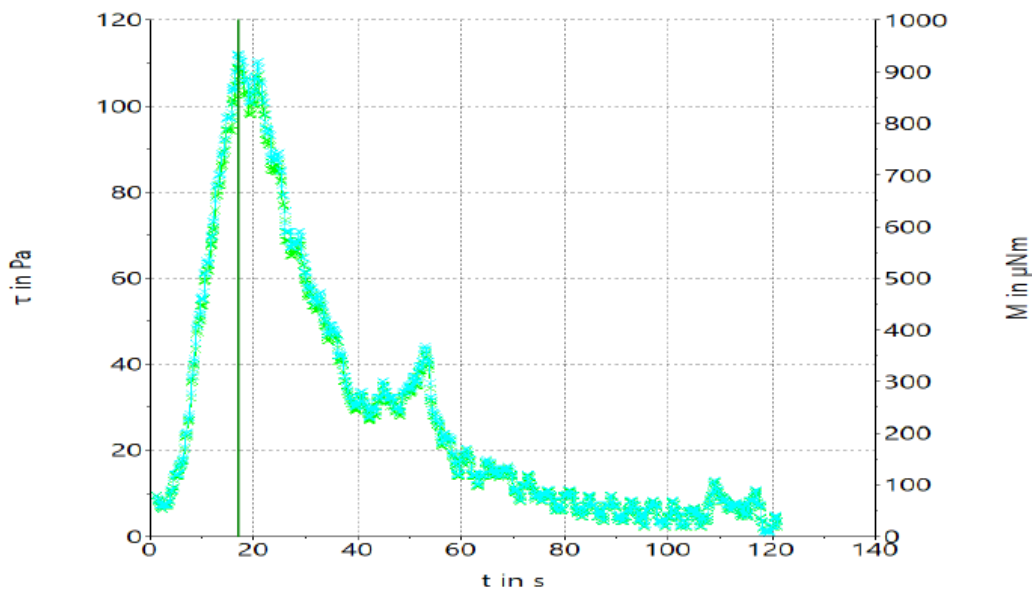


Figure D.13 Melter feed #9b: Shear strength as a function of time after settling for 48 hours.



HAAKE RheoWin 4.86.0002

Filename: C:\Users\D3M966\Desktop\lala\GFCs-Seung Min FY 2020\GFC 10\_2021\Rheology 2021-EWG-TI-164\2021-10-21 LAW Slurry Feed-RT-1-1-1.1

Job: C:\Users\Public\Documents\Thermo\RheoWin\Jobs\VT550 - 1.6×1.6 cm vane shear strength.rwj

C:\Users\D3M966\Desktop\lala\GFCs-Seung Min FY 2020\GFC 10\_2021\Rheology 2021-EWG-TI-164\2021-10-21 LAW Slurry Feed-RT-1-1-1.1.rwd

ID 7-4: Curve discussion :

Method	t in s	τ in Pa
-----		
Greatest value	16.95	108.8

Figure D.14 Melter feed #1-1: Shear strength as a function of time after settling for 48 hours.

## D.2 Yield stress versus shear rate

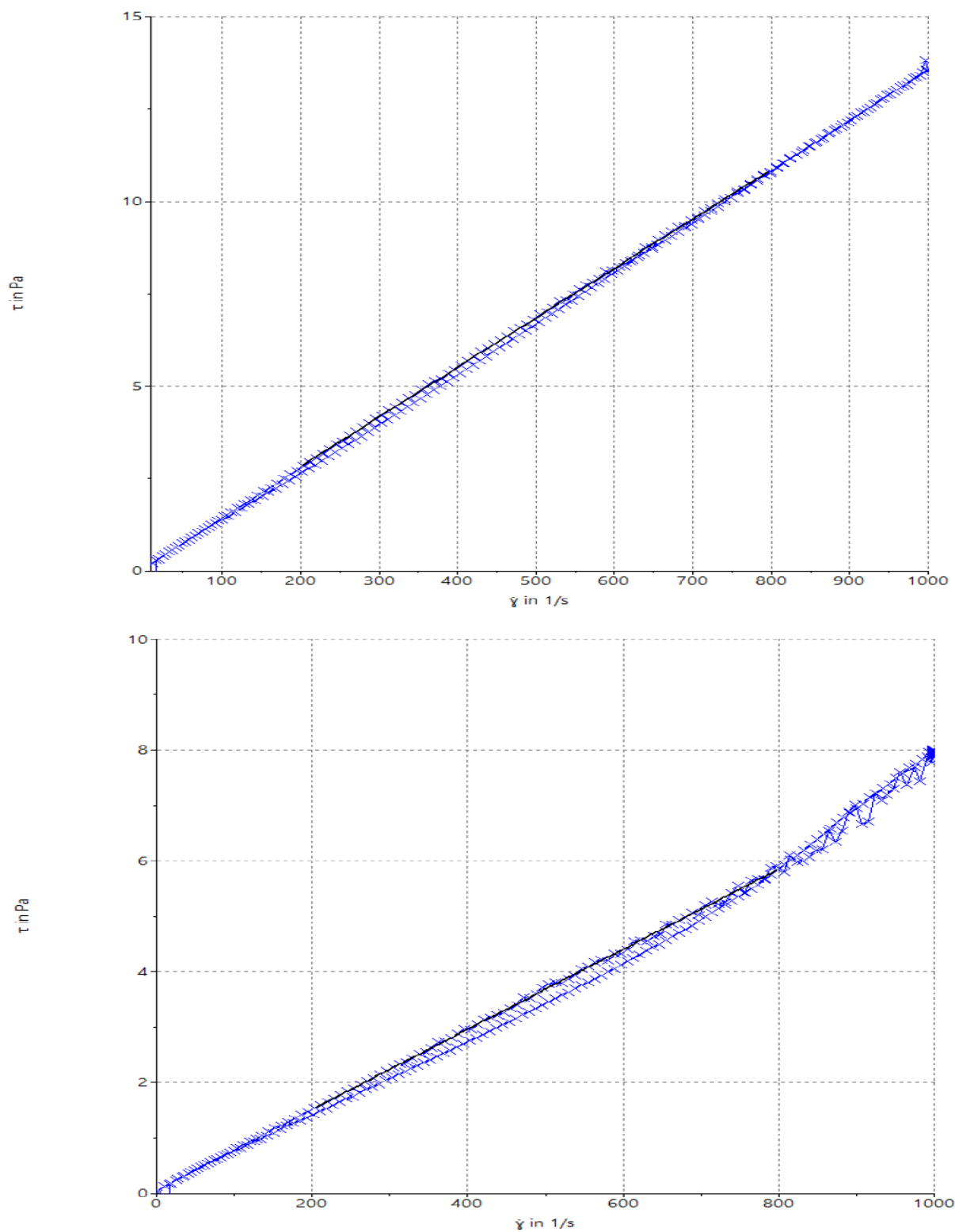


Figure D.15. Slurry feed #1a: Yield stress versus shear rate at 20 °C (top) and 40 °C (bottom)

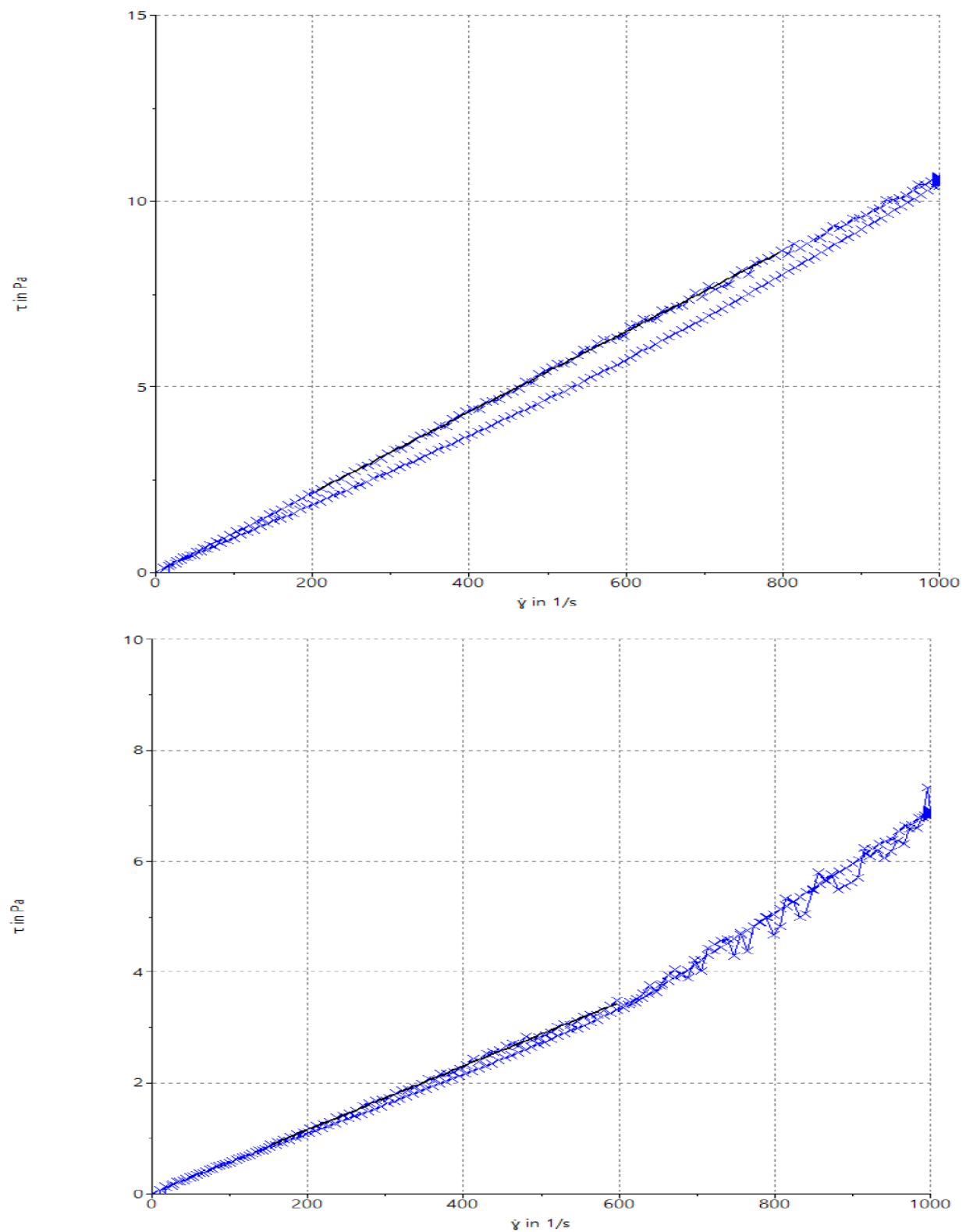


Figure D.16. Slurry feed #6a: Yield stress versus shear rate at 20 °C (top) and 40 °C (bottom)

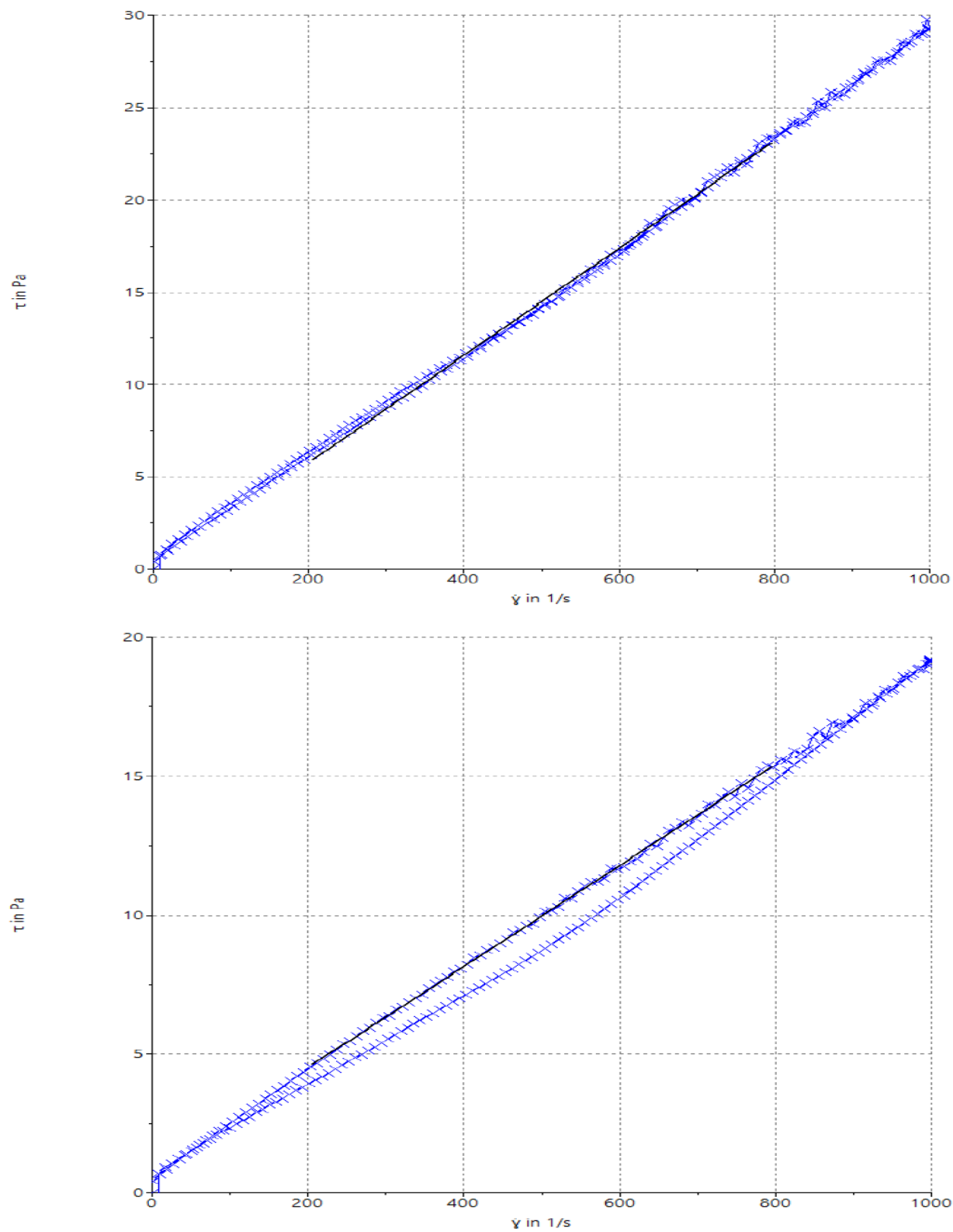


Figure D.17. Slurry feed #9a: Yield stress versus shear rate at 20 °C (top) and 40 °C (bottom)

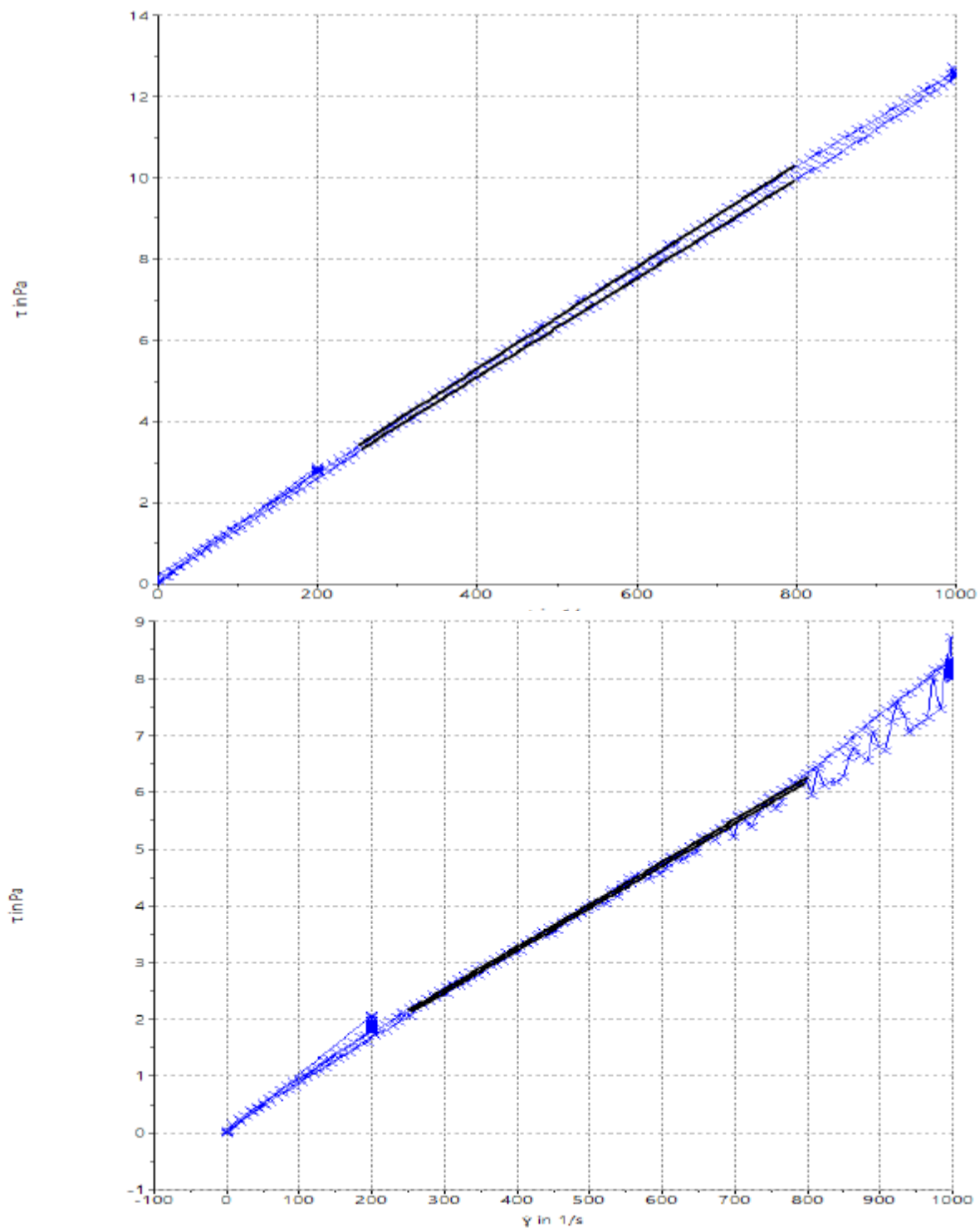


Figure D.18 Melter feed #1b: Yield stress versus shear rate at 20°C (top) and 40°C (bottom).



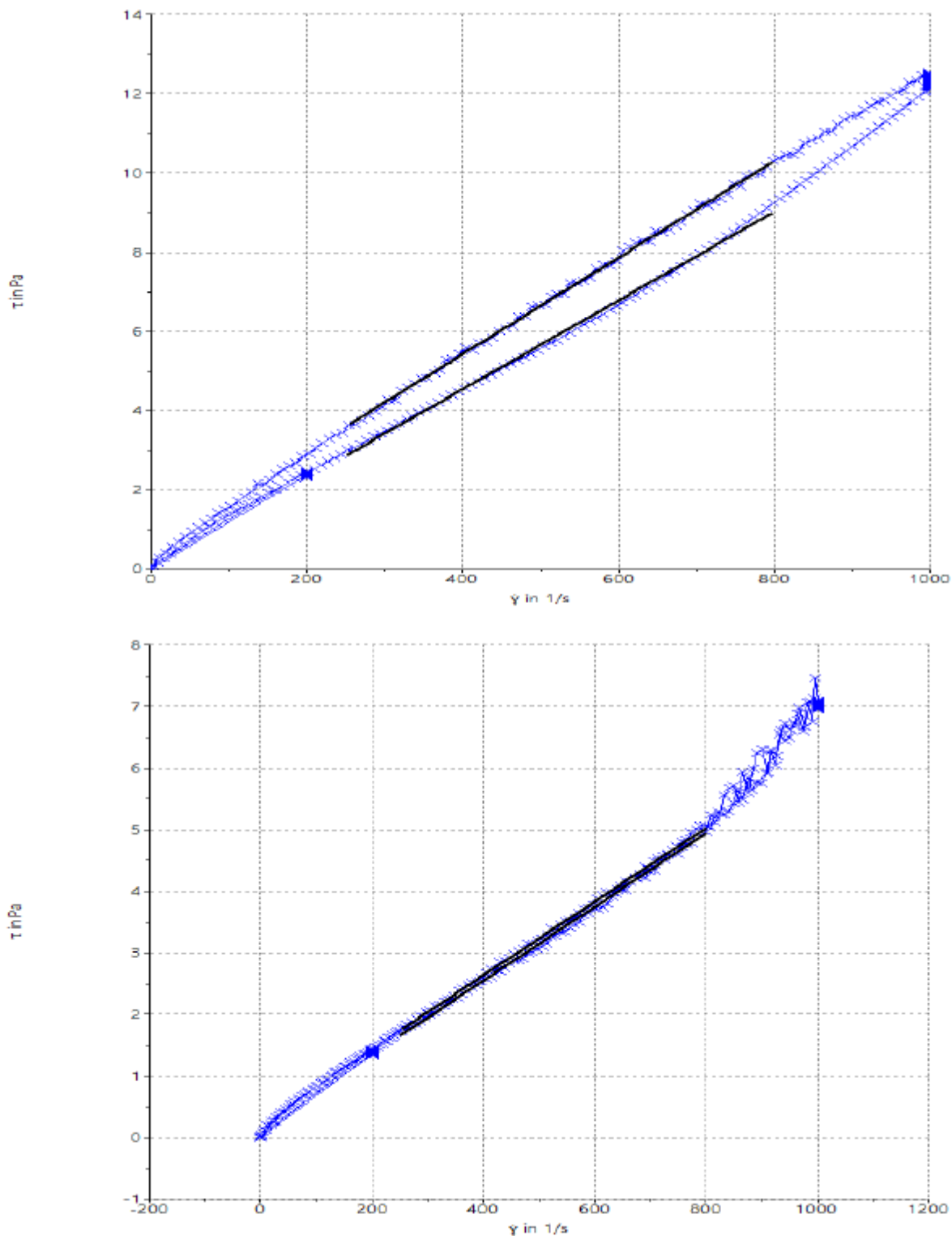


Figure D.19 Melter feed #6b: Yield stress versus shear rate at 20°C (top) and 40°C (bottom).

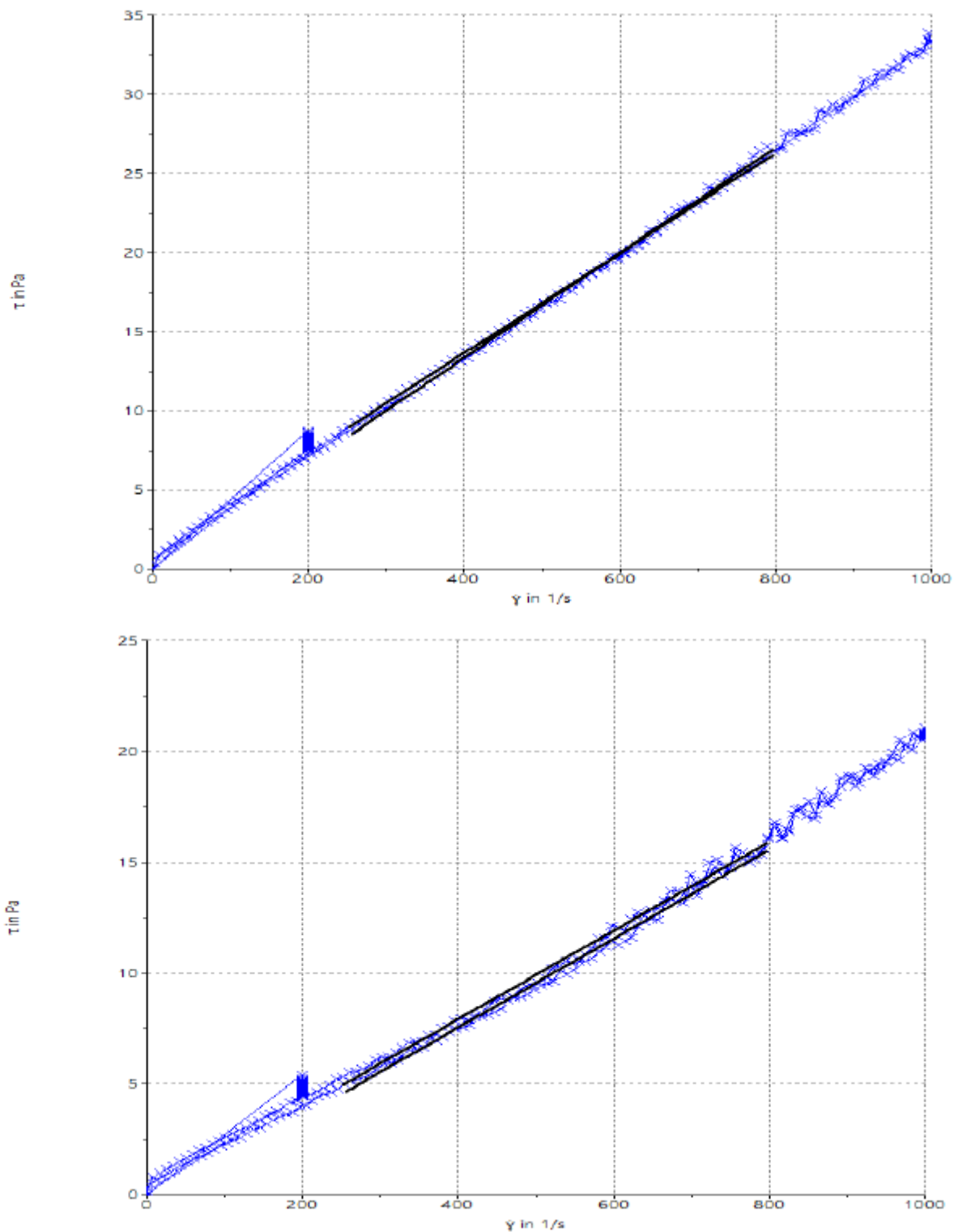


Figure D.20 Melter feed #9b: Yield stress versus shear rate at 20°C (top) and 40°C (bottom).

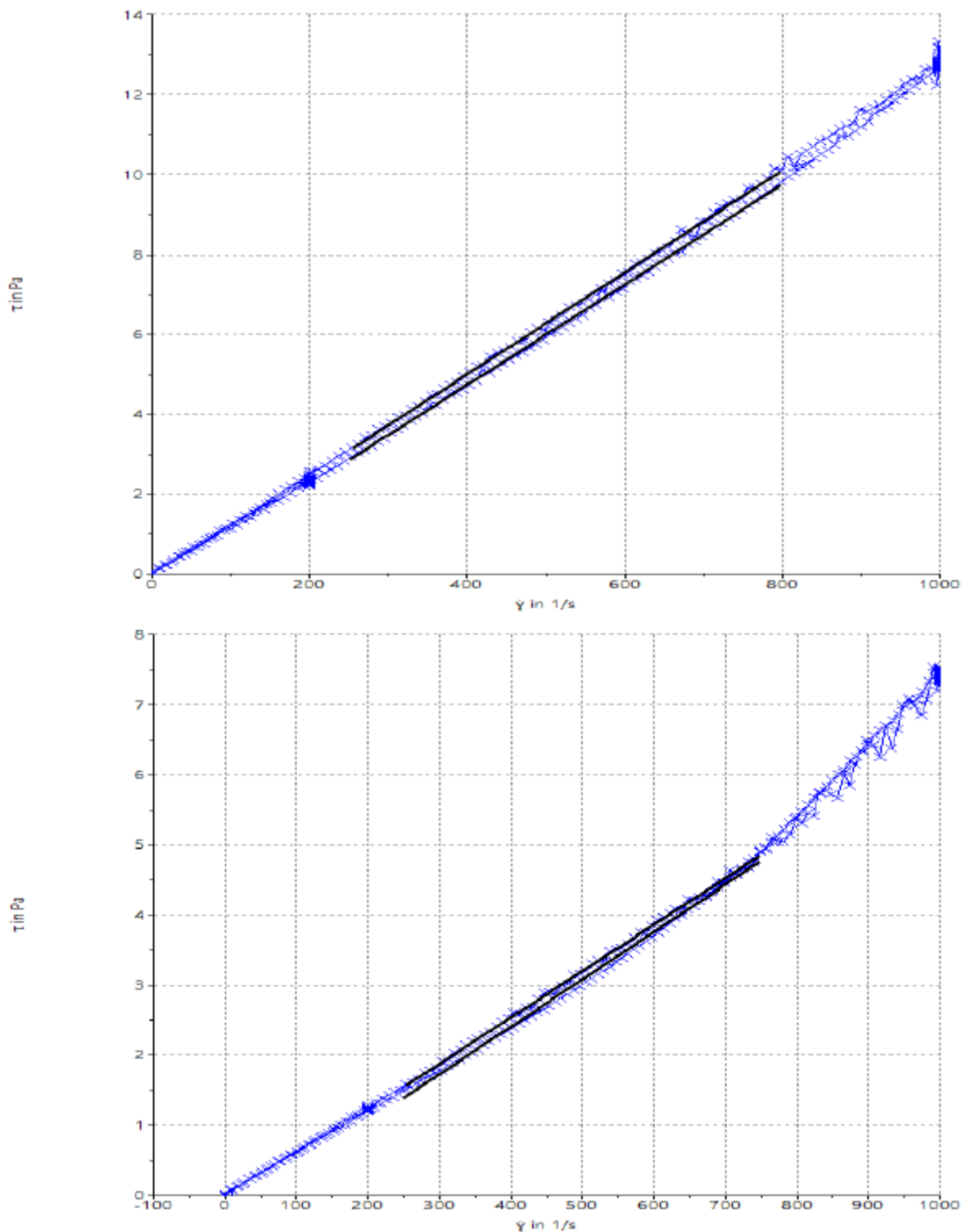


Figure D.21 Melter feed #1-1: Yield stress versus shear rate at 20°C (top) and 40°C (bottom).

## Appendix E – Original Particle Size Distribution Data Measured at PNNL

This appendix provides the original results of the particle size distribution for individual GFCs and their mixtures generated by Pacific Northwest National Laboratory.

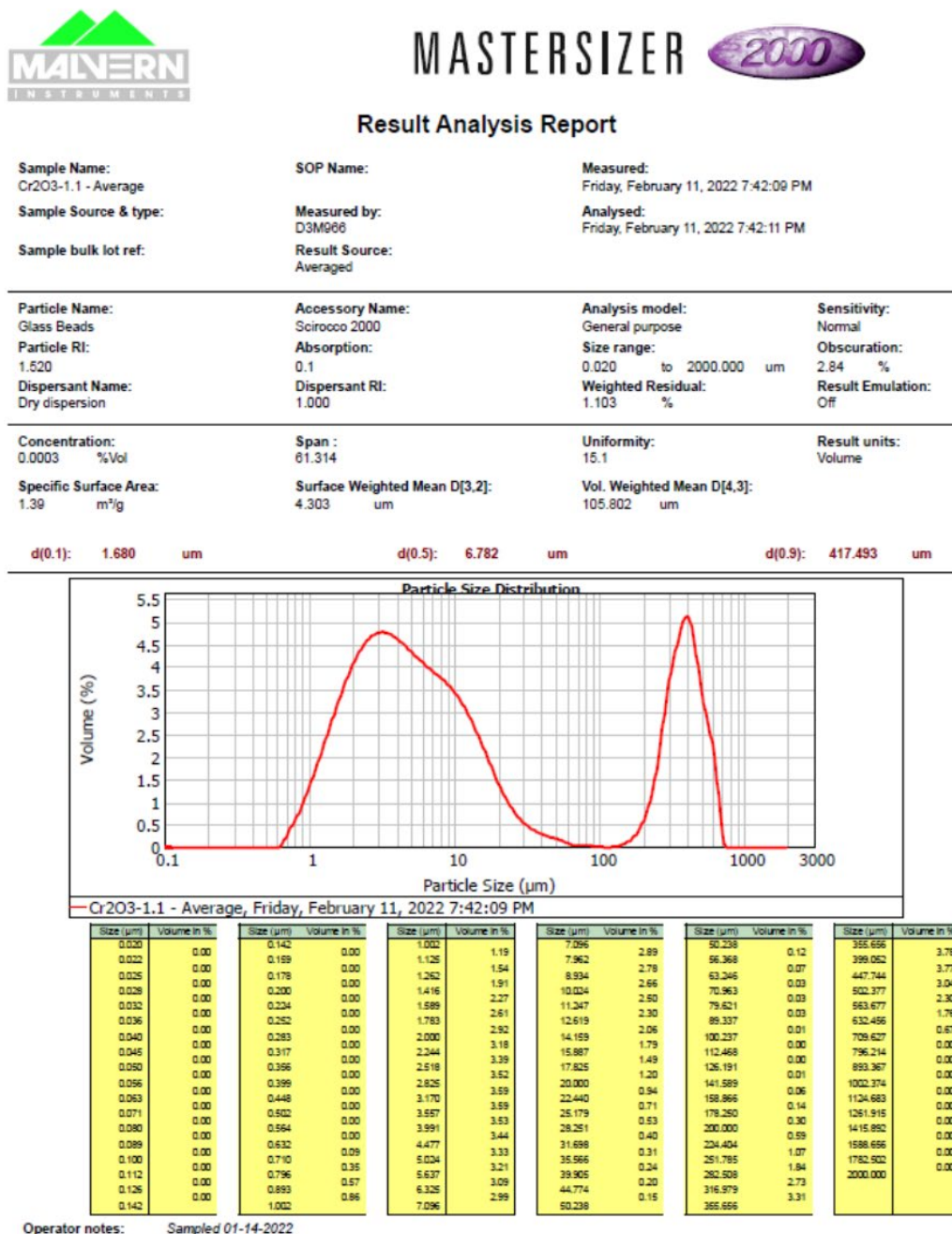


Figure E.1. Particle size distribution for Cr<sub>2</sub>O<sub>3</sub>



# MASTERSIZER



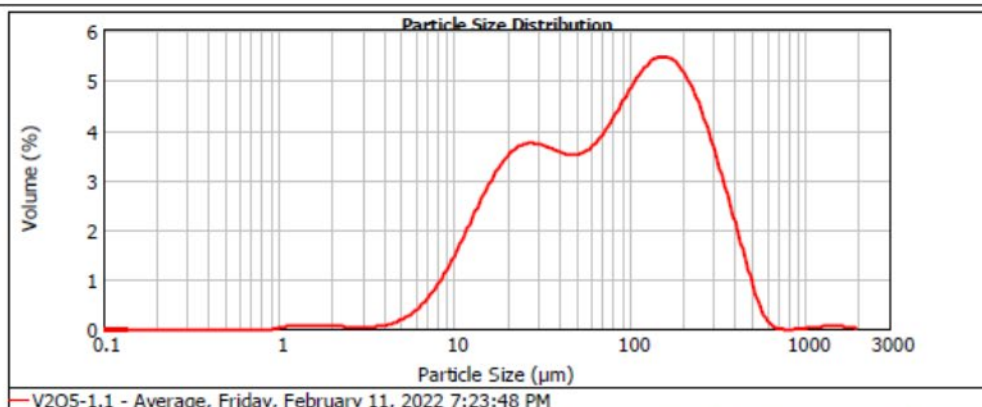
## Result Analysis Report

Sample Name: V2O5-1.1 - Average      SOP Name:      Measured: Friday, February 11, 2022 7:23:48 PM  
Sample Source & type:      Measured by: D3M966      Analysed: Friday, February 11, 2022 7:23:50 PM  
Sample bulk lot ref:      Result Source: Averaged

Particle Name: Glass Beads      Accessory Name: Scirocco 2000      Analysis model: General purpose      Sensitivity: Normal  
Particle RI: 1.520      Absorption:      Size range: 0.020 to 2000.000 um      Obscuration: 2.31 %  
Dispersant Name: Dry dispersion      Dispersant RI: 1.000      Weighted Residual: 0.301 %      Result Emulation: Off

Concentration: 0.0026 %Vol      Span : 3.205      Uniformity: 1.04      Result units: Volume  
Specific Surface Area: 0.167 m<sup>2</sup>/g      Surface Weighted Mean D[3,2]: 35.925 um      Vol. Weighted Mean D[4,3]: 122.582 um

d(0.1): 15.416 um      d(0.5): 83.720 um      d(0.9): 283.728 um



Size (µm)	Volume in %	Size (µm)	Volume in %	Size (µm)	Volume in %	Size (µm)	Volume in %	Size (µm)	Volume in %	Size (µm)	Volume in %
0.020	0.00	0.142	0.00	1.002	0.04	7.096	0.56	50.238	2.66	355.656	1.84
0.022	0.00	0.159	0.00	1.125	0.06	7.962	0.76	56.368	2.74	399.052	1.37
0.025	0.00	0.178	0.00	1.262	0.06	8.934	0.99	63.246	2.88	447.744	0.91
0.028	0.00	0.200	0.00	1.416	0.06	10.024	1.25	70.963	3.06	502.377	0.46
0.032	0.00	0.224	0.00	1.589	0.06	11.247	1.52	79.621	3.28	563.677	0.16
0.036	0.00	0.252	0.00	1.783	0.06	12.619	1.80	89.337	3.52	632.456	0.03
0.040	0.00	0.283	0.00	2.000	0.06	14.159	2.08	100.237	3.74	709.627	0.00
0.045	0.00	0.317	0.00	2.244	0.06	15.887	2.32	112.468	3.93	796.214	0.00
0.050	0.00	0.356	0.00	2.518	0.03	17.825	2.53	126.191	4.06	893.367	0.01
0.056	0.00	0.399	0.00	2.825	0.03	20.000	2.68	141.589	4.13	1002.374	0.03
0.063	0.00	0.448	0.00	3.170	0.04	22.440	2.78	159.866	4.11	1124.683	0.04
0.071	0.00	0.502	0.00	3.557	0.05	25.179	2.82	179.250	4.00	1261.915	0.05
0.080	0.00	0.564	0.00	3.991	0.07	28.251	2.81	200.000	3.81	1415.892	0.05
0.089	0.00	0.632	0.00	4.477	0.11	31.698	2.77	224.404	3.53	1588.656	0.04
0.100	0.00	0.710	0.00	5.024	0.18	35.966	2.71	251.785	3.18	1782.902	0.03
0.112	0.00	0.796	0.00	5.637	0.27	39.905	2.66	282.508	2.78	2000.000	0.00
0.126	0.00	0.893	0.01	6.325	0.40	44.774	2.64	316.979	2.32		
0.142	0.00	1.002	0.01	7.096	0.56	50.238	2.64	355.656	2.32		

Operator notes: Sampled 01-14-2022

Figure E.2. Particle size distribution for V<sub>2</sub>O<sub>5</sub>



# MASTERSIZER



## Result Analysis Report

**Sample Name:**  
SnO-1.1-Average Result

**Sample Source & type:**

**Sample bulk lot ref:**

**SOP Name:**

**Measured by:**  
D3M966

**Result Source:**  
Averaged

**Measured:**

Friday, February 11, 2022 6:33:35 PM

**Analysed:**

Friday, February 11, 2022 7:11:52 PM

**Particle Name:**

Glass Beads

**Particle RI:**

1.520

**Dispersant Name:**

**Accessory Name:**

Scirocco 2000

**Absorption:**

0.1

**Dispersant RI:**

1.000

**Analysis model:**

General purpose

**Size range:**

0.020 to 2000.000  $\mu\text{m}$

**Weighted Residual:**

1.023 %

**Sensitivity:**

Normal

**Obscuration:**

3.84 %

**Result Emulation:**

Off

**Concentration:**

0.0043 %Vol

**Specific Surface Area:**

0.175  $\text{m}^2/\text{g}$

**Span :**

1.455

**Surface Weighted Mean D[3,2]:**

34.325  $\mu\text{m}$

**Uniformity:**

0.397

**Vol. Weighted Mean D[4,3]:**

58.967  $\mu\text{m}$

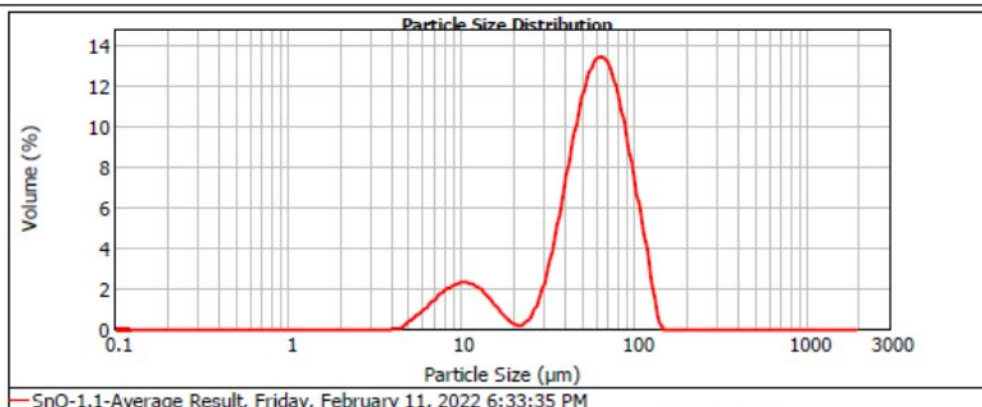
**Result units:**

Volume

**d(0.1):** 12.522  $\mu\text{m}$

**d(0.5):** 58.446  $\mu\text{m}$

**d(0.9):** 97.546  $\mu\text{m}$



Size ( $\mu\text{m}$ )	Volume in %	Size ( $\mu\text{m}$ )	Volume in %	Size ( $\mu\text{m}$ )	Volume in %	Size ( $\mu\text{m}$ )	Volume in %	Size ( $\mu\text{m}$ )	Volume in %	Size ( $\mu\text{m}$ )	Volume in %	Size ( $\mu\text{m}$ )	Volume in %
0.020	0.00	0.142	0.00	1.002	0.00	7.096	1.27	50.238	9.21	355.656	0.00		
0.022	0.00	0.159	0.00	1.125	0.00	7.962	1.52	56.368	10.00	399.052	0.00		
0.025	0.00	0.178	0.00	1.262	0.00	8.934	1.69	63.246	10.11	447.744	0.00		
0.028	0.00	0.200	0.00	1.416	0.00	10.024	1.75	70.963	9.50	502.377	0.00		
0.032	0.00	0.224	0.00	1.589	0.00	11.247	1.66	79.621	8.28	563.677	0.00		
0.036	0.00	0.252	0.00	1.783	0.00	12.619	1.42	89.337	6.59	632.456	0.00		
0.040	0.00	0.283	0.00	2.000	0.00	14.159	1.08	100.237	4.77	709.627	0.00		
0.045	0.00	0.317	0.00	2.244	0.00	15.887	0.69	112.468	2.98	796.214	0.00		
0.050	0.00	0.356	0.00	2.518	0.00	17.825	0.34	126.191	0.86	893.367	0.00		
0.056	0.00	0.399	0.00	2.825	0.00	20.000	0.15	141.589	0.00	1002.374	0.00		
0.063	0.00	0.448	0.00	3.170	0.00	22.440	0.08	158.866	0.00	1124.683	0.00		
0.071	0.00	0.502	0.00	3.557	0.00	25.179	0.24	178.250	0.00	1261.915	0.00		
0.080	0.00	0.564	0.00	3.991	0.00	28.251	0.69	200.000	0.00	1415.892	0.00		
0.089	0.00	0.632	0.00	4.477	0.01	31.698	1.58	224.404	0.00	1588.656	0.00		
0.100	0.00	0.710	0.00	5.024	0.43	35.966	4.46	251.785	0.00	1782.902	0.00		
0.112	0.00	0.796	0.00	5.637	0.67	39.905	6.22	282.508	0.00	2000.000	0.00		
0.126	0.00	0.893	0.00	6.325	0.98	44.774	7.87	316.979	0.00				
0.142	0.00	1.002	0.00	7.096		50.238		355.656	0.00				

Operator notes: Average of 5 measurements from GFC Powder measurements 2022.mea

Figure E.3. Particle size distribution for SnO





# MASTERSIZER

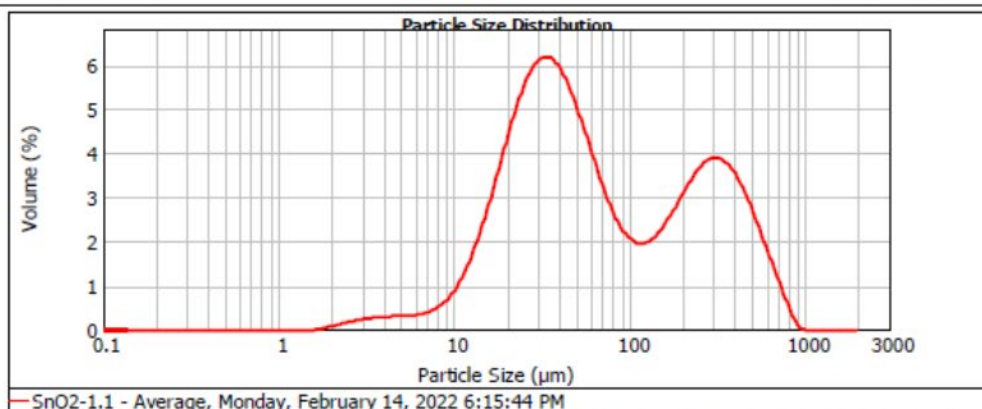


## Result Analysis Report

**Sample Name:** SnO2-1.1 - Average  
**Sample Source & type:** D3M966  
**Sample bulk lot ref:** Averaged  
**SOP Name:** Measured: Monday, February 14, 2022 6:15:44 PM  
**Measured by:** D3M966  
**Result Source:** Averaged  
**Analysed:** Monday, February 14, 2022 6:15:45 PM

<b>Particle Name:</b> Glass Beads	<b>Accessory Name:</b> Scirocco 2000	<b>Analysis model:</b> General purpose	<b>Sensitivity:</b> Normal
<b>Particle RI:</b> 1.520	<b>Absorption:</b> 0.1	<b>Size range:</b> 0.020 to 2000.000 um	<b>Obscuration:</b> 3.37 %
<b>Dispersant Name:</b> Dry dispersion	<b>Dispersant RI:</b> 1.000	<b>Weighted Residual:</b> 0.209 %	<b>Result Emulation:</b> Off
<b>Concentration:</b> 0.0038 %Vol	<b>Span :</b> 7.157	<b>Uniformity:</b> 2.11	<b>Result units:</b> Volume
<b>Specific Surface Area:</b> 0.175 m <sup>2</sup> /g	<b>Surface Weighted Mean D[3,2]:</b> 34.268 um	<b>Vol. Weighted Mean D[4,3]:</b> 140.087 um	

**d(0.1):** 16.866 um      **d(0.5):** 53.161 um      **d(0.9):** 397.347 um



Size (µm)	Volume in %	Size (µm)	Volume in %	Size (µm)	Volume in %	Size (µm)	Volume in %	Size (µm)	Volume in %	Size (µm)	Volume in %	Size (µm)	Volume in %
0.020	0.00	0.142	0.00	1.002	0.00	7.096	0.33	50.238	3.96	355.656	2.77		
0.022	0.00	0.159	0.00	1.125	0.00	7.962	0.42	56.368	3.09	399.052	2.53		
0.025	0.00	0.178	0.00	1.262	0.00	8.934	0.57	63.246	2.63	447.744	2.21		
0.028	0.00	0.200	0.00	1.416	0.00	10.024	0.78	70.963	2.22	502.377	1.89		
0.032	0.00	0.224	0.00	1.589	0.01	11.247	1.08	79.621	1.88	563.677	1.42		
0.036	0.00	0.252	0.00	1.783	0.05	12.619	1.46	89.337	1.50	632.456	1.02		
0.040	0.00	0.283	0.00	2.000	0.08	14.159	1.92	100.237	1.54	709.627	0.61		
0.045	0.00	0.317	0.00	2.244	0.12	15.887	2.44	112.468	1.57	796.214	0.25		
0.050	0.00	0.356	0.00	2.518	0.15	17.825	2.98	126.191	1.54	893.367	0.02		
0.056	0.00	0.399	0.00	2.825	0.18	20.000	3.51	141.589	1.70	1002.374	0.00		
0.063	0.00	0.448	0.00	3.170	0.20	22.440	3.98	158.866	1.92	1124.683	0.00		
0.071	0.00	0.502	0.00	3.557	0.22	25.179	4.35	178.250	2.18	1261.915	0.00		
0.080	0.00	0.564	0.00	3.991	0.23	28.251	4.58	200.000	2.45	1415.892	0.00		
0.089	0.00	0.632	0.00	4.477	0.24	31.698	4.66	224.404	2.68	1588.656	0.00		
0.100	0.00	0.710	0.00	5.024	0.24	35.966	4.57	251.785	2.85	1782.902	0.00		
0.112	0.00	0.796	0.00	5.637	0.25	39.905	4.34	282.508	2.93	2000.000	0.00		
0.126	0.00	0.893	0.00	6.325	0.28	44.774	3.99	316.979	2.91				
0.142	0.00	1.002	0.00	7.096	0.33	50.238	3.96	355.656	2.77				

Operator notes: Sampled 01-14-2022 Balls in fine basket

Figure E.4. Particle size distribution for SnO<sub>2</sub>



## Result Analysis Report

Sample Name:  
ZrSiO<sub>4</sub>-1.1-Average Result

Sample Source & type:

Sample bulk lot ref:

SOP Name:

Measured by:  
D3M066

Result Source:  
Averaged

Measured:

Friday, February 11, 2022 8:03:37 PM

Analysed:

Friday, February 11, 2022 8:03:39 PM

Particle Name:

Glass Beads

Particle RI:

1.520

Dispersant Name:

Dry dispersion

Accessory Name:

Scirocco 2000

Absorption:

0.1

Dispersant RI:

1.000

Analysis model:

General purpose

Size range:

0.020 to 2000.000  $\mu$ m

Weighted Residual:

0.457 %

Sensitivity:

Normal

Obscuration:

2.48 %

Result Emulation:

Off

Concentration:

0.0082 %Vol

Specific Surface Area:

0.061 m<sup>2</sup>/g

Span :

0.647

Surface Weighted Mean D[3,2]:

98.440  $\mu$ m

Uniformity:

0.203

Vol. Weighted Mean D[4,3]:

104.606  $\mu$ m

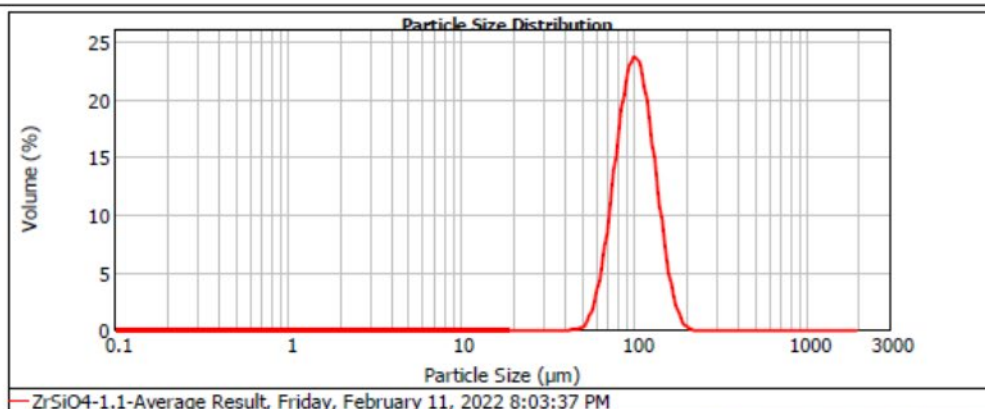
Result units:

Volume

d(0.1): 73.803  $\mu$ m

d(0.5): 101.529  $\mu$ m

d(0.9): 139.527  $\mu$ m



Size ( $\mu$ m)	Volume in %	Size ( $\mu$ m)	Volume in %	Size ( $\mu$ m)	Volume in %	Size ( $\mu$ m)	Volume in %	Size ( $\mu$ m)	Volume in %	Size ( $\mu$ m)	Volume in %
0.020	0.00	0.142	0.00	1.002	0.00	7.096	0.00	50.238	0.44	355.656	0.00
0.022	0.00	0.159	0.00	1.125	0.00	7.962	0.00	56.368	0.44	399.052	0.00
0.025	0.00	0.178	0.00	1.262	0.00	8.934	0.00	63.346	1.96	447.744	0.00
0.028	0.00	0.200	0.00	1.416	0.00	10.024	0.00	70.963	4.90	502.377	0.00
0.032	0.00	0.224	0.00	1.589	0.00	11.247	0.00	79.621	9.30	563.677	0.00
0.036	0.00	0.252	0.00	1.783	0.00	12.619	0.00	89.337	14.03	632.456	0.00
0.040	0.00	0.283	0.00	2.000	0.00	14.159	0.00	100.237	17.29	709.627	0.00
0.045	0.00	0.317	0.00	2.244	0.00	15.887	0.00	112.468	14.96	796.214	0.00
0.050	0.00	0.356	0.00	2.518	0.00	17.825	0.00	126.191	10.42	893.367	0.00
0.056	0.00	0.399	0.00	2.825	0.00	20.000	0.00	141.589	5.78	1002.374	0.00
0.063	0.00	0.448	0.00	3.170	0.00	22.440	0.00	158.866	2.44	1124.683	0.00
0.071	0.00	0.502	0.00	3.657	0.00	25.179	0.00	178.250	0.68	1261.915	0.00
0.080	0.00	0.564	0.00	3.991	0.00	28.251	0.00	200.000	0.03	1415.892	0.00
0.089	0.00	0.632	0.00	4.477	0.00	31.698	0.00	224.404	0.00	1588.656	0.00
0.100	0.00	0.710	0.00	5.034	0.00	35.566	0.00	251.795	0.00	1782.502	0.00
0.112	0.00	0.796	0.00	5.637	0.00	39.905	0.00	282.508	0.00	2000.000	0.00
0.126	0.00	0.893	0.00	6.325	0.00	44.774	0.07	316.979	0.00		
0.142	0.00	1.002	0.00	7.096	0.00	50.238	0.00	355.656	0.00		

Operator notes: Average of 4 measurements from GFC Powder measurements 2022.mea

Figure E.5. Particle size distribution for ZrSiO<sub>4</sub>





# MASTERSIZER



## Result Analysis Report

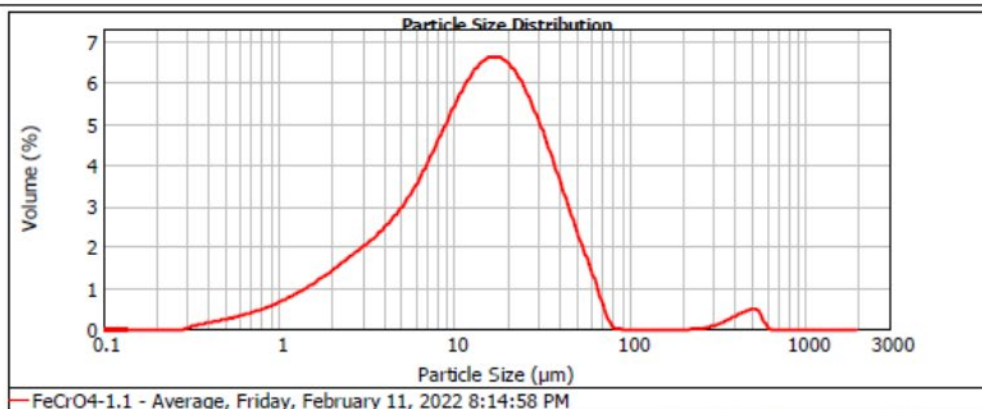
<b>Sample Name:</b> FeCrO4-1.1 - Average	<b>SOP Name:</b>	<b>Measured:</b> Friday, February 11, 2022 8:14:58 PM
<b>Sample Source &amp; type:</b>	<b>Measured by:</b> D3M966	<b>Analysed:</b> Friday, February 11, 2022 8:14:59 PM
<b>Sample bulk lot ref:</b>	<b>Result Source:</b> Averaged	

<b>Particle Name:</b> Glass Beads	<b>Accessory Name:</b> Scirocco 2000	<b>Analysis model:</b> General purpose	<b>Sensitivity:</b> Normal
<b>Particle RI:</b> 1.520	<b>Absorption:</b> 0.1	<b>Size range:</b> 0.020 to 2000.000 um	<b>Obscuration:</b> 2.38 %
<b>Dispersant Name:</b> Dry dispersion	<b>Dispersant RI:</b> 1.000	<b>Weighted Residual:</b> 0.375 %	<b>Result Emulation:</b> Off

<b>Concentration:</b> 0.0004 %Vol	<b>Span :</b> 2.683	<b>Uniformity:</b> 1.25	<b>Result units:</b> Volume
<b>Specific Surface Area:</b> 0.991 m <sup>2</sup> /g	<b>Surface Weighted Mean D[3,2]:</b> 0.053 um	<b>Vol. Weighted Mean D[4,3]:</b> 23.570 um	

d(0.1): 2.674 um      d(0.5): 13.601 um      d(0.9): 39.171 um



Size (µm)	Volume in %	Size (µm)	Volume in %	Size (µm)	Volume in %	Size (µm)	Volume in %	Size (µm)	Volume in %	Size (µm)	Volume in %	Size (µm)	Volume in %
0.020	0.00	0.142	0.00	1.002	0.53	7.096	3.21	50.238	1.56	355.656	0.20		
0.022	0.00	0.159	0.00	1.125	0.61	7.962	3.56	56.368	1.12	399.052	0.28		
0.025	0.00	0.178	0.00	1.262	0.70	8.934	3.91	63.246	0.67	447.744	0.34		
0.028	0.00	0.200	0.00	1.416	0.79	10.024	4.25	70.963	0.19	502.377	0.38		
0.032	0.00	0.224	0.00	1.589	0.90	11.247	4.54	79.621	0.00	563.677	0.08		
0.036	0.00	0.252	0.00	1.783	1.01	12.619	4.78	89.337	0.00	632.456	0.00		
0.040	0.00	0.283	0.01	2.000	1.12	14.159	4.93	100.237	0.00	709.627	0.00		
0.045	0.00	0.317	0.08	2.244	1.24	15.887	4.99	112.468	0.00	796.214	0.00		
0.050	0.00	0.356	0.10	2.518	1.36	17.825	4.94	126.191	0.00	893.367	0.00		
0.056	0.00	0.399	0.14	2.825	1.49	20.000	4.81	141.589	0.00	1002.374	0.00		
0.063	0.00	0.448	0.17	3.170	1.62	22.440	4.57	159.866	0.00	1124.683	0.00		
0.071	0.00	0.502	0.20	3.557	1.77	25.179	4.25	179.250	0.00	1261.915	0.00		
0.080	0.00	0.564	0.24	3.991	1.93	28.251	3.87	200.000	0.00	1415.892	0.00		
0.089	0.00	0.632	0.29	4.477	2.12	31.698	3.43	224.404	0.00	1588.656	0.00		
0.100	0.00	0.710	0.34	5.024	2.34	35.966	2.97	251.785	0.02	1782.902	0.00		
0.112	0.00	0.796	0.39	5.637	2.60	39.905	2.49	282.508	0.06	2000.000	0.00		
0.126	0.00	0.893	0.46	6.325	2.89	44.774	2.03	316.979	0.12				
0.142	0.00	1.002	0.53	7.096	3.21	50.238	1.56	355.656	0.20				

Operator notes: Sampled 01-14-2022

Figure E.6. Particle size distribution for FeCr<sub>2</sub>O<sub>4</sub>



# MASTERSIZER



## Result Analysis Report

**Sample Name:**  
Law Batch #1a-1.1 - Average

**Sample Source & type:**

**Sample bulk lot ref:**

**SOP Name:**

**Measured by:**  
D3M966

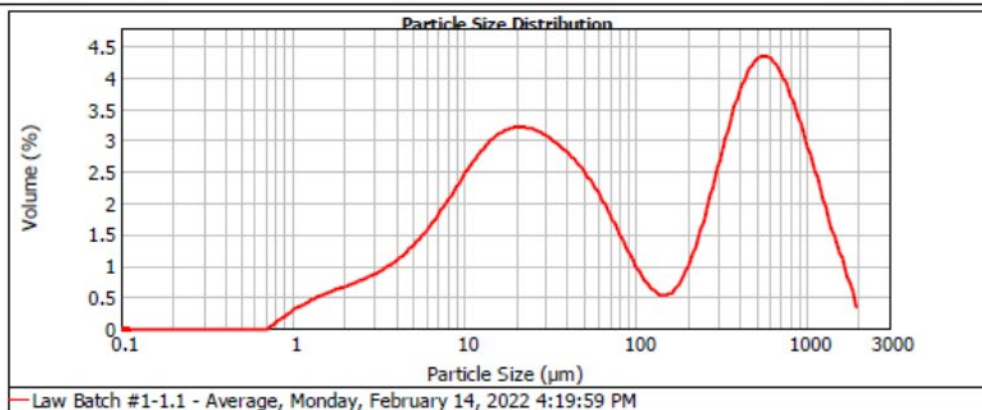
**Result Source:**  
Averaged

**Measured:**  
Monday, February 14, 2022 4:19:59 PM

**Analysed:**  
Monday, February 14, 2022 4:20:00 PM

<b>Particle Name:</b> Glass Beads	<b>Accessory Name:</b> Scirocco 2000	<b>Analysis model:</b> General purpose	<b>Sensitivity:</b> Normal
<b>Particle RI:</b> 1.520	<b>Absorption:</b> 0.1	<b>Size range:</b> 0.020 to 2000.000 $\mu\text{m}$	<b>Obscuration:</b> 2.44 %
<b>Dispersant Name:</b> Dry dispersion	<b>Dispersant RI:</b> 1.000	<b>Weighted Residual:</b> 0.299 %	<b>Result Emulation:</b> Off
<b>Concentration:</b> 0.0011 %Vol	<b>Span :</b> 14.809	<b>Uniformity:</b> 4.72	<b>Result units:</b> Volume
<b>Specific Surface Area:</b> 0.395 $\text{m}^2/\text{g}$	<b>Surface Weighted Mean D[3,2]:</b> 15.199 $\mu\text{m}$	<b>Vol. Weighted Mean D[4,3]:</b> 295.860 $\mu\text{m}$	

d(0.1): 6.084  $\mu\text{m}$       d(0.5): 58.480  $\mu\text{m}$       d(0.9): 872.107  $\mu\text{m}$



Size ( $\mu\text{m}$ )	Volume In %	Size ( $\mu\text{m}$ )	Volume In %	Size ( $\mu\text{m}$ )	Volume In %	Size ( $\mu\text{m}$ )	Volume In %	Size ( $\mu\text{m}$ )	Volume In %	Size ( $\mu\text{m}$ )	Volume In %
0.020	0.00	0.142	0.00	1.002	0.25	7.096	1.45	50.238	1.80	355.656	2.85
0.022	0.00	0.169	0.00	1.125	0.31	7.962	1.60	56.368	1.65	399.052	2.95
0.025	0.00	0.178	0.00	1.262	0.31	8.934	1.60	63.246	1.65	447.744	2.95
0.028	0.00	0.200	0.00	1.416	0.36	10.024	1.75	70.963	1.46	502.377	3.15
0.032	0.00	0.224	0.00	1.589	0.40	11.247	1.92	79.621	1.26	563.677	3.25
0.036	0.00	0.252	0.00	1.793	0.45	12.619	2.07	89.337	1.05	632.456	3.25
0.040	0.00	0.283	0.00	2.000	0.52	14.159	2.19	100.237	0.85	709.627	3.14
0.045	0.00	0.317	0.00	2.244	0.56	15.887	2.29	112.468	0.66	796.214	2.94
0.050	0.00	0.356	0.00	2.518	0.56	17.825	2.36	126.191	0.51	893.367	2.67
0.056	0.00	0.399	0.00	2.825	0.60	20.000	2.40	141.589	0.42	1002.374	2.36
0.063	0.00	0.448	0.00	3.170	0.65	22.440	2.41	158.866	0.40	1124.683	2.03
0.071	0.00	0.502	0.00	3.557	0.71	25.179	2.40	178.250	0.46	1261.915	1.68
0.080	0.00	0.564	0.00	3.991	0.77	28.251	2.37	200.000	0.61	1415.892	1.31
0.089	0.00	0.632	0.00	4.477	0.85	31.698	2.31	224.404	0.85	1588.656	1.01
0.100	0.00	0.710	0.00	5.024	0.94	35.566	2.24	251.785	1.16	1782.502	0.68
0.112	0.00	0.796	0.03	5.637	1.04	39.905	2.15	282.508	1.52	2000.000	0.40
0.126	0.00	0.893	0.11	6.325	1.15	44.774	2.06	316.979	1.91		
0.142	0.00	1.002	0.19	7.096	1.30	50.238	1.94	355.656	2.30		

Operator notes: Sampled 01-14-2022

Figure E.7. Particle size distribution for LAW batch #1a



## Result Analysis Report

Sample Name:  
Law Batch #6a-1.1 - Average

Sample Source & type:

Sample bulk lot ref:

SOP Name:

Measured by:  
D3M966

Result Source:  
Averaged

Measured:

Monday, February 14, 2022 4:45:15 PM

Analysed:

Monday, February 14, 2022 4:45:17 PM

Particle Name:

Glass Beads

Particle RI:

1.520

Dispersant Name:

Dry dispersion

Accessory Name:

Scirocco 2000

Absorption:

0.1

Dispersant RI:

1.000

Analysis model:

General purpose

Size range:

0.020 to 2000.000 um

Weighted Residual:

0.268 %

Sensitivity:

Normal

Obscuration:

3.41 %

Result Emulation:

Off

Concentration:

0.0015 %Vol

Specific Surface Area:

0.386 m<sup>2</sup>/g

Span :

13.502

Surface Weighted Mean D[3,2]:

15.540 um

Uniformity:

4.25

Vol. Weighted Mean D[4,3]:

244.856 um

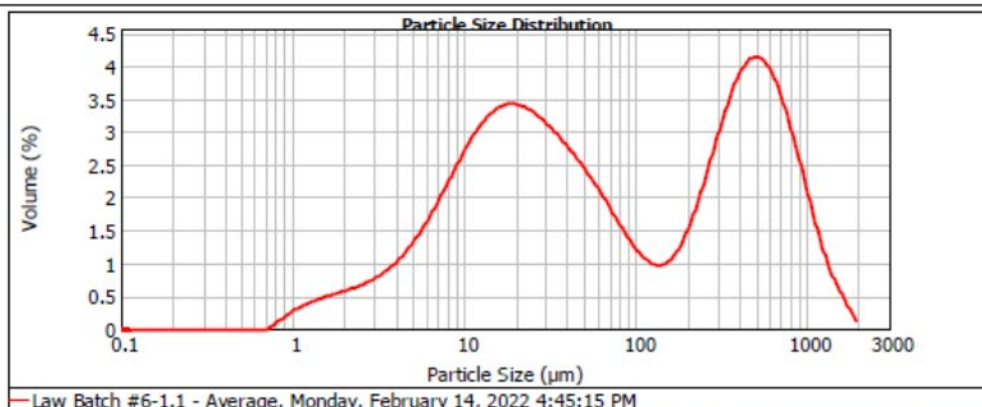
Result units:

Volume

d(0.1): 6.468 um

d(0.5): 53.234 um

d(0.9): 725.208 um



Size (µm)	Volume in %	Size (µm)	Volume in %	Size (µm)	Volume in %	Size (µm)	Volume in %	Size (µm)	Volume in %	Size (µm)	Volume in %
0.020	0.00	0.142	0.00	1.002	0.24	7.096	1.57	50.238	1.77	355.656	2.79
0.022	0.00	0.159	0.00	1.125	0.28	7.962	1.76	56.368	1.62	399.052	3.00
0.025	0.00	0.178	0.00	1.262	0.33	8.934	1.95	63.246	1.47	447.744	3.11
0.028	0.00	0.200	0.00	1.416	0.39	10.024	2.13	70.963	1.30	502.377	3.11
0.032	0.00	0.224	0.00	1.589	0.39	11.247	2.28	79.621	1.14	563.677	3.00
0.036	0.00	0.252	0.00	1.783	0.42	12.619	2.41	89.337	0.99	632.456	2.79
0.040	0.00	0.283	0.00	2.000	0.46	14.159	2.50	100.237	0.86	709.627	2.49
0.045	0.00	0.317	0.00	2.244	0.49	15.887	2.56	112.468	0.77	796.214	2.15
0.050	0.00	0.356	0.00	2.518	0.53	17.825	2.58	126.191	0.73	893.367	1.77
0.056	0.00	0.399	0.00	2.825	0.58	20.000	2.56	141.589	0.75	1002.374	1.39
0.063	0.00	0.448	0.00	3.170	0.64	22.440	2.52	159.866	0.85	1124.683	1.02
0.071	0.00	0.502	0.00	3.557	0.72	25.179	2.45	179.250	1.01	1261.915	0.72
0.080	0.00	0.564	0.00	3.991	0.81	28.251	2.36	200.000	1.25	1415.892	0.50
0.089	0.00	0.632	0.00	4.477	0.93	31.698	2.26	224.404	1.54	1588.656	0.31
0.100	0.00	0.710	0.03	5.024	1.06	35.566	2.15	251.785	1.86	1782.902	0.15
0.112	0.00	0.796	0.11	5.637	1.21	39.905	2.03	282.508	2.20	2000.000	
0.126	0.00	0.893	0.17	6.325	1.38	44.774	1.91	316.979	2.52		
0.142	0.00	1.002		7.096		50.238		355.656			

Operator notes: Sampled 01-14-2022 Balls in basket

Figure E.8. Particle size distribution for LAW batch #6a





# MASTERSIZER



## Result Analysis Report

**Sample Name:**  
Law Batch #9a-1.1 - Average

**Sample Source & type:**

**Sample bulk lot ref:**

**SOP Name:**

**Measured by:**  
D3M966

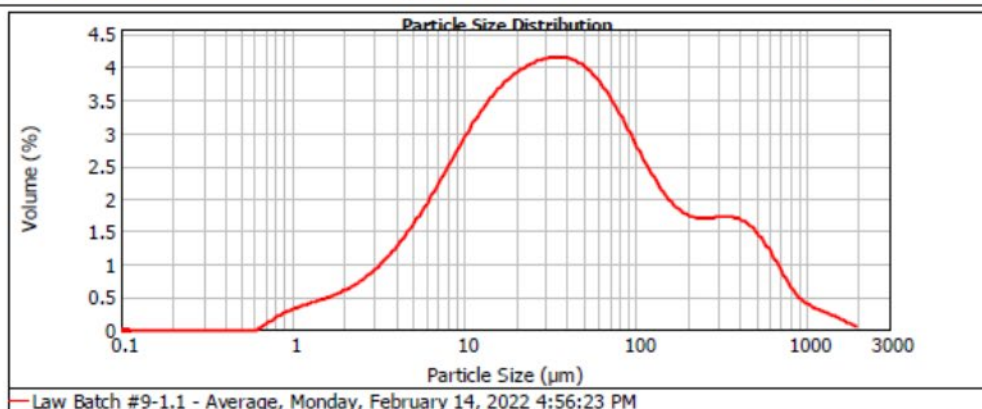
**Result Source:**  
Averaged

**Measured:**  
Monday, February 14, 2022 4:56:23 PM

**Analysed:**  
Monday, February 14, 2022 4:56:25 PM

<b>Particle Name:</b> Glass Beads	<b>Accessory Name:</b> Scirocco 2000	<b>Analysis model:</b> General purpose	<b>Sensitivity:</b> Normal
<b>Particle RI:</b> 1.520	<b>Absorption:</b> 0.1	<b>Size range:</b> 0.020 to 2000.000 um	<b>Obscuration:</b> 3.95 %
<b>Dispersant Name:</b> Dry dispersion	<b>Dispersant RI:</b> 1.000	<b>Weighted Residual:</b> 0.164 %	<b>Result Emulation:</b> Off
<b>Concentration:</b> 0.0015 %Vol	<b>Span :</b> 8.768	<b>Uniformity:</b> 2.65	<b>Result units:</b> Volume
<b>Specific Surface Area:</b> 0.454 m <sup>2</sup> /g	<b>Surface Weighted Mean D[3,2]:</b> 13.230 um	<b>Vol. Weighted Mean D[4,3]:</b> 109.908 um	

d(0.1): 5.674 um      d(0.5): 35.804 um      d(0.9): 319.591 um



Size (um)	Volume In %	Size (um)	Volume In %	Size (um)	Volume In %	Size (um)	Volume In %	Size (um)	Volume In %	Size (um)	Volume In %
0.020	0.00	0.142	0.00	1.002	0.25	7.096	1.76	50.238	2.98	355.656	1.28
0.022	0.00	0.159	0.00	1.125	0.29	7.962	1.94	56.368	2.87	399.052	1.25
0.025	0.00	0.178	0.00	1.262	0.32	8.934	2.11	63.246	2.74	447.744	1.18
0.028	0.00	0.200	0.00	1.416	0.35	10.024	2.29	70.963	2.59	502.377	1.07
0.032	0.00	0.224	0.00	1.589	0.39	11.247	2.44	79.621	2.41	563.677	0.93
0.036	0.00	0.252	0.00	1.783	0.43	12.619	2.58	89.337	2.22	632.456	0.85
0.040	0.00	0.283	0.00	2.000	0.47	14.159	2.71	100.237	2.03	709.627	0.76
0.045	0.00	0.317	0.00	2.244	0.53	15.887	2.81	112.468	1.84	796.214	0.69
0.050	0.00	0.356	0.00	2.518	0.60	17.825	2.90	126.191	1.68	893.367	0.63
0.056	0.00	0.399	0.00	2.825	0.68	20.000	2.98	141.589	1.53	1002.374	0.57
0.063	0.00	0.448	0.00	3.170	0.78	22.440	3.03	158.866	1.42	1124.683	0.52
0.071	0.00	0.502	0.00	3.557	0.88	25.179	3.08	178.250	1.34	1261.915	0.48
0.080	0.00	0.564	0.00	3.991	1.00	28.251	3.11	200.000	1.30	1415.892	0.44
0.089	0.00	0.632	0.00	4.477	1.13	31.698	3.13	224.404	1.28	1588.656	0.40
0.100	0.00	0.710	0.05	5.024	1.27	35.966	3.13	251.785	1.28	1782.902	0.36
0.112	0.00	0.796	0.11	5.637	1.43	39.905	3.10	282.508	1.29	2000.000	0.32
0.126	0.00	0.893	0.21	6.325	1.59	44.774	3.05	316.979	1.30		
0.142	0.00	1.002	0.21	7.096	1.76	50.238	3.05	355.656	1.30		

Operator notes: Sampled 01-14-2022 Balls in fine basket

Figure E.9. Particle size distribution for LAW batch #9a



# MASTERSIZER

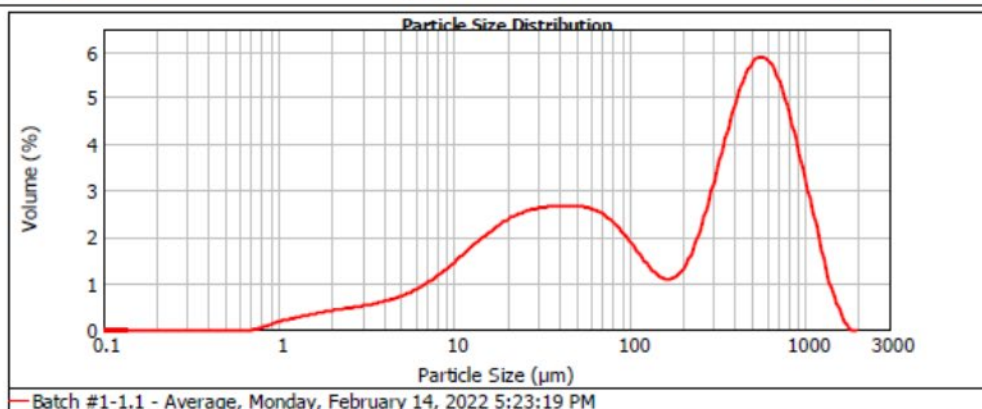


## Result Analysis Report

Sample Name: Batch #1b-1.1 - Average  
SOP Name:  
Measured: Monday, February 14, 2022 5:23:19 PM  
Sample Source & type: D3M966  
Measured by:  
Analysed: Monday, February 14, 2022 5:23:21 PM  
Sample bulk lot ref: Result Source: Averaged

Particle Name: Glass Beads	Accessory Name: Scirocco 2000	Analysis model: General purpose	Sensitivity: Normal
Particle RI: 1.520	Absorption: 0.1	Size range: 0.020 to 2000.000 um	Obscuration: 2.48 %
Dispersant Name: Dry dispersion	Dispersant RI: 1.000	Weighted Residual: 0.422 %	Result Emulation: Off
Concentration: 0.0017 %Vol	Span : 4.572	Uniformity: 1.56	Result units: Volume
Specific Surface Area: 0.255 m <sup>2</sup> /g	Surface Weighted Mean D[3,2]: 23.512 um	Vol. Weighted Mean D[4,3]: 321.969 um	

d(0.1): 10.510 um d(0.5): 178.677 um d(0.9): 827.485 um



Size (µm)	Volume In %	Size (µm)	Volume In %	Size (µm)	Volume In %	Size (µm)	Volume In %	Size (µm)	Volume In %	Size (µm)	Volume In %
0.020	0.00	0.142	0.00	1.002	0.15	7.096	0.82	50.238	2.00	355.656	3.42
0.022	0.00	0.159	0.00	1.125	0.18	7.962	0.92	56.368	1.97	399.052	3.89
0.025	0.00	0.178	0.00	1.262	0.22	8.934	1.03	63.246	1.91	447.744	4.23
0.028	0.00	0.200	0.00	1.416	0.25	10.024	1.16	70.963	1.82	502.377	4.41
0.032	0.00	0.224	0.00	1.589	0.27	11.247	1.28	79.621	1.69	563.677	4.40
0.036	0.00	0.252	0.00	1.783	0.30	12.619	1.41	89.337	1.52	632.456	4.20
0.040	0.00	0.283	0.00	2.000	0.32	14.159	1.53	100.237	1.34	709.627	3.83
0.045	0.00	0.317	0.00	2.244	0.34	15.887	1.64	112.468	1.14	796.214	3.33
0.050	0.00	0.356	0.00	2.518	0.36	17.825	1.74	126.191	0.97	893.367	2.73
0.056	0.00	0.399	0.00	2.825	0.39	20.000	1.82	141.589	0.86	1002.374	2.14
0.063	0.00	0.448	0.00	3.170	0.41	22.440	1.89	158.866	0.82	1124.683	1.52
0.071	0.00	0.502	0.00	3.557	0.44	25.179	1.94	178.250	0.89	1261.915	0.98
0.080	0.00	0.564	0.00	3.991	0.48	28.251	1.97	200.000	1.09	1415.892	0.47
0.089	0.00	0.632	0.00	4.477	0.52	31.698	1.99	224.404	1.41	1588.656	0.12
0.100	0.00	0.710	0.02	5.024	0.58	35.966	2.01	251.785	1.84	1782.902	0.00
0.112	0.00	0.796	0.06	5.637	0.64	39.905	2.01	282.508	2.34	2000.000	
0.126	0.00	0.893	0.11	6.325	0.72	44.774	2.01	316.979	2.90		
0.142	0.00	1.002	0.15	7.096	0.82	50.238	2.01	355.656	3.42		

Operator notes: Sampled 01-14-2022 Balls in fine basket

Figure E.10. Particle size distribution for LAW batch #1b







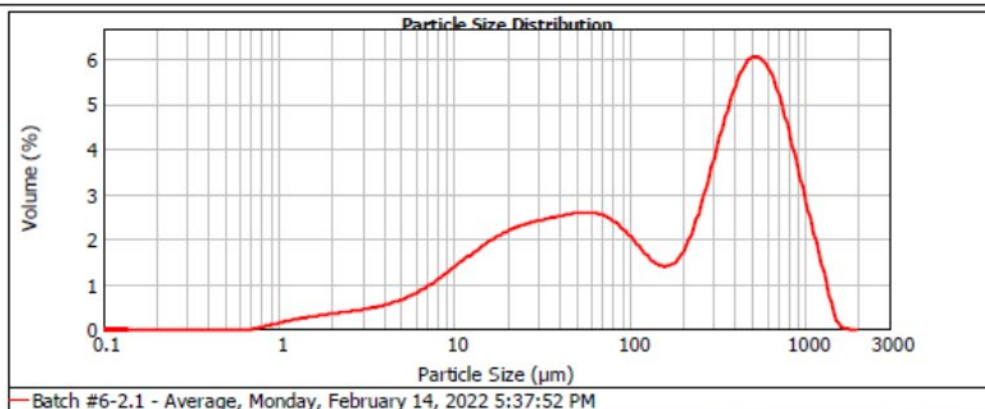
# MASTERSIZER 2000

## Result Analysis Report

Sample Name: Batch #6b-2.1 - Average  
SOP Name:  
Measured: Monday, February 14, 2022 5:37:52 PM  
Sample Source & type: Measured by: D3M966  
Analysed: Monday, February 14, 2022 5:37:54 PM  
Sample bulk lot ref: Result Source: Averaged

Particle Name: Glass Beads	Accessory Name: Scirocco 2000	Analysis model: General purpose	Sensitivity: Normal
Particle RI: 1.520	Absorption: 0.1	Size range: 0.020 to 2000.000 um	Obscuration: 2.79 %
Dispersant Name: Dry dispersion	Dispersant RI: 1.000	Weighted Residual: 0.423 %	Result Emulation: Off
Concentration: 0.0022 %Vol	Span: 3.686	Uniformity: 1.25	Result units: Volume
Specific Surface Area: 0.228 m <sup>2</sup> /g	Surface Weighted Mean D[3,2]: 26.311 um	Vol. Weighted Mean D[4,3]: 313.637 um	

d(0.1): 11.724 um d(0.5): 209.826 um d(0.9): 785.041 um



Size (µm)	Volume in %	Size (µm)	Volume in %	Size (µm)	Volume in %	Size (µm)	Volume in %	Size (µm)	Volume in %	Size (µm)	Volume in %	Size (µm)	Volume in %	Size (µm)	Volume in %
0.020	0.00	0.142	0.00	1.002	0.12	7.096	0.76	50.238	1.96	355.656	3.86				
0.022	0.00	0.159	0.00	1.125	0.15	7.962	0.87	56.368	1.96	399.052	4.25				
0.025	0.00	0.178	0.00	1.262	0.18	8.934	0.97	63.246	1.93	447.744	4.50				
0.028	0.00	0.200	0.00	1.416	0.20	10.024	1.09	70.963	1.87	502.377	4.56				
0.032	0.00	0.224	0.00	1.589	0.23	11.247	1.20	79.621	1.77	563.677	4.43				
0.036	0.00	0.252	0.00	1.783	0.25	12.619	1.31	89.337	1.63	632.456	4.12				
0.040	0.00	0.283	0.00	2.000	0.27	14.159	1.42	100.237	1.47	709.627	3.65				
0.045	0.00	0.317	0.00	2.244	0.28	15.887	1.51	112.468	1.30	796.214	3.09				
0.050	0.00	0.356	0.00	2.518	0.30	17.825	1.60	126.191	1.15	893.367	2.48				
0.056	0.00	0.399	0.00	2.825	0.33	20.000	1.67	141.589	1.06	1002.374	1.98				
0.063	0.00	0.448	0.00	3.170	0.35	22.440	1.72	158.866	1.06	1124.683	1.28				
0.071	0.00	0.502	0.00	3.657	0.38	25.179	1.77	178.250	1.17	1261.915	0.71				
0.080	0.00	0.564	0.00	3.991	0.42	28.251	1.81	200.000	1.42	1415.852	0.14				
0.089	0.00	0.632	0.00	4.477	0.47	31.698	1.84	224.404	1.79	1586.656	0.01				
0.100	0.00	0.710	0.01	5.024	0.52	35.956	1.87	251.785	2.26	1782.922	0.00				
0.112	0.00	0.796	0.06	5.637	0.59	39.905	1.90	282.508	2.80	2000.000					
0.126	0.00	0.893	0.09	6.325	0.67	44.774	1.93	316.979	3.35						
0.142	0.00	1.002	0.09	7.096		50.238		355.656							

Operator notes: Sampled 01-14-2022 Balls in fine basket

Figure E.12. Particle size distribution for LAW batch #6b



# MASTERSIZER



## Result Analysis Report

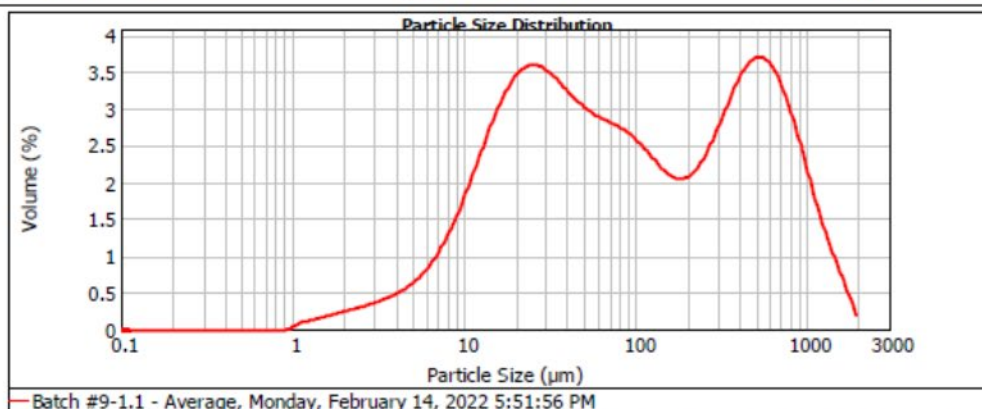
<b>Sample Name:</b> Batch #9b-1.1 - Average	<b>SOP Name:</b>	<b>Measured:</b> Monday, February 14, 2022 5:51:56 PM
<b>Sample Source &amp; type:</b>	<b>Measured by:</b> D3M966	<b>Analysed:</b> Monday, February 14, 2022 5:51:57 PM
<b>Sample bulk lot ref:</b>	<b>Result Source:</b> Averaged	

<b>Particle Name:</b> Glass Beads	<b>Accessory Name:</b> Scirocco 2000	<b>Analysis model:</b> General purpose	<b>Sensitivity:</b> Normal
<b>Particle RI:</b> 1.520	<b>Absorption:</b> 0.1	<b>Size range:</b> 0.020 to 2000.000 um	<b>Obscuration:</b> 1.98 %
<b>Dispersant Name:</b> Dry dispersion	<b>Dispersant RI:</b> 1.000	<b>Weighted Residual:</b> 0.225 %	<b>Result Emulation:</b> Off

<b>Concentration:</b> 0.0017 %Vol	<b>Span :</b> 8.935	<b>Uniformity:</b> 2.74	<b>Result units:</b> Volume
<b>Specific Surface Area:</b> 0.225 m <sup>2</sup> /g	<b>Surface Weighted Mean D[3,2]:</b> 26.626 um	<b>Vol. Weighted Mean D[4,3]:</b> 255.644 um	

d(0.1): 11.578 um      d(0.5): 82.344 um      d(0.9): 747.297 um



Size (um)	Volume in %	Size (um)	Volume in %	Size (um)	Volume in %	Size (um)	Volume in %	Size (um)	Volume in %	Size (um)	Volume in %	Size (um)	Volume in %
0.020	0.00	0.142	0.00	1.002	0.06	7.096	0.87	50.238	2.23	355.656	2.47		
0.022	0.00	0.159	0.00	1.125	0.09	7.962	1.04	56.368	2.18	399.052	2.64		
0.025	0.00	0.178	0.00	1.262	0.11	8.934	1.24	63.246	2.13	447.744	2.75		
0.028	0.00	0.200	0.00	1.416	0.13	10.024	1.47	70.963	2.09	502.377	2.79		
0.032	0.00	0.224	0.00	1.589	0.15	11.247	1.71	79.621	2.04	563.677	2.73		
0.036	0.00	0.252	0.00	1.783	0.15	12.619	1.71	89.337	2.04	632.456	2.73		
0.040	0.00	0.283	0.00	2.000	0.17	14.159	1.95	100.237	1.98	709.627	2.59		
0.045	0.00	0.317	0.00	2.244	0.20	15.887	2.17	112.468	1.90	796.214	2.37		
0.050	0.00	0.356	0.00	2.518	0.22	17.625	2.37	126.191	1.80	893.367	2.10		
0.056	0.00	0.399	0.00	2.825	0.28	20.000	2.64	141.589	1.61	1002.374	1.47		
0.063	0.00	0.448	0.00	3.170	0.31	22.440	2.70	158.866	1.55	1124.683	1.15		
0.071	0.00	0.502	0.00	3.557	0.34	25.179	2.70	178.250	1.54	1261.915	0.89		
0.080	0.00	0.564	0.00	3.991	0.39	28.251	2.65	200.000	1.59	1415.892	0.67		
0.089	0.00	0.632	0.00	4.477	0.44	31.698	2.58	224.404	1.69	1588.656	0.43		
0.100	0.00	0.710	0.00	5.024	0.51	35.966	2.48	251.785	1.85	1782.902	0.23		
0.112	0.00	0.796	0.00	5.637	0.51	39.905	2.39	282.508	2.04	2000.000			
0.126	0.00	0.893	0.01	6.325	0.72	44.774	2.30	316.979	2.26				
0.142	0.00	1.002	0.01	7.096		50.238		355.656					

Operator notes: Sampled 01-14-2022 Balls in fine basket

Figure E.13. Particle size distribution for LAW batch #9b



# **Pacific Northwest National Laboratory**

902 Battelle Boulevard  
P.O. Box 999  
Richland, WA 99354  
1-888-375-PNNL (7665)

***[www.pnnl.gov](http://www.pnnl.gov)***